Ultrastructural, morphological and molecular characterization of heterotopic cells in the hippocampus in epileptic Dcx knockout (KO) mice

Reham Khalaf-Nazzal

THESE DE DOCTORAT DE

L'UNIVERSITE PIERRE ET MARIE CURIE

Spécialité

Génétique et Neurodéveloppement

(Ecole doctorale Complexité du vivant)

Présentée par

REHAM KHALAF-NAZZAL

Pour obtenir le grade de

DOCTEUR de l'UNIVERSITÉ PIERRE ET MARIE CURIE

Titre de la thèse :

Caractérisation ultrastructurale, morphologique, et moléculaire des cellules hétérotopiques dans un modèle d'épilepsie hippocampique, chez les souris inactivées pour le gène *Dcx*

Soutenue le 19 November 2012

Devant le jury composé de:

Pr. Rose Katz Président

Dr. Alfonso Represa Rapporteur

Dr. Stéphane Auvin Rapporteur

Dr. Catherine Fallet-Bianco Examinateur

Pr. Richard Miles Examinateur

Dr. Fiona Francis Directeur de thèse

TITRE ET RESUME:

Caractérisation ultrastructurale, morphologique, et moléculaire des cellules hétérotopiques dans un modèle d'épilepsie hippocampique, les souris inactivées pour le gène *Dcx*

Des mutations dans le gène doublecortine (DCX) sont responsables de lissencéphalie de type 1 ou d'hétérotopie laminaire sous-corticale, un spectre de malformations corticales associées à de sévères crises d'épilepsie ainsi qu'à des déficits cognitifs. Les souris invalidées pour le gène Dcx sont épileptiques et présentent des anomalies hippocampiques, avec notamment la présence de deux couches de cellules pyramidales spécifiquement dans l'aire CA3 de cette structure. Le sujet de cette thèse concerne la caractérisation de ces neurones «hétérotopiques ». Cette hétérotopie hippocampique est associée à une hyperexcitabilité susceptible de perturber la fonction du réseau neuronal. Notre but est d'identifier les mécanismes moléculaires et cellulaires responsables de cette hyperexcitabilité chez les souris Dcx. Pendant ma thèse, et grâce à la technique de microdissection au laser suivie d'une étude de transcriptome, j'ai pu isoler les neurones mal-positionnés de la région CA3 de l'hippocampe des souris inactivées pour le gène Dcx, afin de comparer leurs profils d'expression génique à ceux des neurones de la région CA3 des souris contrôles. Les analyses comparatives globales de leurs profils d'expression génique ont permis de révéler des informations importantes sur leur génération et leur migration, nous aidant ainsi à mieux comprendre l'origine de l'hétérotopie. Les résultats au stade P0 (jour de la naissance des souris), montrent que les profils d'expression génique de chacune des deux couches hétérotopiques présentes chez les souris Dcx, diffèrent significativement entre eux ainsi qu'en comparaison avec les profils de la couche pyramidale des souris contrôles. Sur le plan fonctionnel, cette étude indique des perturbations au niveau des organelles intracellulaires, tels que les endosomes, les mitochondries et l'appareil de Golgi. En étudiant séparément les profils associés à chacune des deux couches des souris Dcx, nous avons mis en évidence des différences de degrés de maturité neuronale entre chacune des couches, suggérant des fenêtres temporelles distinctes de production des neurones. L'utilisation de marqueurs moléculaires spécifiques aux couches en combinaison avec des expériences d'injections de bromo-désoxy-uridine (BrdU) à différents moments du

développement suggère une inversion des couches neuronales présentes chez les souris Dcx en comparaison avec les souris contrôles. En complément des données d'expression génique, et en collaboration avec la plateforme de microscopie électronique de notre institut, j'ai également réalisé des analyses morphologiques et notamment des propriétés ultrastructurales des neurones anormaux en comparaison avec celles des neurones contrôles, au stade P0. Ces expériences ont ainsi permis de préciser la nature du défaut de lamination ainsi que les défauts morphologiques des cellules CA3 dans le modèle Dcx. Ces études indiquent que les cellules hétérotopiques des souris Dcx, présentent des anomalies d'organelles intracellulaires, avec notamment des défauts de mitochondries et des modifications de l'appareil de Golgi. Qui plus est, nos données montrent une augmentation significative de la mort cellulaire dans les régions CA1 et CA3 de l'hippocampe. Aussi, nous avons également montré que les couches hétérotopiques étaient hétérogènes, présentant notamment des distributions anormales des précurseurs d'oligodendrocytes et des interneurones exprimant la somatostatine, ce qui n'est pas le cas chez les souris contrôles. L'ensemble de ces données devrait nous permettre de mieux comprendre les dysfonctionnements des neurones pyramidaux chez les souris Dcx adultes. Ces résultats ouvrent donc de nouvelles perspectives pour mieux comprendre la physiopathologie de ces maladies graves associées à des hétérotopies neuronales dans le cerveau, de l'épilepsie et des déficits cognitifs.

TITLE & ABSTRACT:

Ultrastructural, morphological and molecular characterization of heterotopic cells in the hippocampus in epileptic Dcx knockout (KO) mice.

Mutations in the doublecortin gene (DCX) are responsible for type 1 lissencephaly and subcortical band heterotopia, malformations that lead to intellectual disability and epilepsy. This thesis work concerns the characterization of abnormally positioned 'heterotopic' neurons present in the Dcx knockout (Dcx KO) mouse model, which exhibits hippocampal dysplasia and epilepsy. The pyramidal cell layer of the hippocampal CA3 region in Dcx KO mutants is divided into two heterotopic cell layers instead of a single layer observed in the wild type (WT) controls. Heterotopic neurons show hyperexcitability, which is likely to lead to a perturbation of network function and subsequent epilepsy. Using the Dcx KO model, our work investigates the molecular and cellular mechanisms leading to hyperexcitability. During my thesis, I was able to isolate abnormally positioned heterotopic neurons using laser capture microdissection, from the CA3 region of the Dcx KO hippocampus, and compare them to WT neurons. Using transcriptome experiments, I aimed to determine the specific gene expression profiles of such cells. Global gene expression analyses of the knockout neurons revealed information concerning their generation and migration, which helps us understand why their positioning is abnormal. Knockout layers were shown to differ from each other and from WT at postnatal day 0. Common perturbed mechanisms affect intracellular organelles including endosomes, mitochondria and Golgi apparatuses. Studying perturbed mechanisms specific to the individual KO layers shows defined but distinct neurogenesis time windows of each layer, that correspond to a different maturity status in early postnatal stages. Layer specific molecular markers and bromo-deoxyuridine (BrdU) birth dating experiments in KO and WT mice, suggest that there is an inversion of the neuronal layers of the Dcx KO CA3 region, compared to wild type. Complementing these gene expression data, and in collaboration with the electron microscopy facility of our institute, I carried out ultrastructural and morphological analyses of abnormal Dcx KO neurons compared to WT, in their tissue environment of the developing brain (postnatal day 0). This revealed the nature of the lamination defect and the state of CA3 cells in this model. Potential organelle abnormalities, including mitochondrial defects and modifications

of the Golgi apparatus, were identified in Dcx KO cells, as well as significantly increased cell death in CA1 and CA3 regions. Oligodendrocyte precursor cells and somatostatin-positive interneurons were found interspersed within the pyramidal cell layers in early postnatal stages, and this was not the case in wild-type. These combined data may provide clues to the abnormal functioning of pyramidal neurons in the adult. These results therefore open up new directions in order to better understand the pathophysiology of a sepectrum of severe disorders associated with heterotopic neurons in the brain, presenting in human patients with severe epilepsy and, developmental delay, and intellectual disability.

ACKNOWLEDGEMENT:

It would not have been possible to write this doctoral thesis without the help and support of the kind people around me, who made this experience an unforgettable one for me, to only some of whom it is possible to give particular mention here.

I would like to start by expressing my gratitude to the thesis jury members. I thank Dr. Alfonso Represa and Dr. Stéphane Auvin for critically reading the thesis manuscript and their constructive comments that had important impact on its improvement. My special thanks to the thesis jury examiners, Dr. Catherine Fallet-Bianco and Pr. Richard Miles, not only for accepting to be examiners members in the jury, but also for following my scientific development in the past four years. My sincere thanks to Pr. Rose Katz, the thesis jury President. This thesis arose in the context of bilateral exchange between the UPMC and the Palestinian medical schools, for which Pr. Katz is a key member in the durable success of this scientific project.

I would like to express my deepest sense of gratitude to my thesis supervisor, Dr. Fiona Francis. I thank you for establishing this distinguished backbone of research theme and so this thesis, combining the clinical and fundamental research to study brain pathologies. I would like to thank you for your continuous advice, supervision, and crucial contribution to the advancement of my work. I deeply thank you for your scholarly inputs and consistent encouragement during the last four years. Thank you for your patience and enthusiasm when I was first initiated in doing scientific experiments, experiments as simple as DNA extraction to the complicated ones. Thank you for your unconditional support and making yourself available during thesis writing, continuously guiding me to improve the text despite my “limited and poor” English writing skills.

I will forever be sincerely thankful to my initiator on developmental neurosciences and neurogenetics, Pr. Anwar Dudin, the dean of An-Najah medical school. Your foremost vision, intelligence, hard work and confidence that you donate to people working with you makes you stand as a role model. As I told you once, I’m deeply proud to be your fellow. And as you suggested once, I will try to be an ambitious big dreamer. My special thanks to Dr. Samar Musmar, dean assistant for clinical affairs. To Pr. Rami Hamdallah, An-Najah University president, I acknowledge my gratitude,

for the heavy load you are bearing, to improve and revolutionize the higher education in Palestine. For your continuous support, and the opening avenues you are offering to establish a clinical research activity in the university. I would like to acknowledge An-Najah National University for the financial support during my thesis, and for the continuous support provided for my near future return project.

I express my gratitude to my thesis committee members. I thank Dr. François Giudicelli, Pr. Eric Leguern, and again Pr. Ricard Miles. I also thank the doctoral school represented by Ms. Elizabeth Clement and Dr. Muriel Umbhauer for their continuous orientation and care.

I thank all the past and present members of Fiona Francis group. Special thanks to Françoise Phan Dinh Tuy and Katia Boutourlinsky, for receiving me when first arrived to Paris. For your unforgettable help in performing the initial experiments, and the valuable support in learning to speak French, I loved your nice French expressions that you articulate from time to time. You made the tough task greatly enjoyable! I am indebted to Audrey Roumegous, your unconditional support in performing the experiments, your unique organization skills, and non-vanishing smile transformed my lab life into a real joy! I vividly thank you for being as great as you are! My very sincere thanks to Richard Belvindrah, with you, hippocampus *in utero* electroporation was miraculously successful! I deeply appreciated our insightful scientific discussions that tethered me further to the domain of developmental neurosciences. Thank you Richard for your efforts in comprehensively answering any rising question in my mind, and for your constructive feedback for the thesis manuscript. I thank also Elodie Bruel-Jungerman and Sara Bizzotto for your help in writing thesis manuscript, and the moments we shared together.

I express my sincere thanks to Iffat Sumia, the multi-skillful and intelligent M1 student. Your commitment, wisdom, and nice humor turned your rotation into an unforgettable life experience. I express my deep appreciation towards you, and wish you a wonderful future, for which you got all of the needed elements.

I was extraordinarily fortunate in being a member of the Institute du Fer à Moulin. I thank all people I encountered there. I thank Dr. Jean-Antoine Jirault, the director of the institute and Dr. Patricia Gaspar and Dr. Andre Sobel, the co-directors, for the

endless care you are providing to this place making it a unique and rich scientific environment. Some members of the Institute have been very kind enough to extend their help at various phases of my stay, whenever I approached them, and I do hereby acknowledge all of them. I vividly thank Jocelyne Bureau for the joyful experience we had together, studying and reasoning at the electron microscope. Jocelyne: I appreciate your sympathy, commitment, and faith, and I will eternally keep a good memory of you. I thank Mythili Savariradjane, Jean Paul –Rio, Jocelyne Chevallier, Christine Vaillant, Marianne Coutures, Geraldine, Ghislaine, Evelyne, and Sylvie Clain. My field study and my life was made less obstacle-ridden because of the presence of a few individuals, I express my deep gratitude to my two valuable friends Imane Moutkine and Ahlem Assali. I thank 4th floor people particularly Lucie Viou, Charlotte Plestant, and Sara Devaux. I thank my office colleague Stéphanie Chauvin. I am particularly indebted to animal house facility personnel, without whom this thesis would have never been possible. I thank the IFM Olympics' team. I really enjoyed it!

I vividly thank all of our collaborators, without whom this thesis would have never seen the day. I sincerely thank Dr. Robert Olaso, Mrs. Sylvie Dumont, Dr. Wassila Carpentier, and Mr. Benoit Albaud. I thank Dr. Sophie Hamelin and Dr. Antoine Depaulis. I acknowledge my gratitude to Pr. Richards' Miles group and Dr. Nadia Bahi-Buisson.

Collective and individual acknowledgments are also owed to my Parisian friends, who accompanied me in the discovery of this wonderful city. I thank you for the family core that we established here together and for the moral support and the continuous care you surrounded me during my happiness and sorrows. I thank again Ahlem and Imane, but also Manar, Marc and Zeinab, Amanie, Azza, Suhaib, Saleh, Motee', Nadia, Jawad, and Nasim. I am deeply thankful to Jill, Jane and John for the special holidays we spent together in the UK.

I take this opportunity to express the profound gratitude from my deep heart to my beloved parents, for their love and continuous spiritual support. I thank you for all what you gave to your little spoiled girl. I will never forget these moments, when this eerily strong maternal instincts sense would drive my mother to call, when I'm in my tears, missing you badly.

My greatest sense of gratitude is addressed to my husband whose dedication, love and persistent confidence in me, has taken the load off my shoulder, even when we spent four years, thousands of miles apart. I owe you for being unselfishly loving, temporarily scarifying our couple life to let your passions and ambitions collide with mine. I'm eternally indebted to you!

And not to forget to thank the soul of my beloved uncle. The tender love, courage, and sympathy you provided me, your faith in my strength, and your emphasis on achieving my dreams were the nurture that fed my heart. Unable to be between us in this occasion, I dedicate all of this work to your memory.

Above all, I owe it all to Almighty God for granting me the wisdom, health and strength to undertake this research task and enabling me to its completion.

I dedicate this thesis to my family, my husband, Mahmoud, and the memory of my beloved uncle for their constant support and unconditional love.
I love you all dearly.

TABLE OF CONTENTS:

List of Figures:

List of Abbreviations:

5HT3aR	serotonin receptor 5HT3a
AIS	axon initial segment
AIS	axon initial segment
AnkG	AnkyrinG
ANR	anterior neural ridge
AP	apical progenitors
BDNF	brain-derived neurotrophic factor
BLBP	brain lipid binding protein
BMPs	Bone morphogenetic proteins
BrdU	Bromodeoxyuridine
C-DC	C-terminal conserved DCX domain
CA	cornu ammonis
CAM	L1 cell adhesion molecule
CaMKII	Ca2+/ calmodulin dependent proteinkinase II
CDK5	cyclin-dependent kinase 5
CGE	Caudal ganglionic eminence
CNS	central nervous system
CNTF	ciliary neurotrophic factor
CoP	commissural plate
CP	cortical plate
CR	Cajal-Retzius
Crl	calretinin
CSF	colony stimulating factor-1
DC domain	conserved doublecortin domain
Dcx	Doublecortin
DG	dentate gyrus
DG	dentate gyrus
EE	enriched environment
EM	Electron microscopy
FGF	fibroblast growth factor
GABA	gamma-aminobutyric acid
GAD	glutamic acid decarboxylase
GLAST	astrocyte-specific glutamate transporter
Hes	Hairy/Enhancer of Split
IN	interneuron
IP	intermediate progenitor
IPB	the infrapyramidal bundle
IPSP	inhibitory post-synaptic potential
IS	irregular-spiking
IZ	intermediate zone
JIP-1	JNK interacting protein
JNK	c-Jun N-terminal kinase
KCC2	potassium- chloride cotransporter 2
LGE	Lateral ganglionic eminence
LIF	leukaemia inhibitory factor
LIS	Classical lissencephaly
LMT	large mossy fiber terminal
LP	lateral pallium
LTP	long term potentiation
MAP	microtubule associated protein
MB	the major bundle, the suprapyramidal bundle
MGE	Medial ganglionic eminenece
MRI	Magnetic resonance images
MT	microtubule
MZ	marginal zone
N-DC	N-terminal conserved DCX domain
NE	neuroepithelial
NF	Neurofascin
NKCC1	Na+–K+–2Cl- co-transporter
NPY	neuropeptide Y
NRG1	neuregulin 1
NT4	neurotrophin4
OPC	oligodendrocyte precursor cell
oRG	outer radial glial
PAFAH1 B1	platelet-activating factor acetylhydrolase 1B a subunit
PF	protofilaments
POA	preoptic area
PP	preplate
PP1	protein phosphatase 1
PP2A	Protein Phosphatase 2A
PSB	pallial–subpallial boundary
PSC	post synaptic current
PV	parvalbumin
RGC	radial glial cell
RP	roof plate
SBH	subcortical band heterotopia
Shh	Sonic hedgehog
SP	subplate
SsT	somatostatin
SVZ	subventricular zone
TA	terminal arborization
TA	terminal arborization
TF	transcription factor
TGFβ	transforming growth factor β
Unc5	uncoordinated 5
VAMP2	vesicle-associated membrane protein 2
VP	ventral pallium
VZ	ventricuar zonel
WT	wild type

CHAPTER 1: INTRODUCTION

PREAMBLE

The behavioral and cognitive tasks performed by the adult brain depends on its structural organization and a correct sequence of developmental events occurring during embryonic and early postnatal life, that will assure correct connectivity between several millions of neurons. This thesis discusses a neurodevelopmental problem and hence different developmental steps are presented here. Despite its complexity, the brain starts as a sheath of non-specified neuroepithelium. Elaborate early processes of patterning events, including neuronal identity specification at the anterior end of the neural plate, and territorial definition and arealization, will result in the formation of the telencephalon. This structure gives rise principally to two major progenitor domains; a dorsally positioned cortical ventricular zone that will generate the majority of glutamatergic excitatory (pyramidal) neurons, and ventrally positioned ganglionic eminences, that will contribute to the generation of inhibitory GABAergic interneurons in the adult cortex and hippocampus. A tightly coordinated program of neurogenesis, neuronal migration, differentiation and maturation of neuronal circuits is fundamental to assure normal brain development and adult functions.

From the earliest stages of neurogenesis, neuronal molecular identity and laminar fate are determined. This fate will be further refined during later processes of neuronal migration and differentiation, during which synapse formation, neurotransmitter release and cell to cell electrical signaling will permit the individual cell to incorporate intrinsic genetic and extrinsic environmental factors, that will allow the cell to interact in synchrony with other cells of the same or distinct types, contributing to the overall brain function.

Disruptions at various stages of cortical development lead to a wide spectrum of disorders presenting frequently in children with developmental delay and epilepsy. In 1996, Barkovich introduced the term Malformation of Cortical Development (MCD) to include a spectrum of cerebral cortical malformations that were detected and classified according to magnetic resonance imaging findings. With the huge advancement of genetic techniques, including most recently high throughput genomic and exome sequencing, the hunt for new disease-causing genetic mutations has largely widened our knowledge in this field. New syndromes have been described, and many new genes and mutations have been identified. In addition, the advancement in molecular and cell biological techniques has helped us to model these

disease-causing mutations in other species, opening the avenue to new discoveries, and better understanding of the role of each of these genes and mutations in cerebral cortical development in humans and model organisms. Therefore, the integration of genetic together with the cellular and molecular data has led to a better understanding and classification of MCDs; for example, we know now that while disorders of neurogenesis give rise to abnormalities in cerebral cortical size, disorders of neuronal migration give rise to aberrantly positioned 'heterotopic' neurons, either close to the ventricular surface or within the white matter.

The work of my thesis was focused on the study of perturbed developmental programs and subsequent morphological, molecular and ultrastructural phenotypes of malpositioned, 'heterotopic' neurons in the hippocampus of the doublecortin knockout (Dcx KO) mouse model of neuronal migration defects and spontaneous epilepsy. More specifically, my first objective was to characterize molecular profiles of heterotopic cells in the hippocampal CA3 region of Dcx KO mouse during development and in the adult. In my second objective, I aimed at studying the morphological and ultrastructural characteristics, and the maturation program of these heterotopic cells at perinatal period. Therefore, in the introduction of my thesis, I will address the major steps of cerebral cortex development focusing on neuronal phenotype specification, neurogenesis, neuronal migration, generation of cellular type diversity, and synaptogenesis, processes that will culminate in the generation of normal mature neuronal circuits. The development of the hippocampus, a structure with a particular layout of cells and fiber pathways that has historically attracted the attention of neuroscientists, and is particularly affected in Dcx KO mice will be presented. Being attracted by the beauty and the particularity of this structure, I will address in some depth the seminal work that revealed the elegance of developmental programs culminating in its formation. The distinct cellular events and molecular programs that fingerprint the unique hippocampal architecture, development, and connectivity patterns from other cortical areas, will be addressed here. In the last section of the introduction, I will summarize what we know about Dcx protein function, human patient phenotypes mutated for DCX, and I will briefly present the available mouse models of Dcx loss of function, that helped in shedding light on important aspects of its function and interaction with other molecular partners during cerebral cortex development.

SECTION 1: CEREBRAL CORTEX DEVELOPMENT, PATTERNING AND NEURONAL CELL FATE SPECIFICATION

The cerebral cortex is a layered structure derived from the dorsal pallium which is basically a cylindrical layer surrounding fluid-filled ventricles. Other telencephalic structures are derived from pallium including the medial pallium (MP), which gives rise to the archicortex, and the hippocampus; the lateral pallium (LP), which generates the olfactory cortex; and the ventral pallium (VP), from which the claustroamygdaloid complex is generated.

The ventral telencephalon consists of two distinct progenitor domains, the lateral (LGE) and medial (MGE) ganglionic eminences, generating the striatum and pallidum, respectively. These telencephalic subdivisions are traced on the basis of differences in morphology, connectivity and neurochemical profiles, and by distinct patterns of gene expression, reflecting the initial acquisition of regional identity by progenitor populations during early embryonic development.

The neocortex represents the brain structure that has been subjected to a major expansion in its size and complexity during the course of mammalian evolution. The achievement of such a highly complex architecture relies on a precise orchestration of the proliferation of progenitors, onset of neurogenesis, spatiotemporal generation of distinct cell types and control of their migration and differentiation. Complex molecular mechanisms participate in coordinating growth and patterning of the developing cortex

The cerebral cortex is organized into 6 layers of neurons, which are arranged in an in-side-out lamination sequence (Angevine and Sidman, 1961; Rakic, 1972). Cortical layers are not simply stacked one over the other; there exist characteristic connections between different layers and neuronal types, which span all the thickness of the cortex. These cortical microcircuits are grouped into cortical columns and minicolumns, the latter of which have been proposed to be the basic functional units of cortex (Jones and Rakic, 2010). Functional properties of the cortex change abruptly between laterally adjacent points; however, they are continuous in the direction perpendicular to the surface. Functionally distinct cortical columns have been shown in the visual cortex, auditory cortex, and associative cortex (Maduzia and Padgett, 1997; Meyer et al., 2010a, 2010b).

Patterning cues in the developing cerebral cortex are governed by both intrinsic and extrinsic signals of neuronal progenitors. Early anterioroposterior and dorsoventral patterning of the developing embryo, and generation of progenitor domains and neuronal specification into major classes of telencephalic cells, together with the precise coordination of cell cycle control, differentiation and spatiotemporal control of cell fate along both the radial and tangential dimension of the developing cerebral cortex are crucial steps required for the patterning of early cortical territories (regionalization) and of postnatal cortical areas (arealization).

1.1 Intrinsic control of cerebral cortex development through patterning centers and transcription factor (TF) gradients

Multiple signaling centers or 'organizers' are involved in the induction and patterning of early brain territories through the expression of specific TFs. Secreted molecules (morphogens and growth factors) at signaling centers affect cortical growth and patterning at short range at early developmental stages. Four patterning centers are responsible for early induction and patterning of the telencephalon in the mouse embryo (Figure 1):

1. The anterior neural ridge /commissural plate at the rostral midline forming the border between neural and non-neural ectoderm. During neurulation and closure of the neural tube, Fgf8 is expressed at the rostral midline in the anterior neural ridge, thus defining the anterior patterning center. Later on, at E10.5–E12.5, after the expansion of the telencephalic vesicles, the fibroblast growth factors (Fgf8, Fgf15, Fgf17, Fgf18) are expressed anteriorly in nested domains at the commissural plate (CoP) and septum.
2. The roof plate (RP) and cortical hem at the dorsal/caudal midline and immediately adjacent territories, the Wnts and Bone morphogenetic proteins (Bmps) are localized at the dorsal/caudal midline in the RP and cortical hem.
3. The prechordal plate (PP)/ventral telencephalon signaling units, Sonic hedgehog (Shh) is localized in the ventral telencephalon at the PP.

4. The pallial–subpallial boundary (PSB) or anti-hem get involved later to coordinate growth and spatial patterning as growth proceeds and the distance between patterning centers increases (E11.0–E13.5). The PSB localizes at the lateral edge of the pallium and expresses of Fgf7, Sfrp2, and Tgfa (Assimacopoulos et al., 2003).

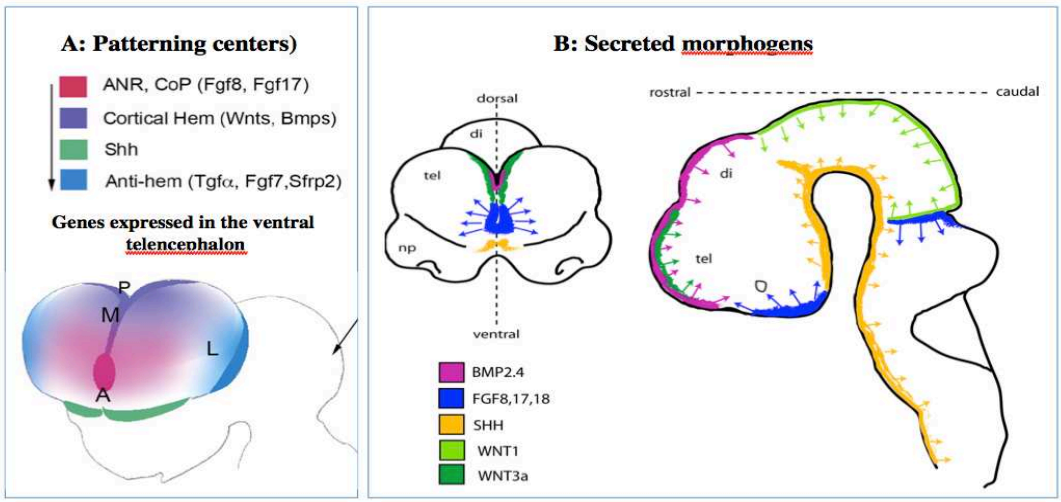

Figure 1: Schematic representation of the role patterning centers and secreted morphogens in telencephanlon development:
Adapted from (O'Leary and Sahara, 2008; Stevens et al., 2010).

During neurulation and closure of the neural tube, Fgf8 is expressed at the rostral midline in the ANR, Shh is expressed at the ventral midline in the PP, and Wnts/Bmps are localized at the dorsal midline in the RP. After the expansion of the telencephalic vesicles, the Fgfs are expressed anteriorly at the CoP and septum. The Wnts and Bmps are localized at the dorsal/caudal midline in the RP and cortical hem and Shh in the ventral telencephalon in addition to the PP. At this stage the the anti-hem localizes at the lateral edge of the pallium.

Fgfs in telencephalic progenitors and Shh and Wnts in other CNS regions accelerate the cell cycle by shortening the G1 phase, thus enhancing cell cycle exit (Pierani and Wassef, 2009). This represents an intrinsic effect that will ultimately have a crucial role in controlling the area-specific and, possibly, species- specific rates of neuron production.

1.2 Extrinsic signals that control cerebral cortex patterning

Although patterning centers and their secreted morphogens play a crucial role in the initial territorial shaping of the developing telencephalon, the proceeding of growth and the increase in the distance between signaling centers require the addition of other

patterning mechanisms. Diffusion works efficiently at short distances, but alone cannot pace with the expanding size. The emergence of other efficient signals that combine speed and functionality sounds fundamental, and a postmitotic neuronal compartment, together with migrating and differentiating cells seem needed to assure a correct fine-tuning of developing brain.

The ventricular fluid, which has been shown to contain signaling molecules like bFGF or Slits, could serve as a vehicle for forebrain growth signals through the formation of gradients mediated by the synchronized beating of cilia (Sawamoto et al., 2006). Additionally, migrating cells could act as mobile patterning cues where through their motility; they can mediate long distance transport of signaling molecules. Cajal-Retzius (CR) cells represent a transient class of earliest born neurons that populate the marginal zone of the developing cerebral cortex from early stages of development when regionalization takes place. CR cells secrete Reelin, an extracellular matrix protein that plays an important role in normal lamination of developing cortex. They are composed of a combination of molecularly distinct subtypes arising from restricted locations at the borders of the developing pallium, which actually represent the major patterning centers, namely the hem, the pallium–subpallium border and the septum (Figure 2) (Bielle et al., 2005; Pierani and Wassef, 2009). After generation, CR cells migrate from sites of origin and distribute in specific cortical regions. Fgf8, expressed at the rostral patterning center, and Tgfb, expressed at the caudal patterning center, induce the production of CR subtypes, which modulate early cortical patterning by transporting signaling molecules over a long distance (Griveau et al., 2010).

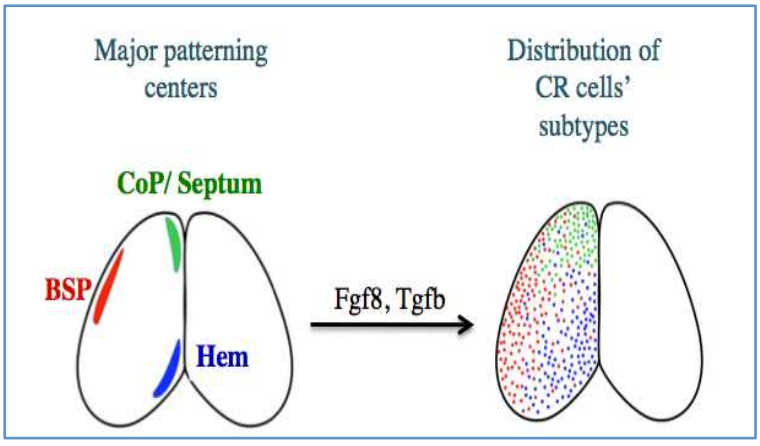

Figure 2: Patterning over a long distance.
Adapted from Borello and Pierani, 2010

Fgf8 and Tgfb expressed at the rostral and caudal patterning centers respectively, induce the production of CR subtypes, which modulate early cortical patterning by transporting signaling molecules over a long distance.

Additionally, a new class of migrating projection neurons, cortical plate (CP) transient cells, as well as the meninges and the invading vasculature also play a role in fine-tuning the developing telencephalon (Vasudevan et al., 2008; Siegenthaler et al., 2009).

Altogether, a complementary interplay between intrinsic and extrinsic patterning mechanisms seems pivotal for the early events that help in correctly instruction telencephalon development and patterning.

SECTION 2: CEREBRAL CORTEX HISTOGENESIS, NEUROGENESIS AND SPECIFICATION OF NEURONAL PHENOTYPES IN THE DEVELOPING TELENCEPHALON

The histogenesis of the cerebral cortex starts from the time when the cerebral hemispheres develop from the wall of the telencephalic vesicle. The neuroepithelial cells initially span the thickness of the wall, and as they continue to undergo cell division, the area of the hemispheres expands. At this early stage of development, the progenitor cells are thought to undergo primarily symmetric cell divisions, and their progeny both remain in the cell cycle. Soon, however, a few cells withdraw from the cycle to develop as the first cortical neurons. These neurons migrate a short distance to form a distinct layer, just beneath the pial surface, known as the preplate (Bayer and Altman, 1990) (Figure 3). The preplate and its derivatives contain projection neurons, collectively named as pioneer neurons, whose axonal arborizations establish the earliest corticofugal projection systems during cortical development (Soria et al., 1999; Soria and Fairén, 2000). The CP develops within the preplate, so that preplate neurons become redistributed between the marginal zone, containing a group of large, stellate-shaped CR cells, and a deeper zone of cells called the intermediate zone (IZ)/SP, where most of the glutamatergic pioneer neurons are located and increasing numbers of incoming axons (Allendoerfer and Shatz, 1994; López-Bendito et al., 2002; Morante-Oria et al., 2003; Espinosa et al., 2009). A minor group of preplate pioneer neurons are not found later in the subplate (SP), they are rather divided into two groups and are found in the marginal zone, and the CP respectively (Espinosa et al., 2009). The two groups of non-SP pioneer neurons show distinct early locations in the preplate and later on, express distinct neurochemical properties (figure 3).

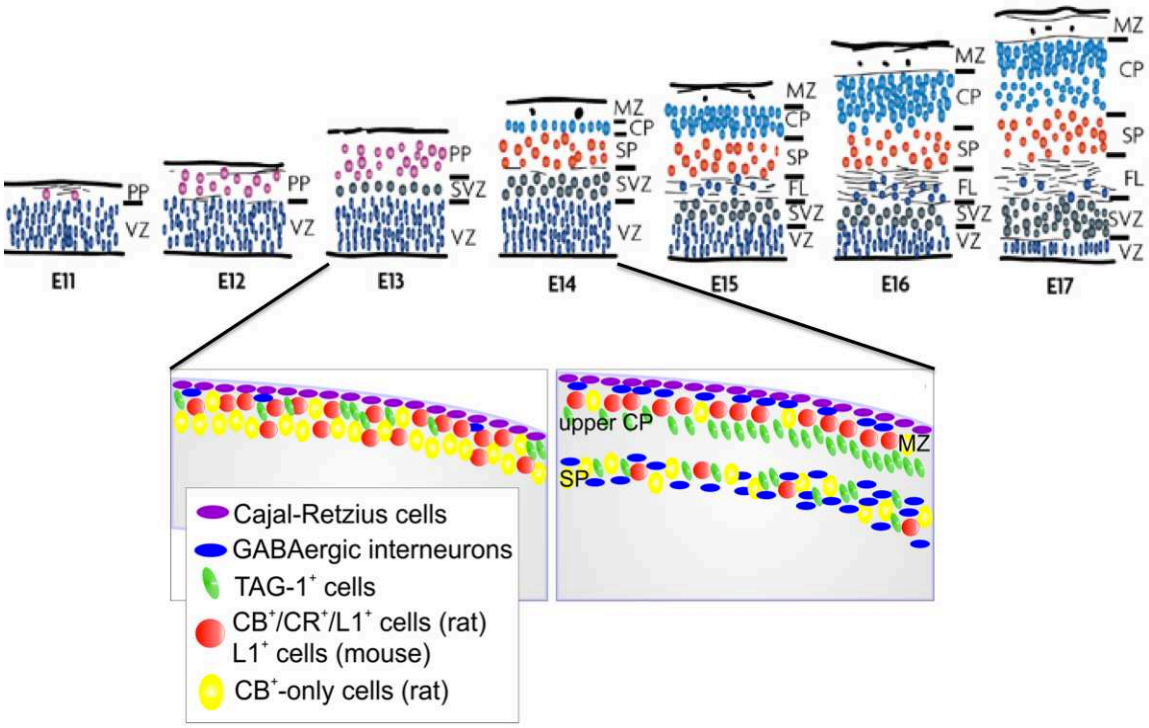

Figure 3: The developmental processes that will lead to organization of the neocortex into distinct neuronal layers.
Adapted from (Dehay and Kennedy, 2007; Espinosa et al., 2009)

Schematic presentation of the sequential layering events in the mouse and rat embryonic cortex. VZ: ventricular zone, SVZ: subventricular zone, PP: preplate, SP: subplate, CP: cortical plate, MZ: marginal zone, FL: fiber layer.

In rats, non-SP pioneer neurons situated in the upper part of the preplate before its partition will express the calcium binding proteins calbindin and calretinin, and the cell adhesion molecule L1. However, a second subtype of non-SP pioneer neurons is located deeper in the preplate. They will specifically express the adhesion molecule TAG-1, and will be transiently located in the upper CP (Espinosa et al., 2009). In mice, similar populations of pioneer non-SP neurons also exist. However, the more superficial cells express the adhesion molecule L1, but not the calcium binding proteins calbindin and calretinin. Interestingly, the two populations of non-SP pioneer neurons show different projection patterns. Axons of L1 neurons project to the ganglionic eminences and the anterior preoptic area, whereas axons of TAG-1 pioneer neurons only project to the lateral parts of the ganglionic eminences at the early stages of cortical histogenesis (Dehay and Kennedy, 2007; Espinosa et al., 2009).

From the earliest stages of cortical development, the processes of the apical progenitor cells span the entire thickness of the cortex (Miyata et al., 2001; Nadarajah et al., 2001). The first cortical neurons that are generated use the predominantly radial

orientation of their neighboring progenitor cells to guide their migration. However, the accumulation of neurons within the CP results in a marked increase in cortical thickness. As a result, the processes of later born cells no longer are able to extend to the external surface of the cortex. Nevertheless, the newly generated cortical neurons still migrate primarily in a radial direction guided by a remarkable set of cells, known as radial glia, which provide a scaffold (Rakic, 1978; Nadarajah et al., 2001; Nadarajah and Parnavelas, 2002).

These glial cells have long processes that extend from the ventricular zone all the way to the pial surface. They form a scaffold that neurons migrate along. Serial section electron microscopic (EM) studies by Pasko Rakic first clearly demonstrated the close association of migrating neurons with radial glial cells in the cerebral cortex (Figure 4). The migrating neurons wrap around the radial glial processes, and move in a saltatory way, with migrating neurons frequently starting and stopping along the way.

The next phase of cortical histogenesis is characterized by the gradual appearance of defined layers within the CP. As increasing numbers of newly generated neurons migrate from the ventricular zone (VZ) into the CP, they settle in progressively more peripheral zones. Meanwhile, the earlier generated neurons start to differentiate. Thus, later generated neurons migrate past those generated earlier. This results in an inside-out development of cortical layers (Rakic, 1978; Nadarajah et al., 2001; Nadarajah and Parnavelas, 2002). Richard Sidman used the 3H-thymidine birthdating technique, to mark newly born neurons from the VZ to their settling point in the CP, and was the first to

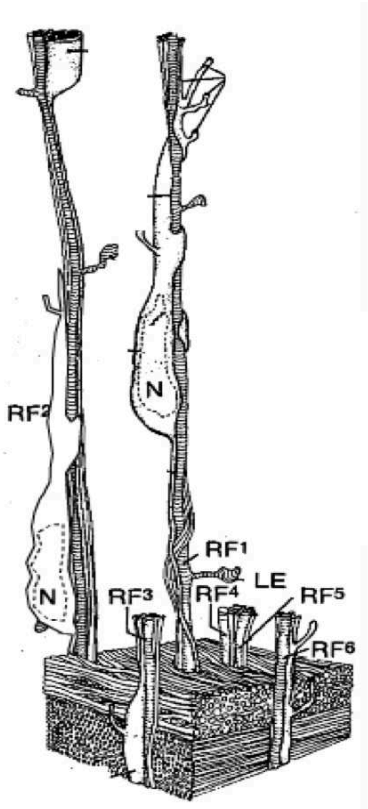

Figure 4: a three-dimensional reconstruction of a migrating neuron along the surface of a radial glial fiber
Adapted from (Rakic, 2003)

Neurons are generated in the proliferative ventricular zone. They traverse the expanding cerebral wall and pass through the layer of earlier generated neurons in the deep layers, before settling in at the top of the developing cortex. Migrating neuron is attached to the radial glial fiber, which guides the neurons to the appropriate layers of the cerebral cortex. RF: radial fiber, N: neuron.

demonstrate the inside-out pattern of cerebral cortical histogenesis. The neurons labeled in the cortex of pups born from pregnant female rats injected with thymidine on the 13th day of gestation were located in the deeper layers of the cortex, whereas the neurons labeled after a thymidine injection on the 15th day of gestation were found more superficially. This inside-out pattern of cortical neurogenesis is conserved across mammalian species. Thymidine injections at progressively later stages of gestation result in progressively more superficial layers of cerebral cortical neurons being labeled. Each cortical layer has a relatively restricted period of developmental time over which it is normally generated (Angevine and Sidman, 1961; Caviness and Rakic, 1978; Caviness, 1982; Fairén et al., 1986).

Time-lapse imaging of labeled neuroblasts (Nadarajah et al., 2001; Noctor et al., 2004) shows clearly that many of the neuroblasts migrate just as predicted from the EM reconstructions of Rakic. However, direct visualization of the migration process also revealed that many of the neuroblasts move via a very different process, a process termed somal translocation. In this case, in early stages of corticogenesis, the migrating cell has a leading process that extends to the pial surface, while the cell body is still near the VZ. Then, with progressive shortening of the process, the cell soma is drawn to the pial surface (Nadarajah et al., 2001).

In addition to their function in supporting migrating neurons, radial glial cells are also neuronal progenitors. They undergo several cell divisions, and the progeny are not always additional radial glia but migrating immature neurons that migrate along the radial glia that generated them and label for neuron specific markers, while the radial glial cell that generated them expresses proteins typical of radial glia (Noctor et al., 2002; Lui et al., 2011).

In addition to this predominantly radial migration of the newly generated neurons, it has been shown that other populations of cortical cells migrate tangentially to the cortical surface. These correspond to different populations of GABAergic interneurons, oligodendrocytes, Cajal-Retzius cells and endothelial cells.

Indeed there was an important discovery of a subset of cortical neurons that do not arise in the pallial VZ, but instead, originate in distinct subpallial regions (Wonders and Anderson, 2006). Fate mapping experiments and loss-of-function analyses in rodents have shown that cortical interneurons arise predominantly from the medial

and caudal (CGE) ganglionic eminences, and from the embryonic preoptic area (POA) (Gelman et al., 2009). However, recent observations in fetal human and monkey brains have suggested that, in these two species, a substantial proportion of cortical interneurons may arise from the lateral ventricular epithelium starting from the second half of gestation (Letinic et al., 2002; Yu and Zecevic, 2011).

Abundant evidence indicates that cortical interneurons comprise distinct neuronal subpopulations as defined by their morphological, neurochemical and electrophysiological properties (Butt et al., 2005). It has been suggested that the generation of the different subpopulations is linked to regional differences, defined by the expression of particular combinations of TFs, in the specification of progenitor cells in the subpallium, and these differences are key contributors to the generation of interneuron diversity in the cerebral cortex. These topics will be detailed in this section.

2.1 NEUROGENESIS : FROM NEUROEPITHELIAL STEM CELLS TO RADIAL GLIAL CELLS

During development, neuroepithelial (NE) cells are the neural stem cells that give rise to all the neurons of the mammalian central nervous system. They are the source of the two types of neurons, cortical projection neurons and interneurons, as well as, astrocytes and oligodendrocytes. NE stem cells are self-renewing for a certain number of cell divisions; they first undergo symmetric, proliferative divisions, each of which generates two daughter stem cells (McConnell, 1995; Rakic, 1995). These divisions are followed by approximately 5-6 asymmetric, self-renewing divisions. Each of these divisions generates a daughter stem cell, plus a more differentiated neuronal precursor.

At the neural tube stage, the NE cell layer is composed of highly polarized pseudostratified epithelial cells, with the nuclei of these cells migrating up and down the apicobasal axis during the cell cycle (interkinetic nuclear migration) (Huttner and Brand, 1997). Tight junctions are present at the most apical end of the lateral plasma membrane and receptors for basal lamina constituents such as integrins contact the basal lamina (Wodarz and Huttner, 2003). With the generation of neurons, the neuroepithelium transforms into a more specialized tissue for neuron production. In

the VZ, the most apical cell layer that contains most of the progenitor cell bodies, neuroepithelial cells switch to neurogenesis and downregulate certain epithelial features (Aaku-Saraste et al., 1996). Astroglial markers appear and a distinct, but related, cell type — radial glial cells — which exhibit residual neuroepithelial as well as astroglial properties appear (Kriegstein and Götz, 2003). Radial glial cells represent more fate-restricted progenitors than neuroepithelial cells and successively replace the latter. As a consequence, all of the projection neurons in the brain are derived, either directly or indirectly, from radial glial cells.

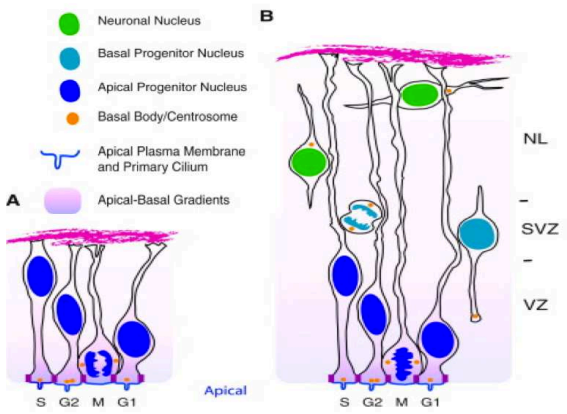

Figure 5: Neuronal progenitors
Taken from (Taverna and Huttner, 2010)

Apical-basal polarity of NE cells (A) and apical progenitors (B). AP mitosis (M) occurs at the apical surface, whereas S phase takes place at a more basal location, with apical-to-basal nuclear migration in G1 and basal-to-apical nuclear migration in G2. Mention basal progenitors.

I. Types of neuronal progenitors in the developing telencephalon

Cortical neurons are exclusively generated from progenitors located within the dorsolateral wall of the telencephalon. Heterogeneity within this progenitor population has been shown, with apical progenitors (APs) (some of which are radial glial cells) located along the luminal wall and intermediate "basal" progenitors (IPs) which delaminate from the VZ and divide at a distance from the lumen (Figure 5) (Kriegstein et al., 2006).

1. Apical progenitors (APs)

At the time of corticogenesis (E10 in the mouse), NE cells switch and give rise to other neuronal progenitor populations: radial glial cells (RGCs) and short neural

precursors (SNPs) both still residing in the VZ. APs exhibit apical-basal polarity, with the apical plasma membrane lining the lumen of the ventricle, the primary cilium protruding from the apical plasma membrane, and the interphase centrosomes located at the apical plasma membrane. AP nuclei occupy different positions along the apical-basal axis depending on the phase of the cell cycle and undergo interkinetic movement (Figure 5). Both these cell types will be further detailed here.

a. Radial glial cells:

As NE cells, RGCs exhibit an apico-basal polarity and span the entire cortical wall with an apical process contacting the ventricle and a basal process extending to the basement membrane. RGCs and NE cells also share expression of the intermediate filament protein Nestin, as well as expression of RC2 and the TF Pax6, but RGCs are further delineated by the expression of astroglial markers such as the astrocyte-specific glutamate transporter (GLAST), vimentin and the brain lipid binding protein (BLBP) (Pinto and Götz, 2007). With the onset of corticogenesis, RGCs comprise the predominant progenitor population within the VZ. They play a dual role in providing migratory guides for newly born neurons, and they are able to generate neurons or neuronal progenitors following asymmetric division, thereby giving rise, directly or indirectly, to most projection neurons of the cerebral cortex (Noctor et al., 2004). Like NE cells, RGCs show interkinetic nuclear migration, with their nuclei undergoing mitosis at the apical surface of the ventricular zone and migrating basally for S phase of the cell cycle (Figure 5). However, whereas in neuroepithelial cells the nuclei migrate through the entire length of the cytoplasm, this is not the case in RGCs. This interkinetic nuclear movement underlies the pseudostratification of the VZ. It allows the limited apical space to be used efficiently for AP mitoses, and functions by influencing the AP fate by controlling the exposure of AP nuclei to different, proliferative versus neurogenic, signals localized along the apical-basal axis (Noctor et al., 2004).

Time lapse imaging experiments have shed light on the molecular and cellular mechanisms of interkinetic nuclear movement. This movement appears completely independent of centrosome behavior and occurs along the MT network spanning the entire length of the progenitor cell. RNA interference (RNAi) experiments using *in utero* electroporation to inhibit the expression of dynein, block apically directed but

not basally directed nuclear movement. Basally directed movement, however, was inhibited by RNAi of the unconventional kinesin heavy chain protein, kinesin 3 (Kif1a) (Tsai et al., 2010). Thus, interkinetic nuclear movement is regulated by very specific molecular motors.

b. Short neuronal progenitors SNPs:

The identification of SNPs as a distinct progenitor population added further evidence to the heterogeneity of VZ cells (Gal et al., 2006). RG cells remain the main progenitor population. SNPs can be morphologically characterized by the presence of a short basal process, which does not contact the basal lamina (figure 6), as well as by the activity of the tubulin alpha1 promoter, suggesting that they are restricted neuronal progenitors; their true origin (NE cell- or RGC-derived cells) remains unknown. Despite differing in cellular and molecular features, NE cells, RGCs and SNPs all display strong apico-basal polarity as well as having a specialized membrane domain facing the ventricular lumen that is limited by apical junctional complexes. Remarkably, they all undergo interkinetic nuclear migration. Based on the location of their nuclei during mitosis, all three above-mentioned progenitor cell types can thus be referred to as APs (Fish et al., 2008).

2. Intermediate 'basal' progenitors (IPs):

As soon as neurogenesis begins, a different type of progenitor, called intermediate (basal) progenitors, arise from a division event from an AP (e.g. NE cell or RGC), they detach from the VZ to form the subventricular sone (SVZ) at later stages of neurogenesis. In the SVZ, IPs undergo mitosis and contribute to both early and late born neurons (Miyata et al., 2004; Noctor et al., 2004). IPs contribute to neurogenesis by undergoing symmetric cell division and might function to increase the number of neurons generated from an apical division (Haubensak et al., 2004). In contrast to APs, IPs do not exhibit interkinetic nuclear migration, nor display any apparent signs of polarity and typically lack both an apical and a basal process contacting the ventricle and the basal membrane, respectively (Figure 5, 6). Moreover, IPs are molecularly distinct from APs and exclusively express the TF Tbr2, and Cux1; a progressive attenuation of Pax6 expression concomitant with the appearance of Tbr2

transcripts characterizes the transition of APs to IPs (figure 6) (Englund et al., 2005). The non-coding RNA Svet-1 and the TF Cux2 (Nieto et al., 2004) are also expressed in subsets of IPs during the generation of upper layer neurons.

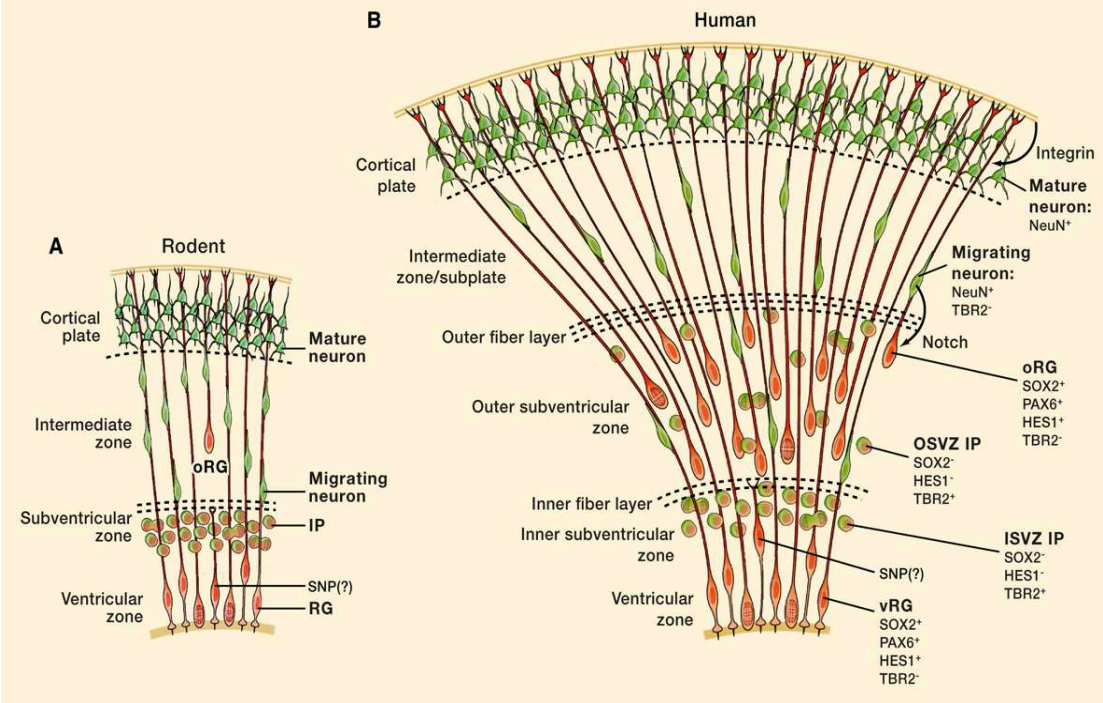

Figure 6: Rodent (A) and human neocortical development (B).
Adapted from (Lui et al., 2011)
In rodents RG cells generate intermediate progenitor (IP) cells that divides to produce pairs of neurons, which use RG fibers to migrate to their final destination. oRG cells exist in the mouse as well as in humans, but they are much less frequent in the mouse. SNPs, are also shown.

APs and IPs produce neurons by distinct mechanisms. During neurogenesis, APs undergo mostly asymmetric, self-renewing divisions, each of which generates an AP and an IP, or an AP and a neuron. IPs (at least in rodents) in most cases (90%) divide once, and nearly always symmetrically to produce two neurons with the same birthdate (Noctor et al., 2004). APs and IPs therefore represent two modes of neuron production, with a self-renewing progenitor pool and a "consumptive", non-self-renewing pool for neuron production, respectively. For neuron production, the APs act as the self-renewing compartment where asymmetric divisions maintain the pool of progenitors while producing neuronal cells (direct neurogenesis). The self-renewal capacity of APs appears intimately linked to their epithelial-like features such as the apico-basal polarity and apical junctional complexes (Cappello et al., 2006). Mitotic

spindle and cleavage orientations determine if polarity is retained. The loss of these key features seems to be associated with neuronal differentiation and may also be causative for the loss of self-renewal and neurogenic potential at the end of neurogenesis. As for the IPs, these may be considered a neurogenic transit amplifying progenitor population that expands the number of particular neuronal populations (indirect neurogenesis). As both modes of neurogenesis take place simultaneously throughout cortical development, a crucial issue is whether they generate different subtypes of cortical neurons.

3. Outer radial glial cells (oRGCs):

A new class of neuronal progenitors is found in the outer part of the SVZ, termed outer radial glial (oRG) cells. These cells have been described in different species including mouse (Shitamukai et al., 2011; Wang et al., 2011), ferret (Fietz et al., 2010; Reillo et al., 2011), marmoset (García-Moreno et al., 2012; Kelava et al., 2012) and human (Hansen et al., 2010; Lui et al., 2011). Interspecies differences in number and abundance have been described for oRGs, with humans and higher mammals having much more numerous oRGs when compared to rodents (Lamonica et al., 2012). This difference could be one of the evolutionary mechanisms adopted by higher mammals to expand the tangential cerebral cortex surface area and form a gyrencephalic brain. Unlike RG cells, oRG cells are located far from the ventricle, with no apical contact to the luminal surface, but they possess a long basal fiber that often extends to the pial surface (Figure 6). They express Pax6 and Sox2, but not Tbr2 (Hansen et al., 2010; Reillo et al., 2011).

Time lapse imaging experiments have shown common fundamental features between these oRG cells among mammals; they are generated directly from RG cells in the VZ, and migrate away to the superficial SVZ via mitotic somal translocation rather than interkinetic nuclear migration. However, an important difference between species does exist. In mice, oRG cells undergo self-renewing asymmetric division to generate neurons directly, while human oRG cells generate transit-amplifying cells that in turn generate neurons (Wang et al., 2011).

The limited number of oRG cells and their rapid terminal differentiation in mice justifies the fact that the contribution of oRG cells to neurogenesis and cortical layer formation in rodents is small compared to higher mammals, and this may explain why

genetic mutations causing severe brain malformation phenotypes in human do not necessarily cause the same dramatic phenotype in rodents (Pulvers et al., 2010).

II. The subventricular zone: a secondary zone of neurogenesis

This secondary zone of neurogenesis is established upon migration of IPs that are generated from NE and RGCs at the apical surface of the neuroepithelium/VZ and migrate to the basal side of the NE/VZ. In rats, from E11 to E14, mitoses occur exclusively at the ventricular surface; however, at E16, the SVZ forms, subadjacent to the VZ, and the SVZ continues to generate neurons and glia long after the VZ has ceased cell division at E19 (Tarabykin et al., 2001; Martínez-Cerdeño et al., 2012).The majority of the glia of the forebrain are thought to be derived from the SVZ. In recent years, the SVZ has become the subject of intense investigation owing to its maintenance in the adult brain. The rostral migratory stream represents another specialized migratory route found in the brain of some animals along which neuronal precursors that originated in the SVZ of the postnatal brain migrate to reach the main olfactory bulb. After the initial burst of gliogenesis (see above), most of the neuronal precursors generated in the SVZ during the postnatal period and in mature rodents migrate to the olfactory bulb (Lois et al., 1996). The cells migrate in chains, along extended astrocyte networks. These networks are complex but in general have rostral-caudal orientation. One might imagine that the association of migrating SVZ cells is analogous to the migration of cortical neurons along radial glia; however, the SVZ cells do not appear to require the glia. The migration of SVZ cells has been termed chain migration and is hence distinct from the migration of neurons along radial glia. The SVZ cells form a chainensheathed by astrocytic processes, and migrate by sliding along one another. Thus, glia might help to orient SVZ migration but are not essential for it (Nam et al., 2007).

2.2 SPECIFICATION

I. Neuronal versus glial cell fate choice in the telencephalon

One of the first decisions that neural progenitors must make during development is whether to adopt a neuronal or a glial cell fate. Neuronal stem cells alter their output

over time; they initially give rise to committed neuronal precursors and only later to glial precursors (Qian et al., 2000).

1.1 The role of Notch signaling:

Notch signaling has a permissive rather than instructive role in promoting an uncommitted NSC state in the telencephalon (Henrique et al., 1997). Hairy/Enhancer of Split (Hes) genes are downstream mediators of Notch signaling that function by inhibiting the expression or activity of positively acting bHLH proneural proteins (Figure 7). In Hes1 single and Hes1/Hes5 double mutants, telencephalic NSCs have a reduced self-renewal capacity and undergo premature neuronal differentiation. Ectopic expression of Hes genes in telencephalic progenitors delays differentiation without biasing cells towards a neuronal or glial identity (Ohtsuka et al., 2001). This confirms the Notch pathway as a permissive rather than instructive mediator.

1.2 Proneural proteins and neuronal cell fate determination

Mash1 and Ngn2 proneural bHLH proteins are intrinsic mediators of the neuronal over glial fate decision. Loss-of-function and *in vitro* gain-of-function studies have shown that both Mash1 and Ngn2 promote the specification of a neuronal over a glial fate in the embryonic telencephalon (Sun et al., 2001). However, overexpression studies *in vivo* suggest that Mash1 and the Ngns are not very efficient at converting progenitors in the cortex to a neuronal fate. A likely explanation for this is that forced expression of bHLH factors *in vivo* is not sufficient to counteract the effect of extracellular signals that promote a glial fate, in part, by interfering with bHLH activity. This result supports the idea that the transition from neurogenesis to gliogenesis may involve inhibition of proneural protein activity, in addition to transcriptional repression of proneural genes, as well as glial-promoting signals. Thus, NSCs must integrate a variety of neuronal and glial promoting cues that change over time. As a result, neuronal determinants (e.g. Ngns) are induced during the period of neurogenesis, and these neuronal determinants are later inhibited and astrocytic determinants are activated during the subsequent period of gliogenesis, at late embryonic/postnatal stages (Qian et al., 2000; Hand et al., 2005; Heng et al., 2008a) (Figures 7, 8).

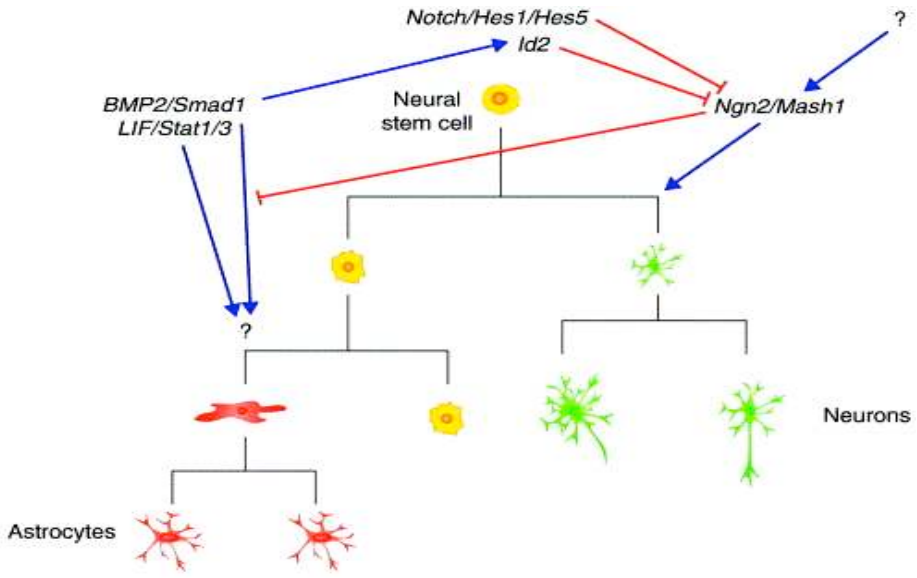

Figure 7: Neuronal versus glial cell fate specification
From (Schuurmans and Guillemot, 2002)

1.3 Gliogenic signals

Several extracellular factors, including leukemia inhibitory factor Lif, Bmp2, and fibroblast growth factor2 (Fgf2) influence glial fate decisions in an instructive fashion in the telencephalon (Nakashima et al., 2001) (Figure 7).

- Bmp2 and its downstream effector Smad1 promote astrocytic differentiation, in cooperation with Lif and its downstream effector Stat3, through the formation of gliogenic Smad1/Stat3/p300 transcriptional complexes.
- Bmp2/Smads induce expression of Hes5 and bHLH proteins of the Id family, which are known to interfere with Ngn1, another neurogenesis inducing proneural protein (Nakashima et al., 1999). Ngn1 has been shown to have reciprocal, dual functions, independently promoting neurogenesis through transcriptional activation of neuronal differentiation genes, and suppressing gliogenesis by associating with Smad1/p300 complexes and by competing for the formation of the gliogenic Smad1/Stat/p300 complexes (Sun et al., 2001).

II. Specification of neuronal phenotypes in the ventral telencephalon

The subdivision of the telencephalic VZ by the regionalized expression of TFs is followed by the differentiation of distinct types of neurons in each of these

subdivisions. In the basal telencephalon, differentiating neurons are primarily γ-amino butyric acid GABAergic and are characterized by expression of the homeodomain proteins Dlx5 and Dlx6 (Wilson and Rubenstein, 2000), and by Nkx2.1, Lhx6 and Lhx7 expression for neurons born in the MGE (Grigoriou et al., 1998). GABAergic interneurons found in the adult cortex, hippocampus and olfactory bulb express these molecular markers. Results from a number of genetic studies, clonal analysis and migration assays demonstrated that many interneuron populations are generated in the basal telencephalon, primarily in the MGE, and later migrate into the overlying cortex (Anderson et al., 1997).

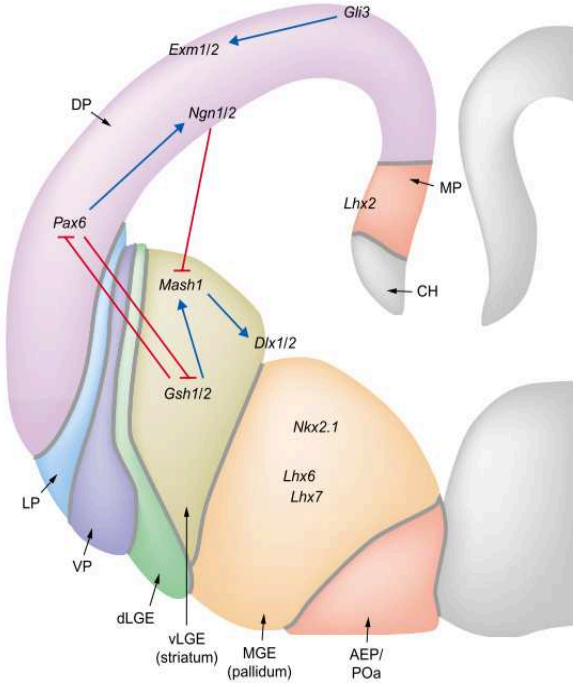

Figure 8: Specification of neuronal phenotypes in the developing telencephalon
From (Schuurmans and Guillemot, 2002)

Unique gene expression patterns define dorsal and ventral domains of the developing telencephalon, and will regulate the spatiotemporal differentiation of different cell types present in the adult brain. Dorsal telencephalic progenitors express high levels of the bHLH TFs Ngn1 and Ngn2, and the homeodomain proteins Emx1, Emx2, Lhx2 and Pax6. Ventral progenitors express Mash1 and the Gsh1, Gsh2, Dlx1, Dlx2, Dlx5 and Dlx6. Important cross-regulatory interactions between Ngn1/2 and Mash1 and Pax6 and Gsh2 participate in the maintenance of telencephalic progenitor identity.

The specification of GABAergic interneurons, as well as oligodendrocytes, at long distances from their final destination thus allows the physical segregation of inductive cues, thereby increasing the capacity for cell diversity.

Intrinsic factors are involved in the specification of a GABAergic phenotype. In rodent, Mash1 respecifies cortical neurons when misexpressed in dorsal progenitors, inducing the expression of Dlx genes and directing the differentiation of a GABAergic phenotype. Dlx2 induces the biosynthetic enzyme glutamic acid

decarboxylase (GAD) 67, when ectopically expressed in cortical explants (Anderson et al., 1999). Therefore, a genetic pathway Mash1-Dlx-GAD operates during GABAergic differentiation in the telencephalon. However, some redundancy in this system is suggested by the persistant expression of Dlx and GAD67 in the ventral telencephalon of Mash1 mutant mice (Shieh et al., 2011), and ventral telencephalic neurons acquire a GABAergic phenotype in the absence of both Dlx1 and Dlx2. Factors that participate in the specification of neuronal phenotypes other than GABAergic that are found in the basal ganglia, play a role; Nkx2.1 mutants lack almost all striatal interneurons and 50% of cortical interneurons, including all neuropeptide Y (NPY), nitric oxide synthase and somatostatin (Sst), suggesting a role for this gene in the specification of distinct neuronal populations (Kawauchi et al., 2010). There is also evidence that Lhx6 participates in the specification of striatal interneurons and that Lhx7 is involved in the specification of cholinergic interneurons in the striatum (Marin et al., 2000).

III. Specification of neuronal phenotypes in the dorsal telencephalon (the developing cerebral cortex), (Figure 8)

The cerebral cortex is a six-layered structure comprised primarily of glutamatergic projection neurons, originating from dorsal telencephalic progenitors, and of interneurons of ventral origin. Cortical projection neurons are distinguished early on by their expression of the T box TF Tbr1 and several bHLH proteins including NeuroD1, NeuroD2, Math2 and Math3 acting in regulatory cascades orchestrating neuronal differentiation (Fode et al., 2000; Pleasure et al., 2000). Lhx5, which is required for the proper proliferation and differentiation of hippocampal precursors but not for their initial specification, also has characteristics of a neuronal differentiation gene (Zhao et al., 1999). In contrast to the role of Mash1 in specifying a GABAergic phenotype ventrally, the dorsally restricted bHLH gene Ngn2 does not appear to have an instructive role in the specification of neuronal identity in the dorsal telencephalon; Ectopic replacement of Mash2 by Ngn2 in ventral telencephalic progenitors, did not convert ventral telencephalon into a cortical phenotype (Parras et al., 2002). Thus, the function of Ngn2 in the specification of neuronal identity is that of a permissive

cofactor, acting in conjunction with as yet unidentified instructive factors (Mizuguchi et al., 2001).

Little is known about the genes involved in the specification of laminar identity of cortical projection neurons. Transplant studies have demonstrated that laminar identities are specified just prior to a progenitor's last mitosis and that laminar potential is progressively lost during development (McConnell and Kaznowski, 1991). Tarabykin et al. have modified this idea by proposing a model whereby deep and upper layer neurons derive from distinct cortical progenitor populations, located in the VZ and SVZ, respectively (Tarabykin et al., 2001). As discussed earlier in this section, AP and IP located in the VZ and SVZ, respectively, are two types of progenitors well known to differ with respect to their proliferative properties, and the final destination of neurons derived from them (Takahashi et al., 1995, 1999; Noctor et al., 2004). This model is further confirmed by the discrete and non-overlapping gene expression patterns in both upper and lower layer neurons. Upper layer neurons generated from SVZ progenitors, express the gene Svet1, which specifically marks SVZ progenitors and upper layer neurons. The expression of Svet1 is reduced in the SVZ of Pax6 mutants and fewer upper layer neurons are produced in these mutants (Tarabykin et al., 2001). Otx1 has a complementary expression to Svet1, being restricted to VZ progenitors and deep layer neurons (Tarabykin et al., 2001). However, the analysis of Otx1 mutants failed to reveal early defects in the specification of deep layer identity, suggesting that other factors may be involved in the complex processes of laminar specification. Tbr1 is one of the few known genes with a role in the generation of a defined subpopulation of cortical neurons. Tbr1 is expressed at high levels in early born neurons, and Tbr1 mutant defects are restricted to early born neurons of the marginal zone, SP and layer 6 (Hevner et al., 2001). Similarly, the COUP-TF1 orphan nuclear receptor may play a role in the specification of SP identity, as this layer is specifically missing in COUP-TF1 mutants (Zhou et al., 1999).

SECTION 3: CELL TYPE DIVERSITY IN THE BRAIN

The developing and mature CNS is populated by a wide diversity of cells that perform discrete but complementary functions, culminating in the precise formation of mature functional electrical circuits.

3.1 CAJAL-RETZIUS CELLS

Cajal-Retzius cells represent a transient class of neurons found at the surface of the developing cerebral cortex of mammals. Santiago Ramón y Cajal and Gustaf Retzius, first described them at the end of the 19th century. These 'special cells', as Cajal initially called them, populate the marginal zone (layer I) of the cortex from early stages of development, and thus have a strategic position to influence its organization. CR cells have a peculiar morphology with distinctive horizontal dendrites, and they release the neurotransmitter glutamate. CR cells are among the first neurons to be generated in the embryonic telencephalon. They start invading the preplate at E10.0–E10.5 in mice (König et al., 1977, 1981; del Río et al., 1995) and are subsequently localized in the most superficial layer (marginal zone (MZ)/layer I) of the developing cortex. Their best-documented function is to control the radial migration of neurons and the formation of cortical layers by secreting the extracellular glycoprotein Reelin. They act as 'project managers' in the construction of the cerebral cortex; the absence of Reelin or other molecules from its signaling pathway results in a severe disruption of the laminar organization of the cortex (Meyer and Wahle, 1999). Additional functions for CR cells have been proposed at late stages of development, such as the regulation of the radial glia phenotype (Larroche, 1981), and the development of hippocampal connections (Del Río et al., 1997). The rare finding of CR cells in adult brain could be due to a limited production of these cells very early during development, thus the distance between cells increases progressively and this could account for their apparent scarcity in the adult cortex. However, some studies suggest that most CR cells are eliminated through cell death during early postnatal stages, only a small proportion differentiating into nonpyramidal glutamatergic cells and this may account for their scarcity in the adult cortex.

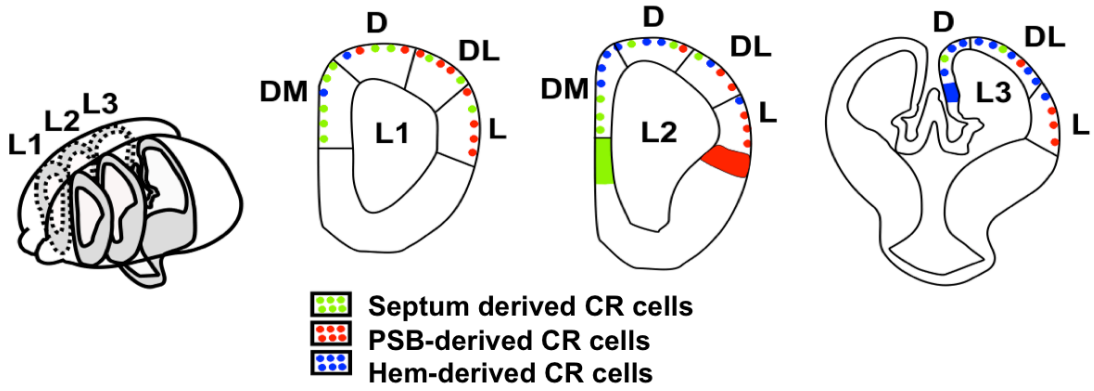

Figure 9: Schematic representation showing multiple origins and distribution of Cajal-Retzius cells in the brain.
Adapted from (Kerjan and Gleeson, 2007)

The dorso-medial part of the telencephalon (L1 level) is mainly populated by septum-derived cells. Very few hem-derived cells can be detected. No PSB-derived CR ($Dbx1^{+)}$ cells are detected at this level. At the dorso-lateral level (L2 level), more hem-derived cells are detected compared to L1, positioned dorsally to septum-derived cells. PSB-derived CR ($Dbx1^{+)}$ cells are exclusively found at the septum and at the PSB (green and red domains, respectively). At caudal levels (L3 level), hem-derived CR cells are the main population accounting for 85–95% of CR cells in caudo-medial territories, whereas PSB-derived CR cells represent 50–60% CR cells along the dorso-caudal and lateral territories.

CR cells are generated at signaling centers and migrate over long distances to cover the entire surface of the cerebral cortex. Genetic tracing experiments have described at least three sites of origin of CR neurons at the borders of the developing pallium, which corresponds to the major patterning centres in the developing telencephalon: the PSB (or anti-hem) laterally, the pallial septum (also called commissural plate) rostromedially, and the cortical hem caudomedially (Bielle et al., 2005) (Figure 9).

Hem-derived CR neurons have been shown to predominantly populate the caudomedial and dorsolateral pallium at E12.5. The expression of the homeodomain TF Dbx1 at the septum and the PSB gives rise to two molecularly distinct subtypes of CR cells that migrate over long distances from their origins to primarily populate the rostromedial and lateral developing pallium, respectively (Bielle et al., 2005). The choroid plexus and the thalamic eminence have also been suggested to generate CR neurons which invade caudoventral telencephalic regions (Abellan et al., 2010). The simultaneous production of CR cells at several sites guarantees a complete coverage of all regions of the cerebral cortex. From these sites molecularly distinct CR subtypes move by tangential migration over long distances to cover the cortical primordium by E11.5 and distribute in specific subtype combinations into pallial territories at the time of cortical regionalization (Bielle et al., 2005). All three sites of

CR generation coincide with patterning centres, and it has been recently shown that Fgf8 and Tgfb signaling are involved in the generation of rostral and hem CR subtypes, respectively. The different CR subtypes express specific repertoires of signaling factors. Genetic ablation of one subpopulation leads to a highly dynamic redistribution of the two others. This results in defects in expression of TFs and in progenitor cell proliferation, which correlate with the resulting changes in the size and positioning of cortical areas. These ablation experiments confirm the participation of CR cells in the regulatory hierarchy of cortical patterning and point to a strategy of morphogen delivery over long distance by migrating cells (Zimmer et al., 2010).

3.2 PROJECTION NEURONS

3.2.1 Laminar fate specification of projection neurons

During development, the various subtypes of projection neurons are produced in a temporal sequence and subsequently migrate radially to specific laminar positions. Neurons in layers V and VI project to subcortical targets, with thalamic projections arising from neurons in layer VI (known as corticothalamic projection neurons) and neurons in layer V (known as subcerebral projection neurons) projecting to the midbrain, hindbrain and spinal cord. Neurons that send their axons to other cortical areas (as well as those projecting to the contralateral hemisphere via the corpus callosum) are particularly abundant in layers II and III (known as corticocortical projection neurons). Finally, there are also neurons in layers I and IV that form axonal connections locally within the cortical hemisphere (Figure 10).

Insights have been gained into the mechanisms of areal specification, including the contribution of graded morphogens and TFs in the generation of diverse types of cortical neurons generated from embryonic stem cells (Monuki et al., 2001; Muzio et al., 2002; Hanashima et al., 2004; Shen et al., 2006). This molecular link between areal and laminar patterning may provide the first hints as to how different areas are composed of the same six layers, but in distinct proportions. However, the extent of diversity of neural progenitors remains underestimated. Molecular mechanisms that allow cortical progenitors to change competence in a time-dependent fashion, and how the various features of the identity of a cortical neuron are coordinated to achieve

a proper match between laminar position and connectivity, as well as how this is related to the differentiation of cortical areas are not fully understood.

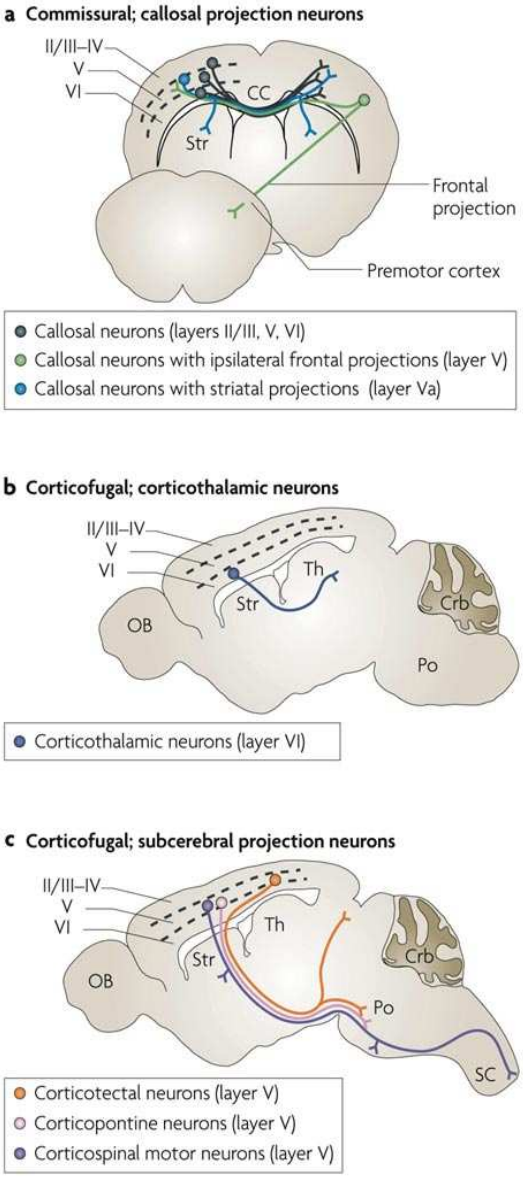

Figure 10: Projection neuronal types in the cerebral cortex
Adapted from (Molyneaux et al., 2007)

a. Commissural projection neurons: Small to medium pyramidal sized neurons are primarily located in layers II/III, V and VI, and extend an axon across the corpus callosum to three major sites; single projections to the contralateral cortex (black); dual projections to the contralateral cortex and ipsilateral or contralateral striatum (blue); and dual projections to the contralateral cortex and ipsilateral frontal cortex (green).
b. Corticothalamic (subcortical) projection neurons: These neurons are located in the deeper cortical layers; VI and layer V to a lesser extent. They project subcortically to different nuclei of the thalamus (Th).
c. Subcerebral projection neurons. Large sized neurons located primarily in deep-layer V and extend projections to the brainstem and spinal cord. They are subdivided into several distinct projection neuron subtypes according to their subcortical projection;
   i. Corticotectal neurons are located in the visual area of the cortex and maintain primary projections to the superior colliculus, with secondary collateral projections to the rostral pons (Po).
   ii. Corticopontine neurons (pink) maintain primary projections to the pons.
   iii. Corticospinal motor neurons (purple) are located in the sensorimotor area of the cortex and maintain primary projections to the spinal cord, with secondary collaterals to the striatum, red nucleus, caudal pons and medulla.

3.2.2 Molecular specification of cortical projection neurons

A Specification of cortical identities

In the developing telencephalon, crosstalk between morphogens secreted by patterning centers establishes the graded expression of four major TFs, Emx1 and 2, Pax6, Lhx2 and FoxG1, in neuronal progenitors. These TFs play an important role in positional identity and fate specification of telencephalic neurons. At the molecular

level, these TFs act by promoting the establishment of cortical neuron phenotypes as well as by repressing adjacent cell fates.

As early as E9 in the mouse, Pax6 shows a regionalized expression pattern that is confined to the neuroepithelium of the pallium in a rostral/lateral high to caudal/medial low gradients and contributes to pallial vs. subpallial specification. In the Pax6 Small eye mutant, cortical progenitors fail to express some cortical markers and ectopically express markers of subpallium such as Mash1, Gsh2 and Dlx1/2 (Stoykova et al., 2000). Emx1 and Emx2 are expressed in cortical progenitors in an opposite gradient pattern with regards to Pax6, and Emx1/2 mutations result in a size reduction of the cortex (Bishop et al., 2000). Emx2 is also required, in concert with Pax6, for establishing the dorsal identity of dorsal progenitors. In Pax6/Emx2 double mutant embryos, the cortex is absent and subpallial domains expand across the entire telencephalon (Muzio et al., 2002). Lhx2 is expressed in the whole telencephalic neuroepithelium, except in the cortical hem. In the dorsal telencephalic primordium, Lhx2 functions as a selector gene to cell-autonomously specify hippocampal and cortical fate and to suppress adjacent cell fates. The absence of Lhx2 results in the spreading of adjacent structures: the cortical hem and anti-hem (a putative secondary signaling center at the lateral extreme of the pallium) (Mangale et al., 2008). FoxG1 is expressed in a cortical rostral/lateral high to caudal/medial low gradient in the telencephalic primordium as early as E9 in the mouse. Foxg1 is critical for establishing cortical neuron identity. Early deletion of FoxG1 will result in cortical neurons that express Reelin (a marker for Cajal–Retzius cells) while losing cortical plate- neuronal specific markers (Hanashima et al., 2004). This effect represents a medial to lateral repatterning of the cortical field, which is respecified as cortical hem and hippocampus in the absence of FoxG1. Additionally, loss of FoxG1 after the onset of corticogenesis also results in the production of Reelin-expressing cells, indicating that persistent expression of FoxG1 is required to maintain cortical progenitor identity (Shen et al., 2006).

In addition to the positional identity instruction encoded by the regionalized, combined expression of these TFs to NE cells in the pallium, they also drive additional and interlinked crucial functions during corticogenesis, such as self-renewal, transition from APs to IPs, neuronal commitment, and subtype specification. For example, Pax6 directly activates an enhancer element of the proneural TF

Neurog2 in APs (Scardigli et al., 2003), which in turn restricts APs to a neuroprogenitor fate, as well as driving neuronal subtype specification in postmitotic neurons. Levels of Pax6 are critical for the proliferation of APs and the absence of Pax6 in *Sey* mutants favours the generation of IPs by promoting asymmetric division of APs (Estivill-Torrus et al., 2002; Quinn et al., 2007). In *Sey* mutants, axon guidance is disrupted, and the majority of thalamocortical axons fail to enter the ventral telencephalon and those that do are unable to innervate their cortical targets. In addition, the expression of upper layer markers Svet-1 and Cux2 is lost in the SVZ and in upper layer neurons suggesting that Pax6 might selectively regulate transcriptional programs to specify upper layer neurons and regulate subsequent thalamo-cortical connectivity (Frantz and McConnell, 1996; Jones et al., 2002; Molyneaux et al., 2007). Thus Pax6 is a key TF for cortical development and is likely to play several roles.

B Temporal specification of cortico-laminar identities

Both intrinsic properties of progenitors and extrinsic factors cooperate to define the laminar fate of projection neurons. Furthermore, this cooperation seems to be essential for determining the number of upper layer neurons.
The specification of projection neurons follows a coordinated temporal sequence as neurons from different layers are progressively generated. Pioneering transplantation experiments demonstrated that the cell intrinsic determinants of laminar fate are present in progenitors (prior to mitosis), and that cortical progenitors become progressively restricted in their potency to populate the different cortical layers as neurogenesis proceeds. Thus, early cortical progenitors are multipotent. They usually produce deep layer neurons, but can be competent to generate later born neurons after transplantation into older hosts(McConnell and Kaznowski, 1991; Nguyen et al., 2006). Conversely, late cortical progenitors produce only neurons of upper layers even when transplanted into an early permissive environment (younger embryo) (Wu et al., 2005). Remarkably, *in vitro* culture of early cortical progenitors or neural progenitors derived from embryonic stem cells leads to clones that generate layer-specific neurons in an appropriate temporal order resembling that observed *in vivo*. In addition, changes in cell cycle length appear to correlate with the timing of

neurogenesis (Marín-Padilla, 1992), supporting the idea that cell cycle control mechanisms are involved in the fate determination process (Reiner, 1991). Altogether, these data indicate that both intrinsic properties of progenitors and extrinsic factors cooperate to define the laminar fate of projection neurons. Furthermore, this cooperation seems to be essential for determining the number of upper layer neurons (Marín-Padilla, 1992). Accordingly, thalamocortical afferents, as mentioned above, and GABAergic interneurons that reach the developing cortex during corticogenesis have been proposed to participate in the timing of neurogenesis. Interestingly, factors secreted by thalamic axons and the neurotransmitter GABA have been shown to influence the proliferation of cortical progenitors (Smart et al., 2002; Kriegstein et al., 2006). As mentioned above, during neurogenesis, certain genes are selectively expressed by cortical progenitors, which correlate with their layer specific neuronal identity. Many of these genes continue to be expressed at various levels in their progeny, making them attractive candidates to control either fate specification or maintenance of a specific neuronal lineage. One such example is the TF FezF2 which is expressed by APs and is persistently detectable in deep layer (layers V and VI) neurons as they mature. During their genesis, deep layer neurons express FezF2 at low levels in the VZ and more robustly in the developing CP, consistent with the position of newborn deep layers neurons (Bohner et al., 1997). Postnatally, FezF2 is expressed primarily in subcerebral projection neurons of layer V, with lower levels of expression in corticothalamic neurons of layer VI. Targeted deletion of this gene in mutant mice has demonstrated that FezF2 acts to specify the fate of subcerebral projection neurons of layer V (Chen et al., 2008), with the most striking phenotype being a respecification of subcerebral projections towards a callosal projection fate (Chen et al., 2008). Interstingly, the respecification of projection neurons in Fezf2−/− cortex, resulted also in abnormal radial distribution of interneuronal populations, and altered GABAergic inhibition (Lodato et al., 2011). In another example, expression of the non-coding RNA Svet-1 and the TF Cux2 in subsets of IPs in the SVZ correlates with the generation of upper layers neurons that still express these markers. Recent elegant in vivo genetic fate mapping and in vitro clonal analysis experiments have shown that a RGC sublineage present early on in the VZ, expresses the upper layer marker Cux2. These identified RGCs are intrinsically specified to generate the majority of upper layer neurons later on, once they become IPs. These experiments add to the heterogeneity of the progenitor pool that will produce specific cell

population at a specific time point. It also highlight the fact that intrinsic signals in RGCs play a fundamental role in generating proper layer-specific neuronal populations (Franco et al., 2012). However, whether these signals act independently as key determinants for the specification of these neurons remains to be determined as there is evidence that the SVZ constitutes a unique "permissive" environment to synchronize migration by isochronically generated projection neurons and interneurons and subsequent acquisition of their appropriate laminar identity (Kriegstein and Noctor, 2004). Providing further support to this hypothesis is that the newborn projection neurons have been observed to pause in the SVZ for up to 24h before initiating their radial migration, thereby entertaining this hypothesis. Nevertheless, the relative contributions by cell-intrinsic and extrinsic factors towards the establishment of the laminar identity of cortical neurons remains to be further clarified, with special effort made to determine at which precise step during the specification process are instructions imparted by these factors (e.g. does the switch between a corticofugal towards a callosal fate observed in FezF2 mutant result from lack of FezF2 expression in the progenitor cell or in the newborn neuron?).

C Subtype specification of projection neurons

Layer and neuron subtype specificity are identified not only by neuronal birth but also through postmigratory differentiation and expression of specific molecular markers (Figure 11). Two major classes in the cortex are specified by different genetic mechanisms:

- Callosal projection neurons, which are present through layers II–VI (though are particularly abundant in upper layers II–IV)
- Corticofugal neurons, which reside in deep layers V and VI.

3.1. Specification of corticofugal vs. callosal projection neurons

Two genes, are exclusively expressed in distinct subsets of cortical projection neurons and are essential for specification of their respective neuronal populations (Britanova et al., 2008). Ctip2, encoding a zinc finger transcriptional co-factor, is specifically expressed in early born corticofugal neurons, with a high expression level in

subcerebral neurons of layer V and a much lower level in corticothalamic neurons of layer VI. Satb2, a DNA-binding protein, is exclusively expressed in callosally projecting neurons (layers II–VI) (Britanova et al., 2008). The expression of each of these genes in cortical neurons is almost mutually exclusive, thus they serve roles exclusive to their respective subpopulations. Accordingly, Satb2 antagonizes the expression of Ctip2 by direct binding to MAR (matrix attachment region) sequences in the regulatory regions adjacent to the Ctip2 gene. As a result, the switch in axonal targeting observed in Satb2 mutants is accompanied by a recovery of Ctip2 expression. Importantly, both these genes are instructive for their subtype specification function, since with loss of Ctip2 function; neurons fail to extend axons towards the spinal cord (Rallu et al., 2002), whereas in the absence of Satb2, neurons that would normally project axons across the corpus callosum instead extend axons towards subcortical targets. The ectopic expression of Ctip2 or Satb2 is sufficient to redirect their axons towards subcortical targets or the corpus callosum, respectively (Britanova et al., 2008).

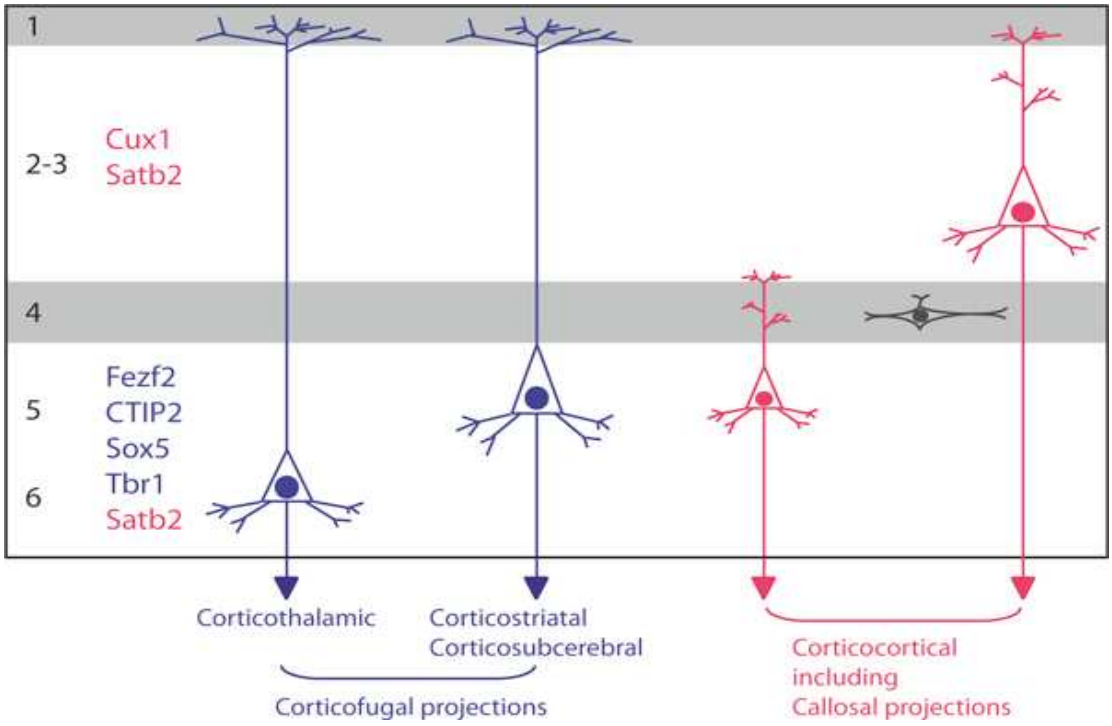

Figure 11: Gene expression correlation to axonal projection and cortical layer organization.
Adapted from (Gaspard and Vanderhaeghen, 2011)

Neurons sending corticofugal projections (in blue) reside exclusively in the deep layers V and VI of the cortex, and express Fezf2, CTIP2, Sox5, Tbr1 and Satb2 TFs. Neurons sending projections within the cortex (in red), are located primarily in the upper layers, and express Cux1 and Satb2 TFs.

Ctip2 is a major downstream effecter of FezF2; and they play a common role in the specification of layer V neurons. The expression of Ctip2 is lost in FezF2 −/− mutant cortex, and rescue of Ctip2 expression in FezF2 mutant neurons can partially ameliorate their axonal miswiring phenotype (Bohner et al., 1997).

3.2. Specification of corticofugal projection neuron subtype

Several other TFs have recently been shown to play crucial roles in the specification of corticofugal projection neuron identity.

Tbr1 is expressed soon after cortical progenitors begin to differentiate, and is highly expressed in the preplate and in layer VI neurons. Tbr1 is a key determinant in the generation of these cortical neurons and loss of Tbr1 expression in genetically modified mice leads to specific molecular and functional defects in SP and corticothalamic neurons (Hevner et al., 2001).

Sox5, belonging to the SRY-box-containing gene family, is expressed by subcortically projecting neurons in layers V, VI and the SP (low levels detected in layer V neurons, with higher levels in SP and layer VI neurons) and is largely excluded from intracortically projecting neurons. Sox5−/− mutant cortices exhibit failed preplate splitting, defects in laminar positioning and aberrant axonal projections (Kwan et al., 2008). Sox5 has been proposed to control the temporal maturation sequence of deep layer neurons (first with the production of SP neurons, followed by corticothalamic then subcerebral projection neurons of layer V), since loss of Sox5 leads to a premature acquisition of subcerebral projection neuron features by early-born SP neurons (Lai et al., 2008). While this model implies that Sox5 acts early to control this sequential corticofugal projection neuron subtype production, an alternative view is interpret a post-mitotic, post-migratory function for Sox5 in controlling subtype specification through direct transcriptional repression of FezF2, which in turns suppresses Ctip2 expression (Kwan et al., 2008).

The TF Otx1 acts at a later stage than FezF2, Ctip2 and Sox5 in the specification program for subcortically projecting neurons. It is specifically expressed by some subcerebral layer V projection neurons, during the period of refinement and elimination of a subset of long-distance projections. In Otx1 mutant mice, layer V neurons maintain exuberant axonal projections suggesting that Otx1 might control the

refinement of axon collaterals (Weimann et al., 1999). Furthermore, Otx1 protein localization in these neurons shifts from the cytoplasm to the nucleus, and could suggest a transcription regulatory role for its control of axonogenesis. Thus Otx1 acts at later stage than FezF2, Ctip2 and Sox5 in the specification program for subcortically projecting neurons, though this remains to be completely elucidated (Weimann et al., 1999).

3.2.3 Migration of projection neurons

A Inside-out lamination

Newly born neurons adopt two main strategies to disperse throughout the CNS, designated as radial and tangential migration (Hatten, 1999; Marín and Rubenstein, 2003). These two modes of migration are adopted by glutamatergic cortical projection neurons (pyramidal cells) and GABAergic interneurons respectively. Some of the basic mechanisms underlying the movement of cells using each of these two modes of migration are different. Radially migrating neurons principally use radial glial fibers as substrate and follow a trajectory that is perpendicular to the ventricular surface. Tangentially migrating neurons do not require radial glial fiber support. They move in trajectories that are parallel to the ventricular surface and orthogonal to radial glial processes. However, both types of migration share common principles, in particular those directly related to the cell biology of movement (Marín et al., 2006).

The neocortex develops with new waves of neurons that occupy progressively more superficial positions within the CP (Gupta et al., 2002). As mentioned previously, birthdating studies have shown that layers in the cortical plate (future cortical layers 2–6) are established according to an inside-outside pattern, where the deeper layers contain cells that become postmitotic earlier than the cells in more superficial layers (Angevine and Sidman, 1961; Rakic, 1972). Thus, neurons born simultaneously (in terms of cell-cycle sequence rather than time of neurogenesis *per se*) (Takahashi et al., 1999) migrate and stop migrating roughly at the same time, so they all occupy the same cortical layer. In parallel to this process, GABAergic interneurons migrate to the cortex, where they disperse tangentially via highly stereotyped routes in the MZ, SP,

and lower IZ/SVZ. Interneurons then switch from tangential to radial migration to adopt their final laminar position in the cerebral cortex (Tanaka et al., 2003).

Cortical pyramidal cells and most interneurons both follow an inside-out layering sequence. Inside-out layering means that each neuronal precursor has to migrate outward from the ventricle, pass beyond its predecessors and then stop, in a cortical layer corresponding to its birthdate, undergo terminal differentiation and establish its synaptic connections (Marín and Rubenstein, 2003). The region where migration stops is defined by the layer of pioneer CR cells. CR cells secrete Reelin and other factors in the MZ; where neurons stop moving. Reelin induces detachment of neurons from radial glia, possibly by downregulating integrin adhesive molecules (Sanada et al., 2004), which causes neurons to stop migrating, thus providing a potential explanation for mechanisms of inside- out cortical layering.

Interestingly, radially migrating neurons and tangentially migrating interneurons that are born at the same time, share the same laminar fate (Marín and Rubenstein, 2003). Interneurons migrate across a much longer distance and are not exposed to the same microenvironmental cues as radially migrating neurons until late in their migratory path. This suggests that a precise interplay between the two neuronal populations is needed to assure correct final positioning. To achieve this, interneurons, upon arrival in the CP, are capable of sensing layer fate determinant cues from the cortical microenvironment and might need to descend to the VZ in order to receive the correct layer specification cues from the local microenvironment (Polleux et al., 2002; Tanaka et al., 2009; Hernández-Miranda et al., 2010). On the other hand, cortical projection neurons spend time in the exploratory, multipolar stage (Altman and Bayer, 1990a), probably “searching” for the incoming interneurons arriving from the ventral telencephalon. The ‘sojourning’ of pyramidal neurons in the SVZ might delay their migration sufficiently for isochronically-generated GABAergic cells to complete their tangential migration into the dorsal cortex. This interplay will finally help both cell types to reach the same layer at the same time.

B Cellular and molecular mechanisms involved in neuronal migration

Cortical pyramidal neurons migrate toward the CP in three phases: in phase one, neurons born in the cortical VZ pause or sojourn in the SVZ in a multipolar stage (Altman and Bayer, 1990a). In phase two multipolar neurons become highly polarized (bipolar) in the direction of their movement and migrate along radial glial fibers by locomotion. During the last phase of migration, close to the MZ, neurons undergoing locomotion adopt the somal translocation mode of migration, where they detach from radial glial fibers and reach their final laminar position (Noctor et al., 2004) by shortening their leading process attached to the pial surface.

Somal translocation and radial glia guided locomotion represent two different but complementary modes of migration. Birth date and the time of neurogenesis seems to be the major factor that determines the original mode of migration of a neuron; early-generated cortical neurons adopt a simplified mode of migration that is unaffected by the cascade of signaling mechanisms that regulate the glia-guided migration of later-generated CP neurons. They reach the developing cortex by somally translocating from the VZ to their positions beneath the pial surface, where a migrating neuron extends a single long leading process with branched ends attached to the pial surface. By shortening this process, the cell body is progressively pulled to superficial regions (Nadarajah and Parnavelas, 2002) (Figure 12). This basic migratory cycle is adopted in early born pyramidal neurons or during the last cycle of later born neurons, which have undergone radial glial-guided locomotion.

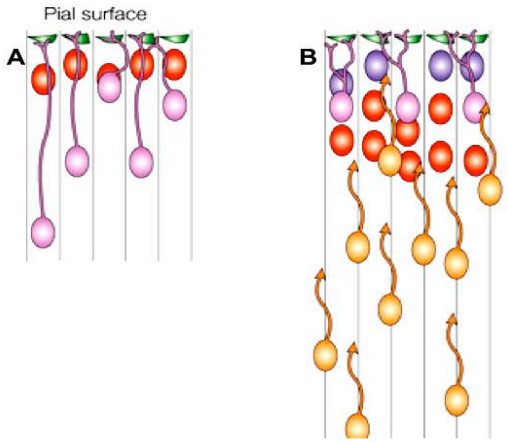

Figure 12: The two distinct forms of cortical neuron movement during migration.
Adapted from (Gupta et al., 2002)

A: Somal translocation, in which young neuroblasts translocate their somata through radially oriented processes, occurs predominantly in early corticogenesis. B: Glial-guided locomotion, in which neurons use radially oriented glial fibers as a scaffold to reach the CP, is more prevalent in later corticogenesis

Neurons undergoing locomotion follow three synchronized steps to move (Ayala et al., 2007). First, the cell extends a short unbranched leading process that is attached to

a radial glial process. Second, the nucleus translocates into the leading process, a step referred to as nucleokinesis. In the final step, the migrating neuron eliminates its trailing process, which leads to the net movement of the cell. The subsequent remodeling of the leading process will initiate a new migratory cycle, which will be repeated until the neuron reaches its final destination (Noctor et al., 2004).

Leading Process Dynamics

The leading process plays an important role in guiding migrating neurons by sensing the surrounding microenvironment and selecting the direction of migration in response to chemotactic cues. The leading process also reflects the state of polarization of migratory neurons. Newly born pyramidal cells have a single process as they leave the VZ (Noctor et al., 2002), they become transiently multipolar for a short period of time in the SVZ (Tabata and Nakajima, 2003). Subsequently, pyramidal cells become highly polarized again and establish a leading process that remains in contact with radial glial fibers until they reach their final destination.

Defects in the extension or maintenance of the leading process, and its interaction with radial glial fibers, leads to aberrant migration. Cdk5, a serine/threonine cyclin-dependent kinase, modulates the extension of the leading process through phosphorylation of Pak1 and p27Kip1, two important actin regulators (Kawauchi et al., 2006). Pak1 phosphorylation by Cdk5 down-regulates Pak1 activity, thereby modulating the actin dynamics in the growth cone (Nikolic et al., 1998). On Cdk5 phosphorylation, p27Kip1 is stabilized in neurons, and this stabilization is critical to keep the proper level of F-actin in the leading processes (Kawauchi et al., 2006).

Connexin 26 (Cx26) and connexin 43 (Cx43) are gap junction proteins expressed at the contact points between radial fibers and migrating neurons. These two gap junction proteins provide dynamic adhesive contacts between the internal actin cytoskeleton of a pyramidal cell and radial glial fibers, thus mediating leading process stabilization along radial fibers and subsequent nucleokinesis (Elias et al., 2007).

Endocytic trafficking of adhesion receptors plays a pivotal role in controlling leading process dynamics and neuronal migration; insertion of new adhesion receptors in front of the cell body generates traction that pulls cell components forward, while removal of adhesive elements in the rear may facilitate forward translocation (Figure

13, 14). Clathrin-coated pits are located closely proximal to neuron–glial junctions of radially migrating neurons (Shieh et al., 2011), where N-cadherin and integrin molecules, which are involved in neuron–neuron or neuron–glial adhesion, are localized to the endocytic compartment. Endocytic adaptor proteins are located primarily in the portion of the leading process just proximal to the neuronal cell body and endocytic recycling of activated integrin receptors is required for growth cone turning and the tangential migration of SVZ neurons in the adult (Hines et al., 2010). Specific and non-specific inhibition of endocytosis, via small-molecule endocytosis inhibitors or overexpression of dominant-negative dynamin constructs respectively, block neuronal migration and lead to an accumulation of adhesion receptors at the rear of the migrating neuron (Shieh et al., 2011). Finally, endocytic trafficking pathways involving the Rab5, Rab7 and Rab11 proteins (small Ras-related GTPases regulating discrete stages of endocytosis) control neocortical radial migration. Rab5 and Rab11 pathways regulate surface expression of N-cadherin in migrating neurons such that inhibition of endocytosis leads to increased surface N-cadherin, excessive adhesion and perturbation in migration. Rab7 appears to regulate final somal translocation within the cortical plate (Kawauchi et al., 2010). Thus, endocytic trafficking of adhesion receptors dynamically orchestrates adhesive interactions required for normal neuronal migration.

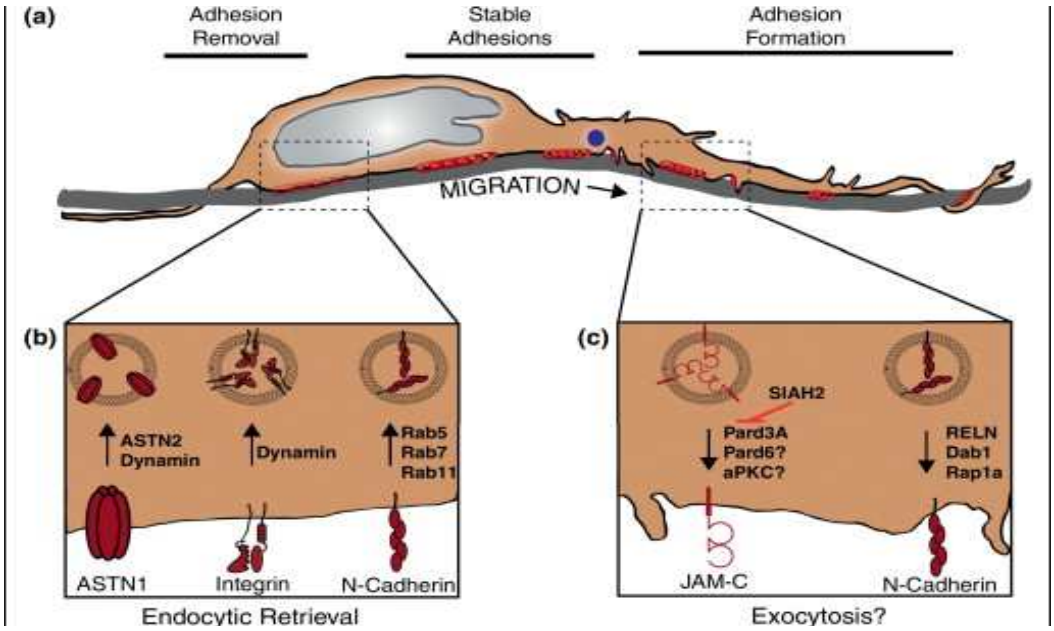

Figure 13: Adhesion dynamics of migrating neurons leading to the extension and maintenance of the leading process.
Adapted from (Solecki, 2012)

a: A gradient of adhesive contacts is generated during the process of migration; new adhesions are primarily located in the leading process, stable adhesions near the soma and adhesions are removed near the rear of the soma. b: Summary of recently reported signaling pathways that control adhesion receptor endocytosis: integrin receptor endocytosis occurs at the rear of migrating SVZa neurons via dynamin and N-cadherin surface levels are regulated via endocytic recycling controlled by the Rab5, 7 and 11 GTPases. c: Summary of recently reported signaling pathways that control adhesion trafficking to the neuronal cell surface. A Reln Dab1 and Rap1A dependent pathway controls multipolar transition and final cortical plate positioning by regulating N-cadherin. (Gray shading: glial fiber. Red: adhesions)

Leading process dynamics differ in tangentially migrating interneurons. These cells have two branches oriented toward the front of the cell and have a dynamic, exploratory behavior until the cell decides what direction to follow. At this point, only one of the branches keeps extending, whereas the other begins retracting. This event is followed by nucleokinesis. These steps are repeated continuously with the generation of a new branch in the leading process in each migratory cycle (Bellion et al., 2005). The ability of tangentially migrating neurons to generate a branched leading process appears to be intimately linked to their guidance. In these cells, chemoattractants and chemorepellents induce the biased formation of new leading processes already oriented toward or against, respectively, the source of the guidance molecule (Martini et al. 2009;Ward et al. 2005). This seems to allow migrating neurons to rapidly change direction without having to reorient pre-existing branches representing a very efficient method for the exploration of the microenvironment (Britto et al., 2009).

Lissencephaly 1 (Lis1) and Doublecortin (Dcx), two MT associated proteins are involved in regulating leading process branching in migrating interneurons (Kappeler et al., 2006; Nasrallah et al., 2006; Gopal et al., 2010). The leading process of Dcx-deficient interneurons branches more frequently than normal, but new branches are unstable. In contrast, the leading process of interneurons heterozygous for a Lis1 mutation branches less frequently and, consequently, is longer than in normal cells (Nasrallah et al., 2006). Together, these data indicate that Lis1 and Dcx play complementary roles in leading process dynamics.

Nucleokinesis

Nucleokinesis occurs in two steps. First, a cytoplasmic swelling forms in the leading process, immediately proximal to the nucleus (Bellion et al., 2005). The centrosome, which is normally positioned in front of the nucleus, moves into this swelling accompanied by additional organelles, including the Golgi apparatus, mitochondria, and the rough endoplasmic reticulum (Tsai and Gleeson, 2005) (Figure 14b). Second, the nucleus follows the centrosome (Figure 14c,d). These two steps are repeated producing the typical saltatory movement of migrating neurons. These processes originally shown in interneurons and then also later seen in radially migrating neurons (Bellion et al., 2005; Schaar and McConnell, 2005; Tsai and Gleeson, 2005; Solecki et al., 2009).

During nucleokinesis, forces generated within the leading process are transmitted to the centrosome, which moves forward. The centrosome is linked to the nucleus through a MT network that envelops the nucleus in a cage like structure. Following centrosome movement, the nucleus is pulled toward it by dyneins associated with the MT network. In addition, actomyosin contraction in the rear of the cell contributes to drive the nucleus forward during nucleokinesis (Malone et al., 2003; Xie et al., 2003; Tanaka et al., 2004a; Tsai and Gleeson, 2005).

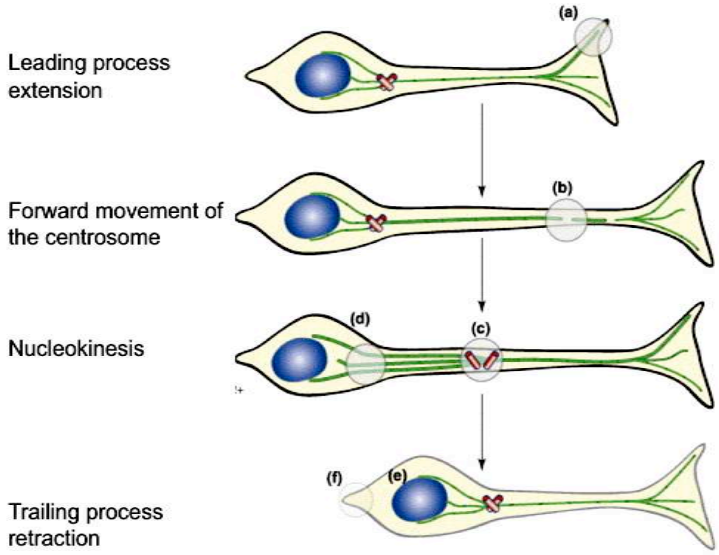

Figure 14: Cellular and molecular mechanisms of neuronal migration

Adapted from (Marín et al., 2006)

a: Microtubule plus ends are recruited to the cortical actin meshwork. b: In the intermediate segment of the leading process, microtubule destabilization through the stathmin family of proteins will render them loose enough to enable forward movement of the centrosome. γ-Tubulin and the microtubule-related protein ninein show a wide distribution in migrating neurons. c: Forward movement of the centrosome. Both centrioles split during the advance of the soma. d, e: Nucleokinesis, requires a microtubule motor complex based on dynein; proteins interacting within this include dynactin, Lis1, Ndel1, Disc1 and Dcx. Dcx molecules are found attached to microtubules that extend from the centrosome to the perinuclear 'cage'. Ca^{2+} signaling might also operate at this stage. f: Trailing-process retraction. Actomyosin contraction has a role in driving the nucleus towards the centrosome.

The movement of the centrosome and the nucleus is highly dependent on the integrity of a rich network of MTs with different post-transcriptional modifications that extends between both of them. Lis1, and the motor protein dynein and its partner Ndel1, belong to a highly conserved complex of proteins that are associated with MTs and that regulate nuclear migration in filamentous fungi, an event that is similar to nucleokinesis in migrating neurons (Morris, 2000). Lis1 associates with MTs and a proportion of Lis1 protein localizes to the centrosome. It promotes MT stability by inhibiting MT catastrophe (Sapir et al., 1997). Ndel1 facilitates the interaction between Lis1 and dynein and is capable of targeting dynein, through Lis1, to the plus end of MTs (Li et al., 2005a). Ndel1 is also required for targeting Lis1 and dynein to the centrosome, and facilitates the nucleation and anchoring of MTs to the centrosome. In addition, Ndel1 facilitates the interaction between Lis1 and dynein and regulates dynein-mediated retrograde transport. Disruption of Lis1, Ndel1, or dynein function abolishes centrosome- nucleus coupling, increasing the distance between the two organelles (Gupta et al., 2002; Li et al., 2005a).

Dcx is a MT-associated protein (Francis et al., 1999; Gleeson et al., 1999) that also may participate in the regulation of nucleokinesis during neuronal migration. Interneurons lacking Dcx have nucleokinesis abnormalities; the centrosome-containing cytoplasmic swelling can move backward toward the nucleus in Dcx mutant neurons, indicating a problem in the polarization of organelles in these cells (Kappeler et al., 2006). Consistently, knockdown of Dcx in pyramidal cells leads to an abnormally hyperactive centrosome, with loss of directional movement and lack of spatial correlation with the nucleus (Sapir et al., 2008). In addition, the centrosome-nucleus uncoupling observed in Lis1 or dynein-deficient cells is rescued by Dcx expression (Tanaka et al., 2004a), confirming that Dcx can function in the maintenance of the MT network for coupling the centrosome and the nucleus in migrating neurons.

Mark2 (MT affinity- regulating kinase 2, also known as Par-1), one of the proteins involved in cell polarity (Sapir et al., 2008), plays an important role in coordinating the movement of the centrosome and the nucleus in each migratory cycle. Loss of Mark2 function impairs migration probably due to excessive MT stabilization. Dcx is a substrate of Mark2, and loss of Dcx function increases MT dynamics, co-reduction of Mark2 and Dcx resulted in a partial restoration of normal neuronal migration *in*

vivo. This highlights the fact that the kinetic behavior of the centrosome, regulated by different molecular mechanisms, is important to ensure successful nucleokinesis and proper neuronal migration (Sapir et al., 2008).

The motor protein myosin II is localized to both the leading process of most neurons and at the rear of neurons undergoing movement (Solecki et al., 2009). The presence of activated myosin II at the trailing edge is often correlated with a cup-like shape of the cell rear that is suggestive of the cell soma being contracted. Pharmacological blocking of Myosin II ATPase activity inhibits nucleokinesis, suggesting that rear contraction of actomyosin fibers plays a complementary role and provides additional forces required for nucleokinesis and neuronal migration (Bellion et al., 2005; Schaar and McConnell, 2005). Additionally, F-actin and Myosin II motors are enriched in the proximal region of the leading process of migrating cerebellar granule cells. Rapid F-actin turnover powered by Myosin II in this region appears to contribute to the forward movement of the centrosome, which in turn facilitates the subsequent displacement of the nucleus (Solecki et al., 2009).

Cues regulating radial migration; reelin signaling and its role as in cerebral cortex lamination

Reelin is a large secreted extracellular matrix glycoprotein that helps regulate processes of neuronal migration and positioning in the developing brain by controlling cell–cell interactions (Franco et al., 2011; Jossin and Cooper, 2011). During brain development, reelin is secreted in the cortex and hippocampus by Cajal-Retzius cells which are predominantly found in the MZ of the developing cortex and in the hippocampal stratum lacunosum-moleculare and the upper marginal layer of the dentate gyrus (Alcántara et al., 1998). Reelin's function is mediated by its binding to two members of low density lipoprotein receptor gene family: Vldlr and the ApoER2 (Trommsdorff et al., 1999). This binding induces tyrosine phosphorylation of the adaptor protein, Dab1 (Hack et al., 2007). Mouse mutants helped in deciphering the Reelin signaling pathway and its fundamental role in neuronal migration and cerebral cortex layering. The naturally occurring *reeler*, *scrambler* and *yotari* mouse mutants, as well as the engineered mutants that are double homozygous null for the genes *Vldlr* and *Lrp*8 (which encode Vldlr and ApoER2) show defects in preplate splitting, with

SP cells remaining adjacent to the MZ (Caviness et al., 1972; Howell et al., 1997; Sheldon et al., 1997; Trommsdorff et al., 1999). Moreover, birth dating experiments showed an inverted lamination pattern of the *reeler* cortex (Caviness, 1982). Consequently, the CP is established underneath a superplate and is itself severely affected, as layering is inverted and indistinct (Kerjan and Gleeson, 2007).

Dab1 phosphorylation is translated into the regulation of MT dynamics, as supported by several lines of evidence. First, tyrosine phosphorylation of Dab1 is coupled to the activation of PI3K in the leading processes of migrating neurons. This in turn activates Akt and induces the serine phosphorylation of Gsk3b, which inhibits its activity (Beffert et al., 2004). One of the major substrates of Gsk3b is the MT associated protein tau, which stabilizes MTs in its unphosphorylated state. Under physiological conditions, activation of Dab1 might function to maintain tau's dephosphorylation, thereby promoting MT stability. Accordingly, both *reeler* and *Vldlr*/ *ApoER*2 double mutant mice show hyperphosphorylation of tau at Ser202 and Thr205, two Gsk3b sites (Hiesberger et al., 1999; Ohkubo et al., 2002, 2003). On the other hand, Reelin signaling can also induce the phosphorylation of Gsk3b at its tyrosine residue, leading to its activation. Activated Gsk3b functions synergistically with Cdk5 to phosphorylate another MT associated protein, Map1b (González-Billault et al., 2005). Phosphorylation of Map1b is believed to regulate both MT stability and the cross talk between MTs and actin filaments in axonal growth cones (Kawauchi et al., 2005). These opposite effects on Map1b and tau phosphorylation likely reflect a very dynamic regulation of MT dynamics by Reelin signaling, depending on the context of the cellular compartment or phases of migration. Third, Dab1 interacts with Lis1, and this interaction depends on the tyrosine phosphorylation of Dab1 (Assadi et al., 2003). Furthermore, LIS1 mutations associated with severe phenotypes in humans disrupt the LIS1-Dab1 interaction. In addition, the compound Reelin/Lis1 heterozygous mice show a greater degree of cortical malformation than the individual heterozygotes, suggesting an epistatic relationship of the two genes (Assadi et al., 2003). Taken together, these studies suggest that the Reelin signaling pathway regulates MT dynamics through multiple signaling components.

Interestingly, the aberrant behaviour of Reelin signaling-deficient neurons are characterized by two components, implying that the biological functions of the Reelin

signaling pathway are multifaceted, affecting several aspects of neuronal migration and possibly the development of radial glial processes:

(1) The early inability of the first-migrating neurons to split the preplate, a process mediated principally by migrating neurons that carry out somal translocation, the glia independent mode of migration. To split the preplate, the leading edge of a translocating neuron concentrates Vldlr or ApoER2 on its surface. When the leading edge attaches to the pial surface, either of the two receptors is able to bind to Reelin secreted by the CR cells of the developing MZ. The Reelin–receptor interaction results in tyrosine phosphorylation of Dab1, which activates downstream signaling events that propel the cell soma towards the leading edge to split the preplate successfully (Beffert et al., 2004).

(2) The late inability of glial-guided cells to migrate past each other, when locomoting cells need to detach from radial glia to complete their journey by somal translocation. During this step, Reelin interacts with cell adhesion molecules including integrins and cadherins.

Downregulation of α3β1 integrin is important for the radial detachment of neurons as they migrate closer toward the MZ. Reelin binds to α3β1 integrin and forms a complex with Vldlr and ApoER2. This binding induces the tyrosine phosphorylation of Dab1, which promotes the endocytosis of the entire complex. Endocytosis results in the degradation of Reelin and Dab1 and the modulation (decrease) of α3β1 integrin receptor levels leading to a switch from a gliophilic adhesion system to a neurophilic adhesion system, such that the migratory neuron detaches from the radial glial fiber and begins to differentiate in its “home” cortical layer (Dulabon et al., 2000).

Cadherins are a group of cell adhesion molecules that have broad roles in neocortical development and have been shown to interact with the Reelin signaling pathway. N-cadherin is highly expressed in the MZ, where Reelin controls glia-independent somal translocation. Reelin binding to its receptors triggers Dab1 phosphorylation and the activation of their downstream effector Rap1. Rap1 regulates neuronal adhesive properties of N-cadherin, which act downstream to control terminal translocation of migrating neurons (Franco et al., 2011). Thus, Reelin is a really important molecule regulating cortex development in several different ways, via its effects on migrating neurons.

3.3 INTERNEURONS

GABAergic interneurons mostly originate from precursors located in the subpallium and migrate tangentially to invade the cortex and hippocampus to occupy the different cortical layers. Interneurons comprise around 20% of the cortical neuronal population. They are locally projecting to pyramidal cells to control and synchronize their output (McBain and Fisahn, 2001; Zsiros and Maccaferri, 2005). Through mostly inhibitory mechanisms, interneurons control hyperexcitability, by controlling the timing of pyramidal cell firing, synchronizing network activity, and the generation of cortical rhythms. Thus, they play an important role by responding to dynamic changes in excitation, and maintaining the excitatory and inhibitory balance necessary for the transfer of information. The required precision of this function depends on the existence of a variety of interneuron types. Understanding interneuron diversity is thus critical to understand information processing within the cerebral cortex (Ascoli et al., 2008). Moreover, malfunction or deficiency of these neurons has been implicated in a number of diseases such as epilepsy (Cossart et al., 2001; Noebels, 2003; Cobos et al., 2005).

Multiple distinct types of interneurons exist; they are defined by a constellation of molecular, neurochemical, anatomical and electrophysiological characteristics (Yuste, 2005; Wonders and Anderson, 2006; Gelman and Marín, 2010; Hernández-Miranda et al., 2010; Cossart, 2011; Jovanovic and Thomson, 2011). Several attempts to classify interneurons into distinct classes gathering different characteristics have been attempted (The Petilla Interneuron Nomenclature Group PING, 2008). The embryological origin of interneurons has been shown to be crucially related to interneuron structure and function. Different classes of interneurons originate from three main sources in the developing subpallium: the MGE, the CGE and the POA, and reach the cortex following different migratory routes (Anderson et al., 1997; Wichterle et al., 2001; Nery et al., 2002; Xu et al., 2004; Welagen and Anderson, 2011). Three major groups of interneurons exist, with each group expressing a specific molecular marker, and including several subtypes of interneurons that differ in morphological and electrophysiological properties and likely have different functions in cortical circuits. These major groups include the Ca2+-binding protein parvalbumin (PV) expressing interneurons, the neuropeptide somatostatin (Sst) expressing interneurons, and the ionotropic serotonin receptor 5HT3a (5HT3aR)

expressing interneurons. These groups account for nearly 100% of neocortical interneurons, and further subdivisions of interneurons arise from the combinatorial expression of other molecular markers (Lee et al., 2010; Rudy et al., 2011).

3.3.1 Migration of interneurons from the ventral telencephalon to developing cortex

As mentioned previously, interneurons generated in the subpallium migrate tangentially before they arrive in the cortex, and employ other modes of intracortical migration, to populate different cortical layers at the end of their journey. Immature interneurons derived from the MGE, LGE/CGE, and POA have an impressive capacity for migration (Figure 15). In vitro experiments show that LGE cells migrate more than 100 um per day, and MGE cells migrate almost three times faster (Eisenstat et al., 1999; Long et al., 2009). A constellation of orchestrating guidance systems is needed to direct these diverse migrating cells.

A : Tangential neuronal migration

Motogenic factors:

Several factors have been shown to possess motogenic activity, stimulating the undirected movement of neurons from their original position. Neurotrophic factors have been implicated in controlling the rate of migration of neurons derived from the subpallial telencephalon. Addition of brain-derived neurotrophic factor (BDNF) and neurotrophin 4 (NT4), both of which are high-affinity ligands for the tyrosine kinase receptor TrkB, produce heterotopic accumulations of neurons in the MZ of the cortex (Brunstrom et al., 1997). These heterotopias are probably caused by increased migration, and they contain neurons that resemble GABA-containing subpial granule cells (Meyer et al., 1998). Consistent with the idea that TrkB receptor activation might stimulate neuronal migration in the developing telencephalon, tyrosine kinase inhibitors block BDNF-induced migration in cortical slice cultures (Behar et al., 1997). It is not yet known if the distinct migratory behaviour of CGE- and MGE-derived precursors depends on the differential expression of receptors for these motogenic factors.

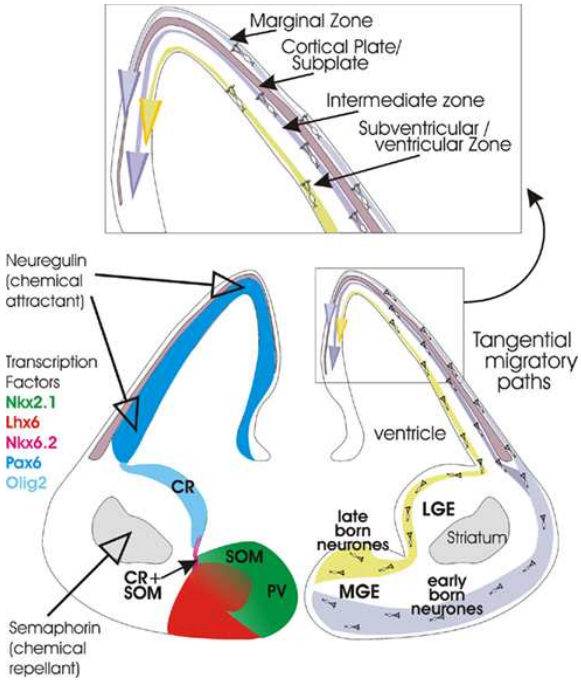

Figure 15: Origin and migratory routes of cortical interneurons.
Adapted from (Jovanovic and Thomson, 2011)

Coronal section through the brain of an embryonic mouse at E14.5. Expression patterns of the transcription factors that play a role in differentiation and migration of interneurons. The birthplaces of Sst, PV, Clr, and Clr + Sst interneurons are indicated.
Neuropilin receptors mediate the repulsive actions of class 3 semaphorins on axons. Due to the repellent action of semaphorin 3, neuropilin-expressing interneurons will avoid the striatum and invade the developing cerebral cortex. Early born interneurons follow a ventral route before migrating through the MZ overlying the developing cortex (superficial stream). Later born neurons migrate through the IZ. Later on, neurons follow a more dorsal route and then migrate through the SVZ.

Extracellular substrates.

Tangentially migrating cells in the IZ of the cortex seem to be closely associated with corticofugal axons (Denaxa et al., 2001), indicating that migrating neurons might use other neuronal processes as the substrate for their migration (axonophilic migration). The number of interneurons migrating to the cortex in slice cultures is severely reduced by adding antibodies against the neuronal adhesion molecule TAG-1 (contactin 2), which is expressed on corticofugal axons (Denaxa et al., 2001). However, the in vivo analysis TAG-1 mutants have shown its essential role in interneurons migrationg to the caudal medulla, but not to the cerebral cortex (Denaxa et al., 2005). Therefore it is still unclear whether most interneurons that migrate to the cortex interact with fibre tracts *in vivo* (Wichterle et al., 2001).

Guidance factors.

Tangential migration in the telencephalon is a highly directional process. Several families of ligands/receptors are candidates for guiding the trajectories of tangentially migrating interneurons (Fig. 15). Neuropilins are transmembrane receptors that mediate the repulsive actions of class 3 semaphorins on axons. In the subpallial telencephalon, neuropilins are expressed by interneurons that migrate to the cortex, but not by interneurons that invade the developing striatum. Expression of neuropilins

allows migrating cortical interneurons to respond to a chemorepellent activity in the striatal mantle, of which the class 3 semaphorins Sema3a and Sema3f are likely components . Loss of neuropilin function increases the number of interneurons that migrate into the striatum and decreases the number that reaches the embryonic cortex. So, the final destination of tangentially migrating interneurons (striatum or cortex) is determined by the expression of the class 3 semaphorin receptors neuropilin 1 and neuropilin 2. Moreover, by channeling migrating cortical interneurons into superficial and deep pathways, the chemorepellent activity in the developing striatum might also help to distribute cortical interneurons differentially into superficial (MZ) and deep (SVZ/lower IZ) positions within the cortex (Marín et al., 2001).

The neuregulin 1 (NRG1) family of proteins is essential for interneurons to leave the MGE and enter the cortical wall. First, the membrane bound isoform of NRG1 (type III) is found highly expressed by so-called corridor cells present in the SVZ but not the VZ of the LGE. Together with the inhibitory action of semaphorins emanating from the striatum, a permissive corridor is created through the SVZ for interneurons to traverse the LGE. Second, the secreted isoforms of NRG1 (types I and II), which are expressed in the neocortex, act as a long-range chemoattractant for migrating interneurons. This helps them cross the corticostriatal notch. It has been shown that the complete loss of NRG1 in the forebrain leaves interneurons incapable of leaving the MGE (Flames et al., 2004; Batista-Brito and Fishell, 2009).

B: Intracortical migration of interneurons

Once interneurons arrive in the cortex, they need to switch from tangential migration and employ a radial migration mode to enter the CP. Both inward radial migration towards the CP from the MZ and outward radial migration towards the CP from the IZ/SVZ can be employed (Tanaka et al., 2006).

The switch from tangential to radial migration is dependent on neurite branching dynamics (Tanaka et al., 2009). While migrating in tangential migratory streams, interneurons maintain the orientation of the leading neurite parallel to the ventricular surface/pia. Once they receive the signal to move into the CP, the angle of the leading branch changes from small to nearly orthogonal, and the switch from tangential to a radial migratory mode is achieved (Martini et al., 2009). Candidate molecular cues

governing this switch have been identified; the downregulation of connexin 43 expression in interneurons significantly decreased the percentage of radially oriented cells, with a concomitant increase in tangential cell orientation (Elias et al., 2010). The downregulation of cues required for anchoring interneurons in the MZ during the horizontal dispersion phase could be a second mechanism. The chemokine CXCL12 and its receptors CXCR4 and CXCR7 attract cortical interneurons in the MZ and SVZ, and loss of CXCL12 signaling increases interneuron branching and dramatically disrupts tangential migration, resulting in the premature entry of interneurons into the CP and abnormal lamination. Thus, CXCL12/CXCR signaling may play a dual role, initially attracting interneurons to the neocortex and subsequently maintaining their migration in the tangential streams until the correct radial signal is received (Tiveron et al., 2006; López-Bendito et al., 2008).

C: Differentiation and maturation of interneurons

Upon arrival at their final destination, interneurons perceive that they have reached their target position and continue to differentiate into mature neurons. Early patterns of neuronal activity generated in the target region may influence this process. Migrating interneurons, for example, sense ambient GABA and glutamate on their way to the cortex via their $GABA_A$ and AMPA/NMDA receptors (Bortone and Polleux, 2009). At early stages of cortical development, both neurotransmitters seem to depolarize migrating cells, inducing intracellular Ca2+ transients that promote cell movement. Upon arrival in the cortex, interneurons upregulate the expression of the potassium/chloride (K+/Cl-) exchanger KCC2, which modifies their response to GABA from depolarizing to hyperpolarizing. This later event leads to a reduction in the Ca2+ influx, and since this is ultimately needed for movement, the net result is that neurons end up halting their migration (Bortone and Polleux, 2009). According to this model, KCC2 expression determines the end of the migratory period for cortical interneurons. To this end, it would be interesting to further understand the dynamics of KCC2 expression in interneurons, as these cells tend to invade the cortex in different waves according to their birth date (Miyoshi and Fishell, 2011).

3.3.2 Major classes of cortical interneurons

A: Parvalbumin (PV) Interneuron Group

PV expressing cells constitute the major type of cortical interneuron, accounting for about 40% of all. There are two types of PV neurons: basket cells, neurons that make synapses at the soma and proximal dendrite of target neurons and have a multipolar morphology, and chandelier cells, which target the axon initial segment (AIS) of pyramidal cells (Cauli et al., 1997; Kawaguchi and Kubota, 1997; Ascoli et al., 2008). Fate mapping experiments have shown that PV expressing interneurons originate exclusively from the MGE mainly at E13.5 in embryonic mouse.

PV expression has been associated with a fast spiking firing pattern (Kawaguchi et al., 1987). Acquisition of the fast-spiking characteristics and expression of PV seem to be defined by the concerted action of Nkx2-1, Dlx5, Dlx6, Lhx6 and Sox6, five genes expressed by specific cohorts of cortical interneurons (Azim et al., 2009; Wang et al., 2011).

The fast-spiking, basket cells are identified by their innervation at the soma and proximal dendrite of target neurons (both pyramidal and GABAergic) (Freund, 2003). They are also identified by their fast kinetics; including high-frequency repetitive firing and brief single spikes. They innervate postsynaptic targets close to the site of action potential initiation, the axon initial segment. Therefore, they provide strong inhibitory control over postsynaptic cell firing and are the main class of cells to provide feedforward inhibition resulting in precise control of neuronal output (Pouille and Scanziani, 2001). Moreover, PV basket cells contact a vast number of postsynaptic cells to mediate fast, precise, and powerful inhibition of target neurons. This characteristic renders them the major neuronal subtype capable to synchronize the firing of large groups of neurons and likely the dominant inhibitory system in the cortex (Jonas et al., 2004). They have been also implicated in the establishment and maintenance of fast (gamma frequency) cortical rhythms (Traub et al., 2004).

Chandelier (or axo-axonic) cells are one of the most distinctive types of GABAergic interneurons in the cortex. They exclusively innervate pyramidal cells, and do not make synapses with other cell types (Martínez et al., 1996). These cells have a distinctive axonal arbor, with parallel arrays of short vertical sets of presynaptic terminals, which resemble the candlesticks of a chandelier lamp. Each chandelier cell

targets many dozens of pyramidal neurons and establishes several synapses in their axonal initial segment (DeFelipe et al., 1985). The functions of chandelier cells are controversial. Although they are traditionally considered inhibitory neurons, where some reports indicate a predominantly hyperpolarizing effect of chandelier cells on their postsynaptic targets (Glickfeld et al., 2009), data from rat and human neocortical preparations suggest that chandelier cells can in some circumstances have a depolarizing effect on pyramidal neurons at resting membrane potential, and can even activate synaptic chains of neurons (Szabadics et al., 2006; Molnár et al., 2008; Woodruff et al., 2009). This depolarizing effect, could be mediated by local differences in the expression of the Na–K–2Cl transporter NKCC1 (Woodruff et al., 2006) and the the K+/Cl− co-transporter KCC2 (Szabadics et al., 2006) that changes Cl- concentration, and hence the reversal potential of GABAA receptors, at the pyramidal cell AIS. Despite the strong evidence of depolarizing effect of chandelier cells on their postsynaptic pyramidal cells, it is it is not yet clear if this effect could actually be excitatory and lead to spiking activity in the whole circuit. Determination of the effect of these cells in quiescent as well as excited fields is still needed to understand the physiologic relevance of these cells and their contribution to the electrical activity of the brain under certain stimuli.

B: Somatostatin (Sst) Interneuron Group

Sst-containing interneurons are primarily generated in the MGE. They represent a group of GABAergic interneurons abundant in layer V, although they can be found throughout layers II-VI, with ascending axons that arborize in layer I spreading horizontally to neighboring columns and making synapses on the apical and basal dendrites of pyramidal neurons. Synaptic contacts are found mainly on dendritic shafts and on spines. As a result of this feature, repetitive activity in a single pyramidal cell can drive a somatostatin interneuron to fire and provide feedback inhibition to pyramidal neurons across layers and columns (Silberberg and Markram, 2007). Sst cell-mediated inhibition is selective by inhibiting more strongly excitatory inputs arriving at the dendrite in close proximity to the location of the interneuron inputs (Silberberg and Markram, 2007).

There are two main subpopulations of Sst cells in the neocortex; Sst+/Calretinin (Clr)+ interneurons which account for 30% of Sst interneurons, and Sst+/Clr -

interneurons. The two cell populations have differences in intrinsic firing properties, the expression of molecular markers, connectivity, and in embryonic origins. Although both Sst+/Clr+ cells and Sst+/Clr - cells exhibit similar cell anatomical features and have similar adapting spike-firing patterns, they differ in the horizontal extension of their dendritic fields and number of primary processes. In layers II/III, the two subtypes of Sst interneurons have different connectivity. Sst+/Clr - cells receive strong excitatory input from both layers II/III and IV, while Sst+/Clr + cells receive excitatory input mainly from layers II/III where they are concentrated and only weakly from layer IV (Xu and Callaway, 2009). Another feature suggesting a difference between the two populations is evidenced by the difference in their embryonic origin with the Sst+/ Clr+ population mainly arising from the dorsal Nkx6-2-positive region of the MGE (Sousa et al., 2009).

C: 5HT3aR Interneuron Group

Although PV and SST expressing interneurons are mainly derived from the MGE, the CGE is the origin of most interneurons that do not express these markers (Miyoshi et al., 2010). This includes the reelin-expressing late-spiking neurogliaform cells as well as bipolar/bitufted VIP-expressing cells. A recent report suggests that most, if not all, GABAergic neurons in the cortex that do not express PV or SST express the 5HT3a receptor; these 5HT3aR-positive interneurons comprise 30% of GABAergic neurons in somatosensory cortex (Lee et al., 2010; Rudy et al., 2011). The VIP expression interneurons, which do not overlap with those that express PV or SST, account for 40% of the 5HT3aR population. All VIP and at least 90% of 5HT3aR neurons originate in the CGE (Lee et al., 2010).

VIP cells are particularly enriched in layers II/III. A significant fraction of VIP neurons (40%) express Clr, which, as described earlier, is also expressed in a fraction of Sst neurons, as well as in interneurons that do not express VIP or Sst (Lee et al., 2010; Miyoshi et al., 2010). These VIP+/Clr+ cells have a bitufted morphology with a vertically oriented descending axon reaching deep layers. They are often referred to as irregular-spiking (IS) cells (Lee et al., 2010; Miyoshi et al., 2010). Non-VIP cells account for 60% of 5HT3aR neurons. More than 80% of these interneurons express reelin, and they reside in layer I where more than 90% of neurons in this layer belong

to this group (Miyoshi et al., 2010). This reelin-positive, VIP-/Sst- 5HT3aR group includes the neurogliaform cells, which have a characteristic morphology consisting of a small, round soma from which multiple dendrites spread radially in all directions and have a wider round axonal plexus composed of fine branches (Lee et al., 2010). Neurogliaform cells are the only cortical interneuron type, which establish electrical synapses not only with each other but also with other interneuron types. Thus, neurogliaform cells play a central role in generating and shaping synchronized activity of neuronal circuits (Simon et al., 2005). Moreover, neurogliaform axonal varicosities containing synaptic vesicles were often not associated with classical synaptic contacts, although they produced hyperpolarizing responses in a large fraction of neighboring neurons. These results led to the suggestion that neurogliaform cells influence target neurons by volume release of GABA, thus eliciting slow, long lasting inhibitory post-synaptic potential (IPSP) on pyramidal cells and other interneurons, through a combined activation of slow $GABA_A$ and $GABA_B$ receptors (Oláh et al., 2009).

3.4 MACROGLIA, ASTROCYTES AND OLIGODENDROCYTES

Astrocytes and oligodendrocytes are macroglial cells derived from the neuroepithelium and are found throughout the mature CNS, accounting for more than 50% of the total cells in the mature rodent brain. In the developing brain, radial glial cells give rise to all neurons and macroglia in the adult brain (Qian et al., 2000). By contrast, the other group of glia; microglia has a mesodermal origin (Alliot et al., 1999).

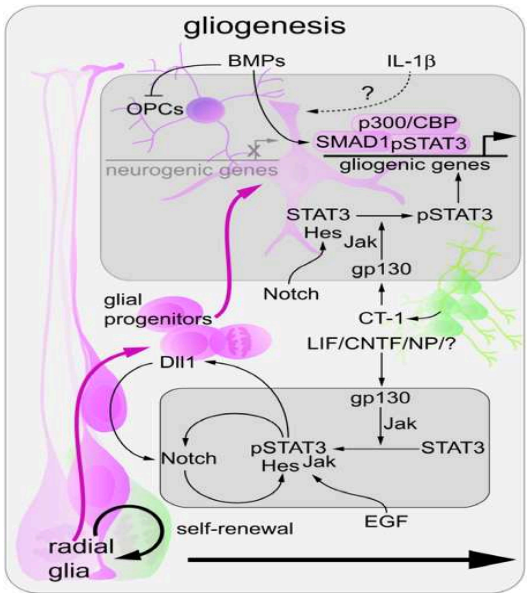

Figure 16: Signaling cascade that results in the generation of glial precursors from RGCs
Adapted from (Deverman and Patterson, 2009)

The specification of macroglial cells is similar to the development of the diverse neuron types. Spatiotemporal factors restrict the pools of RGCs and commit them to produce astrocytes and

oligodendrocytes, at later stages during embryonic development (Qian et al., 2000; Tomita et al., 2000; Viti et al., 2003; Anthony et al., 2004). The neuron to glial switch is mediated by several intrinsic (genetic) and extrinsic (environmental) mechanisms. Activation of Notch signaling in radial glia promotes astrogenesis (Namihira et al., 2009), in part, through HES proteins, which inhibit neurogenic bHLH factors, but also through epigenetic mechanisms that will promote cytokine- mediated activation of the JAK–STAT pathway (Kamakura et al., 2004; Deverman and Patterson, 2009) (Figure 7, 16). Demethylation of the two-astrocyte promoters, GFAP and S100B, will render the neuroepithelial cells sensitive to cytokine signals (Takizawa et al., 2001). Neurons secrete the gliogenic cytokines-IL-6 family members, including leukaemia inhibitory factor (LIF), ciliary neurotrophic factor (CNTF) and cardiotrophin 1 which bind to a receptor complex that contains the α-subunit of the LIF receptor and gp130, activating the gp130–JAK–STAT pathway in cortical precursor cells and promoting gliogenesis (figure16) (Bonni et al., 1997; Ochiai et al., 2001; Barnabé-Heider et al., 2005). Thus, a neuronal feedback mechanism seems to be involved to regulate the developmental switch to gliogenesis.

Although the gp130–JAK–STAT pathway is crucial for promoting gliogenesis in cortical precursor cells, it is not necessarily sufficient to commit precursors to astrocytic fate; cells stimulated to express GFAP by LIF remain multipotent and self-renew, at least *in vitro* (Bonaguidi et al., 2005). The presence of BMP signaling seems to be crucial to transform multipotent progenitors into the mature form of adult astrocytes with the typical stellate morphology (Figure 16), (Bonaguidi et al., 2005). Mouse mutants lacking type I Bmp receptors Bmpr1a and Bmpr1b have 25-40% reduction of GFAP and S100B positive cells in the cervical spinal cord (See et al., 2007). Thus BMP signaling seems to play a dual role in glial cell fate switch; it regulates neurogenesis during the neurogenic period and astrogenesis during the gliogenic period. Intrinsic factors have also been implicated in the specification of oligodendrocyte precursor cell (OPC) identity, including the bHLH proteins Olig1 and Olig2, which label OPCs in the spinal cord (Lu et al., 2000; Zhou et al., 2000). In the telencephalon, Olig genes are expressed in a more widespread manner than expected of OPC-specific genes, suggesting that their function is not limited to oligodendrocyte specification.

While the presence of bipotent cells in the cortex in the late developmental stages, that give rise to both neurons and glia has been confirmed (Costa et al., 2009), the presence of a bipotent progenitor precursors pool that give rise to astrocytes and oligodendrocytes is widely debated (Richardson et al., 2006). On the one hand, some studies showed the presence of two types of astrocyte precursor *in vitro* (type 1 and type 2 astrocytes) and indicated that type 2 astrocytes and oligodendrocytes developed from a common oligodendrocyte-type 2 astrocyte precursor (Raff et al., 1983). In addition, Herrera et al., showed the presence of a bipotent oligodendrocyte-astrocytes from glial-restricted precursor cells that were able to generate both oligodendrocytes and astrocytes (Herrera et al., 2001). However, *in vivo* retroviral fate mapping studies targeting proliferating cells, indicated that mixed astrocyte and oligodendrocyte clones were rarely or never observed in the studied embryos (Costa et al., 2009).

Using the Cre-lox approach in transgenic mice to follow the development of distinct OPC populations in the developing telencephalon has shown the presence of three different spatiotemporal origins of oligodendrocytes (Figure 17), (Kessaris et al., 2005); an early wave of OPCs (OPC1) were generated in the *Nkx*2.1-expressing MGE and anterior entopeduncular area around E12.5 and subsequently migrated widely into all parts of the telencephalon, entering the cerebral cortex after E16. By postnatal day 10, there were very few *Nkx*2.1-derived OPCs or oligodendrocytes in the cortex. At this stage, they have been replaced by OPCs arising from a second group of precursors expressing the homeobox gene *Gsx*2 in the MGE and LGE, starting at E15.5 (OPC2); and a third group (OPC3) arising from precursors expressing the homeobox gene *Emx*1 in the cortex, starting at birth (Figure 17) (Kessaris et al., 2005).

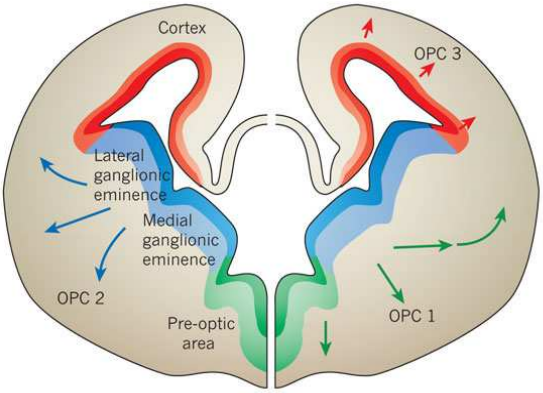

Figure 17: Competing waves of oligodendrocytes in the developing forebrain
Adapted from (Rowitch and Kriegstein, 2010)

Three sequential waves of OPCs are generated from different regions of the forebrain ventricular zone: OPC 1 (green arrows) arises from Nkx2.1-expressing precursors in the medial ganglionic eminence; OPC 2 (blue arrows) arises from precursors expressing Gsx2 in the LGE and MGE; and OPC 3 (red arrows) arises from precursors expressing the homeobox gene Emx1 in the cortex.

I. Migration and functional differentiation of of astrocytes and oligodendrocytes

Similar to other cell types in the developing brain, astrocytes and OPCs are highly migratory. Being generated from multiple distant sites in the developing brain, OPCs need to migrate long distances. This migration is mediated in part by interactions between the OPCs (identified by the unique expression of platelet derived growth factor receptor alpha, PdgfA) and growing axons (Ono et al., 1997). OPCs intended for the optic nerve for example, will interact with the chemorepellent molecules, netrin-1 and the semaphorins (Sugimoto et al., 2001; Spassky et al., 2002). The cessation of migration of these cells upon arrival is mediated probably by the extracellular matrix molecule tenascin C (Kiernan et al., 1996). Growing numbers of studies have started to unscramble the molecular mechanisms involved in directing OPC migration along significant distances in the developing cortex, a task that has been long complicated by the wide variety and multiple origins of OPCs. Axonophilic mechanisms are suggested to play a role in OPC migration and the ephrin and Eph receptors have been suggested to be possible candidates for this (O'Leary and Wilkinson, 1999). Also, Nogo-A, an inhibitor of axonal regeneration, is expressed by maturing oligodendrocytes, and Nogo-A-deficient mice exhibit a marked delay of oligodendrocyte differentiation and transient hypomyelination (Pernet et al., 2008) (Pernet et al., 2008). Several growth factors regulate OPC behavior, including Pdgfa which has been shown to be critical for myelination, and Fgf2 (Baron et al., 2000; Vora et al., 2011). Both of these interact with receptor tyrosine kinases, and regulate migration via activation of the extracellular regulated kinase (Erk) pathway (Vora et al., 2011). Also, a localized concentration of the cytokine Cxcl1 (a homologue of interleukin-8) will act as a stop signal for migrating OPCs (Tsai and Miller, 2002; Tsai et al., 2002). Activation of the Cxcl1 receptor, Cxcr2, leads to inhibition of PdgfA induced oligodendrocyte progenitor migration (Vora et al., 2012).

Unlike OPCs, astrocytes originate from multiple domains of the NE and constitute a heterogenous cell population (Miller and Szigeti, 1991). Direct differentiation of radial glial cells into astrocytes represents one of their sources, and these cells do not need to migrate significant distances to their final location (Voigt, 1989; Hunter and Hatten, 1995). A second origin of astrocytes is the subventricular zone of the developing cortex and elegant tracer studies suggest these cells migrate radially into

overlying white and gray matter (Zerlin et al., 1995). Insights into astrocyte migration have been drawn from transplantation experiments, where astrocytes were injected into organotypic slice cultures in different regions and at different developmental stages (Jacobsen and Miller, 2003). These studies have shown that the pattern and extent of dispersion of transplanted astrocytes are dependent on both the age of the host brain in which the cells are transplanted and the area of the brain into which these cells are placed, with younger hosts having more dispersed astrocytes, preferentially occupying myelinated white matter tracts rather than in gray matter or unmyelinated tracts (Andersson et al., 1993).

II. Function of astrocytes and oligodendrocytes in adult brain

Function of astrocytes in adult brain:

Astrocytes are the most abundant cells in the mammalian CNS. They play critical roles in the developing and adult brain. During development, they take part in inducing formation of the blood brain barrier, which protect the CNS from substances in the systemic circulation (Abbott et al., 2006). In the adult, astrocytes play variable critical roles to maintain the homeostasis of the CNS. By regulating hydrogen and potassium ion concentrations, they can modulate pH and water balance in the brain (Papadopoulos and Verkman, 2007). They can modulate neuronal synaptic activity by sequestering and releasing neurotransmitters like GABA (Schousboe and Waagepetersen, 2006) and glutamate (Bergles and Jahr, 1997) as well as synthesizing their precursors (Hertz et al., 1999). Astrocytes contribute to the maintenance of the metabolic homeostasis in the brain by the detoxification of ammonium (Johansen et al., 2007) and reactive oxygen species (Liddell et al., 2006), and providing neurons with energy substrates such as glucose, lactate and pyruvate (Pellerin et al., 2007; Rouach et al., 2008).

Function of oligodendrocytes in adult brain:

Oligodendrocytes are the myelin producing cells of the CNS. There are five basic phases of the oligodendrocyte development: generation, migration, proliferation, differentiation and myelination. Myelin reduces ion leakage and decreases the capacitance of the cell membrane. It also increases impulse speed, as saltatory

propagation of action potentials occurs at the nodes of Ranvier in between Schwann cells (of the peripheral nervous system) and oligodendrocytes (of the CNS). In contrast, satellite oligodendrocytes are functionally distinct from most other oligodendrocytes. They are located primarily in the grey matter and are not attached to neurons and, therefore, do not serve an insulating role (van Landeghem et al., 2007). They remain apposed to neurons and regulate the extracellular fluid and provide metabolic support to principal neurons (Takasaki et al., 2010). Upon demyelinating injury, satellite oligodendrocytes are responsible for remyelination of gray matter axons (van Landeghem et al., 2007). A role of these cells in regulating extracellular glutamate levels in the brain after injury has been suggested by the spatiotemporal alterations in their expression of glutamate transporter proteins upon ischemic injury (van Landeghem et al., 2007).

3.5 MICROGLIA

Microglia are abundant nonneuronal cells derived from myeloid progenitors that take up residence in the brain of vertebrates during development are found in the neural plate as soon as it is formed (Herbomel et al., 2001). Their heavily branched morphology, response to pathological tissue changes, and similarity to macrophages have led researchers to propose that they might have a surveillance or maintenance role in brain function. In mice, the major increase in microglial number occurs postnatally from day 6 (Cohen et al., 2002). Microglia have been ascribed many roles most frequently relating to immunological, apoptotic cell clearance and repair activities (Glezer et al., 2007; Lalancette-Hébert et al., 2007; Streit and Xue, 2009). It has also been suggested that they have a role in neuronal development by guiding axons (Milligan et al., 1991) and eliminating neuronal projections (Berbel and Innocenti, 1988). Synaptic pruning by microglia is necessary for normal brain development and normal maturation of neurons (Paolicelli et al., 2011). In addition, roles in neurogenesis, neuronal survival and synaptogenesis have been proposed (Michaelson et al., 1996; Walton et al., 2006; Bessis et al., 2007; Thored et al., 2009). Macrophages are primarily regulated by the growth factor, colony stimulating factor-1 (CSF-1, also known as macrophage-CSF) (Chitu and Stanley, 2006). CSF-1 signals via a Class III transmembrane receptor tyrosine kinase CSF-1R. CSF-1R mouse

mutants, where no functional activated microglia can be found, have perturbations in brain architecture. Although early brain development proceeds normally with no gross defects, a gradual increase in the volume of the ventricular system is observed, becoming very severe by 3 weeks of age, when the lateral ventricles are significantly enlarged and the abutting brain regions are reduced and/or misshapen including the cerebral cortex, olfactory bulb and hippocampus. This late progression of pathology could be due to true non-atrophic hydrocephalic condition, pointing to microglia involvement in blood brain barrier development. The interference of normal outflow of cerebrospinal fluid could be related also to accumulating cellular debris, especially high during developmental programmed cell death, that would normally be significantly cleared by phagocytic microglia in the parenchyma (Erblich et al., 2011).

SECTION 4: AXON GUIDANCE, SYNAPTOGENESIS, AND MATURATION OF DEVELOPING NEURONAL CIRCUITS

Normal functions of the brain including sensation, motor control and behaviour depend on the correct wiring up of neuronal circuits during embryonic and postnatal development. The correct sequential program of neuronal generation, specification, migration, and differentiation must be followed by the events of terminal differentiation, axogenesis, and synaptogenesis. Early perinatal experience plays critical roles in the final-shaping of mature neuronal circuits.

Axon growth and navigation

The longest components of neuronal circuits, the neuronal axons, sprout from immature neurons and elongate precisely through diverse tissues to reach synaptic partners located throughout the developing body. This embryonic axonal navigation is accomplished by the motile structure at the distal tip of an elongating neuronal axon, called a growth cone.

The growth cone is a specialized flattened, fan-shaped amoeboid structure at the tip of an extending axon that is able to navigate through the surrounding environment and sense the 'guiding cues' that can be either attractive or repulsive. A graded distribution of attractive and repulsive guidance cues controls the direction of growth cone and subsequent axonal growth (Henley et al., 2004; Li et al., 2005b; Wang and Poo, 2005; Togashi et al., 2008). When an axon is delivered to its approximate target, it sends multiple branches and contacts postsynaptic targets at very specific points.

When a growth cone migrates in a guidance cue gradient, the side of the growth cone facing higher concentrations of the cue will experience higher asymmetric receptor occupancy, which will eventually polarize the growth cone for turning towards or away from the cue (Wang and Poo, 2005; Togashi et al., 2008). Turning of the growth cone involves the asymmetric calcium mediated activation of second messengers that control multiple cellular mechanisms including vesicular membrane trafficking, adhesion molecules and cytoskeleton re-organization (Figure18).

Dynamic calcium elevations mediate growth cone responses to extracellular attractive and repulsive signals upon their binding to receptors. Attractive signals will result in

high amplitude calcium elevations by calcium influx through calcium gated ion channels. Calcium influx can be further amplified and extended in space and duration by secondary release from the endoplasmic reticulum, a cAMP mediated process (Figure 18) (Zheng, 2000).

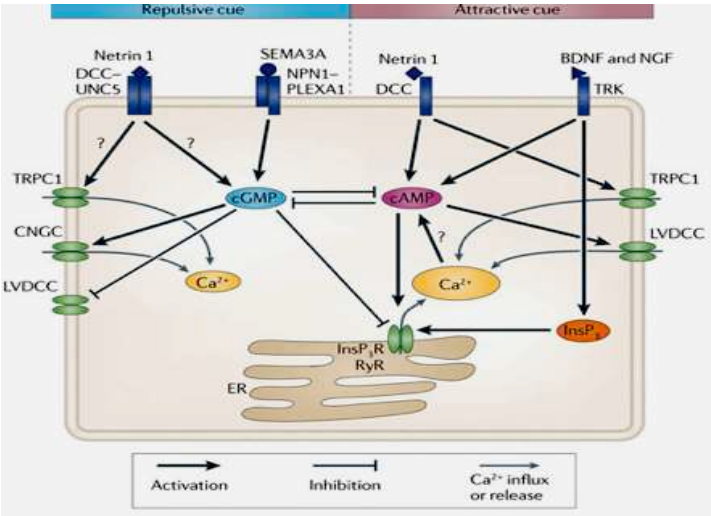

Figure 18: Dynamic calcium oscillations mediate growth cone responses to axon guidance cues, involving cGMP and cAMP.
Adapted from (Tojima et al., 2011)

In contrast, repulsive cues cause low amplitude calcium influx that does not release calcium from the endoplasmic reticulum. Additionally, elevation of the intracellular concentration of cGMP, mediated by binding of repulsive cues, including Sema3a and Netrin 1, to their receptors, will inhibit further cAMP mediated release of calcium from endoplasmic reticulum (Figure 18) (Togashi et al., 2008).

In order to accomplish growth cone turning, the external signals that have been interpreted, amplified and transduced need to result in changes in growth cone morphology, mediated by the cytoskeleton, which facilitates plasma membrane protrusion and adhesion complex insertion, mediating membrane anchoring to the extracellular matrix. This steering machinery is organised in an asymmetrical pattern in response to guidance cues, thus the growth cone turns preferentially toward the side with cytoskeletal and adhesion complexes. This effect of cytoskeleton dynamics is mediated by a number of effector proteins, including Rho-family GTPases, actin depolymerization factor/cofilin, adenomatous polyposis coli protein, calpain, focal adhesion kinase (FAK) and Src-family kinases. Local translation or degradation of cytoskeletal components and their regulators also participates in growth cone guidance (Hu et al., 2001; Robles et al., 2003, 2003; Li et al., 2004, 2008).

Asymmetric Ca2+ signals attract and repel growth cones also via Ca2+/ calmodulin dependent protein kinase II (CaMKII) and calcineurin signaling (Figure 19), respectively. Both the magnitude and subcellular localization of Ca2+ signals dictate which effector pathways are activated, and consequently favor either exocytosis or endocytosis, two fundamental processes for growth cone turning (Rusnak and Mertz, 2000; Hudmon and Schulman, 2002; Wen et al., 2004).

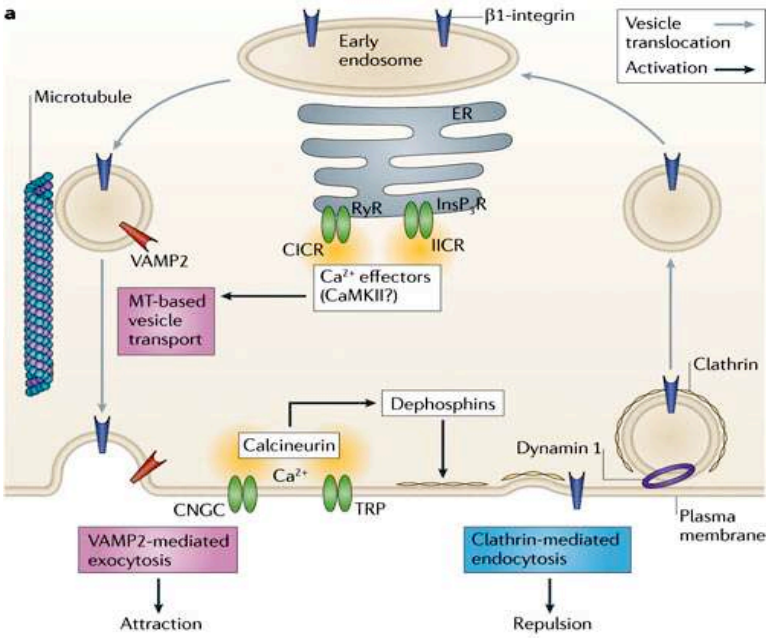

Figure 19: Cellular response and subsequent calcium oscillations in response to attractive and repulsive cues during axon guidance.
Adapted from (Tojima et al., 2011)

Regulated exocytosis and endocytosis occur asymmetrically across the growth cone in response to guidance cue gradients. A gradient of chemoattractants promotes vesicle transport and vesicle-associated membrane protein mediated exocytosis on the gradient side of the growth cone, and subsequent surface availability of relevant receptors such as deleted in colorectal cancer, uncoordinated 5 (UNC5) and neuropilin1 (Bouchard et al., 2004; Bartoe et al., 2006). Conversely, a chemorepellent gradient causes asymmetric clathrin-mediated endocytosis on the side facing the gradient. Endocytosis of the relevant receptors transiently desensitizes the growth cone to collapse-inducing activities of Sema3A and netrin-1 (Piper et al., 2005). Protein synthesis is required for the reappearance of receptors on the growth cone surface. However, a partial recovery of cell surface receptor does occur in the absence of protein synthesis, which is due to recycling from the endosomal compartment back to the plasma membrane. Thus, receptor endocytosis is necessary for the full regeneration of intracellular guidance signals from early endosomes (Mann et al., 2003).

Attractive Ca2+ signals facilitate two distinct but successive processes: vesicle translocation into the growth cone periphery and regulated exocytosis in a CamKII dependant manner. They promote MT-based transport of membrane vesicles and their subsequent VAMP2-mediated exocytosis on the side with elevated Ca2+ (Figure 19). The attractive Ca2+ signals might locally activate CaMKII, which could phosphorylate motor proteins like myosin-V and KIF17 and trigger release of these motors from cargo vesicles. After releasing these motors, the vesicles could be incorporated into a readily-releasable pool of vesicles docked beneath the plasma membrane, followed by Ca2+-dependent activation of synaptotagmins and other effector proteins on the vesicle membrane that regulate exocytosis (Tojima et al., 2007).

Repulsive Ca2+ signals elicit asymmetric clathrin-mediated endocytosis in a calcineurin-dependent manner (Figure 19). The role of calcineurin in clathrin-mediated endocytosis has been extensively studied in presynaptic terminals (Marks and McMahon, 1998). Calcineurin dephosphorylates, and thereby activates, dephosphins, a group of at least eight endocytic-adaptor proteins. In synaptic transmission, activated dephosphins facilitate synaptic vesicle endocytosis after exocytic neurotransmitter release. In growth cones, the requirement for calcineurin activity in repulsive turning and clathrin-mediated endocytosis suggests that dephosphins play a similar role in axon guidance (Tojima et al., 2010).

Synapse formation in the developing brain

Synapses represent cell-to-cell contact sites, where information propagation from one cell to the other occurs. Most synapses in the CNS are chemical synapses, where neurotransmitter release from the presynaptic terminal and its binding to postsynaptic receptors, mediates signal transmission (Li and Sheng, 2003). Two distinct types of synapses can be categorized based on where the synapses locate within the axon: terminal synapses and en passant synapses. Terminal synapses are formed at the end of the axon projections, whereas en passant synapses locate along the axon shaft and can be far away from the axon terminal. Both types of synapses are quite abundant in the vertebrate CNS (Sabo et al., 2006).

Multiple overlapping mechanisms are required for the formation of new stable synapses and eventual circuit formation in the brain. This begins early on, with cell fate specification, when each neuron adopts a distinct morphology, axonal and dendritic trajectory, and synaptic property at the level of synaptic specificity and neurotransmitter content. Later on, navigating axons possess intrinsic abilities to pattern their presynaptic terminals. Evidence for this was drawn from dissociated cortical neuron culture experiments, where the initial formation of presynaptic terminals occurred preferentially at predefined sites within the axons, not determined by contact with neighboring neurons or glia. Transporting synaptic vesicle precursors paused repeatedly at these sites, even in the absence of neuronal or glial contact, and "attract" dendrite filopodia to form stable synapses (Sabo et al., 2006). Additionally, nonsynaptic clusters of postsynaptic proteins can form in young neurons (Washbourne et al., 2004). Stable sites of accumulation of stationary protein complex clusters containing neuroligin, PSD-95, GKAP and Shank in postsynaptic dendrites exist, and can recruit synaptophysin-positive axonal transport vesicles. These complexes appear to be located at predefined sites in dendrites that can induce the formation of a postsynaptic terminal specifically (Gerrow et al., 2006). Taken together, these results suggest that sites of new synapse formation are not a completely stochastic event and that intrinsic factors in the growing axon and dendrite may predefine sites that determine where synapses can form along these processes.

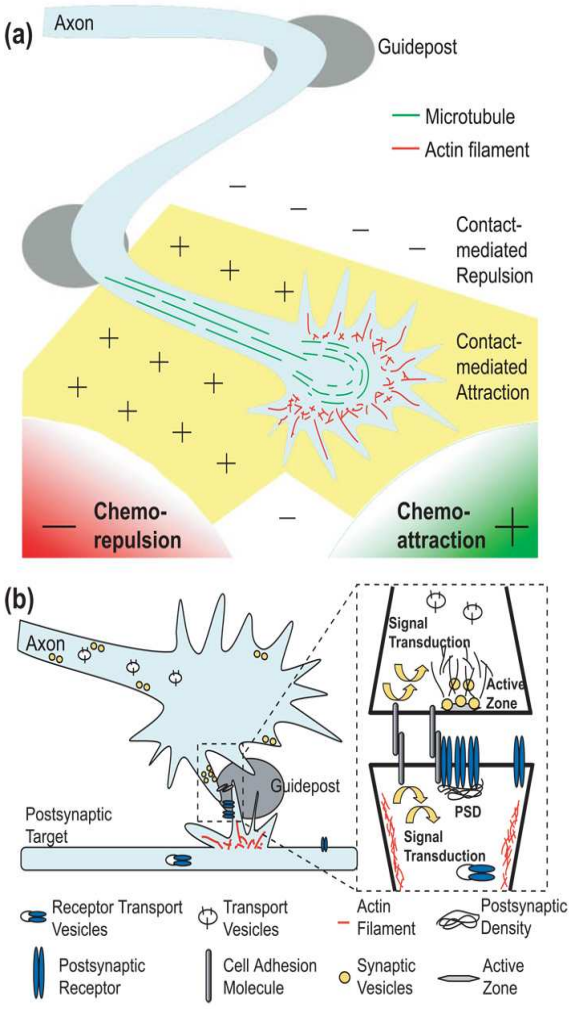

Figure 20: Mechanisms of axon guidance and molecules involved in synapse formation.
Adapted from Chen and Cheng, 2009

As well as intrinsic mechanisms, it is also accepted that new synapse formation starts when the growth cone encounters a pro-synaptogenic signal (Figure 20a) (Plachez and

Richards, 2005). Upon reaching and contacting its target, the filopodia of the growth cone transforms into a presynaptic specialization capable of transducing synaptic signals to the postsynaptic target. The contacts between the presynaptic and postsynaptic compartments are favored by the recruitment of additional cell adhesion molecules (Giagtzoglou et al., 2009). This will result in the stabilization of initial synaptic contacts by adhesive protein interactions (Wang et al., 2009), organization of presynaptic and postsynaptic specializations by scaffolding proteins (Berkel et al., 2010), regulation of growth by intercellular signaling pathways, reorganization of the actin cytoskeleton (Rodal et al., 2008), and proper endosomal trafficking of synaptic growth signaling complexes (Wu et al., 2009)(Figure 20b).

Thus, the initial contact between the growing axon and its target depends on molecular attractions that have pro-synaptogenic effects. These effects are maintained through precisely opposed presynaptic and postsynaptic domains of adhesion protein complexes that operate in parallel to ensure proper synaptic alignment (Figure 20a). Postsynaptic neuroligins and their cognate presynaptic receptors neurexins, are two such families of synapse-specific adhesion molecules critically involved in establishing and maintaining CNS connectivity (Dean and Dresbach, 2006). Neurexin–neuroligin interaction is vital to initially align postsynaptic sites with presynaptic terminals. Additionally, the intracellular domain of neuroligin alone play a role in some postsynaptic assembly events, such as the recruitment of PSD95 (Dean and Dresbach, 2006).

After the initial contact, chemoattractants help regulate subcellular cytoskeletal dynamics to facilitate functional synapse formation by recruiting synaptic components to build up neurotransmission machinery in pre- and post-synaptic cells. Scaffolding proteins (eg the PDZ containing protein PSD95) are critical mediators of this process. Scaffolds are composed of multiple protein– protein interaction domains, and form a physical link between adhesion proteins, ion channels, neurotransmitter receptors, intercellular signaling cascades, and the actin cytoskeleton. Thus preassembled packets of proteins localize to the presynaptic compartment to form the active zone and the synaptic vesicle release machinery. Simultaneously, neurotransmitter receptors, signaling molecules, and structural proteins cluster at the postsynaptic site (Ziv and Garner, 2004).

Contact Stabilization:

The forming axo-dendritic contact needs to get stabilized and mature into a functional synapse. Stabilization of these contacts is accompanied by dendritic calcium waves (Lohmann and Bonhoeffer, 2008). Cell surface expressed proteins like ephrinB/EphB, cadherins, SynCaM, as well as neurexin/neuroligin, are known to regulate synapses and control axo-dendritic contact stabilization. EphrinB/EphB interacting molecules on the membranes of axon nerve terminals and target dendrites act as bidirectional ligands/receptors to transduce signals into both the Eph-expressing and ephrin-expressing cells to regulate cytoskeletal dynamics (Lai and Ip, 2009). Cadherin superfamily proteins, including cadherin 11 and cadherin 13 are involved in synapse formation and are required for proper stabilization of both glutamatergic and GABAergic synapse densities (Abe et al., 2004; Paradis et al., 2007). They likely stabilize transient axo-dendritic contacts via cell–cell adhesion or facilitate the clustering of synaptic proteins. Similarly, N- cadherin regulates the maturation of dendritic spines and excitatory synapses in part through stabilization of dendrite filopodia and spines (Togashi et al., 2002).

Synapse maturation:

Recruitment of pre- and postsynaptic proteins to sites of contact including presynaptic accumulation of transmitter-filled vesicles is a hall- mark process in the functional maturation of synapses in the CNS. The cross communication between the pre- and postsynaptic terminals is essential for the coordinated assembly at both sides of the synapse.

Although the initial assembly of a synapse can be quite rapid (occurring within minutes of contact), the development of a mature synapse is generally prolonged and needs the development of mature ultrastructural components (Figure 21) (Ahmari and Smith, 2002) and electrophysiological properties (Mohrmann et al., 2003). In general, synaptic maturation consists of synapses growing larger and the amount of pre- and postsynaptic protein increasing considerably. This growth is maintained in part by the same mechanisms that lead to synapse stabilization. Additionally, neuronal activity plays a critical role in final synapse shaping and terminal differentiation into functional excitatory or inhibitory synapses (Flavell and Greenberg, 2008; Kozorovitskiy et al., 2012).

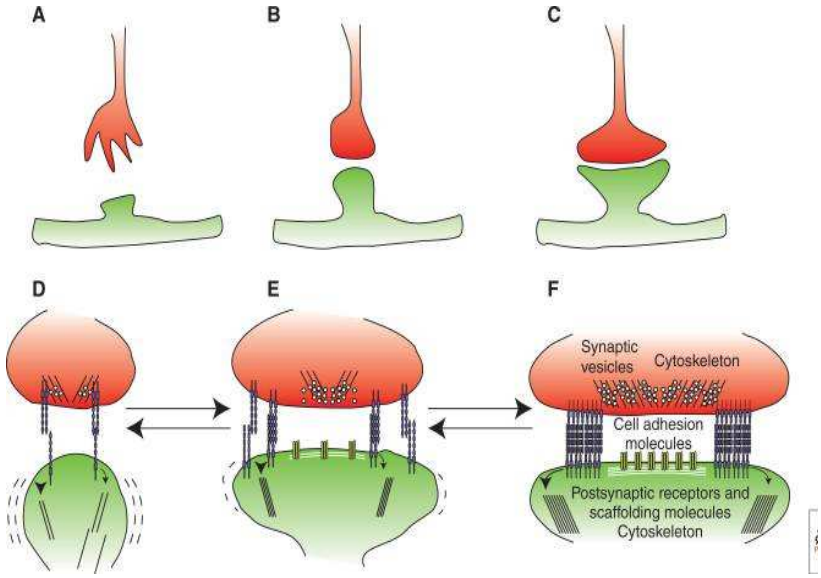

Figure 21: Successive events leading to contact stabilization and maturation of developing synapses. *Adapted from (Giagtzoglou et al., 2009)*

Secreted molecules have also been shown to play a crucial role in synaptic assembly and growth of both presynaptic and potsynaptic compartments (Figure 22). Secreted Wnt proteins function as retrograde signals to regulate axon remodeling and the accumulation of presynaptic proteins. Wnt-7a stimulates presynaptic protein clustering and facilitates presynaptic neurotransmitter release probability in CA3-CA1 hippocampal synapses (Cerpa et al., 2008). In addition, Wnts may also play roles in postsynaptic mechanisms of synaptogenesis and plasticity; Wnt-5a induces clustering of PSD-95 in dendritic spines through a JNK-dependent signaling pathway, and Wnt-5a also modulates glutamatergic synaptic transmission through a postsynaptic mechanism (Figure 22), (Farías et al., 2009). EphBs appear to promote synapse formation through both extracellular and intracellular mechanisms by regulating cell–cell adhesion, activation of F-actin remodeling, recruiting synaptic proteins to the nascent synapse, and as mentioned above, activating ephrinB reverse signaling (Figure 22).

Transsynaptic control of vesicle accumulation and subsequent excitatory synapse maturation is mediated by a cooperative interplay between two synaptic adhesion systems N-cadherin and neuroligin-1. In the absence of N-cadherin, a strong impairment of vesicle accumulation in presynaptic compartments was observed. In fact N-cadherin acts by postsynaptically aiding the accumulation of neuroligin-1 and

activating its function via the scaffolding molecule S-SCAM, leading, in turn, to presynaptic vesicle clustering (Stan et al., 2010).

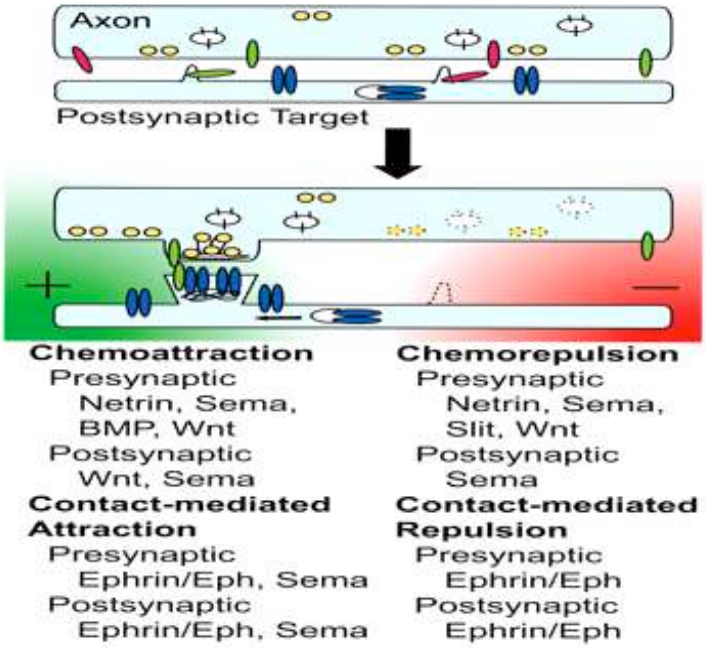

Figure 22: Molecular mechanisms involved in synapse growth and stabilization.
Adapted from Chen and Cheng, 2009

In excitatory synapses, several trans-synaptic complexes – collectively referred to as 'synaptic organizing proteins' – initiate and stabilize early synaptic contacts via recruitment of synaptic vesicles to the presynaptic active zone, and N-methyl-D-aspartate (NMDA) receptors to the postsynaptic density (Siddiqui and Craig, 2011). As mentioned previously, PDZ domain proteins such as PSD-95 serve as scaffolds for recruitment of synaptic components required. Initial flurries of excitatory synaptogenesis give way to an abundance of silent NMDA receptor-containing synapses subject to activity-dependent strengthening or elimination. Recruitment of α-amino-3-hydroxy-5-methyl-4-isoxazolepropionic acid (AMPA) receptors to the postsynaptic membrane augments glutamatergic transmission and is a critical process in excitatory synapse maturation (Kim and Sheng, 2004).

During the early postnatal period, when synapse maturation and differentiation take place, environmental factors play a critical role in synapse maturation. Natural stimulation of neonatal mice pups through enriched environment (EE) rearing promotes GABAergic neurotransmission and accelerated maturation of GABAergic and glutamatergic synapses. Whole-cell recordings from CA1 pyramidal neurons in

acute hippocampal slices of EE-reared mice showed higher amplitudes of miniature GABAergic postsynaptic currents, as well as accelerated transition of GABA action from excitation to inhibition, compared with mice reared under standard housing conditions. This was accompanied by elevated levels of GABAA receptors, KCC2 and increased levels of excitatory synaptic components, including NMDA and AMPA receptors and PSD95 in the forebrain/hippocampus of EE- reared mice during the first two postnatal weeks (He et al., 2010).

SECTION 5: HIPPOCAMPAL DEVELOPMENT

The hippocampus constitutes a remarkable structure of the brain. It is one of the structures of the limbic system, and is implicated in both normal physiological functions and pathology. It plays important roles in the consolidation of information from short-term memory to long-term memory and spatial navigation. It has also attracted the attention of many clinicians and neuroscientists for its involvement in a wide spectrum of pathological conditions, including epilepsy, intellectual disability, Alzheimer disease and others.

The hippocampus is functionally connected to related brain regions that together comprise the hippocampal formation. The hippocampus proper is composed of multiple subfields including the dentate gyrus (DG) and the cornu ammonis (CA) fields. The DG contains the fascia dentata and the hilus, while the CA is differentiated into fields CA1, CA2, CA3 and CA4. The other regions of the hippocampal formation include the subiculum, presubiculum, parasubiculum, and entorhinal cortex. The CA fields are also structured depthwise in clearly defined stratum (Anderson et al., 2006) (Figure 23A).

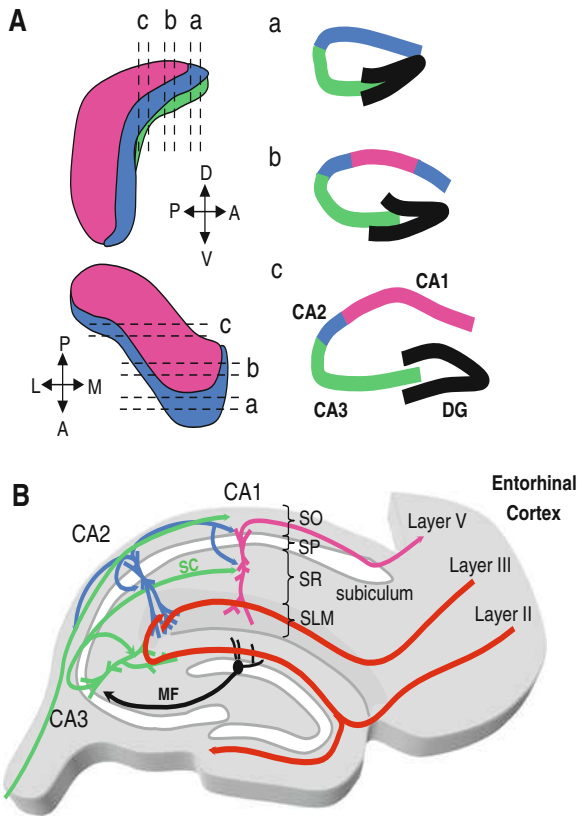

Figure 23: The organization of hippocampal fields and stratum
Adapted from (Piskorowski and Chevaleyre, 2012)

A (Left): Schematic representation of a 3 dimensional view of the hippocampus, showing the CA1-3 fields and the DG. Dashed lines indicate the location of three separate sections along the transverse axis shown on the right. B: Diagram of a transverse section of the hippocampus. The different classes of pyramidal neurons and different hippocampal layers are shown. SC Schaffer collaterals, MF mossy fibers, SO stratum oriens, SP stratum pyramidale, SR stratum radiatum, SLM stratum lacunosum moleculare. A anterior, P posterior, D dorsal, V ventral, M median, L lateral.

The unidirectional progression of the excitatory pathway links each region of the hippocampal formation and forms a trisynaptic circuit in the hippocampus (Figure 24). The trisynaptic circuit starts from the layer II, and layer III to a less extent, of the entorhinal cortex, where neuronal axons transmit the sensory information to the DG and CA3 region through the perforant pathway (EC2 Figure 24) (Steward, 1976). The projection from the entorhinal cortex follows a precise laminar pattern where medial entorhinal cortex axons terminate within the middle portion of the molecular layer of the DG, and those from the lateral entorhinal cortex terminate in the outer third of the molecular layer. These two parts of the perforant pathway also terminate in a similar laminar pattern in the stratum lacunosum-moleculare of CA3 and CA2 (Figure 24). Those axons arising from the medial entorhinal cortex terminate in the stratum lacunosum- moleculare which is close to CA3; while those from the lateral entorhinal cortex end in the portion of the stratum lacunosum-moleculare that is at the border between CA1 and the subiculum (Steward, 1976). Following a similar laminar projection pattern, neurons in layer III of the entorhinal cortex project to CA1 and the subiculum (EC3 pink, Figure 24). These terminate on the distal dendrites of CA1 pyramids. Thus, CA1 neurons are only weakly excited by these inputs. Thus, layer III inputs are greatly attenuated by the dendritic cable and are thought to act as CA1 function modulators (Spruston, 2008).

In the dentate gyrus, the DG cells give rise to mossy fibers (MF) that terminate on the proximal dendrites of CA3 pyramidal cells (Spruston, 2008). The MF also contact mossy cells and interneurons in the hilus. The CA3 pyramidal cells project to CA1 through Schaffer collaterals, and to other levels of the CA3 (Chronister and DeFrance, 1979). CA1 pyramidal cells project to both the subiculum and deep layers of the entorhinal cortex (Figure 24). The deep layers of the entorhinal cortex, in turn, give rise to projections back to many of the same cortical areas that originally projected to the hippocampus (Köhler, 1986). Thus, sensory information

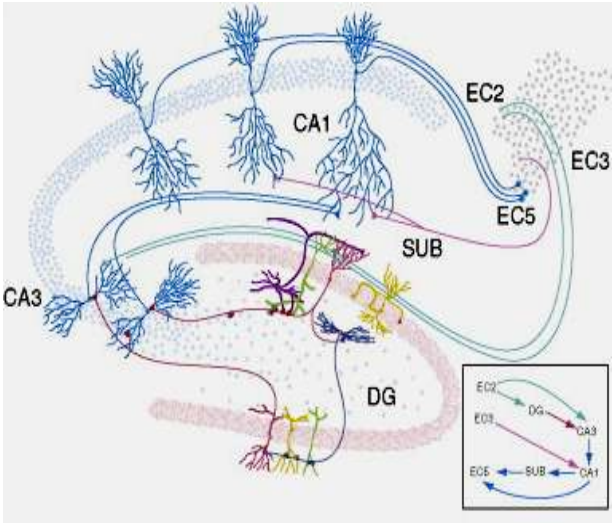

Figure 24: The hippocampal network
Adapted from (Li et al., 2009)

converging on the entorhinal cortex from specific cortical areas proceeds through the hippocampal circuit and then returns back to the cortical region of origin.

A relatively recent report has shed light on the presence of a di-synaptic circuit involving the CA2 region of the hippocampus, a region which has long been obscure and thought to form a minor pathway linking CA3 to CA1 (Figure 25), (Sekino et al., 1997). In this report, researchers have shown that layer II and III entorhinal cortex neurons send strong excitatory inputs to the distal dendrites of CA2 neurons (Figure 25A). These neurons in turn form strong synaptic inputs onto CA1 neurons which drives a strong output and undergoes a robust long-term potentiation (LTP) (Chevaleyre and Siegelbaum, 2010). The existence of two effective pathways from the entorhinal cortex to CA1 (trisynaptic layer II – DG – CA3 – CA1, and disynaptic layer III – CA2 – CA1 pathway) can explain why ablation of either CA3 or layer III input have by themselves only limited effects on hippocampal functions such as contextual learning (Chevaleyre and Siegelbaum, 2010; Piskorowski and Chevaleyre, 2012). Interestingly, this study shows evidence that entorhinal input to the distal dendrites of CA2 has a much stronger effect than CA3 input, which terminates on the proximal dendrites of CA2 neurons; LTP can occur at entorhinal-CA2 but not at CA3-CA2 synapses. Understanding the dendritic structure and the unique mechanisms underlying the differences in the integration and the propagation of input in the di-synaptic circuit is needed if we are to better understand how neuronal activity causes pyramidal cells to fire *in vivo*.

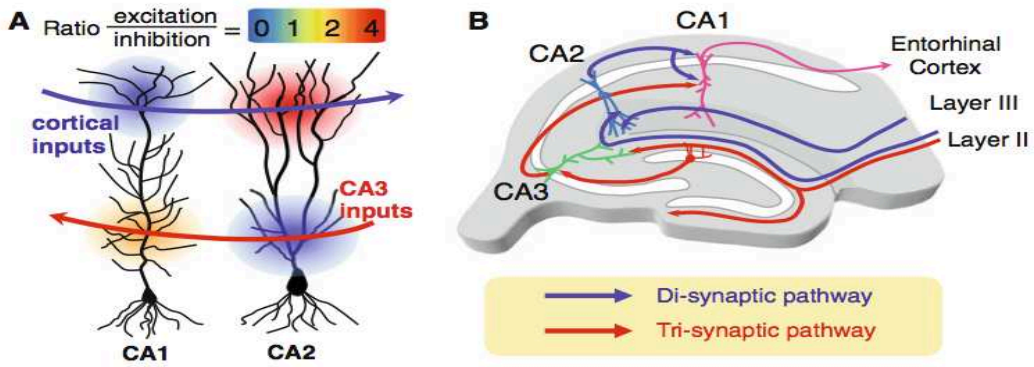

Figure 25: The organization and overall contribution of the di-synaptic and tri-synaptic circuits in the adult hippocampus
Adapted from Piskorowski and Chevaleyre, 2012

In the various hippocampal fields, principal neurons follow common mechanisms controlling their production and differentiation, thus the hippocampus displays a grossly uniform structure with a complex axonal projection pattern. However, combined genomic-neuroanatomic experiments have revealed cellular heterogeneity and very well respected boundaries between and within hippocampal fields (Tole et al., 1997; Tole and Grove, 2001; Lein et al., 2004, 2007; Thompson et al., 2008). Defined maps are established during early developmental stages by molecular markers corresponding to particular cell populations in the hippocampus. Interestingly, these marker boundaries are believed to correlate tightly with specific aspects of the functional complexity in the hippocampus (Thompson et al., 2008).

In the adult, the laminated structure of the hippocampus forming the series of cytoarchitecturally discrete subregions can be distinguished on the basis of neuron morphology, connectivity, and electrophysiological properties and the above-mentioned molecular markers. All fibres originating from a particular afferent source terminate at identical dendritic segments. The pyramid-shaped cells of the hippocampus have become the most intensively studied neurons in the brain. Light has been shed upon the mechanisms controlling the uniform production, relatively short distance migration and differentiation of hippocampal pyramidal cells as well as the inhibitory interneurons and oligodendrocytes that are generated in distant areas in the ventral telencephalon, and migrate long journeys to settle in the hippocampus.

5.1 PATTERNING EVENTS AND FIELD SPECIFICATION IN THE DEVELOPING HIPPOCAMPUS

During telencephalon development, the dorsal midline region invaginates and gives rise to two telencephalic vesicles at embryonic day E10 in the mouse. The medial edge of the invaginating telencephalic vesicles is re-organized into two important structures, the cortical hem and the choroid plexus. The future hippocampus develops in-between these two structures.

Similar to the surrounding telencephalic structures, the cortical hem constitutes a continuous sheet of pseudostratified cortical neuroepithelium that expresses the proneural genes Ngn1 and 2 (Sommer et al., 1996). However, it represents features of

a classical signaling centre that instructs the functional organization of the developing cortex into distinct functional domains, including the hippocampus. Its location at the medial edge of the telencephalon, and its rich expression of regulatory signaling morphogens including Wnt and BMP signaling molecules, highlights its fundamental role in instructing hippocampal development.

5.1.1 Cortical hem boundary specification

Medio-lateral and rostro-caudal boundaries of the developing medial telencephalon are formed by a cross regulation of transcription factors that result in the precise definition of the cortical hem as a unique tissue with distinct cytologic and gene expression boundaries, and its relation to the choroid plexus on one side and to the developing dorsal cortex on the other side (Figure 26, 27).

I: Rostro-caudal boundaries:

Definition of this boundary determines the relationship between the cortical hem and the developing caudal cerebral cortex.

1. Fgfs expressed by the anterior neural ridge (ANR) are fundamental regulators of midline patterning. They activate the midline expressing transcription factor Foxg1 and repress Lhx2 (a cortical maker) thus helping to establish a midline domain within the telencephalon prior to invagination (Figure 26A). Fgfs also repress Wnt genes rostrally whose expression defines the cortical hem (Figure 26A). This cross regulation between two groups of secreted signals helps to define a caudo-medial position for the hem (Shimogori et al., 2004).

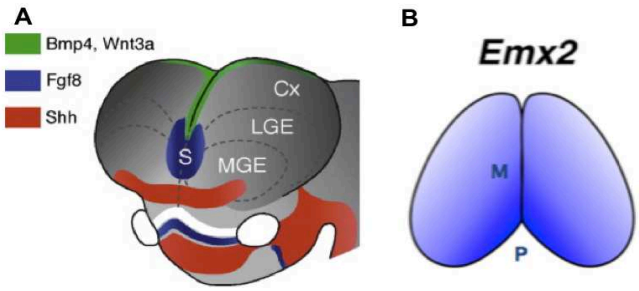

Figure 26: Pattern of expression of TF that will define rostro-caudal bondaries of the cortical hem
Adapted from Pierani and Wassef, 2009 and Hoch et al., 2009.

2. Emx2 expressed highest in progenitors that generate posteriomedial areas of neocortex, and lowest in progenitors that generate the anterolateral areas (Figure 26B), acts at two stages of boundary definition. Early on, it acts by restricting the anterior region of Fgf gene expression, thus helps in refining the caudo-medial domain for the cortical hem as well as the hippocampus. Later, it mediates the effects of hem signaling during further development of this region by acting as an effector of the canonical Wnt signaling from the hem to regulate proliferation within this region (Muzio et al., 2005).

II: Medio-lateral boundaries:

Defining this boundary determines the relationship between the cortical hem and the adjacent choroid plexus, and between the cortical hem and the cortex on the other side. The specification of choroid plexus requires unique Bmp signaling from the roof plate (Figure 26A), which will directly activate the enrichment of Hes genes in the putative choroid plexus (Hébert et al., 2002). At the same time, this region downregulates Ngn gene expression, which continues to be maintained in the adjacent cortical hem. This downregulation of Ngn expression is important in establishing choroid plexus fate and therefore delineating the hem–choroid plexus boundary (Figure 27) (Imayoshi et al., 2008). The specific expression of Wnt3a in the cortical hem as early as E9.5, and of other Wnt molecules including Wnt5a and Wnt2b at the medial edge later on, defines the lateral boundary between the hem and the cerebral cortex.

A Molecular markers of the cortical hem

Specific non-overlapping molecular marker signatures accompany boundary definitions in the developing medial telencephalon. These markers assign distinct identities, for both the cortical hem and the choroid plexus. By E11.5, the homeobox gene Msx1 for example, is strongly expressed in the choroid plexus (Grove et al., 1998). The strong expression of TGF-β family members Bmp4 and 7 confirms further the identity of this structure (Bulchand et al., 2001).

Although the cortical hem weakly expresses Bmp family molecules, expression of Wnt family proteins defines it as a unique structure from the surrounding choroid

plexus and the rest of the cerebral cortex (Figure 27A, C) (Grove et al., 1998). The cortical hem is first identifiable by Wnt3a expression at E9.5 when the telencephalon is a single vesicle. Later on, the specific expression of other Wnt molecules Wnt5a and Wnt2b at the medial edge, defines the hem from the cerebral cortex and its organizer role in instructing hippocampal development (Grove et al., 1998).

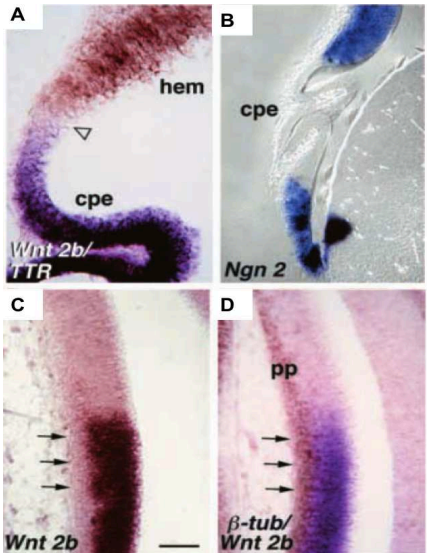

Figure 27: Molecular and morphological features of the hem and the nearby choroid plexus epithelium and cortical neuroepithelium.
Adapted from (Grove et al., 1998)

A: Choroid plexus epithelium (cpe) strongly expresses the marker TTR (purple), the cortical hem is marked by Wnt2b expression (brown).The junctional epithelium between the cpe and hem expresses neither TTR nor Wnt2b. B: Expression of Ngn2 (blue) marks cerebral cortex neuroepithelium, including the hem but avoiding the choroid plexus epithelium. C: Sections through the caudal hem and adjacent embryonic cerebral cortex where Wnt2b is expressed at the ventricular side of the hem, but not in cells close to the pial surface (arrows). D: Wnt2b- negative cells express the neuronal marker, class III-tubulin (brown), and represent a continuation of the developing PP of the embryonic cerebral cortex into the hem.

The extra-toes mutant mouse, which carries an intragenic deletion of the Gli3 gene (Schimmang et al., 1992), does not develop telencephalic choroid plexus, and shows Wnt gene misregulation in the cortical hem (Grove et al., 1998). Gli3 is not expressed in the embryonic choroid plexus epithelium itself (Hui and Joyner, 1993; Grove et al., 1998), but is expressed in embryonic head mesenchyme. It acts downstream of Shh signaling, and regulates expression of Wnt and Bmp genes in the mouse dorsal telencephalon (Grove et al., 1998). Therefore, Gli3 deficiency disrupts inductive interactions between the developing choroid plexus epithelium and the cortical hem, disrupting functional Wnt3a expression at the cortical hem which is required for normal hippocampal development (Grove et al., 1998; Grove and Tole, 1999; Lee et al., 2000).

B Organizer function of the cortical hem

The role for the cortical hem as hippocampal organizer was suggested by experiments showing that the entire hippocampus was missing when the hem was deleted, or when

the hem specific expression of Wnt3a molecules was disrupted (Lee et al., 2000; Yoshida et al., 2006). Definitive evidence of the role of the cortical hem in hippocampal development came from chimeras in which Lhx2 null cells, surrounded by wild-type cortical neuroepithelium, differentiated into ectopic hem tissue. Lhx2 expression is restricted to cortical precursor cells, and is excluded from the cortical hem and adjacent choroid plexus. Lhx2 acts autonomously to specify cortical identity and suppress alternative fates. When Lhx2 is deleted, cells adopt cortical hem identity, which can induce and organize ectopic hippocampal fields. These findings confirm that the cortical hem is a hippocampal organizer (Mangale et al., 2008).

5.1.2 Field pattern specification in developing hippocampus and the role of cortical hem

As discussed earlier in this section, the hippocampus is divided into three major distinct fields, CA1, CA3 and the DG. Each of these is defined depending on distinct morphology, physiological properties and connectivity. Specific molecular markers also indicate the divisions between the hippocampal fields. The two classes of CA1 and CA3 pyramidal neurons mingle in the small transitional field, CA2. Thus, morphologically, the transition from CA1 to CA3 is marked by a simple shift from one major pyramidal cell type to another. However, as mentioned above, the function of CA2 is quite specific.

A panel of CA1, CA2, and CA3 pyramidal cell markers has been identified as differentially expressed in the hippocampus (Tole et al., 1997; Tole and Grove, 2001; Datson et al., 2004, 2009; Lein et al., 2004, 2007; Newrzella et al., 2007; Thompson et al., 2008; Dong et al., 2009; Fanselow and Dong, 2010; Kjonigsen et al., 2011). Such markers distinguish between the cell classes and subclasses and label all, or almost all, cells in a category. Two robust field-specific markers were originally identified to label CA3 and CA1 cells. KA1, a glutamate receptor subunit, and SCIP, a POU-domain gene, are expressed in the pyramidal neurons of CA3 and CA1 respectively (He et al., 1989; Tole et al., 1997) (Figure 28). *In situ* hybridization experiments have shown that these two markers show consistent patterns of expression from the embryo to the adult. They are expressed in postmitotic migrating neurons in the hippocampal IZ and in already settled cells, with exclusion of

expression from the VZ. KA1 expression is weakly detectable in CA3 at E14.5, but becomes very strong one day later. SCIP starts to be expressed at E15.5 in CA1 in the mouse. Marker expression starts at the poles (dentate and subicular zones) and fuses only at birth in the CA2 region, giving these two markers the unique pole-inward patterns of expression (Tole et al., 1997).

Although field specific markers as well as field morphological properties are not obvious in the developing hippocampus before E14.5 in the CA3 region, and E15.5 in the CA1 region. However, elegant medial telencephalon explant experiments with explants harvested at E12.5, when none of the field markers are yet expressed, have shown that hippocampal explants upregulate autonomously the expression of field-specific markers in culture, when analysed three days later. Thus, the initial specification of hippocampal fields begins at least as early as E12.5 and does not require the surrounding environment (Tole and Grove, 2001). Cell lineage analyses have excluded that precursor populations of hippocampal progenitors are permanently specified, or committed, to produce neurons for a single field. Rather, interactions between hippocampal cells and the surrounding environment is the main factor that determines final field identity development in the hippocampus (Bulchand et al., 2001).

The cortical hem seems to play a pivotal role in field development; in mice deficient for Wnt3a, a Wnt gene expressed selectively at the cortical hem, the hippocampus is largely absent and represented only by minor, residual cell populations. Analysis of Wnt3a-mutant mice at E15.5 or E18.5, revealed few KA1-expressing CA3 cells (Tole and Grove, 2001). Nonetheless, E12.5 (3 DIV) explants from which the cortical hem was eliminated already contain substantial populations of both SCIP and KA1-expressing cells in the correct topographic position. These observations suggest that Wnt3a is most critical to the developing CA fields before E12, when the cortical hem plays its instructive role by expressing signals required for hippocampal field specification and amplification (Lee et al., 2000; Tole and Grove, 2001).

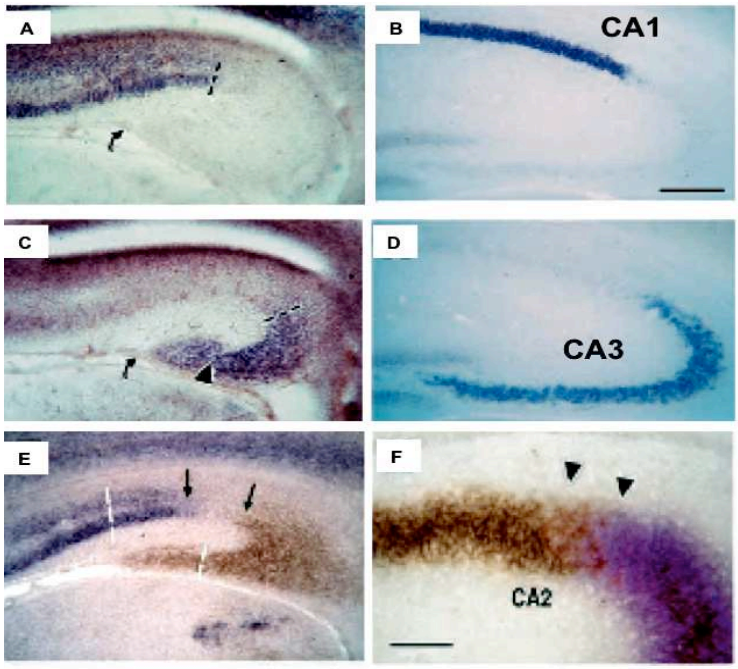

Figure 28: Embryonic and mature hippocampal pyramidal cells are identified by the expression of field specific markers.

Adapted from (Tole et al., 1997)

SCIP, a CA1 specific marker is expressed in the embryonic hippocampus as early as E15.5 (A), and persists into adulthood (B). KA1, a CA3 specific marker is expressed in the embryonic CA3 region (C), and persists into the adult life (D). Marker expression starts at the poles and fuses only at birth in the CA2 region (E, F)

5.1.3 Field sub divisions and the complex genomic and functional anatomy of the hippocampus

Besides the molecular signatures just described that classically define hippocampal fields, a more refined intra-hippocampal field boundary definition has more recently been described. This identification was made possible by the use of high throughput *in situ* hybridization techniques combined with more traditional manual anatomical boundary mapping (Lein et al., 2007). This approach helped to assess the molecular and cellular architecture of the hippocampus, and to generate a molecularly defined anatomical map that can be correlated with the differential functional domains throughout the hippocampus.

Strong evidence of anatomical and functional differentiation along the long hippocampal septotemporal axis exists. The perforant path is divided into several input bands projecting from the entorhinal cortex to different septotemporal levels of the DG (van Groen et al., 2003). Amygdalar afferents selectively target temporal portions of CA3, CA1 and subiculum (Petrovich et al., 2001). Septal hippocampal lesions result in selective impairment in spatial memory tasks, whereas temporal lesions result in different impairments (Bannerman et al., 2002). In models of hippocampal pathology, slices through temporal hippocampus exhibit greater

epileptiform bursting in high potassium. In contrast, septal CA1 shows selective vulnerability to ischemic insults (Thompson et al., 2008). In the kainate mouse model of mesial temporal lobe epilepsy, status epilepticus and recurrent epileptiform activity was stronger in temporal hippocampus, and this septotemporal pattern is tightly correlated with the spatial pattern of cell proliferation and neurogenesis, both being substantially increased in the temporal hippocampus (Häussler et al., 2012).

The functional organization along the septotemporal axis in the hippocampus is evident early on, in the developing perinatal brain. Giant depolarizing potentials (GDPs), endogenous spontaneous GABA- mediated oscillatory events in the immature brain, are initiated at a higher rate in septal hippocampus and propagate to temporal parts. GDPs give rise to neuronal synchronized firing and calcium oscillations, which are crucial events for synapse development and maturation of developing neuronal circuits (Häussler et al., 2012). Given the fact that GABAergic transmission is the major driving force of GDPs, the septotemporal gradient of GDP activity could be related directly to the differential maturation of interneurons in the septal and temporal fields of the developing hippocampus, which most likely play a role in this gradient (Ben-Ari et al., 1989; Buzsáki et al., 1990)

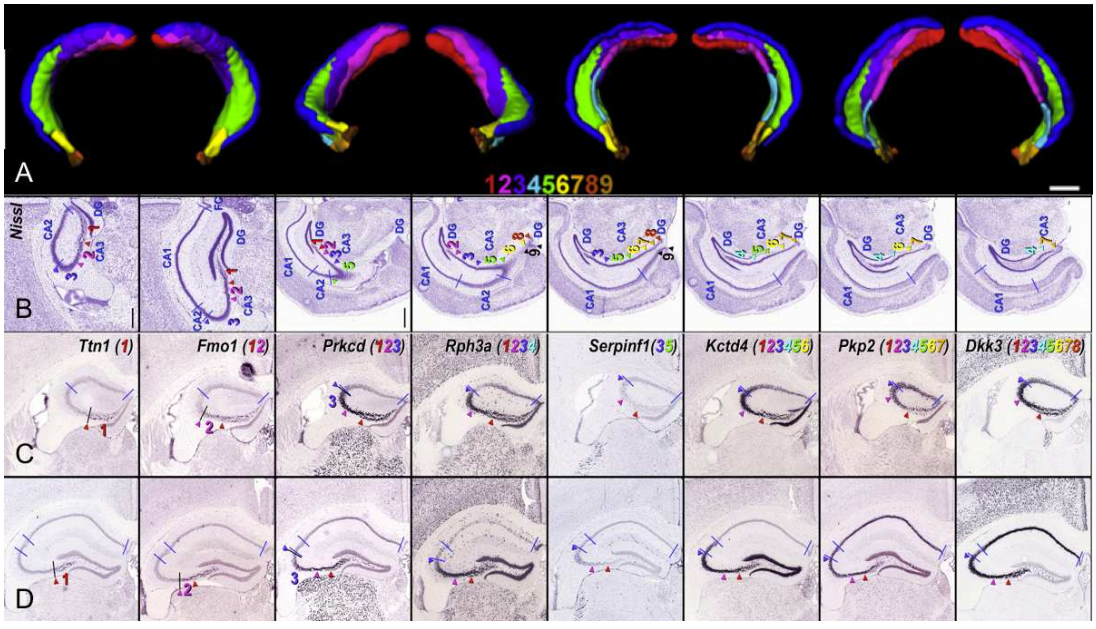

Figure 29: Representation of three-dimensional molecular signatures along the septotemporal axis of the hippocampal CA3 region.
Adapted from (Thompson et al. 2008)

A: Four different orientations demonstrate the organization of CA3 subdivisions, which can be seen to divide septal CA3 into a series of diagonal bands oriented septal-distal (toward CA2, dark blue) to

temporal-proximal (toward DG) and represented in coronal sections of Nissl stained sections (B). C and D: Example of genes (*in situ* hybridization) expressed in the nine molecular septotemporal domains of the CA3 pyramidal cell layer, displayed in one section from rostral (C) to more caudal (D).

In accordance with this morphological and functional organization, mutually exclusive molecular signatures delineate the hippocampal septotemporal axes (Thompson et al., 2008). The CA3 region represents an interesting example, where individual gene expression patterns are observed along septotemporal, proximal/distal, and radial dimensions. For example, the septal two-thirds of CA3 is clearly divided into a series of diagonal bands oriented into septal-distal (toward CA2) to temporal-proximal domains (toward the DG; Figure 29). This banding is highly reminiscent of the organization of recurrent associational projections (Thompson et al., 2008). Interestingly, these nonoverlapping septotemporal domains are detectable at postnatal day P14, and are stable across later adult stages. Suggesting a preserved intrinsic functional properties for each of these domains.

Gene expression specificities along the radial unit axis in the hippocampal CA3 region have also been described (Thompson et al., 2008; Slomianka et al., 2011). A single-cell- thick band of neurons along the border of the pyramidal cell layer and *stratum oriens* strongly expresses a small set of genes including the procollagen gene *Col6a*1 and suppressor of tumorigenicity 18 (Figure 30) (Thompson et al., 2008). Also a recent report described a transgenic 'sparse' Thy1 mouse line (Lsi1 line), where a high-level membrane GFP (mGFP) transgene is expressed in a small subset of neuronal cells within CA3, CA1 and DG. Global gene expression experiments show that these neuronal populations represent homogenous groups of cells in each of the above-mentioned fields. Study of CA3 GFP positive cells shows that Col6a1 and St18 are highly enriched in this specific Lsi1 cell population (Figure 30). Bromodeoxyuridine (BrdU) birth dating experiments show that adult Lsi1 GFP positive neurons are born at a specific time point and represent the earliest born hippocampal neurons. These cells have a matched pattern of synaptogenesis and maturity status between the DG, CA3 and CA1 neurons produced at the same time

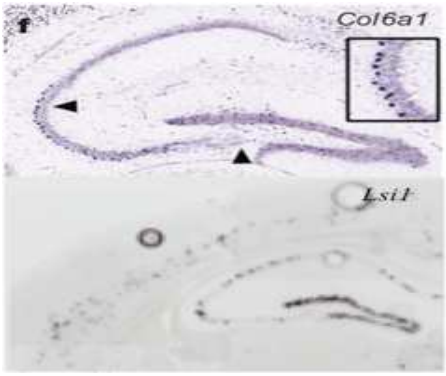

Figure 30: Molecular markers along outer boundary of the radial unit of hippocampla CA3 field.
Adapted from Thompson et al., 2008, Deguchi et al., 2011

point, and show selective connectivity patterns during the development of the trisynaptic circuit. Altogether, this data suggest that neuronal subpopulations which are committed to a specific developmental program, including a specific birthdate, migration, synaptogenesis, maturation and connectivity, share specific field and layer-specific molecular markers which are tightly linked to adult function (Deguchi et al., 2011).

5.2 CELL HETEROGENEITY AND THE DEVELOPMENT OF NEURONAL TYPE DIVERSITY IN THE ADULT HIPPOCAMPUS

Similar to other parts of the brain, several cell types of different lineage and sites of origin reside in the adult hippocampus. These cells are comparable with other cell types that reside in the cerebral cortex and include glutamatergic pyramidal cells, dentate granular cells, GABAergic groups of interneurons, glial cells and oligodendrocytes.

5.2.1 Hippocampal projection neurons

A Histology

As already mentioned, hippocampal projection neurons show a wide range of diversity depending on the field that they are located in, the radial distribution in each field, molecular markers, neurochemical properties and connectivity patterns. Added to the molecular signatures that specify pyramidal cells in each of the hippocampal fields, non-synchronous spatio-temporal hippocampal pyramidal cell morphogenesis processes occur; by which cells differentiate from simple bipolar to complex shapes characteristic of the adult pattern of different hippocampal fields. Cells in the CA4 field undergo morphological differentiation at earlier stages, prenatally, compared to CA3 cells, and these in turn earlier than CA1 cells. Furthermore, core morphological differences between mature adult CA1 and CA3 pyramidal cells exist (López-Gallardo and Prada, 2001).

1. Pyramidal cells in CA1 have one main dendrite arising from the apical pole of the cell body which branches profusely in the *stratum lacunosum-moleculare* and several short side branches leaving from the stem dendrite on its course through the *stratum radiatum*, whereas the apical dendrite of CA3 cells branches more proximally, in some cases immediately after emerging from the cell body.
2. Mature pyramidal cell bodies are larger in CA3 than in CA1.
3. The presence of postsynaptic structures 'thorny excrescences' exist on the proximal dendrites of CA3 pyramidal cells, but not on CA1 pyramids.
4. Basal dendrites of CA3 cells are more extensive than those of CA1 cells.

Additionally, two main types of pyramidal cells are described along the radial axis of the hippocampus, deep (closer to *stratum oriens*) and superficial (closer to *stratum radiatum*) ones (Slomianka et al., 2011). The superficial pyramids are arranged in one or two very dense rows. The deep pyramids are grouped into several less dense rows below. The deep pyramids are less numerous in lower mammals (mouse, rabbit, dog, cat) than in primates (monkey, man). In mouse and rat CA1 region for example, the deep pyramids can be seen clearly at the distal and temporal parts of CA1, as a sublayer of loosely arranged cells. It is interesting to note that this superficial to deep division along the radial axis has important consequences on the connectivity pattern between pyramidal cells and interneurons such as basket cells (Slomianka et al., 2011).

B Neurogenesis and neuronal migration of projection neurons in the developing hippocampus

Traditionally, developmental processes such as neurogenesis, patterns of migration and connectivity development have been studied in a descriptive manner by monitoring the formation of mature structures from simpler, undifferentiated stages. Molecular and genetic techniques have supported previous results and helped in a more exact description of the developmental processes involved in the formation of different brain regions including the hippocampus. Nevertheless, these techniques have also opened up important but not yet answered questions. The data resumed here has mainly been accumulated in the mouse embryo, although similar processes are observed in the rat and in primates.

Similar to the cerebral cortex, the hippocampus represents a nicely laminated structure, with an inside-out layering pattern and deep to superficial molecular and connectivity specificities. This pattern is induced and established early on during development, so newly born neurons carry an intrinsic character that establishes their adult phenotype.

Neurogenesis in the hippocampus occurs over a long period of time starting at embryonic day E10 in mice, and extends well beyond birth. The pyramidal neurons in CA1-CA3 are generated by an extensive area of neuroepithelium and migrate radially to the Ammon's horn, while dentate granule cells are generated by a narrow area of neuroepithelium adjacent to the fimbria called the dentate neuroepithelium (primary dentate matrix) and migrate tangentially through the subpial area to form the C-shaped cortical structure (Figure 31). The neurons in each field of the hippocampus arise in overlapping, but still significantly different waves, gradients, and peaks (Bayer, 1980a, 1980b, Pleasure et al., 2000).

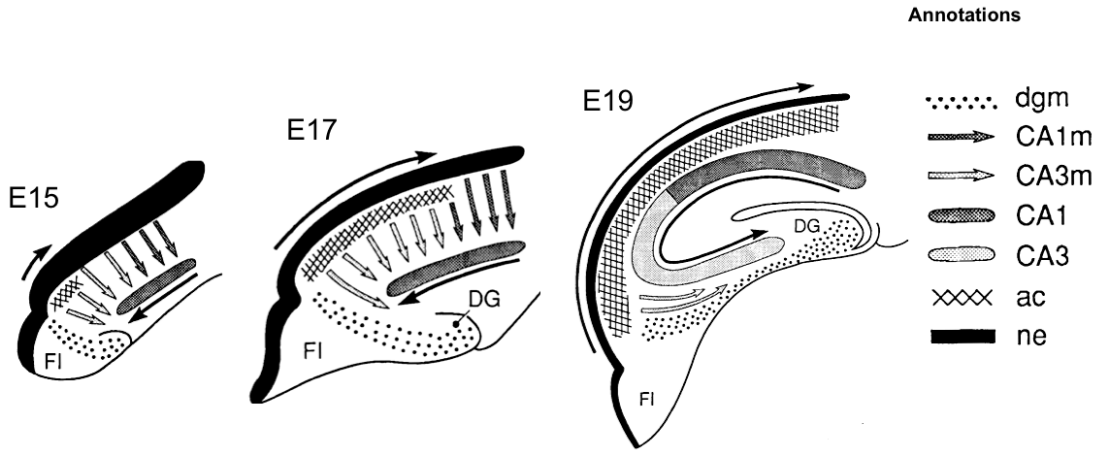

Figure 31: Summary diagram of waves of neurogenesis and migration of pyramidal cells in the hippocampus.
Adapted from Altman and Bayer, 1990c

DG: gentate gyrus, FI:Fimbria, dgm: dentate gyrus migratory cells, CA1m: CA1 migratory cells,CA3m: CA3 migratory cells, ac: alveolar channels, ne: neuroepithelium.

The time of origin and gradients of neurons along the length of pyramidal cell layer are considerable. The earliest cells born at E10 are found to reside in the deep layers of CA1 and CA2 fields. At this time point, no CA3 cells are generated (Angevine, 1965, Stanfield and Cowan, 1979). The generation of CA3 cells starts one day later, at E11, and these neurons will reside in deepest hippocampal layers. Neurogenesis continues in the hippocampus thereafter, and at E14, the generation of CA3 neurons

reaches its peak (Angevine, 1965). Although CA1 neurogenesis starts one day earlier compared to CA3, it peaks one day later, at E15 (Stanfield and Cowan, 1979; Bayer, 1980a). Neurogenesis in the dentate gyrus will extend over a longer period of time during hippocampal development. Starting early on, at E10, it peaks at E16, and continues until the first postnatal week (Bayer, 1980a, 1980b).

C Sojourn of newly born cells in the developing hippocampus

In the developing cortex, newly generated neuroblasts sojourn in the IZ before they continue their migratory stream. Upon detachment of cells from the VZ they display a multipolar morphology with fine processes (Tabata and Nakajima, 2003b). This applies to cells in the hippocampus as well as the cortex, however, the time of sojourn varies greatly between cortical and hippocampal pyramidal cells and even between hippocampal cells in different fields. While cortical pyramidal cells sojourn for one day, before they continue their glia guided migration, neurons in the developing hippocampus sojourn for longer periods. CA1 cells sojourn 2-3 days before continuing their glia-guided migration. CA3 cells pause for an even longer time, 4 days, before they continue their migration. Different hypotheses have been suggested to explain this sojourn of pyramidal cells in general, and this longer sojourn of pyramidal cells in the hippocampus in particular (Altman and Bayer, 1990c).

It has been suggested in the past that the temporary pause of young neocortical neurons outside the neuroepithelium may be associated with the outgrowth of their axons prior to settling in the CP (Altman and Bayer, 1990b, 1990c). Also some of the horizontally oriented cells in the cortical IZ migrate laterally to reach cortical areas where there is no neuroepithelium underneath the CP (Altman and Bayer, 1990c).

In the hippocampus, the different dynamic properties of sojourning neurons have multiple explanations. For obvious reasons, neither the distance nor the complexity of the migratory fields can be a factor because it is the cortical IZ that has the more elaborate organization compared to the hippocampal IZ. In contrast, the longer sojourn in the hippocampus could be related to the necessity of coordinating between the diversity of cellular types, including granule cells and pyramidal cells that are located in different layers within the same structure. Added to that, combined

complex morphogenic events should assure correct and synchronous CA fields and DG assembly; pyramidal cells destined to settle in the CA3 region, should be contacted by granule cells axons (the mossy fibers), and have to wait for the later formation of the granular layer on days E17-E18 (Altman and Bayer, 1990c). Interneurons (residing in the hippocampus are derived from distant ventral parts of the developing telencephalon, and will need longer migration times to reach the hippocampus, when compared to interneurons in the developing cortex (Tricoire et al., 2011). Tangentially migrating interneurons must encounter and assemble with radially migrating cells, in order to form the proper spatio-temporal sequence of migration gradients. Therefore, the migration of pyramidal neurons and GABAergic interneurons is cross-regulated: glutamate released from projection neuroblasts will facilitate interneuron migration, whereas the release of GABA from interneurons facilitates the migration of glutamatergic neuroblasts (Manent et al., 2005). This sequence of events could justify the prolonged sojourn of hippocampal neuroblasts in the SVZ. Afferent and efferent fibres in the cortex have an unconstrained path of distribution through the white matter situated underneath the entire expanse of the cortical gray matter. In the hippocampus the bulk of the fibres (specifically the efferents) are funneled through a narrow bottleneck region where the fimbria is located. Thus fundamental differences in the anatomical organization of the two systems could be the reason behind this long sojourn (Angevine and Sidman, 1961).

D Migration of neuroblasts in the developing hippocampus:

In the developing hippocampus, pyramidal cells follow the same two modes of migration as those in the neocortex; glia guided migration and somal translocation. Radial glial cells, which play an essential role in guiding neuronal migration, extend long vertical processes from the hippocampal VZ to the pial surface. Glial fibers persist until P9, at which age they disappear from the Ammon's horn (Altman and Bayer, 1990b). Both the nucleus and the cytoplasm of migrating cells are relatively electron-dense and the latter contains organelles typical of young neurons as described in other brain regions (Nowakowski and Rakic, 1979).

A Golgi and electron microscopic analysis in foetal rhesus monkey shed light on the similarities between cortical and hippocampal neuroblast migration. However, some differences do exist, which are mostly related to the anatomic localization as well as to the complex connectivity pattern in the hippocampus when compared to the developing cerebral cortex. The use of foetal rhesus monkey brains to study hippocampal neuronal migration allowed the study of different phases of neuronal migration, a task that can be difficult in rodents due to the short distance between the VZ and *stratum pyramidale*. In foetal rhesus monkey, the IZ is divided into an inner deeper and an outer more superficial zone. The authors found that neurons migrating along radial glial processes in the inner part of the IZ are radially oriented (Figure 32, panel A, C1, see the leading process of these cells opposed to the radial glial fiber F). The authors also found that their apical leading processes, usually one per cell, end in the form of a bulb-shaped growing tip. These migrating cells also have one thinner trailing process, which is not attached to the ventricular surface. In addition, the migrating young neurons have several thin short processes emanating horizontally from their cell bodies. This pattern hence describes what is now accepted to be the characteristics of radially migrating neurons (Nowakowski and Rakic, 1979; Nakahira and Yuasa, 2005) (Figure 32 ,panel A and A' C1).

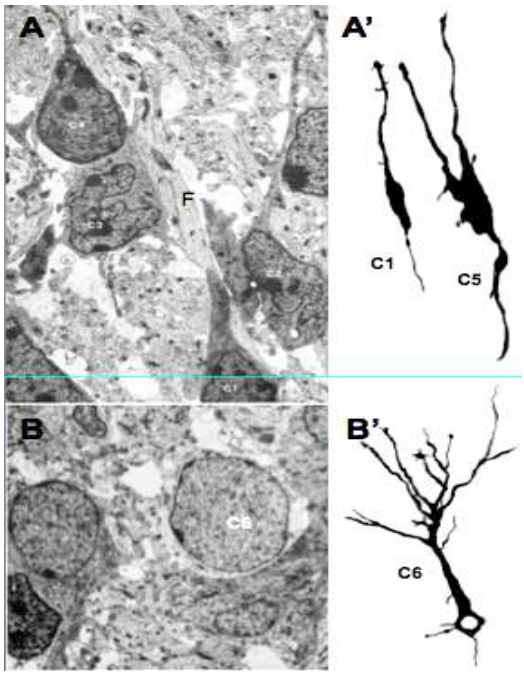

Figure 32: Structural and morphologic characteristics of migrating neurons at different stages.
Adapted from (Nowakowski and Rakic, 1979)

Ultrastructural and morphologic appearnce of migrating pyramidal cells in lower (A, A') and upper intermediate zone (B, B').

In this same study the authors found that in the outer portion of the IZ, the radial alignment of migrating neurons is less pronounced. After reaching this level, the migrating cells usually develop one or two thick, horizontally oriented processes (Figure 32, panel A' C5), and often the nucleus becomes eccentrically located in the perikaryon. The migrating cells whose nuclei reside in the upper IZ generally have at

least one long process extending into the CP. This morphologic change is correlated with the last step in neuronal migration, when the cell translocates its soma to reach its final destination.

The ultrastructural appearance of the migrating hippocampal neurons is similar to that described for migrating cells in other brain regions. The nucleus is usually ovoid in shape, occasionally lobulated, and has moderately-dispersed chromatin and electron-dense karyoplasm (Figure 32, panel A). The cytoplasm of these cells has an electron-dense matrix characteristic of immature neurons; it contains mitochondria, ribosomes, rough and smooth endoplasmic reticulum and the Golgi apparatus. The leading process usually contains a higher concentration of mitochondria and a prominent Golgi apparatus. The migrating cell is apposed along its entire length to a MT-filled glial fibre or to a fascicle of such fibres. The less obvious apposition of the young neurons to the radial fibres in the outermost part of the IZ (Figure 32, panel B), could be due to dissociation of the young neurons from the guiding fibres, to allow them to translocate their soma and settle in their final destination. At this stage, cells in this position are slightly less electron-dense than radially-opposed migrating ones. This difference in electron density between is a reflection of the progress of en route maturation of migrating hippocampal neurons (Figure 32, panel B) (Nowakowski and Rakic, 1979).

Neuronal migration in the CA fields:

As mentioned earlier, after neurogenesis, cells exhibit a long sojourn (up to 5 days after generation) where they show multipolar morphology, and are independent of radial glial fibers. By P2, most of the sojourning cells will have arrived at their final destination in the pyramidal cell layer. Although cells follow a classical inside-out migration and lamination pattern in the hippocampus, in the CA3 region, they adopt a more complex pattern due to the extended curved route of migration from their ventricular germinal zone to the developing extraventricular part of CA3 (Stanfield and Cowan, 1979; Sheldon et al., 1997), and the proximal (early) to distal (late) patterns of CA3 pyramidal generation.

Neuronal migration in the CA1 region is a glia guided migration with sojourning pyramidal cells in the IZ longer than the cortex, but less than the CA3 region. The lamination of the CA1 region is a typical inside-out lamination pattern with earliest

born neurons in most deep layers, and later born neurons residing in more superficial layers.

As described earlier, Lsi1 and Lsi2 transgenic mouse lines (*Thy1-mGFP*^{Si1} and *Thy1-mGFP*^{Si2}) express membrane-targeted GFP (mGFP) in small neuronal subsets that correspond to distinct but partially overlapping neuronal subpopulations that emerge during early hippocampal neurogenesis (Deguchi et al., 2011). Lsi1 neurons represent the earliest principal neurons in the hippocampus born before E11.5, Lsi2 neurons are born one day later, around E12.5. This fine difference in the birth dates corresponds to subtle temporal distinctions pronounced during hippocampal circuit assembly, since Lsi1 neurons mature and establish synapses ahead of Lsi2 neurons, and both precede the synaptogenesis of most other principal neurons. This example provides evidence that commitment to Lsi1 and Lsi2 subpopulation fates occurs early during hippocampal neurogenesis, and that at least early hippocampal neurogenesis proceeds according to non-random spatial patterns, that correspond to well defined developmental programs (Deguchi et al., 2011).

E En route differentiation

One major difference exists between migrating cortical and hippocampal neuroblasts. Migrating hippocampal neurons situated at progressively more superficial levels of the IZ become progressively more differentiated and complex. The young neurons in the outer portion of the IZ exhibit some of the characteristics of mature pyramidal neurons. In particular, they have a single, relatively thick, elongated apical process that extends up from the perikaryon before branching into several processes (Figure 32, panel B') (Nowakowski and Rakic, 1979). Electron microscopic examination of cells situated at various depths in the IZ reveals that cells in the outer IZ are slightly less electron-dense than those situated in the inner portion of the IZ (Figure 32, panel B). At still more superficial levels just below the ammonic plate, the migrating cells are only slightly more electron-dense than those neurons already situated in the ammonic plate. They acquire several additional cytoplasmic processes and occasionally a long thin axon-like process which courses into the incipient alveus. These cells have somewhat larger somata and less electron-dense nuclei and

cytoplasm than the migrating neurons still situated in the inner part of the IZ. These morphological and ultrastructural differences between the migrating cells in the inner versus outer portions of the IZ is a reflection of the progress of their maturation while en route (Nowakowski and Rakic, 1979).

Because the hippocampus comprises multiple cell types, each of which has its particular developmental, morphological and physiological profile, molecular access to individual cell groups in their native environment is required to specifically decipher the developmental and molecular mechanisms in each of these types. The development of the *in utero* electroporation technique (IUE), in which a series of voltage pulses are used to transfect target pyramidal neurons via their neural precursors with plasmid DNA at a specific embryonic time point has been useful in this respect (Figure 33). Embryonic targeting of pyramidal neuronal precursors using this technique results in persistent expression of the transgene from early developmental time points up to adulthood (Nakahira and Yuasa, 2005; Navarro-Quiroga et al., 2007). The work by Nakahira and Yuasa, and by Navarro-Quiroga have hence confirmed and refined the earlier seminal works of the authors cited in this section.

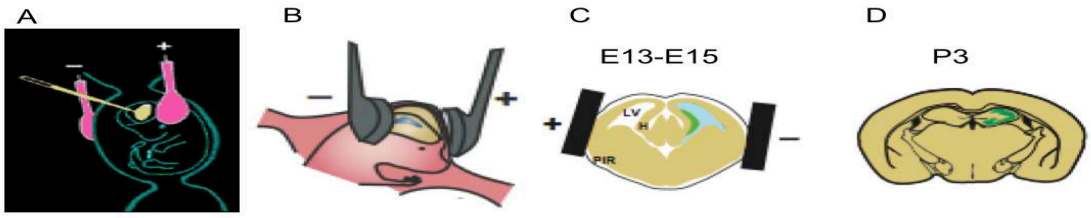

Figure 33: Hippocampus-specific gene targeting by in utero electroporation.
Adapted from (Taniguchi et al., 2012)

A: Injection of DNA solution into lateral ventricle, B and C: The *ammonic* neuroepithelium is targeted via dorsal lateral placement of the electrodes. D: targeted cells can be studies at a later stage.

Migration of dentate gyrus cells:

Dentate gyrus cells are generated in the ventricular zone, adjacent to the fimbria (Altman and Bayer, 1990a, 1990b; Pleasure et al., 2000). Newly generated DG cells exit the VZ to the primary dentate matrix, where they display a multipolar morphology, and migrate in a glia independent matter (Nakahira and Yuasa, 2005). After they exit the primary dentate matrix and enter the subpial space, migratory dentate granule cells form a compact stream of migrating cells; they follow the

tangentially oriented RG fibers, and migrate in a glia dependent fashion. (Nakahira and Yuasa, 2005). Early stages of migration from the primary dentate matrix consist of a mixture of postmitotic neurons destined to differentiate into granule cells and precursor cells that form the primary dentate granule cell layer and continue to divide to produce new granule cells in situ in the dentate gyrus (Altman and Bayer, 1990a, 1990b; Pleasure et al., 2000). Upon arrival at the secondary dentate matrix, Migrating cells will proliferate and produce large numbers of granule cells through the first month of postnatal life before settling in the SGZ and gradually reducing their output of new granule cells to a lower basal rate through adulthood. Stratification take place for the DG cells 5-6 days later, at P1-2 (Nakahira and Yuasa, 2005).
Mutations in the genes involved in the Reelin signaling pathway (Stanfield and Cowan, 1979; Sheldon et al., 1997; Trommsdorff et al., 1999) induce the malformation of the unipolar astrocytes and disarrangement of granule cells in the dentate gyrus (Frotscher et al., 2003). However, subpial migration is not very severely impaired, because it follows glial fibers but may be partially dependent on glial guidance.

5.2.2 Hippocampal interneurons

Like their cortical counterparts, hippocampal interneurons are characterized by the synthesis and release of the neurotransmitter GABA. They are classified into several subgroups according to their axonal projection pattern, neurochemical content and physiological properties. Axonal projection pattern correlates with the modulatory effect of these cells on excitatory hippocampal cells and other interneurons. For example, basket cells make synapses specifically with the cell bodies and proximal dendrites of pyramidal cells, while chandelier or axo-axonic cells contact the axon initial segment of principal neurons. These specific contact sites are ideally located to control the genesis of action potentials (Miles et al., 1996). The *oriens-lacunosum-moleculare* cells, are located in the *stratum oriens* but contact the distal most part of the apical dendrites of pyramidal neurons in the *stratum lacunosum-moleculare*. Thus, these cells may specifically control dendritic calcium spikes (Miles et al., 1996) and have an important role in controlling excitatory inputs from the entorhinal cortex,

which also terminate specifically on the distal- most part of the apical dendrites of pyramidal neurons (Figure 34).

Specific projection patterns are correlated to some extent with the neurochemical markers expressed by certain groups of interneurons (Freund and Buzsaki, 1996; Fig. 2). Chandelier cells express the calcium-binding protein parvalbumin (Kosaka et al., 1987). The calcium-binding protein calbindin or the neuronal nitric oxide synthase enzyme is expressed by interneurons contacting the dendritic shafts of pyramidal neurons (Gulyás and Freund, 1996; Seress et al., 2005). Besides its particular somatic localization and axonal projection, the *oriens-lacunosum- molecular* cell is also characterized by the expression of the neuropeptide somatostatin (Freund and Buzsáki, 1996; Jaglin et al., 2012). However, the expression of a particular neurochemical marker or physiological property may not be sufficient to allocate an interneuron to a particular subgroup. Additionally, interneurons exhibit further diversity based on their firing patterns and response to modulating transmitters (Parra et al., 1998). Thus classification schemes based on individual criterion do not correlate with each other in a simple way, and different categories of properties appear at times to vary independently, leading to a possible conclusion that an unlimited number of potential GABAergic subtypes exist.

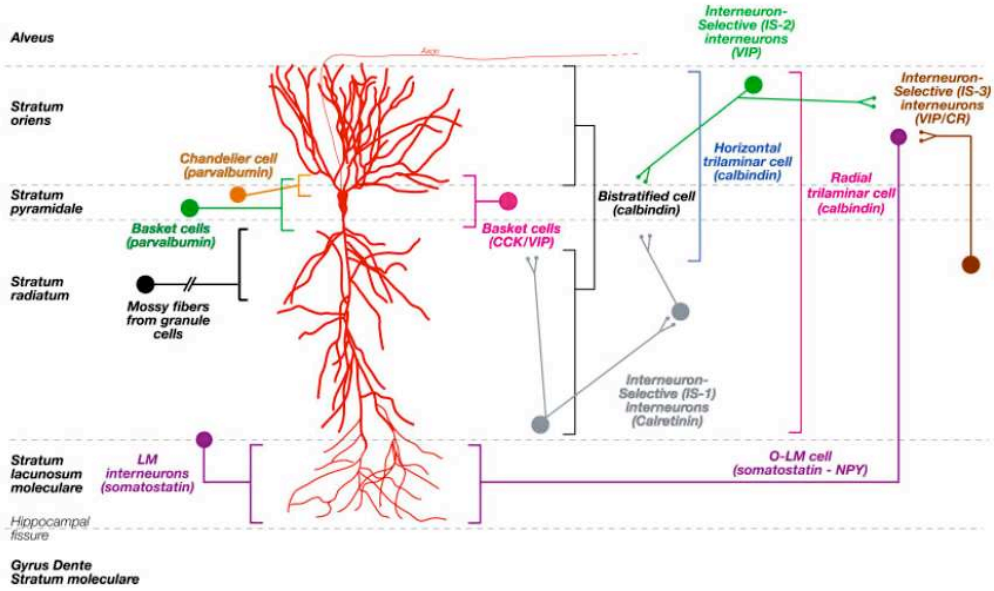

Figure 34: Hippocampal interneurons can be classified by their calcium-binding protein content, and by their synapse sites on hippocampal pyramidal cells.

Adapted from(Danglot et al., 2006)

A Developmental processes culminating in the generation and migration of hippocampal interneurons

Given the wide variety of cortical and hippocampal interneurons, early developmental processes will have important impact on defining the ultimate identity of an interneuron within a given cortical circuit. This will be influenced by both birth location and date (Butt et al., 2005; Miyoshi et al., 2007; Miyoshi and Fishell, 2011). An interneuron born at a specific time point and place is expected to recognize specific membrane molecules and target pyramidal neurons to establish specific inhibitory connections. Although much remains to be elucidated concerning these processes, altogether, these observations confirm the importance of early developmental processes in establishing the inhibitory network in the developing hippocampus.

All hippocampal interneurons originate in the medial and the caudal ganglionic eminences, MGE and CGE respectively. The same specification and neuronal induction signals that govern cortical interneuron development govern hippocampal interneurons as well. Hippocampal interneurons are produced in two neurogenic waves between E9–12 and E12–16 from MGE and CGE respectively. They follow similar routes of migration from their site of genesis to the hippocampus, migrating through both the MZ and the IZ/SVZ streams to invade the hippocampus by E14. As mentioned, interneurons migrating to the hippocampus will take a longer migration time when compared to those migrating to the cerebral cortex, 48-72 hours instead of 24-48 hours, respectively (Tricoire et al., 2011). Similar to the developing cortex, later born interneurons will migrate at a higher speed when compared to early born ones, probably indicating a shift in the balance between attractive and repulsive guidance cues within the MZ and IZ/SVZ migratory paths (Marín et al., 2010). Migrating interneurons to the hippocampus migrate mainly along the MZ path, contrary to cortical interneurons which migrate mainly along the IZ/SVZ path (Manent et al., 2006). The first interneurons enter the hippocampus on or slightly after E14 with peak invasion occurring between E15 and E18. Interneurons reach the hippocampus first through a MZ migratory path and later through both MZ and

IZ/SVZ migratory paths (Manent et al., 2006). They invade first the subiculum and the CA1 fields, and reach the CA3 field no earlier than E16, and the DG primordium one day later, at E17 (Manent et al., 2006). CGE- derived interneurons are added with a minor temporal delay when compared to MGE-derived interneurons (Rubin et al., 2010; Tricoire et al., 2011).

Upon arrival at the hippocampus, MGE and CGE- derived interneurons populate all strata with a majority of the migrating interneurons following the MZ stream into *stratum lacunosum moleculare*. In the mature hippocampus CGE-derived interneurons primarily localize to superficial regions in *strata lacunosum moleculare* and deep *radiatum* while MGE-derived interneurons readily populate all regions with preference for *strata pyramidale* and *oriens* (Tricoire et al., 2011). At later postnatal stages, a reduction in interneuron density is noticed in the hippocampus, this could be due to a dilution effect in the expanding brain volume, combined with neuronal death between P4 and P8 (Verney et al., 2000).

Recent combined molecular, anatomical, and electrophysiological studies have shown that the MGE produces parvalbumin-, somatostatin-, and nitric oxide synthase-expressing interneurons including fast-spiking basket, bistratified, axo-axonic, oriens-lacunosum moleculare, neurogliaform, and ivy cells. In contrast, CGE-derived interneurons contain cholecystokinin, calretinin, vasoactive intestinal peptide, and reelin including non-fast-spiking basket, Schaffer collateral-associated, MF-associated, trilaminar, and additional neurogliaform cells (Tricoire et al., 2011).

Overall, the temporal profiles of hippocampal PV+, Sst +, VIP+, and reelin+ interneuron generation are similar to those of the neocortex but with a slight shift toward earlier embryonic stages (Miyoshi et al., 2007; Batista-Brito and Fishell, 2009). In contrast, Clr+ interneurons, which often coexpress VIP in the neocortex, are generated at much later stages if they are destined for the hippocampus.

B Maturation of hippocampal interneurons and synaptogenesis: signals from postsynaptic neurons trigger GABAergic synaptogenesis.

At birth, interneurons at different stages of development are intermingled in the same layer (Hennou et al., 2002). However, only the interneurons at a certain degree of morphological maturation receive functional synaptic inputs, first from GABAergic and then from glutamatergic neurons. The same phenomenon is observed for pyramidal neurons, but with a delay (Tyzio et al., 1999). These observations could suggest that the degree of maturation of postsynaptic neurons is the limiting factor for the establishment of synapses. They are in agreement with heterochronic co-culture experiments, showing that axons are competent to establish synapses before the postsynaptic somato-dendritic compartment (Fletcher et al., 1994). Several other aspects of GABAergic synaptogenesis in the hippocampus also support this hypothesis. The maturation of GABAergic terminals on CA1 pyramidal cell bodies is delayed when compared with that on CA3 pyramidal neurons, which are generated earlier (Altman and Bayer, 1990b; Marty et al., 2002). In the granule cell layer, basket cells establish their first synapses with the more mature dentate granule cells, at the border of the molecular layer (Seress and Ribak, 1990). These results suggest that neurons reaching a certain stage of their development start to express molecules triggering synaptogenesis with nearby GABAergic axons.

5.3 FACTORS AFFECTING NEURONAL MIGRATION IN THE DEVELOPING HIPPOCAMPUS

Immature neurons express GABA and glutamate receptors as early as prenatal day E17. The expression of these receptors in silent neurons of the developing hippocampus, which have no functional synapses, has been shown to have an important functional role in mediating tonic, spontaneous, and evoked currents in embryonic and neonatal CA1 neurons (Demarque et al., 2002), and in modulating neuronal migration (Manent et al., 2005). Elegant hippocampal organotypic slice coculture assay experiments in which E17–E18 hippocampal slices from GFP and wild-type mice were cocultured in tight apposition at the level of the neuroepithelium of the CA1 region to study the migration of hippocampal neuroblasts have shown that applications of antagonists of $GABA_A$ or NMDA receptors led to a strong impairment of neuronal migration (Manent et al., 2005). In the presence of the antagonists, cells failed to migrate and remained distributed into the migration area (neuroepithelium

and *stratum oriens*) instead of invading the pyramidal cell layer. Morever, the study of organotypic slice cultures from GAD67–EGFP transgenic mouse line have shown that glutamate acting through AMPA but not NMDA receptors exert a permissive role enhancing interneuron migration (Manent et al., 2006). Thus, excitatory and inhibitory neurotransmitters have selective permissive roles modulating the migration of radially-migrating glutametergic and tangentially-migrating GABAergic neuronal populations, respectively. These glutamatergic and GABAergic migrating neuronal populations modulate their migration in a synergistic and cooperative manner.

5.4 COORDINATED SYNAPTOGENESIS

As mentioned previously, the hippocampus is a highly organized laminated structure that receives extrinsic and intrinsic inputs terminating in segregated non-overlapping fields and layers. Thus, entorhinal afferents recognize their appropriate targets in the CA3 region and the DG, terminating on the distal dendrites of the *stratum lacunosum-moleculare* and the outer molecular layer, respectively. The commissural/associational fibers terminate in *stratum oriens*, *stratum radiatum*, and the inner molecular layer (Marín et al., 2010). The sequential ingrowth of hippocampal afferents correlates very well with their position on the target cells' dendritic arbors. Early formed projections such as the entorhino-hippocampal projections terminate on distal dendrites, whereas projections generated later such as axons of the late-generated dentate granule cell-MF contact dendritic portions closer to the cell body of CA3 pyramidal neurons by establishing characteristic synapses with large excrescences originating from proximal dendrites (Amaral and Dent, 1981; Gonzales et al., 2001). Despite this temporal correlation, tracing and slice culture experiments have shown that reversing the normal sequence of developing axons does not affect their proper recognition of their final terminations (Frotscher and Heimrich, 1993). Thus lamination of these fiber systems may not be due to the sequence of arrival of afferents, rather, specific layer targeting is guided by local cellular and molecular signals interacting with specific proteins present in the growing axons.

CR cells are a special class of pioneer neurons that transiently occupy the MZ of developing cortex and hippocampus. They are present at the time of growth of

entorhinal axons into the developing hippocampus and the latter establish transient synapses with CR cells (Supèr et al., 1998). It has been suggested that the axons of CR cells that project from the hippocampus to the entorhinal cortex provide a template or a guiding scaffold for the outgrowing axons of the entorhinal cortex (Ceranik et al., 2000). In *Reeler* mice, the extracellular matrix protein Reelin, which is secreted by CR cells before and during the arrival of entorhinal afferents, is absent. Although the entorhino-hippocampal pathway is formed in the absence of Reelin, a reduction in axonal branching, and an increase in the number of misrouted aberrant fibers confirms the fundamental role of CR cells secreting Reelin in proper laminar targeting and correct synaptogenesis of developing entorhino-hippocampal terminals (Borrell et al., 1999).

Dab1 is an intracellular adaptor protein that is phosphorylated in response to Reelin signaling. Dab1 mutants also have alterations in the development of the entorhino-hippocampal pathway, where the pattern of termination of hippocampal afferents are largely similar to those described for *reeler* mice. This phenotype in Dab1 mutants indicates that Reelin modulates entorhino-hippocampal axonal targeting through the adaptor protein Dab1 (Borrell et al., 2007).

Mossy fibers:

Entorhinal cortex afferents contact DG cells forming a step in the trisynaptic circuit. DG cells, in turn, grow MFs that terminate on the proximal dendrites of CA3 pyramidal cells and mossy cells of the dentate hilus, as well as a number of interneurons in the two areas. MFs display a number of unique features with regard to their development, axonal projection specificity, terminal structures targeting and synaptic contacts. The synapses formed by MFs on pyramidal cells are one of the most complex synapses that develop during the postnatal period in rodents (Amaral and Dent, 1981). They are characterized by unique multi-headed dendritic spines termed thorny excrescences, which are engulfed by massive presynaptic MF boutons, which are 50–100 times larger in volume than a typical asymmetric synapse and can contain over 30 separate vesicle release sites. These large synaptic boutons onto pyramidal neurons in CA3 are few in number (8–11 per MF in the mouse), easily identifiable morphologically, and unusually potent (Henze et al., 2002; Rollenhagen et al., 2007).

One of the unique features of MF is their ability to preferentially contact CA3 cell dendrites, but not CA1 or DG cells (Figure 35B, C, D, and E). Using cell and synapse specific markers in hippocampal microisland assays and cell microculture experiments, some of the molecular mechanisms that drive initial formation and maturation of these unique hippocampal MF synapses have been unscrambled (Williams et al., 2011). This unique synapse formation does not require directed axon guidance; instead, specific molecular cues promote DG synapses with CA3 neurons. Cadherin-9 encodes a classic type II cadherin which signals via homophilic binding and is expressed specifically in DG and CA3 neurons, where it provides a bidirectional target recognition cue between them. *In vivo*, downregulation of cadherin-9 in either MFs or CA3 pyramidal cell dendrites, results in severe disruption of these contact sites. Presynaptic boutons are consistently reduced in size, and complexity upon cadherin-9 knockdown and postsynaptic spine formation is severely disrupted as well, suggesting a transsynaptic role of this homophilic protein in DG-CA3 MF synapse development (Williams et al., 2011).

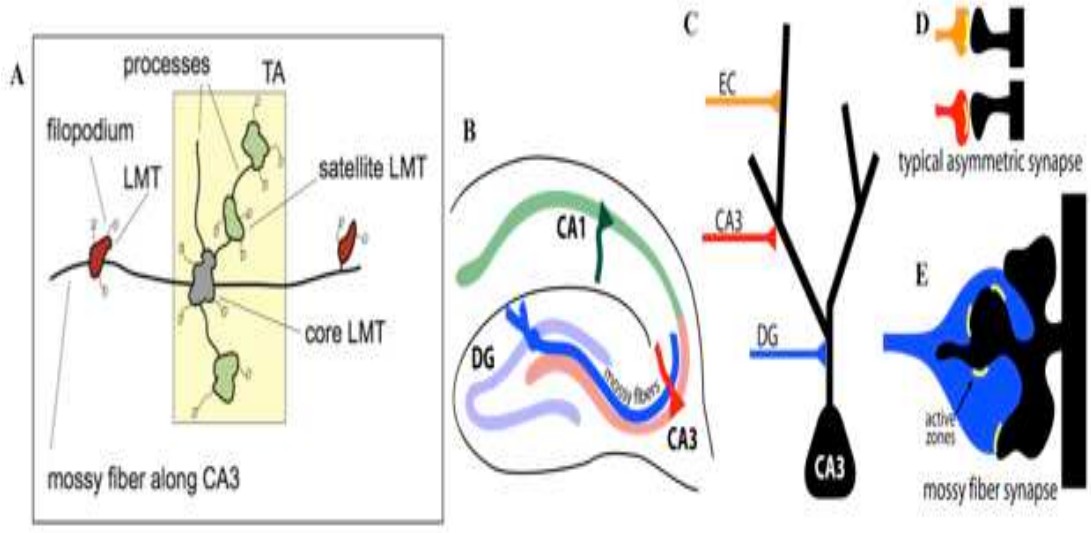

Figure 35: The unique structure and the specificity of synaptic connections in the hippocampus.
Adapted from Galimberti et al., 2010 and Williams et al., 2011

LMT, large mossy fiber terminal, TA, terminal arborization, EC, entorhinal cortex. Mossy fibre terminals can be either core or satellite and connected to each other.

Another particularly important feature of MFs is the characteristic arrangement; consisting of a core and satellite terminations connected to each other through processes forming a terminal arborization (TA) (Figure 35A). Interestingly, these represent a structurally plastic region where satellite termination frequencies are

positively influenced by hippocampal dependent learning and environmental enrichment (van Praag et al., 2000; Ramírez-Amaya et al., 2001; Galimberti et al., 2010).

Subpopulations of hippocampal GCs in the mouse exhibit 0 (50%–55% of all GCs), 1 (60%–70% of TA positive GCs), or >2 TAs per MF along the CA3 region. Notably, mGFP-positive MFs from Lsi1 and Lsi2 mice mentioned previously (Deguchi et al., 2011) exhibit 1 and >2 TAs, respectively. Disruption of EphA4 signaling or PSA-NCAM specifically in developing hippocampal circuits, resulted in disruption of single-TA MFs and the establishment of >2 TAs uniquely in Lsi1 neurons, but not Lsi2 or other later born DG cells. Altogether, this suggests that TAs are specified during critical periods in juvenile circuits, through mechanisms involving the retention of synaptic complexes at the GC contact sites along the CA3 region according to a precise topographic map (Galimberti et al., 2010).

In developing neuronal circuits, growing axons send off multiple collateral projections to ensure global coverage of all potential contact targets. Consequently, collaterals contacting inappropriate targets need to be refined through an extensive and specific process called stereotyped axonal pruning (O'Leary et al., 1990). This stereotyped pruning ensures the development of precise connectivity while removing subsets of transient, inappropriately targeted long axon collaterals. This is a predictable process, where transient branches to be removed are identifiable. In the developing hippocampus, MFs originating from DG cellss and contacting CA3 pyramids and interneurons are fasiculated into two major bundles, the suprapyramidal and the infrapyramidal bundles (IPBs). The suprapyramidal bundle, the major bundle (MB), extends in the *stratum lucidum*, just above and adjacent to the apical dendrites of the CA3 pyramidal cell layer. The IPB runs below the pyramidal cells adjacent to their basal dendrites and extends to the apex of the curvature of the CA3 region early on, at P5. However, in the adult, the axons of the IPB extend a very short distance before ascending to join the MB (Claiborne et al., 1986). This topographic difference is related to the fact that IPB axons undergo a process of stereotyped pruning between P20 and P30, and the final shape of MF axons is achieved around P45 when the axons are confined largely to the DG hilus (Bagri et al., 2003).

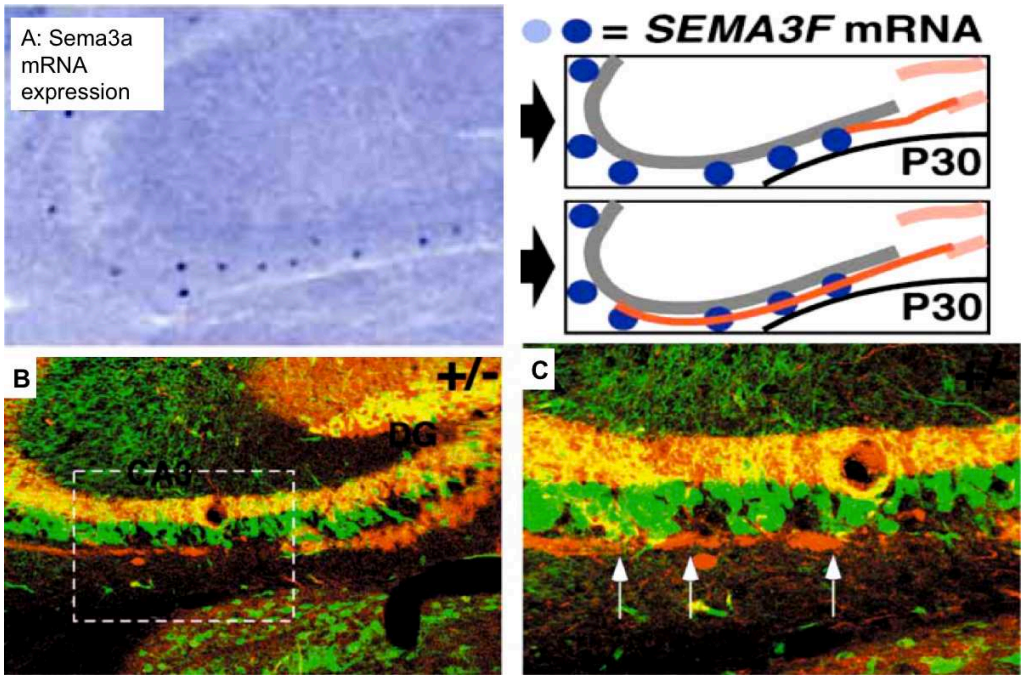

Figure 36: Cell autonomous pruning defect of the IPB in Plexin-A3 mutants.

Adapted from Bagri et al., 2003

Sema 3F is a secreted protein activating the receptor complex of neuropilin2 and Plexin-A3. This receptor complex functions as a retraction inducer to trigger stereotyped pruning of specific hippocampal MFs and pyramidal axon branches. In P25 mouse hippocampus, when pruning is actively taking place, Sema3F is strongly expressed in isolated large cells within the IPB region and *stratum oriens* of CA3 which are thought to represent a subset of NPY positive interneurons, and this expression pattern is consistent with a receptor role for Plexin-A3 in regulating IPB pruning (Figure 36A) Plexin-A3 expression is restricted to the inner third of the granular cell layer, where the youngest DG cellss are located and extends along a significant portion of the axons in the IPB (Bagri et al., 2003). In Plexin-A3 or Neuropilin-2 mutants, the IPB fails to undergo normal pruning, suggesting a role for these receptor in regulating pruning of IPB (Bagri et al., 2003). In the hippocampus of compound heterozygous females of Plexin-A3, which is an X-linked gene, and X-GFP, chimeric animals help in distinguishing WT and mutant axons in compound heterozygous females due to random X-activation. At P30, all MF axons stain for calbindin (red, figure 36B and C), and only Plexin-A3 WT axons will be positive for GFP (green, figure 36B and C). Thus, yellow axons contain both calbindin and GFP

originate from dentate granule cells expressing WT Plexin-A3, whereas red axons contain only calbindin and therefore originate from dentate granule cells expressing the mutant Plexin- A3 allele. In adult animals (WT, yellow) axons within the IPB were short, and all the abnormally long axons extending underneath the pyramidal layer within the IPB were red (i.e., mutant), regardless of whether WT (green) or mutant (black) pyramidal cells populated the pyramidal layer overlying the long IPB axons (Figure 36); many WT (yellow) axons were observed in the main bundle. The absence of WT (yellow) axons in the unpruned IPB regardless of the genotype of the environment argues strongly that loss of Plexin-A3 within granule cells is necessary for the pruning defect, consistent with a cell-autonomous role for Plexin-A3 as a receptor within dentate granule cells regulating pruning (Bagri et al., 2003).

Developmental events leading to maturation of hippocampal circuits:

A rich body of scientific literature describes key developmental processes orchestrating developing neuronal circuits and resulting in fine-tuning of its components for eventual proper wiring and functionality in the adult brain. Successive molecular, cellular, and electrical events operate sequentially resulting in progressive neuronal maturation. GABA, which largely acts as an inhibitory neurotransmitter in adult brain, has been shown to be a core player in functional maturation of developing circuits including the hippocampus (Leinekugel et al., 1997; Fukuda et al., 1998; Rivera et al., 1999). GABA typically acts by gating a chloride-selective ion channel. When the chloride reversal potential is maintained close to or negative to the resting membrane potential, the activity of interneurons acts to reduce postsynaptic activity by a combination of hyperpolarisation and shunting inhibition. The chloride reversal potential is controlled by the activity of two chloride transporters, KCC2, which normally lowers the intracellular chloride concentration by extruding chloride ions, and the Na+–K+–2Cl- co-transporter NKCC1, that typically imports chloride thus raising its intracellular concentration. Expression of these transporters is developmentally regulated; the early predominance of NKCC1 expression in immature neurons and the later expression of KCC2 renders the intracellular concentration of chloride of immature neurons relatively high, with

consequent efflux of chloride upon activation of GABA-A receptors and excitation of immature neurons (Leinekugel et al., 1997; Fukuda et al., 1998; Rivera et al., 1999).

Patch-clamp recording and *post hoc* reconstruction experiments of CA1 pyramidal neurons in rat hippocampal slices at P0 have shown that the same population of pyramidal cells is structurally and functionally heterogenous. The majority of the studied neurons (80%) were "silent" with no spontaneous or evoked postsynaptic currents (PSCs). These neurons had small somata and no dendrites. A minor group of the studied neurons (10%) had a small apical dendrite restricted to the *stratum radiatum* and PSCs mediated only by GABAA receptors; and another10% of neurons had a more advanced maturation state with an apical dendrite that reached the *stratum lacunosum moleculare* and basal dendrites, and expressed PSCs mediated by both GABAA and glutamate receptors. None of the recorded neurons had glutamate without GABAergic PSCs (Tyzio et al., 1999). Altogether, these experiments demonstrate that GABAergic synapses are formed and are operative before glutamatergic ones on hippocampal pyramidal cells during critical periods of early neonatal maturation of developing hipocampal networks.

In contrast to these results, patch clamp recordings from CA1 interneurons at P0 have shown an opposite trend of synaptic maturity of interneurons when compared to pyramidal cells. The majority of recorded neurons (87%) had both GABAergic and glutamatergic synapses, while only 5% of these interneurons were silent. This observation correlates tightly with the sequential developmental programs of pyramidal cells and interneurons, where interneurons are generated before pyramidal cells. This tightly controlled developmental program where excitatory GABAA synapses are active at a time when most principal cells are quiescent with no synaptic connections, seems mandatory to drive network activity and circuit maturity, and further confirms GABA signaling as a central player in these events (Hennou et al., 2002).

SECTION 6: DOUBLECORTIN, A NEURONAL MIGRATION GENE

6.1 CLASSICAL LISSENCEPHALY

Lissencephaly (including both agyria and pachygyria) is a neurodevelopmental disorder characterized by the lack of cortical convolutions and an abnormally thick cortex (Barkovich et al., 1991; Pilz et al., 1998; Dobyns et al., 1999; Cardoso et al., 2002; Kerjan and Gleeson, 2007; Morris-Rosendahl et al., 2008). It results from defective neuronal migration during the development of the cerebral cortex (Iannetti et al., 1996; Barkovich et al., 2001; Verrotti et al., 2010). Mutations of at least six genes have been associated with forms of lissencephaly including LIS1, DCX, TUBA1A, RELN, VLDLR and ARX, whereas co-deletion of LIS1 along with many other telomeric genes, especially 14-3-3e, produces a more severe form of lissencephaly and distinct facial features, a syndrome known as Miller-Dieker syndrome (Reiner et al., 1993; des Portes et al., 1998; Gleeson et al., 1998; Pilz et al., 1998; Zaki et al., 2007). RELN, VLDLR and ARX pathologies differ however, from LIS1, DCX and TUBA1A, especially because of accompanying and constant defects in other brain structures.

In classical lissencephaly (LIS), affected individuals have an abnormal cortex, but no other major brain malformations. This is the only type of lissencephaly that is associated with subcortical band heterotopia. To date, three distinct genetic causes for LIS have been identified. Heterozygous mutations in platelet-activating factor acetylhydrolase 1B a subunit (PAFAH1B1, located in 17p13.3, and encoding the LIS1 protein), hemizygous mutations in the the X-linked gene doublecortin (DCX) and heterozygous mutations in tubulin A 1A (TUBA1A) each produce varying severities of classical lissencephaly. Mutations of LIS1, DCX and TUBA1A account for 65%, 12% and an 1-4% of patients with LIS, respectively (Reiner et al., 1993; des Portes et al., 1998b; Gleeson et al., 1998; Pilz et al., 1998; Keays et al., 2007; Kumar et al., 2010) The proteins coded by these genes all affect microtubule (MT) function and interfere with neuronal migration (discussed earlier in section 3).

Classical lissencephaly and subcortical band heterotopia (SBH) comprise a spectrum of cortical malformations where the most severe form of lissencephaly consists of absent gyri (agyria); the intermediate form consists of abnormally shallow gyri

(pachygyria) and the least severe forms are represented by SBH (Kato and Dobyns, 2003). DCX is the major gene mutated in SBH (des Portes et al., 1998a). Children born with this disorder suffer from varying degrees of severe epilepsy, intellectual disability, and premature death in the most severe cases (Barkovich et al., 1991; Dobyns et al., 1992).

6.1.1 Neuropathology

Some data about the detailed histopathological characteristics of this disorder have been described. In DCX-mutated cases of classical lissencephaly, gross brain examination revealed a smoothening of the surface, with an agyric or a pachygyric convolution pattern. The phenotype is most severe anteriorly in the frontal lobes (Friocourt et al., 2011). Corpus callosal abnormalities were common in the studied cases, and range from complete agenesis, thinning, or even an abnormally thick corpus callosum (Dobyns et al., 1999; Kappeler et al., 2007; Friocourt et al., 2011). The abnormally thick corpus callosum was identified also during human neurofoetopathological analyses at 35 gestational weeks (35 GW), a time when the formation of the corpus callosum is complete. This finding is suggestive of either defective pruning of callosal fibers, swelling of fiber tracts, or misguided crossing of fibers. The latter hypothesis is further suggested by the finding of callosal agenesis in the same analysed fetal brain but at different rostro-caudal levels (Kappeler et al., 2007). Microscopic examination revealed increased cortical thickness (between 10 and 20 mm instead of 4 mm from birth) (Ross et al., 1997; Forman et al., 2005). Examination of one 35WG DCX- mutated embryonic brain showed that the cortical ribbon is thick and poorly separated from the IZ and is composed of four layers (Friocourt et al., 2011). In the postnatal brain, the superficial cortical layers layers I, II and III had a milder phenotype when compared to deeper layers (Forman et al., 2005). Layer I contained CR neurons. Layer II was a thin layer containing few pyramidal neurons. Layer III was poorly delimited and paucicellular, made up of granule and immature neurons with sparse myelination. However, this layer contains more neurons than brains with LIS1 mutations (Forman et al., 2005). Layer IV was thickened with a striking transition between the lissencephalic cortex characterized by the presence of multiple small nodules of subcortical heterotopia at the junction

between the grey and white matter arranged in a radially and columnar pattern. These nodules were composed of later born neurons and interneurons which are arrested in the periventricular areas or the striatum (Forman et al., 2005; Friocourt et al., 2011). These cells seem to mix with the layer VI that is actually widely distributed through the deep white matter and the striatum. The hippocampal formation is hypoplastic (Kappeler et al., 2007).

Histologic examination of the brain from LIS1- lissencephaly brains revealed similarities but also important differences compared to cases with DCX-mutations. The posterior parts of the brains are most severely affected, the gyri are broad, small in number and coarse, with a failure or a delayed opercularization of the Sylvian fissure. In less severe cases, primary temporal and occipital fissures may be observed and the hippocampal area, as well as the adjacent cortex, may have a normal gyration. The cytoarchitecture of the different hippocampal fields appears to be generally preserved with occasional decrease in pyramidal cell density. The cerebral cortex is thickened, layer I is composed of CR cells close to the pia. Layer II is composed of densely packed pyramidal neurons and is thicker than in DCX-lissencephaly brains. Layer III consists of scattered fusiform, rounded or multipolar neuronal elements. Layer IV is particularly poorly separated from the underlying white matter and composed of misoriented pyramidal neurons. The reduced white matter contains multiple arrested post-mitotic neuroblasts (Forman et al., 2005; Friocourt et al., 2011).

6.1.2 Genotype-phenotype correlation and molecular diagnosis of classical lissencephaly

The imaging findings of lissencephaly vary with the causative gene as well as with the severity of the mutation (Leventer et al., 2001; Leger et al., 2008). When very severe, the cortex is markedly thickened and almost no sulci are formed (Figure 37 A and A'), whereas in less severe cases, the cortex is less thickened and a variable number of shallow sulci separate broad gyri (Figure 37 B and B').

A classification system considering both the severity of the anomalies and their anterior (A) or posterior (P) predominance has been developed: the spectrum varies from complete or near complete agyria (grades 1 and 2) (Figure 37 A and A') to

pachygyria (grade 4) and SBH (grade 6) (Figure 37 C). Intermediate grades consist of mixed agyria–pachygyria (grade 3) (Figure 37 B and B') and mixed pachygyria–SBH (grade 5) (Dobyns and Truwit, 1995; Dobyns et al., 1999; Kato and Dobyns, 2003). A recognizable gradient in which the malformation is more severe anteriorly (DCX) or posteriorly (LIS1 and TUBA1A) is also identified (Dobyns and Truwit, 1995; Pilz et al., 1998; Dobyns et al., 1999; Saillour et al., 2009; Kumar et al., 2010; Friocourt et al., 2011). Thus imaging studies can help predict the causative genetic mutation in many cases. It also plays an important role in predicting the degree of neuromotor impairment which was shown to be in tight accordance with the severity of lissencephaly as judged by MRI diagnostic studies (Leger et al., 2008; Saillour et al., 2009).

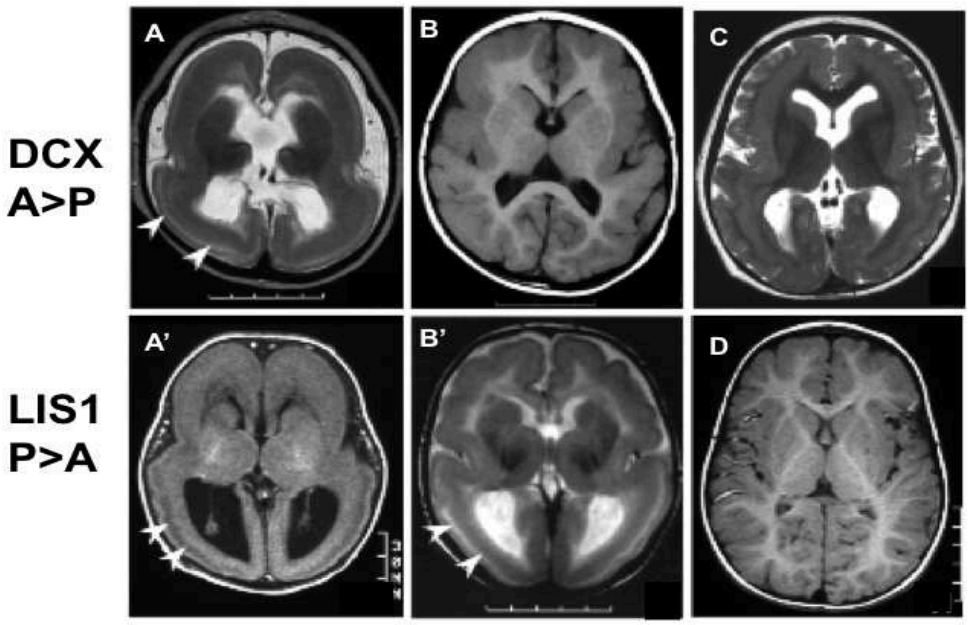

Figure 37: Magnetic resonance images (MRI) at the level of basal ganglia showing different degrees of LIS severity.
Adapted from Kato et al., 2003

In contrast to a normal control (D), all types of LIS have broad or absent gyri and an abnormally thick cortex, except for LIS grade 6 or SBH, in which the sulci separating gyri are very shallow. Notice the anterior to posterior gradient of LIS is strictly correlated with the causative gene. Specifically, mutations of DCX or RELN result in an anterior more severe than posterior (a > p) gradient (A and B), while mutations of LIS1 or ARX lead to a posterior more severe than anterior (p > a) gradient (A' and B'). In heterozygous females, mutations of DCX result in SBH (C).

Genotype-phenotype correlation studies, where the clinical presentation and its severity is correlated with the causative gene mutation have shed light on important functional domains in the mutated genes and proteins, which could be tightly correlated to its altered function (Leger et al., 2008; Saillour et al., 2009). Sequence and structural analyses of DCX proteins from various organisms and mutation analysis in humans have shown that DCX is a 361 amino acid protein composed of two highly conserved tandem domains, an N-terminal internal repeated domain (N-DC; aa 46-139) and a C-terminal domain (C-DC; aa 173-263), the two domains share a common ubiquitin-like fold (Sapir et al., 2000; Taylor et al., 2000; Kim et al., 2003). C-DC is followed by a serine/proline-rich tail. Interestingly, most disease-causing mutations are missense mutations, clustered in the two conserved N-DC and the C-DC domains (des Portes et al., 1998b; Matsumoto et al., 2001; Leger et al., 2008). The region of the protein containing the N- and C-DC domains is known to bind to MTs, however, it is still unclear if DCX interacts through its N-DC, or C-DC domain, or both. Recent, genotype-phenotype studies, have clearly demonstrated that LIS and SBH causing mutations cluster in both domains (Leger et al., 2008, Bahi-Buisson et al., submitted). However, lissencephaly patients having mutations in the N-DC domain may in some cases have a more severe clinical grade when compared to C-DC domain patients (Leger et al., 2008). However, the same is not strictly true when considering patients with SBH (see below, Bahi-Buisson et al., submitted). Genotype-phenotype relationships support experimental data on the functional importance of these two evolutionary conserved repeated regions in DCX and their role in MT binding.

Genotype-phenotype correlation studies to uncover critical domains in the LIS1 gene have not shown significant results. Large deletions of the LIS1 gene account for most lissencephaly cases (Pilz et al., 1998). Most of the disease-causing point mutations are found to be truncation mutations distributed all over the gene. Missense mutations are less frequently observed (Cardoso et al., 2002). Recently, through studying a large cohort of patients with mutations in the LIS1 gene, it has been confirmed that the mutation type and location can not predict the severity of the clinical and radiological phenotypes in the LIS1-related lissencephaly cases (Saillour et al., 2009).

6.1.3 Subcortical band heterotopia

SBH is a related disorder in which bilateral bands of gray matter are located between the ventricular wall and the cortex, separated from the cortex by a thin band of white matter (Figure 37 C) (Matsumoto et al., 2001). The gyral pattern in the overlying cortex can be normal, or can be simplified to shallow sulci (Guerrini and Parrini, 2010). Histopathology demonstrates that heterotopic neurons settle close to the 'true' cortex in a pattern suggestive of laminar organization and these may be smaller in size than normal compared to those in the overlying cortex (Guerrini and Parrini, 2010).

SBH is mainly caused by mutations in two genes: LIS1 and DCX, although one mutation in TUBA1A also gives rise to this disorder (these are not the key references so I think here it's best not to cite any. Generally speaking, DCX mutations cause lissencephaly in hemizygous males and SBH in heterozygous females, and is responsible for most cases of SBH (des Portes et al., 1998a; Pilz et al., 1998). DCX mutations have been found in all familial cases and in 53–84% of patients with sporadic anteriorly predominant band heterotopia, which represent the most common form of SBH (Mei et al., 2007). In one report, 80% of sporadic female cases, and 25% of sporadic male cases of SBH were due to DCX mutations (Matsumoto et al., 2001). Somatic mosaicism has been shown to be the cause of SBH in male patients mutated for the DCX gene and male and female patients with LIS1 gene mutation (D'Agostino et al., 2002; Sicca et al., 2003; Quélin et al., 2012). Most of DCX gene mutations causing SBH are point mutations. (Pilz et al., 1998; D'Agostino et al., 2002a; Leger et al., 2008, Bahi-Buisson et al., submitted). A recent report also described a sporadic male patient with SBH carrying somatic mosaicism for deletion of exon 6 in the DCX gene (Quélin et al., 2012).

A robust genotype-phenotype correlation of DCX mutated-SBH patients has been recently performed in a large-scale study where more than 70 cases of familial and sporadic cases were examined (Bahi-Buisson et al,. submitted). In this study, it is clearly shown that the degree of neurological impairment is related to the overlying cortical abnormalities and band heterotopia thickness assessed by quantitative MRI volumetric analysis. Band thickness is also correlated with the degree of overlying cortical abnormalities including the degree of pachygyria and ventricular enlargement (Bahi-Buisson et al,. submitted). Mutation analysis has further confirmed that most of

the disease-causing mutations were missense mutations distributed approximately equally between the N-DC and the C-DC domains (Bahi-Buisson et al,. submitted). Skewed X inactivation has been demonstrated to be one of the severity-modifying factors, responsible for a less severe phenotype or even asymptomatic inherited and sporadic carrier state in female patients (Bahi-Buisson et al,. submitted). It was shown that carriers females with skewed X inactivation could transmit severe mutations to their offspring males, a finding that helps in explaining some severe familial cases of DCX related lissencephaly and other atypical situations (Bahi-Buisson et al,. submitted). This could add to the complexity to the genotype-phenotype prediction and clinical diagnosis, especially when we keep in mind skewing is not identical between different tissues in the same individual.

A severity difference between *de novo* and inherited mutations was noticed, where *de novo* ones commonly resulted in a more severe phenotype (Bahi-Buisson et al,. submitted). This finding goes with what was already identified in male lissencephaly cases. A plausible explanation could be related to the important functional impairment related to severe mutations that renders the transmission of these mutations to future generations highly improbable, an adaptive evolutionary selection method.

While identified mutations in LIS1 and DCX genes account for the vast majority of cases, a minority of patients with the lissencephaly-SBH spectrum remains without a molecular diagnosis. One of the reasons contributing to this is the molecular heterogeneity in different types of mutation mechanisms. Several reports have recently identified intragenic deletions and duplications of the LIS1 and DCX genes as disease-causing mutations (Mei et al., 2007; Haverfield et al., 2009), explaining a certain number of apparently ‘negative’ cases. Together with the cases of somatic mosaicism (Sicca et al, Quelin et al) and skewed X inactivation this adds further to the wide variety of disease causing mechanisms in the lissencephaly-SBH spectrum of cortical malformations. Detection of all types of mutations of the known genes thus remains a major challenge. New genes will also almost certainly help explain remaining cases.

6.2 DOUBLECORTIN, AN MT ASSOCIATED PROTEIN INVOLVED IN NEURONAL MIGRATION AND DIFFERENTIATION

DCX is a member of a neuronal MT associated protein (MAPs) family (Moores et al., 2004). In the developing CNS, MAPs are involved in a wide range of cellular processes including cell division, migration, polarity formation, and differentiation (Conde and Cáceres, 2009). DCX is expressed specifically in postmitotic migrating and differentiating neurons, where it plays crucial roles in regulating MT dynamics (Francis et al., 1999; Gleeson et al., 1999).

6.2.1 The interaction between DCX and microtubules

MTs are long polymers of tubulin that are essential for brain development and function. MT dynamics involve several processes, α- and β-tubulin heterodimers are formed into MT protofilaments (PFs) in a process called nucleation, which can require γ-tubulin protein complexes (Erickson, 2000) or other nucleating factors. During nucleation, α- and β-tubulin heterodimers associate head to tail to form PFs and laterally to form the cylindrical MT wall.

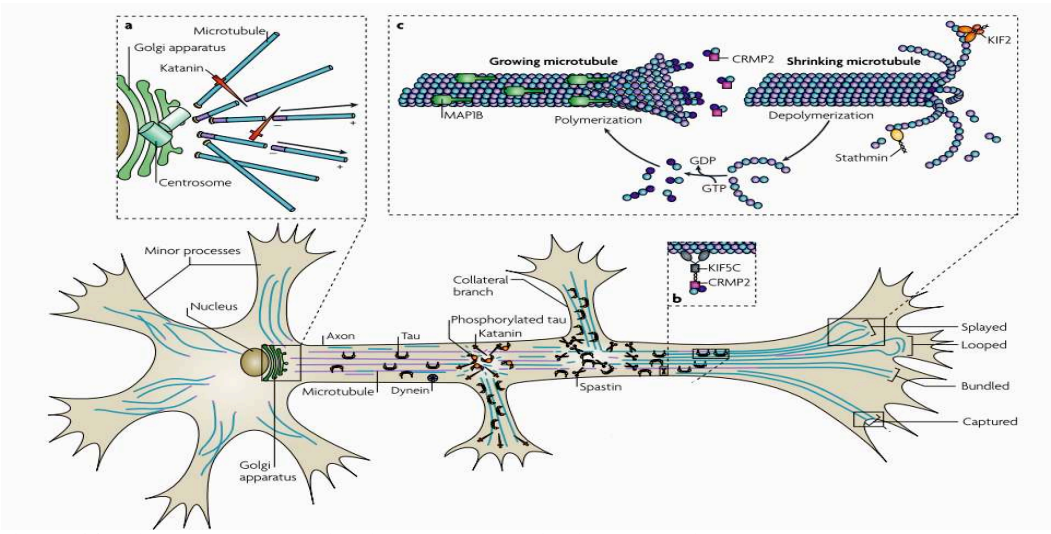

Figure 38 Microtubule organization and dynamics in developing neurons.
Adapted from Conde and Cáceres, 2009.

In vivo, most MTs are built from 13 parallel PFs (Figure 38C), (Tilney et al., 1973; Nogales et al., 1998, 1998). Formed MTs go through cycles of elongation and shortening and can be stabilized and destabilized. Destabilized MTs will collapse in a

process known as MT catastrophe (Conde and Cáceres, 2009). The head-to-tail association of the αβ heterodimers makes MTs polarized structures, and they have different polymerization rates at the two ends. In each PF, the αβ heterodimers are oriented with their β-tubulin monomer pointing towards the faster-growing end (plus end) and their α-tubulin monomer exposed at the slower-growing end (minus end). The MT can switch between the growing and shrinking phases dynamically at the plus end (Conde and Cáceres, 2009). During polymerization, both the α- and β-subunits of the tubulin dimer are bound to a molecule of GTP. Since tubulin adds onto the end of the MT only in the GTP-bound state, there is a cap of GTP-bound tubulin at the tip of the MT, protecting it from disassembly. While the GTP bound to α-tubulin is stable, the GTP bound to β-tubulin may be hydrolyzed to GDP shortly after assembly. The GDP-tubulin subunit at the tip of a MT is prone to depolymerization and undergoes a structural transition from a strained polymerised conformation to a bent, depolymerisation- favouring conformation and a will fall off (Ravelli et al., 2004). Thus the MT begins rapid depolymerization and shrinkage (Figure 38) (Manna et al., 2007).

DCX contributes to brain development through the stabilization of MTs in the leading process of migrating neurons and other neuronal processes (Horesh et al., 1999). Dcx is enriched along the lengths of MTs in the leading process of migrating neurons, extending in immature neurites (Francis et al., 1999; Gleeson et al., 1999) and growth cones (Tint et al., 2009). In cultured neurons, Dcx/actin filament patches are present along the axonal shaft, where they display dynamic movements similar to what is described in growth cones (Figure 38), (Tint et al., 2009). Dcx knockdown results in decreased collateral branching, axon elongation, and dendritic arborization (Deuel et al., 2006; Tint et al., 2009). Its deletion in mice results in branching defects of migrating neurons (Kappeler et al., 2006; Koizumi et al., 2006).

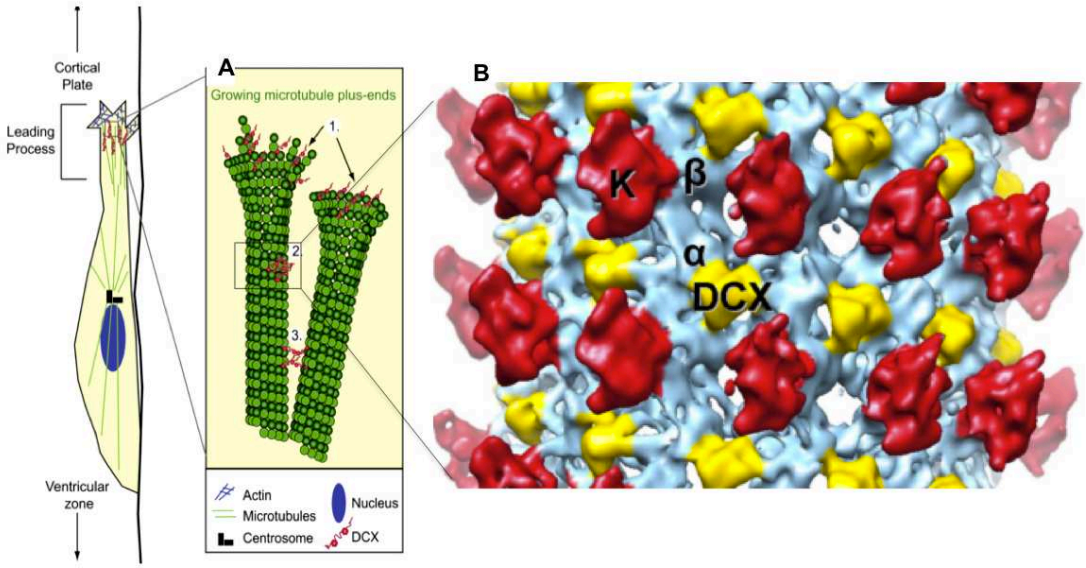

Figure 39: A proposed model of DCX interaction with MT in the in the leading process of migrating neurons showing cooperative DCX binding to MT and an affinity for growing microtubule.
Adapted from (Fourniol et al., 2010; Stumpff, 2012)

As mentioned above, DCX is enriched in neuronal processes, at extremities of migrating and differentiating neurons, a region which is devoid of γ-tubulin (Baas and Joshi, 1992). In these sites, DCX selectively binds and polymerizes 13 pf MTs (Moores et al., 2004) and thus possesses a potent nucleation activity, by laterally linking together adjacent PFs and counteracting their outward depolymerising bending conformation (Figure 38, 39A) (Moores et al., 2006). This leads to MT elongation, preventing them from catastrophe and decreasing the rate of post-catastrophe shrinkage (Moores et al., 2006; Fourniol et al., 2010). Structural biology experiments have confirmed that DCX specifically recognizes the corner of four tubulin dimers, and binds at the interdimer longitudinal junction between α- and β -tubulin, which forms the exchangeable GTP site (Figure 39B) (Nogales et al., 1998). DCX overrides the GTP/GDP nucleotide dependence of MT polymerization and architecture (Moores et al., 2006). Thus, the DCX-MT stabilization mechanism is a plastic mechanism that can stabilize both lateral and longitudinal contact sites and nucleate MTs independent of the tubulin-bound nucleotide, a mechanism different from γ-tubulin mediated stabilization (Friocourt et al., 2003; Fourniol et al., 2010). The density attributable to DCX at each binding site is 1/4 of the protein, corresponding to a DC domain (Moores et al., 2004; Fourniol et al., 2010); the atomic

structure of the N-DC fits very well to the described binding site. However, up-to-date, no evidence rules out the involvement of the C-DC domain in this binding (Fourniol et al., 2010).

Recently, *in vitro* single-molecule fluorescence microscopy assays helped provide insight into the molecular mechanisms underlying the DCX-MT interaction. It has been shown that DCX recognizes 13-pf MTs through a cooperative interaction between adjacent DCX molecules, meaning that a single DCX molecule does not bind specifically to 13-pf MTs, but groups of DCX molecules do (Figure 39A) (Bechstedt and Brouhard, 2012). Additionally, the presence of neighboring molecules causes DCX to remain bound to the MT longer. This cooperative-interaction model seems to be valid *in vivo* as well; DCX molecules with missense mutations identified in SBH patients had a significantly decreased cooperative interaction. Both N-DC mutations and C-DC mutations showed a severely impaired response, indicating that both domains may play a role in this cooperative interaction. Moreover, mutations resulting in the more severe ‘‘thick’’ SBH cases had more dramatic effects than ‘‘thin’’ SBH, while a ‘‘moderate’’ SBH mutation lay in between. Altogether the penetrance of an individual mutation, that is tightly correlated with the clinical phenotype (Nadia-Bahi-Buisson et al., submitted), seems to correlate also with the degree of cooperative interaction between DCX and the MT backbone (Bechstedt and Brouhard, 2012).

While genotype-phenotype correlation studies did not clearly reveal the importance of the MT-binding function of the DC domain, protein structural analyses suggested that the N-DC domain is more adapted to interact with MT pfs (Moores et al., 2004). However, less is known about how the C-DC domain might interact with MTs, and structural analysis of DCX molecules harboring missense mutations in either domain resulted in severe decline of DCX- mediated MT cooperative binding (Bechstedt and Brouhard, 2012). This signifies that both domains can be involved in MT stabilization. Nevertheless, DCX involvement in MT stabilization can well extend beyond direct MT interaction. Indirect effects of DCX mutations can probably result in localization defects, premature degradation (Bahi-Buisson et al, submitted), aberrant posttranslational modifications (eg the S47N mutation affects a phosphorylation site), or modification of DCX binding to other molecular partners, resulting in reduced MT stability, migration defects and a pathologic phenotype.

6.2.2 The role of phosphorylation in regulating DCX function

Several protein partners have been described to interact with DCX mediating or modulating its functions (Refs). The subcellular localization of Dcx and its affinity to MTs are maintained by a balance of phosphatase and kinase activities at the perinuclear space and the leading edge of the migrating neuron, which will control the MT binding activity of Dcx in response to extrinsic guidance cues (Refs). Cyclin-dependent kinase 5 (Cdk5) is a member of the Cdk family of serine/threonine kinases that is ubiquitously expressed in the developing brain. It is an atypical kinase in that it is not involved in cell-cycle control, but in neuronal migration and differentiation (Tanaka et al., 2001, 2004). The activity of Cdk5 is tightly controlled by binding to its neuron-specific activators p35 and p39. p35 has an expression pattern in the developing cortex that photocopies DCX expression. Additionally, strong Cdk5 and p35 immunoreactivity was detected in the perinuclear cell soma and the leading process (Tanaka et al., 2004), where Dcx is enriched and localizes to MTs (Francis et al., 1999; Gleeson et al., 1999). p35 co-immunoprecipitates with Dcx, which co-assembles with Cdk5 on MTs (Tanaka et al., 2004). *Cdk5* activity is required for proper localization of Dcx to fine perinuclear MTs where it phosphorylates Dcx at Ser297 *in vivo* (Tanaka et al., 2004b). Phosphorylation of Dcx by Cdk5 lowers its affinity for MTs, and impairs MT polymerizing activity (Tanaka et al., 2004b). Altogether, this data supports the fact that Cdk5-mediated phosphorylation of Dcx fine tunes its function in binding and stabilizing perinuclear MTs, a process essential for the dynamic regulation of the centrosome-nucleus coupling and nucleokinesis during neuronal migration.

The c-Jun N-terminal kinase (JNK) and JNK interacting protein (JIP-1) work upstream of Dcx. The localization of Dcx at neurite tips is determined by its interaction with JIP-1 which in turn interacts with a conventional kinesin; a plus-end directed molecular motor (Gdalyahu et al., 2004). Interestingly, overexpression of a mutated JIP- 1 (lacking the last 11 amino acids essential for interaction with kinesin) resulted in accumulation of Dcx closer to the cell soma. Thus, JIP-1 interaction with Dcx promotes kinesin-mediated transport of Dcx from the cell soma to the neurite.

Morever, Dcx colocalizes with JNK in the perinuclear area as well as in the neurites. And JNK mediated phosphorylation of Dcx affects neurite extension and slows *in vitro* cortical neuronal migration (Gdalyahu et al., 2004; Jin et al., 2010). The phosphorylation of Dcx by JNK lowers its binding to tubulin (or MTs?). And treatment of neurons with JNK inhibitors increased the amount of Dcx bound to tubulin (or MTs?) (Jin et al., 2010). Neurabin II, an actin binding protein that successfully mediates the interaction between Dcx and the actin cytoskeleton (Tsukada et al., 2005), binds to protein phosphatase1 (PP1), where it regulates PP1 mediated dephosphorylation of Dcx on sites phosphorylated by JNK (Shmueli et al., 2006). However, the role of this interaction on neuronal migration needs to be determined. But see spinophilin/Dcx paper Bielas et al.

PKA and MARK kinases act also as negative regulators of Dcx binding to MTs. The serine residue S47 in the Dcx protein, which is mutated in lissencephaly patient cohorts (Bahi-Buisson et al; submitted, and marks the beginning of the N-DC domain (Kim et al., 2003), represents a substrate for MARK phosphorylation, and mediates the negative regulation of Dcx MT affinity upon MARK phosphorylation. Protein phosphatase 2A (PP2A) inhibitors increased the amount of dephosphorylated DCX and de-localized DCX from the neurite tips to cell soma (Schaar et al., 2004). Thus phosphatase activity is crucial to maintain Dcx localization at neurite tips. Dcx function *in vivo* is therefore balanced by several factors that stabilize-destabilize MTs and assure correct migration.

In conclusion, coordinated and reciprocal action of serine/threonine (Ser/Thr) protein kinases and phosphatases produces transient phosphorylation, a fundamental regulatory mechanism in MT dynamics. Altogether, the above-mentioned examples add to the progress that has been made in proposing mechanisms and signaling pathways that will transfer external signals such as cell adhesion molecules and chemoattractants into increased cellular dynamics, growth cone turning, and neuronal migration.

6.2.3 Dcx's role in enhancing long-distance cellular transport

MTs represent a structural support within neurons involved in various dynamic processes. They are the engines generating power during neuronal migration and they also act as the principal tracks for long-distance cellular transport of enzymes, organelles, mRNAs and cytoskeletal components. In particular, the growth cone of a migrating neuron requires a steady stream of cellular components to be channelled to its tip and such transport is performed by plus-end–directed kinesin motors (Guzik and Goldstein, 2004).

In addition to Dcx's function in supporting neuronal motility through MT stabilization, it seems to be very important for providing stable tracks for anterograde transport and vesicular trafficking. Evidence for this has been suggested by experiments of MTs bound to DCX which did not block kinesin-dependent transport in neurons, thus DCX allows MT growth and stabilization without interfering with other critical cytoskeletal reorganizations (Moores et al., 2006). Moreover, the DCX binding site is in between MT PFs, only one-part of the DCX molecule is in the inter-PF groove and the rest of the DCX molecule is exposed, probably participating in other MT mediated functions (Moores et al., 2006; Fourniol et al., 2010). The participation of Dcx in vesicular trafficking was confirmed by studying *Dcx*/*Dclk* (*Doublecortin-like kinase*) double mouse mutants which display a severely compromised intracellular neuronal transport (Deuel et al., 2006). Specifically, they have defects in Kif1a-mediated trafficking of the presynaptic vesicle-associated membrane protein 2 (Vamp2). Fewer Vamp2- vesicles exit the cell body toward the neurites in both *Dcx*- and *Dcx*/*Dclk*1-deficient neurons, and instead, accumulate in the soma (Liu et al., 2012). Additionally, *in vitro* studies have demonstrated that DCX enhances binding of the ADP-bound Kif1a motor domain to MTs thus mediating specific increases of Kif1a MT binding and run length (Moores et al., 2006). Moreover, RNAi knockdown of Kif1a in neurons mimics several effects of *Dcx*/*Dclk*1 deficiency. Dcx mutated at S47R, a mutation described in lissencephaly patients, not only caused retention of Dcx in the soma, but also resulted in a significant reduction in the number of Vamp2 vesicles exiting into neurites (Liu et al., 2012).

While Dcx-MT binding is regulated by dephosphorylation of Dcx through specific interactions with PP1 and PP2A phosphatases in the soma and the distal regions of neurites, stimulating Kif1a-Vamp2 anterograde transport in a dynamic and localized fashion is mediated through DCX-MT assembly. In contrast, the release of DCX from MTs, is mediated by kinases which also play important roles in neuronal development and function, such as CDK5, MARK, and JNK. Therefore, vesicle trafficking to assure differential anterograde delivery of cargo from cell soma to neurites is tightly regulated by spatial and temporal signals that act down stream to extracellular cues and growth factors, connecting the actin cytoskeleton to MT motors, and DCX is likely to play a fundamental role in this process.

6.2.4 DCX's interaction with LIS1

Transport is one of the major functions of MTs and is mediated by individual MT-based motors (Vale, 2003). Motors are directional; as suggested above kinesins transport cargoes away from the cell body to distal parts of the axon (plus-end-directed MT motor), and dynein mediates transport back toward the cell body (minus-end-directed MT motor). The LIS1 protein is associated with dynein and regulates its function at various cellular and molecular levels (McKenney et al., 2010). It affects neuronal progenitor cell division (Faulkner et al., 2000), it is involved in the regulation of neuronal migration by enhancing nucleokinesis (Dujardin et al., 2003) and it regulates the extension of the leading processes of neurons by regulating both reorientation of the MT-organizing center and actin-based motility (Faulkner et al., 2000; Gupta et al., 2002). Additionally, together with Nudel, LIS1 regulates dynein, which mediates transport back toward the cell body towards MT minus ends (Liang et al., 2004; Li et al., 2005). On the other hand, LIS1 may interact with DCX; they partially colocalize in the soma and in neurites and may function in the same protein complex in the developing brain. DCX may be abnormally localized in Miller–Dieker syndrome (involving LIS1 deletion) brains (Qin et al., 2000). When dephosphorylated, DCX is mobilized from neurite tips and associates with MT bundles, where it may influence LIS1.Interplay between DCX and LIS1 may involve common regulatory mechanisms affecting retrograde minus-end-directed MT

transport and common pathways that regulate neuronal migration and differentiation may exist between two proteins which when mutated lead to a common pathology.

6.2.5 DCX's interaction with Neurofascin (NF)

NF belongs to a family of L1 cell adhesion molecules (CAMs), which are transmembrane proteins of the immunoglobulin superfamily that engage in stable protein interactions at the membrane as well as signaling pathways (Hortsch, 1996). During cortical development, and upon local signaling of neurotrophins in culture, DCX modulates the subcellular distribution of NF and targets it to the axon initial segment (AIS) at the time of axogenesis (Kizhatil et al., 2002; Yap et al., 2012). DCX specifically binds phosphorylated NF at the intracellular FIGQY motif, and promotes the clathrin dependent endocytosis of NF from the neuronal plasma membrane in the soma and dendrites and redistributes it to the AIS. Once at the AIS, FIGQY-Neurofascin becomes de-phosphorylated promoting its binding to AnkyrinG (ankG) (Tuvia et al., 1997) which tethers it to the AIS. Accumulated and stabilized NF at the AIS is essential for the formation, maintenance, and stabilization of the AIS and cell specific synaptogenesis (Burkarth et al., 2007; Kriebel et al., 2011).

DCX also interacts with μ1 and μ2 subunits of the protein adaptor complexes AP-1 and AP-2 respectively, which are involved in clathrin-dependent protein sorting (Friocourt et al., 2001). AP-2 is particularly involved in clathrin-mediated endocytosis and receptor sorting at the plasma membrane (Friocourt et al., 2001). And the μ subunits have been shown to mediate the capture of specific proteins (often integral membrane proteins) in clathrin-coated vesicles (Ohno et al., 1998). Therefore, it sounds plausible that DCX-mediated clathrin dependent endocytosis of NF is accomplished via the DCX-AP2 interaction.

6.3 MIGRATION DEFECTS AND SPONTANEOUS EPILEPSY IS A COMMON FEATURE OF DIFFERENT DCX MUTANTS' MODELS

DCX plays important roles during brain development in rodents and humans. However, phenotypic differences between species do exist. While human patients with disease-causing mutations in the DCX gene will have a spectrum of lissencephaly and SBH, constitutional Dcx KO mice have grossly normal isocortex, with disorganization of the hippocampus. Lamination defects is mostly appreciated in the CA3 region, which is divided into two layers. A loose layering of cells is noticed in all the Cornus Ammonia fields (Corbo et al., 2002; Kappeler et al., 2007). Lamination defects in hippocampal fields are detected during embryonic periods; at E17.5 an increased density of cells in the intermediate zone adjacent to the developing pyramidal cell layer was observed. Additionally, two cell layers were observed in the CA3 region and CA1 to a lesser extent at this stage. At postnatal stages, fewer heterotopic cells were detected in the CA1 region while lamination defect persisted in the CA3 region into adulthood. In the adult, the CA3 pyramidal cell layer was divided into a thin superficial neuronal layer close to *stratum oriens*, and a deep thicker band of neurons close to *stratum radiatum*, an abnormality that was detected along the rostrocaudal level of the hippocampus (Kappeler et al., 2007; Nosten-Bertrand et al., 2008; Bazelot et al., 2012). Disturbances in the morphology of pyramidal cell layers in the CA3 region was noticed in the two heterotopic layers. Apical dendrites of pyramidal cells in the SPE were typically shorter than those of WT pyramidal cells, while basilar dendrites of cells of the SPI layer were less profuse (Bazelot et al., 2012).

Time-lapse imaging has demonstrated defects in the migration dynamics of ventrally derived interneurons, originating from the medial ganglionic eminance. Tangentially migrating interneurons in *Dcx* mutants had more frequent, less stable formation of new branches in the growth cone. This resulted in cells migrating in a disorganized manner, making shorter nuclear jumps. Despite this abnormality, migration speed and distance was identical to the WT neurons (Kappeler et al., 2006). These experiments provided important insights on cellular roles of *DCX* during interneuron migration. However, the functional consequences of this abnormality in the number and

distribution of several interneuronal populations in mutants' cortex and hippocampus is not yet performed.

Abnormalities in neurons originating from the anterior subventricular zone and migrating along the rostral migratory stream en route to the olfactory bulb have been describes as will. Severe morphological defect in the rostral migratory stream and delayed neuronal migration was detected in Dcx mutants (Koizumi et al., 2006). DCX is required for nuclear translocation and maintenance of bipolar morphology during migration of these cells. Highlighting an essential role of DCX in translocation of the nucleus and the maintenance of cell polarity (Koizumi et al., 2006; Belvindrah et al., 2011).

In addition to the above mentioned anatomical defects, corpus callosum agenesis was detected in Dcx mutants, exclusively maintained in S129*PAS* genetic background (Kappeler et al., 2007). Defects in the formation of the later-formed caudal part of the corpus callosum were detected, while the rostral part was able to form in some cases. Callosal abnormalities resulted in an abnormal position and form of the dorsal part of the hippocampus, thus it seems likely that the callosal agenesis directly affected hippocampal positioning in these mice (Kappeler et al., 2007).

Dcx mutants display hippocampal-onset epileptic seizures with secondary generalization to tonic–clonic convulsions (Nosten-Bertrand et al., 2008). Intracellular recordings of hippocampal pyramidal cells in the CA3 region showed that heterotopic cells are more excitable than WT pyramidal cells (Bazelot et al., 2012). Field recordings from Dcx KO brains' slices suggested that pyramidal cells had the primary contribution to spontaneous epileptiform activity; they receive strong inhibitory inputs during interictal events, and GABAergic signalling seemed preserved (Bazelot et al., 2012).

Despite the absence of the gross cortical migration defects in constitutional Dcx KOs in mice, *in utero* electroporation experiments using RNAi construct against Dcx revealed defective migration of later born, glia- guided radially migrating cortical neurons. (Bai et al., 2003; Ackman et al., 2009; Manent et al., 2009; Lapray et al., 2010). In this model, neurons prematurely stopped migrating to form subcortical band heterotopias within the intermediate zone and the future white matter. Other neurons migrated into inappropriate neocortical lamina within normotopic cortex. Migration

disruption was due to cell-autonomous and cell-non-autonomous defects, suggesting a cooperative radial migration model (Bai et al., 2003). SBH due to Dcx knockdown was associated with spontaneous epileptic activity (Manent et al., 2009; Lapray et al., 2010). The severity of the epileptic manifestations was positively correlated with both the size of the subcortical heterotopia and the age of recorded animals (Lapray et al., 2010). Interestingly, trials to stimulate the migration of aberrantly positioned neurons by reexpressing Dcx during critical postnatal period were successful. Reexpressing Dcx both reduced the SBH size, and the convulsant-induced seizure threshold to a level similar to that in malformation-free controls. These experiments confirmed the potential of successful therapeutic intervention in cases of abnormal migration, during narrow time windows, when the networks are sufficiently plastic and responsive to rescue trials (Manent et al., 2009).

CHAPTER 2: RESULTS

PREAMBLE

Human *DCX* mutations are associated with lissencephaly, subcortical band heterotopia and with syndromes of intellectual disability and epilepsy. DCX is a developmentally regulated microtubule associated protein that is important for cooperative stabilization of MTs in migrating and differentiating neurons during embryogenesis (Francis et al., 1999; Gleeson et al., 1999; Bechstedt and Brouhard, 2012) and newly born neurons in the adult brain (Brown et al., 2003). Neurons lacking DCX have nucleokinesis abnormalities and branching defects (Kappeler et al., 2006), and knockdown of *DCX* in pyramidal cells leads to an abnormally hyperactive centrosome, with loss of directional movement and spatial correlation with the nucleus (Sapir et al., 2008).

In *Dcx* KO mice, CA3 hippocampal pyramidal cells are abnormally laminated (Corbo et al., 2002); a double layer of loosely organized neurons is apparent in the CA3 region of the hippocampus from E17.5 onwards (Kappeler et al., 2007), instead of a single compact pyramidal cell layer present in wild type littermates. This is associated with spontaneous epilepsy (Nosten-Bertrand et al., 2008). *Dcx* KO pyramidal cells show a reduced dendritic length and cells are more excitable than their WT counterparts (Bazelot et al., 2012). Field recordings from *Dcx* KO young adult brain slices suggested that heterotopic pyramidal cells make a primary contribution to the spontaneous epileptiform activity (Bazelot et al., 2012). They receive strong inhibitory inputs during interictal events, and thus GABAergic signalling may be largely preserved (Bazelot et al., 2012).

The hippocampus plays a dual role in the primary or secondary pathogenesis of temporal lobe epilepsy in cases of heterotopia (Aghakhani et al., 2005; López H et al., 2010; Piao et al., 2010; Kitaura et al., 2012). In human patients, aberrantly positioned heterotopic cells in the hippocampus are strongly correlated with severe forms of pharmacoresistent epilepsy (Lehéricy et al., 1995; Watson et al., 1996; López H et al., 2010). Some studies suggest that the hippocampus is the primary epileptogenic focus even in cases of extrahippocampal heterotopias due to the existence of functional connectivity and electrical coupling with the hippocampus (Kitaura et al., 2012). Moreover, the hippocampus display abnormal interictal spiking activity in all cases of

periventricular heterotopia, and it is the unique structure involved in epileptogenesis in some reported cases (Aghakhani et al., 2005).

The development of mispositioned, heterotopic neurons, their molecular profiles, maturation and integration during brain wiring, and their eventual contribution to the genesis of hyperexcitable neuronal circuits have attracted the attention of researchers, trying to actively dissect the functional role of these cells. Several studies have reported that various types of heterotopic or dysplastic neurons present a modified gene or protein expression compared to their homotopic counterparts (Chevassus-Au-Louis et al., 1998; Rafiki et al., 1998; Finardi et al., 2006). The study of the maturation program of heterotopic neurons and their integration in neuronal circuits in the cortex has been performed in rodent models using acute *Dcx* knockdown experiments. In a rat model of *Dcx* knockdown during the embryonic period, a band of functionally active neuronal heterotopias was found to locate below a grossly normal appearing cortex (Bai et al., 2003; Ackman et al., 2009; Manent et al., 2009; Lapray et al., 2010). Interestingly, in this model, neurons located in the heterotopic region retained immature properties, and most of them displayed a delayed maturation of GABA-mediated signaling (Ackman et al., 2009). Homotopic cells were also hyperexcitable. In contrast, in a second model of *Dcx* knockdown in migrating neuroblasts of the rostral migratory stream during early postnatal stages, affected cells had abnormal migration and were found in ectopic positions (Belvindrah et al., 2011). These ectopic neurons matured precociously, and received GABAergic and glutamatergic synaptic inputs earlier when compared to their control counterparts in similar locations (Belvindrah et al., 2011). Thus, striking temporal differences in the maturation program were demonstrated in two different models of heterotopia due to *Dcx* loss of function.

In this project, we hypothesized that heterotopic neurons in the *Dcx* knockout mouse model have aberrant connections and function abnormally, and show different gene and protein expression. We are interested in identifying the intrinsic properties of these cells by studying their molecular profile, and understanding how changing their extrinsic environment due to mispositioning affects the normal developmental program and maturation sequence adopted by these cells. To achieve these goals we set to perform an in-depth characterization of the morphological organization, ultrastructural properties (article 1), and global gene expression profiling of these

cells during perinatal stages (article 2) and in the adult. We assumed that the intrinsic cellular properties of heterotopic neurons are refined and modified by the new environment imposed upon them. We hope that this multi-experimental approach will be combined in the future with translation of the molecular and cellular data obtained during this thesis work into functional characterizations of the properties of *Dcx* KO cells at critical periods and the integration of heterotopic neurons in the epileptic circuits using electrophysiological experiments. These combined experiments are expected to add to the richness of the literature concerning the characterization of heterotopic cells. Global interpretations of the obtained results, taking into account the temporal variation in morphological, cellular, ultrastructural, molecular and electrophysiological properties of these cells at perinatal and adult stages, will contribute to our comprehensive understanding of the implication of heterotopic and homotopic cells in the generation of developmental forms of epilepsy.

Specific objectives of my thesis project were:

1. To describe the general organization of *Dcx* KO heterotopic principal neurons with respect to each other and to other cellular types in the hippocampus, respectively at the postnatal age P0 (article 1).

2. To describe the ultrastructural features of *Dcx* KO neurons at P0 using electron microscopy (article 1).

3. To identify spatiotemporal and stable molecular profiles of *Dcx* KO neurons at P0 and in the adult hippocampus (article 2).

4. To identify perturbed developmental mechanisms and molecular biological functions in heterotopic neurons and their homotopic counterparts at P0 and in the adult, which might explain their potential contribution to the development of hyperexcitable circuits (article 2 and still ongoing).

We decided to study the P0 stage, to assess ultrastructural characteristics and global gene expression in the WT and *Dcx* KO CA3. From a technical point of view, P0 represents a stage when the hippocampal CA3 region of the *Dcx* KO is composed of

two distinct neuronal layers, that can be easily and specifically microdissected from each other. Additionally, from a developmental point of view, in rodents, P0 represents a stage where some late born CA3 neurons are still migrating, and most other neurons are expected to have reached their final destination in the pyramidal cell layer and to be differentiating (Angevine, 1965; Altman and Bayer, 1990). Therefore, this approach helped us in our aim, which was targeted at identifying developmentally regulated molecular markers with specific spatiotemporal expression patterns, and perturbed signalling pathways that are potentially involved in generating hyperactive circuits in the two populations of *Dcx* KO neurons.

In our research laboratory, we chose to use the *Dcx* KO mouse model generated by F. Francis, which is a chronic model generated and maintained on two different genetic backgrounds (Sv129Pas and C57BL/6), with very little inter-individual variability in each of them. While the use of *Dcx* KOs maintained on C56Bl/6 background is ideal for the study of the epileptic phenotype (Nosten-Bertrand et al., 2008), we noticed that in the SV129Pas background the two heterotopic bands are more obviously separated from each other (Kappeler et al., 2007) and this is still associated with hyperexitability in vitro (Bazelot et al., 2012). The clarity of the morphological phenotype on this background encouraged us to use these mice for the morphological and the ultrastructural analysis, and to separate them using laser capture microdissection. Despite the hyperexcitability of the *Dcx* KO cells on the SV129PAS background, it is well documented in the scientific literature that this genetic background is resistant to epileptic seizures (Frankel et al., 2001; McKhann II et al., 2003). Therefore, this was a second reason justifying the use of this background for the molecular profile analysis of these neurons, particularly in adult animals, where epileptic seizures could confound the molecular signatures, related more to consequences of epileptic seizures, rather than being related to the intrinsic properties and unique molecular signatures of heterotopic cellsin a perturbed tissue environment.

Due to technical difficulties of the microarray hybridization protocol beyond our control, and limited amounts of RNA obtained from laser capture microdissection material; the generation of molecular data at P0 and in the adult was delayed. P0 data has now been successfully generated and analyzed. Normalized data was obtained last July, and pathway analyses were then performed. These analyses seem to agree with and complement the ultrastructural results which had been generated previously

(article 1). For adult transcriptome, new data was very recently generated, and pathway analyses still need to be performed, as well as validation of differentially expressed genes by qPCRs. For these reasons, this data is not presented here. It will be of great interest in the future to compare this obtained set of results to the P0 dataset, and to potentially combine it with ultrastructural analyses in the adult. However, in my thesis manuscript, adult data will not be included because of time constrains.

ARTICLE 1:

Characterization of heterotopic neurons at the morphologic and the ultrastructural levels during development is performed, and results are presented in this article.

Pyramidal cells in the different hippocampal fields express unique, field-specific molecular markers. We set to identify the field markers of heterotopic neurons. Using electron microscopy, we were interested in studying the general organization of pyramidal cells in the two heterotopic layers in the *Dcx* KO CA3 region. Ultrastructural characteristics of these cells is described as well. Electron microscopy work was performed in collaboration with the electron microscopy group at the Institute du Fer à Moulin. Obtained results prompted us to study developmental cell death in the *Dcx* KO hippocampus at P2, and the identification of heterogenous non-pyramidal cells that are found abnormally positioned in the *Dcx* KO hippocampus.

Ultrastructural and cellular abnormalities associated with hippocampal heterotopia in neonatal doublecortin knockout mice.

Khalaf-Nazzal R[1-3], Bruel-Jungerman E[1-3], Bureau J[1-3], Sumia I[1-3], Roumegous A[1-3], Martin E[4,5,6], Olaso, R[7], Eirinopoulou T[1-3], Parras C[4,5,6], Rio J-P[1-3], Cifuentes-Diaz C[1-3], Francis F[1-3].

[1] INSERM UMR-S 839, Paris 75005;

[2] Université Pierre et Marie Curie, Paris 75005;

[3] Institut du Fer à Moulin, Paris 75005, France

[4] UPMC-Paris 6, Centre de Recherche de l'Institut du Cerveau et de la Moelle épinière, 75013 Paris, France;

[5]Inserm UMR_S 975, 75013 Paris, France;

[6]CNRS UMR 7225, 75013 Paris, France

[7] Plateforme de Transcriptomique, Laboratoire de Recherche Translationnelle, CEA/DSV/IG-Centre National de Génotypage, 2 rue Gaston Crémieux, 91057 Evry, France

Correspondance to: Fiona Francis, Institut du Fer à Moulin, 17 rue du Fer à Moulin, 75005 Paris France. Email: fiona.francis@inserm.fr

ABSTRACT

Doublecortin (*DCX*) is mutated in subcortical band heterotopia (SBH), a severe human cortical malformation characterized by cortical neuronal somata trapped in the white matter, and associated with epilepsy. Various mouse models exist with forms of heterotopia, but the composition and state of cells developing in heterotopic bands has been little studied. *Dcx* knockout (KO) mice show hippocampal CA3 pyramidal cell lamination abnormalities, appearing from the age of E17.5, associated with spontaneous epilepsy. The *Dcx* KO CA3 region is divided into two layers, thus resembling heterotopia. Here, we further characterized the pyramidal cell abnormalities in these mice postnatally. Electron microscopy revealed that the *Dcx* KO CA3 pyramidal cells layers at postnatal day (P) 0 are distinct and separated by an intermediate layer without neuronal somata. Morphology, organization and cytoplasm content appear different in *Dcx* KO CA3 pyramidal neurons, compared to wild type (WT) cells. Less regular nuclei, with mitochondrial and Golgi apparatus differences were observed. Immunohistochemistry experiments showed that caspase-3 dependent cell death was also increased in both the CA1 and CA3 regions of *Dcx* KO mice at P2.

Each *Dcx* KO CA3 layer at P0 was found to contain pyramidal neurons but also other closely apposed cells, displaying different morphologies. Quantitative PCR and immunohistochemistry for Olig1 revealed increased numbers of oligodendrocyte precursor cells (OPCs) in close proximity to *Dcx* KO pyramidal cells. Immature radial glial (Pax6, Sox2) and astrocytic markers (GFAP) showed no specific labeling in either the WT or KO pyramidal cell layers at this age. *In situ* hybridization experiments on the other hand showed somatostatin (Sst)-positive interneurons more frequently interspersed with KO pyramidal cells in some brain regions. These combined data hence provide a detailed characterization of the *Dcx* KO hippocampus in early post-natal stages and reveal ultrastructural and cellular abnormalities which may contribute to abnormal neuronal function and the development of hyperexcitability in this model.

Introduction

Heterotopic or aberrantly positioned cortical neurons (Chevassus-au-Louis and Represa, 1999) are often associated with epilepsy and intellectual disability. They arise in cortical malformations, the most severe of which are visible with ultrasound or magnetic resonance imaging (MRI) and are confirmed by neuropathological analyses. At least 40% of patients with intractable epilepsy are estimated to have severe abnormalities of cortical development, including white matter heterotopia (Farrell et al., 1992, Guerrini and Marini 2006). Lissencephaly is characterized by a smooth brain surface and a thickened and severely disorganized neocortex, organized in four ill-defined layers including a thick band of disorganized neurons extending into the white matter, as well as abnormally formed hippocampi (Harding, 1996, Kappeler et al., 2007). SBH, a milder cortical malformation of the lissencephaly spectrum, is characterized by a band of heterotopic neurons in the white matter, in addition to a relatively normal cortex (Barkovich et al., 1994). *Doublecortin* (*DCX*), *LIS*1, *reelin* (*RELN*) and *alpha tubulin 1A* (*TUBA1A*) are mutated in these disorders {des Portes, Pinard, et al. 1998 10 /id} with *DCX* being the gene most frequently mutated in SBH (des Portes et al., 1998b; Bahi-Buisson et al., in press).

Heterotopic neurons can arise during development by a variety of mechanisms. For example, neurons born close to the ventricle must migrate across long distances to reach their final position in the cortical plate (Gupta et al., 2002). Slowed or arrested migration can therefore stop neurons in their migratory trajectory, leading to abnormal final positioning (Lambert and Rouvroit, 1998). The physiopathological consequences of heterotopia and especially their link with the emergence of epileptiform activities are not well understood. Rare histological and immunohistochemical studies of human heterotopia have shown that they can contain both pyramidal cells and interneurons, and DiI tracing studies have revealed connections between heterotopic regions and subcortical/cortical regions (Hannan et al., 1999). In rodent models, acute inactivation of *Dcx* in the rat and simultaneous recordings of neurons present in a heterotopia and the overlying cortex has shown synchronous epileptiform activity in both heterotopic and homotopic cells (Ackman et al., 2009). Few studies have addressed the morphology and state of neurons developing in heterotopic bands, which could give clues to their later abnormal function in the adult.

Mouse models mutated for genes involved in SBH and type 1 lissencephaly in human are consistently associated with heterotopic pyramidal cells in the hippocampus. *Reeler* mice are the most severely affected, showing a grossly disorganized hippocampus and isocortex (Lambert and Rouvroit, 1998; Deller et al., 1999). *Lis*1 mutant mice have subtle defects in the isocortex but also severe hippocampal lamination defects, consisting of fragmented CA1 and CA3 pyramidal cell layers, and epilepsy (Fleck et al., 2000, Jones and Baraban 2007). More recently characterized *Tuba1a* mutant mice also have severe hippocampal lamination defects similar to *Lis*1 mutants, and only minor isocortical defects (Keays et al., 2007). *Dcx* KO mice are the least severely affected anatomically, with pyramidal cell disorganization largely restricted to the CA3 region of the hippocampus (Corbo et al., 2002; Kappeler et al., 2006; 2007). At embryonic day 17 (E17), a stage at which hippocampal neurons are still migrating across an intermediate zone (IZ) (Altman and Bayer 1990a), as well as a correctly forming pyramidal cell layer in the *Dcx* KO, an abnormal density of cells is observed in the IZ, particularly in the CA3 region and extending into the CA1 region, and this continues during late stages of embryogenesis (Kappeler et al., 2007). In the adult, two CA3 pyramidal cell layers are observed. Interestingly, these mice suffer from spontaneous epilepsy and show enhanced excitability in the disorganized CA3 region *in vitro* (Nosten-Bertrand et al., 2008). Using intracellular recordings and biocytin fillings, individual adult *Dcx* KO pyramidal cells were shown to have reduced dendritic lengths and to be more excitable than their WT counterparts (Bazelot et al., 2012). Since hippocampal circuits are well characterised, *Dcx* KO mice provide an excellent model to further study specific features of developing heterotopic cells and the way they may generate hyperexcitability.

Interneurons and oligodendrocyte precursor cells (OPCs) are derived from the ventral telencephalon and migrate extremely long distances to reach the hippocampus. The earliest generated interneurons reach the hippocampus by E14 (Danglot et al., 2006; Picardo et al., 2011) with major streams arriving from E15 onwards and to reach the CA3 region by E16 (Pleasure et al., 2000; Danglot et al., 2006, Manent et al., 2006). In late embryonic stages and postnatally, interneurons and OPCs move within the hippocampus to their final position (Danglot et al., 2006; Chen et al., 2008). Dentate gyrus granule cell production is temporally matched with the other cell

types (Deguchi et al., 2011), with numerous cells produced from E16 onwards (Altman and Bayer 1990b), migrating in a tangential subpial stream in the IZ during late stages of embryogenesis, to finally reach the dentate gyrus region (Nakahira and Yuasa, 2005), where production continues postnatally (Danglot et al., 2006). Also during this period, cell death is a physiological phenomenon with peaks of apoptosis observed in the rodent hippocampus between P0 and P2 (Knuesel et al., 2005; Liu et al., 2008; Wakselman et al., 2008). We set out to characterize the *Dcx* KO CA3 region during these postnatal stages.

Few ultrastructural analyses examining the content and aspect of heterotopic cells have been reported previously (Colacitti et al., 1999; Ono-Yagi et al., 2000). Performing an ultrastructural and morphological study to compare the state of CA3 hippocampal pyramidal cells at birth in the *Dcx* KO model revealed the nature of the lamination defect and the state of CA3 cells. Potential organelle abnormalities were identified in *Dcx* KO cells, as well as increased cell death. OPCs and certain interneuron populations were found interspersed within the pyramidal cell layers in early postnatal stages, which was not the case in WT. These combined data may provide clues to the abnormal functioning of pyramidal neurons in the adult.

MATERIALS AND METHODS

Animals

Dcx KO mice (deleted for *Dcx* exon 3) were generated by using the Cre-loxP site-specific recombination system, and crossed onto C57BL/6N and Sv129Pas backgrounds as described previously (Kappeler et al., 2006). Here, Sv129Pas *Dcx* KO mice exhibiting a double pyramidal cell layer in the CA3 region were studied. Dcx is present on the X chromosome, so male hemizygote (-/Y) mice have no functional Dcx protein (Kappeler et al., 2006). For all analyses male hemizygote KO mice were compared with littermate male wild type mice. These were generated by crossing heterozygote females with pure Sv129Pas males (Charles River, France). Mice were genotyped by PCR as described previously (Kappeler et al., 2006). Experiments involving mice were performed according to national and European ethical guidelines. For electron microscopy studies, 3 WT and 3 KO mice were analyzed on the day of birth. To study cell death and 3 WT and 3 KO animals were analyzed on

postnatal day 2 (P2). For immunohistochemistry 2 WT and 2 KO animals were analyzed at P2, and for *in situ* hybridization 2 WT and 2 KO animals were analyzed each at P2 and P60. For laser capture microdissection and quantitative PCRs (qPCRs) 5 WT and 5 KO mice at P0 were used.

In situ hybridization

P4 and adult brains were perfused transcardially and fixed using 4% paraformaldehyde (PFA) in phosphate buffered saline (PBS). Brains were postfixed overnight and were cryoprotected in 30% sucrose, embedded and frozen in OCT, and cut coronally using a cryostat at 20µm thickness. Adult brains were cut using a vibratome into 60 µm thick sections. Specific antisense RNA probes were generated for *Wfs1* (gene ID NM_011716)*, Necab2* (gene ID, NM_054095 and Thompson et al., 2008)*, KA1* (NM_175481) and *Sst* genes (NM_009215). (*Wfs*1 oligonucleotide sequences: forward TACGCCAAGGGCATCATT, reverse CACCAGGTAGGGCACCAG; *Necab*2 forward TACCATCGATTCAGACAACACC, reverse AGGTACTGTCTCAGGGAATCCA; *KA*1 forward CAGCGCATGGAGGTGCCCAT, reverse GGCTCGCTGCTGTTGGTGGT, Sst, forward ACGCTACCGAAGCCGTC, reverse GGGGCCAGGAGTTAAGGA). Frozen cryostat sections were rinsed 3 × 5 min in PBS, postfixed in 4 % PFA, rinsed in PBS 2 × 5 min, and treated with proteinase K (10 µg/ml) for 10 min. Sections were incubated in PBS + glycine (2 mg/ml), rinsed in PBS, and postfixed in 4% PFA, then rinsed in PBS. Tissue sections were hybridized at 70°C overnight with digoxygenin (DIG)-labeled probes diluted 1/100 in hybridization buffer (50% deionised formamide, 10% dextran sulphate, 1 mg/ml Yeast RNA, 1x Denhardt's solution). The next day, sections were sequentially washed in 2X saline sodium citrate (SSC) Tween 0.1% at 70°C then in maleate buffer (Maleic acid 100 mM, NaCl 150 mM, 0.1% Tween20, pH 7.5) at room temperature, following Bally-Cuif and Wassef (1994) For immunological detection of DIG-labeled hybrids, sections were first treated in blocking solution (2% blocking reagent-Roche Diagnostics, France, cat. 1096176, 20% sheep serum in maleate buffer). Sections were then incubated overnight at 4°C in the same solution containing sheep anti-DIG-alkaline phosphatase-conjugated Fab fragments (Roche) diluted 1/2,000. The following day, sections were washed 4 × 15 min in maleate buffer, 30 min in NTMT buffer (100 mM NaCl, 100 mM Tris-HCl, pH 9.5, 50 mM $MgCl_2$, 0.1% Tween 20).

The alkaline phosphatase chromogen reaction was performed in NTMT buffer containing 100 mg/ml nitroblue tetrazolium (Roche) and 50 mg/ml 5-bromo-4-chloro-3-indolyl phosphate (Roche) at room temperature for 1-7 days and stopped with PBS. Sections were mounted on glass slides, dried, counterstained using nuclear fast red and dehydrated in graded ethanol solutions, and coverslipped with Vectamount (Vector Laboratories). Sections were viewed with a Provis Olympus Microscope. Images were acquired with a Coolsnap CCD camera.

Antibodies and immunohistochemistry

For testing cell death, 3 WT and 3 KO pups at P2 were anesthesized (15 min-ice immersion), and then subsequently perfused transcardially with 4% PFA in 0.1 M phosphate buffer, pH 7.4. Brains were removed and placed in the same fixative overnight at 4°C. Brains were then transferred to 30% sucrose in 0.1 M PBS, pH 7.4, and were frozen in OCT and serially cut in 16-µm thickness coronal sections using a cryostat (Leica). Every 12^{th} section was collected on Superfrost Plus slides and dried overnight before being processed for immunofluorescence. Rabbit anti-activated caspase-3 (#559565, BD Pharmingen, France) was used to detect apoptotic cells using immunofluorescence. Briefly, after several rinses with PBS, sections were permeabilized with PBS containing 0.25% Triton-X100 (PBS-T) and then incubated for 1 hr at room temperature in the blocking solution (PBS-T containing 5% Normal Goat Serum). Sections were incubated with the primary antisera (1/500) overnight at 4°C and then rinsed, blocked and incubated with Alexa-568 conjugated goat anti-rabbit antibody (1/600, Invitrogen France) at room temperature for 1 hr. After several rinses, sections were counterstained with DNA dye bisbenzamide (Hoechst 33342, Sigma; 1 µg/mL), and coverslipped under fluoromount-G (SouthernBiotech, Birmingham, AL, USA).

Caspase-3 positive cells were counted in both CA1 and CA3 regions of the dorsal

hippocampus across a surface of approximately 5 x 10^5 (CA1) and 2 x 10^5 (CA3) µm².

A 40x objective mounted on a LEICA DM6000 microscope was used for manual counting. The area of the surface was calculated on corresponding Hoechst images

using Image J software. 7 sections (each 192 µm apart) per animal were analyzed for 3 WT and 3 KO animals. Counting of the number of caspase 3 positive cells was conducted in a blind manner. The density of Caspase-3 positive cells was calculated by dividing their number by the corresponding area. Average densities per animal were estimated and compared between groups with Student t test using the GraphPrism software.

To characterize the cell fate of the ectopic cells found in CA3 DCX mutant layers we used a panel of different neural precursor marker antibodies listed above. Rat anti-Pdgfra (1/800, BD biosciences, cat # 558774) was used as oligodendrocyte precursor marker. Rabbit anti-GFAP (1/1000, Dako # Z0334) and rabbit anti-Ndrg2 (1/500; Okuda et al., 2008, kind gift from T. Miyata) were used as astrocyte markers. Rabbit anti-Pax6 (1/500, Abcam, #ab5790), rabbit anti-Sox2 (1/500, Millipore AB5603) and mouse anti-Nestin (1/500, Millipore MAB353) were used as more immature precursor markers. Immunostaining was carried out according to the same protocol described above. Corresponding secondary antibodies coupled to Alexa-488 (green), Alexa-495 (red) and Alexa-647(far-red) (1/1000, Invitrogen, France) were used for different antibody combinations. Immunofluorescence was visualized with a Zeiss AxioImager Z1-Apotome system microscope. Pictures were taken with a 20X objective as stacks of 3 to 5 mm with 0.5 mm per between sections. Z-projections projections were done in ImageJ and processed with Adobe Photoshop. Figures were made using Adobe Illustrator.

Laser capture microdissection (LCM) and quantitative PCR

To prepare RNA from CA3 pyramidal cell region, laser microdissection was performed. Coronal brain sections (12 µm) containing the rostrocaudal hippocampus from *Dcx* KO and WT mice were prepared using a cryostat at -20°C and mounted on PENmembrane slides (1440–1000, PALM, Bernried, Germany) which were pretreated by RNase ZAP (Ambion) and UV irradiated for 30 min at 254 nm. After sectioning, slides were stored at -80°C for further use within 1 week. On the day of LCM, the slides were removed from the -80°C freezer, and immediately fixed in 70% ethanol prepared in RNase free water (Invitrogen) for 2 min and then in 50% ethanol for 5 sec and stained with cresyl violet 1% (Sigma Aldrich, France) for 1 min.

Subsequently, slides were rinsed and dehydrated using graded series of ethanol (50% for 5 sec, 75% for 5 sec, 100% for 30 sec). Sections were air-dried and subjected to LCM within the next 30 minutes. In WT animals, the single CA3 pyramidal cell layer was microdissected (Zeiss LCM system), in *Dcx* KO animals, internal and external heterotopic CA3 cells were microdissected. Per WT sample (n=5), the entire CA3 structure (bilateral) was excised from 60 sections and pooled, corresponding to an area of 3.2×10^6 μm^2. Per KO sample (n=5), the same was performed for the internal (area of 1.2×10^6 μm^2) and external layers (area of 2.8×10^6 μm^2).

Total RNA was isolated using Arcturus picopure RNA isolation kit according to manufacturer instructions. RNA was eluted in 13µl of the elusion buffer provided in the kit. RNA quantity was measured using a Nanodrop ND-1000 spectrophotometer (ThermoScientific). RNA quality was checked using by analyzing 1 µl of RNA on the Agilent 2100 Bioanalyzer (Agilent Technologies, USA) using the RNA 6000 Pico LabChip Kit (5065-4473, Agilent Technologies, Palo Alto) according to manufacturer's instructions. To generate cDNA for qPCR experiments, RNA reverse transcription and amplification was performed using Nugen Ovation Pico WTA system following manufacturer's instructions.

Real time qPCR assays using the SYBRgreen method followed MIQE guidelines (Bustin et al., 2009). Gene-specific primers for Olig1 (forward CGTCTTGGCTTGTGACTAGCG and reverse GCCAGTTAAATTCGGCTACTGTC) and for GAD1 (forward TGTGACTCGCTTAGCTGAAACCTA and reverse GTCAGTGTATCGGAGGTCTTCAGA) were designed using Primer Express Software (PE Applied Biosystems). Amplicon size were respectively 124 bp and 58 bp. Standard curves were generated from assays made with serial dilutions of cDNA to calculate PCR efficiencies (90 % < efficiency < 105%, with r2 >=0.998). Threshold cycles (Ct) were transformed into quantity values using the formula $(1+\text{Efficiency})^{-Ct}$. Only means of triplicates with a coefficient of variation of less than 10 % were analyzed. Inter-plate variation was below 10 %. Values were normalized to the geometric mean of 3 Normalization Factors (NF) found to be the most stable through all samples using the geNorm approach. These were ATP synthase, H+ transporting mitochondrial F1 complex, beta subunit (Atp5b), eukaryotic translation initiation factor 4A2 (Eif4a2) and prosaposin (Psap).Average values ± standard deviations are

presented for 5 animals of each genotype (individual values are provided in Supplementary Table). Ratios were calculated and *P* values using the Student *t*-test.

Electron microscopy and morphometry

P0 mouse pups were euthanized by immersion in ice for 15 minutes after which they were transcardially perfused with 4% PFA and 2.5 % glutaraldehyde in 0.1 M phosphate buffer (PB). The brains were removed and placed in fresh fixative overnight at 4°C, rinsed in PB, postfixed in 2% OsO_4 (in PB), dehydrated in an ascending series of ethanol, and embedded in epoxy resin. Semi-thin sections (0.5 mm) were stained with toluidine blue and viewed with a Provis Olympus Microscope. Images were acquired with a Coolsnap CCD camera. Ultra-thin sections (40 nm thick) were mounted in either 200 mesh or one slot grids, cut and double stained with uranyl acetate and lead citrate prior to observation with a Philipps (CM-100) electron microscope. Digital images from the CA3 region were obtained with a CCD camera (Gatan Orius).

Morphometric analysis was performed with the software Digital Micrograph on two different mice of each phenotype. For each nucleus, the largest diameter was measured, and mean nuclear diameter was calculated from 50 neuronal nuclei per genotype. Only neurons displaying a clearly visible nucleolus were taken into account. Damaged and non-damaged mitochondria were counted in 20 SPI and 20 SPE cells. Golgi apparatus (GA) was analyzed in 50 cells from two WT animals and 50 from two KO animals.

RESULTS

CA1, 2 and 3 field identity in the hippocampus of *Dcx* KO mice

Histological studies to characterize the *Dcx* KO hippocampus were previously performed at different stages between E17 and P6 (Kappeler et al., 2007). At P0, two clear layers of pyramidal cells are obvious in the CA3 region, and a similar double layer of cells is observed in the adult, although the internal layer is generally thinner than the external layer (Figure 1 and Kappeler et al., 2007; Bazelot et al., 2012). We define these layers here as *stratum pyramidale* internal (SPI, thinnest layer, closest to the *stratum radiatum*) and *stratum pyramidale* external (SPE, thicker layer, closest to the *stratum oriens*).

In order to verify the identities of CA KO cells, we used adult hippocampal field specific markers in *in situ* hybridization experiments. *Wolfram syndrome gene* 1 (*Wfs1*) is a CA1 field specific marker (Lein et al., 2007; Dong et al., 2009; Fanselow and Dong, 2010, Fig 1A). In the *Dcx* KO hippocampus, we identify both normally positioned and a small number of heterotopic CA1 pyramidal cells close to the subiculum expressing this marker (Fig 1B, long arrows). Disorganized cells in the KO CA3 region do not express *Wfs*1. *N terminal EF calcium binding protein* 2 (*Necab*2), labels the CA2/CA3a region (the part of CA3 closest to CA2) and the outer border of the CA3b (the middle portion of CA3) cells in the adult (Fig 1C). This marker reveals where the splitting of the *Dcx* KO pyramidal cell layer occurs in the CA2/CA3 region (Fig 1D, long arrow). In the *Dcx* KO, *Necab2* appears to label CA2 pyramidal cells similar to WT, although we noticed using this marker that the pyramidal layer division extends most probably beyond the CA3 field to the CA2 field, and some *Necab*2 labeled cells in CA3b are observed in the superficial *Dcx* KO SPI layer (Fig 1D, short arrow), whereas they are normally found in the deep pyramidal layer close to the *stratum oriens* in this region in WT (Fig 1C). *KA*1 (glutamate receptor kainate type 1) is a well-known CA3 cell marker, whose expression is specified early on during hippocampal development (Tole et al., 2001). Although the splitting of the CA3 pyramidal layer in the KO model was clearly revealed with this marker, the pattern of labeling was similar in the WT and KO adult hippocampus, intense in the CA3 region and lighter in the CA1 region (Fig 1E, F). Thus in the *Dcx* KO hippocampus, pyramidal cells appear largely correctly specified with appropriate CA field markers, despite their abnormal positioning along the radial axis.

Electron microscopy shows two layers in the P0 CA3 region with different cell types and abnormal cellular profiles

To learn more about *Dcx* KO cells during development, we decided to characterize the double CA3 pyramidal cell layer at P0 using electron microscopy. Semi-thin sections were cut and serial ultrathin sections were mounted in one slot grids for identifying in these sections, the integral cellular layers of the CA3 region.

In coronal semi-thin WT sections, well-organized pyramidal cell nuclei, aligned along the same axis, were identified in a layer bordered by the *stratum oriens*

and the *stratum radiatum* (Fig 2A, C). In the *Dcx* KO sections, two cell layers (marked by black dotted lines) were visualized, present over a larger less cell dense region (Fig 2B, D). The two layers were clearly separated by an intermediary layer (IN) with a neuropil-like aspect. In WT, cells are closely packed and their nuclei display round or oval shapes enclosing one or two nucleoli (Fig 2C). In *Dcx* KO CA3, the SPE layer consisted largely of cells with an aspect of pyramidal neurons, distinguished from neuroepithelial cells in the *stratum oriens* by their neuronal nuclear aspect (Privat and Leblond, 1972) and their contiguous arrangement, without large free spaces that characterize the neuroepithelium (Fig 2D). The nuclei of cells in the SPE layer appeared aligned in at least three or four different superposed layers displaying different sizes and shapes. Nuclei in SPI, closer to the *stratum radiatum*, were found to possess more regular shapes and to be more regularly aligned. SPE and SPI KO nuclei were in general more widely spaced than in the WT layer and the average nuclear diameter was significantly smaller in SPE than in SPI and WT layers ($p<0.0001$, Fig 2E). (WT 9.396 +/- 1.341 μm, SPI 8.839 +/- 1.094 μm, SPE 7.126 +/- 1.192 μm, SPE versus WT Mann-Whitney test, $p<0.0001$). The IN layer separating SPI from SPE was found to be composed essentially of neuritic processes. Sometimes small or flattened nuclei, oriented parallel with respect to the neuroepithelium, neighbouring these processes were observed (Fig 2D).

Examination by electron microscopy at higher magnification (Fig 3A) showed that in WT mice the broad single layer appears regularly arranged in superposed layers of cells with a characteristic neuronal aspect displaying a clear abundant cytoplasm, and homogeneously shaped nuclei. Neurons starting from the border of the *stratum oriens* are found aligned (asterisks) and often display oval shaped nuclei. Superposed layers are composed of neurons in close apposition without specialized junctions (Fig 3C). Dark cellular profiles are sometimes observed in the adjacent soma, corresponding to ribosomes and cellular organelles such as mitochondria. These WT pyramidal neurons show a light cytoplasm (black asterisks, Fig 3C). *Dcx* KO sections examined at higher magnification showed that CA3 layers contain cells which are morphologically different from those observed in WT hippocampi (Fig 3B). A first cell type shows clear cytoplasm and bigger, round or elongated nuclei (black asterisks) enclosing light chromatin, similar in aspect to the neuronal chromatin in WT, with peripherally located nucleoli (Fig 3B). A second type of cell

with denser chromatin and darker cytoplasm (indicated with a white asterisk in Fig 3B) interspersed between neuronal-like cells were observed in both SPE and SPI. Such cells were in some cases found to entirely surround neuronal-like cells (data not shown) and were likely to display several short processes, occasionally present at each pole of the cell. Their nuclei showed irregular contours often smaller than neuronal-like cells. Their cytoplasm displayed a darker cytoplasm rich in organelles (Fig 3D). No specialized junctional complexes were observed between the darker cells and neuronal-like cells. Scarce cytoskeletal elements could also sometimes be observed.

In WT cytoplasm, mitochondriae were generally found to have a normal aspect, with clearly defined cristae (arrow in Fig 3C), whereas neuronal-like cells in both KO layers often showed damaged and swollen mitochondriae (Fig 3D). To further characterize the extent of such abnormalities we assessed the percentage of abnormal mitochondria in a number of randomly selected cells. In 20 analyzed somata of neuronal-like cells from both SPI and SPE, proportions of damaged mitochondria varied, with certain cells showing only 14 % abnormal mitochondria, and others as much as 88 %, with an overall average of 55 % for SPI cells, and 54 % for SPE cells (Supp Table 1). On the other hand, interspersed cells with darker cytoplasm closely juxtaposed to *Dcx* KO neuronal-like cells always showed intact mitochondriae with clearly defined cristae (arrowhead, Fig 3D). Thus probable mitochondrial abnormalities in *Dcx* KO cells appear cell-type specific and likely restricted to neuronal cells.

Nuclei in *Dcx* KO neuronal-like cells often showed an irregular or lobulated form compared to WT (Fig 4 compare A, B to D,E and G,H), and chromatin occasionally appeared clumped (data not shown). Golgi apparatuses also appeared modified in form compared to WT (Fig 4, compare C to F,I,J and Fig 5), exhibiting increases of cisternae with circular disposition (found in 64 % of cells, only 1.9% for WT), and of the presence of more than 10 Golgi vesicles (Fig 4J, and Fig 5 for quantification, 90.2% of cells, 9.1% in WT). Thus overall, the *Dcx* KO layers show cell heterogeneity, and *Dcx* KO neuronal-like cells appear to exhibit mitochondrial and Golgi apparatuses differences, whereas juxtaposed cells seem unaffected.

The *Dcx* KO IN space present in between the two KO pyramidal cell layers contains numerous heterogeneous, neuritic profiles and nuclei were largely absent from this region (Fig 4K-O). Neuritic profiles are not oriented uniformly and hence display heterogeneous forms, ranging from round to elongated. Some display a light cytoplasm containing tubulo-vesicular structures (arrow, Fig 4N) and possessing regions without cytoskeletal elements and with damaged mitochondria (Fig 4M). Microtubules, when obvious in neurites, often appeared less organized and less numerous in *Dcx* KO cells (Fig 6) and occasionally showed a wavy appearance (data not shown). Microtubule tracts could also appear shorter and frequently disconnected (Fig 6). On the other hand, some neighboring well filled neuritic profiles were also observed in the IN with a darker aspect enclosing cytoskeletal elements, ribosomes and rough endoplasmic reticulum (data not shown).

Synaptic contacts were observed at the border of the IN, in some cases likely to be immature, symmetric synapses of GABAergic cells contacting perisomatic regions of pyramidal cells (Fig 4O). They contain vesicles (arrow) opposite the postsynaptic zone. Thus, despite abnormal cellular profiles, at P0 synaptogenesis is already occurring in *Dcx* KO neuronal-like cells. Another potential contact observed, was directly established between apical neurites (black asterisk, Fig 4M) potentially emerging from a neuronal cell located in the SPE and extending to a neuronal soma in SPI (white asterisk, Fig 4L, M). This profile could represent a growing apical dendrite.

Cell death is increased in the *Dcx* KO hippocampus

The cellular aspects revealed at P0 by electron microscopy suggest some ultrastructural modifications at the level of the nuclei, Golgi apparatus and mitochondria. We also decided here to assess cell death in the *Dcx* KO hippocampus. Cells expressing activated caspase-3 were identified across the rostro-caudal extent of the *Dcx* KO dorsal hippocampus compared to WT littermate hippocampi (n=3 animals for each genotype). Previous studies have shown that peaks of developmental caspase-dependent cell death occur at P2 in the CA3 region of the rat (Liu et al., 2008) and P0 for the whole hippocampus of the mouse (Wakselman et al., 2008). In the absence of other studies describing peaks of cell death in the mouse CA3 region,

we performed an experiment at P2, which showed that in both WT and KO, activated caspase-3 labeled cells were present in highest densities in the CA3 region as well as, to a lesser extent, in the CA1 region (Fig 7A-D, white arrowheads). In both CA3 and CA1 regions, caspase-3 positive cells were predominantly present in the *stratum oriens*, although some cells could also be seen in the *stratum pyramidale* (Fig 7E-F). Overall, higher numbers of caspase 3 cells were found across the rostro-caudal extent of the hippocampi of *Dcx* KO animals as compared to the WT. Analyzing CA1 and CA3 regions separately, an approximately two-fold increase of caspase 3-positive cells was present in each hippocampal region in the KO compared to WT (Fig 7G-H, [in CA1 9 cells / 10^6 μm^2 in WT versus 15.8 cells / 10^6 μm^2 in *Dcx* KO, $P<0.05$; in CA3 28.3 cells / 10^6 μm^2 in WT versus 49.8 cells / 10^6 μm^2 in *Dcx* KO, $P<0.05$]). Thus increased cell death is a feature of the developing *Dcx* KO hippocampus.

Further characterization of *Dcx* KO cell types in close proximity to pyramidal cells

We set out to identify heterogeneous cell types, interspersed within, or in close proximity to, the *Dcx* KO pyramidal cell layers, identified by electron microscopy (Fig 3B). Anti-Pax6 and anti-Sox2, two markers of apical radial glial cell progenitors, normally present in the ventricular zone, were first used. Whereas Pax6- and Sox2-positive nuclei were seen in their correct position in the ventricular zone of both WT and KO brains, no positive nuclei were seen ectopically within the pyramidal cell layers (Supp Fig 1A-F). Similarly, we used anti-nestin, which labels intermediate filaments in radial glial cells, including their processes. Nestin immunoreactivity, although showing evidence of processes close to the neuroepithelium, showed no evidence of nestin-positive soma within the pyramidal cell layers (Supp Fig 1C-F). GFAP, a marker of mature astrocytes also showed no labeling at this stage in the vicinity of pyramidal cells in either WT or KO hippocampi (Supp Fig 1G, H), although some labeling was observed in the ventricular zone.

Platelet derived growth factor receptor α (Pdgfrα), a marker of OPCs, was next tested. In the WT CA3 region, cell somata were present in the *strata oriens* and *radiatum* but rarely in the pyramidal cell layer (Fig 8A). However, a number of OPCs were identified within and adjacent to the *Dcx* KO pyramidal cell layers (Fig 8 B-E

and Supp Fig 1). OPC nuclei were either horizontally, or vertically oriented (Fig 8C, arrows) and had extensive arborizations. In order to confirm the higher abundance of OPCs in the *Dcx* KO *stratum pyramidale* compared to WT, quantitative PCR (qPCR) was performed comparing another OPC marker, *Olig*1. For this, laser microdissection was used at P0 to separate the *Dcx* KO CA3 SPE from the SPI, and a similar region of the CA3 *stratum pyramidale* was microdissected in WT. qPCR results of *Olig*1, normalized against the geometric mean of three different reference genes, showed a two-fold upregulation of *Olig*1 in *Dcx* KO SPE compared to WT (Student *t*-test, p = 0.001, Supp Fig 2) and a six-fold up-regulation in *Dcx* KO SPI compared to WT (Student *t*-test, p = 0.004, Supp Fig 2). These combined results support a significant excess of OPCs interspersed within the P0 *Dcx* KO pyramidal cell layers.

Some further unlabeled, vertically oriented nuclei were also observed in the immunohistochemistry studies, suggesting the presence of other cell types. Some had an aspect of migrating neurons based on their oval shaped nuclei (Fig 8D, E1, red arrowheads). In order to further identify heterogeneous cell types intermingled in the pyramidal cell layers in the *Dcx* KO, we performed qPCRs for *Gad*1, a marker of interneurons. An upregulation of *Gad*1 was observed in the *Dcx* KO SPI at P0 (0.047 WT, 0.080 SPI, 1.7 fold upregulated in SPI, *P val.* <0.005, Student *t*-test, Supp Fig 2). We hence further tested interneuron markers, focusing on subpopulations present in the CA3 region perinatally, but not normally associated with the *stratum pyramidale*. At P4, somatostatin (Sst) interneurons were particularly abundant in the *stratum oriens* and we also observed cell bodies in the *stratum radiatum* throughout the WT hippocampus (Fig 9A, C, E, G), and in the hilus (data not shown). In the *Dcx* KO, although observed in such regions, Sst-positive cells were also consistently observed within the SPI or SPE, or the IN region (Fig 9B, D, F, H). The abnormal distribution of Sst interneurons was most pronounced in the rostral-mid parts of the hippocampus, in regions where the separation of the pyramidal cell layer into two distinct layers appeared more severe. Such cells were vertically, obliquely or horizontally oriented and some showed a potentially migratory morphology (Fig 9H, arrow). Thus some interneuron subpopulations in certain hippocampal regions, show disorganization in the early postnatal *Dcx* KO hippocampus, the latter found within and between the *stratum pyramidale*.

DISCUSSION

We characterized here the state of the *Dcx* KO hippocampus at early postnatal ages using field identity markers, electron microscopy, and using immunodetections and qPCRs to characterize cell death and ectopic cell types. Few previous studies have addressed aspects of abnormally positioned cells by electron microscopy, although analyses of the disorganized embryonic *reeler* cortex were previously performed, revealing cell mis-orientation but grossly normal neuronal differentiation (Goffinet, 1980). In the *Dcx* KO model at P0, we show that both SPI and SPE layers of cells are apparently less compact and heterogeneous compared to WT. There are some nuclear, Golgi network and mitochondrial differences compared to WT, specific to *Dcx* KO neuronal-like cells, which has not been previously shown to our knowledge in other mouse models related to type 1 lissencephaly. At P2, cell death is increased approximately two-fold in both CA1 and CA3 regions. Our combined data shed further light on how functional abnormalities might arise in the *Dcx* KO hippocampus, and may provide a basis for better understanding the consequences of the heterotopia and the development of cell hyperexcitability (Nosten-Bertrand et al., 2008; Bazelot et al., 2012).

Hippocampal field identities, recognized by particular genetic markers (e.g. KA1), arise early (Tole et al., 1997; Tole and Grove 2001, Deguchi et al., 2011). Thus, medial telencephalon culture experiments, with explants harvested at E12.5 when none of the field markers are yet expressed, have shown that hippocampal explants upregulate autonomously the expression of field-specific markers in culture, when analyzed three days later. Thus, the initial specification of hippocampal fields begins at least as early as E12.5 and does not require the surrounding cortical environment (Tole and Grove, 2001). We show here that despite pyramidal cell disorganization, due to retarded or arrested migration (Kappeler et al., 2007), cells appear largely correctly specified from subicular to dentate poles.

During development, hippocampal neurons are generated in the ventricular neuroepithelium and migrate across the IZ using radial glial cell processes as a substrate (Altman and Bayer, 1990a, Soriano et al., 1986). Radial glial cells progressively become more mature and this has been shown to be important for correct hippocampal development (Barry et al., 2008). In this study, no obvious

differences in nestin, a marker of radial glial cell processes, were observed. The peak of neurogenesis for the CA3 region occurs at E14 (Stanfield and Cowan 1979) and some CA3 pyramidal cells are still produced at E16 (Nakahira and Yuasa, 2005). Migration occurs across a 4 to 5 day period before cells reach the hippocampal plate, after pausing extensively in the IZ (Altman and Bayer, 1990a), perhaps waiting for coordinating signals from interneurons and dentate gyrus granule cells (Manent et al., 2006; Deguchi et al., 2011). In this study, we looked at the state of cells in early postnatal development, thus at a time when migration is expected to be largely complete (Altman and Bayer, 1990a; Danglot et al., 2006). The presence and position of two KO layers (SPI and SPE) suggests that some cells may become arrested in their migration and remain closer to or within the *stratum oriens* even in the adult (Corbo et al., 2002; Kappeler et al., 2007). Some clues were obtained from the EM data to explain the differences between SPI and SPE neurons. A difference in nuclear diameter was detected, which could be related to maturity (Nowakowski and Rakic, 1979; Madeira et al., 1992), with the SPE showing smaller and more electron-dense nuclei. A previous study of immature hippocampal neurons in foetal monkey brain showed that as migrating cells reach the pyramidal cell layer they become progressively more complex, with larger somata and less electron-dense nuclei (Nowakowski and Rakic, 1979). Our data are consistent with the idea that cells in the SPE are less mature and slowed or arrested in their migration compared to WT. SPI cells, on the other hand, may migrate using Dcx-independent mechanisms. Other abnormalities were identified similarly in both the SPI and SPE layers. Concerning cell heterogeneity, some oval-shaped nuclei were identified in *Dcx* KO SPI and SPE, which may correspond to pyramidal cell or interneurons which are still migrating, or are recently post-migratory. Indeed, electron microscopy images of radially aligned cells with a tapered leading process and often lobulated nuclei containing relatively dense chromatin were previously reported in the developing mouse brain by Pinto-Lord and colleagues (1982). Based on the identification of such cells in the KO SPI and SPE, it is possible that retarded or aberrant migration still continues in the *Dcx* KO during postnatal stages.

Despite migration abnormalities and abnormal cell organization, synaptic contacts are clearly being formed in the *Dcx* KO. Indeed, the IN layer seems to resemble neuropil, containing axons from SPI neurons, interneuronal cell processes,

and incoming mossy fibers. It is also likely to contain growing apical and basal dendrites of SPE and SPI pyramidal cell neurons, respectively. We previously showed in adult *Dcx* KO cells by biocytin labeling that SPE apical dendrites cross the SPI (Bazelot et al., 2012). Neurites from the SPE, observed by electron microscopy at P0 to extend up to and to contact SPI cells, may hence be such dendrites. Mature apical dendrites of SPE cells and basal dendrites of SPI cells in the adult showed reduced length compared to WT (Bazelot et al., 2012). Stunted dendrite growth might be a consequence of such a bi-layered organization. On the other hand, incoming mossy fibers have been shown to connect relatively normally to both layers (Kerjean et al., 2009; Bazelot et al., 2012), although some connections are retained on basal dendrites (Bazelot et al., 2012).

In evolutionary terms, the presence of hippocampal pyramidal cells extending into the *stratum oriens* in the adult has been previously documented in some mammals for the CA1 region (Slomianka et al., 2011). Indeed, a bi-laminar organization of CA1 naturally exists in the wallaby, possum and mole rat, although in this case, only the inner, superficial layer is compact, whereas the 'outer layer' represents a continuum of sparser cells (Slomianka et al., 2011). At P0 in the *Dcx* KO on the other hand, both cell layers seem relatively compact, they are separated by an intermediary layer and can be distinguished from other cell soma in the *stratum oriens,* most probably corresponding to migrating granule cells and neuroblasts, some late migrating pyramidal cells and interneurons (Danglot et al., 2006).

Although *Dcx* KO cells are compacted in layers, their extracellular environment may be permissive or attractive for colonization by OPCs and other cell types which insert themselves into the intercellular spaces. Some cells identified by EM with denser nuclei and somata may therefore be OPCs. It seems likely that these cells, which display normal organelles, do not normally express Dcx, which is largely restricted to the neuronal lineage (Francis et al., 1999; Zhang et al., 2010). Developing OPCs are proliferative cells that originate in the ventricular zones and migrate along axons toward a chemical gradient of Pdgf throughout the CNS (Armstrong et al., 1990; Rosenberg et al., 2008). Other contact-mediated mechanisms (adhesion molecules) and long-range cues (chemotropic molecules) are also likely to control their migration (de Castro and Bribián, 2005). They rapidly increase in number in the developing CNS between P0 and P7 and migrate extensively to populate the developing hippocampus before converting into differentiated

oligodendrocytes (Chen et al., 2008). The final fate of these *Dcx* KO OPCs present at P0 is still not known, although interestingly qPCRs still show up-regulation at P60 (Supp Fig 2). Potential aberrant signaling between neurons and OPCs (Kukley et al., 2010) could contribute to the generation of pro-epileptic circuits.

Concerning interneurons, we previously assessed the number of parvalbumin positive cells in the adult *Dcx* KO hippocampus, showing no overall differences in number compared to WT (Bazelot et al., 2012). Sst-positive cells represent a second major subpopulation, derived from the dorsal medial ganglionic eminence during development (Tricoire et al., 2011), which can co-express either reelin, neuropeptide Y or calretinin markers (Gelman et al., 2010). Sst-positive cell bodies can be found in the *stratum oriens* (Tricoire et al., 2011) and have also been described in the *stratum lacunosum-moleculare* (Danglot et al., 2006). Sst-positive cells are expected to contact the distal-most part of the apical dendrites of pyramidal neurons. Such cells may control dendritic calcium spikes (Miles et al., 1996) and play a role in controlling excitatory inputs from the entorhinal cortex. It is not yet clear if the Sst-positive cells that we observed within the SPI and SPE at P4 will remain permanently disorganized. This point is difficult to assess due to changes in this population with epileptic seizures, as reported by others (Kerjean et al., 2009). It will nevertheless be important to verify if the termini of such cells connect appropriately to both SPI and SPE apical dendrites.

Although more quantifications are required, it seems likely that organelle abnormalities exist in *Dcx* KO neuronal-like cells, with other adjacent cells, perhaps OPCs, spared. To our knowledge, abnormal mitochondria have not previously been reported in classical cortical malformation models, although they are associated with Zellweger syndrome (Baumgart et al., 2001) and more commonly in models of neurodegenerative disorders (Oettinghaus et al., 2012). Such abnormalities could stem from aberrant functioning of the microtubule network leading to organelle transport problems. Abnormal Golgi profiles have also been previously linked to microtubule depolymerization (Mourelatos et al., 1990). Dcx is a microtubule-associated protein (Francis et al., 1999; Gleeson et al., 1999) and subtle microtubule disorganization was previously detected in *Dcx* KO neurons in culture (Bielas et al., 2007). Microtubules were found to be splayed, fragmented, unevenly spaced and not condensed into a single shaft. As well as microtubule functions (Moores et al., 2004; 2006), Dcx may

also link organelles to microtubules by interacting with the μ subunit of the clathrin AP1 and AP2 adaptor complexes (Friocourt et al., 2001), which are involved in vesicle and cargo trafficking. Dcx-microtubules have also been shown to change the parameters of molecular motor (kinesin)-directed movement (Fourniol et al., 2010, Liu et al., 2012). Neurons mutant for two Dcx family members showed abnormalities in axonal transport and synaptic vesicle deficits (Deuel et al., 2006). Thus, mitochondrial abnormalities identified here could be a reflection of microtubule defects.

Alternatively, organelle differences may arise for other reasons eg more generalized cell stress, calcium signaling abnormalities (Napolioni et al., 2011), perturbed neurotrophic factors (Markham et al., 2012), or due to increased oxidative stress (Baumgart et al., 2001). It will be important in the future to identify the causes of these defects and assess the situation in adult *Dcx* KO pyramidal cells. Apoptosis may eliminate severely deficient cells during development, and autophagy may also play a role in their survival (Oettinghaus et al., 2012), allowing them to function in the adult. Acquiring further information of this nature may lead to the identification of novel neuroprotective treatment strategies for this type of lamination disorder.

Acknowledgements

We thank Nicolas Narboux-Neme for *in situ* hybridization advice, Sylvie Dumont for laser microdissection, Benoit Albaud and David Gentien for help with picochip analyses, Virgine Lavilla for help with quantitative PCRs. We thank A. Sobel for his constructive comments on reading of the manuscript. We thank the Inserm Avenir program, the French Agence National de la Recherche (ANR- 08-MNP-013), the Fondation Bettencourt Schueller and the Fondation Jérôme Lejeune for grant support to FF and Paris 6 and An-Najah universities for support to RKN. We thank the Ile de France region through the Neuropole (Nerf) for support of EBJ and animal house facilities and the FRC Rotary for confocal microscope equipment.

Figures:

Figure 1.

Field identity markers show correctly specified fields in the *Dcx* KO.

In situ hybridization results show *Wfs*1 (A,B), *Necab*2 (C,D) and *KA*1 (E,F) markers comparing adult WT (A, C, E) and *Dcx* KO sections (B,D,F). *Wfs*1 is present in the CA1 region and reveals some heterotopic CA1 cells close to the subicular region (arrows, B). *Necab*2 detects the CA2/CA3a region and labeling appears similar in the *Dcx* KO, although the splitting of the pyramidal cell layer into two is observed in this region (arrow, D). The *KA*1 marker most intensely labels the CA3 region, and the *Dcx* KO double cell layer is labeled with this marker. Scale bar, 60 µm.

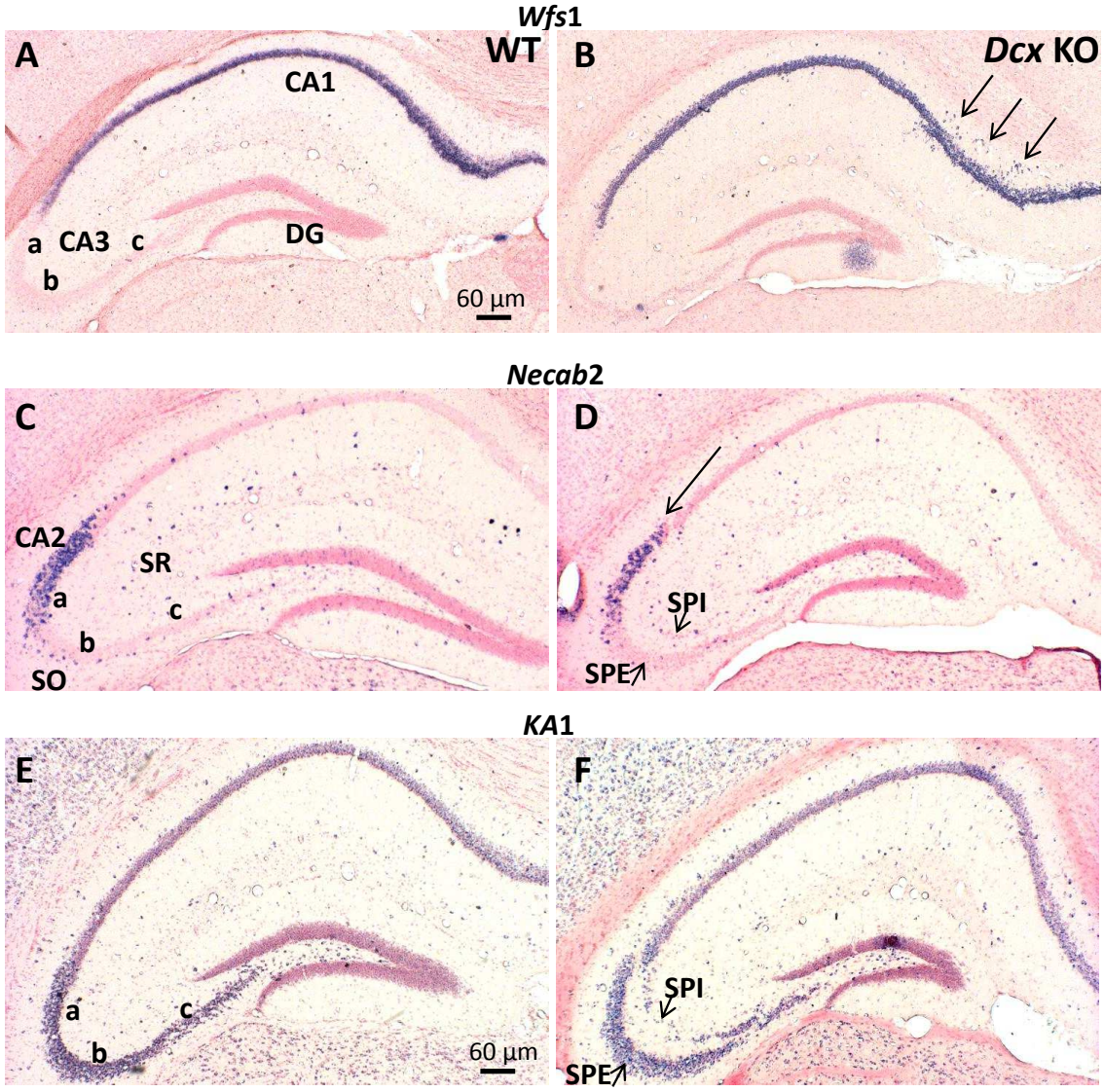

Figure 2

***Dcx* knockout mice display two neuronal layers in the CA3 region at P0 with different morphological features.**

(A, B) Light microscopy images of coronal semi-thin sections of the CA3 hippocampal region in wild-type (A) and KO mice (B), after toluidine blue staining. Neuron nuclei are seen in the CA3 pyramidal layers (delimited by black dotted lines). In WT (A) the pyramidal neurons contain nuclei with a similar aspect. In KO (B), two pyramidal cell layers are visualized, the external layer (SPE) closest to the neuroepithelium bounding the *stratum oriens* (SO), and an internal layer (SPI) in the *stratum pyramidale* region but positioned closer to the *stratum radiatum*. They are separated by an intermediary layer (IN) with a neuropil-like aspect. Each pyramidal cell layer contains nuclei with different shapes and sizes. Scale bars A, B: 15 µm.

(C, D) Electron micrographs from ultrathin sections of the CA3 region. (C) In WT, nuclei from the layer of pyramidal neurons are encircled in red. Neuronal nuclei were identified at higher magnification by their chromatin aspect and their size. They are larger than glial cell nuclei and their chromatin is lighter. Neuronal cells were closely packed and their nuclei display round or oval shapes containing one or two nucleoli. (D) In KO, nuclei of the pyramidal neurons in the SPE (encircled in pink) are often smaller than nuclei of the SPI (in green). In the intermediary layer, neuritic processes only are observed. Scale bar: 20 µm.

(E) Measurements of nuclear diameter. Nuclear diameters from WT and KO (not distinguishing between SPE and SPI), differ significantly (WT 9.39 +/- 1.34 µm, KO 7.98 +/- 1.42 µm, Mann-Whitney test, $p<0.0001$). Nuclear diameters from the SPI and SPE layers in KO mice are also significantly different from each other (SPI 8.84 +/- 1.09 µm, SPE 7.13 +/- 1.19 µm, Mann-Whitney test, $p<0.0001$). SPE nuclei are significantly smaller than WT (Mann-Whitney test, $p<0.0001$) and SPI nuclei not significantly different.

Figure 2

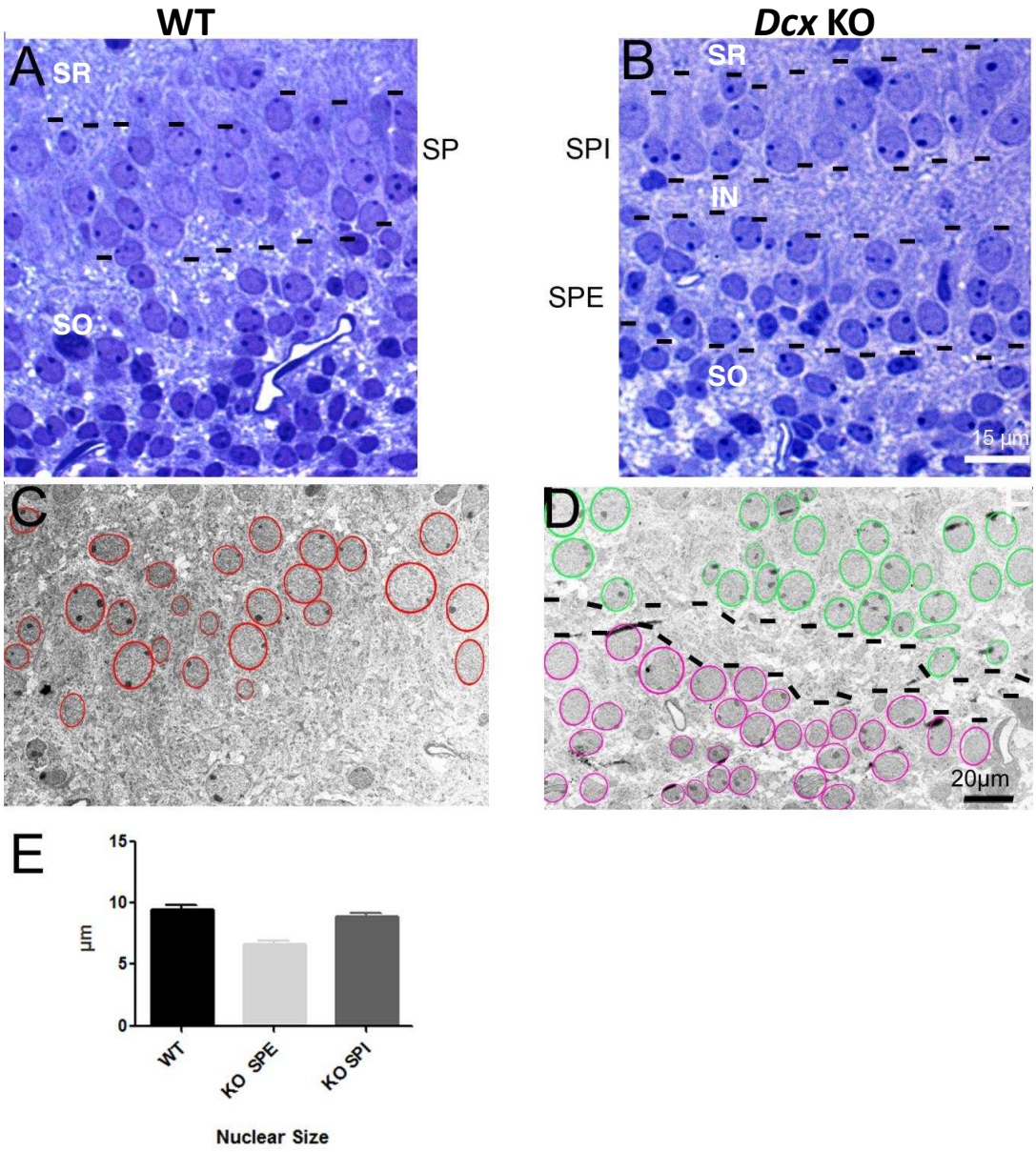
WT
Dcx KO
A
SR
SP
SO
B
SR
SPI
IN
SPE
SO
15 µm
C
D
20µm
E
15
10
5
0
µm
WT
KO SPE
KO SPI
Nuclear Size

Figure 3.

***Dcx* KO CA3 layers show heterogeneous and disorganized cells compared to WT**

A-D. Ultra-thin sections of the hippocampus from WT (A,C) and KO mice (B,D).

(A) In WT, the broad layer of pyramidal neurons (delimited by dashed black lines) shows a more regular arrangement of adjacent columns of cells displaying a characteristic neuronal aspect. Each column of cells has been marked either with an asterisk or a circle. A layer bordering the *stratum oriens* (SO) displays occasional oval elongated shaped nuclei (arrow). All nuclei are surrounded by a light cytoplasm.

(B) The KO external layer (SPE) bounds the SO (lower dashed black line) and the internal layer (SPI) is limited by the *stratum radiatum* (SR, upper dashed black line). In both the external and internal layers two types of cells are shown. One exhibits clear cytoplasm and larger nuclei (black asterisks) with round, elongated or lobulated shapes, enclosing light chromatin, similar in aspect to the neuronal chromatin in WT with peripherally located nucleoli. The second type of cell (white asterisks) has a darker cytoplasm and encloses nuclei with very dense chromatin. They are intermingled between neuronal-like cells and are closely juxtaposed to them. The elongated central cell shown in the SPI may resemble a radial-glial cell.

(C) High magnification of a WT pyramidal neuron showing its cytoplasm (black asterisks) and the cytoplasm of a neurite enclosing normal mitochondriae (arrow).

(D) Detail of two juxtaposed KO neuronal-like cells (recognized by their lighter cytoplasm indicated by black asterisks) with shrunken mitochondriae (arrow) and a cell with darker cytoplasm (white asterisk), exhibiting a normal mitochondria (arrowhead).

Scale bars: A,B: 5 μm; C,D: 0.5 μm.

Figure 3

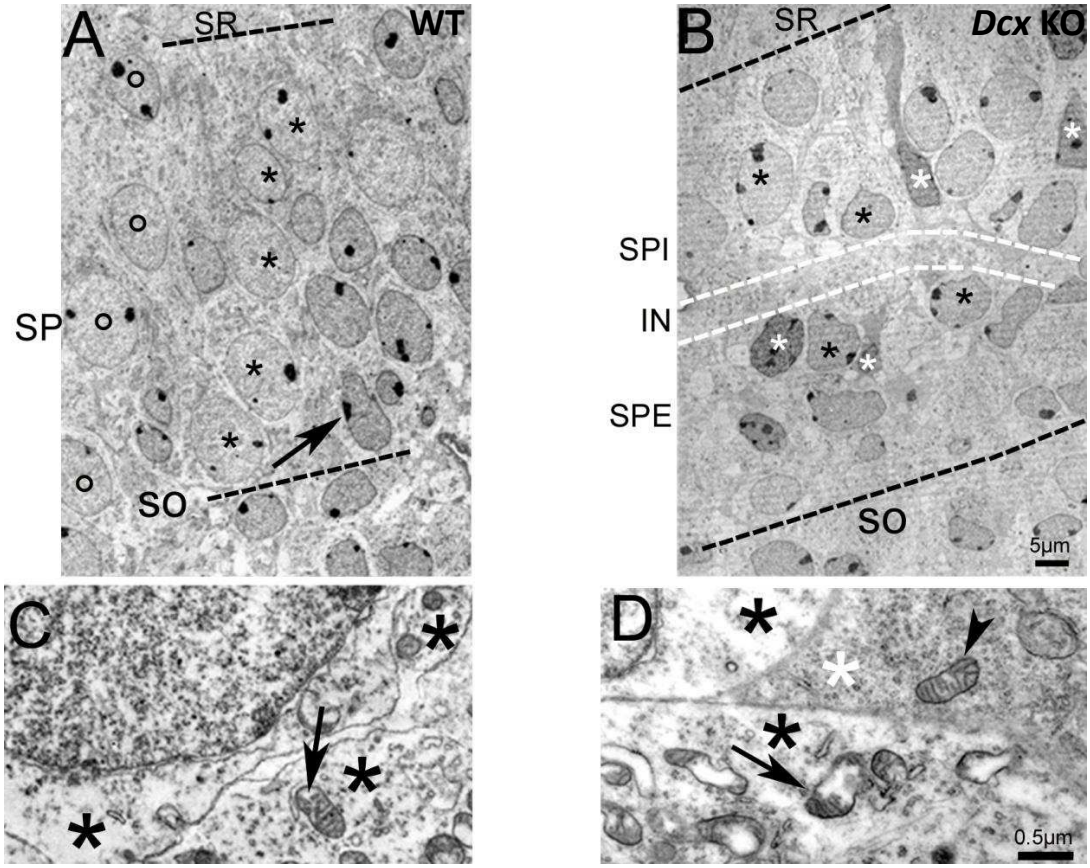

Figure 4

Ultrastructural organization of the *Dcx* KO CA3 SPI, SPE and intermediary layers compared to WT, showing details of nuclei, Golgi apparatus, neuritic profiles and synaptic contacts

Electron micrographs from ultra-thin sections of the hippocampus from WT (A-C) and KO mice (D-O).

(A) The pyramidal neurons are juxtaposed and regularly arranged in WT. The shape of their nuclei and soma are relatively homogeneous.

(B) Higher magnification of a nucleus illustrated in A (circle) showing the homogeneous aspect of the nuclear membrane.

(C) Typical aspect of the Golgi apparatus consisting of a parallel array of tubules and cisternae with few individual vesicles.

(D-F) In the internal layer (SPI), two types of cells are shown, pyramidal neuronal-like cells with a clear cytoplasm (asterisks) and a second cell type with a darker cytoplasm (circle). Their nuclei are visualized at higher magnification in E and F, respectively. Asterisks and circles indicate the same cells at different magnifications. F is a detail from the arrowed region indicated in D, showing the lighter cytoplasm adjacent to the darker cytoplasm. The thin arrow in F points to abnormal Golgi apparatus.

(G, H) In the external layer (SPE) similar cell types with light (asterisks) and dark cytoplasm (circle) are also identified.

(I) A Golgi apparatus is observed with dilated cisternae (arrow) adjacent to flattened curved cisternae.

(J) Two Golgi apparatuses are observed with flattened and curved sacculae and numerous vesicles (arrowhead) enclosed in a cell with light cytoplasm. Similar Golgi were identified in cells in the SPI.

(K) Low magnification showing the intermediary layer (IN) delimited by black dashed lines. Cells from the SPI (white asterisks) and from the SPE (black asterisks) flank numerous neuritic profiles enclosed in the IN layer.

(L) Higher magnification of K. In the IN itself, numerous, dense cellular profiles are visualized, corresponding to neuronal processes (likely to be immature dendrites and

axons) and synaptic contacts (see ‘O’). Arrow, arrowhead and ‘1’ correspond to zones presented at higher magnification in M, N and O respectively.

(M) is a higher magnification of the arrowed region in (K) showing a neurite from a cell located in the external layer (black asterisk) extending to and contacting (arrow) the soma from a cell in the internal layer (white asterisk). Note mitochondria organized on chains along the MT network.

(N) The cellular profiles in the IN display heterogeneous aspects: some of them with a light cytoplasm corresponding to transversal sections of neurites (higher magnification of arrowhead in L), contain tubulo-vesicular structures (arrowhead) and display regions without cytoskeletal elements.

(O) is a detail of an axo-somatic synaptic contact identified in L and M as ‘1’. A number of synaptic vesicles are observed (arrow). Similar synaptic contacts are observed in the SPE layer (not shown).

Scale bars: A, D, G, K: 3 μm; C,F,L,J: 0.2 μm; M: 0.5 μm.

Figure 4

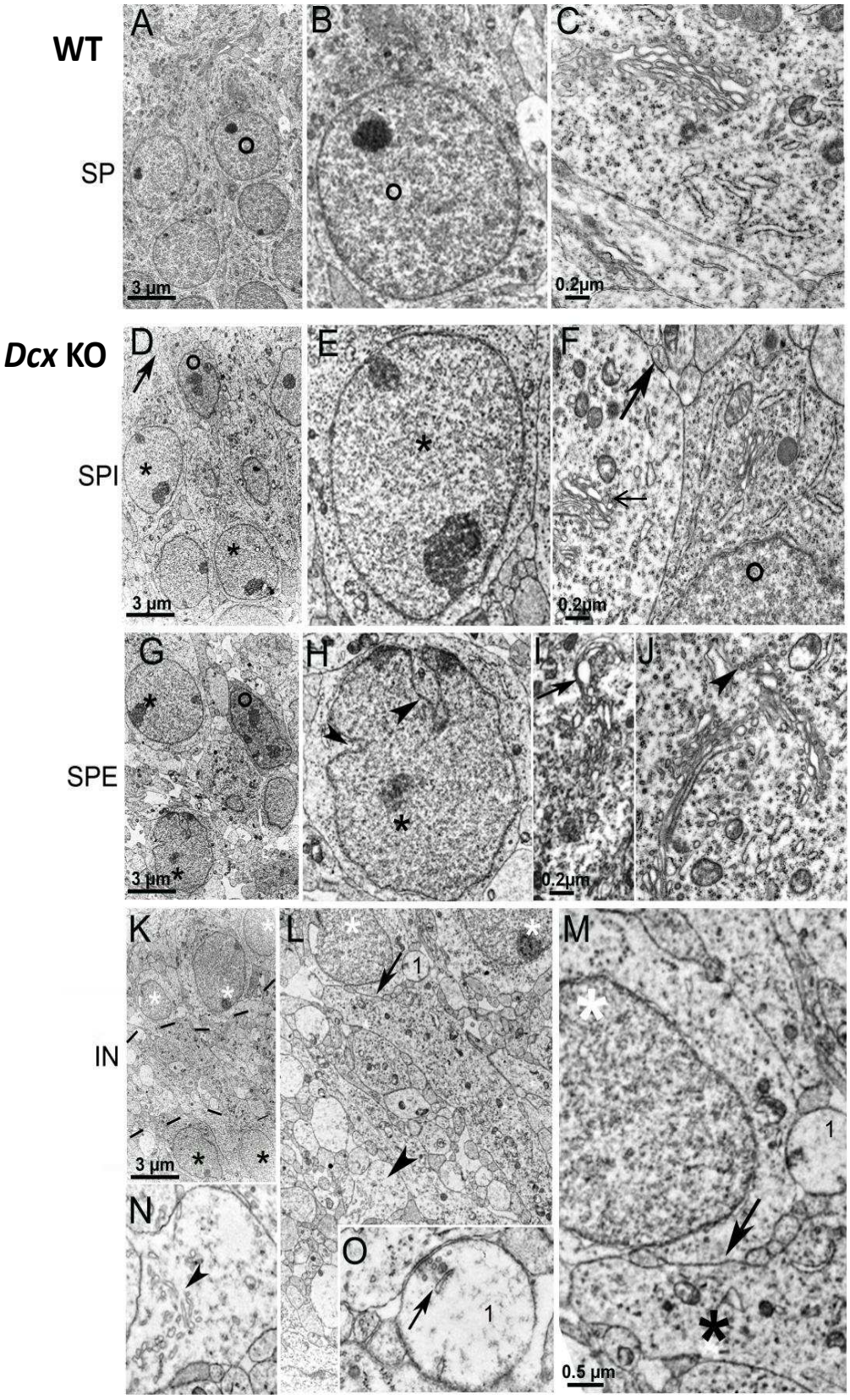
WT
SP
A
B
C
3 µm
0.2µm
Dcx KO
SPI
D
E
F
3 µm
0.2µm
SPE
G
H
I
J
3 µm*
0.2µm
IN
K
L
M
N
O
1
3 µm
0.5 µm

Figure 5

Ultrastructural organization of the Golgi Apparatus from *Dcx* KO and WT CA3 neurons

Examples of WT (A, B) and *Dcx* KO (C,D) Golgi apparatuses.

(A,B) Typical Golgi apparatuses (arrowheads) are observed consisting of a parallel array of tubules and cisternae with few individual vesicles.

(C,D) Golgi apparatuses in KO cells showing the heterogeneous aspect of the Golgi cisternae. Curved (arrow, C) and swollen (arrowhead, D) forms are displayed. Numerous vesicles (arrows, D) are associated with them. In some cases swollen cisternae (arrowhead) are adjacent to shrunk sacculae (double arrows) and several vesicles (arrow).

Scale bars: 0.5 µm.

(E) Quantitative analyses of the modified Golgi apparatus forms between WT and *Dcx* KO hippocampal CA3 cells. Mean percentage of the detected abnormality for each genotype. Note significant differences between the genotypes (significant two tailed *: *P. val*. < 0.05, **: *P val.* <0.005).

Figure 5

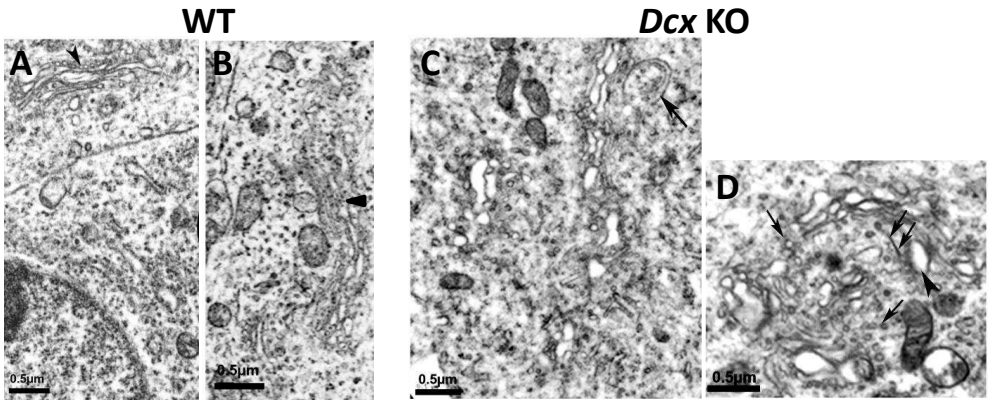
WT
Dcx KO
A
B
C
D
0.5µm
0.5µm
0.5µm
0.5µm

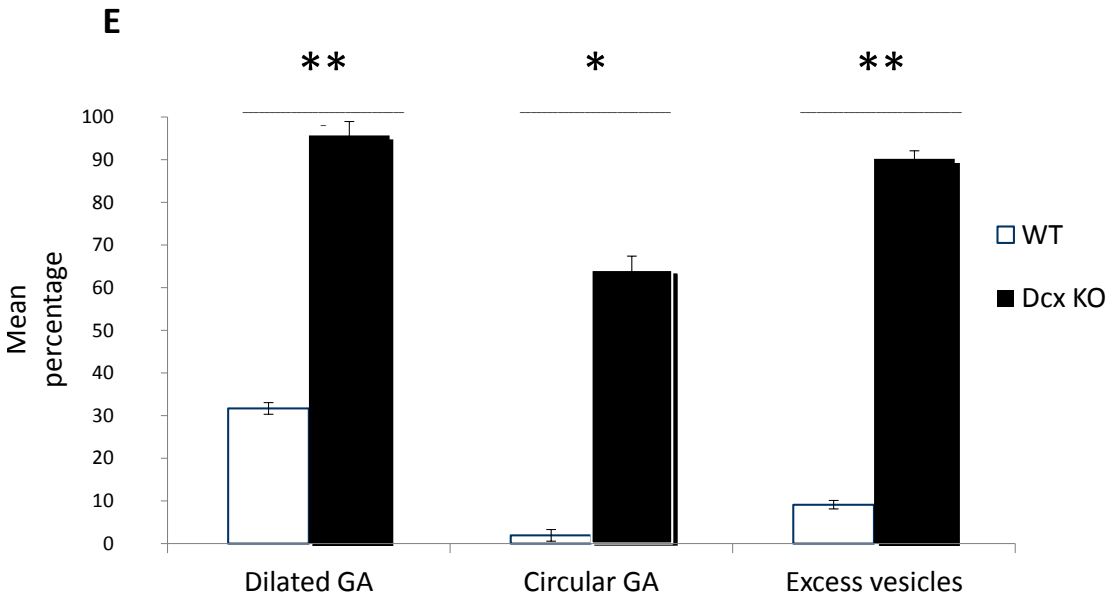
E
**
*
**
100
90
80
70
60
50
40
30
20
10
0
Mean percentage
WT
Dcx KO
Dilated GA
Circular GA
Excess vesicles

Figure 6

Abnormal microtubules in *Dcx* KO cells

Neurites of hippocampal pyramidal neurons from WT (A) and KO (B) mice.

(A) A neurite from a pyramidal cell neighboring the *stratum radiatum*, longitudinally sectioned, contains numerous adjacent microtubules closely arranged in parallel fascicles (arrowhead).

(B) In KO, a neurite from a pyramidal neuron from the internal layer shows sparser, fragmented microtubules (arrowhead).

Scale bar: 5 µm.

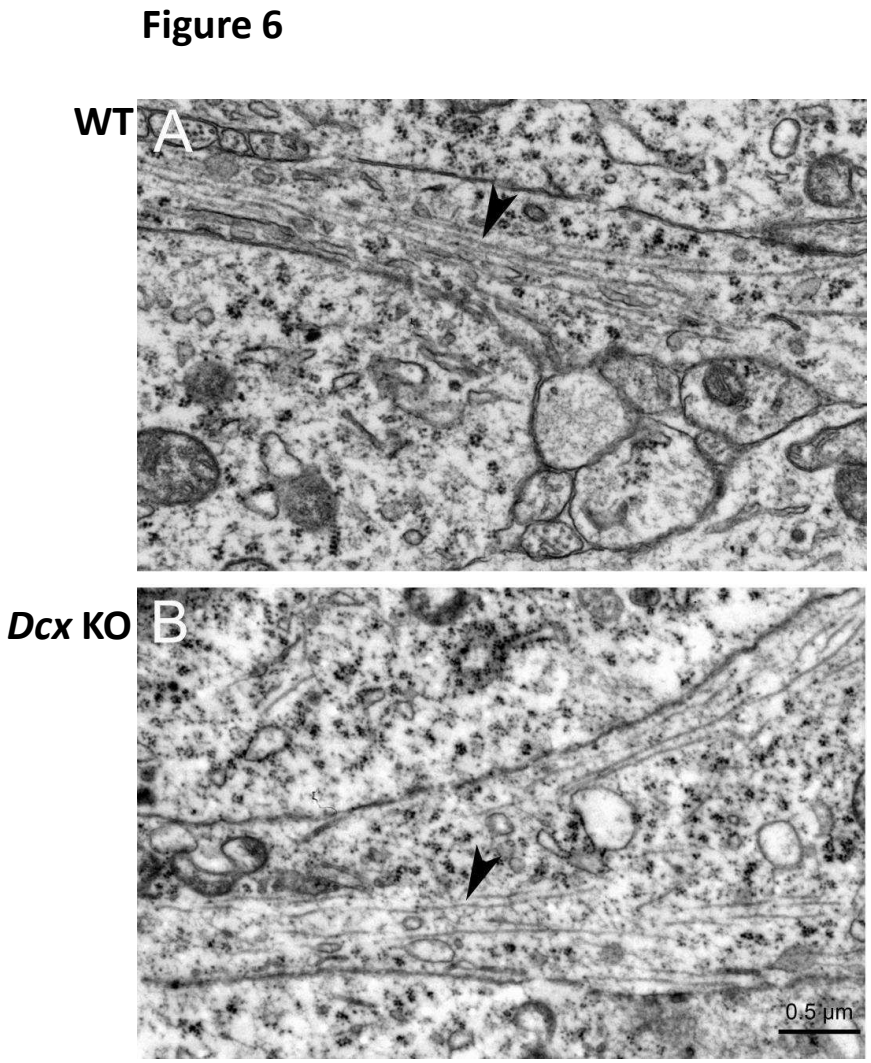

Figure 7

Apoptosis is increased in *Dcx* KO hippocampus.

Immunofluorescent coronal sections of WT (A, C, E) and *Dcx* KO (B, D, F).

(A-F) CA3 region of the hippocampus of P2 WT (A,C,E) and *Dcx* KO (B,D,F) mice showing immunoreactivity to activated caspase-3 (red) and Hoechst (white) at both rostral (A-B) and caudal (C-F) levels. Arrowheads in A-D indicate labeled cells with pyknotic nuclei, typical features for apoptotic cells.

(E-F) Higher magnifications corresponding to the inset regions in C and D. Caspase-3 positive cells are present in both the *stratum oriens* (SO) and the *stratum pyramidale* (SP) of the CA3 region of both KO (F) and WT (E) hippocampi.

(G, H) Bar graphs representing the cellular density of activated caspase-3 expressing cells in CA1 and CA3 regions respectively of WT versus KO hippocampi. $P<0.05$

Scale bars (A-D 100μm; E-F 50μm).

Figure 7

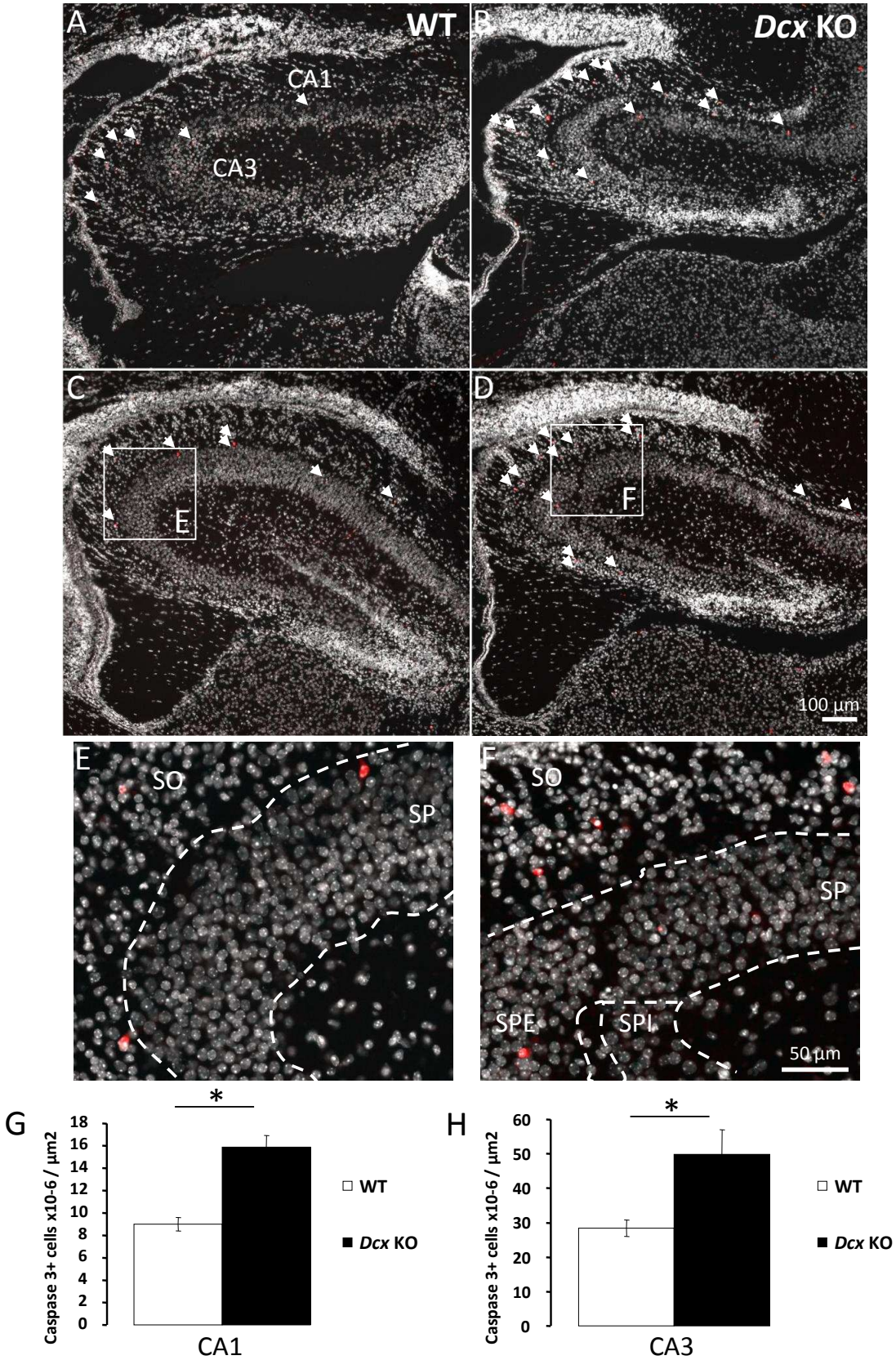
A
WT
CA1
CA3
B
Dcx KO
C
E
D
F
100 µm
E
SO
SP
F
SO
SP
SPE
SPI
50 µm
G
Caspase 3+ cells x10-6 / µm2
18
16
14
12
10
8
6
4
2
0
*
WT
Dcx KO
CA1
H
Caspase 3+ cells x10-6 / µm2
60
50
40
30
20
10
0
*
WT
Dcx KO
CA3

Figure 8.

Oligodendrocyte precursor cells (OPCs) intercalate between *Dcx* KO CA3 neurons.

Immunofluorescent coronal sections of WT (A) and *Dcx* KO (B-E).

(A-E) CA3 region of the hippocampus of P0 wild-type (A) and *Dcx* KO mice (B-E), showing immunoreactivity for Pdgfrα (green, a marker of OPCs) and DAPI staining for cell nuclei (white). Red arrows indicate several Pdgfrα^{+} cells, which are horizontally or vertically oriented, with ovoid nuclei intercalated between the CA3 neurons in *Dcx* mutants (B-E). No Pdgfrα^{+} cells were revealed in the pyramidal cell layer in WT (A). Arrowheads in D, E show ovoid nuclei in the CA3 region of the *Dcx* mutant that are Pdgfrα-negative. C and E are higher magnifications of the areas in the insets of B and D, respectively. Scale bars: 50 μm.

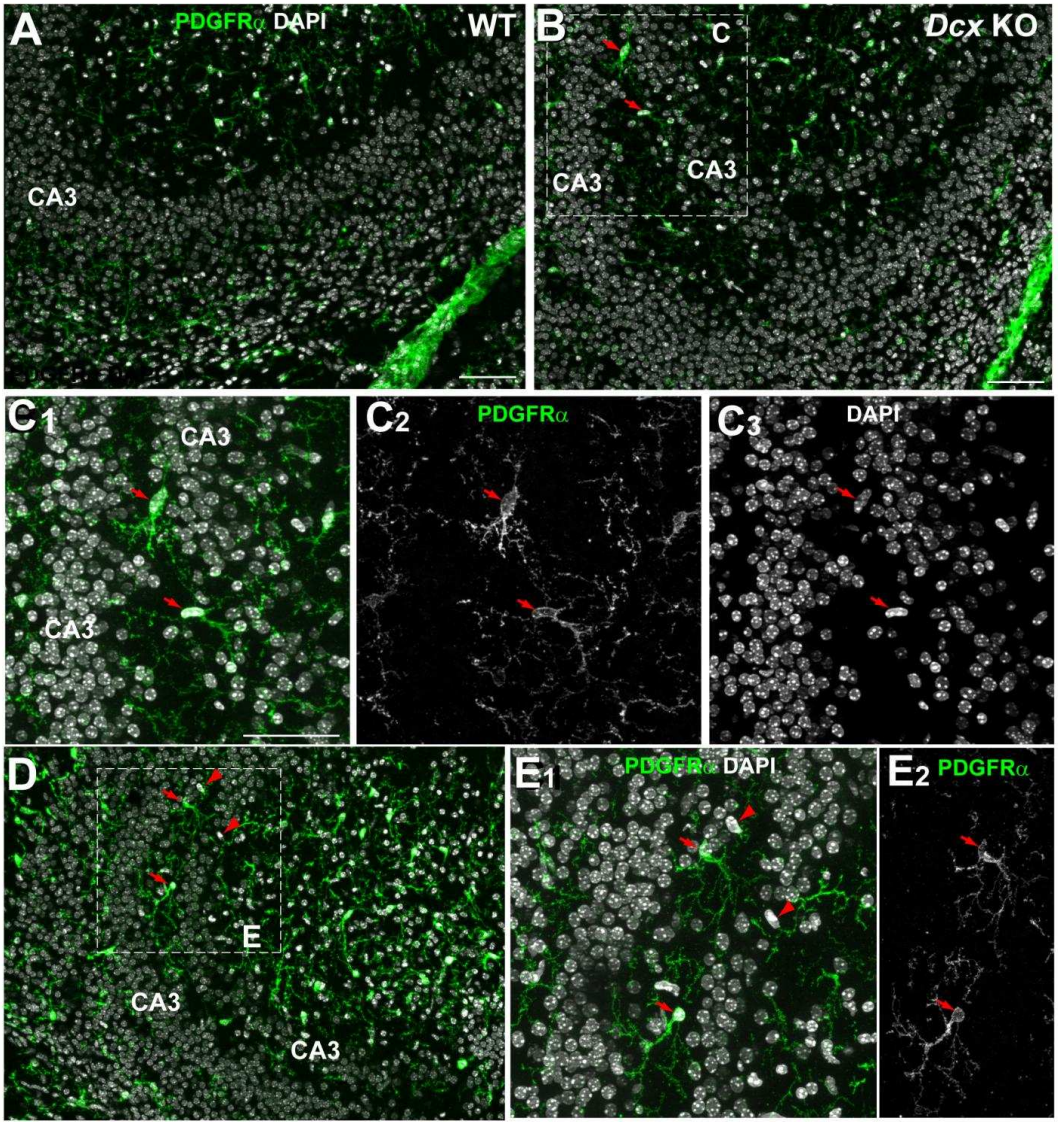

Figure 9.

Somatostatin-positive interneurons are disorganized and also present in the *stratum pyramidale* in rostral-mid regions of *Dcx* KO hippocampi.

Immunoreactivity to Sst in WT (A, C, E, G) and KO (B, D, F, H) coronal brain sections.

In situ hybridization results are shown at two rostro-caudal levels (A-D; E-H). C, D and G, H are higher magnifications of A,B and E,F respectively. In WT, Sst-positive interneurons are mainly restricted to the *stratum oriens* and hilar regions at this age. In the *Dcx* KO, some Sst-positive cells are consistently observed associated with the SPI, IN and SPE, although they are rarely observed associated with the *stratum pyramidale* in WT. Scale bars, A (for A, B, E, F) 100 μm; C (for C, D, G, H) 50 μm.

Figure 9

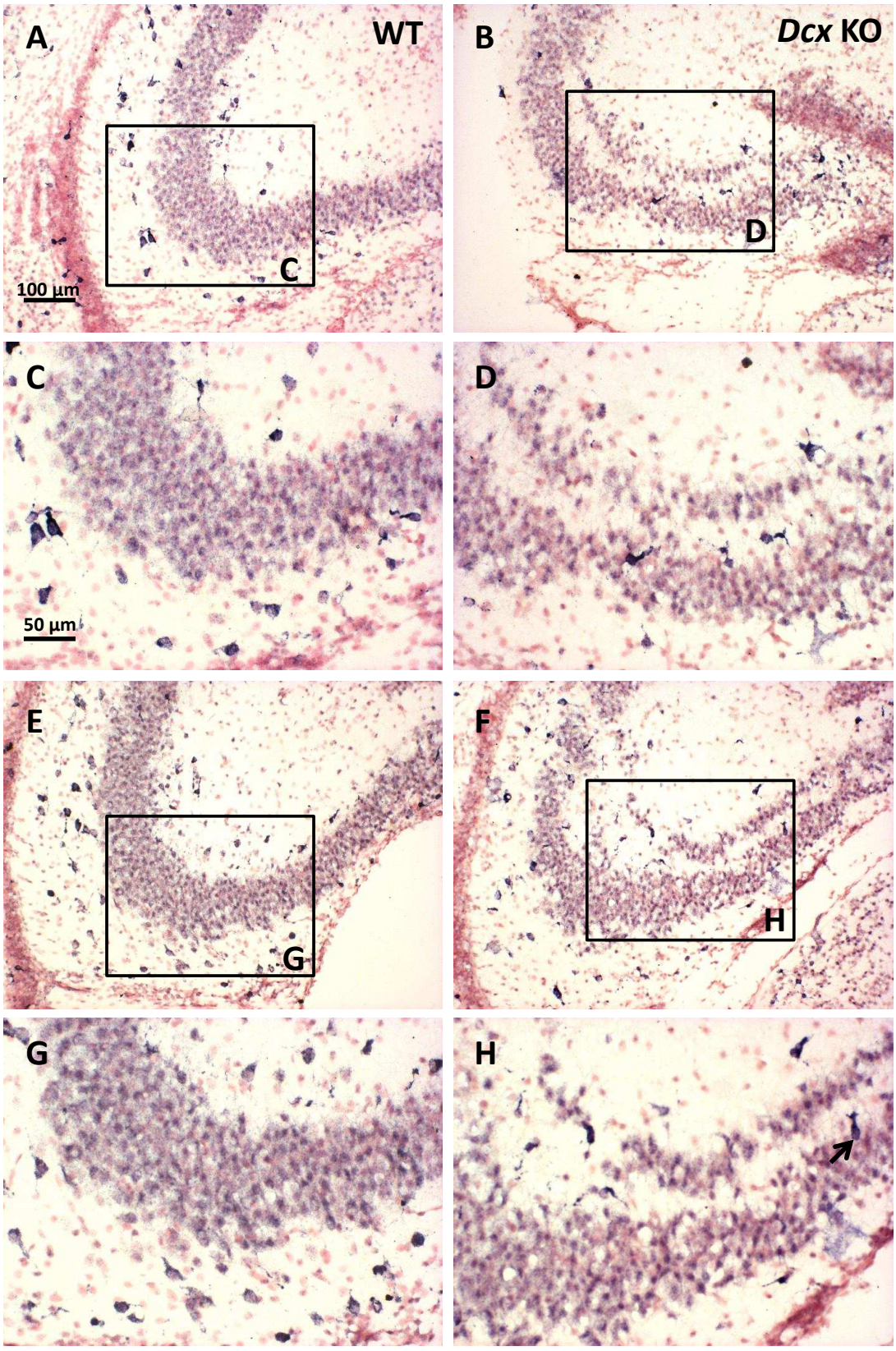

Supplementary Figure 1

OPCs but not astrocytes intercalate between CA3 neurons.

(A-H) Coronal sections through the CA3 region of the hippocampus of P0 WT (A) and *Dcx* KO mice (B-H). (A-B) Sections immunostained for Pdgfrα (red), Pax6 (green) showing that $Pax6^+$ cells are only present in the ventricular region, but no ectopic Pax6 cells are found in the mutant CA3 layers. (C-F) Sections immunostained with Sox2 (red), Pdgfrα (green) and Nestin (light blue) showing that no immature precursors are intercalated between CA3 neurons in *Dcx* mutant hippocampus. Note that some $Sox2^+$ cells (arrowheads) can be found below the CA3 region as a stream of cells migrating towards the dentate gyrus (C) or in the *stratum radiatum* (E, F arrowheads). E, F are magnifications of boxed areas in C, D. (G, H) Sections immunostained with antibodies for astroglial markers Nrdg2 (red), GFAP (pink), and OPC marker Pdgfrα (green) showing that only OPCs but not astrocytes intercalate between the CA3 neurons in *Dcx* mutant hippocampus. Note that astrocytes are close to the ventricular surface (G, arrowheads). H is a higher magnification of the area in the inset of G. Scale bars: 50 μm.

Supp Figure 1

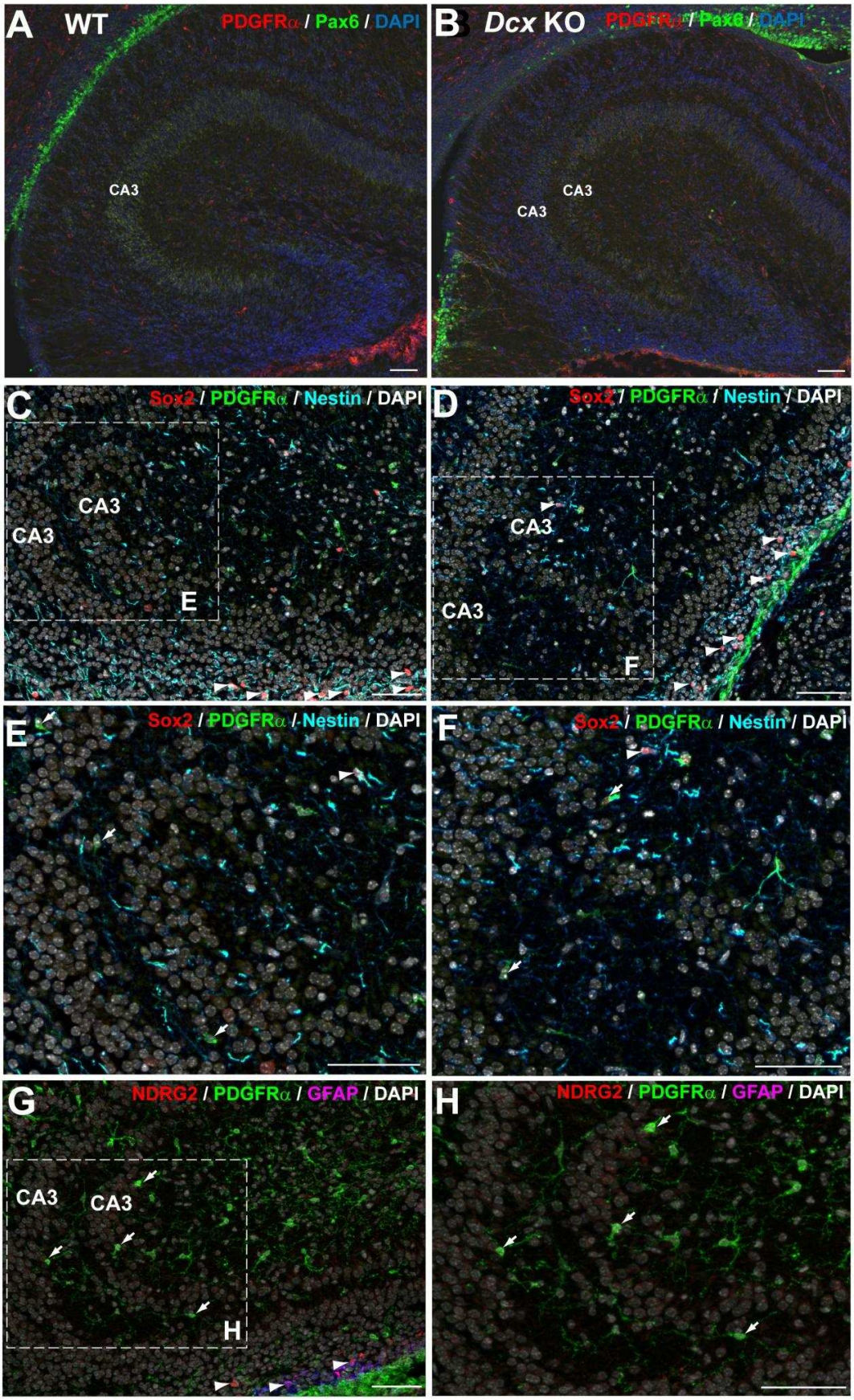

Supplementary Figure 2

RT-qPCR quantifications related to the observed cellular heterogeneity revealed by immunodetections. *:

Significant two tailed *P. val*. < 0.05, **: Very significant two tailed *P val.* <0.005. *Olig*1 is upregulated in both SPI and SPE at P0, and remain significantly up-regulated in SPI in adult (P60). Interestingly, it is downregulated in SPE in the adult. *Gad*1 shows upregulation in SPI at P0 and has not yet been tested in the adult.

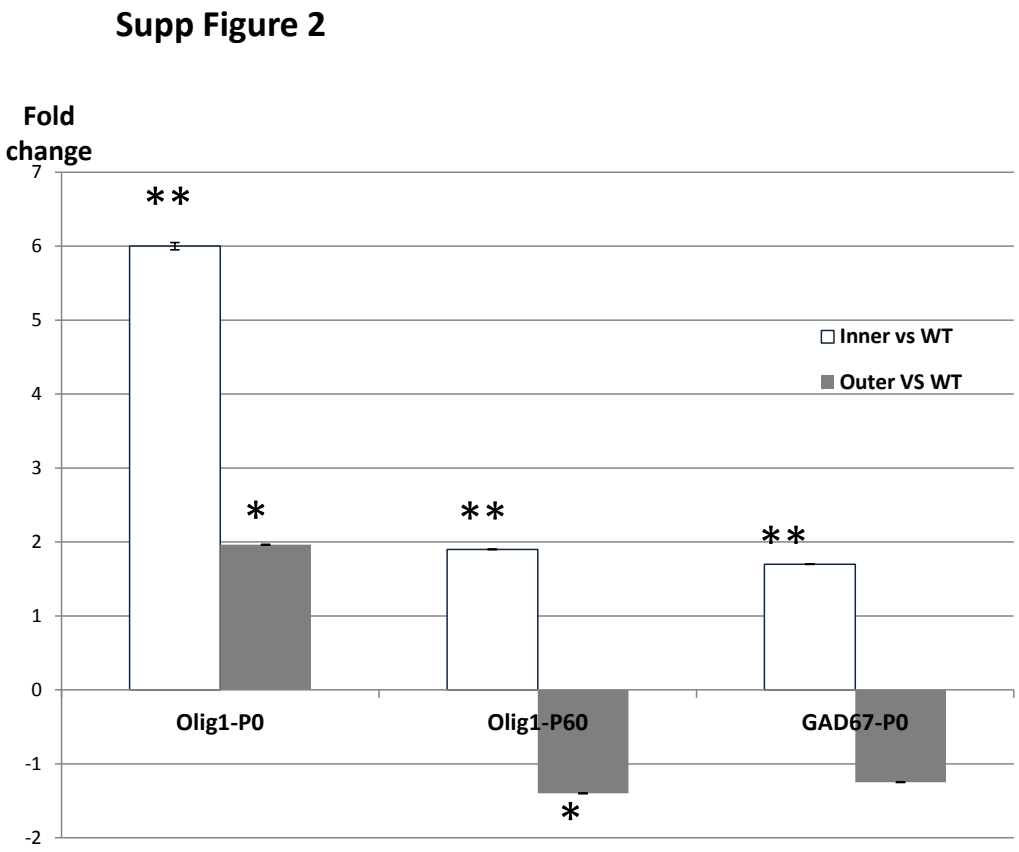

Supplementary Table 1

		Mito non damaged	Mito damaged	**% of damaged over all**		
series 1	1 ko SPI					
cell 1		6	13	0,68421053		
cell 2		1	4	0,8		
cell 3		3	5	0,625		
cell 4		2	5	0,71428571		
cell 5		2	4	0,66666667		
					SPI	
	1 ko SPE				series 1	0,56068296
cell 1		2	7	0,77777778	series 2	0,53997259
cell 2		2	3	0,6		
cell 3		2	6	0,75	**SPE**	
cell 4		2	2	0,5	series 1	0,54583639
cell 5		1	2	0,66666667	series 2	0,53591857
	5 ko SPI					
cell 1		2	2	0,5		
cell 2		8	2	0,2		
cell 3		1	2	0,66666667	**mean SPI**	**0,55032777**
cell 4		3	1	0,25	**mean SPE**	**0,54087748**
cell 5		8	8	0,5		
	5 ko SPE					
cell 1		5	1	0,16666667		
cell 2		2	2	0,5		
cell 3		5	2	0,28571429		
cell 4		2	6	0,75		
cell 5		7	6	0,46153846		
series 2		Mito non damaged	Mito damaged			
	7 ko SPI					
cell 1		3	8	0,72727273		
cell 2		2	14	0,875		
cell 3		4	14	0,77777778		
cell 4		1	7	0,875		
cell 5		6	11	0,64705882		
	7 ko SPE					
cell 1		4	10	0,71428571		
cell 2		3	9	0,75		
cell 3		2	10	0,83333333		
cell 4		3	22	0,88		
cell 5		1	8	0,88888889		
	9 ko SPI					
cell 1		11	7	0,38888889		
cell 2		10	4	0,28571429		
cell 3		11	8	0,42105263		
cell 4		13	4	0,23529412		
cell 5		5	1	0,16666667		
	9 ko SPE					
cell 1		6	1	0,14285714		
cell 2		15	4	0,21052632		
cell 3		14	5	0,26315789		
cell 4		14	8	0,36363636		
cell 5		22	10	0,3125		

LITERATURE CITED

Ackman JB, Aniksztejn L, Crépel V, Becq H, Pellegrino C, Cardoso C, Ben-Ari Y, Represa A. 2009. Abnormal network activity in a targeted genetic model of human double cortex. J Neurosci 29:313-27.

Altman J, Bayer SA. 1990a. Prolonged sojourn of developing pyramidal cells in the intermediate zone of the hippocampus and their settling in the stratum pyramidale. J Comp Neurol 301:343-64.

Altman J, Bayer SA. 1990b. Mosaic organization of the hippocampal neuroepithelium and the multiple germinal sources of dentate granule cells. J Comp Neurol 301:325-42.

Armstrong RC, Harvath L, Dubois-Dalcq ME. 1990. Type 1 astrocytes and oligodendrocyte-type 2 astrocyte glial progenitors migrate toward distinct molecules. J Neurosci Res 27:400-7.

Bahi-Buisson N, Souville I, Fourniol F, Toussaint A, Moores C, Khalaf R, Hully M, Poirier K, Leger PL, Elie C, Boddaert N, SBH-LIS European consortium, Chelly J, Beldjord C, Francis F. In revision. New insights into genotype-phenotype correlations for the *DCX*-related lissencephaly spectrum. Brain

Bally-Cuif L, Wassef M. 1994. Ectopic induction and reorganization of Wnt-1 expression in quail/chick chimeras. Development 120:3379-94.

Barkovich AJ, Guerrini R, Battaglia G, Kalifa G, N'Guyen T, Parmeggiani A, et al. 1994. Band heterotopia: correlation of outcome with magnetic resonance imaging parameters. Ann Neurol 36:609-17.

Barry G, Piper M, Lindwall C, Moldrich R, Mason S, Little E, Sarkar A, Tole S, Gronostajski RM, Richards LJ. 2008. Specific glial populations regulate hippocampal morphogenesis. J Neurosci 28:12328-40.

Baumgart E, Vanhorebeek I, Grabenbauer M, Borgers M, Declercq PE, Fahimi HD, Baes M. 2001. Mitochondrial alterations caused by defective peroxisomal biogenesis in a mouse model for Zellweger syndrome (PEX5 knockout mouse). Am J Pathol 159:1477-94.

Bazelot M, Simonnet J, Dinocourt C, Bruel-Jungerman E, Miles R, Fricker D, Francis F. 2012. Cellular anatomy, physiology and epileptiform activity in the CA3 region of Dcx KO mice: a neuronal lamination defect and its consequences. Eur J Neurosci 35:244-56.

Bielas SL, Serneo FF, Chechlacz M, Deerinck TJ, Perkins GA, Allen PB, Ellisman MH, Gleeson JG. 2007. Spinophilin facilitates dephosphorylation of doublecortin by PP1 to mediate microtubule bundling at the axonal wrist. Cell 129:579-91.

Bustin SA, Benes V, Garson JA, Hellemans J, Huggett J, Kubista M, Mueller R, Nolan T, Pfaffl MW, Shipley GL, Vandesompele J, Wittwer CT. 2009. The MIQE guidelines: minimum information for publication of quantitative real-time PCR experiments. Clin Chem 55:611-22.

Chen PH, Cai WQ, Wang LY, Deng QY. 2008. A morphological and electrophysiological study on the postnatal development of oligodendrocyte precursor cells in the rat brain. Brain Res 1243:27-37.

Chevassus-au-Louis N, Represa A. 1999. The right neuron at the wrong place: biology of heterotopic neurons in cortical neuronal migration disorders, with special reference to associated pathologies. Cell Mol Life Sci 55: 1206-15.

Colacitti C, Sancini G, DeBiasi S, Franceschetti S, Caputi A, Frassoni C, Cattabeni F, Avanzini G, Spreafico R, Di Luca M, Battaglia G. 1999. Prenatal methylazoxymethanol treatment in rats produces brain abnormalities with morphological similarities to human developmental brain dysgeneses. J Neuropathol Exp Neurol 58:92-106.

Corbo JC, Deuel TA. et al. 2002. Doublecortin is required in mice for lamination of the hippocampus but not the neocortex. J Neurosci 22: 7548-57.

Danglot L, Triller A, Marty S. 2006. The development of hippocampal interneurons in rodents. Hippocampus 16:1032-60.

de Castro F, Bribián A. 2005. The molecular orchestra of the migration of oligodendrocyte precursors during development. Brain Res Brain Res Rev 49:227-41.

Deller T, Drakew A, Heimrich B, Förster E, Tielsch A, Frotscher M. 1999. The hippocampus of the reeler mutant mouse: fiber segregation in area CA1 depends on the position of the postsynaptic target cells. Exp Neurol 156:254-67.

Deguchi Y, Donato F, Galimberti I, Cabuy E, Caroni P. 2011. Temporally matched subpopulations of selectively interconnected principal neurons in the hippocampus. Nat Neurosci 14:495-504.

des Portes V, Pinard JM et al. 1998a. A novel CNS gene required for neuronal migration and involved in X-linked subcortical laminar heterotopia and lissencephaly syndrome. Cell 92:

51-61.

des Portes V Francis F, et al. 1998b. doublecortin is the major gene causing X-linked subcortical laminar heterotopia (SCLH). Hum Mol Genet 7: 1063-70.

Deuel TA, Liu JS, Corbo JC, Yoo SY, Rorke-Adams LB, Walsh CA. 2006. Genetic interactions between doublecortin and doublecortin-like kinase in neuronal migration and axon outgrowth. Neuron 49:41-53.

Dong HW, Swanson LW, Chen L, Fanselow MS, Toga AW. 2009. Genomic-anatomic evidence for distinct functional domains in hippocampal field CA1. Proc Natl Acad Sci U S A 106:11794-9. Epub 2009 Jun 26.

Fanselow MS, Dong HW. 2010. Are the dorsal and ventral hippocampus functionally distinct structures? Neuron 65:7-19.

Farrell MA, DeRosa MJ, et al. 1992. Neuropathologic findings in cortical resections (including hemispherectomies) performed for the treatment of intractable childhood epilepsy. Acta Neuropathol 83: 246-59.

Fleck MW, Hirotsune S, et al. 2000. Hippocampal abnormalities and enhanced excitability in a murine model of human lissencephaly. J Neurosci 20: 2439-50.

Francis F, Koulakoff A, et al. 1999. Doublecortin is a developmentally regulated, microtubule-associated protein expressed in migrating and differentiating neurons. Neuron 23: 247-56.

Friocourt G, Chafey P, Billuart P, Koulakoff A, Vinet MC, Schaar BT, McConnell SK, Francis F, Chelly J. 2001. Doublecortin interacts with mu subunits of clathrin adaptor complexes in the developing nervous system. Mol Cell Neurosci 2001 18:307-19.

Fourniol FJ, Sindelar CV, Amigues B, Clare DK, Thomas G, Perderiset M, Francis F, Houdusse A, Moores CA. 2010. Template-free 13-protofilament microtubule-MAP assembly visualized at 8 A resolution. J Cell Biol 191:463-70.

Gelman, D.M., Martini, F.J., Nóbrega-Pereira, S., Pierani, A., Kessaris, N., and Marín, O. (2009). The Embryonic Preoptic Area Is a Novel Source of Cortical GABAergic Interneurons. J. Neurosci. 29, 9380–9389.

Gleeson JG, Allen KM, et al. 1998. Doublecortin, a brain-specific gene mutated in human X-linked lissencephaly and double cortex syndrome, encodes a putative signaling protein. Cell 92: 63-72.

Gleeson JG, Lin PT, Flanagan LA, Walsh CA. 1999. Doublecortin is a microtubule-associated protein and is expressed widely by migrating neurons. Neuron 23:257-71.

Goffinet AM. 1980. The cerebral cortex of the reeler mouse embryo. An electron microscopic analysis. Anat Embryol (Berl) 159:199-210.

Guerrini R, Marini C. 2006. Genetic malformations of cortical development. Exp Brain Res. 173:322-33.

Gupta A, Tsai LH, Wynshaw-Boris A. 2002. Life is a journey: a genetic look at neocortical development. Nat Rev Genet 3:342-55.

Hannan AJ, Servotte S. et al. 1999. Characterization of nodular neuronal heterotopia in children. Brain 122: 219-38.

Harding B. 1996. Gray matter heterotopia. Dysplasias of cerebral cortex and epilepsy. R Guerrini R, Andermann F, Cannapicchi R, Roger J, Zilfkin B, Pfanner P. (eds). Philadelphia, USA, Lippincott-Raven: 81-88.

Hong SE, Shugart YY, et al. 2000. Autosomal recessive lissencephaly with cerebellar hypoplasia is associated with human RELN mutations. Nat Genet 26: 93-6.

Jones DL, Baraban SC. 2007. Characterization of inhibitory circuits in the malformed hippocampus of Lis1 mutant mice. J Neurophysiol 98: 2737-46.

Kappeler C, Saillour Y, et al. 2006. Branching and nucleokinesis defects in migrating interneurons derived from doublecortin knockout mice. Hum Mol Genet 15: 1387-400.

Kappeler C, Dhenain M, Phan Dinh Tuy F, Saillour Y, Marty S, Fallet-Bianco C, Souville I, Souil E, Pinard J-M, Meyer G, Encha-Razavi F, Volk A, Beldjord C, Chelly J, Francis F. 2007. Magnetic resonance imaging and histological studies of corpus callosal and hippocampal abnormalities linked to doublecortin deficiency. J Comp Neur 500:239–54.

Keays D, Tian, AG, et al. 2007. Mutations in alpha-tubulin cause abnormal neuronal migration in mice and lissencephaly in humans. Cell 128: 45-57.

Kerjan G, Koizumi H, Han EB, Dubé CM, Djakovic SN, Patrick GN, Baram TZ, Heinemann SF, Gleeson JG. 2009. Mice lacking doublecortin and doublecortin-like kinase 2 display

altered hippocampal neuronal maturation and spontaneous seizures. Proc Natl Acad Sci U S A 106:6766-71.

Knuesel I, Elliott A, Chen HJ, Mansuy IM, Kennedy MB. 2005. A role for synGAP in regulating neuronal apoptosis. Eur J Neurosci 21(3):611-21.

Kukley M, Nishiyama A, Dietrich D. 2010. The fate of synaptic input to NG2 glial cells: neurons specifically downregulate transmitter release onto differentiating oligodendroglial cells. J Neurosci 30:8320-31.

Lambert de Rouvroit C, Goffinet AM. 1998. The reeler mouse as a model of brain development. Adv Anat Embryol Cell Biol 150:1-106.

Lein ES, Hawrylycz MJ, Ao N, Ayres M, Bensinger A, Bernard A, Boe AF, Boguski MS, Brockway KS, Byrnes EJ, Chen L, Chen L, Chen TM, Chin MC, Chong J, Crook BE, Czaplinska A, Dang CN, Datta S, Dee NR, Desaki AL, Desta T, Diep E, Dolbeare TA, Donelan MJ, Dong HW et al. 2007. Genome-wide atlas of gene expression in the adult mouse brain. Nature 445:168-76.

Liu JS, Schubert CR, Fu X, Fourniol FJ, Jaiswal JK, Houdusse A, Stultz CM, Moores CA, Walsh CA. 2012. Molecular basis for specific regulation of neuronal Kinesin-3 motors by doublecortin family proteins. Mol Cell 47:707-21.

Liu JP, Chang LR, Lai Gao X, Wu Y 2008. Different Expression of Caspase-3 in Rat Hippocampal Subregions During Postnatal Development. Microsc. Res. Tech. 71:633–638.

Madeira MD, Sousa N, Lima-Andrade MT, Calheiros F, Cadete-Leite A, Paula-Barbosa MM. 1992. Selective vulnerability of the hippocampal pyramidal neurons to hypothyroidism in male and female rats. J Comp Neurol 322:501-18.

Manent JB, Jorquera I, Ben-Ari Y, Aniksztejn L, Represa A. 2006. Glutamate acting on AMPA but not NMDA receptors modulates the migration of hippocampal interneurons. J Neurosci 26:5901-9.

Markham A, Cameron I, Bains R, Franklin P, Kiss JP, Schwendimann L, Gressens P, Spedding M. 2012. Brain-derived neurotrophic factor-mediated effects on mitochondrial respiratory coupling and neuroprotection share the same molecular signalling pathways. Eur J Neurosci 35:366-74.

Miles R, Tóth K, Gulyás AI, Hájos N, Freund TF. 1996. Differences between somatic and dendritic inhibition in the hippocampus. Neuron 16:815-23.

Moores CA, Perderiset M, Francis F, Chelly J, Houdusse A, Milligan RA. 2004. Mechanism of microtubule stabilization by doublecortin. Mol Cell 14:833-9.

Moores CA, Perderiset M, Kappeler C, Kain S, Drummond D, Perkins SJ, Chelly J, Cross R, Houdusse A, Francis F. 2006. Distinct roles of doublecortin modulating the microtubule cytoskeleton. EMBO J 25:4448-57.

Mourelatos Z, Adler H, Hirano A, Donnenfeld H, Gonatas JO, Gonatas NK. 1990. Fragmentation of the Golgi apparatus of motor neurons in amyotrophic lateral sclerosis revealed by organelle-specific antibodies. Proc Natl Acad Sci USA 87:4393-5.

Nakahira E, Yuasa S. 2005. Neuronal generation, migration, and differentiation in the mouse hippocampal primoridium as revealed by enhanced green fluorescent protein gene transfer by means of in utero electroporation. J Comp Neurol 483:329-40.

Napolioni V, Persico AM, Porcelli V, Palmieri L. 2011. The mitochondrial aspartate/glutamate carrier AGC1 and calcium homeostasis: physiological links and abnormalities in autism. Mol Neurobiol 44:83-92.

Nosten-Bertrand M, Kappeler C, Dinocourt C, Denis C, Germain J, Phan Dinh Tuy F, Verstraeten S, Alvarez C, Métin C, Chelly J, Giros B, Miles R, Depaulis A, Francis F. 2008. Epilepsy in Dcx knockout mice associated with discrete lamination defects and enhanced excitability in the hippocampus. PLoS ONE 3:e2473.

Nowakowski RS, Rakic P. 1979. The mode of migration of neurons to the hippocampus: a Golgi and electron microscopic analysis in foetal rhesus monkey. J Neurocytol 8:697-718.

Oettinghaus B, Licci M, Scorrano L, Frank S. 2012. Less than perfect divorces: dysregulated mitochondrial fission and neurodegeneration. Acta Neuropathol 123:189-203.

Okuda T, Kokame K, Miyata T. 2008. Differential expression patterns of NDRG family proteins in the central nervous system. J Histochem Cytochem 56:175-82.

Ono-Yagi K, Ohno M, Iwami M, Takano T, Yamano T, Shimada M. 2000. Heterotopia in microcephaly induced by cytosine arabinoside: hippocampus in the neocortex. Acta Neuropathol 100:403-8.

Picardo MA, Guigue P, Bonifazi P, Batista-Brito R, Allene C, Ribas A, Fishell G, Baude A, Cossart R. 2011. Pioneer GABA cells comprise a subpopulation of hub neurons in the developing hippocampus. Neuron 71:695-709.

Pinto-Lord MC, Evrard P, Caviness VS Jr. 1982. Obstructed neuronal migration along radial glial fibers in the neocortex of the reeler mouse: a Golgi-EM analysis. Brain Res 256:379-93.

Pleasure SJ, Anderson S, Hevner R, Bagri A, Marin O, Lowenstein DH, Rubenstein JL. 2000. Cell migration from the ganglionic eminences is required for the development of hippocampal GABAergic interneurons. Neuron 28:727-40.

Privat A, Leblond CP. 1972. The subependymal layer and neighboring region in the brain of the young rat. J Comp Neurol 146:277-302.

Reiner O, Carrozzo R, et al. 1993. Isolation of a Miller-Dieker lissencephaly gene containing G protein beta-subunit-like repeats. Nature 364: 717-21.

Rosenberg SS, Kelland EE, Tokar E, De la Torre AR, Chan JR. 2008. The geometric and spatial constraints of the microenvironment induce oligodendrocyte differentiation. Proc Natl Acad Sci USA 105:14662-7.

Slomianka L, Amrein I, Knuesel I, Sørensen JC, Wolfer DP. 2011. Hippocampal pyramidal cells: the reemergence of cortical lamination. Brain Struct Funct 216:301-17.

Soriano E, Cobas A, Fairén A. 1986. Asynchronism in the neurogenesis of GABAergic and non-GABAergic neurons in the mouse hippocampus. Brain Res 395:88-92.

Stanfield BB, Cowan WM. 1979. The development of the hippocampus and dentate gyrus in normal and reeler mice. J Comp Neurol 185:423-59.

Thompson CL, Pathak SD, Jeromin A, Ng LL, MacPherson CR, Mortrud MT, Cusick A, Riley ZL, Sunkin SM, Bernard A, Puchalski RB, Gage FH, Jones AR, Bajic VB, Hawrylycz MJ, Lein ES. 2008. Genomic anatomy of the hippocampus. Neuron 60:1010-21.

Tole S, Christian C, Grove EA. 1997. Early specification and autonomous development of cortical fields in the mouse hippocampus. Development. 124:4959-70.

Tole S, Grove EA. 2001. Detailed field pattern is intrinsic to the embryonic mouse hippocampus early in neurogenesis. J Neurosci 21:1580-9.

Tricoire, L., Pelkey, K.A., Erkkila, B.E., Jeffries, B.W., Yuan, X., and McBain, C.J. (2011). A blueprint for the spatiotemporal origins of mouse hippocampal interneuron diversity. J. Neurosci. 31, 10948–10970.

Wakselman S, Béchade C, Roumier A, Bernard D, Triller A, Bessis A. 2008. Developmental neuronal death in hippocampus requires the microglial CD11b integrin and DAP12 immunoreceptor. J Neurosci 28:8138-43.

Zhang J, Giesert F, Kloos K, Vogt Weisenhorn DM, Aigner L, Wurst W, Couillard-Despres S. 2010. A powerful transgenic tool for fate mapping and functional analysis of newly generated neurons. BMC Neurosci 11:158.

ARTICLE 2:

Various types of heterotopic or dysplastic neurons present a modified gene or protein expression pattern compared to their homotopic counterparts (Chevassus-Au-Louis et al., 1998; Rafiki et al., 1998; Finardi et al., 2006). Previous reports studied the expression of a few numbers of molecules using classical immunohistochemical methods. Global gene expression data for heterotopic cells is needed. In this part of the work, we take the advantage of the available new technical methods to characterize heterotopic neurons in the hippocampus of the *Dcx* KO mice. Using laser capture microdissectio, we successfully isolated the two populations of SPI and SPE CA3 heterotopic neurons in this model at P0 and in the adult. In this article, I will present gene expression changes and molecular profiles' analyses of these heterotopic cells at P0. Complementary *in situ* hybridization experiments and birthdating studies, confirming built hypothesis based on microarray data analysis are presented as well.

Molecular characterization and layer identity of heterotopic cells in the hippocampal CA3 region of doublecortin knockout mice

Khalaf-Nazzal R[1-3], Olaso R[4], Muresan L[5-7], Roumegous, A[1-3], Lavilla W[4], Belvindrah R[1-3], Carpentier W[8], Moutkine I[1-3], Dumont S[9], Albaud B[10], Roest Crollius H[5-7], Cagnard, N[11], Francis F[1-3].

[1] INSERM UMR-S 839, Paris 75005;

[2] Université Pierre et Marie Curie, Paris 75005;

[3] Institut du Fer à Moulin, Paris 75005, France

[4] Plateforme de Transcriptomique, Laboratoire de Recherche Translationnelle, CEA/DSV/IG-Centre National de Genotypage, 2 rue Gaston Crémieux, 91057 Evry, France

[5] Ecole Normale Supérieure, Institut de Biologie de l'ENS, IBENS, Paris, F-75005 France.

[6] Inserm, U1024, Paris, F-75005 France.

[7]CNRS, UMR 8197, Paris, F-75005 France.

[8] Plateforme post-génomique de la Pitié-Salpêtrière, Faculty of medicine, 75013, Paris.

[9] Anatomy-Pathology Laboratory, Hospital Saint Antoine, 75011 Paris

[10] Plateforme Affymetrix, Institut Curie, Hospital St Louis, Paris

[11] Plateforme Bio-informatique Paris Descartes, Faculté de Necker, 156 rue de Vaugirard, 75730 Paris Cedex 15.

Correspondance to: Fiona Francis, Institut du Fer à Moulin, 17 rue du Fer à Moulin, 75005 Paris France. Email: fiona.francis@inserm.fr

ABSTRACT

Human *doublecortin* (*DCX*) mutations are associated with lissencephaly, subcortical band heterotopia and varying degrees of intellectual disability and epilepsy. In type 1 lissencephaly patients the layering of the neocortex and the hippocampus is disorganized. In *Dcx* knockout (KO) mice, hippocampal pyramidal cells are abnormally laminated, mostly in the CA3 region, where the single pyramidal cell layer observed in wild type (WT) is divided into two abnormal layers. Video EEG recordings have shown previously that *Dcx* KO mice suffer from seizures with spontaneous epileptic activity originating in the hippocampus and propagating to the cortex. Intracellular recordings of hippocampal pyramidal cells in the CA3 region similarly showed that heterotopic cells are more excitable than WT pyramidal cells.

The Dcx protein plays a fundamental role in the regulation of microtubule cytoskeleton dynamics during neuronal migration and differentiation. Intrinsic genetic events as well as extrinsic local signals may be perturbed in *Dcx* KO hippocampal cells causing abnormal migration, differentiation and subsequent circuit development. In this study, we performed transcriptome analyses to search for perturbed gene expression comparing the two abnormal *Dcx* KO CA3 pyramidal cell layers with WT. Global gene expression analyses show that the KO layers differ from each other and from WT. Common perturbed mechanisms affect intracellular organelles including endosomes, mitochondria and Golgi apparatuses. Studying perturbed mechanisms specific to the individual KO layers shows defined but distinct neurogenesis time windows of each layer, that correspond to a different maturity status in early postnatal stages. Layer specific molecular markers and BrdU birth dating experiments to mark adult and developing pyramidal cells respectively in KO and WT mice, suggest that the inside-out layering of the CA3 region of the hippocampus is perturbed in *Dcx* KO animals. Further studies are required to better assess the consequences of such abnormalities on connectivity and network function.

INTRODUCTION

The proper development of neuronal circuits requires a correct sequence of events including cell proliferation, migration, and differentiation, where maturing neurons arriving at their final destination start extending axons and dendrites, allowing them to communicate with other neurons through the process of synaptogenesis. The layered structure of the mature cerebral cortex develops in an inside-out fashion. Layer-specific classes of cortical neurons are derived from neuronal progenitor cells in a sequential order and new waves of generated neurons occupy progressively more superficial positions within the developing cortical plate. Thus, neurons destined for lower layers are generated first, followed by upper-layer neurons (Angevine and Sidman, 1961; Rakic, 1972).

Somal translocation and radial glia guided locomotion represent two different but complementary modes of neuronal migration (Noctor et al., 2004). Early born neurons simply attach their processes to the pial surface and translocate to the cortical plate (Nadarajah and Parnevelas, 2002; Tabata and Nakajima, 2003). Later born neurons have a longer migration distance and depend on radial glia processes as substrates during the majority of their migratory path (Rakic, 1972; Noctor et al., 2004). Thus, birth date seems to be an important causal factor that determines the mode of migration of a neuron (Gupta et al., 2002), while intrinsic and extrinsic determinants will define its laminar identity (Molyneaux et al., 2007).

Similar to the cerebral cortex, the hippocampus is a laminated structure with the pyramidal cell layer showing an inside-out layering pattern with deep to superficial molecular and connectivity gradients (Slomianka et al., 2011). This pattern is induced early on during development, so newly born neurons carry intrinsic properties to help establish their adult phenotypes (Deguchi et al., 2011). Neurogenesis in the hippocampus occurs over a long period of time starting at embryonic day (E)10 in mice, and extends well beyond birth. The pyramidal neurons in CA1-CA3 are generated by an extensive area of neuroepithelium and migrate radially to the Ammon's horn (Altman and Bayer, 1990). Hippocampal field specific markers have been identified and reported to be differentially expressed in the pyramidal cells of CA1, CA2, and CA3 fields (Tole et al., 1997; Tole and Grove, 2001; Thompson et al., 2008; Datson et al., 2009). Specific markers are also differentially expressed along the

radial, as well as the septotemporal axes of the hippocampus, and gene boundaries can be correlated with functional connectivity (Thompson et al., 2008, Häussler et al., 2012). Moreover, it has been shown that subpopulations of neurons in different hippocampal fields share common intrinsic developmental programs including birthdate, synaptogenesis, connectivity patterns, and molecular markers, and this is tightly linked to their structural plasticity and adult function (Galimberti et al., 2010; Deguchi et al., 2011).

Human *doublecortin* (*DCX*) mutations are associated with a wide spectrum of neurodevelopmental syndromes of lissencephaly (LIS) and subcortical band heterotopia (SBH), which present clinically by varying degrees of intellectual disability and epilepsy (des Portes et al., 1998; Gleeson et al., 1998; Barkovich et al., 2001). DCX is a developmentally regulated microtubule associated protein (MAP) that is important for stabilization of MTs in migrating and differentiating neurons during embryogenesis (Francis et al., 1999; Gleeson et al., 1999) and newly born neurons in the adult brain (Brown et al., 2003). It participates in the dynamic regulation of cell morphology changes in immature neurons, regulated itself by the coordinated and reciprocal action of serine/threonine protein kinases and phosphatases acting through signaling pathways that will transfer external signals, such as via cell adhesion molecules and chemoattractants, into increased cellular dynamics, growth cone turning and neuronal migration (Gdalyahu et al., 2004; Tanaka et al., 2004; Schaar et al., 2004; Kappeler et al., 2006; Koizumi et al., 2006; Sapir et al., 2008; Jin et al., 2010).

In *Dcx* KO mice, hippocampal pyramidal cells are abnormally laminated, mostly in the CA3 region, where the single pyramidal cell layer observed in wild type (WT) is divided into two abnormal layers (Corbo et al., 2002; Kappeler et al., 2007). Video EEG recordings show that the *Dcx* KO mice have spontaneous epilepsy with the abnormal electrical activity originating in the hippocampus and secondarily propagating to the cortex (Nosten-Bertrand et al., 2008). Extracellular and whole cell recordings in the *Dcx* KO CA3 region showed that heterotopic cells are more excitable than WT pyramidal cells (Nosten-Bertrand et al., 2008; Bazelot et al., 2012). Field recordings from *Dcx* KO brain slices suggested that pyramidal cells make a primary contribution to the spontaneous epileptiform activity (Bazelot et al., 2012).

They receive strong inhibitory inputs during interictal events, and thus GABAergic signalling may be largely preserved (Bazelot et al., 2012).

Evidence from human patient clinical, histological and electrophysiological studies suggest that aberrantly positioned heterotopic cells in the hippocampus are strongly correlated with severe forms of pharmaco-resistant epilepsy (Lehéricy et al., 1995; Watson et al., 1996; López et al., 2010). Several other studies have reported that various types of cortical heterotopic or dysplastic neurons present a modified gene or protein expression compared to their homotopic counterparts (Chevassus-Au-Louis et al., 1998; Rafiki et al., 1998; Finardi et al., 2006). These studies used *in situ* hybridisation or immunohistochemistry to compare the expression of a limited number of genes or proteins in mature cells. Global gene expression from the cerebral cortex of certain mouse mutants of neuronal migration genes (*Lis*1, *Dcx*, *Ywhae* and *Ndel*1) have identified several biological processes commonly perturbed among these mutants in an overlapping manner (Pramparo et al., 2011). However, global gene expression to identify molecular signatures of developing heterotopic cells has not yet been reported. *Dcx* KO mice with hippocampal heterotopia and abnormal lamination represent an excellent model to study the molecular and cellular mechanisms leading to developmental forms of hyperexcitability. In this study, we set out to understand how migration defects arise and can lead to aberrant formation of the hippocampus, which may contribute to epileptogenesis. We studied both perturbed mechanisms common to both KO layers and mechanisms specific to each KO layer. Common perturbed mechanisms reveal organelle abnormalities. Furthermore, gene expression analyses suggested inversed neurogenesis time windows compared to WT for subsets of superficial and deep layer *Dcx* KO CA3 pyramidal cells, resulting in different maturity statuses at early postnatal stages. Field specific molecular markers and BrdU birth dating experiments to mark adult and developing pyramidal cells respectively, in KO and WT mice, confirmed this, showing that the inside-out layering of the CA3 region of the hippocampus is perturbed in *Dcx* KO animals. Such differences may have consequences on neuron morphology and connectivity, and may contribute to the development of hyperexcitability.

METHODOLOGY

Animals

Dcx KO and WT mice were maintained on the *Sv129Pas* background with more than ten generations of backcrosses (Kappeler et al., 2006, 2007). Genotyping was performed by PCR to verify the inactivation of the *Dcx* gene in KO animals (Kappeler et al., 2006). All experiments were performed in accordance with institutional, national and international guidelines (EC directive 86/609) and were approved by the local ethical committees. The day of confirmation of vaginal plug was defined as embryonic day zero (E0.5?), and the day of birth was defined as postnatal day zero (P0). P0 animals were anesthetized by placing on ice for 5 minutes before decapitation. For laser capture microdissection (LCM), the whole head was immediately frozen in isopentane at -35°C for 1 minute before storing at -80°C for future cryostat cutting. For *in situ* hybridization and immunohistochemistry experiments, animals were perfused, and brains were fixed using 4% paraformaldehyde (PFA) in phosphate buffered saline (PBS). Brains were post-fixed in the same solution overnight. Embryonic and early postnatal brains were cryoprotected in 30% sucrose, embedded and frozen in OCT tissue freezing medium, and cut using a cryostat (Leica) at 20µm thickness, and spread on SuperFrost II slides.

Laser capture microdissection (LCM)

Coronal brain sections (12 µm) containing the rostrocaudal hippocampus were prepared using a cryostat (Leica) maintained at -20°C and mounted on PENmembrane slides (1440–1000, PALM, Bernried, Germany) which were pretreated by RNase ZAP (Ambion) and UV irradiated (in a cell culture hood) for 30 min at 254 nm. After sectioning, the slides were stored in a -80°C freezer for use within 1 week. On the day of LCM, the slides were removed from the -80°C freezer, and fixed in 70% ethanol, prepared in RNase free water for 2 min and then in 50% ethanol for 5 seconds, and stained with 1% cresyl violet (Sigma) for 1 min. Subsequently, slides were rinsed and dehydrated using serial dilutions of ethanol (50% for 5 sec, 75% for 5 sec, 100% for 30 sec). Sections were air-dried and subjected to LCM within the next 30 minutes. Samples were cut using a Zeiss LCM system (PALM Microbeam). In WT animals, the hippocampal CA3 region was microdissected in one piece by LCM. In *Dcx* KO animals, internal *stratum pyramidale* (SPI) and external *stratum pyramidale* (SPE)

CA3 cells in the two layers were separated. Per WT brain, the entire CA3 structure (bilateral) from the dorsal hippocampus was excised (Figure 1). 60 sections per animal were pooled, corresponding to an average CA3 area of 3.2 x 10^6 μm^2 (Zeiss LCM software). Per KO brain, the CA3 SPI heterotopic layer (bilateral) was excised from 60 sections and pooled, corresponding to an average area of 1.2 x 10^6 μm^2. The CA3 SPE heterotopic layer (bilateral) was excised from the same 60 KO sections and pooled, corresponding to an average area of 2.8 x 10^6 μm^2. A test reverse transcriptase (RT) PCR from LCM material confirmed that the microdissected WT and KO cells expressed the CA3 marker *KA*1, but did not express the CA1 marker *Nov*, nor the dentate gyrus marker *Prox*1 (data not shown). Sequences of primers used to amplify these gene products are shown in Supplementary table 1.

RNA isolation, quantity and quality assessment

Total RNA for each brain was isolated from pooled microdissected material using an RNA isolation kit (Arcturus picopure) according to manufacturer instructions. RNA was eluted in 13µl of the elution buffer provided in the kit. RNA quantity was measured using a nanodrop spectrophotometer. RNA quality was checked using an Agilent 2100 Bioanalyzer with the RNA 6000 Pico LabChip Kit (5065-4473, Agilent Technologies, Palo Alto) according to the manufacturer's instructions.

Linear RNA amplification and GeneChip hybridization

15 samples, corresponding to n=5 samples in each studied group were processed using the Illumina TotalPrep RNA Amplification Kit (Ambion, Life Technologies) and the Whole-genome Gene Expression Direct Hybridization Assay (Illumina) according to manufacturers' instructions. Briefly, approximately 200 ng total RNA was used to prepare double-stranded cDNA using a T7 oligo (dT) primer (Illumina protocol). Reverse transcription was followed by *in vitro* transcription in the presence of biotinylated nucleotides. cRNA samples were hybridized to the Illumina Mouse-Ref-8 expression beadchip arrays in the appropriate buffer overnight at 58 °C. After hybridization and washes, fluorescent tagging was achieved by incubation with streptavidin-Cy3. Each array contains approximately 25,600 well-annotated RefSeq transcripts, each present as 30 unique probes, which corresponds to over 19,100 unique genes.

Nugen linear RNA amplification

For some qPCR experiments, RNA was amplified linearly using an Ovation kit (Nugen) adapted for LCM samples.

Data analysis

Intra-sample normalisation

In order to compare gene expression intensities between samples, expression values within samples were first normalised to account e.g. for differences in mRNA library preparation or in mRNA concentrations. To this end, each log-transformed expression value was corrected by subtracting the median of the distribution of log-transformed expression values and dividing by the standard deviation of this distribution (Supp Figure 1A).

Inter-sample normalisation

Samples from the same biological source were distributed on two different slides, requiring a correction for potential experimental or technical differences between slides. A principal component analysis of the expression values of the 15 samples (Supp Figure 1C) showed that the principal eigenvector (Z[1]) is sufficient to separate the samples according to their slide of origin, indicative of a possible slide bias. To account for this, we first measured the bias and then applied a corresponding correction. To measure the bias, we averaged the expression values of each gene across the four SPI and the four SPE samples of slide 1 respectively. We next subtracted this average value from the value of the single SPI and SPE samples on slide 2 to obtain the bias estimate (respectively Δ_I and Δ_E in Supp Figure 1B). If no slide bias exists, then all data points should be close to zero on both axes, indicating that slide 1 and 2 provide the same expression values. While this appears to be true for many genes, we observed a distribution of points along a slope. For genes lying on this diagonal, this indicates a slide bias of the same magnitude for both SPI and SPE samples.

In order to remove this bias, we first performed a gene-wise correction of the SPI samples on slide 1 to be compatible with corresponding samples on slide 2. The corrected value for each gene *j* is obtained as the sum of the original value and an

estimate of the bias error. The estimate of the bias is based on the bias of SPE (since we assume the bias to be independent of the sample, i.e. affecting intensities in the same way on the two slides) weighted with a constant w_I.

The bias correction for SPI samples is:

$$I_j^{corr,slide_1} = I_j^{slide_1} + w_I \cdot \Delta_{E,E,j}$$

$$\text{with:} \quad \Delta_{E,j} = average\left(E_j^{slide_1}\right) - E_j^{slide_2}$$

where *I* and *E* represent the intensity of gene *j* on the slide indicated by the superscript (the subscript of the sample on the slide is omitted for better readability). The constant w_I was determined by minimizing the error between the intensities of the genes on two different slides according to a least square criteria (as in the equations below).

For SPI: $\min_{w_I}\left[\sum_j \left(I_j^{slide_2} - average\left(I_j^{corr,slide_1}\right)\right)^2\right]$

For SPE: $\min_{wE}\left[\sum_j \left(E_j^{slide_2} - average\left(E_j^{corr,slide_1}\right)\right)^2\right]$

Similarly, the SPE samples were corrected on slide 1 with the bias estimated from SPI and thus all samples were aligned to the samples as found on slide 2.

After this bias correction, the same principal component analysis as performed previously showed that SPI and SPE samples from slide 2 respectively cluster with the SPI and SPE samples from slide 1.

Finally the linear model fit of the limma package was applied on these bias-corrected expression values in order to detect the differentially expressed genes pertaining to the three conditions, using a t-test. The Benjamini-Hochberg false discovery rate control (with p=0.05) was applied to correct for multiple testing.

Pathway analysis and functional category clustering

A global overview of the biological processes and enriched functional clusters in SPI and SPE lists was obtained using a Database for Visualization and Integrative Discovery (DAVID) (Dennis et al., 2003). The following sources were used: COG-

Ontology, SP-PIR-Keywords, UP-SEQ-Feature, GOterm-BP-FAT, GOterm-CC-FAT GOterm-MF-FAT, KEGG pathways, and INTERPRO protein information resources. Enrichment for each term was defined relative to the probes presenting with a *P* value <0.005, with at least 4 genes per term per dataset. Fuzzy Heuristical clustering was performed using kappa similarity >0.3, and requiring an enrichment score >1.5.

For specific questions, Ingenuity Systems Pathway Analysis (IPA) (Ingenuity Systems, Mountain View, CA; www.ingenuity.com) was used to define functional categories and pathways which could be enriched and are specific to the developing central nervous system.

Quantitative PCR (qPCR) validation

Real time qPCR assays using the SYBRgreen method followed MIQE guidelines (Bustin et al., 2009). Gene-specific primers were designed using Primer Express Software (PE Applied Biosystems). Standard curves were generated from assays made with serial dilutions of cDNA to calculate PCR efficiencies (90 % < efficiency < 105%, with r2 >=0.998). Threshold cycles (Ct) were transformed into quantity values using the formula $(1+\text{Efficiency})^{-Ct}$. Only means of triplicates with a coefficient of variation of less than 10 % were analyzed. Inter-plate variation was below 10 %. Values were normalized to the geometric mean of 3 Normalization Factors (NF) found to be the most stable through all samples using the geNorm approach. These were ATP synthase, H+ transporting mitochondrial F1 complex, beta subunit (Atp5b), eukaryotic translation initiation factor 4A2 (Eif4a2) and prosaposin (Psap).Average values ± standard deviations are presented for 5 animals of each genotype (individual values are provided in Supplementary Table). Ratios were calculated and *P* values using the Student t-test.

mRNA in situ hybridization

Specific antisense RNA probes (see supplementary table 1 for PCR probe extremities) for *Col6a1*, *Necab2, Grp, Cdh13 and Chl1* genes were used for *in situ* hybridization analyses. Equivalent sense probes were also generated for comparison. Digoxygenin (DIG) probes were synthesized with a labeling kit according to the manufacturer's instructions (Roche Diagnostics). Following a protocol adapted from Bally-Cuif and Wassef (1994), frozen cryostat sections were rinsed 3 × 5 min in PBS, postfixed in

4% PFA, rinsed in PBS 2 × 5 min, and treated with proteinase K (10 µg/ml) for 10 min. Sections were incubated in PBS + glycine (2 mg/ml), rinsed in PBS, and postfixed in a mixture of 4% PFA, followed by a rinse in PBS. Tissue sections were hybridized at 70°C overnight with the DIG-labeled probes diluted 1/100 in hybridization buffer (50% deionised formamide, 10% dextran sulphate, 1 mg/ml Yeast RNA, 1x Denhardt's solution). The next day, sections were sequentially washed in 2X saline sodium citrate (SSC) Tween 0.1% at 70°C then in maleate buffer (Maleic acid 100 mM, NaCl 150 mM, 0.1% Tween20, pH 7.5) at room temperature. For immunological detection of DIG-labeled hybrids, sections were first blocked (2% blocking reagent-Roche Applied Science, cat. 1096176, 20% sheep serum in maleate buffer) and then incubated overnight at 4°C in the same solution containing sheep anti-DIG-alkaline phosphatase-conjugated Fab fragments (Roche Diagnostics) diluted 1/2000. The following day, sections were washed 4 × 15 min in maleate buffer and 30 min in NTMT buffer (100 mm NaCl, 100 mm Tris-HCl, pH 9.5, 50 mm $MgCl_2$, 0.1% Tween 20). The alkaline phosphatase chromogen reaction was performed in NTMT buffer containing 100 mg/ml nitroblue tetrazolium (Roche Diagnostics) and 50 mg/ml 5-bromo-4-chloro-3-indolyl phosphate (Roche) at room temperature for 1-7 days and stopped with PBS. Sections were mounted on glass slides, dried, counter-colored using nuclear fast red and dehydrated in graded ethanol solutions, and coverslipped with Vectamount (Vector Laboratories).

Birth date studies

Pregnant mice were injected intraperitoneally (i.p) once with 200 mg/kg bromo deoxy uridine (BrdU) (body weight) at E11.5, E12.5 and E16.5. Animals were sacrificed at P25. To determine the number of BrdU-positive cells, every eighth section of 20 µm (160 µm intervals) of 1 cerebral hemisphere from each animal was processed for immunohistochemistry.

Immunohistochemistry

Cryostat sections at 20 µm thickness were washed in PBS 1X, and incubated in 2 N HCl at 37°C for 40 min to denature DNA. Sections were thoroughly washed in PBS 1X to neutralize the acid, and incubated in blocking solution (0.1 M PBS, 0.3% Triton X-100, 2% normal goat serum) for two hours at room temperature. This was followed by incubation with the primary antibodies; anti-BrdU (Rat, clone ICR1, ABD serotec

1:400), anti-NeuN (Mouse, clone A60 Millipore, 1:1000), anti-KCC2 (Rabbit, sigma, dilution 1:1000); diluted in blocking solution, for 48 hours at 4°C. Two days later, brain sections were washed three times in PBS 1X and incubated with fluorochrome-conjugated secondary antibodies (1:400, Invitrogen) diluted in blocking solution containing Hoechst fluorescent nuclear counterstain (1:5000). Sections were mounted using fluoromount G (Electron Microscopy Devices) and cover-slipped.

Image acquisition and quantification:

Bright-field *in situ* hybridization images were acquired with a Coolsnap CCD camera fitted to a Provis Olympus Microscope using 4X, 10X and 20X objectives (magnification/numerical aperture).

Fluorescent BrdU and NeuN immunostained sections were acquired using SP5II Leica confocal microscope using a 40X objective. BrdU-labelled cell quantification was performed using the Metamorph cell counting module. BrdU-labelled cells were counted depending on the following criteria: 1. Strong BrdU signal in the form of a circle, crescent, or more than two dots in the nucleus. 2. Co-immunostaining for both BrdU and NeuN to include only pyramidal cells and exclude interneuron or astrocyte- labelled cell populations. Division of the hippocampal CA3 subfields in coronal brain sections into CA3a, CA3b, and CA3c was performed as described previously (Li et al., 1994).

RESULTS

Laser capture microdissection of CA3 cells in *Dcx* KO and WT

We assessed global gene expression in WT and *Dcx* KO CA3 cells at postnatal day (P0). This represents a developmental stage where some late born CA3 neurons are still migrating, and most neurons are expected to have reached their final destination in the pyramidal cell layer and to be differentiating (Angevine, 1965; Altman and Bayer, 1990). This approach helped us identify developmentally regulated molecular markers with specific spatiotemporal expression patterns, and perturbed signalling pathways that are potentially involved in generating hyperactive circuits in the two populations of *Dcx* KO neurons. In the *Dcx* KO hippocampus, the CA3 region is

divided into two bands of pyramidal cells; which we termed *stratum pyramidale* internal (SPI, closest to the *stratum radiatum*) and *stratum pyramidale* external (SPE, closest to the *stratum oriens*) (Figure 1). LCM allowed us to specifically separate the SPI from the SPE, and to excise a similar region in WT CA3. RT-PCR of the LCM material confirmed the purity of the cellular populations, which specifically express *KA1* and *Col6a*1, markers preferentially expressed in the CA3 field, and in a band of cells at the outer border of the CA3 region, respectively (Tole et al., 1997; Tole and Grove, 2001; Lein et al., 2007). *Nov* and *Prox1*, which are CA1 and DG markers, respectively (Pleasure et al., 2000; Lein et al., 2004), were not expressed in LCM CA3 material (data not shown, primer sequences in Supp Table 1).

Surface areas of WT CA3, SPI and SPE were calculated using the LCM software and the number of cells was counted in selected sections. Thus, an estimate was obtained of the number of cells collected for each sample, corresponding to the dorsal hippocampi from both hemispheres of a single animal (Fig 1). Picochip analyses of the RNA quality of LCM samples from the CA3 region of WT, and the SPI and SPE of *Dcx* KO brains (n=5 of each genotype), were compared to a whole section sample that was cut at the cryostat and stained, without being subjected to LCM. The whole section sample had a high RNA integrity number (RIN) value of 9.2, indicating that the starting brain material was of good quality, and that the cryostat cutting and staining protocol had a minimal consequence on RNA quality. The LCM samples displayed a mild to moderate degree of degradation which is expected from this procedure, and showed RIN values of between 5.2 and 7.2 (Fig 1, Supp Table 2). Their overall RNA integrity was considered to be of sufficient quality to proceed with a microarray analysis. For this, a total of 150-200 ng of RNA was used as a starting material, and reverse transcription and amplification were performed according to Illumina protocols.

Differential gene expression between the WT CA3 region and the two *Dcx* KO bands

Of the 25,600 well-annotated transcript probes on the *Illumina MouseRef-8 v2.0 Expression BeadChip* array, 11800 on average demonstrated a detectable level of expression amongst the 15 studied samples. After data normalization (Supp Fig 1),

2360 and 1900 genes were found to be differentially expressed in SPI and SPE cells respectively compared to WT, when the *P* value cutoff was set to <0.01. Of these, 1700 and 1200 genes were highly significantly, differentially expressed in SPI and SPE cells respectively (*P* value <0.005) (Figure 2A). Table 1 lists 10 significantly deregulated genes showing the highest fold changes (up- and down-regulated), when comparing SPI to SPE and each individually to WT. 50 genes in SPI and 8 genes in SPE showed a greater than 1.5 X fold change when compared to WT (*P* value <0.005) (Supp Table 3). For the SPI gene expression changes, an approximately equal number of genes were up- and down-regulated, specifically 52% and 48%, respectively (*P* value <0.005). For SPE, a greater proportion of genes were up-regulated (67%) and only 33% were down-regulated (*P* value <0.005) (Figure 2A).

Performing DAVID (bioinformatics functional annotation clustering) analyses, the functional categories which were found to be enriched when comparing de-regulated genes in SPI and SPE layers to WT, are presented in Supp Table 4. These data are also summarized in Figure 2B for the categories with the highest enrichment scores. We observed that categories differ between SPE and SPI. Concerning up-regulated genes, these cluster in the following most highly enriched categories for SPI: generation of precursor metabolites and energy, calcium ion binding, synapse vesicle and regulation of synaptic process, and for SPE: intracellular organelle lumen, purine nucleotide binding, RNA binding and processing. Concerning functional clustering specifically related to down-regulated genes, RNA processing, non-membrane bound organelle, translation and coupled ATPase activity appear in the SPI down-regulated gene list, whereas vesicular, cytoskeletal, mitochondrial, cellular response to stress and calcium ion binding pathways appear related to down-regulated genes in the SPE list. Thus, certain enriched categories correspond to up-regulated gene clusters in SPI and down-regulated gene clusters in SPE (eg calcium ion binding and cytoskeleton), and *vice versa* (RNA processing, ATPase activity). Thus, this analysis suggests that SPI differs from SPE.

Focusing also on genes that were commonly differentially expressed in both SPI and SPE cells compared to WT, 455 and 272 genes with *P* values of <0.01 and <0.005, respectively were identified. Microarray analyses confirmed that the three cell populations studied expressed invariably the CA3 field specific markers *KA1* (Tole et al., 1997) and *Bok* (Newrzella et al., 2007). Gene expression changes common to SPI

and SPE, compared to WT samples, might be expected to be directly and specifically related to the loss of Dcx. Gene ontology analyses using the DAVID software revealed the major molecular functions, cellular components and biological processes that are jointly perturbed in these two cell populations. Analyzing the 455 commonly de-regulated genes (*P* Value < 0.01, combining up- and down-regulated gene lists), the functional categories of endosome, methylation, molecules associated with the mitochondrial membrane and Golgi apparatus, purine metabolism and ATP binding, oxidative phosphorylation, cellular response to stress and DNA repair, and neuron differentiation appeared most significantly in these analyses (Figure 3A, Supp Table 5). Of particular interest, several of these clusters seem to point to organelle abnormalities, which indeed we previously observed by electron microscopy (Khalaf-Nazzal et al., article 1). Thus, genes functionally clustered in the terms, 'structural components of the mitochondria' (*P* Value, 0.007, enrichment score 1.8) and 'Golgi apparatus' (*P* Value, 0.0004, enrichment score 1.7) showed enriched clustering in the common gene list. Genes related to endosomes were also highly enriched (*P* Value, 0.0006, enrichment score 2.8).

Of mitochondria-associated genes, a number of transporters as well as enzymes located on the inner or the outer mitochondrial membrane (Table 1 and Supp Table 5) showed differential expression. For example, the solute carrier family 25, member 22 (*Slc25a22)*, is a mitochondrial glutamate transporter expressed in the inner mitochondrial membrane. It was significantly upregulated in both SPI and SPE samples, a result that was confirmed by qPCR analysis of LCM material (2.6 and 1.3 fold increased expression in SPI and SPE, respectively, *P* Value < 0.05, Figure 4). Aldolase C (*Aldoc*) is a brain-specific aldolase isoform with restricted expression in hippocampal CA3 and cerebellar Purkinje neurons (Buono et al., 2004). This enzyme which is involved in glycolysis (Ahn et al., 1994), provides neuroprotection to neurons after excitotoxic events (Slemmer et al., 2007), and showed a 2.1 and a 1.3 fold increase in expression in SPI and SPE cells, respectively in the microarray data (Supp Table 3).

Of the genes appearing in the response to stress category, the heat shock protein 90kDa alpha, class B member 1 (*Hsp90ab1)* belongs to HSP90 a family of proteins involved in cell signalling pathways favouring cell survival (Nathan et al., 1997; Arya et al., 2007). *Hsp90ab1* is significantly up-regulated in both SPI and SPE

cells (Table 1). Pleiotrophin *(Ptn)* was also up-regulated in SPI and SPE cells. It is a heparin-binding cytokine (Li et al., 1990) induced by intense stressful stimuli including seizures (Wanaka et al., 1993) and glutamate-induced neurotoxicity, where it acts as a neuroprotective factor, protecting against stress induced cell death (Asai et al., 2011). These common gene changes in both SPI and SPE may hence reflect the anatomical data generated previously.

Neuronal migration genes are differentially expressed between SPI and SPE cells in *Dcx* KO hippocampus at P0

DCX plays fundamental roles in regulating cellular mechanisms involved in neuronal migration, including stabilization of microtubules during leading process extension and centrosome-nucleous coupling during nucleokinesis (Horesh et al., 1999; Tanaka et al., 2004a; Kappeler et al., 2006; Sapir et al., 2008). We actively searched for Dcx molecular partners and other genes involved in neuronal migration in the transcriptome data. Through Ingenuity Pathway Analysis (IPA) biological functional clustering of gene lists, and extensive literature searches, we identified a group of significantly deregulated genes. Several genes that are involved in neuronal migration and lamination of the cerebral cortex, including *Lis1*, and *Dab1* were found up-regulated in both SPI and SPE cells when compared to WT (Supp Table 3). *Tubg1,* a member of the tubulin superfamily which mediates microtubule nucleation, was also jointly and significantly up-regulated in SPI and SPE lists, a result that is further confirmed by qPCR analysis (Figure 4). Dcx nucleates and stabilizes microtubules (Moores et al., 2004) at the extremities of migrating and differentiating neurons (Friocourt et al., 2003), a region which is devoid of γ-tubulin (Baas and Joshi, 1992). The up-regulation of *Tubg*1 may represent as a compensatory mechanism due to Dcx loss of function. *Dclk*1 and *Dclk*2 which are close homologs of *Dcx* which are thought to be involved in functional compensation in cases of Dcx loss of function (Deuel et al., 2006; Tanaka et al., 2006) did not show gene expression changes, a result that is previously suggested by *in situ* hybridisation experiments (Tuy et al., 2008).

Careful examination of genes involved in neuronal migration showed some significant expression pattern differences between SPI and SPE cells, with SPI cells

having significant downregulation of many known neuronal migration genes compared to SPE and to WT cells (Table 2). A striking example is the expression of the Rho-GTPase *Rnd2*. *Rnd2* is a modulator of radial migration in the developing cerebral cortex with a very specific spatiotemporal expression pattern, being strongly expressed in radial glial progenitors and radially migrating neurons (Heng et al., 2008). Its expression is sharply down-regulated once neurons finish migration, settle, and start differentiation. *Rnd2* showed significant down-regulation in SPI cells compared to SPE and WT cells, and was up-regulated in SPE cells. The T-cell lymphoma invasion and metastasis 2 *Tiam2,* a gene involved in neuronal migration, interacts with microtubules and induces focal adhesion disassembly (Rooney et al., 2010) and was significantly down-regulated in SPI cells but not in SPE cells. Also, the alpha-N-acetyl-neuraminide alpha-2,8-sialyltransferase 2, *St8sia2,* is a neuronal migration gene which is highly expressed in migrating neurons, and its expression is down-regulated during neuronal differentiation (Rieger et al., 2008). Its expression was significantly down-regulated in SPI cells compared to SPE and WT cells, whereas it showed no significant changes comparing SPE cells to WT. Thus, although the two *Dcx* KO populations share a common deficit in Dcx, and both differ from WT, they show different molecular patterns which suggest temporal differences in generation and migration, with SPE cells less different from the WT population and potentially still migratory, and SPI cells potentially more advanced in maturity.

Pathway analysis reveals temporal differences in the maturity status of the two heterotopic cell populations in *Dcx* KO hippocampus at P0

Comparing directly SPI and SPE gene lists against each other also identified extensive gene expression differences, with 2647 genes showing significant expression differences between the two *Dcx* KO cell populations (Supp Table 3). Of these 100 genes showed more than 1.5 X fold change difference (*P* Value <0.005). Thus, the SPI population differs significantly from SPE at P0.

To further query the biological processes specific to the development of each of the two *Dcx* KO layers at P0, we performed IPA pathway analyses using a differentially expressed gene list of SPI versus SPE, and concentrating particularly on processes involved in central nervous system (CNS) development. *P* Value <0.005

cutoffs identified the significantly changed categories which differed between SPI and SPE. For the SPI gene list, mitosis, cell cycle progression, formation of axons, branching of neurons, formation of neurites, and long term potentiation of synapses were among the biological functions predicted to be the most significantly activated (z-score >2). Differentiation of oligodendrocytes and movement of brain cells were among the biological functions predicted to be inhibited (z-score <-2). For the SPE gene list; development of central nervous system and cell movement of brain cells were predicted to be the most significantly activated biological functions (z-score >2), while differentiation of brain cells was predicted to be inhibited (z-score <-2).

In order to obtain a global functional clustering confirmation of the enriched pathways, and to reveal pathways specific to each group compared to the other, we again used the DAVID bioinformatics functional annotation clustering tool. We compared SPI to SPE gene expression and generated two lists of clusters composed of the preferentially expressed genes in each category (Figure 3B, C). Notably, SPI cells had clustering enrichment in processes related to glycoproteins, synapse transmission, cell adhesion, vesicle mediated transport, generation of metabolites and cytoskeletal organisation. SPE cells had clustering enrichment related to the regulation of transcription, chromatin modifications, RNA processing and ribonucleoprotein biosynthesis. Synapse transmission and vesicle trafficking are mostly active post-migratory processes up-regulated during neuronal circuit maturation (Nowakowski and Rakic, 1979; Galimberti et al., 2010), while active transcriptional and translational activity is known to be one of the characteristics of migrating neurons (Nowakowski and Rakic, 1979). Although these clustering analyses are not exclusive (eg cell migration occurs in both SPI and SPE), nevertheless the combined pathway and functional clustering analysis might suggest temporal differences in the maturity status between the two *Dcx* KO CA3 cellular layers.

Layer specific genetic markers showed partial inversion of the *Dcx* KO hippocampal CA3 field along its radial plan

The hippocampus is made up of morphologically and functionally distinct pyramidal cells along its radial (deep to superficial) and septal to temporal axes. Molecular differences along these axes are thought to account at least in part for these

phenotypes (Thompson et al., 2008). In WT, *collagen type VI alpha 1 (Col6a1)* is a CA2 and CA3 border specific marker in the adult (Thompson et al., 2008), exclusively expressed in a single-cell-thick band of pyramidal cells along the border of the pyramidal cell layer and *stratum oriens* (Figure 5). On the other hand, in the *Dcx* KO adult CA3 region, the expression of this marker is more pronounced in SPI cells close to the *stratum radiatum*, with only some SPE outer boundary cells also labelled in more temporal regions (Figure 5). Thompson et al (2008) described a battery of boundary specific molecular markers that label CA3 outer boundary neurons. We searched for these molecular markers in our gene expression data and found that *Suppression of tumorigenicity 18 (St18), Cadherin13 (Cdh13), and N-terminal EF-hand calcium binding protein 2 (Necab2)* showed striking and significant up-regulation in SPI neurons at P0 (Table 4 Figure 5). We confirmed the enriched expression of some of these genes by qPCR and *in situ* hybridization experiments (Figure 5). Alternatively, some genes, which are excluded from the outer boundary region itself but are still expressed preferentially in the deep parts of the CA3 close to the *stratum oriens* in WT (Table 3), were shown to be significantly up-regulated in *Dcx* KO SPE (Figure 5). This includes the *cell adhesion molecule with homology to L1CAM (Chl1)* and the *gastrin-releasing peptide Grp*. These findings strongly suggest that some cells destined for the very deepest outer boundary layer of the CA3 pyramidal cell region, potentially born at early stages of CA3 neurogenesis (Altman and Bayer, 1990), are superficially positioned in the *Dcx* KO with respect to the other layers of CA3 pyramidal cells. Other deep layers are however retained in SPE, similar to the WT situation.

Inside-out lamination and birthdating experiments using time point specific injections of BrdU

Similar to the archicortex, lamination of the developing hippocampus proceeds in an inside-out pattern. Field and layer molecular specific marker data suggested that the inside-out layering of the CA3 region of the hippocampus is perturbed in *Dcx* KO mice. To study this in detail, the birth date and final destination of CA3 cells was studied by BrdU injections at different time-points during CA3 neurogenesis. BrdU, a thymidine analogue, incorporates into cells during S-phase. In the WT, injection of

BrdU at E11.5 is expected to label the earliest born neurons along the border of the pyramidal cell layer and *stratum oriens*. Injection of BrdU at E16.5 is expected to label later born neurons, settled in the most superficial layer of the CA3 region, at the border with *stratum radiatum* (Altman and Bayer, 1990; Deguchi et al., 2011).

BrdU labelings were performed to assess the final destinations of neurons born at specific time points in the *Dcx* KO. BrdU was thus injected in pregnant mothers at E16.5 and brains were analysed at P20. In the cortex, labelled neurons were found in layers II-III, confirming the specificity of labelling (data not shown). In the WT hippocampus, the labelled cells were located in the pyramidal cells closest to the *stratum radiatum* in both CA3 and CA1 fields (Figure 6). In the *Dcx* KO CA3 region, labelled cells were mainly located in the most superficial pyramids of the SPE layer, however, with complete exclusion of labelling of the even more superficial SPI cells. No difference was seen in the distribution of BrdU-labelled cells in the CA1 field of the WT and *Dcx* KO (data not shown). Quantification of BrdU labelled cells in CA3a and CA3b regions revealed apparently reduced numbers of BrdU labelled cells in the *Dcx* KO compared to WT. It also showed that (95%) of E16.5 BrdU labelled cells are located in the SPE layer in the *Dcx* KO, with few cells located in other regions, including the SPI layer. BrdU injections performed at E11.5 were difficult to quantify, but showed that labelled cells are located in the outer-most region of the WT CA3 at the border with *stratum oriens*, a labelling corresponding well to the cells marked by *Col6a1* and *St18* molecular markers. However, in the *Dcx* KO, labelled cells were frequently found in the SPI layer in CA3b and CA3c, and only occasionally in the SPE layer of the CA3a region. These data hence confirm at least a partial inversion of layers in the *Dcx* KO hippocampus, which may contribute to abnormal network development and function.

DISCUSSION

In the present study, we performed a global gene expression analysis of the double CA3 layer of the hippocampus of the *Dcx* KO mouse model, which exhibits neuronal migration defects and epilepsy. Laser microdissection from cresyl violet stained sections was successful to isolate RNA of suitable quantity and quality for microarray analyses. The SPI layer is relatively thin at P0, and we estimated that only 3500 cells

were collected per mouse brain. However, even this number of cells provided largely sufficient material for microarray analyses and subsequent qPCRs, and on average 45 % of the transcripts on the microarray showed a detectable level of expression, which falls into an appropriate range of the number of expressed genes expected per tissue, as shown by RNAseq studies (Ramsköld et al., 2009). Cell number estimates showed that SPI represents approximately 15 % of the overall *Dcx* KO CA3 population at P0. The thicker SPE layer is apparently closer in size, cell number and organization to WT. On the other hand, both layers showed appreciable numbers of differentially expressed genes compared to WT, and these were mainly layer-specific. Only 16 % of the SPI differentially expressed genes were commonly de-regulated in SPE, and 22 % of the SPE differentially expressed genes were found commonly de-regulated in SPI. Thus, overall there are substantial differences between each of the two layers and WT CA3.

Molecular changes found common to SPI and SPE seem in fitting with abnormalities previously identified by electron microscopy (Khalaf-Nazzal et al., article 1). Perturbed gene expression pointed to organelle (endosome, mitochondrial and golgi apparatus) structural and functional abnormalities, as well as, cellular response to stress, and activated DNA damage and repair pathways. Ultrastructural analyses of *Dcx* KO neurons in SPI and SPE layers revealed significant abnormalities in the mitochondria and the Golgi apparatus. The mitochondriae were abnormally swollen and vacuolated, and had abnormal cristae. Different ratios of swollen and circular Golgi apparatuses were frequently seen as well (Khalaf-Nazzal et al., article 1). These ultrastructural findings could suggest cellular stress in *Dcx* KO cells, and apoptotic cell death was increased in the hippocampus of *Dcx* KO mice at P2. As well as molecular data revealing functional categories related to the mitochondria and Golgi apparatus, there are also indications of a possible up-regulation of neuroprotective mechanisms. For example, the solute carrier family 25, member 22 (*Slc25a22)* was up-regulated in SPI and SPE neurons. *Slc25a22* which is a mitochondrial glutamate transporter expressed in the inner mitochondrial membrane is involved in metabolism-secretion coupling (Palmieri, 2004). This gene is also mutated in patients with neonatal myoclonic epilepsy (Molinari et al., 2009). The heat shock protein 90kDa alpha, class B member 1 (*Hsp90ab1)* was also up-regulated in both SPI and SPE cells. The HSP90 family are highly conserved molecular

chaperones that play key roles in signal transduction, protein folding, protein degradation, and protection against cell death under stressful conditions (Cid et al., 2005; Chen et al., 2009; Cha et al., 2010). This protein interacts with protein kinases and transcription factors that have crucial roles in developmental processes involved in cell signalling pathways favouring cell survival over death upon exposure to various stressful stimuli (Nathan et al., 1997; Arya et al., 2007). The upregulation of the neurotrophic factor Pleiotrophin *(Ptn)* in SPI and SPE neurons is another example of activated neuroprotective and survival promoting molecular signals. *Ptn* is highly expressed in perinatal brain in neurons as well as glia-derived cells (astrocytes and oligodendrocytes) (Wanaka et al., 1993), where it acts as a neurotrophic factor promoting differentiation and neurite outgrowth (Silos-Santiago et al., 1996; Yanagisawa et al., 2010). In the adult brain, *Ptn* expression is confined to specific neuronal subpopulations in the hippocampus and layer II–IV in the cerebral cortex (Wanaka et al., 1993). *Ptn* expression can be induced by seizures and excitotoxic conditions (Wanaka et al., 1993), to protect against cell death (Asai et al., 2011). Thus, gene expression analyses suggest activated signalling pathways related to the ultrastructural abnormalities observed, as well as neuroprotective, cell survival mechanisms that may have been stimulated by organelle abnormalities, or other unrelated and currently unidentified stressors.

Searching specifically for de-regulated neuronal migration genes, although revealing some up-regulated, potentially compensatory, genes common to both layers, also provided clues to the differences between SPI and SPE. Thus, several genes (e.g. *Rnd2* and *St8sia2*) known to be sharply down-regulated after neurons finish migration (Heng et al., 2008; Rieger et al., 2008) were found expressed in WT and SPE cells, and down-regulated in SPI. Together with pathway analyses revealing processes consistent with migration up-regulated in SPE, and consistent with neuritogenesis and synapse function up-regulated in SPI, these data suggest that SPI are in general more mature than SPE cells. The SPE population may potentially be regarded as still having active migratory processes (Nowakowski and Rakic, 1979), since transcriptional and translational machinery are clearly up-regulated compared to WT, and these processes which are down-regulated in SPI. The position of SPE, extending within the *stratum oriens* may also be more coherent with migration, since this is the area during late embryogenesis where migrating CA3 neurons ‘sojourn’ extensively

before becoming positioned in the pyramidal cell layer (Altman and Bayer, 1990). We previously showed that in the *Dcx* KO hippocampus, an abnormal density of pyramidal cells can be observed histologically in this region from E17.5 onwards (Kappeler et al., 2007), suggesting slowed or indeed, arrested migration. The SPE layer may therefore represent a true heterotopic band in this respect, and it is possible that the gene expression changes at P0 are a reflection of neurons still actively being instructed to migrate. Our BrdU studies, labelling a late-born (E16.5) population are also revealing, showing a largely correct positioning of these neurons along the radial axis within the SPE layer, having migrated to its superficial regions by P20. Nakahira and Yuasa (2005) previously showed, using *in utero* electroporation experiments targeting the hippocampus that E16.5-born neurons migrate first tangentially in the subpial stream, then radially crossing through the pyramidal cell layer to reach superficial regions, closest to the *stratum radiatum*. This suggests that the SPE layer itself, although less superficial than SPI and potentially too deep in the *stratum oriens*, nevertheless forms relatively correctly, respecting inside-out lamination.

The *Dcx* KO SPI layer showed a slightly larger number of differentially expressed genes than the SPE layer. Some gene expression differences of SPI are likely to be related to maturity, but a percentage of differences may also be accounted for by cell heterogeneity, since, other cell types, including oligodendrocyte precursors and interneurons, were previously identified amongst the pyramidal cells (Khalaf-Nazzal et al., article 1). Indeed, *Olig*1, a marker of oligodendrocyte precursors, shows the highest fold change in the SPI versus WT up-regulated gene list. On the other hand, we also observed up-regulation of CA3 outer boundary markers (eg *Cdh*13, *Necab*2), up-regulation of synaptic vesicle markers (eg *Sv2b*) and down-regulation of neuronal migration genes (eg *Rnd2*), which may in each case, be specifically related to the origin and maturity status of P0 SPI pyramidal cells. Thus, comparing SPI to SPE gene lists, suggests strong temporal differences in the migration and maturation status of the two *Dcx* KO cell layers. BrdU labelling studies were particularly revealing for the SPI layer. This layer closest to the *stratum radiatum* was largely not labelled by late-born neurons. Instead we observed appreciable labelling of this layer by performing BrdU injections at E11.5 (data not shown). In the WT, such injections label cells in the deepest part of the CA3 layer, at the border of the *stratum oriens* (Altman and Bayer, 1990; Deguchi et al., 2011). Combined BrdU experiments

therefore suggest that the SPI population are misplaced with respect to SPE and this conclusion is reinforced by *in situ* hybridisation data of CA3 outer boundary (deepest layer) markers (*Col6A1, Cdh13, Necab2*). Some of these markers were initially highlighted by Thompson et al., who studied the genetic anatomy of the hippocampus and defined genes with restricted expression to certain layers or subdivisions along the radial and septo-temporal axes (Thompson et al., 2008). Deguchi et al (2011), who showed coordinated connectivity between early born cell populations in the hippocampus, also identified genes enriched in early-born pyramidal cells, similar to those appearing in the SPI list. Thus, the SPI seems to be formed from early-born CA3 neurons, and this is in fitting with the more advanced maturity of SPI cells at P0, revealed by gene expression differences, as well as preliminary data immunodetecting KCC2 (not shown), and querying cell maturity by distinguishing cytoplasmic (less mature) from plasma membrane (more mature) forms (Khalilov et al., 2011). These combined data are consistent with temporal differences in the developmental programs of SPI and SPE layers, and indeed, an inversed inside-out lamination, specific to early-born, outer boundary cells with respect to all other CA3 pyramidal cells, a finding that is detected at P0 and persists into adulthood.

We show here an advanced analysis of a heterotopic cell situation. The relative positions of SPI and SPE seem to imply that SPI cells migrate correctly to their final destination, with SPE cells migrating less efficiently, and accumulating below, potentially without an outer-boundary. These data might suggest that early-born, outer boundary neurons normally migrate in a Dcx-independent fashion. It remains to be seen what repercussions this relative displacement of early-born, outer boundary cells to more internal regions might have on neuronal differentiation, cell-to-cell communication, connectivity and function. Interestingly, dendritic morphology is already known to be affected, with adult SPI cells showing reduced basal dendritic length and SPE cells, reduced apical dendritic length (Bazelot et al., 2012). Restricted expression of cell adhesion molecules such as cadherins and collagens, have previously been shown to provide topographic specificities for functional connectivity, and along with specific ion channel expression, to determine intrinsic electrophysiological profiles (Thompson et al., 2008). It remains possible that SPI cells, exhibiting a unique molecular identity, still become connected appropriately, even though they are displaced from the environment of SPE cells. The abnormal

neuronal position for SPE cells, extending in the *stratum oriens*, could also have consequences on connectivity. Further studies are required, including investigating synaptogenesis during postnatal stages, and performing gene expression analyses of more mature *Dcx* KO cells, to help answer these questions concerning the consequences of abnormal neuronal position on neuronal and network function.

Acknowledgements

We thank Nicolas Narboux-Neme and Katia Bourtourlinsky for *in situ* hybridization advice, Evelyne Souil for initial advice concerning LCM, David Gentien for advice and use of Picochip chips and Dominique Wendum for the use of the LCM platform. We thank the Inserm Avenir program, the French Agence National de la Recherche (ANR- 08-MNP-013), the Fondation Bettencourt Schueller and the Fondation Jérôme Lejeune for grant support to FF. We thank University Paris 6, and An-Najah University, Palestine for support to RKN. We thank the Ile de France region for support of imaging and animal house facilities.

Figure 1: The experimental procedure of laser capture microdissection (LCM) material preparation for expression profiling in hippocampal cornus ammonis CA3 layers.

A: In the WT (upper images) and *Dcx* KO (lower images), hippocampal CA3 and SPI and SPE fields, respectively, were microdissected from cresyl violet stained coronal P0 brain sections using LCM. Selected regions are drawn around on acquired images using the LCM software, indicating the laser path to be used to cut the tissue. B: The summation of estimated total surface area and number of cells obtained per animal (dorsal hippocampus, both hemispheres) for each type of sample (WT, SPI and SPE). C: Isolated total RNA from the collected tissue fragments subjected to bioanalysis on Picochips (Agilent) to check for RNA integrity number (RIN). Examples of WT (sample 63), SPI (sample 93-1), and SPE (sample 93-2) RIN electropherograms, showing fluorescence on the y-axis and nucleotides on the x-axis. The two major peaks in each plot refer to 18S and 28S ribosomal bands. A corresponding gel image is shown on the right, showing little evidence of RNA degradation.

A

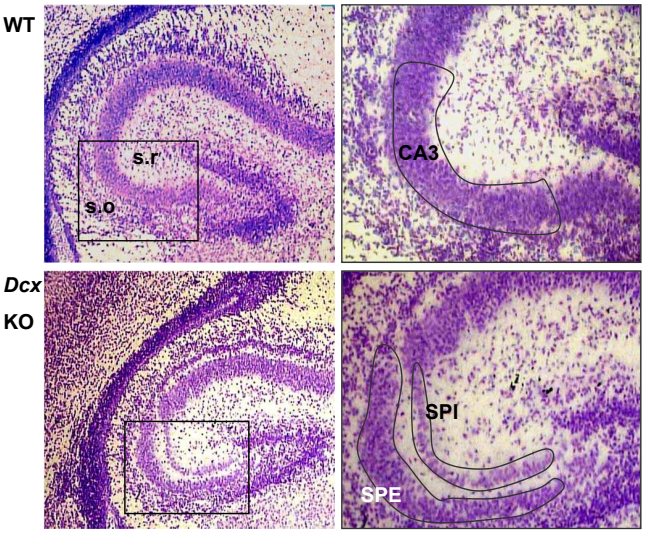

B

Hippocampal area	WT CA3	*Dcx* KO	
		CA3 SPI	CA3 SPE
Total surface area collected in tubes	9400mm²	2340mm²	77800 mm²
Total number of cells collected in tubes	30000 cells	3500 cells	20000 cells

C

WT CA3	KO CA3 SPI	KO CA3 SPE
63	93-1	91-2

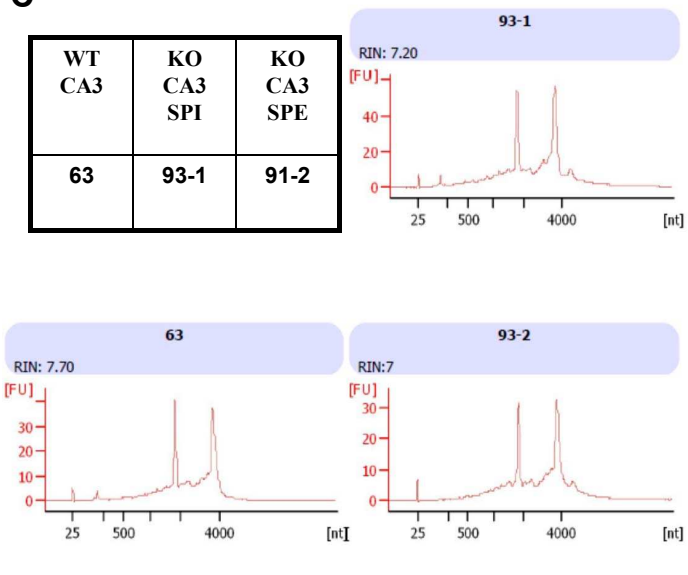

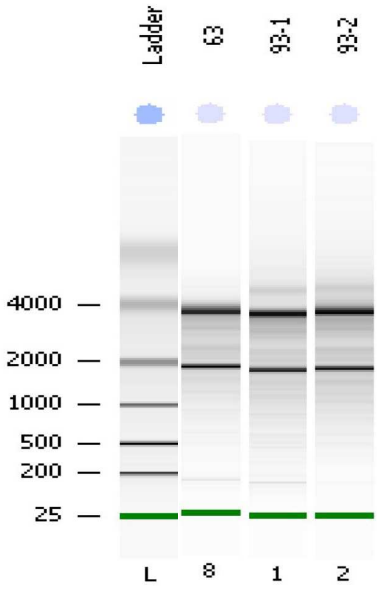

Figure 2: Global gene expression changes in the two *Dcx* KO layers, compared to WT.

A: the increasing number of differentially expressed genes with lowering *P.* value cutoffs. The red color indicates the up-regulated genes, and the green color indicates the down-regulated genes. B: Functional clustering of up-regulated and down-regulated differentially expressed genes appearing when comparing SPE cells to WT and SPI cells to WT, respectively. Each functional category (Y-axis), is plotted against the value of enrichment score (X-axis) obtained using DAVID pathway analysis software.

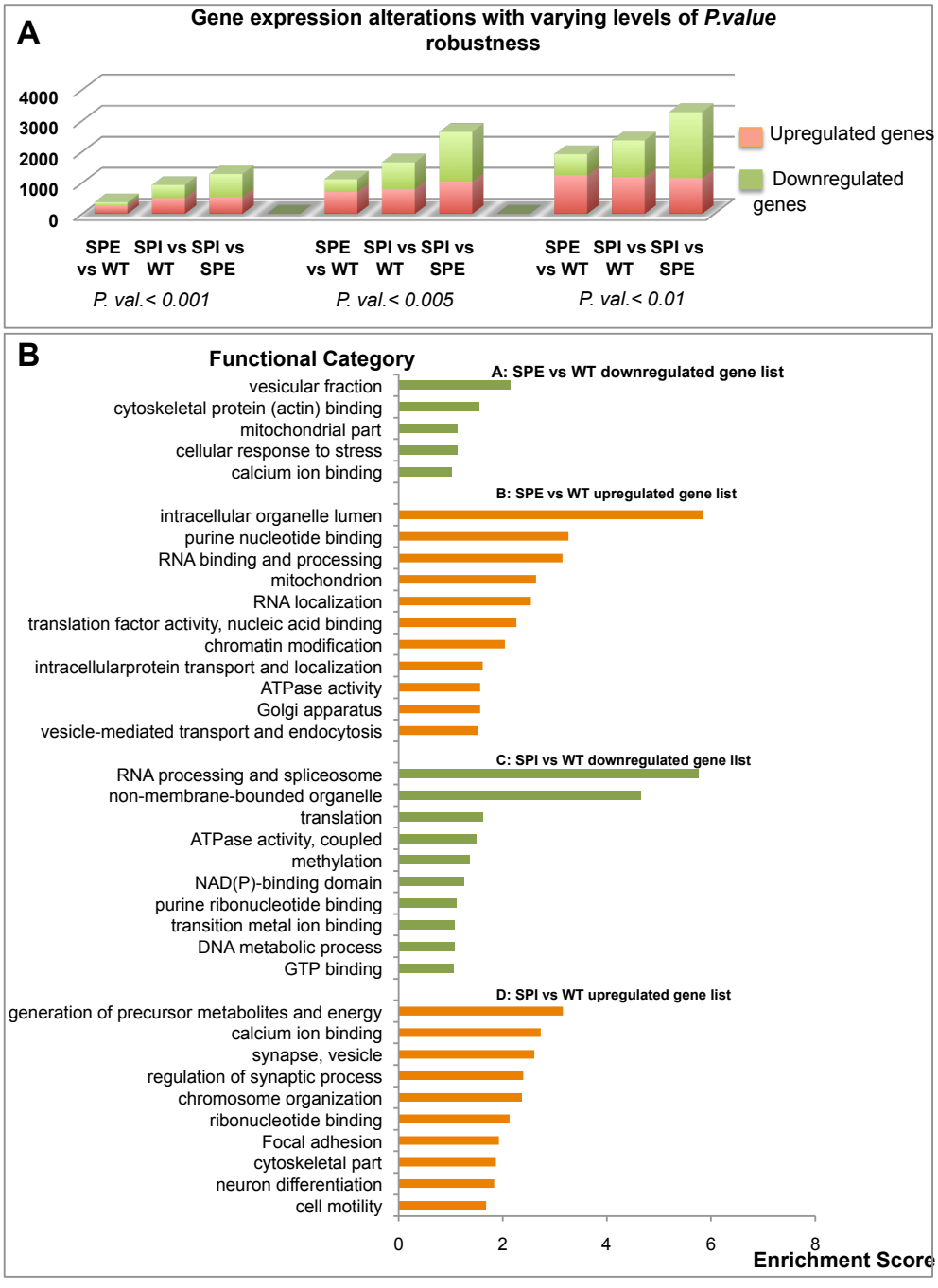

Figure 3: Functional clustering of common and layer-specific gene expression differences.

A: Genes commonly de-regulated in SPI and SPE were subjected to DAVID functional clustering analyses. B: Functional clustering of SPI-specific gene changes. C: Functional clustering of SPE-specific gene changes. Each functional category (Y-axis), is plotted against the value of enrichment score (X-axis).

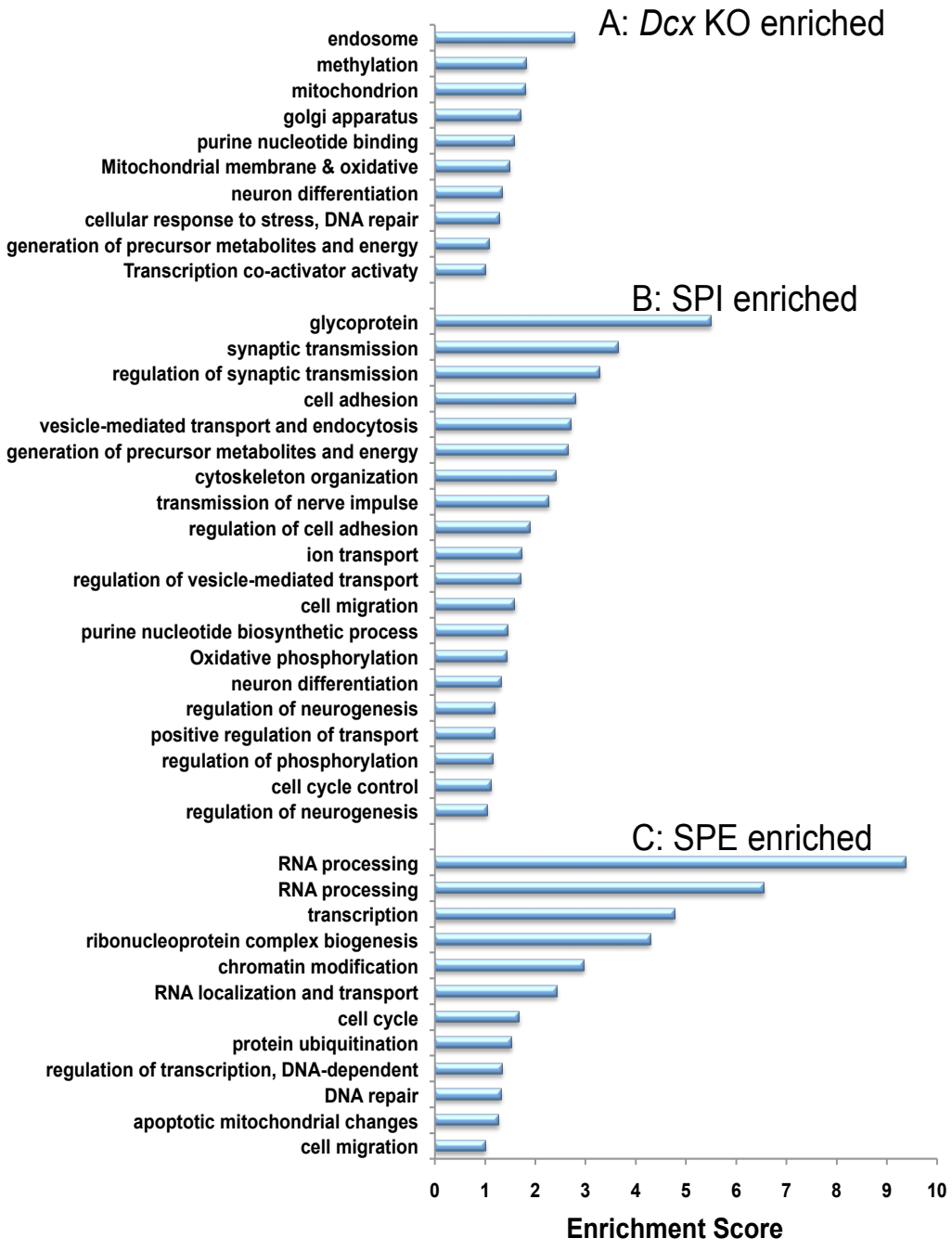

Figure 4: Quantitative RT-PCR validation of deregulated genes in SPI and SPE cells compared to WT.

For each gene, expression is represented as the fold change in SPI (blue) or SPE (grey) cells relative to each other and to the WT. Data shown corresponds to a *P.* Val. < 0.05 when comparing SPI to SPE. Stars correspond to gene changes with a *P.* Val. < 0.05 when compared to WT. Bars indicate +/- standard error.

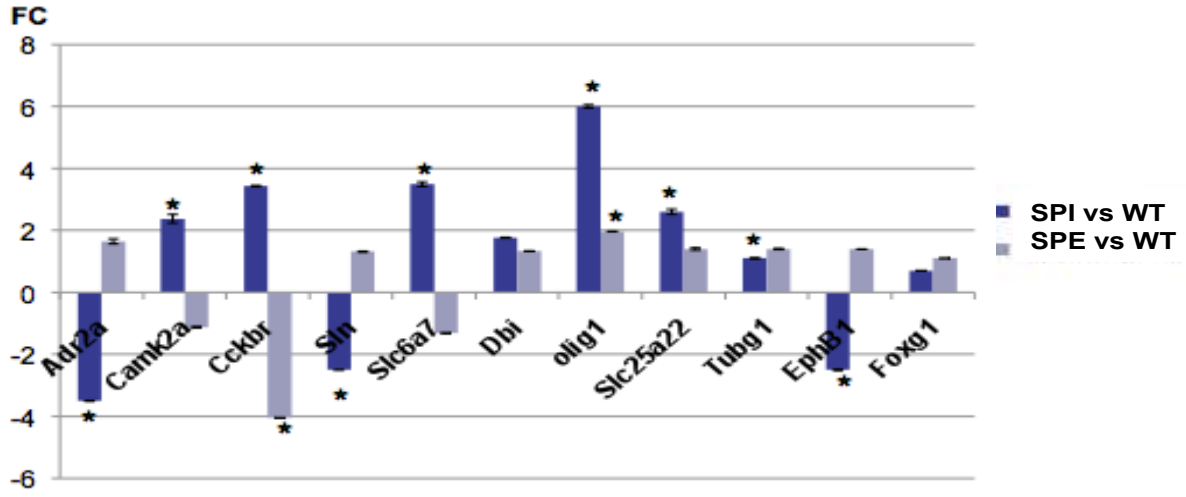

Figure 5: *In situ* hybridization and qRT-PCR results for genes showing layer-specific expression patterns.

A: *Col6A1* expression in adult WT (far left) and *Dcx* KO hippocampus coronal sections (R, rostral, C, caudal). The CA3 region is shown. Blue colour indicates specific labeling. *Col6A1* labels outer-boundary cells closest to the *stratum oriens* in WT, whereas mainly SPI cells are labeled in the *Dcx* KO in septal regions, as well as some outer boundary cells in more temporal regions. B: *Necab*2 expression in similar adult sections. This marker labels CA2 cells and CA3 outer-boundary cells in WT, and similar to *Col6A*1, shows a predominant expression in SPI cells in septal regions. C: qPCR analyses of four genes, two up-regulated in SPI and down-regulated in SPE (*Necab2* and *Cdh13*); and two up-regulated in SPE and down-regulated in SPI (*Grp* and *Chl1*). D: *In situ* hybridization of gene showing WT expression in a deep layer of CA3, internal to the outer-boundary layer, at P0. In the KO, its expression is observed in SPI. Lower (left) and higher (right) magnifications are shown. E: *In situ* hybridization of *Grp* showing WT expression in late-migrating neurons in the intermediate zone at P0 as well as the CA3 pyramidal layer. In the KO, no expression is observed in SPI. Lower (left) and higher (right) magnifications are shown.

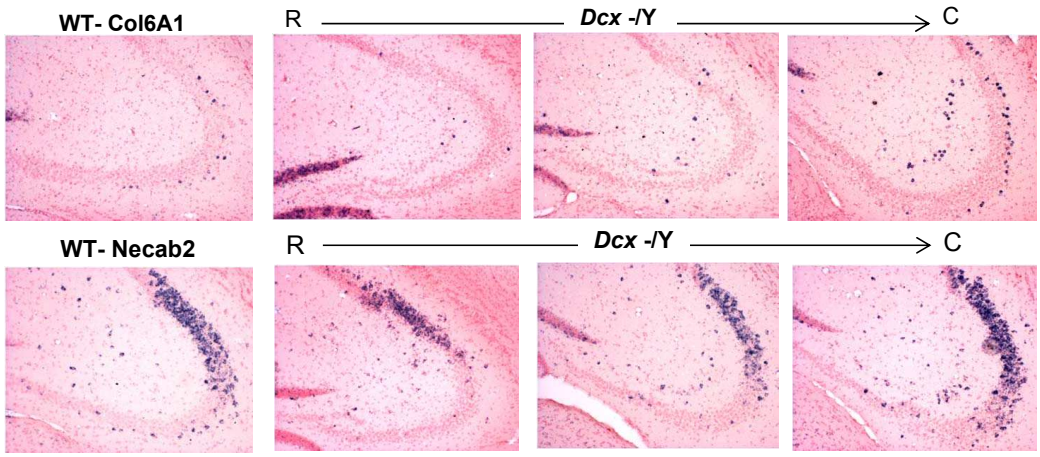
WT- Col6A1
R
Dcx -/Y
C
WT- Necab2
R
Dcx -/Y
C

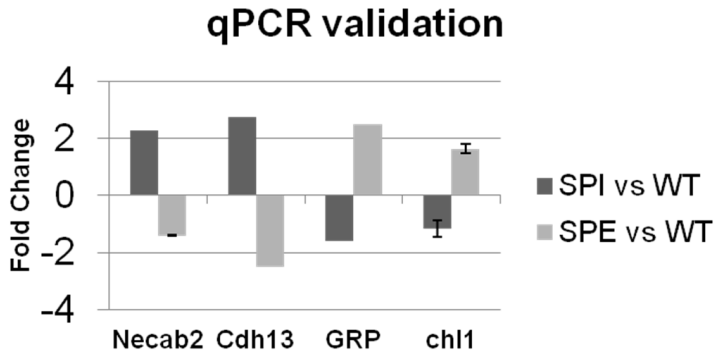
qPCR validation
Fold Change
4
2
0
-2
-4
Necab2
Cdh13
GRP
chl1
SPI vs WT
SPE vs WT

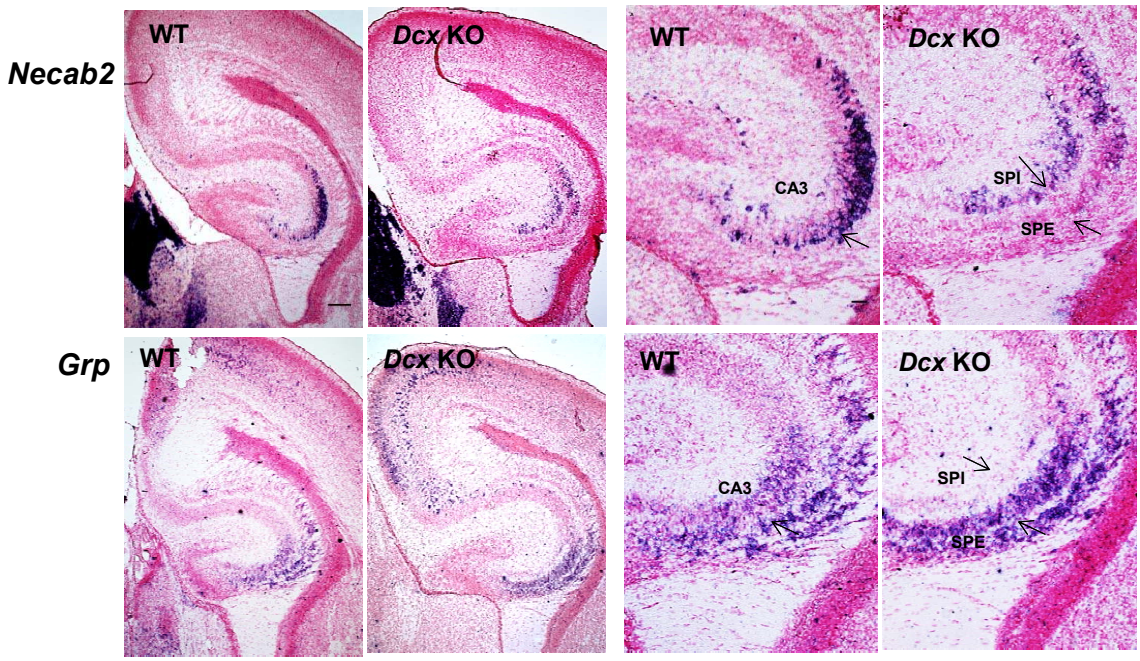
Necab2
WT
Dcx KO
WT
Dcx KO
CA3
SPI
SPE
Grp
WT
Dcx KO
WT
Dcx KO
CA3
SPI
SPE

Figure 6: BrdU labeling of E16.5 born neurons, (preliminary data for n=1 animal).

A: Representative images are shown of BrdU labeling (green) compared to NeuN (red). Three rostral-caudal levels are shown (from upper to lower). Note the thin layer of BrdU labeled cells in the internal region of the WT CA3 pyramidal cell layer (left images). In the KO, cells are similarly positioned in SPE and rarely present in SPI. B: Quantifications of the number of cells present in SPE and SPI. Y-axis, average number of cells. Scale bar 100μm.

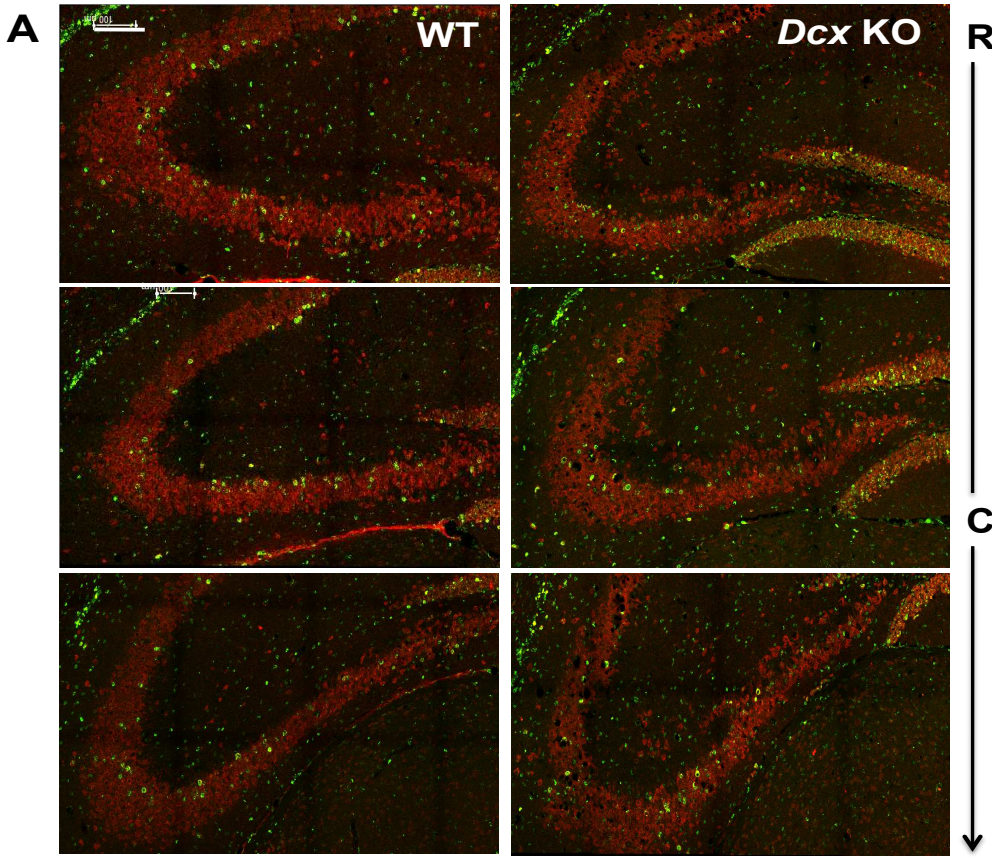

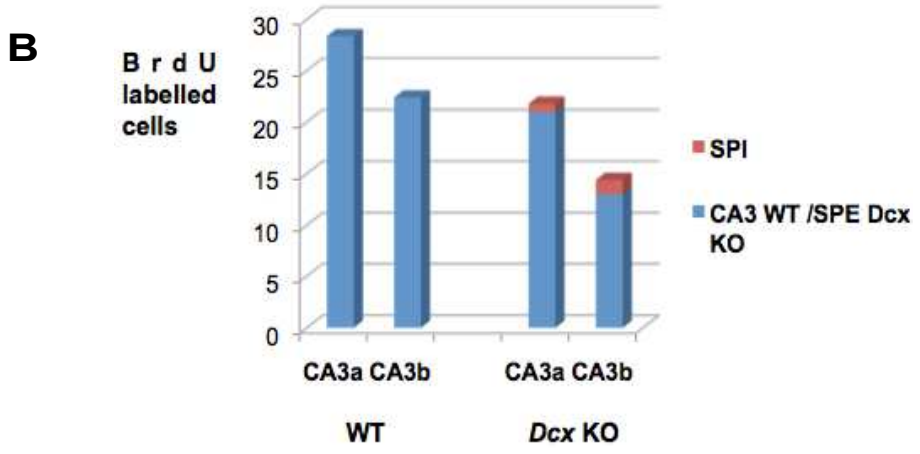

Table 1: A list depicting the most significantly upregulated and downregulated genes when comparing SPI to SPE, SPI to WT, and SPE to WT. *P*. val <0.05

Upregulated genes with highest ratio difference, *P.val*<0.005

SPI vs SPE	Ratio	SPI vs WT	Ratio	SPE vs WT	Ratio
metallothionein 1 (Mt1).	2.51	oligodendrocyte transcription factor 1 (Olig1).	2.38	zinc finger protein 238 (Zfp238), transcript variant 2.	1.56
RAS guanyl releasing protein 1 (Rasgrp1).	2.37	aldolase C, fructose-bisphosphate (Aldoc).	2.12	heat shock protein 90kDa alpha (cytosolic), class B member 1 (Hsp90ab1).	1.55
actin, beta (Actb).	2.36	pleiotrophin (Ptn).	1.94	PREDICTED: similar to Matrin 3 (LOC100046320), misc RNA.	1.55
solute carrier family 17 (sodium-dependent inorganic phosphate cotransporter), member 7 (Slc17a7).	2.11	RIKEN cDNA 1200009O22 gene (1200009O22Rik).	1.90	seryl-aminoacyl-tRNA synthetase (Sars).	1.52
interleukin 11 receptor, alpha chain 1 (Il11ra1).	2.11	calcium/calmodulin-dependent protein kinase II alpha (Camk2a), transcript variant 2.	1.84	gastrin releasing peptide (Grp).	1.48
metallothionein 3 (Mt3).	2.10	RAS guanyl releasing protein 1 (Rasgrp1).	1.83	membrane-associated ring finger (C3HC4) 6 (March6).	1.48
calcium/calmodulin-dependent protein kinase II alpha (Camk2a), transcript variant 2.	2.06	metallothionein 1 (Mt1).	1.81	lengsin, lens protein with glutamine synthetase domain (Lgsn).	1.48
sparc/osteonectin, cwcv and kazal-like domains proteoglycan 3 (Spock3).	2.04	synaptic vesicle glycoprotein 2 b (Sv2b).	1.74	heat shock protein 90kDa alpha (cytosolic), class B member 1 (Hsp90ab1).	1.47
RIKEN cDNA 4930511J11 gene (4930511J11Rik).	1.96	sparc/osteonectin, cwcv and kazal-like domains proteoglycan 3 (Spock3).	1.73	Von Willebrand factor homolog (Vwf).	1.47
visinin-like 1 (Vsnl1).	1.94	sparc/osteonectin, cwcv and kazal-like domains proteoglycan 1 (Spock1).	1.72	heterogeneous nuclear ribonucleoprotein A1 (Hnrpa1), transcript variant 2.	1.46

Downregulated genes with highest ratio difference, *P.val*<0.005

SPI vs SPE	Ratio	SPI vs WT	Ratio	SPE vs WT	Ratio
adrenergic receptor, alpha 2a (Adra2a).	-2.22	adrenergic receptor, alpha 2a (Adra2a).	-2.34	enolase 3, beta muscle (Eno3).	-1.99
insulin-like growth factor binding protein-like 1 (Igfbpl1).	-2.18	insulin-like growth factor binding protein-like 1 (Igfbpl1).	-1.93	actin, beta (Actb).	-1.78
chondrolectin (Chodl).	-2.03	calbindin 2 (Calb2).	-1.78	troponin T1, skeletal, slow (Tnnt1).	-1.50
gastrin releasing peptide (Grp).	-1.85	Rho family GTPase 2 (Rnd2).	-1.60	solute carrier family 17 (sodium-dependent inorganic phosphate cotransporter), member 7 (Slc17a7).	-1.47
Rho family GTPase 2 (Rnd2).	-1.84	insulinoma-associated 1 (Insm1).	-1.57	cholecystokinin B receptor (Cckbr).	-1.47
cysteine rich BMP regulator 2 (chordin like) (Crim2).	-1.79	cysteine rich BMP regulator 2 (chordin like) (Crim2).	-1.57	RIKEN cDNA 4930511J11 gene (4930511J11Rik).	-1.40
calbindin 2 (Calb2).	-1.77	chondrolectin (Chodl).	-1.56	lamin A (Lmna), transcript variant 2.	-1.37
single-stranded DNA binding protein 2 (Ssbp2), transcript variant 1.	-1.74	elastin microfibril interfacer 2 (Emilin2).	-1.55	calcium/calmodulin-dependent protein kinase II alpha (Camk2a), transcript variant 2.	-1.34
insulinoma-associated 1 (Insm1).	-1.68	Meis homeobox 2 (Meis2), transcript variant 2.	-1.53	titin-cap (Tcap).	-1.33
single-stranded DNA binding protein 2 (Ssbp2), transcript variant 1.	-1.67	relaxin family peptide receptor 3 (Rxfp3).	-1.52	visinin-like 1 (Vsnl1).	-1.32

Table 2: Migration genes showing significant gene expression when comparing SPI cells to SPE cells

Definition	Search Key	FC-SPI vs SPE	*P.val.* SPI vs SPE
Migration genes upregulated in SPE, and downregulated in SPI cells			
Rho family GTPase 2 (Rnd2)	ILMN_221456	0.54	0
T-cell lymphoma invasion and metastasis 2 (Tiam2)	ILMN_219894	0.67	1.00E-05
nuclear receptor subfamily 2, group F, member 2 (Nr2f2), transcript variant 2	ILMN_218443	0.71	5.00E-05
ST8 alpha-N-acetyl-neuraminide alpha-2,8-sialyltransferase 2 (St8sia2)	ILMN_219178	0.72	8.00E-05
lamin B1 (Lmnb1)	ILMN_220293	0.77	0
ephrin B1 (Efnb1)	ILMN_218638	0.80	0.00024
katanin p60 (ATPase-containing) subunit A1 (Katna1)	ILMN_223573	0.83	0.00044
tubulin, gamma complex associated protein 2 (Tubgcp2)	ILMN_195059	0.837	3.00E-05
neurogenin 2 (Neurog2)	ILMN_214239	0.84	3.00E-05
PTK2 protein tyrosine kinase 2 (Ptk2)	ILMN_211438	0.86	0.00018
p21 (CDKN1A)-activated kinase 4 (Pak4)	ILMN_213768	0.90	0.00297
motor neuron and pancreas homeobox 1 (Mnx1)	ILMN_223550	0.90	0.00056
Migration genes downregulated in SPE and upregulated in SPI cells			
nuclear distribution gene E homolog 1 (A nidulans) (Nde1)	ILMN_186852	1.14	0.00198
amyloid beta (A4) precursor protein-binding, family B, member 1 (Apbb1)	ILMN_212171	1.15	0.00014
chitinase 3-like 1 (Chi3l1)	ILMN_210847	1.16	0.00088
angiopoietin 2 (Angpt2)	ILMN_213914	1.18	0.00018
mitogen activated protein kinase kinase 4 (Map2k4)	ILMN_235654	1.19	0.00015
endothelin receptor type B (Ednrb)	ILMN_208799	1.2	0.00155
unc-5 homolog C (C. elegans) (Unc5c)	ILMN_188618	1.24	1.00E-05
growth arrest specific 6 (Gas6)	ILMN_217682	1.3	0
solute carrier family 1 (glial high affinity glutamate transporter), member 3 (Slc1a3)	ILMN_213165	1.37	0.00019

Table3 : regionalized expression patterns of deep (close to *stratum oriens*) or superficial (close to *stratum radiatum*) molecular markers along the septotemporal axis of the pyramidal cell layer of the hippocampus.

Genes enriched in SPE cell layer representing deep cell markers in the WT																				
Definition	**SPI/ SPE**	**Pyramidal cell layers**									***St. Oriens* border layer**									
		1	**2**	**3**	**4**	**5**	**6**	**7**	**8**	**9**	**1'**	**2'**	**3'**	**4'**	**5'**	**6'**	**7'**	**8'**	**9'**
gastrin releasing peptide (Grp)	0.54								8											
potassium channel, subfamily K, member 1 (Kcnk1)	0.62	**1**	**2**	**3**	**4**	5	6	7												
neuronal growth regulator 1 (Negr1), transcript variant 1	0.69	1	2	3	4	5	6	7	8	9										
natriuretic peptide receptor 3 (Npr3), transcript variant 1	0.80				4	5	6	**7**	**8**	**9**										
Ngfi-A binding protein 1 (Nab1)	0.86	1	2	3	4	5	6	7	8	9										
catenin (cadherin associated protein), alpha 2 (Ctnna2), transcript variant 2	0.86	**1**	**2**	3	4	5	6													
Genes enriched in SPI cell layer representing outer boundary markers in the WT																				
Definition	**SPI/ SPE**	**Pyramidal cell layers**									***St. Oriens* border layer**									
		1	**2**	**3**	**4**	**5**	**6**	**7**	**8**	**9**	**1'**	**2'**	**3'**	**4'**	**5'**	**6'**	**7'**	**8'**	**9'**
solute carrier family 30 (zinc transporter), member 3 (Slc30a3)	1.1	1	2						8	9			3'		5'	6'	7'			
cadherin 13 (Cdh13)	1.2													4'	5'	6'				
StAR-related lipid transfer (START) domain containing 13 (Stard13)	1.22												3'	4'	5'	6'	7'			
Ly6/Plaur domain containing 1 (Lypd1)	1.41							7	8	9			3'	4'	5'	6'				
FXYD domain-containing ion transport regulator 7 (Fxyd7)	1.64	**1**	**2**	**3**	**4**				8	9					5'					
suppression of tumorigenicity 18 (St18)	1.64											2'	3'	4'	5'	6'	7'	8'	9'	
N-terminal EF-hand calcium binding protein 2 (Necab2)	1.69			3		**5**	**6**	**7**	8				3'	4'	5'	6'				
sparc/osteonectin, cwcv and kazal-like domains proteoglycan 3 (Spock3)	2.03	**1**	**2**	**3**	4	5														

Supplementary Material:

Supplementary figure 1: Schema depicting the statistical analysis for normalization and bias correction.

(A) Each log-transformed expression value was normalized by subtracting the log-median intensity value and dividing with the standard deviation of the log-intensities (see methods). Next, the samples on slide 1 were corrected to account for a possible bias between slides: the bias of the SPE category (defined as the difference of intensities of SPE sample on slide 2 and the mean of SPE samples on slide 1) was used to correct the SPI samples, while the bias of SPI (defined in a similar way) corrected the SPE samples. (B) The gene-wise bias of SPI plotted against the bias of SPE shows that the majority of genes cluster around zero on the X and Y axis (no bias between slides), but some genes outside of this cluster need correction. The correction is weighted by w, computed as the coefficient that minimizes the least square distance between the samples of the same category on slide 1 and slide 2 respectively (see methods). Finally, the bias corrected samples were used as input for the differential gene expression search as implemented in the R-package limma (A). The projections of the data on the first three principal eigenvectors are shown, before (C) and after (D) bias correction. SPI samples on slide 1 are represented in red, SPE samples on slide 1 in green, SPI and SPE on slide 2 respectively in magenta and cyan, and wild type on slide 2 in black. Note that before bias correction, the first eigenvector (Z[1,]) splits the samples according to the slide they belong to (reflecting a bias), while the samples after correction are more clearly grouped by the biological sample of origin. Data analysis was done in collaboration with the group of Roest Crollius H./ ENS.

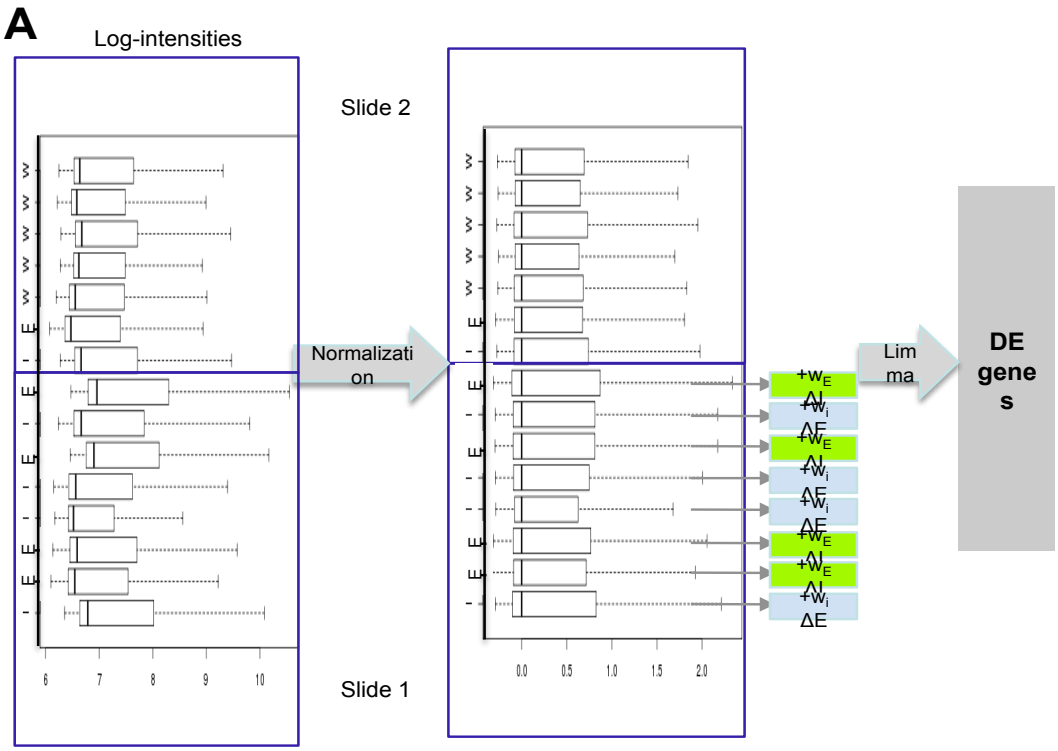

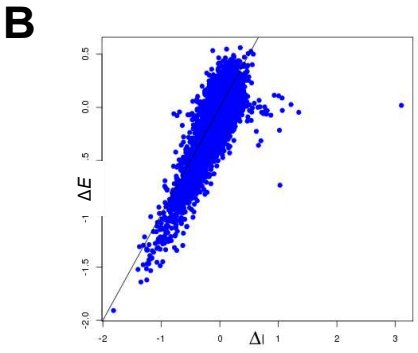

Choice of bias correction weights :

$$min_{wI}\,[I_{slide2} - mean(I_{slide1} + w_I.\Delta_E)]^2$$

$$min_{wE}\,[E_{slide2} - mean(E_{slide1} + w_E.\Delta_I)]^2$$

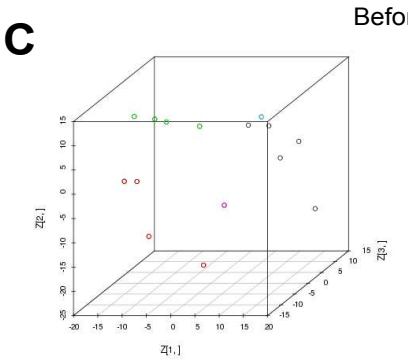

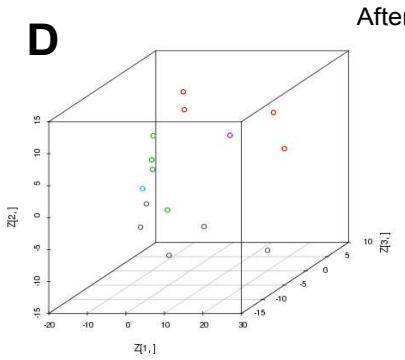

List of supplementary tables

Supplementary table 1: Primer sequences for RT-PCR and ISH experiments

Supplementary table 2: RNA concentration and RIN values.

Supplementary table 3: Differentially expressed gene lists showing ratios of fold changes compared to WT.

Supplementary table 4: Joint SPI and SPE versus WT DAVID analyses (upanddown_0.005)-results summarized in figure 3.

Supplementary table 5: DAVID analyses SPI and SPE commonly de-regulated genes (455 genes) results summarized in figure 2.

Supplementary table 6: SPI-SPE vs WT_IPA_0.005.

Supplementary table 1: Primer sequences for RT-PCR and ISH experiments

Gene name	Forward primer	Reverse primer
Col6a1	GAGATGCACACTCTTTGCTTTG	GAGATAGCTGGCTTGGATCAG
Wfs1	TACGCCAAGGGCATCATT	CACCAGGTAGGGCACCAG
KA1	CAGCGCATGGAGGTGCCCAT	GGCTCGCTGCTGTTGGTGGT
Cdh13	CATTGTGGTGTCCCCCAT	GGGTTGGTGTGGATCTCG
Necab2	TACCATCGATTCAGACAACACC	AGGTACTGTCTCAGGGAATCCA
Chl1	A CAGACAAGAATCCCCAGAACAT	TGTTGAGTTGAGGTTGGAGAGA
GRP	CACGGTCCTGGCTAAGATGTAT	CCAGTAGAGTTGACGTTTGCAG
SST	ACGCTACCGAAGCCGTC	GGGGCCAGGAGTTAAGGA
KA1	TGGCCAAGAACCGTATCAAC	TGTTGCTGATGATGGAGCTG
Nov	GCTGCCCTACAACCACATTT	CTCACTCCTTGGTCGGTGAT
Col6a1	CCAGACAGTCTCCAGGAAGG	GGGCGGGATCTAGGAG
Prox1	GCTCATCAAGTGGTTCAGCA	ATCCAGCTTGCAGATGACCT

Supplementary table 2: RNA concentration and RIN values.

Sample name	Area concerned	RNA concentration	RIN value
LCM 22	CA3	40.9	6.1
LCM 24	CA3	36.4	6.8
LCM29	CA3	NA	NA
LCM31	CA3	65	6.3
LCM33	CA3	68.4	6.7
LCM 25/2	SPE	30.76	7.2
LCM42/2	SPE	71.6	5.6
LCM43/2	SPE	78	6.5
LCM45/2	SPE	54	6.6
LCM40/1	SPE	49	6.2
LCM 25/1	SPI	12.77	5.8
LCM40/2	SPI	30	6.1
LCM42/1	SPI	30.6	5.2
LCM43/1	SPI	46	5.3
LCM45/1	SPI	84	6.3

Supplementary table 3: Differentially expressed gene lists showing ratios of fold changes compared to WT

A: Gene expression changes in SPI cells compared to WT

Definition	SearchKey	FC- SPI vs WT	P.val-SPI vs WT
adrenergic receptor, alpha 2a (Adra2a).	ILMN_190996	0.426908857	0
doublecortin (Dcx), transcript variant 4.	ILMN_214635	0.470739232	0
insulin-like growth factor binding protein-like 1 (Igfbpl1).	ILMN_259511	0.518350551	0
doublecortin (Dcx), transcript variant 4.	ILMN_214635	0.520510799	0
calbindin 2 (Calb2).	ILMN_209607	0.562529242	0
Rho family GTPase 2 (Rnd2).	ILMN_221456	0.62546454	0
insulinoma-associated 1 (Insm1).	ILMN_218993	0.635956503	0
cysteine rich BMP regulator 2 (chordin like) (Crim2).	ILMN_253999	0.63860688	2.00E-05
chondrolectin (Chodl).	ILMN_222851	0.639492791	0.00015
elastin microfibril interfacer 2 (Emilin2).	ILMN_250777	0.644834125	0
Meis homeobox 2 (Meis2), transcript variant 2.	ILMN_254922	0.655651007	0
relaxin family peptide receptor 3 (Rxfp3).	ILMN_217754	0.65747138	0.00028
T-cell lymphoma invasion and metastasis 2 (Tiam2).	ILMN_219894	0.669427628	1.00E-05
phosphofructokinase, platelet (Pfkp).	ILMN_192121	1.639209215	1.00E-05
metallothionein 3 (Mt3).	ILMN_223483	1.646040691	2.00E-05
Kruppel-like factor 9 (Klf9).	ILMN_222878	1.655193632	0
ATPase, Na+/K+ transporting, alpha 2 polypeptide (Atp1a2).	ILMN_220489	1.657489809	0
cadherin 13 (Cdh13).	ILMN_185061	1.665551542	0
histone cluster 1, H2bc (Hist1h2bc).	ILMN_216940	1.666706414	0
arylacetamide deacetylase-like 1 (Aadacl1).	ILMN_218297	1.677136369	0
insulin-like growth factor binding protein 7 (Igfbp7).	ILMN_213162	1.697015803	0
neurocalcin delta (Ncald). XM_921409 XM_921419 XM_921424	ILMN_214828	1.708819482	0
histone cluster 1, H1c (Hist1h1c).	ILMN_235246	1.717130873	0
sparc/osteonectin, cwcv and kazal-like domains proteoglycan 1 (Spock1).	ILMN_208879	1.719512972	0
sparc/osteonectin, cwcv and kazal-like domains proteoglycan 3 (Spock3).	ILMN_212613	1.729074463	0
synaptic vesicle glycoprotein 2 b (Sv2b).	ILMN_219866	1.73748437	0
metallothionein 1 (Mt1).	ILMN_209514	1.813780658	0.00395
RAS guanyl releasing protein 1 (Rasgrp1).	ILMN_208941	1.825130977	0

B: Gene expression changes in SPE cells compared to WT

Definition	SearchKey	FC- SPE vs WT	P.val-SPE vs WT
doublecortin (Dcx), transcript variant 4.	ILMN_214635	0.485990494	0
enolase 3, beta muscle (Eno3).	ILMN_222979	0.503477775	0.00392
actin, beta (Actb).	Actb	0.56097174	0.00306
doublecortin (Dcx), transcript variant 4.	ILMN_214635	0.576742803	0
troponin T1, skeletal, slow (Tnnt1).	ILMN_189308	0.667111585	0.00351
solute carrier family 17 (sodium-dependent inorganic phosphate cotransporter), member 7 (Slc17a7).	ILMN_211658	0.681601304	0.00019
cholecystokinin B receptor (Cckbr).	ILMN_218089	0.682073917	0.0011
RIKEN cDNA 4930511J11 gene (4930511J11Rik).	ILMN_216758	0.715984371	3.00E-05
lamin A (Lmna), transcript variant 2.	ILMN_209635	0.727994774	0.00098
calcium/calmodulin-dependent protein kinase II alpha (Camk2a), transcript variant 2.	ILMN_209509	0.746906729	2.00E-05
titin-cap (Tcap).	ILMN_218508	0.754190038	0.00176
visinin-like 1 (Vsnl1).	ILMN_186814	0.756808396	2.00E-05
mevalonate (diphospho) decarboxylase (Mvd).	ILMN_214187	0.758909626	9.00E-05
MARCKS-like 1 (Marcksl1).	ILMN_211564	1.407368375	0.00037
RNA (guanine-7-) methyltransferase (Rnmt).	ILMN_191320	1.407368375	0.00157
host cell factor C1 (Hcfc1).	ILMN_220569	1.409320755	0.00067
heterogeneous nuclear ribonucleoprotein D-like (Hnrpdl).	ILMN_217979	1.41519416	0.00018
CUG triplet repeat, RNA binding protein 1 (Cugbp1), transcript variant 2.	ILMN_216161	1.419123356	0.00061
neuron specific gene family member 1 (Nsg1).	ILMN_212430	1.423063461	0.00199
myosin light chain, regulatory B (Mylc2b).	ILMN_210875	1.426025717	9.00E-05
oligodendrocyte transcription factor 1 (Olig1).	ILMN_223162	1.429984986	0
cDNA sequence BC085271 (BC085271).	ILMN_226460	1.433955248	0.00048
PREDICTED: hypothetical protein LOC100046136 (LOC100046136).	ILMN_216416	1.459020344	2.00E-05
heterogeneous nuclear ribonucleoprotein A1 (Hnrpa1), transcript variant 2.	ILMN_257803	1.462057448	0.00016
Von Willebrand factor homolog (Vwf).	ILMN_195886	1.468150636	3.00E-05
heat shock protein 90kDa alpha (cytosolic), class B member 1 (Hsp90ab1).	ILMN_216468	1.474269217	0.00018
membrane-associated ring finger (C3HC4) 6 (March6).	ILMN_189549	1.476314406	0.00014

C: Gene expression changes in SPI cells compared to SPE

Definition	SearchKey	FC- SPI vs SPE	P.val-SPI vs SPE
adrenergic receptor, alpha 2a (Adra2a).	ILMN_190996	0.45031299	0
insulin-like growth factor binding protein-like 1 (Igfbpl1).	ILMN_259511	0.459456442	0
chondrolectin (Chodl).	ILMN_222851	0.492774668	0
gastrin releasing peptide (Grp).	ILMN_216485	0.541112322	2.00E-05
Rho family GTPase 2 (Rnd2).	ILMN_221456	0.544121221	0
cysteine rich BMP regulator 2 (chordin like) (Crim2).	ILMN_253999	0.557483109	0
calbindin 2 (Calb2).	ILMN_209607	0.563700206	0
single-stranded DNA binding protein 2 (Ssbp2), transcript variant 1.	ILMN_215622	0.575943821	0
insulinoma-associated 1 (Insm1).	ILMN_218993	0.593779833	0
single-stranded DNA binding protein 2 (Ssbp2), transcript variant 1.	ILMN_215622	0.597081594	0
yippee-like 1 (Drosophila) (Ypel1).	ILMN_188637	0.616426163	0
pleckstrin homology domain containing, family G (with RhoGef domain) member 2 (Plekhg2).	ILMN_210871	0.621144141	0
potassium channel, subfamily K, member 1 (Kcnk1).	ILMN_237297	0.622005827	0
Meis homeobox 2 (Meis2), transcript variant 2.	ILMN_254922	0.623732786	0
tachykinin receptor 3 (Tacr3).	ILMN_216524	0.62546454	1.00E-05
host cell factor C1 (Hcfc1).	ILMN_220569	1.409320755	0.00067
heterogeneous nuclear ribonucleoprotein D-like (Hnrpdl).	ILMN_217979	1.41519416	0.00018
CUG triplet repeat, RNA binding protein 1 (Cugbp1), transcript variant 2.	ILMN_216161	1.419123356	0.00061
neuron specific gene family member 1 (Nsg1).	ILMN_212430	1.423063461	0.00199
myosin light chain, regulatory B (Mylc2b).	ILMN_210875	1.426025717	9.00E-05
oligodendrocyte transcription factor 1 (Olig1).	ILMN_223162	1.429984986	0
cDNA sequence BC085271 (BC085271).	ILMN_226460	1.433955248	0.00048
	ILMN_210976	1.449946833	0.00088
PREDICTED: hypothetical protein LOC100046136 (LOC100046136).	ILMN_216416	1.459020344	2.00E-05
heterogeneous nuclear ribonucleoprotein A1 (Hnrpa1), transcript variant 2.	ILMN_257803	1.462057448	0.00016
Von Willebrand factor homolog (Vwf).	ILMN_195886	1.468150636	3.00E-05
heat shock protein 90kDa alpha (cytosolic), class B member 1 (Hsp90ab1).	ILMN_216468	1.474269217	0.00018
membrane-associated ring finger (C3HC4)	ILMN_18954		

References

Ahn, A.H., Dziennis, S., Hawkes, R., and Herrup, K. (1994). The cloning of zebrin II reveals its identity with aldolase C. Development *120*, 2081–2090.

Altman, J., and Bayer, S.A. (1990). Prolonged sojourn of developing pyramidal cells in the intermediate zone of the hippocampus and their settling in the stratum pyramidale. J. Comp. Neurol. *301*, 343–364.

Angevine, J.B., Jr (1965). Time of neuron origin in the hippocampal region. An autoradiographic study in the mouse. Exp Neurol Suppl Suppl 2:1–70.

Angevine, J.B., and Sidman, R.L. (1961). Autoradiographic Study of Cell Migration during Histogenesis of Cerebral Cortex in the Mouse. , Published Online: 25 November 1961; | Doi:10.1038/192766b0 *192*, 766–768.

Arya, R., Mallik, M., and Lakhotia, S.C. (2007). Heat shock genes - integrating cell survival and death. J. Biosci. *32*, 595–610.

Asai, H., Morita, S., and Miyata, S. (2011). Effect of pleiotrophin on glutamate-induced neurotoxicity in cultured hippocampal neurons. Cell Biochemistry and Function *29*, 660–665.

Baas, P.W., and Joshi, H.C. (1992). Gamma-tubulin distribution in the neuron: implications for the origins of neuritic microtubules. J. Cell Biol. *119*, 171–178.

Barkovich, A.J., Kuzniecky, R.I., Jackson, G.D., Guerrini, R., and Dobyns, W.B. (2001). Classification system for malformations of cortical development: update 2001. Neurology *57*, 2168–2178.

Brown, J.P., Couillard-Després, S., Cooper-Kuhn, C.M., Winkler, J., Aigner, L., and Kuhn, H.G. (2003). Transient expression of doublecortin during adult neurogenesis. J. Comp. Neurol. *467*, 1–10.

Buono, P., Barbieri, O., Alfieri, A., Rosica, A., Astigiano, S., Cantatore, D., Mancini, A., Fattoruso, O., and Salvatore, F. (2004). Diverse human aldolase C gene promoter regions are required to direct specific LacZ expression in the hippocampus and Purkinje cells of transgenic mice. FEBS Letters *578*, 337–344.

Cha, B., Lim, J.W., Kim, K.H., and Kim, H. (2010). HSP90beta interacts with Rac1 to activate NADPH oxidase in Helicobacter pylori-infected gastric epithelial cells. Int. J. Biochem. Cell Biol. *42*, 1455–1461.

Chen, H., Xia, Y., Fang, D., Hawke, D., and Lu, Z. (2009). Caspase-10-mediated heat shock protein 90 beta cleavage promotes UVB irradiation-induced cell apoptosis. Mol. Cell. Biol. *29*, 3657–3664.

Chevassus-Au-Louis, N., Rafiki, A., Jorquera, I., Ben-Ari, Y., and Represa, A. (1998). Neocortex in the hippocampus: an anatomical and functional study of CA1 heterotopias after prenatal treatment with methylazoxymethanol in rats. J. Comp. Neurol. *394*, 520–536.

Cid, C., Alvarez-Cermeño, J.C., Salinas, M., and Alcázar, A. (2005). Anti-heat shock protein 90beta antibodies decrease pre-oligodendrocyte population in perinatal and adult cell cultures. Implications for remyelination in multiple sclerosis. J. Neurochem. *95*, 349–360.

Corbo, J.C., Deuel, T.A., Long, J.M., LaPorte, P., Tsai, E., Wynshaw-Boris, A., and Walsh, C.A. (2002). Doublecortin is required in mice for lamination of the hippocampus but not the neocortex. J. Neurosci. *22*, 7548–7557.

Datson, N.A., Morsink, M.C., Steenbergen, P.J., Aubert, Y., Schlumbohm, C., Fuchs, E., and de Kloet, E.R. (2009). A molecular blueprint of gene expression in hippocampal subregions CA1, CA3, and DG is conserved in the brain of the common marmoset. Hippocampus *19*, 739–752.

Deguchi, Y., Donato, F., Galimberti, I., Cabuy, E., and Caroni, P. (2011). Temporally matched subpopulations of selectively interconnected principal neurons in the hippocampus. Nat. Neurosci. *14*, 495–504.

Dennis, G., Jr, Sherman, B.T., Hosack, D.A., Yang, J., Gao, W., Lane, H.C., and Lempicki, R.A. (2003). DAVID: Database for Annotation, Visualization, and Integrated Discovery. Genome Biol. *4*, P3.

Deuel, T.A.S., Liu, J.S., Corbo, J.C., Yoo, S.-Y., Rorke-Adams, L.B., and Walsh, C.A. (2006). Genetic interactions between doublecortin and doublecortin-like kinase in neuronal migration and axon outgrowth. Neuron *49*, 41–53.

Ezratty, E.J., Partridge, M.A., and Gundersen, G.G. (2005). Microtubule-induced focal adhesion disassembly is mediated by dynamin and focal adhesion kinase. Nat. Cell Biol. *7*, 581–590.

Finardi, A., Gardoni, F., Bassanini, S., Lasio, G., Cossu, M., Tassi, L., Caccia, C., Taroni, F., LoRusso, G., Di Luca, M., et al. (2006). NMDA receptor composition differs among

anatomically diverse malformations of cortical development. J. Neuropathol. Exp. Neurol. *65*, 883–893.

Fourniol, F.J., Sindelar, C.V., Amigues, B., Clare, D.K., Thomas, G., Perderiset, M., Francis, F., Houdusse, A., and Moores, C.A. (2010). Template-free 13-protofilament microtubule-MAP assembly visualized at 8 A resolution. J. Cell Biol. *191*, 463–470.

Friocourt, G., Koulakoff, A., Chafey, P., Boucher, D., Fauchereau, F., Chelly, J., and Francis, F. (2003). Doublecortin Functions at the Extremities of Growing Neuronal Processes. Cereb. Cortex *13*, 620–626.

Galimberti, I., Bednarek, E., Donato, F., and Caroni, P. (2010). EphA4 signaling in juveniles establishes topographic specificity of structural plasticity in the hippocampus. Neuron *65*, 627–642.

Gdalyahu, A., Ghosh, I., Levy, T., Sapir, T., Sapoznik, S., Fishler, Y., Azoulai, D., and Reiner, O. (2004). DCX, a new mediator of the JNK pathway. EMBO J. *23*, 823–832.

Gleeson, J.G., Allen, K.M., Fox, J.W., Lamperti, E.D., Berkovic, S., Scheffer, I., Cooper, E.C., Dobyns, W.B., Minnerath, S.R., Ross, M.E., et al. (1998). Doublecortin, a brain-specific gene mutated in human X-linked lissencephaly and double cortex syndrome, encodes a putative signaling protein. Cell *92*, 63–72.

Gupta, A., Tsai, L.-H., and Wynshaw-Boris, A. (2002). Life is a journey: a genetic look at neocortical development. Nature Reviews Genetics *3*, 342–355.

Häussler, U., Bielefeld, L., Froriep, U.P., Wolfart, J., and Haas, C.A. (2012). Septotemporal position in the hippocampal formation determines epileptic and neurogenic activity in temporal lobe epilepsy. Cereb. Cortex *22*, 26–36.

Henkemeyer, M., Itkis, O.S., Ngo, M. et al. (2003) Multiple EphB receptor tyrosine kinases shape dendritic spines in the hippocampus. J Cell Biol 163, 1313-1326.

Heng, J.I.-T., Nguyen, L., Castro, D.S., Zimmer, C., Wildner, H., Armant, O., Skowronska-Krawczyk, D., Bedogni, F., Matter, J.-M., Hevner, R., et al. (2008). Neurogenin 2 controls cortical neuron migration through regulation of Rnd2. Nature *455*, 114–118.

Horesh, D., Sapir, T., Francis, F., Wolf, S.G., Caspi, M., Elbaum, M., Chelly, J., and Reiner, O. (1999). Doublecortin, a Stabilizer of Microtubules. Hum. Mol. Genet. *8*, 1599–1610.

Jin, J., Suzuki, H., Hirai, S.-I., Mikoshiba, K., and Ohshima, T. (2010). JNK phosphorylates Ser332 of doublecortin and regulates its function in neurite extension and neuronal migration. Dev Neurobiol *70*, 929–942.

Kappeler, C., Dhenain, M., Phan Dinh Tuy, F., Saillour, Y., Marty, S., Fallet-Bianco, C., Souville, I., Souil, E., Pinard, J.-M., Meyer, G., et al. (2007). Magnetic resonance imaging and histological studies of corpus callosal and hippocampal abnormalities linked to doublecortin deficiency. J. Comp. Neurol. *500*, 239–254.

Kappeler, C., Saillour, Y., Baudoin, J.-P., Tuy, F.P.D., Alvarez, C., Houbron, C., Gaspar, P., Hamard, G., Chelly, J., Métin, C., et al. (2006). Branching and nucleokinesis defects in migrating interneurons derived from doublecortin knockout mice. Hum. Mol. Genet. *15*, 1387–1400.

Karle, K.N., Möckel, D., Reid, E., and Schöls, L. (2012). Axonal transport deficit in a KIF5A(-/-) mouse model. Neurogenetics *13*, 169–179.

Kawauchi, T., Chihama, K., Nabeshima, Y., and Hoshino, M. (2003). The in vivo roles of STEF/Tiam1, Rac1 and JNK in cortical neuronal migration. The EMBO Journal *22*, 4190–4201.

Kuiper, J.W.P., Oerlemans, F.T.J.J., Fransen, J.A.M., and Wieringa, B. (2008). Creatine kinase B deficient neurons exhibit an increased fraction of motile mitochondria. BMC Neurosci *9*, 73.

Lehéricy, S., Dormont, D., Sémah, F., Clémenceau, S., Granat, O., Marsault, C., and Baulac, M. (1995). Developmental abnormalities of the medial temporal lobe in patients with temporal lobe epilepsy. AJNR Am J Neuroradiol *16*, 617–626.

Lein, E.S., Hawrylycz, M.J., Ao, N., Ayres, M., Bensinger, A., Bernard, A., Boe, A.F., Boguski, M.S., Brockway, K.S., Byrnes, E.J., et al. (2007). Genome-wide atlas of gene expression in the adult mouse brain. Nature *445*, 168–176.

Lein, E.S., Zhao, X., and Gage, F.H. (2004). Defining a molecular atlas of the hippocampus using DNA microarrays and high-throughput in situ hybridization. J. Neurosci. *24*, 3879–3889.

Li, X.G., Somogyi, P., Ylinen, A., and Buzsáki, G. (1994). The hippocampal CA3 network: an in vivo intracellular labeling study. J. Comp. Neurol. *339*, 181–208.

Li, Y.S., Milner, P.G., Chauhan, A.K., Watson, M.A., Hoffman, R.M., Kodner, C.M., Milbrandt, J., and Deuel, T.F. (1990). Cloning and expression of a developmentally regulated protein that induces mitogenic and neurite outgrowth activity. Science *250*, 1690–1694.

Liu, J.S., Schubert, C.R., Fu, X., Fourniol, F.J., Jaiswal, J.K., Houdusse, A., Stultz, C.M., Moores, C.A., and Walsh, C.A. (2012). Molecular Basis for Specific Regulation of Neuronal Kinesin-3 Motors by Doublecortin Family Proteins. Mol. Cell.

López H, E., Fohlen, M., Lelouch-Tubiana, A., Robain, O., Jalin, C., Bulteau, C., Dorfmüller, G., Dulac, O., and Delalande, O. (2010). Heterotopia associated with hippocampal sclerosis: an under-recognized cause of early onset epilepsy in children operated on for temporal lobe epilepsy. Neuropediatrics *41*, 167–175.

Molinari, F., Kaminska, A., Fiermonte, G., Boddaert, N., Raas-Rothschild, A., Plouin, P., Palmieri, L., Brunelle, F., Palmieri, F., Dulac, O., et al. (2009). Mutations in the mitochondrial glutamate carrier SLC25A22 in neonatal epileptic encephalopathy with suppression bursts. Clin. Genet. *76*, 188–194.

Molyneaux, B.J., Arlotta, P., Menezes, J.R.L., and Macklis, J.D. (2007). Neuronal subtype specification in the cerebral cortex. Nat. Rev. Neurosci. *8*, 427–437.

Moores, C.A., Perderiset, M., Francis, F., Chelly, J., Houdusse, A., and Milligan, R.A. (2004). Mechanism of Microtubule Stabilization by Doublecortin. Molecular Cell *14*, 833–839.

Moores, C.A., Perderiset, M., Kappeler, C., Kain, S., Drummond, D., Perkins, S.J., Chelly, J., Cross, R., Houdusse, A., and Francis, F. (2006). Distinct roles of doublecortin modulating the microtubule cytoskeleton. EMBO J. *25*, 4448–4457.

Nadarajah B, Parnavelas JG. (2002) Modes of neuronal migration in the developing cerebral cortex. Nat Rev Neurosci. 2002 Jun;3(6):423-32. Review.

Nakahira E, Yuasa S. (2005) Neuronal generation, migration, and differentiation in the mouse hippocampal primoridium as revealed by enhanced green fluorescent protein gene transfer by means of in utero electroporation. J Comp Neurol. 2005 Mar 14;483(3):329-40.

Nathan, D.F., Vos, M.H., and Lindquist, S. (1997). In vivo functions of the Saccharomyces cerevisiae Hsp90 chaperone. Proc. Natl. Acad. Sci. U.S.A. *94*, 12949–12956.

Newrzella, D., Pahlavan, P.S., Krüger, C., Boehm, C., Sorgenfrei, O., Schröck, H., Eisenhardt, G., Bischoff, N., Vogt, G., Wafzig, O., et al. (2007). The functional genome of CA1 and CA3 neurons under native conditions and in response to ischemia. BMC Genomics *8*, 370.

Noctor, S.C., Martínez-Cerdeño, V., Ivic, L., and Kriegstein, A.R. (2004). Cortical neurons arise in symmetric and asymmetric division zones and migrate through specific phases. Nat. Neurosci. *7*, 136–144.

Nowakowski, R.S., and Rakic, P. (1979). The mode of migration of neurons to the hippocampus: a Golgi and electron microscopic analysis in foetal rhesus monkey. J. Neurocytol. *8*, 697–718.

Palmieri, F. (2004). The mitochondrial transporter family (SLC25): physiological and pathological implications. Pflügers Archiv European Journal of Physiology *447*, 689–709.

Pleasure, S.J., Collins, A.E., and Lowenstein, D.H. (2000). Unique expression patterns of cell fate molecules delineate sequential stages of dentate gyrus development. J. Neurosci. *20*, 6095–6105.

des Portes, V., Pinard, J.M., Billuart, P., Vinet, M.C., Koulakoff, A., Carrié, A., Gelot, A., Dupuis, E., Motte, J., Berwald-Netter, Y., et al. (1998). A novel CNS gene required for neuronal migration and involved in X-linked subcortical laminar heterotopia and lissencephaly syndrome. Cell *92*, 51–61.

Pramparo, T., Libiger, O., Jain, S., Li, H., Youn, Y.H., Hirotsune, S., Schork, N.J., and Wynshaw-Boris, A. (2011). Global developmental gene expression and pathway analysis of normal brain development and mouse models of human neuronal migration defects. PLoS Genet. *7*, e1001331.

Rafiki, Chevassus-au-Louis, Ben-Ari, Khrestchatisky, and Represa (1998). Glutamate receptors in dysplasic cortex: an in situ hybridization and immunohistochemistry study in rats with prenatal treatment with methylazoxymethanol. Brain Res. *782*, 142–152.

Rakic, P. (1972). Mode of cell migration to the superficial layers of fetal monkey neocortex. The Journal of Comparative Neurology *145*, 61–83.

Ramsköld D, Wang ET, Burge CB, Sandberg R (2009) An Abundance of Ubiquitously Expressed Genes Revealed by Tissue Transcriptome Sequence Data. PLoS Comput Biol 5(12): e1000598.

Rieger, S., Volkmann, K., and Köster, R.W. (2008). Polysialyltransferase expression is linked to neuronal migration in the developing and adult zebrafish. Dev. Dyn. *237*, 276–285.

Rooney, C., White, G., Nazgiewicz, A., Woodcock, S.A., Anderson, K.I., Ballestrem, C., and Malliri, A. (2010). The Rac activator STEF (Tiam2) regulates cell migration by microtubule-mediated focal adhesion disassembly. EMBO Reports *11*, 292–298.

Sapir, T., Shmueli, A., Levy, T., Timm, T., Elbaum, M., Mandelkow, E.-M., and Reiner, O. (2008). Antagonistic effects of doublecortin and MARK2/Par-1 in the developing cerebral cortex. J. Neurosci. *28*, 13008–13013.

Schaar, B.T., Kinoshita, K., and McConnell, S.K. (2004). Doublecortin Microtubule Affinity Is Regulated by a Balance of Kinase and Phosphatase Activity at the Leading Edge of Migrating Neurons. Neuron *41*, 203–213.

Silos-Santiago, I., Yeh, H.J., Gurrieri, M.A., Guillerman, R.P., Li, Y.S., Wolf, J., Snider, W., and Deuel, T.F. (1996). Localization of pleiotrophin and its mRNA in subpopulations of neurons and their corresponding axonal tracts suggests important roles in neural-glial interactions during development and in maturity. J. Neurobiol. *31*, 283–296.

Slemmer, J.E., Haasdijk, E.D., Engel, D.C., Plesnila, N., and Weber, J.T. (2007). Aldolase C-positive cerebellar Purkinje cells are resistant to delayed death after cerebral trauma and AMPA-mediated excitotoxicity. European Journal of Neuroscience *26*, 649–656.

Slomianka, L., Amrein, I., Knuesel, I., Sørensen, J.C., and Wolfer, D.P. (2011). Hippocampal pyramidal cells: the reemergence of cortical lamination. Brain Struct Funct *216*, 301–317.

Tabata, H., and Nakajima, K. (2003). Multipolar migration: the third mode of radial neuronal migration in the developing cerebral cortex. J. Neurosci. *23*, 9996–10001.

Tanaka, T., Koizumi, H., and Gleeson, J.G. (2006). The doublecortin and doublecortin-like kinase 1 genes cooperate in murine hippocampal development. Cereb. Cortex *16 Suppl 1*, i69–73.

Tanaka, T., Serneo, F.F., Higgins, C., Gambello, M.J., Wynshaw-Boris, A., and Gleeson, J.G. (2004a). Lis1 and doublecortin function with dynein to mediate coupling of the nucleus to the centrosome in neuronal migration. J. Cell Biol. *165*, 709–721.

Tanaka, T., Serneo, F.F., Tseng, H.-C., Kulkarni, A.B., Tsai, L.-H., and Gleeson, J.G. (2004b). Cdk5 Phosphorylation of Doublecortin Ser297 Regulates Its Effect on Neuronal Migration. Neuron *41*, 215–227.

Thompson, C.L., Pathak, S.D., Jeromin, A., Ng, L.L., MacPherson, C.R., Mortrud, M.T., Cusick, A., Riley, Z.L., Sunkin, S.M., Bernard, A., et al. (2008). Genomic anatomy of the hippocampus. Neuron *60*, 1010–1021.

Tole, S., Christian, C., and Grove, E.A. (1997). Early specification and autonomous development of cortical fields in the mouse hippocampus. Development *124*, 4959–4970.

Tole, S., and Grove, E.A. (2001). Detailed field pattern is intrinsic to the embryonic mouse hippocampus early in neurogenesis. J. Neurosci. *21*, 1580–1589.

Tuy, F.P.D., Saillour, Y., Kappeler, C., Chelly, J., and Francis, F. (2008). Alternative transcripts of Dclk1 and Dclk2 and their expression in doublecortin knockout mice. Dev. Neurosci. *30*, 171–186.

Verstreken, P., Ly, C.V., Venken, K.J.T., Koh, T.-W., Zhou, Y., and Bellen, H.J. (2005). Synaptic mitochondria are critical for mobilization of reserve pool vesicles at Drosophila neuromuscular junctions. Neuron *47*, 365–378.

Wanaka, A., Carroll, S.L., and Milbrandt, J. (1993). Developmentally regulated expression of pleiotrophin, a novel heparin binding growth factor, in the nervous system of the rat. Developmental Brain Research *72*, 133–144.

Watson, C., Nielsen, S.L., Cobb, C., Burgerman, R., and Williamson, B. (1996). Medial temporal lobe heterotopia as a cause of increased hippocampal and amygdaloid MRI volumes. J Neuroimaging *6*, 231–234.

Yanagisawa, H., Komuta, Y., Kawano, H., Toyoda, M., and Sango, K. (2010). Pleiotrophin induces neurite outgrowth and up-regulates growth-associated protein (GAP)-43 mRNA through the ALK/GSK3beta/beta-catenin signaling in developing mouse neurons. Neurosci. Res. *66*, 111–116.

CHAPTER3: DISCUSSION

The study of the heterotopic neurons and their implication in the generation of hyperexcitable neuronal circuits is important for our understanding of causes of pharmacoresistant epilepsy. We set out to characterize hippocampal CA3 heterotopic neurons in the *Dcx* KO mouse model, which exhibits migration defects and spontaneous epilepsy. We used a multi-experimental approach to characterize these cells at the morphological, ultrastructural and molecular levels. This was combined with specific experiments to examine the developmental origins and the evolution of these neurons in the adult.

Our analysis revealed alterations in the organization of these cells. The WT hippocampal CA3 region is made up of a single, relatively compact and homogenous pyramidal cell layer. The CA3 region of *Dcx* KO animals is divided into two heterotopic layers; we termed them SPI and SPE layers, corresponding to an internal and external position. The cells in these two layers are loosely organized, and contain heterogeneous cell groups, including OPCs and Sst positive interneurons, cell types that are not usually present within the CA3 cell layer in the WT.

Using electron microscopical examination of the CA3 region from P0 pups, we demonstrated potential abnormalities in the cytoplasm content of pyramidal cells in both SPI and SPE layers. Abnormalities in the mitochondria in these cells were noted, in the form of abnormal swelling and vacuolation. We are currently quantifying these observed mitochondrial abnormalities, in order to define the absolute number and the percentage of affected mitochondria in SPI and SPE cells compared to WT, in both the somatic compartment and in the developing neuronal processes.

Golgi apparatus modifications were also observed. In the WT, the Golgi apparatus is made up of a series of 5-6 flattened cisternae with occasional terminal swelling, and vesicles exclusively at the trans end of the Golgi apparatus. This organization was almost always disrupted in SPI and SPE KO cells, where the Golgi apparatus had terminal as well as internal swellings, presented with circular forms in certain cells, and had an excessive vesicular content that was not confined to the trans end, but was seen at the cis end also in some cells. Quantification of these observed abnormalities showed statistically significant differences in Golgi apparatus forms between WT and KO cells. Dilated, circular and vesicular Golgi apparatuses were found in 95%, 64%, and 90% of the KO cells, respectively, compared to 30%, 2%, and 9% in the WT

cells, respectively. These ultrastructural findings at P0 could be an indication of cellular stress in *Dcx* KO cells, indeed, apoptotic cell death at P2 was two times increased in the CA1 and CA3 regions of the hippocampus of *Dcx* KOs (article 1). These combined data advance our understanding of the nature of the pyramidal cell lamination defect, the disorganization of other cell types including oligodendrocyte precursors, which could be secondary to the pyramidal cell defects and the state of *Dcx* KO neuronal-like cells in postnatal stages.

The use of laser capture microdissection technique enabled us to specifically isolate the SPI and SPE heterotopic cells from each other and from the surrounding hippocampal CA3 region strata. We also isolated WT CA3 cells in a similar way for comparison. This experiment was successfully performed at the P0 stage and in the adult. It has allowed us up till now to study the temporal molecular profiles of heterotopic neurons at P0. Interestingly, molecular analysis and functional clustering of enriched genes showed perturbed pathways related to endosomes, methylation, molecules associated with the mitochondrial membrane and Golgi apparatus, purine metabolism and ATP binding, oxidative phosphorylation, cellular response to stress and DNA repair in SPI and SPE *Dcx* KO cells. These pathways correspond tightly to the abnormalities observed by microscopy and highlight some important molecules that may be linked to such abnormalities. A significant upregulation of genes involved in neuroprotective mechanisms was also observed.

Additionally, comparing the gene expression between SPI and SPE cells revealed important differences in molecular signatures between these two cell populations. Neuronal migration genes were differentially expressed between SPI and SPE cells at P0. Downregulation and upregulation of an important set of genes involved in pyramidal cell migration was observed in SPI and SPE cells, respectively. Using this molecular data, we detected also complementary temporal differences in the maturity status of the two heterotopic cell populations with SPI cells showing signs of having advanced maturity compared to SPE cells (article 2).

Altogether, we believe that this advanced maturity status of SPI neurons at P0 is convincing because of the following reasons:

1. Ultrastructural examination of SPI cells demonstrated a cellular profile corresponding to mature neurons, with clear cytoplasmic content, compared to a denser cytoplasm in SPE cells and some WT cells as well. Additionally, quantitative measurement of the nuclear diameter of neurons in SPI and SPE and WT neurons revealed that SPI cells had a higher nuclear diameter than SPE cells, a finding that can be correlated with an advanced maturity status.
2. The expression of *Rnd*2, a neuronal migration gene which is known to be abruptly turned off in differentiating neurons, is downregulated in SPI cells when compared to SPE cells and to the WT.
3. BrdU birth-dating experiments suggested that SPI neurons are early born. BrdU labelling of late born hippocampal neurons at E16.5 did not label SPI cells.
4. *In situ* hybridization experiments, using stable molecular markers of earliest born hippocampal cells, revealed that SPI cells express markers described to be enriched in earliest born cells, normally present in the most external regions in WT. Thus SPI cells are the earliest born. Consequently, it seems very logical that they demonstrate an advanced maturation status.
5. To confirm the advanced maturation status of SPI cells at the functional level, we are studying the expression of KCC2 expression in these cells. Preliminary results showed that some SPI cells express KCC2 on the plasma membrane at this stage. This experiment is mentioned later on in this discussion.

Interpretation of these data in the context of the electrophysiologic properties of these heterotopic neurons during their differentiation will be one of our future goals.

1. Ultrastructural abnormalities in hippocampal heterotopic neurons of Dcx KO mice:

Mitochondria are the primary cellular producer of energy mainly in the form of ATP. Developing and mature neurons are particular in having a striking diversity of distant functional zones including dendrites, axons, growth cones or synapses, areas with a high energy consumption rate. Active and coordinated bidirectional (anterograde and retrograde) transport of mitochondria along the neuronal microtubule network to and from sites of high energy demand represents a fundamental mechanism needed by neurons to assure correct energy balance (Verstreken et al., 2005). Stabilized microtubules act as the principal tracks for long-distance anterograde and retrograde cellular transport of enzymes, organelles, mRNAs and cytoskeletal components (Guzik and Goldstein, 2004). Thus microtubule stability and coordinated function seems indispensable for normal mitochondrial transport, propelled by motor proteins, such as kinesins and dyneins (DiMauro and Schon, 2008). This transport assures the maintenance of energy homeostasis in neurons. Both increased and decreased velocity of mitochondrial transport have been related to pathology (Kuiper et al., 2008; Karle et al., 2012). Defects in genes involved in mitochondrial dynamics have already been associated with several neurodegenerative disorders, such as mutations in hereditary spastic paraplegia type 10 (*SPG10*) and mutations in a gene encoding one of the kinesins (*KIF5A*) (Fichera et al., 2004), in Huntington disease (Dompierre et al., 2007), and in disorders of neuronal migration, such as deletions of *YWHAE* with Miller–Dieker lissencephaly (Toyo-oka et al., 2003).

DCX is a MAP that functions in supporting microtubule stabilization (Moores et al., 2004, 2006; Fourniol et al., 2010). *Dcx*/*Dclk* (*Doublecortin-like kinase*) double mouse mutants display a severely compromised intracellular neuronal transport of Kif1a-mediated trafficking of the presynaptic vesicle-associated membrane protein 2 (Vamp2), which accumulates in the soma of these neurons (Deuel et al., 2006; Liu et al., 2012). *In vitro* knockdown of Dcx expression did not affect the percentage and run length of mobile mitochondria during anterograde transport, it even showed a tendency towards increased velocity and run length of moving mitochondria (Liu et al., 2012). However, defective retrograde microtubule-mediated mitochondrial transport could be a plausible explanation for the mitochondrial abnormalities

revealed by electron microscopy and gene expression analyses. Alternatively, a more severe disruption of microtubule tracks in the knockout might lead to more severe mitochondrial mobility abnormalities. Such defects could in turn be one of the factors contributing to cellular stress, DNA damage and repair, imbalance in purine nucleotide metabolism, and cell death and survival deregulation, perturbed processes that were found functionally enriched upon analysis of the molecular profiles of *Dcx* deficient neurons.

Acetylated microtubule forms stable tracks for the transport of cellular organelles and signalling molecule-containing vesicles. Failure of effective transport of such components can result in defective localization of neurotrophic and neuroprotective signalling components. For example, failure of anterograde and retrograde transport of BDNF-containing vesicles resulted in cytotoxicity and mitochondrial damage observed in a mouse model of Huntington disease (Dompierre et al., 2007). Thus, failure of intracellular transport mechanisms in a variety of ways can lead to mitochondrial damage and cytotoxicity either directly through failure in mitochondrial transport, or indirectly through failure in the transport of other neuroprotective components. Both mechanisms may be a possible explanation for the observed cyto-toxic changes observed in *Dcx*-deficient heterotopic neurons.

Some rare reports suggest that mitochondrial dysfunction may play a role in the pathogenesis of brain malformations and that mitochondrial and DCX functions may share some common cellular and molecular mechanisms during neuronal migration, neuroprotection and neurodegeneration. Inborn errors of metabolism are frequently associated with brain malformations and migration defects (Nissenkorn et al., 2001; Prasad et al., 2007). A case-report of the association of mitochondrial DNA myopathy ‘‘MELAS” mutation and polymicrogyria has been described (Keng et al., 2003). Another report described a female patient presenting with mitochondrial myopathy and diffuse SBH. This patient was found to have double mutation in the *DCX* gene and the common mitochondrial DNA myopathy ‘‘MELAS” mutation (Scuderi et al., 2010). According to authors, the brain malformation in the form of SBH and diffuse agyria/pachygyria in this particular patient was not fully explained by the severity of the mutation in the *DCX* gene. Skewed X-inactivation was excluded in patient lymphocytes, making this possibility a less probable explanation for the severe

phenotype. One plausible explanation for the severe brain phenotype is the co-existence of DCX and mitochondrial disease-causing mutations in this patient (Scuderi et al., 2010). Moreover, Zellweger syndrome, a (cerebro-hepato-renal syndrome) is a peroxisomal biogenesis disorder, associated with neuronal migration defects in the cerebral cortex and the cerebellum in both humans patients and mouse models (Janssen et al., 2003; Krysko et al., 2007). Severe alterations of the mitochondrial ultrastructure, and respiratory chain complexes, resulting in severe oxidative stress was suggested as a major contributing factor in the pathogenesis of this disorder (Baumgart et al., 2001).

Although it is not yet mechanistically confirmed, pathogenic mechanisms common between mitochondrial diseases and migration disorders are possible. Defective energy metabolism resulting in free radical production and oxidative stress could be shared between mitochondrial diseases and migration defects due to failure of microtubule-based mitochondrial transport to zones of high energy demand (Naderi et al., 2006; Zemlyak et al., 2009; Shi et al., 2010).

Moreover, failure in the maintenance of calcium homeostasis could be another common pathway (Dayanithi et al., 2012; Fluegge et al., 2012; Mórotz et al., 2012). Mitochondria can sequester and release large amounts of calcium, which helps to adjust energy production to cellular needs. Basal ionized calcium levels and calcium sequestering are perturbed in fibroblasts from MELAS patients (Rothman, 1999). Correct calcium balance probably through modulation of cAMP and IGF1 signalling is essential for normal neuronal migration and maturation (Komuro and Rakic, 1992, 1996). Modulating calcium intracellular spike frequencies rescued the migration phenotype in both Weaver and fetal Minamata disease mouse models (Liesi and Wright, 1996; Fahrion et al., 2012). Our molecular data revealed disturbances in calcium ion homeostasis and purine nucleotide metabolism in both SPI and SPE heterotopic neuronal populations. Altogether, the above mentioned observations might highlight a possible link between DCX loss of function affecting mitochondrial function in maintaining intracellular homeostasis to assure normal neuronal development and function.

The Golgi apparatus is built of stacks of flattened, closely opposed cisterna and small vesicles, and takes part in modification, sorting, and transport of secretory products,

lysosomal enzymes, and membrane components (Palade, 1975). Microtubules play a dual role in maintaining the structural stability of the Golgi apparatus close to the endoplasmic reticulum (Thyberg and Moskalewski, 1985), and in supporting its function by forming stable tracks for the bidirectional transport of vesicular and tubular structures between the ER and the Golgi stacks on the one hand and between the Golgi stacks and the plasma membrane on the other hand (Matter et al., 1990). Detyrosinated and acetylated subpopulations of microtubules represent the stable part of the microtubule cytoskeleton that is engaged in transporting newly synthesized secretory proteins from the endoplasmic reticulum to the Golgi apparatus (Mizuno and Singer, 1994). Microtubule depolymerization results in a successive multistep structural modification of the Golgi apparatus that will eventually lead to swelling, fragmentation of the system of interconnected stacks, separation of the cisternal stacks from each other, and Golgi dispersion in the cytoplasm (Wehland et al., 1983; Turner and Tartakoff, 1989). Accordingly, intracellular transport, processing and extracellular release of secretory proteins are disturbed upon microtubule instability as well. This microtubule instability leading to abnormal Golgi apparatus morphology and function can be induced experimentally by pharmacological drugs causing depolymerization of microtubules (Stults et al., 1989; Robin et al., 1995). Also this is associated with a number of microtubule-associated diseases including neurodegeneration in Parkinson disease (Lin et al., 2009), Alzheimer's disease (Tanemura et al., 2002), dystonia musculorum sensory neuropathy (Ryan et al., 2012), and progressive motor neuronopathy (Schaefer et al., 2007). Additionally, the Golgi apparatus undergoes a process of swelling and fragmentation in cases of cellular stress and neuronal injury preceding neuronal cell death in a range of excitotoxic conditions including amyotrophic lateral sclerosis (Teuling et al., 2008), and cerebral ischemia (Zeng and C. Xu, 2000), as well as in excitotoxic convulsive events affecting the developing perinatal brain (Portera-Cailliau et al., 1997). The cyclin dependent kinase 5 (CDK5) has been shown to be involved in Golgi apparatus fragmentation in differentiated neuronal cells and primary neurons upon exposure to excitotoxic conditions (Sun et al., 2008). As this protein phosphorylates a number of microtubule-related proteins, including DCX (Xie et al., 2003; Tanaka et al., 2004b), such defects may occur via the microtubule cytoskeleton.

The Golgi appparatus is involved in processing proteins synthesized by the endoplasmic reticulum. The extremity of the Golgi apparatus, the trans-end which faces the plasma membrane, is involved in final protein sorting into several carriers forming mature protein vesicles, which are ready to be transported to different cellular subcompartments including the plasma membrane. The major class of trans-Golgi derived transport vesicles concerns clathrin-coated vesicles, which select cargo for delivery to endosomes, and are also important for endocytosis. μ1 and μ2 subunits of the adaptor complex AP-1 and AP-2, respectively, are involved in clathrin-dependent protein sorting and endocytosis. DCX interacts and co-immunoprecipitates with AP-1 and AP-2 complexes in developing brain extracts (Friocourt et al., 2001). Electron microscopic examination of heterotopic neurons in the *Dcx* KO mouse at P0 revealed swollen and fragmented Golgi with excessive accumulation of vesicles. The accumulated vesicles were mostly located at the trans-end of Golgi complex (data not shown), likely to be mature clathrin-coated round vesicles. Microtubule instability due to *Dcx* loss of function is a strongly plausible explanation for the observed Golgi fragmentation. Moreover, accumulated vesicles could be either related to impaired vesicular trafficking between the endoplasmic reticulum and Golgi apparatus, or between Golgi apparatus and long distance tubulin routing of mature protein vesicles(Storrie and Nilsson, 2002; Daboussi et al., 2012). The fact that the commonly observed accumulated vesicles were at the trans-Golgi side raises the possibility that vesicular trafficking and clathrin mediated exocytosis between the Golgi apparatus and plasma membrane, or indeed endocytosis from the plasma membrane, are seriously impaired in *Dcx* deficient heterotopic neurons, a possibility that may culminate in defective migration and final position of these cells. Indeed, clathrin-mediated endocytosis is involved in adhesion disassembly, that if disrupted, leads to the development of persistent, large focal adhesions that prevent normal migration (Ezratty et al., 2005; Chao and Kunz, 2009; Kawauchi et al., 2010).

Dcx KO mice have spontaneous epilepsy originating in the hippocampus (Nosten-Bertrand et al., 2008), with pyramidal cells being hyperexcitable a likely cause of this phenotype (Bazelot et al., 2012). Although the earliest age of seizures in these mice has not yet been determined, a disproportionate excitation-inhibition balance at P0 is highly probable. Interestingly, epileptic seizures are a common feature associated with inherited mitochondrial diseases. Excessive excitatory input could contribute to

increased metabolic demand and oxidative cellular stress in heterotopic cells, partially contributing to the development of the described abnormalities at the level of mitochondria and the Golgi apparatus. Whether the observed abnormalities in *Dcx* deficient neurons are a pure consequence of microtubule instability due to *Dcx* loss of function, or due to cellular stress caused by excessive excitation for other reasons needs to be determined. The latter possibility is further suggested by the electron microscopic observation of the presence of normal mitochondriae in non-mature, electrically less active cells at P0, located in the SVZ. These cells could correspond well to immature migrating neuroblasts, or to non-neuronal (glial) cells which do not normally express Dcx (Francis et al., 1999). In either case, the presence of functioning DCX protein seems instrumental in maintaining normal neuronal cell ultrastructural and mitochondrial function.

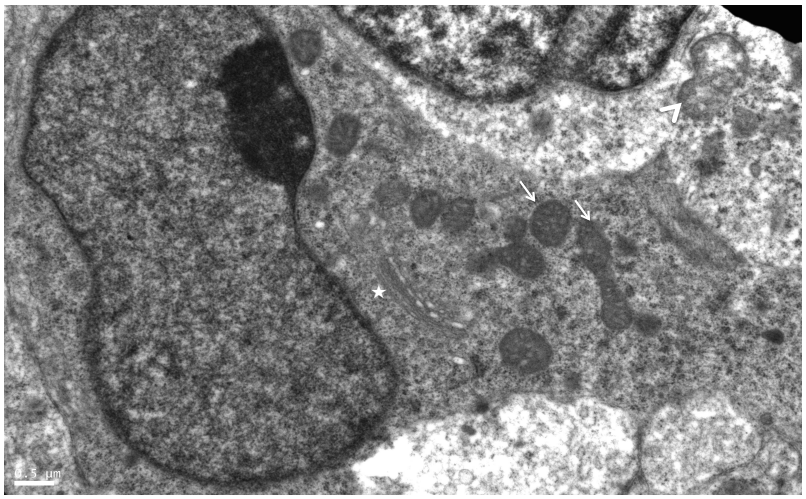

Figure 40: Ultrastructural features of immature cell located in the SVZ in *Dcx* KO CA3 region.

Note the preserved mitochondria (arrows) and the flattened horizontal cisternae charachteristic of Golgi apparatus (Star). Note the abnormal swollen and vaculated mitochondria in a nearby cell with a mature neuronal aspect.

2. *Temporal differences in migration and differentiation programs of the two heterotopic cell populations:*

In this study, our data suggests that the hippocampal lamination defect in the CA3 region of *Dcx* KO mouse is due to inverted layering most probably related to defective migration rather than aberrant *in situ* generation of ectopic CA1, CA2, or dentate gyrus projection neurons, nor due to ectopic accumulation of a non-pyramidal cell type such as interneurons, astrocytes and oligodendrocytes. Both SPI and SPE heterotopic layers are made up of pyramidal cells as a major cellular component. Hippocampal field specific marker *in situ* hybridisation and RT-PCR analyses

confirmed that both heterotopic cell layers express the pyramidal-cell, CA3-specific marker *KA1*, but not CA1, or dentate gyrus molecular markers, *Wfs*1 or *Nov, and Prox1,* respectively. Electron microscopical examination revealed that the two layers are majorly composed of cells with neuronal rather than non-neuronal cellular aspects. Electron microscopical and immunohistochemical examination indicated also the presence of heterogeneity in SPI and SPE layers, and characterized the neuropil between the two heterotopic layers. Potential indications of differences between SPI and SPE from electron microscopy data were nuclear diameter (smaller in immature neurons and in SPE) and also potentially differences in electron density of nuclei (more dense in less mature migrating neurons and in SPE and less dense in post-migratory neurons and in SPI, see discussion article 1).

Heterogeneity in the molecular profiles reflecting non-matching developmental stages between SPI and SPE cells was noted at P0. Both layers had unique expression profiles of neuronal migration genes. The downregulation of *Rnd2,* a gene whose expression is sharply turned off when neurons finish migration (Heng et al., 2008b), in SPI neurons, compared to SPE and WT neurons, suggests that SPI neurons are postmigratory and settled earlier than SPE neurons, and perhaps that they follow a radial glial independent migration mode. The former possibility is further supported by the downregulation in SPI of other neuronal migration genes, e.g. *Tiam2*. *In vivo* loss of function experiments expressing a dominant negative form of *Tiam2* caused inhibition of neuronal migration in the cerebral cortex (Kawauchi et al., 2003). *Tiam2* regulates cell migration by interacting with microtubules and regulating focal adhesion disassembly (Rooney et al., 2010). This involves dynamin-driven endocytosis (Ezratty et al., 2005), and microtubule-dependent activation of the Rho-like GTPase Rac, which controls focal adhesion size and causes their disassembly (Rooney et al., 2010). The alpha-N-acetyl-neuraminide alpha-2,8-sialyltransferase 2 *St8sia2* was also downregulated in SPI neurons. *St8sia2* is highly expressed in migrating neurons, and its expression has been shown previously to be downregulated during neuronal differentiation (Rieger et al., 2008). Thus, several genes support the hypothesis that SPI neurons are post-migratory and settle earlier than SPE neurons.

On the contrary, the above-mentioned neuronal migration genes were significantly upregulated in SPE neurons, suggesting that they may still be migratory at P0. We

also noticed significant upregulation of another two genes, coding for proteins potentially interacting with DCX or involved in neuronal migration in the hippocampus. The *close homolog of L1 (Chl1)* belongs to the family of L1 neural cell recognition molecules that includes *L1, Chl1, Neurofascin* and *NrCAM* (Maness and Schachner, 2007). Neurofascin is an interacting partner of DCX (Kizhatil et al., 2002) but this has not yet been shown for CHL1. A conserved motif in the cytoplasmic domain of L1 family members (FIGQ/AY) recruits ankyrin, which couples to F-actin through direct spectrin association (Herron et al., 2009). As shown for neurofascin, when the motif is tyrosine phosphorylated, DCX is recruited, to potentially encourage endocytosis of this transmembrane molecule. Linkage of L1 family proteins to F-actin, microtubules or both may be important for receptor clustering and signal transduction during cell migration, axon growth, and growth cone collapse (Garver et al., 1997; Jenkins et al., 2001). The absence of *Dcx* affects CA3 cell dendritic form and mossy fiber connectivity (Nosten-Bertrand et al., 2008; Bazelot et al., 2012), resembling the phenotype of Chl1 mutant mice (Montag-Sallaz et al., 2002) indicating a possible molecular convergence in migration and axon guidance signaling pathways. In transcriptome and *in situ* hybridisation (data not shown) analyses, we identified *Chl1* and *ankyrin3* as upregulated genes in *Dcx* KO CA3 neurons at P0. It will therefore be important to investigate whether the upregulation of *Chl1* and *Ankyrin-3* in the *Dcx* KO hippocampus contributes to the disruption of cellular events associated with the abnormal migration and morphology of mutant CA3 neurons.

The gastrin releasing peptide, Grp, belongs to the neuropeptide family of molecules whose expression is enriched in specific zones of the developing and adult brain (Moody et al., 1988; Wada et al., 1990; Kamichi et al., 2005). *Grp* and its receptors are upregulated in various cancers including neuroblastomas and glioblastomas, where they act as growth factors enhancing proliferation and metastasis (Qiao et al., 2008). Overexpression of the *Grp* receptor, ubiquitously expressed in the developing cortex, resulted in laminar disorganization in the telencephalon, tectum and in the cerebellum of chick embryos, and this was associated with abnormal radial glia morphology (Iwabuchi et al., 2006). We detected significant upregulation of *Grp* in SPE migratory cells at P0. *In situ* hybridization analyses of *Grp* expression at P0 and E17.5 stages revealed specific and enriched expression in migrating neuroblasts in the intermediate zone and the hippocampal primordium of the WT CA3 field specifically.

Thus *Grp* appears to be specific to the CA3 region in the developing hippocampus, which is interesting in light of the *Dcx* KO CA3-specific phenotype. Compared to WT, a similar expression pattern was detected in migrating cells and SPE of *Dcx* KO brains, with exclusion of expression in SPI neurons (Figure 5, article 2). This result may reinforce the idea that SPI cells are more mature than SPE, the latter still expressing migration machinery, including Grp.

The upregulation of *Chl1 and Grp* in SPE neurons, and their *in situ* hybridization expression patterns in migrating neuroblasts in the intermediate zone raises the possibility that these are both neuronal migration genes that have potential roles in hippocampal lamination.

3. *Molecular and cellular mechanisms for migration and lamination defects in Dcx mutants:*

Layering of the developing cortex and hippocampus follows an inside-out pattern. Cells exiting the cell cycle will sojourn in the intermediate zone in the multipolar stage, before becoming bipolar and continuing their migration (Altman and Bayer, 1990c; Tabata and Nakajima, 2003). Neurons resuming a bipolar morphology will migrate to the developing cortical plate in two different but complementary modes; early on, when the cortical plate is sufficiently thin, the earliest born neurons will extend their leading processes to the marginal zone, shorten their leading processes and move their cell bodies to their final destination in a process called somal translocation (Nadarajah et al., 2001). Later born neurons will migrate longer distances bypassing earlier-born already settled ones, and will depend on radial glial cell processes during their migration in a process called glia-guided-locomotion (Rakic, 1978; Noctor et al., 2004). Upon arrival in the marginal zone, the migrating neurons will detach from radial glia processes and somally translocate to their final destination (Nadarajah et al., 2001). After the transition from the multipolar to bipolar morphology, migrating neuroblasts resume migration along radial glial processes in a process named locomotion (Noctor et al., 2004). Near the marginal zone, migrating neurons attach their leading processes to the marginal zone and switch to glia-independent somal translocation mode. *Dab1*-mediated *reelin* signaling, and their

downstream targets *Rap1* and *cadherins* regulate cortical lamination by controlling this last step of glia-independent somal translocation in early and late born neurons (Franco et al., 2011).

Complex molecular signalling pathways and cellular machinery are orchestrated to control the succession of events and assure correct migration and layering in the developing cerebral cortex. Mouse mutants for neuronal migration genes have shed light on these machineries and helped researchers to define several critical steps in neuronal migration. For example, positioning of late-born, but not early-born neurons is defective upon disruption of *Cdk5/p35/p39* (Chae et al., 1997; Gilmore et al., 1998; Ko et al., 2001), *Lis1* (Tsai et al., 2007) and *Ndel1* (Shu et al., 2004). In contrast, perturbation of other signaling pathways such as *reelin/Apoer2/Vldlr/Dab1* (Howell et al., 1997; Sheldon et al., 1997; Trommsdorff et al., 1999) causes perturbations in early and late born neuronal positioning.

The coordinated transition from one step of migration to the next (eg multipolar to bipolar) is a tightly regulated process at the molecular and the cellular level. The *forkhead box transcription factor* (*FoxG1)* is transiently downregulated when migrating neuroblasts enter the multipolar cell phase and is re-expressed as they proceed onward into the cortical plate. Failure to downregulate *FoxG1* at the beginning of the multipolar phase transiently indulges migrating neuroblasts to move within the lower intermediate zone as a result of failure to express *Unc5D*. Cells perturbed in this fashion become ultimately displaced to more superficial layers than expected from their birthdate, and their laminar identity was respecified accordingly (Miyoshi and Fishell, 2012). Impaired transition from multipolar to bipolar phase during neuronal migration is a common feature when knocking down genes involved in positioning of late born neurons including *CDK5* (Ohshima et al., 2007), *Lis1* (Tsai et al., 2005), and *Dcx* (Bai et al., 2003). In our microarray data, we found significant upregulation of *Foxg1* in SPE neurons. Although this upregulation itself does not necessarily fit with *Foxg1* expression dynamics during multipolar to bipolar transit,, it could still suggest that disturbances in *Foxg1* expression dynamics are at the core of the failure of multipolar to bipolar state transition of *Dcx* KO SPE migrating neuroblasts. Further *Foxg1* expression analysis at different developmental stages and functional experiments will be needed to validate or rule out this hypothesis.

Although it has never been formally demonstrated in the hippocampal CA3 region, that the earliest born neurons migrate using the somal translocation mode to form the deepest cell layer close to *stratum oriens,* this nevertheless remains likely, following mechanisms shown in the isocortex (Nadarajah et al., 2001). Recently, it has also been shown that intrinsic cellular mechanisms that determine the temporal developmental sequence of certain neuronal populations in the developing hippocampus will eventually link neurogenesis time windows, maturation programs, connectivity patterns and molecular markers (Galimberti et al., 2010; Deguchi et al., 2011). *Col6a1* and *St18* are two molecular markers of deep-located, earliest-born neurons. They label a single-cell- thick band of neurons along the border of the pyramidal cell layer and *stratum oriens* in the CA3 and CA2 hippocampal fields (Thompson et al., 2008; Deguchi et al., 2011).

Global gene expression profiles of the two heterotopic cell layers in *Dcx* KO hippocampus at P0 revealed that *St18* expression was significantly upregulated in the more superficially-located SPI cells close to *stratum radiatum. In situ* hybridization experiments in adult *Dcx KO* hippocampus confirmed the persistent expression of *Col6a1* in this neuronal population, but not in SPE neurons. Moreover, preliminary BrdU birthdating experiments in *Dcx* KO embryos have shown that earliest born pyramids at E11.5 are located in the SPI instead of being located in deeper cell-layers, as in WT. Additionally, the latest born neurons, labelled with BrdU at E16.5, were located in the most superficial part of the SPE hetrotopic layer (Figure 40). Thus earliest born neurons, potentially adopting somal translocation as the principal mode of migration, are located in the more superficial rather than the deepest layers along the radial axis of the CA3 field in *Dcx* KO hippocampus. A finding that highly suggest that the SPI and SPE neuronal populations not only have differences in molecular markers, neurogenesis time windows, and differentiation programs, but may also adopt two distinct modes of migration during development. Thus the SPI cell population, corresponding to the earliest born neurons, are predicted to adopt the somal translocation mode of migration. SPE cells are likely to be later born, and may potentially depend upon radial-glia guided migration. E16.5 BrdU experiments suggest also that despite their failure in bypassing SPI cells, the SPE heterotopic population have maintained the inside-out lamination pattern, within its own neuronal population itself, and that the latest born cells are neither located in the deepest nor

most superficial poles along the radial axis, instead, they are sandwiched in between, contributing further to the overall disorganization in the CA3 region.

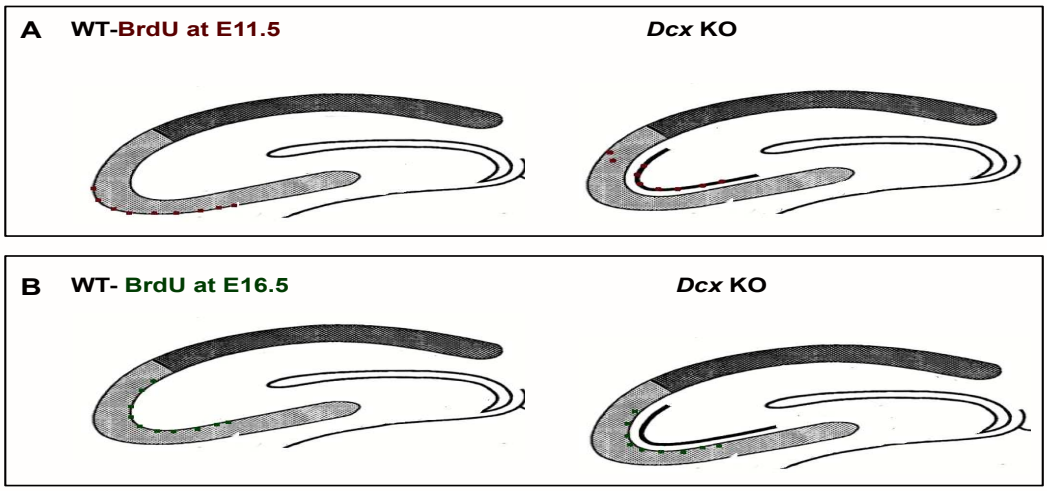

Figure 40: Figure 41: Schematic presentation of the observed birth date and layer fate of BrdU labeled neurons in the WT (left), and the Dcx KO (right)

Dcx mutants do not manifest gross cortical layering defects in mouse (Corbo et al., 2002; Kappeler et al., 2007), most probably due to compensation and genetic redundancy. Acute knockdown of *Dcx* using the RNAi approach resulted in defective migration of upper layer cortical neurons, which remained stalled in the intermediate zone forming a heterotopic band (Bai et al., 2003; Manent et al., 2009; Lapray et al., 2010). Thus, the participation of *Dcx* in radial glia guided migration has been experimentally confirmed. However, *Dcx* knockdown experiments to study its role in migration mechanisms adopted by earlier born neurons, which uses exclusively the somal translocation mode has not been yet performed. Time-lapse imaging of the final step of radially migrating neurons, detaching from radial glial fibers and somally translocating to their final position, has also never been performed. Therefore, a potential function of *Dcx* in any of these steps during cortical layering remains a valid hypothesis. The migration defects observed in *Dcx* KO hippocampus may suggest its involvement in multiple subcellular processes during neuronal migration. However, the ability of the earliest-born, somally- translocating SPI neurons to migrate a long distance, and the failure of SPE neurons to bypass SPI cells could highlight the fact that Dcx is involved in radial-glia guided migration rather than somal translocation. Time-lapse imaging experiments studying the migration dynamics of Dcx deficient neurons during both modes of migration will be needed to confirm this hypothesis.

The CA3 field of the hippocampus is the only part of mouse telencephalon where neuronal migration is severely affected by constitutional *Dcx* knockout (Corbo et al., 2002; Kappeler et al., 2007). Redundant compensatory genetic programs are thought to account for the mild and even absent gross phenotype in other cortical areas. It is still undetermined why it is the CA3 region that is particularly affected. This region of the hippocampus has several unique characteristics; neurons migrating to the CA3 need to migrate a longer distance from areas of generation in the neuroepithelium to the Ammon's horn. Additionally, they need to follow a curved rather than a straight migratory path (Altman and Bayer, 1990c; Nakahira and Yuasa, 2005). In the CA3 field, migrating neuroblasts will spend the longest time sojourning in the multipolar phase, 4-5 days, compared to 2-3 days for CA1 neurons, or 24 hours for cortical neurons (Altman and Bayer, 1990c). With the complex anatomical setup of the CA3 region, SPE neurons may either be facing difficulties in transition from multipolar to bipolar phase, or maybe migrating at a lower speed. These factors may culminate in delayed migration and ectopic positioning of SPE neurons, being unable to reach their final destinations.

Glutamatergic and GABAergic migrating neurons share a synergistic cooperative migration mode, where GABA acting through GABAA receptors and glutamate acting through AMPA receptors play permissive roles promoting the migration of pyramidal cells and interneurons, respectively (Manent et al., 2005, 2006). Consequently, isochronic coordination between the two populations, to assure synchronous migration in close proximity is very essential. The first interneurons invade the CA3 field no earlier than E16, much later than the CA1 or the cortex. Branching and nucleokinesis defects have been described in *Dcx* deficient interneurons (Kappeler et al., 2006). A mild temporal delay in interneurons invading the CA3 region of *Dcx* KO will result in disorganization of this cooperative isochronic migration of glutamatergic and GABAergic populations, culminating in the impaired migration of pyramidal cells and resulting in a more evident disorganization. Detailed analysis of interneuron migration streams at different developmental stages in *Dcx* KO embryos will help determine if glutamatergic and GABAergic neuronal migration synergy is impaired or not in *Dcx* mutants.

4. Maturation of developing hippocampal circuits in Dcx KO mice and possible developmental causes of hyperexcitable circuits:

Understanding the complexity of mature functional hippocampal circuits requires an understanding of the emergence of electrical activity and wiring and the regulatory hierarchy during critical periods of neuronal development. Additionally, mouse models of neuronal pathology help us to gain insights on key components of these developing circuits. In the hippocampus, a temporally coordinated sequence of events will connect neuronal subpopulations sharing unique molecular profiles, birthdates, morphological properties, maturation and connectivity patterns, and help them insert into hippocampal circuits during a specified time window (Deguchi et al., 2011). For example, the earliest born Lsi1 neuronal population possesses a unique identity defined by a unique molecular profile, and a temporally advanced maturation and synaptogenesis status when compared to other later born neuronal populations (Deguchi et al., 2011). Additionally, identity specification in Lsi1 granule cell neurons will also define spatially restricted structural plasticity by forming mossy fiber terminal arborisations specifically with only other Lsi1 pyramidal cells in the CA3 region in a predefined topographic organization (Galimberti et al., 2010; Deguchi et al., 2011).

Neuronal maturation and synaptic transmission also follows a temporal sequence; with GABAergic and then glutamatergic neurons establishing functional synapses (Hennou et al., 2002). At birth, three types of principal hippocampal neurons can be identified depending on their synaptic activity; a majority of later born, electrically silent neurons, a small fraction of earlier born with GABA receptor mediated electrical activity, and a third small fraction of earliest-born electrically active neurons, in whom the electrical activity is mediated by both $GABA_A$ and glutamate receptors (Tyzio et al., 1999). Giant depolarizing currents (GDPs) are network-driven polysynaptic events restricted to the early developing neuronal circuits (Ben-Ari et al., 1989; Menendez de la Prida et al., 1996; Khazipov et al., 2001; Aguado et al., 2003) They are generated predominantly by GABA, which at these stages is depolarizing and excitatory (Khazipov et al., 1997, 2004; Garaschuk et al., 1998). They are initiated through a small population of gap junction-coupled neurons, after which

GDPs appear. They are present simultaneously in hundreds of neurons and propagate to the entire network, shifting the network from a voltage-gated localized pattern involving selected neuronal assemblies to a synaptic one that reaches most neurons via excitatory GABA and glutamatergic synapses (Moody and Bosma, 2005). It seems persuasive that neuronal populations in this network with advanced maturity status, expressing functional GABA and glutamate receptors will play pioneering roles in synchronizing these circuits, potentiating the maturity of these developing networks, and probably contributing to pro-epileptic phenotypes in pathologic conditions. Thus even if neuronal birthdate is not the ultimate determinant of neuronal fate, it plays an instrumental role in the maturation sequence of neurons, being a default factor of determining their contribution to eventual normal or pathologic circuits.

Intrinsic cellular properties orchestrate with strictly defined developmental programs to define not only birth date but also maturity status during critical periods when neurons are highly plastic in preparation to adopt their defined adult function. Despite this strict temporal sequence during perinatal critical periods, neuronal circuits are not hard-wired, and they are sufficiently plastic to modify themselves in cases of pathology. For example, in a rat model of SBH caused by Dcx knockdown, manipulation of abnormally migrated epileptogenic heterotopic neurons and circuits during the postnatal periods resulted in unexpected extensive plastic responses, arrested neurons resumed migration, decreasing the SBH thickness, and with a significant decrease in epileptic threshold and severity (Manent et al., 2009).

Field potential recordings from young adult *Dcx* KO hippocampal slices showed that both SPI and SPE layers received strong inhibitory inputs when compared to WT; the mean frequency amplitude of field inhibitory postsynaptic currents were larger in *Dcx* KOs than in WT (Bazelot et al., 2012). Developing neuroblasts blocked due to *Dcx* knockdown in the rostral migratory stream and developing in ectopic positions matured precociously and received GABAergic and glutamatergic synaptic inputs earlier when compared with their control counterparts in similar locations (Belvindrah et al., 2011). The chloride transporter KCC2 plays an important role in the postnatal excitatory to inhibitory switch of GABA actions in the hippocampus. Its absence is correlated with disturbances in GABAergic and glutamatergic synapse formation and

is associated with the development of spontaneous and evoked epileptiform activities (Khalilov et al., 2011). Using immunohistochemistry, we observed alterations in KCC2 expression between the SPI and SPE neuronal populations, with a subset of earliest born SPI cells expressing this transporter in the cytoplasm and at the plasma membrane in some cases at P0, when SPE neurons either do not express it, or occasionally express it in the cytoplasm (Figure 41). Interestingly hippocampal layer disorganization did not result in disturbances in intrinsic cellular properties and selective connectivity in Reelin mutants (Deguchi et al., 2011). On the other hand, the disturbances in KCC2 expression together with the inversion of lamination and mis-localization of the earliest born, functionally earliest active neuronal population in the *Dcx* KO hippocampus could suggest that altering neuronal migration may influence the early functional maturation of hippocampal networks. These observations raise the possibility that the immature hippocampal network in the *Dcx* KO during its differentiation will participate in the generation of pro-epileptic phenotype observed in adult mice.

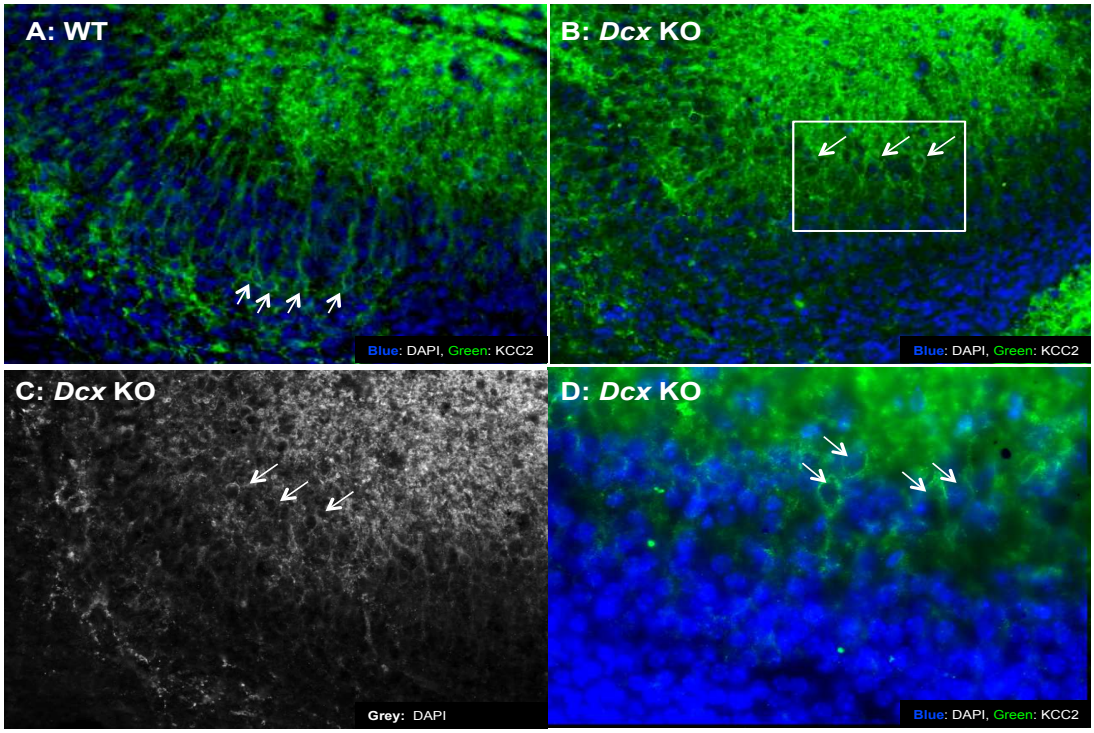

Figure 42: Expression pattern of the potassium- chloride cotransporter 2 (KCC2) in the WT (A), and the Dcx KO (B, C, D) at P0.

(A) Some deep- seated, outer border WT cells express KCC2 (arrows), with a cytoplasmic rather than membranous expression. (B) Some SPI cells express KCC2, with almost no detectable expression in SPE cells. (D) Higher magnification showing KCC2 expression in cells pointed in (B), KCC2 has a combined cytoplasmic and membranous expression, indicating a relatively advanced maturity status.

To summarize, a predefined developmental program is followed at least by earliest born hippocampal principal neurons. This neuronal population will differentiate and mature before later born ones, and will have an earlier expression of functional GABA and later on glutamate receptors. Consequently, it will participate in the generation of GDPs and network synchronization early on. Ectopic localization of this neuronal population is associated with an epileptic phenotype in *Dcx* KO mice. Gaining insights into the behaviour and the participation of this neuronal population in the generation of pro-epileptic circuits at perinatal stages may help in deciphering the role of developmental brain malformations, heterotopias and dysphasia in the generation of neurodevelopmental hippocampal epilepsy.

5. *Dcx KO mouse as a model to study developmental origins and therapeutic strategies in childhood epilepsies:*

Epilepsy is a common neurologic condition with a varying incidence between developing and developed countries (Ngugi et al., 2011), but is supposed to affect about 1% of the general population. Paediatric epilepsy accounts for one fourth of the global epilepsy population, with 25% of epileptic patients being below the age of 15 years (Guerrini, 11). Understanding the pathophysiological mechanisms of hyperexcitable circuits leading first to seizures and then developing into epilepsy is fundamental in testing causation hypotheses, understanding the modification of the brain circuits after these attacks, and testing new therapeutic strategies. Existing animal models commonly used for studying epilepsy use pharmacological agents that will lead to severe epileptic attacks, consequently leading to severe neuronal damage, cell death, and frank modifications in the circuits. Although these models have been instrumental in understanding the long term consequences of severe epilepsy, they have limited use in studying the developmental origins of epilepsy, and the acute short-term consequences of mild to moderate epileptic attacks.

The *Dcx* mouse model of hippocampal dysplasia and spontaneous epilepsy remains one of the available models, of which its use has pros and cons. Despite having hippocampal dysplasia in all *Dcx* KO animals, video EEG recordings were able to

detect spontaneous epileptic activity in only 40-50% of these mutants ((Nosten-Bertrand et al., 2008, Hamelin S. et al., in preparation). However, field recordings from *Dcx* KO hippocampal slices were able to detect interictal and ictal-like activity in all tested samples (Bazelot et al., 2012). The presence of a hippocampal morphological abnormality, resulting from aberrant embryonic development of the hippocampus renders this model more closely related to certain paediatric epilepsy syndromes.

Another feature of the *Dcx* KO mouse model is the absence of hippocampal sclerosis in epileptic animals. Massive cell death after epileptic attacks, mossy fibre sprouting and reactive gliosis were not detected in tested animals (data not shown). Therefore, the *Dcx* KO model maybe a weak model for studying the consequences of epilepsy on hippocampal architecture, but it remains a good model to study milder, more common causes of epilepsy. Moreover, epileptic *Dcx* KO animals have upregulation of neuroprotective mechanisms. *De novo* synthesis of the neuropeptide NPY was detected in mossy fiber terminals of epileptic animals (Nosten-Bertrand et al., 2008). Thus the *Dcx* KO mouse could stand as a good model to study the role of neuroprotection in epilepsy. Global gene expression analyses in the hyperexcitable adult heterotopic SPI and SPE neurons is ongoing. Results are expected to provide us with new insights regarding potential mechanisms that could be perturbed in these cells, potentially providing new therapeutic targets.

CHAPTER 4: ANNEX

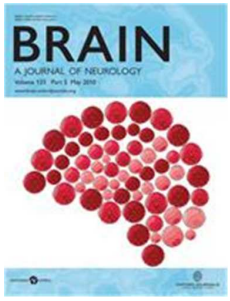

New insights into genotype-phenotype correlations for the doublecortin related lissencephaly spectrum

Journal:	*Brain*
Manuscript ID:	BRAIN-2012-00909.R2
Manuscript Type:	Original Article
Date Submitted by the Author:	n/a
Complete List of Authors:	Bahi-Buisson, Nadia; Necker Enfants Malades, APHP, Paris V, Pediatric Neurology Souville, ISabelle; Cochin, Fourniol, Franck; Institute of Structural Molecular Biology, Biology Toussaint, Aurelie; Cochin, Moores, Carolyn; Birbeck College, Biology Houdusse, Anne; Institut Curie, Lemaitre, Herve; INSERM CEA, Khalaf, Reham; IFM, Hully, Marie; Necker, Poirier, Karine; INSERM U1016, Leger, Pierre Louis; Necker, Elie, Caroline; Necker, Boddaert, Nathalie; Necker, Beldjord, Cherif; Cochin, Chelly, Jamel; INSERM U1016, Francis, Fiona; IFM,
Key Words:	
Please choose up to 5 keywords from the list:	cortical malformations, neuronal morphology

New insights into genotype-phenotype correlations for the *DCX*-related lissencephaly spectrum

Nadia Bahi-Buisson *(1,2,3), Isabelle Souville (4), Franck J Fourniol (5), Aurelie Toussaint (4), Carolyn A Moores (5), Anne Houdusse (6), Jean Yves Lemaitre (7), Karine Poirier (2,3), Reham Khalaf-Nazzal (8-10), Marie Hully (1), Pierre Louis Leger (1), Caroline Elie (11), Nathalie Boddaert (7,12), SBH-LIS European consortium, Cherif Beldjord (4) Jamel Chelly (2,3), Fiona Francis (8-10).

1- Neurologie pédiatrique, Hopital Necker Enfants Malades, Université Paris Descartes, APHP, Paris. France
2- Institut Cochin, Université Paris-Descartes, CNRS (UMR 8104), Paris, France
3- Inserm, U1016, Paris, France
4- Biologie Moléculaire et Génétique, Hôpital Cochin, AP-HP, Université Paris Descartes, Paris, France
5- Institute of Structural Molecular Biology, Birkbeck College, London
6-. Motilité Structurale, Institut Curie CNRS, UMR 144, Paris
7- INSERM U1000 "Imagerie et Psychiatrie", INSERM - CEA - Faculté de Médecine
Paris Sud 11,France
8- INSERM UMR-S839, F75005, Paris, France
9-. Universite Pierre et Marie Curie, F75005, Paris, France
10-. Institut du Fer à Moulin, F75005, Paris, France
11- Biostatistics Hopital Necker Enfants Malades, Université Paris Descartes, APHP, Paris. France
12- Radiologie Pédiatrique, Hopital Necker Enfants Malades, Université Paris Descartes, APHP, Paris. France.

Corresponding author's information

Nadia Bahi-Buisson, MD, PhD

Pediatric Neurology Hopital Necker Enfants Malades, Université Paris Descartes, APHP,
149 rue de Sevres 75015 Paris
Email: nadia.bahi-buisson@nck.aphp.fr
Telephone +33 1 42192699
Fax +33 1 42192692
Institut Cochin - INSERM U1016 - CNRS U8104 Equipe "Génétique et Physiopathologie des retards mentaux et des anomalies du développement du cerveau "75014 Paris

Key Words: Band heterotopia; lissencephaly; doublecortin; microtubules

Characters count for the title: 83
Running title: Genotype-phenotype correlations in DCX-related lissencephaly
Count for running title: 56
Summary word count: 350 words
Total word count with references: 7813 words
Supplemental Data: Figure 1 and 2 ; Table 1 and 2

We confirm that we have read the Journals position on issues involved in ethical publication and affirm that this report is consistent with those guidelines.

We confirm that we have read the Journals position on issues involved in ethical publication and affirm that this report is consistent with those guidelines.

Abstract

X-linked isolated lissencephaly sequence (LIS) and subcortical band heterotopia (SBH) are allelic human disorders associated with mutations of doublecortin (*DCX)* giving both familial and sporadic forms. DCX encodes a microtubule-associated protein involved in neuronal migration during brain development. Structural data show that mutations can fall either in surface residues likely to impair partner interactions or in buried residues likely to impair protein stability. Despite the progress in understanding the molecular basis of these disorders, the prognosis value of the location and impact of individual *DCX* mutations has largely remained unclear. To clarify this point, we investigated a cohort of 180 patients who were referred with the agyria-pachygyria-SBH spectrum.

***DCX* mutations were identified in 136 individuals. Analysis of the parents' DNA revealed the *de novo* occurrence of *DCX* mutations in 76 cases (62 females out of 70 screened (88.5%) and 14 males out of 60 screened (23%) while in the remaining cases, mutations were inherited from asymptomatic (n=14) or symptomatic mothers (n=11). This represents 100% of families screened. In *DCX* mutation females, patients demonstrated 3 degrees of clinical-radiological severity: a severe form with a thick band (n=54), a milder form (n=24) with either an anterior thin or an intermediate thickness band, and asymptomatic carrier females (n=14) with normal MRI.** A higher proportion of nonsense and frameshift mutations were identified in patients with *de novo* mutations. An analysis of predicted effects of missense mutations showed that those destabilizing the structure of the protein were often associated with severer phenotypes. We identified several severe and mild effect mutations affecting surface residues and observed that the substituted amino acid is also critical in determining severity. Recurrent mutations representing 34.5% of all *DCX* mutations often lead to similar phenotypes, for example, either severe in sporadic SBH due to Arg186 mutations or milder in familial cases due to Arg196 mutations.

Taken as a whole, these observations demonstrate that *DCX* related disorders are clinically heterogeneous with severe sporadic and milder familial SBH, each associated with specific *DCX* mutations. There is a clear influence of the individual mutated residue and the substituted amino acid in determining phenotype severity.

Genetically inherited disorders of neuronal migration represent important causes of epilepsy and intellectual disability. Subcortical band heterotopia (SBH) - also known as "double cortex" syndrome - is a neuronal migration disorder characterized by ribbons of grey matter within the central white matter between the cortex and the ventricular surface. The gyral pattern ranges from normal to simplified with broad convolutions, and cortical thickness is often increased (Barkovich *et al.* , 1994, Dobyns *et al.* , 1996). Together, SBH and lissencephaly (LIS) comprise a spectrum of malformations associated with deficient neuronal migration that are caused by alterations in at least three genes *LIS1* (also known as *PAFAH1B1*) (Lo Nigro *et al.* , 1997, Reiner *et al.* , 1993), *DCX* (Gleeson *et al.* , 1998, des Portes *et al.* , 1998a) and *alpha 1 tubulin* (also known as *TUBA1A*) (Keays *et al.* , 2007, Poirier *et al.* , 2007). **Mutations in other tubulin genes (*TUBB2B*, *TUBA8* and *TUBB3)* were also reported in malformations of cortical development, usually polymicrogyria with microcephaly (Abdollahi *et al.* , 2009 , Jaglin *et al.* , 2009 , Tischfield *et al.* , 2010 , Poirier *et al.* , 2010).**

Patients with SBH have a variable clinical course ranging from mildly to severely impaired. The brain malformation is often revealed by onset of seizures within the first decade. These usually evolve to refractory and multifocal epilepsy. Neurological examination is normal in most cases but hypotonia, poor fine motor control and behavioural disturbances may be present (Barkovich *et al.* , 1994, Barkovich *et al.* , 1989). Clinical severity varies with the cortical abnormalities, the band thickness and the degree of ventricular enlargement (Barkovich *et al.* , 1994, Palmini *et al.* , 1991). Patients with correlated pachygyria, thicker heterotopic bands, and severe ventricular enlargement have worse prognoses for neuromotor development. Additionally, they have earlier seizure onset and develop symptomatic generalized epilepsy that resembles Lennox Gastaut syndrome (LGS). Additionally,

periventricular and subcortical white matter T2 hypersignals are correlated with delayed motor development (Barkovich *et al.* , 1994).

Most SBH cases are females with at least 100 SBH cases previously reported (Gleeson *et al.* , 1998, des Portes *et al.* , 1998a, des Portes *et al.* , 1998b, Pilz *et al.* , 1998, Dobyns *et al.* , 1999, Aigner *et al.* , 2000, Aigner *et al.* , 2003, Gleeson *et al.* , 2000, Gleeson *et al.* , 2000, Gleeson *et al.* , 1999, Matsumoto *et al.* , 2001, Poolos *et al.* , 2002, Guerrini *et al.* , 2003, Demelas *et al.* , 2001 , Mei *et al.* , 2007, Haverfield *et al.* , 2009). Although most patients are sporadic, a syndrome of familial SBH with X linked inheritance has been described in which the majority of females have SBH and affected males usually present isolated LIS with more severe abnormalities over anterior brain regions (Pilz *et al.* , 1998, Gleeson *et al.* , 2000, Dobyns *et al.* , 1999). *DCX* mutations cause SBH in heterozygous carrier females and LIS in hemizygous males(Gleeson *et al.* , 1998, des Portes *et al.* , 1998a, Pilz *et al.* , 1998), although rare males with SBH and mosaic *DCX* mutations have been reported (Guerrini *et al.* , 2003, Pilz *et al.* , 1999). *DCX* mutations have been found in all familial cases and in 53% (Gleeson *et al.* , 2000) to 84 % (Matsumoto *et al.* , 2001) of patients with SBH. The frequency of mutations in the most common forms of sporadic SBH is approximately 80% (Matsumoto *et al.* , 2001). Recently, large genomic deletions and duplications were also found to account for a proportion of unexplained cases (Mei *et al.* , 2007, Haverfield *et al.* , 2009).

The DCX protein is the best described member of a family of neuronal microtubule associated proteins (MAPs) that are involved in cell division and / or cell migration (Gleeson *et al.* , 1998). DCX is expressed in migrating and differentiating neurons, it is centrally involved in organising the MT cytoskeleton and this function is essential for neuronal migration (Francis *et al.* , 1999, Gleeson *et al.* , 1999, Kappeler *et al.* , 2006, Koizumi *et al.* , 2006). The DCX MT binding domain is made up of two DC (Doublecortin-homology) domains, namely an N-terminal (N-DC; aa 46-139) and a C-terminal (C-DC; aa 173-263) domain. Lissencephaly-

causing missense mutations mainly cluster within these tandem DC domains, supporting the significance of MT binding for DCX function (Sapir *et al.* , 2000, Taylor *et al.* , 2000). In contrast nonsense mutations occur randomly throughout the protein. The N-DC domain can directly bind to MTs (Kim *et al.* , 2003), whereas the C-DC domain has also been implicated in binding free tubulin and other cellular partners (Caspi *et al.* , 2000, Kizhatil *et al.* , 2002, Tsukada *et al.* , 2003, Friocourt *et al.* , 2005). DCX binds at an unusual site on the MT lattice (Moores *et al.* , 2004; Moores et al., 2006). This confers specificity for MT architecture so that DCX preferentially nucleates and stabilises 13-protofilament MTs, the *in vivo* MT architecture (Tilney *et al.* , 1973).

The availabilities of the three dimensional structure of N-DC of DCX (Kim *et al.* , 2003), of C-DC of DCDC2 (2DNF.PDB in the protein databank), and a sub-nanometer resolution structure of DCX interacting with MTs (Fourniol *et al.* , 2010) has allowed us to predict the impact of disease-causing point mutations on DCX function. Mutations in buried sites are likely to lead to a loss or a reduction in stability, while mutation of surface residues can influence interactions with MTs or other binding partners. Although a small number of mutations were previously evaluated structurally (Kim *et al.* , 2003), here we have analyzed *DCX* mutations from a unique and large European cohort of 136 patients including 25 families. Overall, we present data for 93 SBH females and compare these with the corresponding features in 43 males. In order to better define the phenotypic spectrum, brain Magnetic Resonance Imaging (MRI) and the clinical phenotype of patients was characterized. Using clinical, imaging, molecular and structural data in combination with X inactivation studies where possible, we provide new insights into genotype-phenotype correlations for the DCX-related lissencephaly spectrum.

Patients and methods

Patients selection

As part of our ongoing lissencephaly and cortical malformation collection, 180 patients with agyria-pachygyria-SBH spectrum, were referred to our laboratory for molecular screening **(APHP-Cochin Hospital). This cohort included 70 sporadic females with SBH, 46 patients from 18 families (with either 2 brothers with LIS, 2 sisters with SBH, or affected mothers with SBH and a son with LIS, or foetal male cases with LIS)**, **and 60 sporadic males** with LIS. Patients included were from 20 centres in France, Israël and Switzerland. All patients were known personally to at least one of the authors.

Mutation analysis

Clinical data and blood samples were obtained with informed consent from patients and DNA was extracted using a standard protocol. Mutation analysis of the coding sequence of *DCX* (RefSeq NM_00119553) and *LIS1* was performed in all patients as described previously (des Portes *et al.* , 1998a). DNA samples of the parents were screened in all cases. Mutation detection was performed by direct sequencing of genomic DNA, and if negative, by multiplex ligation-dependent probe amplification (MLPA) analysis combined with single multiplex semiquantitative fluorescent PCR analysis (SQF-PCR) to validate MLPA findings as described previously (Mei *et al.* , 2007). The investigators were unaware of the mutation detected, at the time of initial review of the neuroimaging data. The mutations for pedigrees 9, 11, 15, have been reported previously, and the patients were reevaluated for this study and were respectively referred to as family 1, family 3, and family 2 (des Portes *et al.* , 1998a, des Portes *et al.* , 1998b). Mutations for sporadic patients DCX_SBH_46, DCX_SBH_82, DCX_SBH_83, DCX_SBH_86 were also described previously referred to as case O.D, J.A, B.T, and M.L respectively (des Portes *et al.* , 1998b)

X inactivation studies were performed using the androgen receptor (AR)-specific HpaII/PCR assay, described elsewhere, to assess X inactivation patterns (Monteiro *et al.* , 1998, Collins and Jukes, 1994). X inactivation patterns were classified as random (ratio 50:50 < 75:25) or skewed (ratio > 75:25).

Clinical review

Detailed information regarding family history, pre and perinatal events, age of seizure onset, psychomotor development, cognitive function, and neurological examination were collected. Protocols were approved by the appropriate institutional Review Board Human Subjects Committee.

A revised terminology was used for classification of seizures and epileptic syndromes, (Berg *et al.* , 2010). Levels of cognitive function were graded based on available clinical information. When IQ had not been tested, cognitive function was estimated by using adaptive behavioural criteria.

Brain imaging studies

MR images were available for all patients, were reviewed independently by two of the authors (NB and NBB) and classified using previously developed rating scales that were further modified for this study (Dobyns *et al.* , 1999). MR images were analysed for the degree of pachygyria (number of gyri and depth of sulci), location of the band and the presence of other brain anomalies. For statistical analyses, lissencephaly was graded according to the following patterning scale, referred to as the Dobyns LIS grade. Grades 1-6 denote the overall severity as seen on neuroimaging, with the LIS grade 1 being the severest (complete agyria) and the LIS grade 6 being the least severe (SBH). Bands were graded as previously described (Barkovich *et al.* , 1994). Band thickness was graded 1 (<4 mm at the thickest point) 2 (4-7 mm), 3 (8-10 mm) or 4 (>12 mm). Sulcal pattern was graded from normal to overt pachygyria and additional abnormalities were also recorded.

Volumetric analysis

Structural MRIs of patients with SBH were segmented into grey matter, white matter and cerebro-spinal fluid maps using Statistical Parametric Mapping (SPM8, http://www.fil.ion.ucl.ac.uk/spm/software/spm8/) and VBM8 toolbox (http://dbm.neuro.uni-jena.de/vbm/). Grey matter probability maps were multiplied by the SPM white matter prior map to give more weight to the grey matter present in the subcortical band. These SBH-weighted maps were thresholded to a height-threshold of 50 % and an extent-threshold of 4 cm3. Total grey matter and subcortical band volumes were then computed for each patient from the entire grey matter map and the thresholded SBH-weighted map respectively.

Statistical analysis

Age differences between different groups were analysed using the Kruskal-Wallis rank sum test. Differences in neurological symptoms, cognitive function, behavioural disturbances, imaging characteristics of the SBH and presence of additional brain abnormalities were analysed using Chi-square test or Fisher's exact test, as appropriate.

Structural analysis

Atomic structures were visualized and docked into the sub-nanometer resolution cryo-electron microscopy reconstruction of the DCX-MT interface using UCSF Chimera (Pettersen *et al.* , 2004). To build the potential C-DC-MT interface, a homology model of DCX C-DC (residues 179-263) was generated with MODELLER (Sali and Blundell, 1993), based on the atomic structure of the DCDC2 C-DC domain (2DNF.PDB; 32% sequence identity with DCX C-DC). Missing residues forming the linker N-terminal to C-DC (174-178) were modeled and moved manually into the cryo-electron microscopy reconstruction using UCSF Chimera.

Results

DCX Mutations

As part of our ongoing diagnosis of patients and families with the LIS-SBH spectrum, ***DCX*** **mutations were identified in 62/70 sporadic females with SBH (88.5%), and in 46 patients from 18 families with SBH/LIS (representing all familial cases) and in 21/60 apparently sporadic males with the LIS condition (35%), although 7 were subsequently found to have inherited *DCX* mutations from asymptomatic female carrier mothers, and were subsequently considered as "familial cases".**

Distinct mutations were found in females and males (figure 1 and 2). Among the **83** apparently sporadic cases with *DCX* mutations, analysis of the parents' DNA revealed the *de novo* occurrence of mutations in **76 cases (62 females and 14 males). 59 different *DCX* mutations were identified *de novo* and of these, 24 were novel, and 14 were detected several times in unrelated patients (Table 1 and 2).**

Forty five different *DCX* mutations were found in 62 sporadic females with SBH, that were either missense (26/45; 58%), nonsense (7/45; 15.6%), frameshift (8/45; 17.8%) with insertion or deletion of one or two base pairs leading to premature protein termination, splice site mutations (3/45; 6.7%) or deletion of exon 1-2 (1/45; 2.2%). Most missense mutations (24/26; 92.3%) were distributed between N-DC (13/24; 54.2%) and C-DC (11/24; 45.8%) (Figure 1, table 1). Two additional missense mutations fell in the linkers, p.A33P in the N-terminal linker upstream of N-DC, and p.V177G in the N-DC-C-DC interdomain linker. Interestingly, several recurrent mutations defining potential hot spots were found, the most frequent being mutations affecting Arg186 (p.R186C, p.R186H or p.R186L) observed in 13 females (20.9%) (Figure 1). Other recurrent missense (p.R78C, p.R78H, p.R78L, p.R192W) or nonsense (p.R39X, p.R303X) mutations were found in 2-3 cases each. Altogether, these hot spot mutations represent 38.7% of *de novo DCX* SBH mutations. **True sporadic males**

with LIS carried 14 different *de novo DCX* mutations, that were never found in sporadic females with SBH or inherited SBH/LIS conditions (13/14), except for one splice mutation (c.705+1 G>A) that was also identified in one female (Figure 1-2 and Table 2). Most were missense mutations (8/13), clustered in C-DC (5/8) and in N-DC (3/8). Others were either frameshift in one case (c.403_404delAA p.K135fsX164) and an in-frame insertion-deletion (c.560_568del8insTGGTTACCATCATC) in the C-DC domain in another. Finally, three additional patients harboured mosaic mutations, respectively nonsense mutations in the N- (p.R19X) and C- (p.R303X) terminal linkers and a deletion encompassing *DCX* exon 6.

Twenty inherited *DCX* mutations were identified in 60 individuals from 25 families (see supplementary figure 1) (Figure 1 and 2). These comprised 11 families (25 individuals, 15 females and 10 males) in whom the mother presented SBH and 7 families (21 individuals, 9 females and 12 males) in whom the mother was asymptomatic with either two affected sons (n=5) or 2 female cousins (n=1), or two brothers whose mother's DNA and clinical data were not available (n=1). The remaining 7 families (14 individuals, 7 females and 7 males) were initially referred for sporadic LIS in males, and the asymptomatic mother was subsequently diagnosed with a *DCX* mutation. Most carried missense mutations (n=16) with two recurrent mutations affecting Asp62 and Arg196. Missense mutations were located either in the N terminal or the interdomain linker (4/16), in N-DC (4/16) or C-DC (8/16). The remaining were nonsense (p.R272X), or affecting the first methionine of *DCX* (c.2T>C; pMet1?), or converting the stop codon into a Phe residue leading to 48 extra amino acids (c.1144T>A; p.X361PheX48), or an inframe deletion of exon 3 and 4, and a duplication of exon 4 -7 (Table 1, Supplementary table 1 and Supplementary figure 1).

Notably, the majority of mutations identified in asymptomatic mothers were different from those detected in those identified in sporadic SBH and more interestingly in symptomatic mothers. Moreover, we identified a recurrent mutation located in Arg196 (p.R196C, p.R196H) found in 4 asymptomatic carrier females and their sons (n=5), representing 4/14 inherited mutations with asymptomatic mothers (Figure 1 and 2). Finally, in 10 female carriers, we had the opportunity to screen for *DCX* mutations in grandmothers. Notably, 9/10 female carriers (that included 2 symptomatic and 7 asymptomatic patients) harboured *de novo* mutations. Only one asymptomatic mother carried a mutation (p.T42P) inherited from her asymptomatic mother. One of two asymptomatic female carriers carrying the mutation p.D9N showed skewed X inactivation but had a daughter without neurological symptoms and without any bias, suggesting that this mutation also has a mild effect on DCX function.

The patients for whom *DCX* screening was negative, were tested for *LIS1* mutations. Of these, 2 females and 2 males were found with mosaic *LIS1* mutations, and were therefore not included here.

Skewed X inactivation (>75%) was found in 6/16 tested **female carriers** (3 symptomatic and 3 asymptomatic) compared to 6/38 tested sporadic SBH patients (p=0.15). While the majority of *DCX* mutations are different between **patients with *de novo* and inherited mutations**, two mutations (i.e. p.R272X and p.R192W) were found in both groups (des Portes *et al.* , 1998a, des Portes *et al.* , 1998b). For both mutations, skewed inactivation accounts for the clinical variability. Also of note are **p.Y125H (inherited) and p.Y125D (*de novo*)** mutations because although both were associated with severe phenotypes in children, neither clinical nor X inactivation data were available to explain a presumed milder phenotype in the transmitting female.

Clinical and radiological presentation of SBH patients and outcome

The SBH cohort comprised 62 **females with *de novo* mutations and 16 cases with inherited mutations (10 symptomatic female carriers and 6 daughters)** (supplementary table 1 and 2). Of note, **the symptomatic carriers showed minor neurological signs in all cases and were diagnosed with SBH during pregnancy (n=3) or when their son(s) were diagnosed with LIS. Fourteen other *DCX* mutated mothers were asymptomatic, i.e. no history of epilepsy, normal neurological development and normal MRI (n=13) and one carrier female in whom no data were available.**

In female patients with SBH, presenting symptoms were epileptic seizures (47%) including infantile spasms or developmental delay (16.6%). At last evaluation, all SBH patients except 2 had intellectual disability assessed to be moderate to severe. Impairments included abnormal language development and use (67.1%) and moderate to severe behavioural disturbances (59.7%). The latter mainly consisted of hyperkinetic movements, crying and automutilation, and occasionally, autistic features with perseveration, echolalic language and stereotypical behaviour. A significant proportion of patients displayed an abnormal neurological examination, usually truncal hypotonia or spasticity (29%) and microcephaly (15.6%). Seizure disorders were present in 84.9% patients where seizures started mainly in infancy (34.5%) or during childhood (45%). At onset and at last evaluation, most SBH cases had either polymorphic seizures with a combination of atonic and tonic seizures, atypical absences, and/or epileptic spasms or focal seizures. Classifying these patients by epileptic syndrome, we identified 31 patients presenting with LGS, 10 with focal epilepsy, and 17 with generalised epilepsy. Seizure control is highly variable with a high proportion of drug resistance (78.3%) (supplementary tables 1 and 2).

Brain MRI was performed in all patients (summarized in Table 1 and Supplementary table 2) at a mean age of 14.5 years (median 8 years, ranging from 6 months to 60 years). Brain MRI revealed two major groups: (i) the most severe form with a thick (>8 mm) continuous band

around the entire brain (SBH Grade 3-4) (Figure 3) (n=42). Close to this SBH pattern is a pattern suggestive of lissencephaly on T1-weighted images with increased cortical thickness and poor differentiation of the cortex and underlying white matter and thick heterotopic bands on T2 weighted images (Figure 4); this latter pattern was identified in 12 children younger than 2 years for whom MRI data was already available because of early onset epilepsy. A milder form with a thin band (SBH Grade 1-2; 4-7 mm) was identified either only present in the frontal lobe or restricted to the frontal and temporal lobes with intermediate thickness. This pattern was observed either in **symptomatic female carriers (13/25; 52%) or sporadic patients (11/61; 18%).**

Brain abnormalities observed in SBH are mostly prominent in cortical structures. Considering the corpus callosum abnormalities which were identified, these included a dysmorphic (n=24) or thin corpus callosum (n=6), and one case of posterior corpus callosum agenesis. No significant white matter abnormalities were noted. Cerebellar abnormalities are also variable and comprised mild vermian hypoplasia in 3 cases. Dilatation of the fourth ventricles without pontocerebellar abnormalities was noted in 14 cases. Finally, the occurrence of microcephaly was 15.6%.

Quantitative volumetric analysis of the cortex and the heterotopic bands was performed in 8 patients for whom the resolution of the images as well as the availability of 3D T1 weighted sequences were available (Supplementary figure 2). **Although data are preliminary due to the small number of cases analysed, the ratio of the subcortical band volumes in patients with SBH Grade 1-2 ranged from 5.67 to 9.26% of the total grey matter volume, while in those with severer SBH grade 3-4, the ratio was evaluated from 12.21 to 27.2%, confirming the 2D evaluation of the thickness of the band.**

In order to determine whether MRI can contribute to the prediction of the history and clinical outcome of SBH patients, we compared the severity of intellectual disability,

behavioural disturbances and epilepsy, with band thickness and the degree of cortical abnormalities (Table 3). Two groups could be defined according to band thickness. Patients with diffuse thick bands with anterior predominance (n=54), showed significantly more shallow or very shallow sulci in frontal regions ($p<0.001$), moderate to severe ventricular enlargement ($p<0.001$) and prominent perivascular spaces in subcortical or periventricular regions or both ($p<0.001$). Clinical presentation is also determined by band thickness, with a higher proportion of epileptic encephalopathy at onset (68.6%) or developmental delay (31.4%) ($p<0.001$) in patients with a thicker band. At last evaluation, most patients with a thicker band were severely intellectually impaired ($p<0.001$), with only two patients having age appropriate language, while most had either no words or poor verbal skills (84%) ($p <0.001$). Moreover, they showed a higher proportion of severe behavioural disturbances (77.8%) ($p<0.001$). At the other end of the spectrum, patients with thin SBH (15.2%) displayed a normal cortical aspect or slightly shallow sulci, with no ventriculomegaly. None demonstrated intellectual disability or severe behavioural disturbances. Seizure occurrence was not determined by band thickness, since most patients with thicker bands (82%) show epilepsy consisting of the LGS type (55.3%). Similarly, 91.3% of patients with thin bands have epilepsy with a large proportion of LGS (50%). However, most patients with thicker bands started seizures early in infancy (with a median age of onset 2.2 years) compared with those with a thinner band (median age of seizure onset 10 years -$p=0.0002$). Female carriers with normal MRI (n=14) without a visible band were clinically normal and demonstrated neither neurological symptoms nor epileptic seizures. These data outline the importance of band thickness in the determination of the neurological prognosis of SBH patients.

Clinical and radiological presentations of male patients with DCX mutations

Our previous data suggested that sporadic males **with *de novo DCX* mutations** have a more severe presentation but the trend did not reach statistical significance. To improve statistical

power, we added 4 new **males with inherited mutations** and 5 with *de novo* mutations to the patients described in the previous study (Leger *et al.* , 2008). Altogether, 43 male patients with LIS, were evaluated, including 29 **with inherited mutations** and 14 with *de novo* mutations (see Table 2 *de novo* mutations and Supplementary Table 2 for families). We now confirm that male patients with *de novo DCX* mutations tend to have more severe neurological presentation, including a higher proportion of seizures at onset and more frequently diffuse agyria. *De novo* mosaic mutations (3/14) gave a milder phenotype with anterior pachygyria and SBH (LIS grade 6) (Dobyns and Truwit, 1995). **LIS cases with inherited mutations** showed a more homogeneous phenotype with anterior agyria or pachygyria (LIS grade 3-4 86.4%) (Figure 5) and developmental delay at onset (Table 4). Interestingly, similarly to females with either thin or thick SBH, no differences in seizure occurrence and response to AEDs were found between the groups suggesting that the epileptogenicity is not strictly related to the degree of agyria-pachygyria.

Genotype Phenotype correlations

To gain further insight into the relationship between mutation type and phenotype, we compared the characteristics of *DCX* mutations among the cohort of SBH patients (Table 1 and 3).

Firstly, it is noteworthy that the most severe group (SBH Grade 3-4) shows a large proportion of *de novo* mutations, while only 4 patients had inherited mutations. In this group in which 38 different mutations were identified, one third of mutations were nonsense, frameshift or deletion while the remaining were missense. In contrast, approximately half of the milder forms (SBH Grade 1-2) were due to inherited mutations (54.2%), the majority found in symptomatic female carriers.

Secondly, none of the ***de novo* SBH *DCX*** mutations were responsible for LIS in sporadic males, except one splice mutation (c.705+1G>A), suggesting that the severity and the impact

of these mutations on *DCX* are different. Nonsense mutations were never associated with LIS, except mosaic cases not included in our statistical analyses. **No major overall differences were found in the distribution of the mutations according to their location in either N-DC or C-DC, representing respectively 25.3% and 30.3% of *DCX* mutations. This represents 28.9% versus 24.4% in *de novo* mutations in females, 21.1% versus 35.7% in *de novo* mutations in males, and 20% versus 40% in inherited cases. Of note,** the higher percentage of inherited cases with C-DC mutations increases further if recurrent mutations are included. Thus, C-DC mutations in general appear quite prominent.

We next examined SBH patients with recurring missense mutations at either Arg186, Arg196, or Arg78. We observed that these mutations are associated with distinct phenotypes. The mutation Arg196 located on the surface of C-DC (Table 1) was carried only in **inherited cases** (n=6; supplementary table 2). Moreover, the phenotype was milder in both genders with females demonstrating either normal MRI and clinical presentation (4/6) or thin SBH (2/6) with minor epilepsy. Affected boys showed anterior pachygyria (LIS grade 4), ability to walk and partial to complete seizure control. Conversely, three recurrent mutations Arg186, Arg78, Arg303 were found exclusively in SBH patients with *de novo* mutations. Arg186 mutations (n=13) leading to 3 different substituted residues (p.R186C, p.R186H, p.R186L) were clearly associated with a severe phenotype, with thicker SBH (92.3%) and severe intellectual disability (83.3%), whatever the substituted residue. Because no skewed inactivation was observed in lymphocyte DNA, this phenotype is probably directly related to the importance of this residue for C-DC stability. Other recurrent mutations on Arg303 (n=3) and Arg78 (n=3) were associated with heterogeneous clinical and radiological presentations. In the case of Arg303X, the different presentations may be related to skewed inactivation. Arg78 is a **surface residue and predicted to directly participate in MT-binding,** phenotypic variability is likely therefore to be explained by the different amino acid substitutions leading

to variable alterations of **N-DC function.** Thus, both the affected residue and the substituted amino acid determine the severity of the phenotype, with some mutations probably enabling more residual protein function than others.

We performed a finer analysis of predicted effects of missense mutations on N- or C-DC structure and function (Figure 6, Table 1), taking into account local or global destabilization of the domains. In males, we found that most of the missense mutations in N- and C-DC leading to severe phenotypes are destabilizing (6/8). Highly destabilizing mutations affect buried residues (p.Y125H, p.L228R and p.V182F); less destabilizing mutations affect either buried residues (p.D62N and p.F57Y) or surface residues where mutation is likely to influence the structure of the loop they are found in (p.D241Y). In addition, one further surface mutation is predicted to affect local interactions with MTs (p.Y64N), and one final mutation leading to a severe phenotype in males (p.K193E) is on the surface but faces away from the MT interface, and may affect interactions with other binding partners. In females, severe phenotype missense mutations are also mainly destabilizing (p.R59H, p.R76P, p.V101L, p.L119P, p.G122W, p.Y125D/H, p.S129L, p.V177G, p.P179L, p.R186C/H/L, p.R192W, p.L198P, p.G223E, p.V236E, p.I250T). Of these, four are predicted to be less destabilizing, but also to perturb the interaction with MTs (p.R76P, p.V177G, p.P179L, p.L198P). One further mutated residue is unlikely to be destabilizing but is predicted to perturb the interaction with MTs (p.R78C/L). Two further apparently less destabilizing mutations that produce severe phenotypes are either unlikely to be at the MT interface (p.V101L), or the interaction with MTs is less certain (p.S129L). Thus, the majority of severe female missense mutations in N- and C-DC either destabilize the domain, or affect interactions with MTs. Interestingly, Arg59 in N-DC aligns with Arg186 in C-DC, both are destabilizing and give rise to severe phenotypes. These residues are conserved between the domains most likely because they

are important for folding of the DC domain. Of note, highly destabilizing mutations in general give more severe phenotypes.

Moderate phenotypes in males are associated with either destabilizing effects (p.D62E, p.R192W, p.D263G), or surface residues likely to interact with (p.S47N, p.R76S), or possibly interacting with (p.R196C/H) MTs. It is possible that mutations of these latter residues only affect affinity but still allow MT binding, which might explain the less severe phenotype. S47 is subject to phospho-regulation (Schaar et al., 2004) but the p.S47N mutation also gives only a mild phenotype in a female showing non-biased X inactivation. p.D62E and p.R192W are predicted to be highly destabilizing and the explanation for a moderate and not severe phenotype is therefore not obvious. Undetected mosaicism may be one possible explanation. Of the mild phenotypes in males, one is a surface mutation not predicted to interact with MTs (p.K227N), two further are surface mutations where interactions with MTs are possible but not certain (p.K134T, p.T203S), one is a residue in the interdomain linker (K174E) which might however also interact with MTs, and finally one mutation of a surface residue with a partially buried side chain (T183I) may be lightly destabilizing. Thus, no highly destabilizing mutations are associated with mild phenotypes in males and residues clearly interacting with MTs are also less evident.

Finally, in females, milder mutations have a range of predicted effects: the surface residues, p.S47N (discussed above), p.R78H and p.R102C are predicted to interact with MTs, p.K134E and p.R196S/H may interact with MTs; and p.F243S probably does not interact with MTs. One lightly destabilizing mutation (p.D62N), and several highly destabilizing (p.D62E, p.Y125H, p.V182F, p.R186H, p.R192W, I214T), also give milder phenotypes. It should be noted that the X inactivation status of the majority of these patients is not known, however p.R192W patients are known to have biased inactivation.

Finally, unaffected female carriers, for which X inactivation status was either non-biased or not known, had the following mutation types: surface and interacting with MTs (p.K174E but present in a linker), surface and possibly interacting (p.R196C/H), surface and not interacting (p.K193E) and mildly destabilizing (p.T183I). Of note, none of the unaffected female carriers had highly de-stabilizing mutations.

Discussion

This study presents a mutation analysis in the largest cohort of patients yet reported with sporadic SBH and LIS, and familial SBH/LIS. Fourteen years after the discovery of *DCX*, the aim of our analysis was to provide new insights into the spectrum of phenotypes of patients with *DCX* mutations. We investigated mutation position in the protein, taking into account structural biology data, and compared this to detailed clinical characterisations. Our study examined the clinical and brain MRI characteristics of 136 individuals harbouring 87 *de novo* or inherited mutations in the *DCX* gene, of which 24 mutations are described for the first time here.

The overall information that can be drawn from this study is that: 1) the range of central nervous system involvement is wider than originally described **with a significant proportion of asymptomatic female carriers found to carry *DCX* mutations when their affected son is diagnosed with LIS;** 2) the degree of neurological impairment is related to the band heterotopia thickness and the overlying cortical abnormalities; 3) skewed X inactivation plays a role in explaining familial cases of *DCX* with 'severe effect' mutations, and other atypical situations; 4) there are several hot-spot mutations in *DCX* explaining collectively 34.5 % of SBH cases, **respectively 38.7% of *de novo* mutations and 24% of inherited mutations;** 5) varying ratios of classes of mutations (missense in different domains and linkers, nonsense and other) were identified in the different categories of patients, which are also associated with distinct mutations, **and phenotype severity can often apparently be correlated with genotype;** 6) for a subset of mutated surface residues, the substituted amino acid also appears to be critical in determining phenotype severity.

Female patients with SBH: Two distinct groups rather than a continuum

With this large cohort, two groups of female patients with *DCX* mutations clearly emerge: a milder phenotype mainly affecting carrier females compared to a more severe presentation

usually observed in sporadic patients. The first group is characterized by either thin frontal bands or mostly normal MRIs. These female carriers are usually diagnosed during their pregnancy or when their affected sons are diagnosed with LIS. The majority of these female carriers (9/10) harbour *de novo DCX* mutations. A few cases of mother-daughter transmission with similar milder forms and non-biased X inactivation, suggest the milder effect of these mutations on DCX function. The occurrence of familial SBH is lower than sporadic SBH cases, representing one third of the population of *DCX* mutation females, but we cannot exclude that these patients are underdiagnosed. At the other end of the spectrum, the more frequent (66.7%) and severe presentation is characterized by thicker SBH, combined with moderate to severe intellectual disability, behavioural disturbances and epilepsy, which is often drug resistant. In these cases, severe intellectual impairment, in turn, may cause a reproductive disadvantage, increasing the likelihood for sporadic occurrence.

Similarly, male LIS patients fall into two groups according to the occurrence of *DCX* mutations, inherited or *de novo (ital)*, although the difference is not as striking as for females. **LIS males with *de novo* mutations** are either more severely affected with a large proportion exhibiting diffuse agyria (more than half in our series) or show a milder SBH phenotype with SBH with or without pachygyria (in one third of patients) and are likely to be mosaics. Thus, **males with *de novo* mutations are more severely affected than those with inherited mutations, and are** correlated with the involvement of more 'severe effect' mutations (see Table 2 and 4). In contrast, **LIS patients with inherited mutations** consistently demonstrate a more moderate phenotype with anterior agyria (Lis grade 3) or pachygyria (Lis grade 4) in the majority of patients (here, 79.3% patients).

In *DCX* mutated female patients, the band thickness determines the neurological phenotype

Previous work, which did not involve genetic analysis, has underlined the importance of band thickness in the outcome of SBH patients in a series not studied at the genetic level (Barkovich et al. , 1994, Palmini et al. , 1991). Following this seminal work, genetic data has thus far contributed to the identification of three SBH genes, *DCX* that accounts for 100% of familial cases, and 53% to 80% of sporadic cases, mosaic mutations of *LIS1* (Sicca et al. , 2003) and mutations in *TUBA1A* (Poirier et al. , 2007) accounting for some further rare cases. Here, with a large cohort of 136 patients with confirmed *DCX* mutations and detailed clinical and radiological data, we confirm the predictive value of band thickness. According to previous data, four categories were defined, from the mildest (grade 1) characterized by a thin band restricted to the frontal lobes, to the most severe (grade 4), characterized by a thick and complete band around the entire cerebrum, the thinnest part being in the temporal and occipital lobes. Although this segmentation represents an interesting predictive tool in late childhood and adulthood, our data demonstrate that in young patients, band thickness is difficult to determine. Here, 12 sporadic patients younger than 2 years had T1 weighted images close to the lissencephaly pattern while T2 images showed the heterotopic band. This change in cortical thickness according to age is reminiscent of the changing aspect described in polymicrogyria (Takanashi and Barkovich, 2003). Although serial images were not performed in these patients, this pattern does not seem to represent a difference in morphology but rather changes in the maturity of the cortex and underlying white matter. In clinical practice, the distinction of two categories is convenient. Thicker SBH (> 8mm) is the most frequent presentation of SBH (61.4% in accordance with the Barkovich series, 62.9%) (Barkovich et al. , 1994) and more specifically in sporadic patients (81.9%). Thicker bands are more frequently associated with frontal pachygyria with shallow to very shallow sulci, moderate to severe ventricular enlargement and prominent perivascular spaces in subcortical or periventricular regions, when compared with patients with thin SBH (< 8 mm). This

suggests that the neuronal arrest that leads to the formation of the band is also likely to impair the development of cortical gyri and cerebral white matter. This has previously been suggested in periventricular heterotopia (Hannan et al. , 1999 , Ferland et al. , 2009) and in SBH animal models (Croquelois et al. , 2009, Ackman et al. , 2009). Thicker bands lead to more severe intellectual impairment, more behavioural disturbances and are also responsible for polymorphic epileptic seizures, usually of the LGS type, with earlier age of onset and showing more resistance to AEDs.

In LIS, our previous study found that the majority of *DCX* mutated male patients displayed either a LIS grade 3 or 4 (i.e. anterior agyria or pachygyria). Similar to SBH, the severity of neurological impairment in LIS is determined by the degree of agyria (Dobyns et al. , 1992). Here with a larger cohort, our data reinforce these results with 53.5% patients showing LIS grade 3 or 4. **More importantly, our present results confirm previous data, suggesting that the LIS grade is less severe in inherited *DCX* mutations compared with those with *de novo* (Leger et al. , 2008).** This suggests that ***de novo* mutations** may have a severer effect on *DCX* function.

Little is known about the connectivity and function of heterotopic neurons. Although the band has a disorganized disposition of pyramidal cells, there is evidence that connectivity within the band, and with normal cortical or subcortical neurons is maintained (Palmini et al. , 1991). The functional role of this double cortex has not yet been completely clarified even if functional MRI (fMRI), positron emission tomography, and diffusion tensor imaging have contributed in part to understanding the neurophysiology. By depth electrode recordings, nerve cells within the SBH have been shown to exhibit epileptiform activity similar to and synchronous with those observed in the overlying cortex (De Volder et al. , 1994, Pinard et al. , 2000, Spreer et al. , 2001). Electrophysiological data with EcoG-fMRI (Tyvaert et al. , 2008) and an SBH rat model (Ackman et al. , 2009, Lapray et al. , 2010) shows that both heterotopia

and the overlying cortex contribute to epileptic manifestations. Hence, major alterations not only affect the neurons that fail to migrate but also their programmed target areas. Altogether, these data suggest that despite integration of the heterotopia into networks, the more severe clinical phenotypes associated with thicker bands lead to appreciable abnormal functioning of either the lesion or the overlying cortex, or both.

Proposed mechanisms for phenotypic heterogeneity in SBH

In SBH, one population of neurons forms a relatively normal cortex whereas a second population apparently arrests during migration leading to a collection of neurons beneath the cortex. Because SBH is predominantly an X linked disorder, the phenotype of females is thought to result from a mosaic state due to X inactivation in which neurons express either a normal or a mutant copy of *DCX*. **Previous data suggest that somatic mosaicism can produce the same result (Aigner et al. , 2003, Gleeson et al. , 2000).** A third possibility might be the influence of milder mutations.

Some previous studies suggest that skewed X inactivation does not significantly contribute to the SBH phenotype (Matsumoto et al. , 2001, Demelas et al. , 2001). Here, we found a significant proportion of skewed X inactivation cases in carrier females (37.5%) in accordance with results from one smaller series (Guerrini et al. , 2003). In contrast, skewed X inactivation is rarer (14.7%) in SBH cases with ***de novo DCX*** mutations. This suggests that a biased inactivation may partially account for phenotypic variability at least for familial cases. In support of this, skewed X inactivation may explain phenotypic heterogeneity between familial and sporadic patients with the same mutations. This situation was found in mildly symptomatic female carriers with biased inactivation and two more severely affected sporadic patients, all carrying the same mutation, p.R192W. Analogously for the only nonsense mutation p.R272X found in familial and sporadic cases, skewed X inactivation found in the carrier female is likely to explain her milder phenotype, while others have reported thick

heterotopic bands with balanced X inactivation (Gleeson et al. , 1998, Matsumoto et al. , 2001). Of note, this observation of the same mutation in both *de novo* and inherited cases is extremely rare in the literature and in our series. Also it is noteworthy that, variable degrees of X inactivation were observed in similarly affected patients with recurrent mutations (i.e. p.R196H, p.D9N) suggesting that other mechanisms may account for these less severe presentations, including a milder effect of these mutations on protein function. Altogether, these results suggest that although skewing of X inactivation may have a significant role in phenotypic heterogeneity, it ultimately is not demonstrated in all cases.

Somatic and germline mosaicisms associated with phenotypic heterogeneity in SBH were previously found in 10% of unaffected mothers whose children presented with either SBH or LIS (Aigner et al. , 2003, Gleeson et al. , 2000). Several authors suggest that there may be a critical percentage of mosaicism in peripheral blood that is associated with phenotypic features of SBH (Gleeson et al. , 2000, Poolos et al. , 2002, Kato et al. , 2001). With less than 30% mosaicism, patients are clinically unaffected whereas those with more than 30% mosaicism are symptomatic with SBH. In our cohort, mosaicism of less than 30% was found in 3 males with ***de novo*** nonsense mutations and an exonic deletion of *DCX*. This naturally leads to milder phenotypes with SBH in all three cases. Intriguingly, mosaic mutations were suspected but not demonstrated in blood lymphocytes of several familial cases (here, family 25 and family 11) in which both mothers were clearly asymptomatic, had one of two children including females, with a severe phenotype i.e. SBH grade 4. The possibility of somatic mosaicism in neural cells in these cases cannot be ruled out.

DCX mutations: Is there a genotype-phenotype correlation for lissencephaly and SBH?

To better understand the pathophysiological basis for the dichotomy between patients with ***de novo DCX*** mutations **and inherited mutations**, and to provide further proof of the phenotypic effect of the mutations, we analysed mutation type and location and searched for

genotype-phenotype correlations. **Our data clearly show that a correlation does exist in these *DCX* related conditions, in both SBH and LIS. This is supported by the similar phenotypes associated with recurrent mutations. For example, the most frequent substitution of the C-DC surface residue Arg196 (24% of inherited DCX mutations) is consistently associated with less severe SBH, either pauci-symptomatic or asymptomatic female carriers, or in affected LIS boys with a milder presentation. This recurrent mutation was never previously reported to be a hot spot, reflecting probably different ethnic origins of our population and those previously reported. Other recurrent mutations are strongly associated with severe SBH. Of these, the substitutions of Arg186, accounting for 20.9% of *de novo DCX* mutations in our series, invariably result in severe forms. Interestingly, structural predictions suggest that this residue is crucial for the stability of C-DC, with mutations at Arg59 in N-DC having a similar effect.**

On the other hand, some missense mutations of the same residue (e.g. p.R78L/H/C) have variable consequences. R78 is predicted to be in a loop of N-DC that participates in MT binding. In this case, it is likely that the severity of the phenotype is related to the substituted residue. The mutation p.R78H, associated with a milder phenotype, is predicted to have less of an effect on the charge of the side chain which contacts tubulin, whereas the substitutions p.R78L and p.R78C, associated with more severe phenotypes, are likely to more strongly impair the interaction with MTs.

While nonsense mutations are spread throughout the *DCX* gene, missense mutations are clustered in N-DC and C-DC, supporting the significance of these two domains for DCX function. However, the variable severity among SBH patients was not correlated with a particular distribution of mutations in either the N-DC or C-DC domains. **By separating mutations according to their predicted consequences on DCX structure or ability to bind MTs, we found that highly destabilizing mutations in general tend to give more severe**

phenotypes. It is noteworthy that this type of mutation is observed less frequently in males, further reinforcing their potential detrimental consequences on DCX. Thus structural data provide insights to predict phenotype severity. Moreover, some severe surface mutations in females (p.R78C/L) and in males (p.Y64N) which do not destabilize the protein are predicted to be in direct contact with MTs, and presumably lead to a critical loss of function. On the other hand, other mutations potentially affecting MT interaction led to less severe effects (p.S47N, p.R76S, p.R78H, p.R102C, p.K134E and p.R196C/S/H), perhaps only reducing affinity of interaction, due to their position or the substituted residue. Other residues facing away from the MT interface (e.g. K193E) presumably are important for other partner interactions. Clinical data thus also contributes to the identification of such residues and the fine analysis of DCX's function. Concerning different types of *DCX* mutations it is noteworthy that only 5/93 SBH females were found to carry an intragenic deletion or duplication of the DCX gene. This result contrasts with previous results (Mei et al. 2007; Haverfield et al. 2009), describing the presence of DCX intragenic deletions/duplications in about one third of their SBH patients, and we currently do not have explanations for this difference.

Both N-DC and C-DC play a major role in the function of DCX

Although most structural studies to date have focused on the N-DC domain (Kim et al. , 2003, Fourniol et al. , 2010), our analyses reinforce the idea that both DC domains are important for the full functionality of DCX (Taylor et al. , 2000, Horesh et al. , 1999). For the purposes of our current analysis, we assumed that N-DC and C-DC make equivalent contacts with MTs, although since C-DC can bind tubulin heterodimers (Taylor et al. , 2000, Kim et al. , 2003) as well as MTs and other partners, it may play additional roles to N-DC. Individual mutations occur in N and C-DC with similar frequencies, although recurrent mutations increase the overall number in C-DC. Thus, the C-DC domain is clearly essential for MT-related and other

functions of DCX. Further correlations of structural predictions of mutations with phenotype in the future will continue to help elucidate the functions of DCX.

Conclusion

Taken as a whole, these observations demonstrate that *DCX* related disorders represent a clinically heterogeneous syndrome. In SBH females, two groups clearly emerge with a milder form mainly affecting carrier females that are potentially underdiagnosed and a more severe and frequent presentation usually observed in sporadic patients. Hot spot mutations are more prevalent than previously reported. **Radiological and clinical data combined with structural data point to the fact that it is possible to make genotype-phenotype correlations taking into account X inactivation status, the residue affected by the mutation, the likelihood of the mutation to destabilize the protein, as well as in the case of surface residues, the substituting amino acid.**

Acknowledgements

We are grateful for financial support from the Agence National de Recherche (ANR- 08-MNP-013; FF and NBB, ANR 2010 - Blanc 1103 01; JC), as well as from INSERM, including the Avenir program (FF), the Fondation Bettencourt Schueller (FF), the Fédération pour la recherche sur le cerveau (FRC for FF and AH), the FRM (JC – Equipe FRM 2007) and ANR-Eranet-Erare. FJF and CAM were supported by The Wellcome Trust and New Life.

Figure legends

Figure 1 Schematic representation of the DCX protein and summary of the mutations identified **in asymptomatic and symptomatic females with SBH.**

Each *DCX* nucleotide mutation is numbered with the reference to the ATG. The predicted DCX protein alteration is numbered with reference to the amino acid (aa) residue number. Aa substitution mutations are referenced by the wild type aa and position followed by the mutant aa. For example D9N indicates that the wild type aa D at position 9 is mutated to an N. One or two base-pair deletions or insertions result in a translational reading frameshift followed by a protein termination codon.

Mutations are indicated on the protein sequence of DCX that comprises two evolutionary conserved domains clustered in two repeats, namely N-DC aa 46-139 and C-DC aa 173-263 depicted as pink boxes and the N-terminal, the interdomain and the C-terminal linker are shown as light blue boxes. The mutations found in symptomatic females are indicated above the gene and the deleted portions of the gene as thick lines and mutations found in asymptomatic females are shown in black boxes below the gene schema. An asterisk denotes the mutations described in this paper. **In red, severe forms with SBH Grade 3-4, in black milder forms with SBH Grade 1-2. Underlined are inherited mutations.**

Figure 2 Schematic representation of the DCX protein and summary of the mutations identified **males with LIS.**

Each *DCX* nucleotide mutation is numbered with the reference to the ATG. The predicted DCX protein alteration is numbered with reference to the amino acid (aa) residue number. Mutations are indicated on the protein sequence of DCX that comprises two evolutionary conserved domains clustered in two repeats, namely N-DC aa 46-139 and C-DC aa 173-263 depicted as pink boxes and the N-terminal, the interdomain and the C-terminal linker are shown as light blue boxes. The inherited mutations are indicated above the gene, the families with two brothers affected are figures in black boxes, and *de novo* mutations found are shown below the gene scheme and the deleted portions of the gene as thick lines. An asterisk denotes the mutations described in this paper. **In red, severe forms with LIS Grade 1-2, in black intermediate forms with LIS Grade 3-4, and in light grey boxes are the milder forms with LIS Grade 5-6. Underlined are inherited mutations.**

Figure 3 Variable extent and thickness of band in sporadic SBH cases. Representative MRI scans in patients with either a thick, continuous band around the entire brain (Grade 3-4)

(A,B, E, F) or a thinner band only present in the frontal lobe (G) or restricted to the frontal and temporal lobe with intermediate thickness (Grade 2) (C). Thick and continuous band around the entire brain in two patients respectively aged 2 years and 11 months (A) and 3 years and 6 months (E). The bands appear to fuse with the outer cortex in the frontal regions. Intermediate diffuse SBH in two patients aged 15 (B) and 16 years (F). Thin band only present in the frontal lobe (G) or restricted to the frontal and the temporal lobe (C) in two patients aged 24 years and 11 years. **D, H are from control patients respectively aged 3 and 15 years.**

Figure 4 Representative axial MRI in young children respectively aged 7 months (A,E), 14 months (B,F) and 17 months (C,G)

T1 weighted images show poor differentiation of the cortex and underlying white matter, with an aspect reminiscent of diffuse pachygyria (in younger child, A), or frontoparietal pachygyria combined with band heterotopia in posterior regions (in patients older than one year of age, B, C). At the same level, on T2 weighted images, the band is visible (E,F,G)**. Control MRI : T1 weighted image (D) and T2 weighted image (H) in normal 15 month old girl.**

Figure 5 Representative T1 (A,B,C) and T2 (E,F,G) weighted axial section of MRI in 3 males with *DCX* mutations representing the most prominent LIS grade in this study. Anterior pachygyria (LIS grade 4) in a 2 year-old boy (familial case) (A,E). SBH with anterior pachygyria in a 5 year-old boy (familial case) (B,F). Severe lissencephaly (LIS Grade 2) more severe anteriorly in a sporadic male aged 1 year 3 months (C,G)**. Control MRI : T1 weighted image (D) and T2 weighted image (H) in normal 18 month old boy.**

Figure 6 Localisation of surface residues mutated in DCX in SBH and their relationship with the MT interface

(a) Structure of the DCX-MT interface (cryo-electron microscopy reconstruction displayed as a transparent surface, tubulin in purple, DCX in yellow; EMDB ID 1788; (Kim *et al.* , 2003, Fourniol *et al.* , 2010) **docked with the pseudo-atomic structure of the N-DC-MT interface (ribbons, alpha-tubulin in blue, beta-tubulin in cyan, N-DC in orange; PDB ID 2XRP ;** (Kim *et al.* , 2003, Fourniol *et al.* , 2010)**. Left panel: front view; top right: view from the microtubule plus end; bottom right: view from the centre of the MT outwards. N-DC surface residues subject to missense mutations are displayed as**

spheres, coloured in green for cases with absence of cortex malformations (R102, K134), grey for mild/moderate phenotypes (S47), and orange for severe cases (R59, Y64, R76, R78, S129). Note that when a mutation resulted in more or less severe SBH in different patients, the most severe phenotype was considered in this figure.
(b) Same as (a) but docked with a homology model of C-DC (ribbons, brown). Green spheres : surface residue whose mutation resulted in an absence of phenotype (K193, however X inactivation status for the individual with this mutation is not available and this residue results in a severe phenotype in a male with LIS) ; grey spheres : surface residues whose mutation caused milder SBH (K174, T183, R196, T203, K227, F243, D263) ; orange : severe SBH cases (V177, P179, R186, R192, L198, D241). Of note, milder effect mutations apparently appear more frequently in C-DC than in N-DC.

Supplementary Figure 1: **Schematic representations of pedigrees resuming different situations of patients with *DCX* mutations. (A) The most frequent situation (n=62) shows sporadic SBH patients, with *de novo* (ital) mutations. (B) Sporadic male patients (n=14) with *de novo* (ital) mutations. (C) Inherited *DCX* mutations from asymptomatic mothers (n=13), with either one boy (n=7) with LIS, or 2 affected boys (n=5). (D) Inherited *DCX* mutations from symptomatic mothers (n=10), with either one boy (n=4) or two boys (n=2) or one male with LIS and one or two daughter(s) with SBH (n=2) or a male foetus (n=2). The last case not presented in this category is one family with two affected boys in whom the carrier female data was not available.**

Supplementary Figure 2: **Representative subcortical band segmentation in SBH cases.** Axial **slices of anatomical MRI of patients with thick, intermediate and thin subcortical bands (A, B, C respectively, measured at 147 168 mm^3 band, 70 541 mm^3, 40 678 mm^3). Subcortical band masks are superimposed in red (D, E, F). Respective total grey matter was measured at 533 811.2 mm^3, 577 502 mm^3 and 564 591 mm^3**
The band represents 27.2% of the total grey matter in patient 1 (SBH_DCX067) (A-D), 12.21% of the total grey matter in patient 2 (SBH_DCX023) (B-E), 7.2% of the total grey matter in patient 3 (SBH_DCX032) (C-F).

Table 1 Overview of all *DCX* mutations in females with SBH. Mutations in bold are newly described here. Gr. Grade; XI X Inactivation. N/A Non available. Fem Carrier: Female Carrier **Inh: Inherited cases. NI - non internal residues which are non-destabilizing ; HD highly destabilizing ; LD less destabilizing ; Mt Y/N Interacts with MTs (Y) or not (N) ; "Possible MT binding " indicates residues on the surface of C-DC that based on modeling may interact with MTs but the partners and role of this subdomain is still poorly understood; Surface mutations with partially buried side chains are marked with *. Further structural information is available on request.** Patients previously reported in [1] in (des Portes *et al.* , 1998a) [2] in (des Portes *et al.* , 1998b)

	Status	*de novo* / Inh	Rapport XI	Nomenclature	Mutation Type	Location	3D modelisation and putative consequences on DCX function		Band
							NonInter/destab	Mt Y/N	
DCX_SBH_01	Propositus	de novo	N/A	c.55C>T p.R19X	Nonsense				Gr 2
DCX_SBH_02	Propositus	de novo	N/A	c.55C>T p.R19X	Nonsense				Gr 3
DCX_SBH_03	Propositus	de novo	55/45	**c. 91_92 insA p.H31Qfsx36**	Nonsense				Gr 2
DCX_SBH_04	Propositus	de novo	N/A	c.115C>T p.R39X	Nonsense				Gr 3
DCX_SBH_05	Propositus	de novo	60/40	c.115C>T p.R39X	Nonsense				Gr 4
DCX_SBH_06	Propositus	de novo	N/A	c.115C>T p.R39X	Nonsense				Gr 4
DCX_SBH_07	Propositus	de novo	50/50	**c.285_286delA p.N96TfsX55**	Frameshift				Gr 3
DCX_SBH_08	Propositus	de novo	59/41	**c.366-2A>C**	Splice				Gr 3
DCX_SBH_09	Propositus	de novo	N/A	**c.442_443delG p.V148FfsX3**	Frameshift				Gr 4
DCX_SBH_010	Propositus	de novo	75/25	c.505C>T p.Q169X	Nonsense				Gr 3
DCX_SBH_011	Propositus	de novo	76/24	**c.528_529insT**	Frameshift				Gr 4
DCX_SBH_012	Propositus	de novo	N/A	**c.577A>T p.K193X**	Nonsense				Gr 4
DCX_SBH_013	Propositus	de novo	52/48	**c.579_580delG p.A194LfsX5**	Frameshift				Gr 4
DCX_SBH_014	Propositus	de novo	100/0	**c.681_682insA**	Frameshift				N/A
DCX_SBH_015	Propositus	de novo	57/43	**c.682_683delCT p.L228LfsX13**	Frameshift				Gr 2
DCX_SBH_016	Propositus	de novo	N/A	c.703C>T p.Q235X	Nonsense				Gr 3
DCX_SBH_017	Propositus	de novo	62/38	c.705+1G>A	Splice				Gr 4
DCX_SBH_018	Propositus	de novo	N/A	**c.828+1G>A**	Splice				Gr 4
DCX_SBH_019	Propositus	de novo	16/84	c.814C>T p.R272X	Nonsense				Gr 3
DCX_SBH_020 Fam_1	Propositus	Inh	49/51	c.814C>T p.R272X	Nonsense				Gr 3
DCX_SBH_021	Fem carrier	Inh	80/20	c.814C>T p.R272X	Nonsense				Gr 2

Fam_1									
DCX_SBH_022	Propositus	de novo	20/80	c.907C>T p.R303X	Nonsense				Gr 3
DCX_SBH_023	Propositus	de novo	70/30	c.947C>T p.R303X	Nonsense				Gr 3
DCX_SBH_024	Propositus	de novo	N/A	c.907C>T p.R303X	Nonsense				Gr 4
DCX_SBH_025/ Fam_2	Fem carrier	Inh	100/0	c.2T>A p.Met1?	unclassified				Gr 1
DCX_SBH_026/ Fam_3	Fem carrier	Inh	N/A	c.25G<A p.D9N	Missense	N terminal linker			Abs
DCX_SBH_027/ Fam_4	Fem carrier	Inh	100/0	c.25G<A p.D9N	Missense	N terminal linker			Abs
DCX_SBH_028/ Fam_5	Fem carrier	Inh	56/44	c.124 A>C p.T42P	Missense	N terminal linker			Abs
DCX_SBH_029	Propositus	de novo	55/45	**c.94G>C p.A33P**	Missense	N terminal linker			Gr 4
DCX_SBH_030/ Fam_6	Fem carrier	Inh	N/A	c.140G>A p.S47N	Missense	N terminal linker	NI	Mt Y	Gr 2
DCX_SBH_031/ Fam_7	Fem carrier	Inh	100/0%	c.140G>Ap.S47N	Missense	N terminal linker	NI	Mt Y	Abs
DCX_SBH_032	Propositus	de novo	47/53	c.176G>A p.R59H	Missense	N-DC surface	HD	Mt Possible	Gr 3
DCX_SBH_033	Propositus	de novo	46/54	c.176G>A p.R59H	Missense	N-DC surface	HD	Mt Possible	Gr 3
DCX_SBH_034/ Fam_8	Fem carrier	Inh	N/A	c.186C>G p.D62E	Missense	N-DC buried	HD	Mt N	Gr 1
DCX_SBH_035/ Fam_9 [1,2]	Fem carrier	Inh	N/A	c.184G>A p.D62N	Missense	N-DC buried	LD	Mt N	Gr 2
DCX_SBH_036	Propositus	de novo	31/69	c.227G>C p.R76P	Missense	N-DC surface	LD	Mt Y	Gr 3
DCX_SBH_037 Fam_10	Fem carrier	Inh	N/A	c.226C>A p.R76S	Missense	N-DC surface	NI	Mt Y	Abs
DCX_SBH_038	Propositus	de novo	N/A	c.232C>T p.R78C	Missense	N-DC surface	NI	Mt Y	Gr 4
DCX_SBH_039	Propositus	de novo	36/64	c.233G>A p.R78H	Missense	N-DC surface	NI	Mt Y	Gr 2
DCX_SBH_040	Propositus	de novo	52/48	c.233G>T p.R78L	Missense	N-DC surface	NI	Mt Y	Gr 4
DCX_SBH_041	Propositus	de novo	80/20	**c.263C>A p.T88K**	Missense	N-DC surface	LD	Mt Y	N/A
DCX_SBH_042	Propositus	de novo	53/47	**c.301G>C p.V101L**	Missense	N-DC buried	LD	Mt N	Gr 4
DCX_SBH_043	Propositus	de novo	60/40	**c.304C>T p.R102C**	Missense	N-DC surface	NI	Mt Y	Gr 2
DCX_SBH_044	Propositus	de novo	60/40	**c.356T>C p.L119P**	Missense	N-DC buried	HD	Mt N	Gr 3
DCX_SBH_045	Propositus	de novo	61/39	c.364G>T p.G122W	Missense	N-DC surface	HD	Mt N	Gr 4
DCX_SBH_046 [2]	Propositus	de novo	N/A	c.373T>G p.Y125D	Missense	N-DC buried	HD	Mt N	Gr 4
DCX_SBH_047 Fam_11 [1,2]	Daughter	Inh	N/A	c.373T>C p.Y125H	Missense	N-DC buried	HD	Mt N	Gr 3
DCX_SBH_048 Fam_11 [1,2]	Fem carrier	Inh	N/A	c.373T>C p.Y125H	Missense	N-DC buried	HD	Mt N	Gr 2

DCX_SBH_049	Propositus	de novo	N/A	c.386C>T p.S129L*	Missense	N-DC surface	LD	Mt Possible	Gr 3
DCX_SBH_050	Propositus	de novo	67/33	**c.400A>G p.K134E**	Missense	N-DC surface	NI	Mt Possible	Gr 2
DCX_SBH_051/ Fam_12	Fem carrier	Inh	25/75	c.520A>G p.K174E	Missense	N-DC_C-DC linker	NI	Mt possible	Abs
DCX_SBH_052	Propositus	de novo	59/41	**c.529T>G p.V177G**	Missense	N-DC_C-DC linker	LD	Mt possible	Gr 4
DCX_SBH_053	Propositus	de novo	44/56	c.536C>T p.P179L	Missense	C-DC surface	LD	Mt possible	Gr 4
DCX_SBH_054/ Fam13	Fem carrier	Inh	51/49	c.544g>t p.V182F	Missense	C-DC buried	HD	Mt N	Gr1
DCX_SBH_055/ Fam_14	Fem carrier	Inh	75/25	**c.548C>T p.T183I***	Missense	C-DC surface	LD	Mt N	Abs
DCX_SBH_056	Propositus	de novo	N/A	c.556 C>T p.R186C*	Missense	C-DC surface	HD	Mt possible	Gr 4
DCX_SBH_057	Propositus	de novo	N/A	c.556C>T p.R186C*	Missense	C-DC surface	HD	Mt possible	Gr 4
DCX_SBH_058	Propositus	de novo	25/75	c.556C>T p.R186C*	Missense	C-DC surface	HD	Mt possible	Gr 4
DCX_SBH_059	Propositus	de novo	63/37	c.556C>T p.R186C*	Missense	C-DC surface	HD	Mt possible	Gr 4
DCX_SBH_060	Propositus	de novo	N/A	c.556C>T p.R186C*	Missense	C-DC surface	HD	Mt possible	Gr 4
DCX_SBH_061	Propositus	de novo	80/20	c.556C>T p.R186C*	Missense	C-DC surface	HD	Mt possible	Gr 4
DCX_SBH_062	Propositus	de novo	43/57	c.557G>T p.R186H*	Missense	C-DC surface	HD	Mt possible	Gr 4
DCX_SBH_063	Propositus	de novo	67/33	c.557G>T p.R186H*	Missense	C-DC surface	HD	Mt possible	Gr 4
DCX_SBH_064	Propositus	de novo	31/69	c.557G>T p.R186H*	Missense	C-DC surface	HD	Mt possible	Gr 3
DCX_SBH_065	Propositus	de novo	75/25	c.557G>T p.R186H*	Missense	C-DC surface	HD	Mt possible	Gr 2
DCX_SBH_066	Propositus	de novo	44/56	c.557G>T p.R186H*	Missense	C-DC surface	HD	Mt possible	Gr 4
DCX_SBH_067	Propositus	de novo	100/0	c.557G>A p.R186H*	Missense	C-DC surface	HD	Mt possible	Gr 3
DCX_SBH_068	Propositus	de novo	N/A	c.557G>T p.R186L*	Missense	C-DC surface	HD	Mt possible	Gr 4
DCX_SBH_069/ Fam_15 [1,2]	Fem carrier	Inh	100/0	c.574C>Tp.R192W	Missense	C-DC surface	HD	Mt possible	Gr 1
DCX_SBH_070/ Fam_15 [1,2]	Daughter	Inh	N/A	c.574C>Tp.R192W	Missense	C-DC surface	HD	Mt possible	Gr 2
DCX_SBH_071/ Fam_15 [1,2]	Daughter	Inh	N/A	c.574C>Tp.R192W	Missense	C-DC surface	HD	Mt possible	Gr 2
DCX_SBH_072	Propositus	de novo	44/56	c.574C>T p.R192W	Missense	C-DC surface	HD	Mt possible	Gr 2
DCX_SBH_073	Propositus	de novo	60/40	c.574C>T p.R192W	Missense	C-DC surface	HD	Mt possible	Gr 3
DCX_SBH_074/ Fam_16	Fem carrier	Inh	N/A	c. 576 A>G p.K193E*	Missense	C-DC surface	NI	NI- Mt N	Abs
DCX_SBH_075/ Fam_17	Fem carrier	Inh	53/47	c.586C>T p.R196C	Missense	C-DC surface	NI	Mt possible	Abs
DCX_SBH_076/ Fam_18	Fem carrier	Inh	23/77	c.586C>T p.R196C	Missense	C-DC surface	NI	Mt possible	Abs
DCX_SBH_077/	Fem carrier	Inh	N/A	c.586C>A p.R196S	Missense	C-DC surface	NI	Mt possible	Gr 1

Fam_19									
DCX_SBH_078/ Fam_20	Fem carrier	Inh	N/A	c.587G>A p. R196H	Missense	C-DC surface	NI	Mt possible	Abs
DCX_SBH_079/ Fam_21	Fem carrier	Inh	80/20	c.587G>A p. R196H	Missense	C-DC surface	NI	Mt possible	Abs
DCX_SBH_080/ Fam_22	Fem carrier	Inh	N/A	c.587G>A p. R196H	Missense	C-DC surface	NI	Mt possible	Gr 1
DCX_SBH_081	Propositus	de novo	47/53	**c.593T>C p.L198P**	Missense	C-DC surface	LD	Mt possible	Gr 4
DCX_SBH_082 [2]	Propositus	de novo	N/A	c.640T>C p.I214T	Missense	C-DC buried	HD	Mt N	Gr 2
DCX_SBH_083 [2]	Propositus	de novo	N/A	c.668G>A p.G223E	Missense	C-DC surface	HD	Mt possible	Gr 3
DCX_SBH_084	Propositus	de novo	63/37	**c.707T>A p.V236E**	Missense	C-DC buried	HD	Mt N	Gr 3
DCX_SBH_085	Propositus	de novo	51/49	c.728T>C p.F243S	Missense	C-DC surface	NI	Mt N	Gr 2
DCX_SBH_086 [2]	Propositus	de novo	N/A	c.769T>C p.I250T	Missense	C-DC buried	LD/HD ?	Mt N	Gr 3
DCX_SBH_087	Propositus	de novo	N/A	c.1078delG	Frameshift				Gr 2
DCX_SBH_088/ Fam_23	Fem carrier	Inh	N/A	(c.1144 T>A) X361Phe48X	Unclassified				Gr 1
DCX_SBH_089/ Fam_25	Daughter	Inh	70/30	**Dup Exon 4-7**	duplication				Gr 4
DCX_SBH_090/ Fam_25	Daughter	Inh	63/37	**Dup Exon 4-7**	duplication				Gr 4
DCX_SBH_091/ Fam_25	Fem carrier	Inh	47/53	**Dup Exon 4-7**	duplication				Abs
DCX_SBH_092/ Fam_25	Fem carrier	Inh	60/40	**Dup Exon 4-7**	duplication				Abs
DCX_SBH_093	Propositus	de novo	100/0	**Del exon 1-2**	deletion				Gr 4

Table 2 Overview of neurological data in 14 male patients with *intragenic de novo* mutations in the *DCX* gene. Grey shades are surface mutations potentially involved in tubulin contact (<5 A tubulin); * Surface residues with partially buried side-chains. LIS_Grade (Dobyns *et al.* , 1999); Age refers to age at last evaluation; Yrs : years; sz : seizure ; N/A non available. Bold = newly described mutations. **NI - non internal residues which are non-destabilizing ; HD highly destabilizing ; LD less destabilizing ; Mt Y/N Interacts with MTs (Y) or not (N) ; "Possible MT binding " indicates residues on the surface of C-DC that based on modeling may interact with MT but the partners and role of this subdomain is still poorly understood ; Surface mutations with partially buried side chains are marked with * Further structural information is available on request.** [1] Males previously reported in (Leger *et al.* , 2008).

	Reference	Group	Mutation type	Location	3D modelisation and putative consequences on DCX function		LIS_Grade	Age (yrs)*	Motor development	Epilepsy	
					NonInter/destab	Mt Y/N				Age of onset (yrs)	Sz control
XLIS_03 [1]	DCX026	Missense	c.190T>A p.Y64N	N-DC surface	NI	Mt Y	2	24	Spastic tetraplegia	0.1	Refractory
XLIS_40	This series	Missense	**c.401A>C p.K134T**	**N-DC surface**	NI	Mt possible	5	3	Tetraplegia	0.5	Refractory
XLIS_09	This series	Missense	**c.170 T>A p.F57Y**	**N-DC buried**	LD	Mt N	1	2	Spastic tetraplegia	0.1	Refractory
XLIS 22[1]	DCX025	Missense	c.607A>T p.T203S	C-DC surface	LD	Mt possible	5	5	Normal	0.2	Refractory
XLIS29[1]	DCX015	Missense	c.681A>T p.K227N	C-DC surface	NI	Mt possible	5	7	Normal	2	controlled
XLIS23[1]	DCX024	Missense	c.741G>T p.D241Y	C-DC surface	LD	Mt N	1	4	Tetraplegia	0.2	Refractory
XLIS27	This series	Missense	c. 788 A>G p.**D263G**	C-DC surface	LD	Mt N	3	17	Normal	17	Controlled
XLIS28[1]	DCX021	Missense	c. 683 T>G p. L228R	C-DC buried	HD	Mt N	2	3	Tetraplegia	0.5	Refractory
XLIS30	This series	Splice	c.705 +1 G>A				1		Spastic tetraplegia	0,3	Refractory
XLIS26[1]	DCX030	Frameshift	c.403_404delAA p.K135fsX164				1	3	Tetraplegia	0.3	Refractory
XLIS38[1]	DCX 019	Frameshift	c.560_568del8insTGGTTACCATCATC				6	34	Normal	N/A	N/A
XLIS36[1]	DCX 006	Nonsense (mosaic)	c.55C>T p.R19X				6	28	Normal	6	Refractory
XLIS37[1]	DCX 029	Nonsense (mosaic)	c.947C>T p.R303X				6	12	Normal	17	Partially controlled
XLIS39	This series	Deletion (mosaic)	Deletion Exon 6				6	4	Tetraplegia	0.3	Refractory

Table 3 Comparison of female SBH cases with *DCX* mutations according to the severity

	Severe (SBH Gr3-4)[a]	**Intermediate (SBH Gr1-2)[a]**	**Absent SBH**	**p value**
Total	54	24	14	
Age at last evaluation (median [range])	10 y [1-45]	25 y [5.4-44]	37 y [10-65]	
Status				p < 0.001
Inherited mutations (n=31) (25 females carriers)	3 mutations (4 patients)	11 mutations (13 patients)	11 mutations (14 patients)	
***De novo* mutations (n=61)**	36 mutations (50 patients	11 mutations (11 patients)	0	
DCX mutation type				
Non sense and deletion (n=18*)	14 mutations (20 patients)	5 mutations (5 patients)	1 mutation (2 patients)	
Missense N-DC (n=17**)	11 mutations (10 patients)	6 mutations (6 patients)	1 mutation (1 patient)	
Missense C-DC (n=17***)	9 mutations (18 patients)	7 mutations (10 patients)	4 mutations (6 patients)	
Missense N terminal domain-interdomain (n=6****)/ splicing defect (n=3)	5 mutations (5 patient)	1 mutation (1 patient)	4 mutations (5 patients)	
Unclassified (n=2)	0	2 mutations (2 patient)	0	
Skewed inactivation	6/36 (16.7%)	3/12 (25%)	3/7 (42.9%)	p = 0.29
Moderate to severe ventriculomegaly (n=88)	37/53 (69.8%)	2/21 (9.5%)	0/14 (0%)	p<0.001
Prominent perivascular spaces (n=77)	33/45 (73.3%)	7/19 (36.8%)	0/13 (0%)	p<0.001
Presenting symptoms				p<0.001
Mother carrier	0/51 (0%)	9/23 (39.1%)	14/14 (100%)	
Developmental delay	16/51 (31.4%)	1/23 (4.3%)	0/14 (0%)	
Seizures (including West)	35/51 (68.6%)	13/23 (56.5%)	0/14 (0%)	
Microcephaly (n=68)	7/45 (15.6%)	0/18 (0%)	0/5 (0%)	p=0.24
Moderate to Severe ID (n=86)	47/51 (92.2%)	9/21 (42.9%)	0/14 (0%)	p<0.001
Severe language delay i.e Absent word or poor verbal skills (n=87)	42/50 (84%)	7/23 (30.4%)	0/14 (0%)	p<0.001
Moderate to severe Behavioral disturbances (n=81)	35/45 (77.8%)	5/22 (22.7%)	0/14 (0%)	p<0.001
Patients who developed epilepsy (n=87)	41/50 (82%)	21/23 (91.3%)	0/14 (0%)	p<0.001
Early onset seizures < 1 year (n=55)	18/38 (47.4%)	1/17 (5.9%)		p=0.003
Seizure type at last evaluation (n=58)				p=0.16
Lennox Gastaut type[b]	21/38 (55.3%)	10/20 (50%)		
Focal seizures (including with secondary generalization)	4/38 (10.5%)	6/20 (30%)		
Intractable Epilepsy (n=60)	34/40 (85%)	13/20 (65%)		p=0.1

[a] The number of the denominator indicates the number of patients in whom specific information were available. [b] includes polymorphic seizures i.e. generalized tonic seizures, atypical absences and drop attacks. N/A Not available; SBH subcortical band heterotopia; ID Intellectual Disability; * R272X found in severe and intermediate and dupExon4-7 in absent SBH and severe (from the same family) ** Y125H was found in one family with the female carrier with Gr1-2 and her daughter with Gr 4; *** 3 mutations were found in differents groups : R192W found in the same family with Gr1 in all females, and in 2 cases with *de novo* (ital) mutations with respectively Gr2 and Gr3 SBH. R186H was found in 5 cases with Gr 3-4 SBH in 1 case with SBH Gr2 (intermediate). Also the recurrent mutation R196H was found in the 2 groups abs and intermediate SBH. **** S47N was found in an asymptomatic female carrier (absent SBH) and one symptomatic female carrier.

Table 4 Comparison of male cases with *DCX* mutations according to severity

	LIS Grade 1-2 (Diffuse Agyria) [a]	LIS Grade 3-4 (Anterior Agyria or Pachygyria) [a]	LIS Grade 5-6 (SBH +/- pachygyria)	P value
Total	10	24	9	
Age at last evaluation (median [range])	4 y [0.8-24]	12 y [2-37]	5 y [1.5-34]	p = 0.28
Status				p <0.001
Inherited mutations (n=29)	4/10 (40%)	23/24 (95.8%)	2/9 (22.2%)	
***De novo* mutations (n=14)**	6/10 (60%)	1/24 (4.2%)	7/9 (77.8%)	
DCX mutation type				p = 0.06
Non sense and deletion (n=4*)	1 *de novo* mutation (1 patient)		3 *de novo* mosaic mutation (3 patient)	
Missense N-DC (n=7**)	4 *de novo* mutations (4 patients)	2 inh. mutations (4 patients-2 families)	1 *de novo* mutation (1 patient)	
Missense C-DC (n=12***)	4 *de novo* mutations (4 patients)	4 inh. and 1 *de novo* mutations (9 patients-7 families)	1 inh and 2 *de novo* mutations (3 patients)	
Missense N terminal domain-interdomain (n=6****)	0	4 inh. and 1 *de novo* mutations (9 patients)	1 patient (1 inh. mutation)	
Unclassified (splicing defect n=1-**in frame deletion n=1)**	1 *de novo* mutation (1 patient)		1 *de novo* mutation (1 patient)	
Disease onset (n=42)				p = 0.004
Prenatal diagnosis	0	1 (4.2%)	0	
Developmental delay	1 (11.1%)	15 (62.5%)	1 (11.1%)	
Seizures (including West)	8 (88.9%)	8 (33.3%)	8 (88.9%)	
Microcephaly	8/10 (80%)	6/24 (25%)	1/9 (11.1%)	p = 0.002
Epilepsy (n=42)	10/10 (100%)	18/23 (78.3%)	9/9 (100%)	p = 0.17
Seizure control				p = 0.006
Refractory	8/10 (80%)	3/17 (17.6%)	6/9 (66.7%)	
Partial drug resistance	0	4/17 (23.5%)	2/9 (22.2%)	
Seizure control	2/10 (20%)	10/17 (58.8%)	1/9 (11.1%)	

[a] The number of the denominator indicates the number of patients in whom specific information were available . NS Not significant

References

Barkovich AJ, Guerrini R, Battaglia G, Kalifa G, N'Guyen T, Parmeggiani A, et al. Band heterotopia: correlation of outcome with magnetic resonance imaging parameters. Ann Neurol. 1994 Oct;36(4):609-17.
Dobyns WB, Andermann E, Andermann F, Czapansky-Beilman D, Dubeau F, Dulac O, et al. X-linked malformations of neuronal migration. Neurology. 1996 Aug;47(2):331-9.
Lo Nigro C, Chong CS, Smith AC, Dobyns WB, Carrozzo R, Ledbetter DH. Point mutations and an intragenic deletion in LIS1, the lissencephaly causative gene in isolated lissencephaly sequence and Miller-Dieker syndrome. Human molecular genetics. 1997 Feb;6(2):157-64.
Reiner O, Carrozzo R, Shen Y, Wehnert M, Faustinella F, Dobyns WB, et al. Isolation of a Miller-Dieker lissencephaly gene containing G protein beta-subunit-like repeats. Nature. 1993 Aug 19;364(6439):717-21.
Gleeson JG, Allen KM, Fox JW, Lamperti ED, Berkovic S, Scheffer I, et al. Doublecortin, a brain-specific gene mutated in human X-linked lissencephaly and double cortex syndrome, encodes a putative signaling protein. Cell. 1998 Jan 9;92(1):63-72.
des Portes V, Pinard JM, Billuart P, Vinet MC, Koulakoff A, Carrie A, et al. A novel CNS gene required for neuronal migration and involved in X-linked subcortical laminar heterotopia and lissencephaly syndrome. Cell. 1998a Jan 9;92(1):51-61.
Keays DA, Tian G, Poirier K, Huang GJ, Siebold C, Cleak J, et al. Mutations in alpha-tubulin cause abnormal neuronal migration in mice and lissencephaly in humans. Cell. 2007 Jan 12;128(1):45-57.
Poirier K, Keays DA, Francis F, Saillour Y, Bahi N, Manouvrier S, et al. Large spectrum of lissencephaly and pachygyria phenotypes resulting from de novo missense mutations in tubulin alpha 1A (TUBA1A). Hum Mutat. 2007 Nov;28(11):1055-64.
Abdollahi MR, Morrison E, Sirey T, Molnar Z, Hayward BE, Carr IM, et al. Mutation of the variant alpha-tubulin TUBA8 results in polymicrogyria with optic nerve hypoplasia. Am J Hum Genet. 2009 Nov;85(5):737-44.
Jaglin XH, Poirier K, Saillour Y, Buhler E, Tian G, Bahi-Buisson N, et al. Mutations in the beta-tubulin gene TUBB2B result in asymmetrical polymicrogyria. Nat Genet. 2009 May 24.
Tischfield MA, Baris HN, Wu C, Rudolph G, Van Maldergem L, He W, et al. Human TUBB3 mutations perturb microtubule dynamics, kinesin interactions, and axon guidance. Cell. 2010 Jan 8;140(1):74-87.
Poirier K, Saillour Y, Bahi-Buisson N, Jaglin XH, Fallet-Bianco C, Nabbout R, et al. Mutations in the neuronal {beta}-tubulin subunit TUBB3 result in malformation of cortical development and neuronal migration defects. Hum Mol Genet. 2010 Sep 20.
Barkovich AJ, Jackson DE, Jr., Boyer RS. Band heterotopias: a newly recognized neuronal migration anomaly. Radiology. 1989 May;171(2):455-8.
Palmini A, Andermann F, Aicardi J, Dulac O, Chaves F, Ponsot G, et al. Diffuse cortical dysplasia, or the 'double cortex' syndrome: the clinical and epileptic spectrum in 10 patients. Neurology. 1991 Oct;41(10):1656-62.
des Portes V, Francis F, Pinard JM, Desguerre I, Moutard ML, Snoeck I, et al. doublecortin is the major gene causing X-linked subcortical laminar heterotopia (SCLH). Human molecular genetics. 1998b Jul;7(7):1063-70.
Pilz DT, Matsumoto N, Minnerath S, Mills P, Gleeson JG, Allen KM, et al. LIS1 and XLIS (DCX) mutations cause most classical lissencephaly, but different patterns of malformation. Hum Mol Genet. 1998 Dec;7(13):2029-37.

Dobyns WB, Truwit CL, Ross ME, Matsumoto N, Pilz DT, Ledbetter DH, et al. Differences in the gyral pattern distinguish chromosome 17-linked and X-linked lissencephaly. Neurology. 1999 Jul 22;53(2):270-7.
Aigner L, Fluegel D, Dietrich J, Ploetz S, Winkler J. Isolated lissencephaly sequence and double-cortex syndrome in a German family with a novel doublecortin mutation. Neuropediatrics. 2000 Aug;31(4):195-8.
Aigner L, Uyanik G, Couillard-Despres S, Ploetz S, Wolff G, Morris-Rosendahl D, et al. Somatic mosaicism and variable penetrance in doublecortin-associated migration disorders. Neurology. 2003 Jan 28;60(2):329-32.
Gleeson JG, Luo RF, Grant PE, Guerrini R, Huttenlocher PR, Berg MJ, et al. Genetic and neuroradiological heterogeneity of double cortex syndrome. Ann Neurol. 2000 Feb;47(2):265-9.
Gleeson JG, Minnerath S, Kuzniecky RI, Dobyns WB, Young ID, Ross ME, et al. Somatic and germline mosaic mutations in the doublecortin gene are associated with variable phenotypes. Am J Hum Genet. 2000 Sep;67(3):574-81.
Gleeson JG, Minnerath SR, Fox JW, Allen KM, Luo RF, Hong SE, et al. Characterization of mutations in the gene doublecortin in patients with double cortex syndrome. Ann Neurol. 1999 Feb;45(2):146-53.
Matsumoto N, Leventer RJ, Kuc JA, Mewborn SK, Dudlicek LL, Ramocki MB, et al. Mutation analysis of the DCX gene and genotype/phenotype correlation in subcortical band heterotopia. Eur J Hum Genet. 2001 Jan;9(1):5-12.
Poolos NP, Das S, Clark GD, Lardizabal D, Noebels JL, Wyllie E, et al. Males with epilepsy, complete subcortical band heterotopia, and somatic mosaicism for DCX. Neurology. 2002 May 28;58(10):1559-62.
Guerrini R, Moro F, Andermann E, Hughes E, D'Agostino D, Carrozzo R, et al. Nonsyndromic mental retardation and cryptogenic epilepsy in women with doublecortin gene mutations. Ann Neurol. 2003 Jul;54(1):30-7.
Demelas L, Serra G, Conti M, Achene A, Mastropaolo C, Matsumoto N, et al. Incomplete penetrance with normal MRI in a woman with germline mutation of the DCX gene. Neurology. 2001 Jul 24;57(2):327-30.
Mei D, Parrini E, Pasqualetti M, Tortorella G, Franzoni E, Giussani U, et al. Multiplex ligation-dependent probe amplification detects DCX gene deletions in band heterotopia. Neurology. 2007 Feb 6;68(6):446-50.
Haverfield EV, Whited AJ, Petras KS, Dobyns WB, Das S. Intragenic deletions and duplications of the LIS1 and DCX genes: a major disease-causing mechanism in lissencephaly and subcortical band heterotopia. European journal of human genetics : EJHG. 2009 Jul;17(7):911-8.
Dobyns WB, Berry-Kravis E, Havernick NJ, Holden KR, Viskochil D. X-linked lissencephaly with absent corpus callosum and ambiguous genitalia. Am J Med Genet. 1999 Oct 8;86(4):331-7.
Pilz DT, Kuc J, Matsumoto N, Bodurtha J, Bernadi B, Tassinari CA, et al. Subcortical band heterotopia in rare affected males can be caused by missense mutations in DCX (XLIS) or LIS1. Hum Mol Genet. 1999 Sep;8(9):1757-60.
Francis F, Koulakoff A, Boucher D, Chafey P, Schaar B, Vinet MC, et al. Doublecortin is a developmentally regulated, microtubule-associated protein expressed in migrating and differentiating neurons. Neuron. 1999 Jun;23(2):247-56.
Gleeson JG, Lin PT, Flanagan LA, Walsh CA. Doublecortin is a microtubule-associated protein and is expressed widely by migrating neurons. Neuron. 1999 Jun;23(2):257-71.

Kappeler C, Saillour Y, Baudoin JP, Tuy FP, Alvarez C, Houbron C, et al. Branching and nucleokinesis defects in migrating interneurons derived from doublecortin knockout mice. Hum Mol Genet. 2006 May 1;15(9):1387-400.
Koizumi H, Higginbotham H, Poon T, Tanaka T, Brinkman BC, Gleeson JG. Doublecortin maintains bipolar shape and nuclear translocation during migration in the adult forebrain. Nat Neurosci. 2006 Jun;9(6):779-86.
Sapir T, Horesh D, Caspi M, Atlas R, Burgess HA, Wolf SG, et al. Doublecortin mutations cluster in evolutionarily conserved functional domains. Hum Mol Genet. 2000 Mar 22;9(5):703-12.
Taylor KR, Holzer AK, Bazan JF, Walsh CA, Gleeson JG. Patient mutations in doublecortin define a repeated tubulin-binding domain. J Biol Chem. 2000 Nov 3;275(44):34442-50.
Kim MH, Cierpicki T, Derewenda U, Krowarsch D, Feng Y, Devedjiev Y, et al. The DCX-domain tandems of doublecortin and doublecortin-like kinase. Nat Struct Biol. 2003 May;10(5):324-33.
Caspi M, Atlas R, Kantor A, Sapir T, Reiner O. Interaction between LIS1 and doublecortin, two lissencephaly gene products. Hum Mol Genet. 2000 Sep 22;9(15):2205-13.
Kizhatil K, Wu YX, Sen A, Bennett V. A new activity of doublecortin in recognition of the phospho-FIGQY tyrosine in the cytoplasmic domain of neurofascin. The Journal of neuroscience : the official journal of the Society for Neuroscience. 2002 Sep 15;22(18):7948-58.
Tsukada M, Prokscha A, Oldekamp J, Eichele G. Identification of neurabin II as a novel doublecortin interacting protein. Mechanisms of development. 2003 Sep;120(9):1033-43.
Friocourt G, Kappeler C, Saillour Y, Fauchereau F, Rodriguez MS, Bahi N, et al. Doublecortin interacts with the ubiquitin protease DFFRX, which associates with microtubules in neuronal processes. Mol Cell Neurosci. 2005 Jan;28(1):153-64.
Moores CA, Perderiset M, Francis F, Chelly J, Houdusse A, Milligan RA. Mechanism of microtubule stabilization by doublecortin. Mol Cell. 2004 Jun 18;14(6):833-9.
Tilney LG, Hatano S, Ishikawa H, Mooseker MS. The polymerization of actin: its role in the generation of the acrosomal process of certain echinoderm sperm. The Journal of cell biology. 1973 Oct;59(1):109-26.
Fourniol FJ, Sindelar CV, Amigues B, Clare DK, Thomas G, Perderiset M, et al. Template-free 13-protofilament microtubule-MAP assembly visualized at 8 A resolution. J Cell Biol. 2010 Nov 1;191(3):463-70.
Monteiro J, Derom C, Vlietinck R, Kohn N, Lesser M, Gregersen PK. Commitment to X inactivation precedes the twinning event in monochorionic MZ twins. Am J Hum Genet. 1998 Aug;63(2):339-46.
Collins DW, Jukes TH. Rates of transition and transversion in coding sequences since the human-rodent divergence. Genomics. 1994 Apr;20(3):386-96.
Berg AT, Berkovic SF, Brodie MJ, Buchhalter J, Cross JH, van Emde Boas W, et al. Revised terminology and concepts for organization of seizures and epilepsies: report of the ILAE Commission on Classification and Terminology, 2005-2009. Epilepsia. 2010 Apr;51(4):676-85.
Pettersen EF, Goddard TD, Huang CC, Couch GS, Greenblatt DM, Meng EC, et al. UCSF Chimera--a visualization system for exploratory research and analysis. J Comput Chem. 2004 Oct;25(13):1605-12.
Sali A, Blundell TL. Comparative protein modelling by satisfaction of spatial restraints. J Mol Biol. 1993 Dec 5;234(3):779-815.
Leger PL, Souville I, Boddaert N, Elie C, Pinard JM, Plouin P, et al. The location of DCX mutations predicts malformation severity in X-linked lissencephaly. Neurogenetics. 2008 Oct;9(4):277-85.

Dobyns WB, Truwit CL. Lissencephaly and other malformations of cortical development: 1995 update. Neuropediatrics. 1995 Jun;26(3):132-47.
Sicca F, Kelemen A, Genton P, Das S, Mei D, Moro F, et al. Mosaic mutations of the LIS1 gene cause subcortical band heterotopia. Neurology. 2003 Oct 28;61(8):1042-6.
Takanashi J, Barkovich AJ. The changing MR imaging appearance of polymicrogyria: a consequence of myelination. AJNR American journal of neuroradiology. 2003 May;24(5):788-93.
Hannan AJ, Servotte S, Katsnelson A, Sisodiya S, Blakemore C, Squier M, et al. Characterization of nodular neuronal heterotopia in children. Brain : a journal of neurology. 1999 Feb;122 (Pt 2):219-38.
Ferland RJ, Batiz LF, Neal J, Lian G, Bundock E, Lu J, et al. Disruption of neural progenitors along the ventricular and subventricular zones in periventricular heterotopia. Hum Mol Genet. 2009 Feb 1;18(3):497-516.
Croquelois A, Giuliani F, Savary C, Kielar M, Amiot C, Schenk F, et al. Characterization of the HeCo mutant mouse: a new model of subcortical band heterotopia associated with seizures and behavioral deficits. Cereb Cortex. 2009 Mar;19(3):563-75.
Ackman JB, Aniksztejn L, Crepel V, Becq H, Pellegrino C, Cardoso C, et al. Abnormal network activity in a targeted genetic model of human double cortex. J Neurosci. 2009 Jan 14;29(2):313-27.
Dobyns WB, Elias ER, Newlin AC, Pagon RA, Ledbetter DH. Causal heterogeneity in isolated lissencephaly. Neurology. 1992 Jul;42(7):1375-88.
De Volder AG, Gadisseux JF, Michel CJ, Maloteaux JM, Bol AC, Grandin CB, et al. Brain glucose utilization in band heterotopia: synaptic activity of "double cortex". Pediatr Neurol. 1994 Nov;11(4):290-4.
Pinard J, Feydy A, Carlier R, Perez N, Pierot L, Burnod Y. Functional MRI in double cortex: functionality of heterotopia. Neurology. 2000 Apr 11;54(7):1531-3.
Spreer J, Martin P, Greenlee MW, Wohlfarth R, Hammen A, Arnold SM, et al. Functional MRI in patients with band heterotopia. Neuroimage. 2001 Aug;14(2):357-65.
Tyvaert L, Hawco C, Kobayashi E, LeVan P, Dubeau F, Gotman J. Different structures involved during ictal and interictal epileptic activity in malformations of cortical development: an EEG-fMRI study. Brain : a journal of neurology. 2008 Aug;131(Pt 8):2042-60.
Lapray D, Popova IY, Kindler J, Jorquera I, Becq H, Manent JB, et al. Spontaneous epileptic manifestations in a DCX knockdown model of human double cortex. Cerebral cortex. 2010 Nov;20(11):2694-701.
Kato M, Kanai M, Soma O, Takusa Y, Kimura T, Numakura C, et al. Mutation of the doublecortin gene in male patients with double cortex syndrome: somatic mosaicism detected by hair root analysis. Ann Neurol. 2001 Oct;50(4):547-51.
Horesh D, Sapir T, Francis F, Wolf SG, Caspi M, Elbaum M, et al. Doublecortin, a stabilizer of microtubules. Human molecular genetics. 1999 Sep;8(9):1599-610.
Moores CA, Perderiset M, Kappeler C, Kain S, Drummond D, Perkins SJ, et al. Distinct roles of doublecortin modulating the microtubule cytoskeleton. Embo J. 2006 Oct 4;25(19):4448-57.
Tanaka T, Koizumi H, Gleeson JG. The doublecortin and doublecortin-like kinase 1 genes cooperate in murine hippocampal development. Cereb Cortex. 2006 Jul;16 Suppl 1:i69-73.
Friocourt G, Chafey P, Billuart P, Koulakoff A, Vinet MC, Schaar BT, et al. Doublecortin interacts with mu subunits of clathrin adaptor complexes in the developing nervous system. Mol Cell Neurosci. 2001 Sep;18(3):307-19.
Gdalyahu A, Ghosh I, Levy T, Sapir T, Sapoznik S, Fishler Y, et al. DCX, a new mediator of the JNK pathway. The EMBO journal. 2004 Feb 25;23(4):823-32.

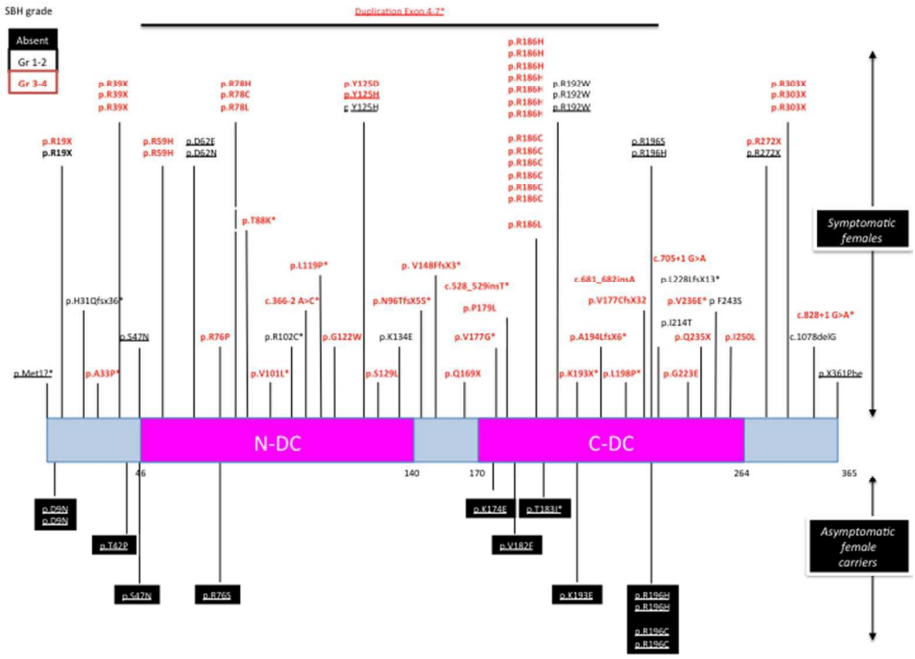

254x190mm (72 x 72 DPI)

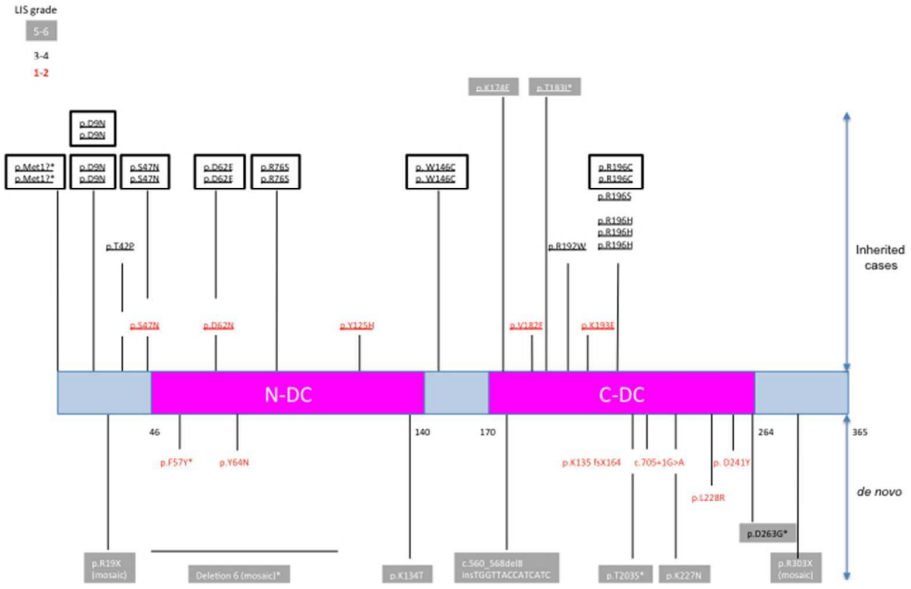

254x190mm (72 x 72 DPI)

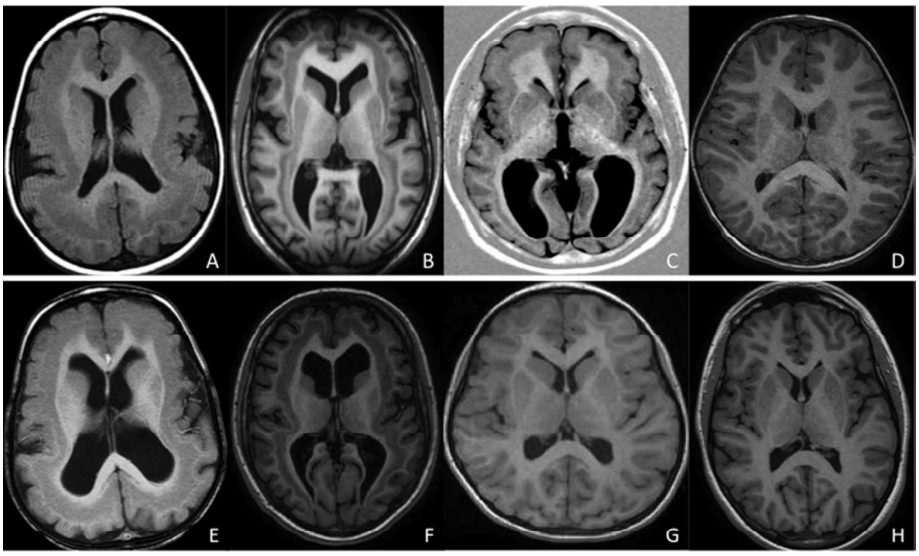

254x190mm (72 x 72 DPI)

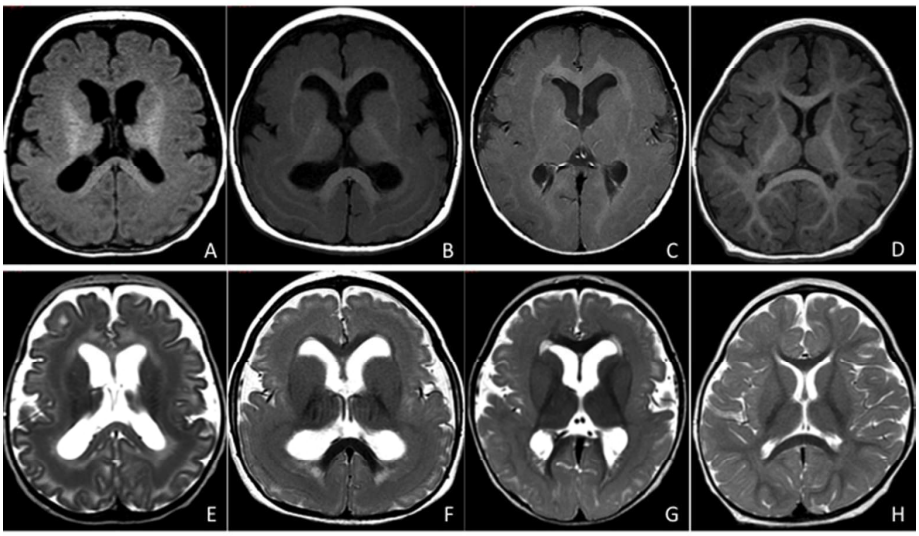

254x190mm (72 x 72 DPI)

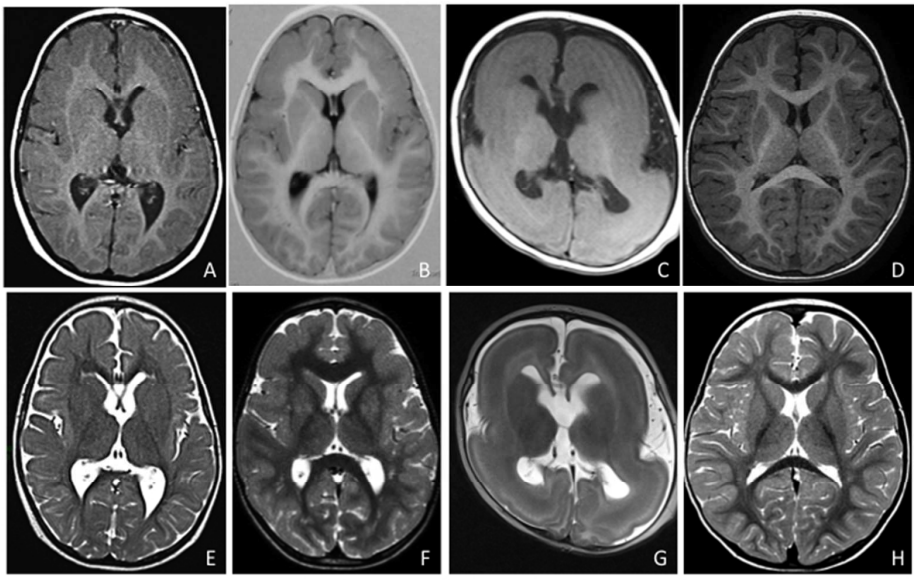

254x190mm (72 x 72 DPI)

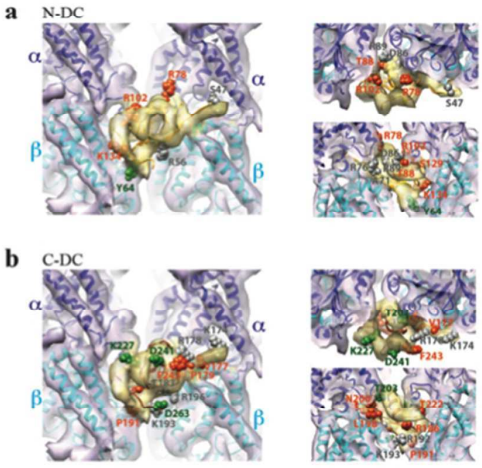

254x190mm (72 x 72 DPI)

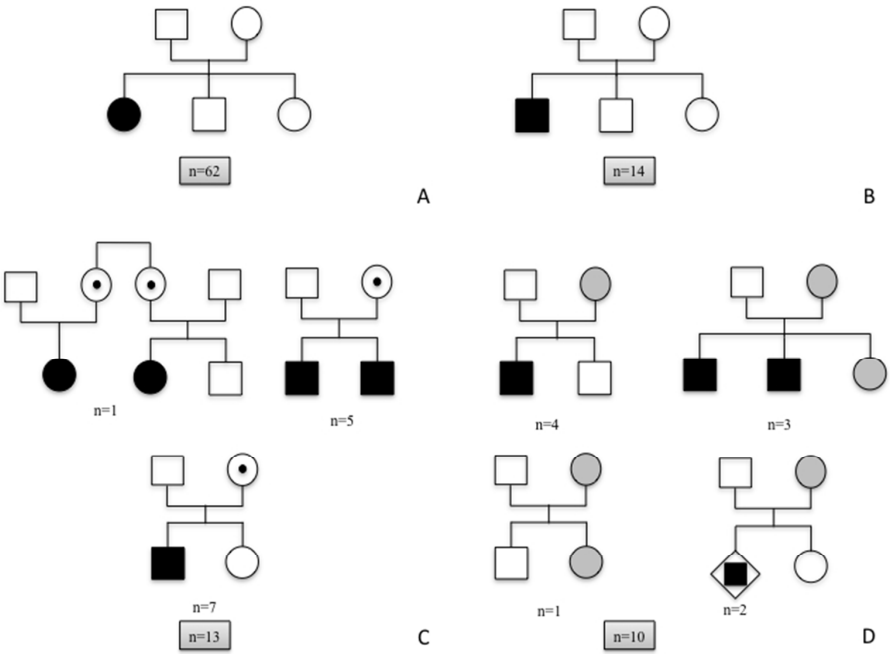

254x190mm (72 x 72 DPI)

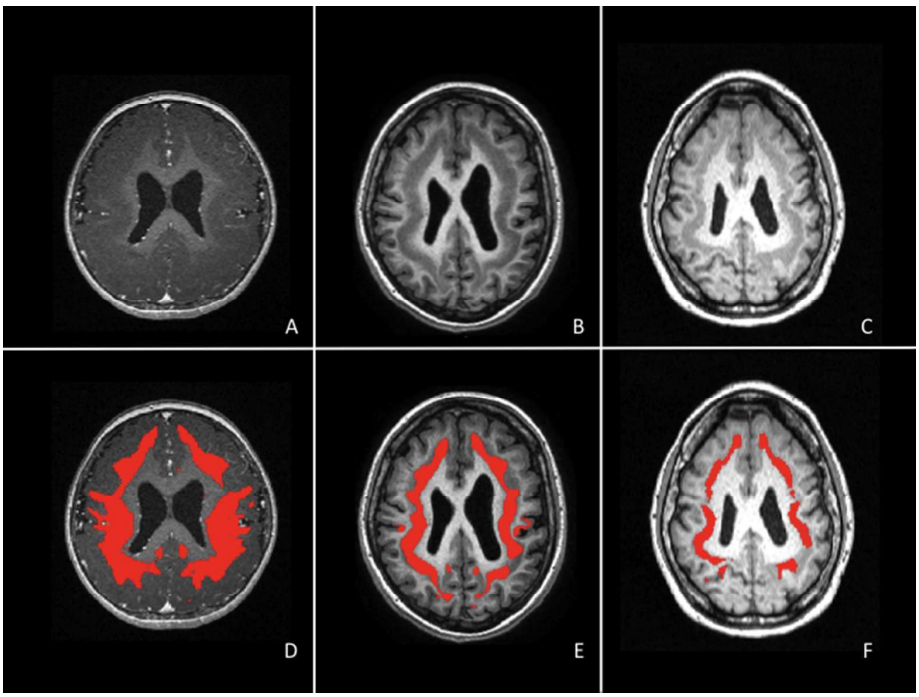

254x190mm (72 x 72 DPI)

Supplementary Table 1 Overview of neurological data in 93 patients with familial and sporadic SBH with mutation in the *DCX* gene *Age at last evaluation; yrs : years; Sz : seizures; DD : developmental delay; Band refers to SBH Grade; CPS : complex partial seizures; DA : drop attacks; AA Atypical Absence; Myo Sz: myoclonic seizures; GTCS : generalized tonic clonic seizures; Foc Sz : focal seizures; TS: tonic seizures; HC : head circumference; AED : antiepileptic drugs; N/A non available. Shown in grey are asymptomatic carrier females. Patients previously reported in [1] in (des Portes *et al.* , 1998a) and [2] in (des Portes *et al.* , 1998b).

	Age * (yrs)	Band	Presenting symptoms	HC	Mental retardation	Level of speech	Behavioral	Age of sz onset (yrs)	Sz type at onset	Current sz type	AED response
DCX_SBH_01	30	Gr 2	Sz	Median	Mild	Normal	Anxiety - delirium	11.5	CPS	DA/ AA /myo sz	partial drug resistance
DCX_SBH_02	28	Gr 3	Sz	Median	Moderate	poor articulation / fair comprehension	Absent	N/A	CPS / GTCS	CPS / GTCS	refractory
DCX_SBH_03	12.5	Gr 2	Sz	Median	Mild	Normal	Absent	11	GTCS	GTCS	controled
DCX_SBH_04	10	Gr 3	Sz	N/A	Moderate	poor verbal skills	frontal inhibition	9	GTCS	GTCS	partial drug resistance
DCX_SBH_05	3	Gr 4	DD	- 1 SD	severe	No language	Absent	No epilepsy			
DCX_SBH_06	2	Gr 4	DD	Median	severe	No word	severe - hyperkinetic-crying-automutilation -Autistic features	No epilepsy			
DCX_SBH_07	23	Gr 3	Sz	N/A	Moderate	poor articulation fair comprehension	frontal inhibition	3	GTCS	DA/ AA /myo sz	refractory
DCX_SBH_08	30	Gr 3	Sz	Median	Moderate	poor verbal skills	frontal inhibition	5	AA / myoclonia	AA / Myo sz / GTS	refractory

DCX_SBH_09	10	Gr 4	DD	Median	severe	No word	severe - hyperkinetic-crying	No epilepsy			
DCX_SBH_010	15	Gr 3	Sz	Median	severe	2-3 words sentences	Autistic - frontal inhibition	4	Foc.S (Temporal sz)	AA / GTS	refractory
DCX_SBH_011	6	Gr 4	West	Median	severe	Babble	frontal inhibition	0.5	Spasms/ DA / Myo sz / GTS	DA / Myo sz / Nocturnal TS	refractory
DCX_SBH_012	11	Gr 4	Sz	Median	severe	severely delayed	N/A	0.5	Myo sz / DA	DA/ AA /myo sz	refractory
DCX_SBH_013	4	Gr 4	DD	- 2SD	severe	Few words	Absent	N/A			
DCX_SBH_014	4.5	N/A	West	- 3 SD	severe	No word	Autistic	0.33	Spasms/GTS	Myo sz/ GTS	partial drug resistance
DCX_SBH_015	24	Gr 2	Sz	N/A	mild	Normal	Absent	6	GTCS	DA/ AA	refractory
DCX_SBH_016	45	Gr 3	Sz	- 2 SD	severe	Few words	frontal inhibition	0.66	CPS / DA / GTS	CPS / DA / GTS	refractory
DCX_SBH_017	20	Gr 4	N/A	N/A	severe	Few words	severe - hyperkinetic-crying	3	GTS / DA / AA	DA/ AA / GTS	refractory
DCX_SBH_018	4.8	Gr 4	Sz	- 2 SD	severe	Few words	Absent	0.75	Foc.S (frontal sz)	CPC	partial drug resistance
DCX_SBH_019	12	Gr 3	Sz	Median	Moderate	Age appropriate	Hyperkinesia	0.5	Spasms/ CPS	Auditive hallucination / nocturnal TS	refractory
DCX_SBH_020 Fam_1	12	Gr 3	Sz	N/A	Moderate	Poor verbal level	Autistic	8	AA / myo sz	AA / Myo sz / GTS	partial drug resistance
DCX_SBH_021 Fam_1	40	Gr 2	Mother	N/A	mild	Age appropriate	Absent	14	AA	AA	sz control
DCX_SBH_022	6	Gr 3	Sz	Median	mild	Age appropriate	Absent	2	DA / GTS	Myo sz	refractory
DCX_SBH_023	25	Gr 3	Sz	Median	Severe	Few words	Autistic features	8	Foc S	DA	refractory
DCX_SBH_	7.9	Gr 4	DD	- 2 SD	Mild	sentence 4-5 words	Temper	5	GTS / DA / AA	DA/ AA	refractory

024							tantrums and violence				
DCX_SBH_025/ Fam_2	33	Gr 1	Mother	N/A	mild	poor verbal skills	frontal - depressive BH	14	CPS	CPS	N/A
DCX_SBH_026/ Fam_3	48	Abs	Mother		Normal	Normal	Absent	No epilepsy			
DCX_SBH_027/ Fam_4	60	Abs	Mother		Normal	Normal	Absent	No epilepsy			
DCX_SBH_028/ Fam_5	28	Abs	Mother	N/A	Normal	Normal	Absent	No epilepsy			
DCX_SBH_029	20	Gr 4	Sz	Median	Moderate	Age appropriate	Psy Frontal inhibition	13	CPS / GCS	CPS (auditive hallucination)	refractory
DCX_SBH_030/ Fam_6	N/A	Gr 2	Mother		N/A	Normal	Absent	No epilepsy			
DCX_SBH_031/ Fam_7	63	Abs	Mother	N/A	Normal	Normal	Absent	No epilepsy			
DCX_SBH_032	14	Gr 3	Sz	- 2 SD	Moderate	Normal	Stereotypic frontal behaviour	0.5	Spasms/CPS	CPC / GCS	partial drug resistance
DCX_SBH_033	22		Sz	Median	Moderale	Normal	Severe	6	Foc Sz (motor)	DA/ AA / GTC	partial drug resistance
DCX_SBH_034/ Fam_8	39	Gr 1	Mother		N/A	Normal	Absent	No epilepsy			
DCX_SBH_035/ Fam_9 [1,2]	40	Gr 2	Mother	Median	Moderate	poor verbal skills	Absent	11	GTS		sz control
DCX_SBH_036	4	Gr 3	N/A	N/A	N/A	N/A	N/A	N/A	N/A	N/A	
DCX_SBH_037 Fam_10	37	Abs	Mother	Median	Normal	Normal	Absent	No epilepsy			
DCX_SBH_038	38	Gr 4	Sz	Median	severe	N/A	severe agressive behavior / crying	N/A	DA / GTS	DA /myo sz /	refractory
DCX_SBH_039	10	Gr 2	Sz	Median	mild	Age appropriate	Absent	8	Foc Sz (Temporal sz)	FS (Temporal sz)	sz control

DCX_SBH_040	5.5	Gr 4	DD	Median	severe	Few words	Absent	No epilepsy			
DCX_SBH_041	10	N/A	N/A	Median	Moderate	N/A	N/A	N/A	AA	Myo sz	N/A
DCX_SBH_042	5	Gr 4	West	-4 DS	severe	poor verbal	severe hyperkinetic	0.5	GTS	AA	partial drug resistance
DCX_SBH_043	25	Gr 3	Sz	Median	Moderate	Normal	Moderate	6	Foc Sz (motor)	DA/ AA / GTC	partial drug resistance
DCX_SBH_044	17	Gr 3	Sz	Median	mild	Normal	Hyperkinesia	15	Foc Sz (sensitive sz)	Foc Sz	refractory
DCX_SBH_045	4	Gr 4	West	Median	Moderate	Slightly delayed	Hyperkinesia	0.4	Spasms/GTS	DA/ Spasms	Sz control
DCX_SBH_046 [2]	15	Gr 4	Sz	Median	severe	Few words	severe frontal BH perseveration echolay inhibition	0.5	GTS / DA / AA	DA/ AA / GTC	refractory
DCX_SBH_047 Fam_11 [1,2]	4.5	Gr 3	Sz	Median	severe	Few words	Absent	0.5	Foc Sz (motor)	CPS	partial drug resistance
DCX_SBH_047 Fam_11 [1,2]											
DCX_SBH_048	34	Gr 3	Sz	Median	Moderate	poor verbal skills	frontal inhibition	5	GTS / DA / AA	DA/ AA / GTS	refractory
DCX_SBH_049	10	Gr 2	Sz	Median	Moderate	Normal	mild frontal features	8	Reflex sz (noise)	AA / GTS / reflex Myo sz	partial drug resistance
DCX_SBH_050/ Fam_12	35	Abs	Mother	N/A	Normal	Normal	Normal	No epilepsy			
DCX_SBH_051	15	Gr 4	Sz	Median	mild	Normal	N/A	2.5	Foc Sz	CPS	refractory
DCX_SBH_052	13	Gr 4	Sz	N/A	N/A	N/A	N/A	N/A	N/A	N/A	
DCX_SBH_053/ Fam13	35		Mother	Median	Moderate	Age Appropriate	Absent	13	GTS / DA / AA	DA/ AA / GTC	partial drug

											resistance
DCX_SBH_054/ Fam_14	32	Abs	Mother	N/A	Normal	Normal	Absent	No epilepsy			
DCX_SBH_055	1.5	Gr 4	DD	-3 DS	Severe	Babble	Stereotypic frontal behaviour	No epilepsy			
DCX_SBH_056	6	Gr 4	Sz	Median	severe	No word	N/A	0.8	Foc Sz	Foc Sz	partial drug resistance
DCX_SBH_057	11	Gr 4	DD	Median	severe	delayed	Autistic - frontal inhibition	12	AA / GTCS	AA / GTCS	partial drug resistance
DCX_SBH_058	6.5	Gr 4	DD	N/A	Moderate	poor verbal skills	N/A	N/A	Foc Sz (Temporal sz)	Foc Sz	partial drug resistance
DCX_SBH_059	18	Gr 4	Sz	- 2 SD	severe	Few words	agressive behaviour	0.33	N/A	N/A	N/A
DCX_SBH_060	1.5	Gr 4	Sz	-3 DS	Severe	No word	N/A	0.5	Spams	Spams	refractory
DCX_SBH_061	4	Gr 4	DD	- 2 SD	severe	single words	severe frontal perseveration echolalic	No epilepsy			
DCX_SBH_062	6	Gr 4	Sz	Median	severe	No word	Hyperkinetic-crying-automutilation -Autistic features	0.9	Febrile sz	CPS / status of CPS	Sz control
DCX_SBH_063	10	Gr 3	West	- 2 SD	severe	poor verbal skills	Hyperkinesia	0.4	Spasms/ CPS / GTS	Spasms/ CPS / GTS	refractory
DCX_SBH_064	15	Gr 2	Sz	Median	Mild	Age appropriate	mild frontal features	1.5	AA / Reflex sz (noise)	DA/ AA /myo sz	refractory
DCX_SBH_065	2.8	Gr 4	DD	- 3 SD	severe	single words	Stereotypic frontal behaviour	No epilepsy			
DCX_SBH_066	2	Gr 3	DD	-4 DS	severe	No word	mild autistic features	No epilepsy			
DCX_SBH_067		Gr 4	N/A		N/A	N/A	N/A	N/A	N/A	N/A	

DCX_SBH_068/ Fam_15 [1,2]	35	Gr 2	Sz	Median	Moderate	Age appropriate	Absent	10	GTS / DA / AA	DA/ AA / GTC	partial drug resistance
DCX_SBH_068/ Fam_15 [1,2]											
DCX_SBH_068/ Fam_15 [1,2]											
DCX_SBH_069	6	Gr 2	N/A		N/A	N/A	Absent	N/A	N/A	N/A	
DCX_SBH_070	10	Gr 3	Sz	Median	Moderate	delayed	autistic and frontal BH	3.5	Foc Sz /GTCS	CPS	Sz control
DCX_SBH_071/ Fam_16	40	Abs	Mother	N/A	Normal	Normal	Absent	No epilepsy			
DCX_SBH_072/ Fam_17	65	Abs	Mother	Median	Normal	Normal	Absent	No epilepsy			
DCX_SBH_073/ Fam_18	32	Abs	Mother	N/A	Normal	Normal	Absent	No epilepsy			
DCX_SBH_074/ Fam_19	44	Gr 1	Mother	Median	mild	Slightly delayed	Absent	N/A	GTCS	GTCS	Sz control
DCX_SBH_075/ Fam_20	40	N/A	Mother	N/A	Normal	Normal	Normal	No epilepsy			
DCX_SBH_076/ Fam_21	38	N/A	Mother	Median	Normal	Normal	Normal	No epilepsy			
DCX_SBH_077/ Fam_22	40	Gr 1	Mother	Median	mild	Normal	Normal	17	CPS	CPS (temporal sz)	sz control
DCX_SBH_078	12	Gr 4	DD	Median	severe	poor verbal skills	Anxiety	11	CPS (temporal sz)	CPS (temporal sz)	refractory
DCX_SBH_079 [2]	20	Gr 2	Sz	Median	severe	2 words in association	frontal inhibition / clastic access / crying	0.8	GTS / DA / AA	DA/ AA / GTC	refractory
DCX_SBH_080 [2]	9	Gr 3	Sz	Median	Moderate	poor verbal skills	N/A	9	Foc Sz		Sz control
DCX_SBH_081	1	Gr 3	Sz	N/A	severe	Babble	Absent	0,4	Spasms	No epilepsy	Sz control
DCX_SBH_	5,4	Gr 2	DD	- 1 SD	severe	Few words	Autistic auto -	2	Febrile sz	No epilepsy	sz control

082							heteroagressivity excessive crying				
DCX_SBH_083	14	Gr 3	DD	Median	severe	poor verbal skills	Autistic - frontal inhibition	4.5	GTS / DA / AA		refractory
DCX_SBH_084	30	Gr 2	Sz	Median	mild	poor verbal skills	Absent	6	Foc Sz	Myo sz/ GTCS / CPS (motor sz)	refractory
DCX_SBH_085/ Fam_23	20	Gr 1	Mother	- 1 SD	Normal	Normal	Absent	15	Foc Sz (sensitive sz)	Foc Sz	partial drug resistance
DCX_SBH_086/ Fam_25	12	Gr 4	DD	- 1 SD	severe	poor verbal skills	Autistic - frontal inhibition	4	GTS	No epilepsy	sz control
DCX_SBH_087/ Fam_25	8	Gr 4	DD	- 1 SD	severe	poor verbal skills	Absent -	No epilepsy			
DCX_SBH_088/ Fam_25	30		Mother	Median	Normal	Normal	Absent	No epilepsy			
DCX_SBH_089/ Fam_25	33		Mother	Median	Normal	Normal	Absent	No epilepsy			
DCX_SBH_090	3		Sz	- 2 SD	severe	No language	Normal	0.4	Spasms/ CPS / GTS	Spasms/ CPS / GTS	refractory

Supplementary Table 2 Overview of neurological data in 60 patients with 25 familial cases of SBH/XLIS. Age* refers to age at last evaluation. Sz : seizures ; Yrs : years ; SBH subcortical band heterotopia ; SBH Grade refers to Barkovich classification (1994) ; LIS lissencephaly, LIS grade refers to Dobyns grade; [1] In both cases, the origin of the mutation is not determined, but the female carriers had one daughter each with a *DCX* mutation and no clinical symptoms. MRI was not performed ; [2] In this case, the mutation was inherited from an asymptomatic grand mother. MRI not done ; [3] Female carriers in whom the *de novo* (ital) occurrence of the *DCX* mutation was demonstrated ; [4] Families previously reported (des Portes *et al.* , 1998a) or (des Portes *et al.* , 1998b) ; [5] Males previously reported in (Leger et al. , 2008) ; [6] Surface residues with partially buried side-chains.

		Structural group	DNA Mutation nucleotide ; protein (origin of the mutation)	Cortical width and pattern	Age *	Neurological examination	Epilepsy (age of sz onset; yrs)	Epilepsy (drug resistance)
	DCX_SBH_025	Unclassified	1st Met [3] *(de novo)*	SBH Gr 1 slightly shallow sulci	33	Normal Depressive behavior	14	Controlled
	XLIS_42 [5]	Unclassified	1st Met [3] *(de novo)*	Anterior pachygyria (LIS grade 4)	3.5	Walk with aid	No epilepsy	
Fam 2	XLIS_43 [5]	Unclassified	1st Met [3] *(de novo)*	Anterior pachygyria (LIS grade 4)	2	Hypotonia	No epilepsy	
	DCX_SBH_026	N term linker	c.25G<A p.D9N [1] (unknown)	Normal	N/A	N/A	N/A	
	XLIS_31 [5]	N term linker	c.25G<A p.D9N	Anterior pachygyria (LIS grade 4)	13	Normal	12	Controlled
Fam 3	XLIS_32 [5]	N term linker	c.25G<A p.D9N	Anterior pachygyria (LIS grade 4)	20	Normal	11	Controlled
	DCX_SBH_027	N term linker	c.25G<A p.D9N [1, 3] *(de novo)*	Normal		Normal	No epilepsy	
	XLIS_33	N term linker	c.25G<A p.D9N	Anterior pachygyria (LIS grade 4)	30	Autistic	15	Controlled
Fam 4	XLIS_34	N term linker	c.25G<A p.D9N	Anterior pachygyria (LIS grade 4)	35	Normal	13	Controlled
	DCX_SBH_028	N term linker	c.124 A>C p.T42P [2] (inherited from grand mother)	Normal		Normal	No epilepsy	
Fam 5	XLIS_35 [5]	N term linker	c.124 A>C p.T42P	Anterior pachygyria (LIS grade 4)	2	Tetraplegia	No epilepsy	
Fam 6	DCX_SBH_030	N term linker	c.140G>A p.S47N (unknown)	SBH Gr 2 slightly shallow sulci		Normal	N/A	

				(foetal case)				
	DCX_SBH_031	N term linker	c.140G>A p.S47N (unknown)	Normal		Normal	No epilepsy	
	XLIS_01 [5]	N term linker	c.140G>A p.S47N	Anterior pachygyria (LIS grade 4b)	30	Normal	17	Partial drug resistance
Fam 7	XLIS_02 [5]	N term linker	c.140G>A p.S47N	Anterior pachygyria (LIS grade 4b)	35	Normal	17	Refractory
	DCX_SBH_034	N-DC_buried site	c.186C>G p.D62E (unknown)	SBH Gr 1 Normal sulci		N/A	N/A	
	XLIS_06 [5]	N-DC_buried site	c.186C>G p.D62E	Anterior agyria and posterior pachygyria (LIS grade 3)	8	Walk with aid (spastic diplegia)	N/A	Controlled
Fam 8	XLIS_07 [5]	N-DC_buried site	c.186C>G p.D62E	Anterior agyria and posterior pachygyria (LIS grade 3)	22	Spastic tetraplegia	N/A	Refractory
	DCX_SBH_035	N-DC_buried site	c.184G>Ap.D62N	SBH Gr 1 Slightly shallow sulci	40	N/A	N/A	
Fam 9 [4]	XLIS_08 [5]	N-DC_buried site	c.184G>Ap.D62N	Generalized agyria (LIS grade 1)	24	Spastic tetraplegia	0.1	Refractory
	DCX_SBH_037	N-DC surface	c.226C>A p.R76S [3] *(de novo)*	Normal		Normal	No epilepsy	
	XLIS_04 [5]	N-DC surface	c.226C>A p.R76S	Anterior pachygyria (LIS grade 4)	5.5	Normal	No epilepsy	
Fam 10	XLIS_05 [5]	N-DC surface	c.226C>A p.R76S	Anterior pachygyria (LIS grade 4)	3.5	Normal	3	Controlled
	DCX_SBH_47 (mother)	N-DC_buried site	c.373T>C p.Y125H *(de novo)*	SBH Gr 2 Slightly shallow sulci	N/A	Normal	N/A	Controlled
	DCX_SBH_48 (sister)	N-DC_buried site	c.373T>C p.Y125H	SBH Gr 4 Frontal very shallow sulci	4.5	Normal	0.5	Partial drug resistance
Fam 11 [4]	XLIS_10 [5]	N-DC_buried site	c.373T>C p.Y125H	Diffuse agyria with shallow sulci in posterior regions (LIS grade 2)	17	Spastic tetraplegia	0.1	Refractory
	XLIS_11 [5]	N-DC-C-DC linker	c.438G>T p.W146C	Anterior agyria and posterior pachygyria (LIS grade 3)	3	Tetraplegia	No epilepsy	
Fam 24	XLIS_12 [5]	N-DC-C-DC linker	c.438G>T p.W146C	Anterior agyria and posterior pachygyria (LIS grade 3)	N/A	Tetraplegia	N/A	
	DCX_SBH_051	N-DC-C-DC linker	c.520A>G p.K174E (unknown)	Normal		Normal	No epilepsy	
Fam 12	XLIS_24 [5]	N-DC-C-DC linker	c.520A>G p.K174E	SBH mixed with anterior pachygyria (LIS grade 5b)	3	Spastic tetraplegia	6	Refractory
Fam 13	DCX_SBH_054	C-DC buried site	c.544G>T p.V182F (unknown)	SBH Grade 1 Normal sulci	35	Normal	13	Partial drug resistance

	XLIS_40	C-DC buried site	c.544G>T p.V182F	Diffuse agyria with shallow sulci in posterior regions (LIS grade 2)	0,8	Tetraplegia	0.3	Refractory
	DCX_SBH_055	C-DC surface	c.548C>T p.T183I [3] (*de novo*)	Normal	32	Normal	No epilepsy	
Fam 14	XLIS_13 [5]	C-DC surface	c.548C>T p.T183I [6]	SBH mixed with anterior pachygyria (LIS grade 5b)	1.5	Spastic tetraplegia	0.1	Refractory
	DCX_SBH_069	C-DC surface	c.574C>T p.R192W (unknown)	SBH Gr 2 slightly shallow sulci	35	Normal	10	Partial drug resistance
	DCX_SBH_070 (daughter)	C-DC surface	c.574C>T p.R192W	SBH Gr 2 slightly shallow sulci	N/A	Normal	N/A	Partial drug resistance
	DCX_SBH_071 (daughter)	C-DC surface	c.574C>T p.R192W	SBH Gr 2 slightly shallow sulci	N/A	Normal	N/A	Partial drug resistance
Fam15 [4]	XLIS_25 [5]	C-DC surface	c.574C>T p.R192W	Anterior agyria and posterior pachygyria (LIS grade 3)	27	Tetraplegia	0.5	Partial drug resistance
	DCX_SBH_074	C-DC surface	c.576A>G p.K193E (unknown)	Normal		Normal	No epilepsy	
Fam 16	XLIS_14 [5]	C-DC surface	c.576A>G p.K193E	Diffuse agyria with shallow sulci in posterior regions (LIS grade 2)	15	Normal	6	Refractory
	DCX_SBH_075	C-DC surface	c.586C>T p.R196C (unknown)	Normal		Normal	No epilepsy	
Fam 17	XLIS_15 [5]	C-DC surface	c.586C>T p.R196C	Anterior agyria and posterior pachygyria (LIS grade 3)	2	Tetraplegia	0.1	Refractory
	DCX_SBH_076 [3]	C-DC surface	c.586C>T p.R196C (*de novo*)	Normal		Normal	No epilepsy	
	XLIS_16 [5]	C-DC surface	c.586C>T p.R196C	Anterior pachygyria (LIS grade 4)	37	Normal	3	Controlled
Fam 18	XLIS_17 [5]	C-DC surface	c.586C>T p.R196C	Anterior pachygyria (LIS grade 4)	30	Normal	8	Controlled
	DCX_SBH_077	C-DC surface	c.586C>A p.R196S (*de novo*)	SBH Gr 1 Slightly shallow sulci	35	Normal	No epilepsy	
Fam 19	XLIS_18 [5]	C-DC surface	c.586C>A p.R196S	Anterior pachygyria (LIS grade 4)	12	Normal	4	Controlled
	DCX_SBH_078	C-DC surface	c.587G>A p.R196H (unknown)	Normal	38	Normal	No epilepsy	
Fam 20	XLIS_19 [5]	C-DC surface	c.587G>A p.R196H	Anterior pachygyria (LIS grade 4)	10	Walk with aid	9	Controlled
	DCX_SBH_079	C-DC surface	c.587G>A p.R196H (unknown)	Normal	40	Normal	No epilepsy	
Fam 21	XLIS_20	C-DC surface	c.587G>A p.R196H	Anterior pachygyria (LIS grade 4)		Hypotonia –Motor delay	No epilepsy	

	DCX_SBH_080	C-DC surface	c.587G>A p.R196H (unknown)	SBH Gr 1 Slightly shallow sulci	40	Normal	17	Partial drug resistance
Fam 22	XLIS_21	C-DC surface	c.587G>A p.R196H	Anterior pachygyria (LIS grade 4)	12	Motor delay	5	Partial drug resistance
Fam 23	DCX_SBH_088[3]	Unclassified	(c.1144 T/A) X361Phe (*de novo*)	SBH Gr 1 slightly shallow sulci (foetal case)	20	Normal	15	Controlled
	DCX_SBH_020	Nonsense	c.814C>T p.R272X	SBH Gr 3 slightly shallow sulci	12	Normal	8	Partial drug resistance
Fam_1	DCX_SBH_021 (mother)	Nonsense	c.814C>T p.R272X (*de novo*)	SBH Gr 2 slightly shallow sulci	40	Normal	14	Controlled
	DCX_SBH_089	duplication	Dup Exon 4-7	SBH Gr 4 Frontal very shallow sulci	12	Hypotonia –Motor delay	4	Controlled
	DCX_SBH_090	duplication	Dup Exon 4-7	SBH Gr 4 Frontal very shallow sulci	8	Hypotonia –Motor delay	No epilepsy	
	DCX_SBH_091 (mother)	duplication	Dup Exon 4-7 (unknown)	Normal	30	Normal	No epilepsy	
Fam_25	DCX_SBH_092 (maternal sister)	duplication	Dup Exon 4-7	Normal	33	Normal	No epilepsy	

HYPERTHERMIC SEIZURES DO NOT ENHANCED HIPPOCAMPAL EPILEPTOGENESIS IN DOUBLECORTIN KNOCKOUT MICE.

Sophie Hamelin[1,2,3,6], MD-PhD, Reham Khalaf[4], MD, Benoit Pouyatos[1,2], PhD, Tanguy Chabrol[1,2], Fiona Francis[4], PhD, Antoine Depaulis[1,2], PhD

[1]Inserm U-836, Grenoble - Institut des Neurosciences, Grenoble, France

[2]Université Joseph Fourier, Grenoble, France

[3]Centre Hospitalier Pierre Oudot, Bourgoin-Jallieu, France

[4]Université Pierre et Marie Curie, Paris, France

[5]Inserm UMR-S839, Institut du Fer à Moulin, Paris, France

[6]Corresponding author: Dr Sophie Hamelin

Grenoble - Institut des Neurosciences

Université Joseph Fourier, Domaine de la Merci

BP170

38042, Grenoble, Cedex 9, France

Tel: 04 56 52 06 59

Tel: 04 56 52 06 56 (Sec.)

Fax: 04 56 52 06 57

Sophie.Hamelin@ujf-grenoble.f

(4) number of characters in the title 96 with spaces

(5) number of word in the abstract: 223

body of the manuscript: 1878, 15 references

(6) number of figures, color figures, and tables

SUMMARY

Purpose

According to the “two hits theory”, the association of cortical dysplasia with febrile seizures should promote the development of mesial temporal lobe epilepsy with hippocampal sclerosis (MTLE). We addressed this hypothesis by examining the consequences of Hyperthermic Seizures (HS) on the hippocampal dysplasia developed by double-cortin knock-out mice (Dcx-KO).

Method

C57BL/6 Dcx-KO, Dcx-heterozygous (Dcx-Hz) and wild-type (WT) littermates were exposed at P10 to either 40°C (HS) or 20°C (Sham) for 30 min. At P70, they were implanted with bipolar hippocampal electrodes and their local field potentials were recorded for up to 20h/mice. Hippocampal neo-expression of neuropeptide Y (NPY) was compared between groups.

Results

In Sham/WT, no seizures were ever recorded (n=11; 240 h of recording) whereas one hippocampal seizure with cortical spread was observed in the HS/WT group (n=12; 288 h). In Sham/Dcx-KO mice, 2 of them developed seizures (15 seizures, n=10; 204 h). In HS/Dcx-KO mice, only one seizure was recorded (n=9; 216 h). No seizure was recorded in both HS/- and Sham/Dcx-Hz mice (N=10/7; 200/184 h). Ectopic expression of NPY was observed in all Dcx-KO mice that displayed seizures, and was three-fold increased in Hz mice that experienced HS.

Discussion

Our results failed to show an increase in the proportion of Dcx-KO seizures after HS, and suggest that HS rather might decrease recurrent seizures via the neo-expression of NPY.

Introduction

Febrile seizure (FS), the most common type of seizures in children, are mostly benign with little evidence of any adverse effects (Knudsen, 1996). However, in about a third of the cases, FS display atypical features qualified as “complex febrile seizures” and constitute a risk factor for mesial temporal lobe epilepsy with hippocampal sclerosis (MTLE) (French et al., 1993). Yet, the sole occurrence of an episode of FS does not appear sufficient to trigger MTLE and it has been suggested that another trauma and/or a genetic predisposition could be necessary to the development of epileptogenesis. Indeed, in patients with MTLE, cortical malformations have been increasingly identified in association with hippocampal sclerosis, a combination referred as “dual pathology” (Lévesque et al., 1991). As a matter of fact, during brain maturation, the presence of a genetic or acquired focal cortical dysplasia might render the brain more susceptible to prolonged FS, therefore increasing the risk of developing MTLE (Hamelin et al., 2009).

Human type I lissencephaly is a form of cortical dysplasia associated with mutations in the gene coding for doublecortin (Dcx), a microtubule-associated protein (Francis et al., 1999; Gleeson et al., 1999). Patients with such a mutation generally display a smooth cortex and a disorganized hippocampus, and suffer from refractory epilepsy, in addition to severe intellectual disability (Portes et al., 1998). Mice in which the Dcx gene has been deleted (Dcx-KO) (Corbo et al., 2002) do not display lamination defects in the isocortex, but present an abnormal organization in the CA3 region with the pyramidal layer divided into at least two distinct layers (Kappeler et al., 2006; 2007). In addition, some of them exhibit rare spontaneous convulsive seizures with a hippocampal origin (Nosten-Bertrand et al., 2008). Using this model, we addressed here whether hyperthermic seizures (HS) at P10 aggravate the development of spontaneous epileptic seizures observed in adults. To this aim, we compared the consequences of HS in both Dcx-KO hemizygous (Dcx-KO) and heterozygous (Dcx-Hz) mice with their wild type (WT) littermates, using the recording of local field potentials (LFP). The expression of NPY in the hippocampus was also explored as it was shown to play a critical role in the modulation of hippocampal seizures (Vezzani et al., 1999) and has been shown to be neo-expressed in the Dcx KO model (Nosten-Bertrand et al., 2008).

MATERIAL AND METHODS

Mice pups were obtained by breeding at the Grenoble Institute of Neuroscience. Dcx-KO mice (deleted for Dcx exon 3 on the X chromosome) were generated by using the Cre-loxP site-specific recombination system, as described elsewhere (Kappeler et al., 2006). These animals were generated with wild-type littermate controls by crossing Dcx-Hz females with C57BL/6N males (Janvier France). To assay Dcx in postnatal stages, protein extracts were analyzed by SDS-PAGE and Western blotting (Kappeler et al., 2006). All procedures were accepted by our local ethical committee in accordance with the guidelines of the European Community's Council Directive of 24 November 1986 (86/609/EEC).

Hyperthermic seizures (HS) were induced for 30-minutes in P10 mice (Dcx-KO, Dcx-Hz, and WT) using a standard hairdryer (41°C) as previously described (Hamelin et al, submitted). The other half of the litter was maintained at 22-24°C (Sham). Adult (P60-70) mice were implanted with (i) two monopolar electrodes over the anterior cortex; (ii) a monopolar electrode over the cerebellum (reference); and (iii) two bipolar electrodes into both hippocampi.

After one-week recovery, freely moving mice were video-LFP recorded (Micromed, sampling rate=1,024 Hz) for a mean duration of 20 hours (3 to 5 sessions) over a one month period. Ictal discharges were defined as the presence of rhythmic recruiting poly-spikes of high-amplitude (>2x the background activity) lasting for at least 6 s. Behaviors associated with limbic seizures in rodents typically included sudden cessation of activity, head bobbing, prolonged immobility then staring, rearing then falling with bilateral clonus. Both electrographic and behavioral correlates were required for the definition of seizure.

Immunohistochemistry was performed at the age of 4 months, using immunoperoxidase detection for anti-NPY (1:10000, rabbit; Sigma), as previously described (Kappeler et al., 2006; Nosten-Bertrand et al., 2008).

Data are expressed as mean + SEM (n= number of independent samples). Differences among the groups were compared using nonparametric Kruskal-Wallis test, and if significant, post-hoc tests were done using Dunn's correction (Prism; GraphPad). Significance was set at 0.05.

RESULTS

DCX-associated hippocampal dysplasia had no influence on HS

We first hypothesized that the CA3 dysplasia would render the mice more prone to HS, as suggested in rats (Scantlebury et al., 2005). We studied 132 pups, issued from 18 litters. Among them, 63 pups (47.7 %) were included in the hyperthermic seizure group (HS). The distribution among genetic background (WT/Dcx-Hz/Dcx-KO) and sex is detailed in Table 1. No differences between WT, Dcx-Hz and Dcx-KO mice were detected neither for temperature seizure threshold, seizure time occurrence and duration, nor mortality before weaning (only 2 in both HS and Sham groups). Stereotyped behavioural seizures were observed among all pups whatever their genetic backgrounds. All pups reacted to the onset of hyperthermia with wild running, followed by an abrupt arrest of movement rapidly associated with distal erratic myoclonus alternating with recurrent increasing nose rubbing, followed by rearing then falling, as we recently described (Hamelin et al, submitted). This behaviour alternated with hypotonia, while pups lost their righting reflexes and were pauci-reactive.

HS did not increase the propensity to convulsive seizures in Dcx KO mice

Video-LFPs were obtained from both hippocampi and anterior cortex in 59 adult mice, for a total time recording of 1,333 hours. There was no difference in the averaged body weight measured before surgery (Table 1). A total of 17 seizures were recorded, mainly (88 %) in the Sham/Dcx-KO group: 15 clonic seizures that included jaw myoclonus, then forelimb clonus, were observed in 2 of the 10 Sham/Dcx-KO mice. The hippocampal discharges associated with these seizures (Fig 1-A,B) showed very reproducible time-frequency pattern and duration, as previously described (Nosten-Bertrand et al., 2008). In contrast, only one seizure was recorded in the HS/Dcx-KO group (Fig 1-C), but its duration was three-times longer than in Sham/Dcx-KO group. In HS/WT mice, only one short clonic seizure was observed, involving the hippocampus first. Seizure duration between the three groups expressing clonic seizure was different, although the difference did not reach the significance threshold (Fig 1-D; $p=0.08$).

Neuropathology and NPY expression

Histological analyses of cresyl-violet-stained sections of mice did not reveal any obvious pyramidal cell loss or granular cell dispersion in any of the 6 groups. We observed in all Dcx-KO mice (Sham and HS), that the CA3 region was divided into several distinct pyramidal cell

layers, as previously described (Nosten-Bertrand et al., 2008). This was also observed in all Dcx-Hz mice, although in a less pronounced manner.

We previously showed that 56 % of Dcx-KO mice neo-expressed NPY in the mossy fibers stemming from the dentate gyrus to the CA3 region and rarely in inter-neurone process in the outer molecular layer (OML), whereas the ectopic expression in Dcx-Hz animals was not investigated (Nosten-Bertrand et al., 2008). Neo-expression of NPY was observed in 75 % of the Sham/Dcx-KO mice (1/8 in OML) and in 62.5 % (2/8 in OML) in HS/Dcx-KO animals (Fig 1-E-F)

Such neo-expression of NPY was observed in 20 % of Sham/Dcx-Hz (0/6 in OML) but was present in 66 % of HS/Dcx-Hz (Chi-Square, alpha 0.15). We never observed any recurrent mossy fibers that traversed the GC layer, as in mice with hippocampal sclerosis.

DISCUSSION

The two main findings of our study are that (i) the existence of a dysplasia in the CA3 did not aggravate HS in immature mice; (ii) HS did not increase epileptogenesis that develops in Dcx-Ko adult mice (iii) but increased the ectopic expression of NPY in Dcx-Hz mice that did not expressed seizures.

(i) CA3 hippocampal dysplasia did not aggravate HS

In rats with cortical cryo-lesion, an increased in HS susceptibility was observed (Scantlebury et al., 2005), whereas in methylazoxymethanol acetate (MAM-E17) pups, the data were controversial (Germano et al., 1996; Park et al., 2010). This suggests that the CA3 dysplasia did not potentiate the HS process, possibly due to the location of the dysplasia (e.g., cortex vs hippocampus).

(ii) HS did not increase epileptogenesis that develops in Dcx-Ko mice.

Our data confirmed that in Dcx-KO mice, clonic seizures are relatively rare (15 seizures in 2 mice out of 8, during 200 hours of recordings) and initiated in the hippocampus without signs of hippocampal sclerosis (Nosten-Bertrand et al., 2008). In contrast with expected results, HS decreased their propensity to develop seizures and disagreed with previous published data in rats. Indeed, either in focal cortical poly-microgyria or cortical dysplasia in MAM-E17 rat model, HS increased the proportion of rats that developed seizures (Park et al., 2010; Gibbs et al., 2011). Nevertheless, our results were somewhat in agreement with clinical data obtained in patients with type 1 focal cortical dysplasia (FCD) and hippocampal sclerosis (Tassi et al., 2010) who showed a significant higher incidence of FS (54 % vs 5 %),

but a lower seizure frequency (10 vs 115) than patients with isolated FCD. To our knowledge, a relationship between seizure frequency and FS in MTLE has not been reported.

(iii) HS increased the ectopic expression of NPY in Dcx-Hz mice

As previously published (Nosten-Bertrand et al., 2008), ≈60 % of Dcx-KO mice displayed an ectopic expression of NPY in mossy fibbers, without modification by HS. Nevertheless, HS highly increased the proportion of Dcx-Hz mice in which this neo-expression was present. The signification of this neo-expression remains poorly understood, and might reflect the pathological process of epileptogenesis. However, this neuropeptide has been suggested to suppress seizures, an effect that may depend on the type of NPY receptor involved. This suggests that an increase of NPY by HS would constitute a form of protective preconditioning.

Our results, contrasting with previously published data on HS that occurred in lesioned immature brain, suggest that HS does not interact with the CA3 dysplasia to potentiate epileptogenesis. On the contrary, our data obtained in Dcx-Hz mice might suggest the existence of a pre-conditioning effect of HS that would rather protect against seizures via an increase expression of NPY.

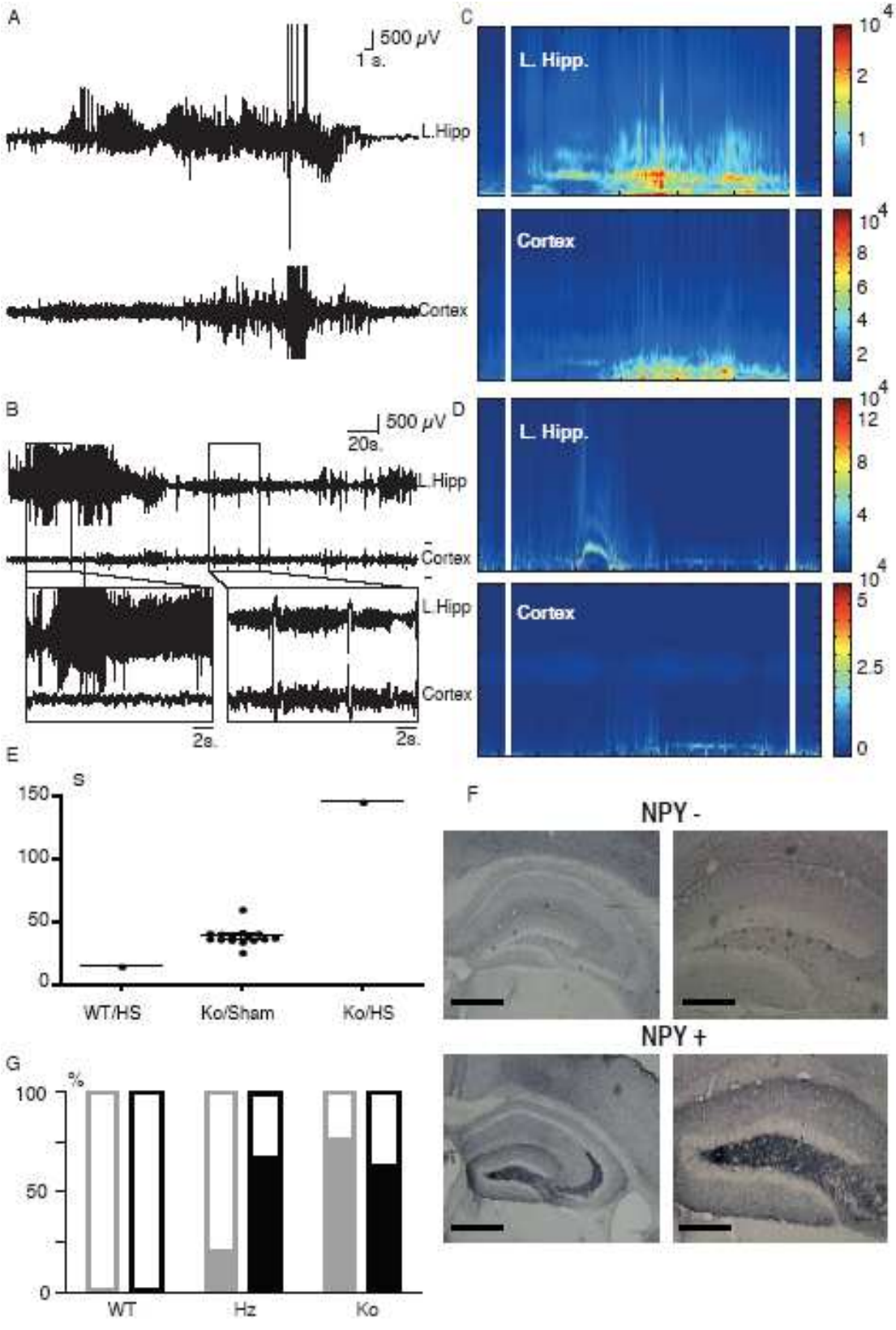
A
500 μV
1 s.
L.Hipp
Cortex
B
500 μV
20s.
L.Hipp
Cortex
L.Hipp
Cortex
2s.
2s.
C
L. Hipp.
Cortex
10^4
2
1
8
6
4
D
L. Hipp.
Cortex
12
5
2.5
0
E
S
150
100
50
0
WT/HS
Ko/Sham
Ko/HS
F
NPY -
NPY +
G
%
100
50
0
WT
Hz
Ko

Figure 1: Hippocampal and cortical local field potential activities during clonic seizures in Sham/Dcx-KO mice (A and B)

Example of LFP recording in hippocampus and cortex during a spontaneous seizure in a freely-moving Sham/Dcx-KO mouse (A) and HS/Dcx-KO mouse (B). **(C and D)** Median average over seizures of LFP power in the time–frequency plane (n=15 seizures) from 2 Sham/Dcx-KO mice (C) and from a HS/Dcx-KO mouse (D). A standard pattern of power during HPDs was derived by normalizing the time axis of the time–frequency representation before median averaging (correspondence of start and end of HPDs was assumed; white lines). **(E)** Individual seizure duration in the different groups HS/WT, Sham/Dcx-KO, and HS/Dcx-KO (Kruskal-Wallis p=0.08) **(F)** NPY-immunolabelling in mice without neo-expression of NPY (top panel), in a Sham/WT mice, and of a neo-expression of NPY in a HS/Dcx-KO mice (bottom panel) **(G)** Percentage of mice that expressed NPY in mossy fibbers in the different groups (Sham are in grey, n=9 WT, 4 Hz, 6 KO, HS are in black, n=6 WT, 5 Hz, 8 KO, Chi-Square:ns).

Table 1:

	Sham			**HS**			
HS	WT	Hz	KO	WT	Hz	KO	p
Male (n=60)	21	0	10	18	0	11	
Female (n=54)	15	10	0	13	16	0	
Total mice (n=114)	36	10	10	31	16	11	
Delay (min.)				7.7±1.0	6.0±0.9	7.3±2.1	0.44
Cage T°C				39.4±0.5	40.2±0.6	40.5±1.1	0.39
Body T°C				35.4±0.5	35.6±0.7	36.3±0.2	0.20
n=				10	12	7	
P60 weight (g)	22.3±1.7	20.4±0.5	24.9±0.7	23.5±1.2	21.25±0.9	27.6±1.2	ns
EEG recordings							
Male (n=31)	6	0	10	6	0	9	
Female (n=28)	5	7	0	6	10	0	
Total (n=59)	11	7	10	12	10	9	
EEG sessions (n)	4.0±0.2	4.0±0.4	3.6±0.4	4.2±0.3	3.8±0.4	4.2±0.3	
EEG mean duration (h/mice)	21,7±1.4	26.4±3.3	20.4±2.8	24.0±1.9	20.0±2.4	24.0±2.5	
EEG total time (h/group)	239.4	184.6	204.2	288.8	200.0	216.4	
Clonic seizures (n)	0	0	15 (2 mice)	1	0	1	
Inter-ictal spikes (n mice (%)	2 (18%)	0	4 (40%)	2 (16%)	1 (10%)	0	

BIBLIOGRAPHY

Corbo, J.C., Deuel, T.A., Long, J.M., LaPorte, P., Tsai, E., Wynshaw-Boris, A., and Walsh, C.A. (2002). Doublecortin is required in mice for lamination of the hippocampus but not the neocortex. Journal of Neuroscience *22*, 7548–7557.

Francis, F., Koulakoff, A., Boucher, D., Chafey, P., Schaar, B., Vinet, M.C., Friocourt, G., McDonnell, N., Reiner, O., Kahn, A., et al. (1999). Doublecortin is a developmentally regulated, microtubule-associated protein expressed in migrating and differentiating neurons. Neuron *23*, 247–256.

French, J.A., Williamson, P.D., Thadani, V.M., Darcey, T.M., Mattson, R.H., Spencer, S.S., and Spencer, D.D. (1993). Characteristics of medial temporal lobe epilepsy: I. Results of history and physical examination. Ann Neurol. *34*, 774–780.

Germano, I., Zhang, Y., Sperber, E., and Moshe, S. (1996). Neuronal migration disorders increase susceptibility to hyperthermia-induced seizures in developing rats. Epilepsia *37*, 902–910.

Gibbs, S., Chattopadhyaya, B., Desgent, S., Awad, P.N., Clerk-Lamalice, O., Levesque, M., Vianna, R.-M., Rébillard, R.-M., Delsemme, A.-A., Hébert, D., et al. (2011). Long-term consequences of a prolonged febrile seizure in a dual pathology model. Neurobiology of Disease *43*, 312–321.

Gleeson, J.G., Lin, P.T., Flanagan, L.A., and Walsh, C.A. (1999). Doublecortin is a microtubule-associated protein and is expressed widely by migrating neurons. Neuron *23*, 257–271.

Hamelin, S., Kahane, P., and Depaulis, A. (2009). Long-term effects of febrile status epilepticus: What animal models can tell us? Epilepsia *50 Suppl 12*, 27–28.

Kappeler, C., Dhenain, M., Phan Dinh Tuy, F., Saillour, Y., Marty, S., Fallet-Bianco, C., Souville, I., Souil, E., Pinard, J.-M., Meyer, G., et al. (2007). Magnetic resonance imaging and histological studies of corpus callosal and hippocampal abnormalities linked to doublecortin deficiency. J. Comp. Neurol. *500*, 239–254.

Kappeler, C., Saillour, Y., Baudoin, J.-P., Tuy, F.P.D., Alvarez, C., Houbron, C., Gaspar, P., Hamard, G., Chelly, J., Métin, C., et al. (2006). Branching and nucleokinesis defects in migrating interneurons derived from doublecortin knockout mice. Hum Mol Genet *15*, 1387–1400.

Knudsen, F.U. (1996). Febrile seizures--treatment and outcome. Brain and Development *18*, 438–449.

Lévesque, M.F., Nakasato, N., Vinters, H.V., and Babb, T.L. (1991). Surgical treatment of limbic epilepsy associated with extrahippocampal lesions: the problem of dual pathology. J. Neurosurg. *75*, 364–370.

Nosten-Bertrand, M., Kappeler, C., Dinocourt, C., Denis, C., Germain, J., Dinh Tuy, F.P., Verstraeten, S., Alvarez, C., Métin, C., Chelly, J., et al. (2008). Epilepsy in Dcx Knockout Mice Associated with Discrete Lamination Defects and Enhanced Excitability in the Hippocampus. PLoS ONE *3*, e2473.

Park, K.-I., Chu, K., Jung, K.-H., Kim, J.-H., Kang, K.-M., Lee, S.-T., Park, H.-K., Kim, M., Lee, S.K., and Roh, J.-K. (2010). Role of cortical dysplasia in epileptogenesis following prolonged febrile seizure. Epilepsia *51*, 1809–1819.

Portes, Des, V., Pinard, J.M., Billuart, P., Vinet, M.C., Koulakoff, A., Carrié, A., Gelot, A., Dupuis, E., Motte, J., Berwald-Netter, Y., et al. (1998). A novel CNS gene required for neuronal migration and involved in X-linked subcortical laminar heterotopia and lissencephaly syndrome. Cell *92*, 51–61.

Scantlebury, M.H., Gibbs, S.A., Foadjo, B., Lema, P., Psarropoulou, C., and Carmant, L. (2005). Febrile seizures in the predisposed brain: a new model of temporal lobe epilepsy. Ann Neurol. *58*, 41–49.

Tassi, L., Garbelli, R., Colombo, N., Bramerio, M., Russo, Lo, G., Deleo, F., Milesi, G., and Spreafico, R. (2010). Type I focal cortical dysplasia: surgical outcome is related to histopathology. Epileptic Disord *12*, 181–191.

Vezzani, A., Sperk, G., and Colmers, W.F. (1999). Neuropeptide Y: emerging evidence for a functional role in seizure modulation. Trends in Neurosciences *22*, 25–30.

CHAPTER 5: REFERENCES

Aaku-Saraste, E., Hellwig, A., and Huttner, W.B. (1996). Loss of occludin and functional tight junctions, but not ZO-1, during neural tube closure--remodeling of the neuroepithelium prior to neurogenesis. Dev. Biol. *180*, 664–679.

Abbott, N.J., Rönnbäck, L., and Hansson, E. (2006). Astrocyte-endothelial interactions at the blood-brain barrier. Nat. Rev. Neurosci. *7*, 41–53.

Abe, K., Chisaka, O., Van Roy, F., and Takeichi, M. (2004). Stability of dendritic spines and synaptic contacts is controlled by alpha N-catenin. Nat. Neurosci. *7*, 357–363.

Abellan, A., Menuet, A., Dehay, C., Medina, L., and Rétaux, S. (2010). Differential expression of LIM-homeodomain factors in Cajal-Retzius cells of primates, rodents, and birds. Cereb. Cortex *20*, 1788–1798.

Ackman, J.B., Aniksztejn, L., Crépel, V., Becq, H., Pellegrino, C., Cardoso, C., Ben-Ari, Y., and Represa, A. (2009). Abnormal network activity in a targeted genetic model of human double cortex. J. Neurosci. *29*, 313–327.

Aguado, F., Carmona, M.A., Pozas, E., Aguiló, A., Martínez-Guijarro, F.J., Alcantara, S., Borrell, V., Yuste, R., Ibañez, C.F., and Soriano, E. (2003). BDNF regulates spontaneous correlated activity at early developmental stages by increasing synaptogenesis and expression of the K+/Cl- co-transporter KCC2. Development *130*, 1267–1280.

Ahmari, S.E., and Smith, S.J. (2002). Knowing a nascent synapse when you see it. Neuron *34*, 333–336.

Alcántara, S., Ruiz, M., D'Arcangelo, G., Ezan, F., de Lecea, L., Curran, T., Sotelo, C., and Soriano, E. (1998). Regional and cellular patterns of reelin mRNA expression in the forebrain of the developing and adult mouse. J. Neurosci. *18*, 7779–7799.

Allendoerfer, K.L., and Shatz, C.J. (1994). The Subplate, A Transient Neocortical Structure: Its Role in the Development of Connections between Thalamus and Cortex. Annual Review of Neuroscience *17*, 185–218.

Alliot, F., Godin, I., and Pessac, B. (1999). Microglia derive from progenitors, originating from the yolk sac, and which proliferate in the brain. Developmental Brain Research *117*, 145–152.

Altman, J., and Bayer, S.A. (1990a). Horizontal compartmentation in the germinal matrices and intermediate zone of the embryonic rat cerebral cortex. Exp. Neurol. *107*, 36–47.

Altman, J., and Bayer, S.A. (1990b). Mosaic organization of the hippocampal neuroepithelium and the multiple germinal sources of dentate granule cells. J. Comp. Neurol. *301*, 325–342.

Altman, J., and Bayer, S.A. (1990c). Prolonged sojourn of developing pyramidal cells in the intermediate zone of the hippocampus and their settling in the stratum pyramidale. J. Comp. Neurol. *301*, 343–364.

Amaral, D.G., and Dent, J.A. (1981). Development of the mossy fibers of the dentate gyrus: I. A light and electron microscopic study of the mossy fibers and their expansions. J. Comp. Neurol. *195*, 51–86.

Anderson, S., Mione, M., Yun, K., and Rubenstein, J.L. (1999). Differential origins of neocortical projection and local circuit neurons: role of Dlx genes in neocortical interneuronogenesis. Cereb. Cortex *9*, 646–654.

Anderson, S.A., Eisenstat, D.D., Shi, L., and Rubenstein, J.L. (1997). Interneuron migration from basal forebrain to neocortex: dependence on Dlx genes. Science *278*, 474–476.

Andersson, C., Tytell, M., and Brunso-Bechtold, J. (1993). Transplantation of cultured type 1 astrocyte cell suspensions into young, adult and aged rat cortex: cell migration and survival. Int. J. Dev. Neurosci. *11*, 555–568.

Angevine, J.B., and Sidman, R.L. (1961). Autoradiographic Study of Cell Migration during Histogenesis of Cerebral Cortex in the Mouse. , Published Online: 25 November 1961; | Doi:10.1038/192766b0 *192*, 766–768.

Ascoli, G.A., Alonso-Nanclares, L., Anderson, S.A., Barrionuevo, G., Benavides-Piccione, R., Burkhalter, A., Buzsáki, G., Cauli, B., Defelipe, J., Fairén, A., et al. (2008). Petilla terminology: nomenclature of features of GABAergic interneurons of the cerebral cortex. Nat. Rev. Neurosci. *9*, 557–568.

Assadi, A.H., Zhang, G., Beffert, U., McNeil, R.S., Renfro, A.L., Niu, S., Quattrocchi, C.C., Antalffy, B.A., Sheldon, M., Armstrong, D.D., et al. (2003). Interaction of reelin signaling and Lis1 in brain development. Nat. Genet. *35*, 270–276.

Assimacopoulos, S., Grove, E.A., and Ragsdale, C.W. (2003). Identification of a Pax6-dependent epidermal growth factor family signaling source at the lateral edge of the embryonic cerebral cortex. J. Neurosci. *23*, 6399–6403.

Azim, E., Jabaudon, D., Fame, R.M., and Macklis, J.D. (2009). SOX6 controls dorsal progenitor identity and interneuron diversity during neocortical development. Nat. Neurosci. *12*, 1238–1247.

Baas, P.W., and Joshi, H.C. (1992). Gamma-tubulin distribution in the neuron: implications for the origins of neuritic microtubules. J. Cell Biol. *119*, 171–178.

Bai, J., Ramos, R.L., Ackman, J.B., Thomas, A.M., Lee, R.V., and LoTurco, J.J. (2003). RNAi reveals doublecortin is required for radial migration in rat neocortex. Nat. Neurosci. *6*, 1277–1283.

Bannerman, D.M., Deacon, R.M.J., Offen, S., Friswell, J., Grubb, M., and Rawlins, J.N.P. (2002). Double dissociation of function within the hippocampus: spatial memory and hyponeophagia. Behav. Neurosci. *116*, 884–901.

Barkovich, A.J., Koch, T.K., and Carrol, C.L. (1991). The spectrum of lissencephaly: report of ten patients analyzed by magnetic resonance imaging. Ann. Neurol. *30*, 139–146.

Barkovich, A.J., Kuzniecky, R.I., Jackson, G.D., Guerrini, R., and Dobyns, W.B. (2001). Classification system for malformations of cortical development: update 2001. Neurology *57*, 2168–2178.

Barnabé-Heider, F., Wasylnka, J.A., Fernandes, K.J.L., Porsche, C., Sendtner, M., Kaplan, D.R., and Miller, F.D. (2005). Evidence that embryonic neurons regulate the onset of cortical gliogenesis via cardiotrophin-1. Neuron *48*, 253–265.

Bartoe, J.L., McKenna, W.L., Quan, T.K., Stafford, B.K., Moore, J.A., Xia, J., Takamiya, K., Huganir, R.L., and Hinck, L. (2006). Protein interacting with C-kinase 1/protein kinase Calpha-mediated endocytosis converts netrin-1-mediated repulsion to attraction. J. Neurosci. *26*, 3192–3205.

Batista-Brito, R., and Fishell, G. (2009). The developmental integration of cortical interneurons into a functional network. Curr. Top. Dev. Biol. *87*, 81–118.

Baumgart, E., Vanhorebeek, I., Grabenbauer, M., Borgers, M., Declercq, P.E., Fahimi, H.D., and Baes, M. (2001). Mitochondrial alterations caused by defective peroxisomal biogenesis in a mouse model for Zellweger syndrome (PEX5 knockout mouse). Am. J. Pathol. *159*, 1477–1494.

Bayer, S.A. (1980a). Development of the hippocampal region in the rat. I. Neurogenesis examined with 3H-thymidine autoradiography. J. Comp. Neurol. *190*, 87–114.

Bayer, S.A. (1980b). Development of the hippocampal region in the rat. II. Morphogenesis during embryonic and early postnatal life. J. Comp. Neurol. *190*, 115–134.

Bayer, S.A., and Altman, J. (1990). Development of layer I and the subplate in the rat neocortex. Exp. Neurol. *107*, 48–62.

Bazelot, M., Simonnet, J., Dinocourt, C., Bruel-Jungerman, E., Miles, R., Fricker, D., and Francis, F. (2012). Cellular anatomy, physiology and epileptiform activity in the CA3 region of Dcx knockout mice: a neuronal lamination defect and its consequences. Eur. J. Neurosci. *35*, 244–256.

Bechstedt, S., and Brouhard, G.J. (2012). Doublecortin recognizes the 13-protofilament microtubule cooperatively and tracks microtubule ends. Dev. Cell *23*, 181–192.

Beffert, U., Weeber, E.J., Morfini, G., Ko, J., Brady, S.T., Tsai, L.-H., Sweatt, J.D., and Herz, J. (2004). Reelin and cyclin-dependent kinase 5-dependent signals cooperate in regulating neuronal migration and synaptic transmission. J. Neurosci. *24*, 1897–1906.

Behar, T.N., Dugich-Djordjevic, M.M., Li, Y.X., Ma, W., Somogyi, R., Wen, X., Brown, E., Scott, C., McKay, R.D., and Barker, J.L. (1997). Neurotrophins stimulate chemotaxis of embryonic cortical neurons. Eur. J. Neurosci. *9*, 2561–2570.

Bellion, A., Baudoin, J.-P., Alvarez, C., Bornens, M., and Métin, C. (2005). Nucleokinesis in tangentially migrating neurons comprises two alternating phases:

forward migration of the Golgi/centrosome associated with centrosome splitting and myosin contraction at the rear. J. Neurosci. *25*, 5691–5699.

Belvindrah, R., Nissant, A., and Lledo, P.-M. (2011). Abnormal neuronal migration changes the fate of developing neurons in the postnatal olfactory bulb. J. Neurosci. *31*, 7551–7562.

Ben-Ari, Y., Cherubini, E., Corradetti, R., and Gaiarsa, J.L. (1989). Giant synaptic potentials in immature rat CA3 hippocampal neurones. J Physiol *416*, 303–325.

Berbel, P., and Innocenti, G.M. (1988). The development of the corpus callosum in cats: a light- and electron-microscopic study. J. Comp. Neurol. *276*, 132–156.

Bergles, D.E., and Jahr, C.E. (1997). Synaptic activation of glutamate transporters in hippocampal astrocytes. Neuron *19*, 1297–1308.

Berkel, S., Marshall, C.R., Weiss, B., Howe, J., Roeth, R., Moog, U., Endris, V., Roberts, W., Szatmari, P., Pinto, D., et al. (2010). Mutations in the SHANK2 synaptic scaffolding gene in autism spectrum disorder and mental retardation. Nat. Genet. *42*, 489–491.

Bessis, A., Béchade, C., Bernard, D., and Roumier, A. (2007). Microglial control of neuronal death and synaptic properties. Glia *55*, 233–238.

Bielle, F., Griveau, A., Narboux-Nême, N., Vigneau, S., Sigrist, M., Arber, S., Wassef, M., and Pierani, A. (2005). Multiple origins of Cajal-Retzius cells at the borders of the developing pallium. Nat. Neurosci. *8*, 1002–1012.

Bishop, K.M., Goudreau, G., and O'Leary, D.D. (2000). Regulation of area identity in the mammalian neocortex by Emx2 and Pax6. Science *288*, 344–349.

Bohner, A.P., Akers, R.M., and McConnell, S.K. (1997). Induction of deep layer cortical neurons in vitro. Development *124*, 915–923.

Bonaguidi, M.A., McGuire, T., Hu, M., Kan, L., Samanta, J., and Kessler, J.A. (2005). LIF and BMP signaling generate separate and discrete types of GFAP-expressing cells. Development *132*, 5503–5514.

Bonni, A., Sun, Y., Nadal-Vicens, M., Bhatt, A., Frank, D.A., Rozovsky, I., Stahl, N., Yancopoulos, G.D., and Greenberg, M.E. (1997). Regulation of gliogenesis in the central nervous system by the JAK-STAT signaling pathway. Science *278*, 477–483.

Borello, U., and Pierani, A. (2010). Patterning the cerebral cortex: traveling with morphogens. Curr. Opin. Genet. Dev. *20*, 408–415.

Borrell, V., Río, J.A.D., Alcántara, S., Derer, M., Martínez, A., D'Arcangelo, G., Nakajima, K., Mikoshiba, K., Derer, P., Curran, T., et al. (1999). Reelin Regulates the Development and Synaptogenesis of the Layer-Specific Entorhino-Hippocampal Connections. J. Neurosci. *19*, 1345–1358.

Bortone, D., and Polleux, F. (2009). KCC2 expression promotes the termination of cortical interneuron migration in a voltage-sensitive calcium-dependent manner. Neuron *62*, 53–71.

Bouchard, J.-F., Moore, S.W., Tritsch, N.X., Roux, P.P., Shekarabi, M., Barker, P.A., and Kennedy, T.E. (2004). Protein kinase A activation promotes plasma membrane insertion of DCC from an intracellular pool: A novel mechanism regulating commissural axon extension. J. Neurosci. *24*, 3040–3050.

Britanova, O., de Juan Romero, C., Cheung, A., Kwan, K.Y., Schwark, M., Gyorgy, A., Vogel, T., Akopov, S., Mitkovski, M., Agoston, D., et al. (2008). Satb2 is a postmitotic determinant for upper-layer neuron specification in the neocortex. Neuron *57*, 378–392.

Britto, J.M., Johnston, L.A., and Tan, S.-S. (2009). The stochastic search dynamics of interneuron migration. Biophys. J. *97*, 699–709.

Brunstrom, J.E., Gray-Swain, M.R., Osborne, P.A., and Pearlman, A.L. (1997). Neuronal heterotopias in the developing cerebral cortex produced by neurotrophin-4. Neuron *18*, 505–517.

Bulchand, S., Grove, E.A., Porter, F.D., and Tole, S. (2001). LIM-homeodomain gene Lhx2 regulates the formation of the cortical hem. Mech. Dev. *100*, 165–175.

Burkarth, N., Kriebel, M., Kranz, E.U., and Volkmer, H. (2007). Neurofascin regulates the formation of gephyrin clusters and their subsequent translocation to the axon hillock of hippocampal neurons. Mol. Cell. Neurosci. *36*, 59–70.

Butt, S.J.B., Fuccillo, M., Nery, S., Noctor, S., Kriegstein, A., Corbin, J.G., and Fishell, G. (2005). The temporal and spatial origins of cortical interneurons predict their physiological subtype. Neuron *48*, 591–604.

Buzsáki, G., Chen, L.S., and Gage, F.H. (1990). Spatial organization of physiological activity in the hippocampal region: relevance to memory formation. Prog. Brain Res. *83*, 257–268.

Cappello, S., Attardo, A., Wu, X., Iwasato, T., Itohara, S., Wilsch-Bräuninger, M., Eilken, H.M., Rieger, M.A., Schroeder, T.T., Huttner, W.B., et al. (2006). The Rho-GTPase cdc42 regulates neural progenitor fate at the apical surface. Nat. Neurosci. *9*, 1099–1107.

Cardoso, C., Leventer, R.J., Dowling, J.J., Ward, H.L., Chung, J., Petras, K.S., Roseberry, J.A., Weiss, A.M., Das, S., Martin, C.L., et al. (2002). Clinical and molecular basis of classical lissencephaly: Mutations in the LIS1 gene (PAFAH1B1). Hum. Mutat. *19*, 4–15.

Caspi, M., Atlas, R., Kantor, A., Sapir, T., and Reiner, O. (2000). Interaction between LIS1 and doublecortin, two lissencephaly gene products. Hum. Mol. Genet. *9*, 2205–2213.

Cauli, B., Audinat, E., Lambolez, B., Angulo, M.C., Ropert, N., Tsuzuki, K., Hestrin, S., and Rossier, J. (1997). Molecular and physiological diversity of cortical nonpyramidal cells. J. Neurosci. *17*, 3894–3906.

Caviness, V.S., Jr (1982). Neocortical histogenesis in normal and reeler mice: a developmental study based upon [3H]thymidine autoradiography. Brain Res. *256*, 293–302.

Caviness, V.S., Jr, So, D.K., and Sidman, R.L. (1972). The hybrid reeler mouse. J. Hered. *63*, 241–246.

Caviness, V.S., and Rakic, P. (1978). Mechanisms of Cortical Development: A View From Mutations in Mice. Annual Review of Neuroscience *1*, 297–326.

Ceranik, K., Zhao, S., and Frotscher, M. (2000). Development of the entorhino-hippocampal projection: guidance by Cajal-Retzius cell axons. Ann. N. Y. Acad. Sci. *911*, 43–54.

Cerpa, W., Godoy, J.A., Alfaro, I., Farías, G.G., Metcalfe, M.J., Fuentealba, R., Bonansco, C., and Inestrosa, N.C. (2008). Wnt-7a modulates the synaptic vesicle cycle and synaptic transmission in hippocampal neurons. J. Biol. Chem. *283*, 5918–5927.

Chae, T., Kwon, Y.T., Bronson, R., Dikkes, P., Li, E., and Tsai, L.H. (1997). Mice lacking p35, a neuronal specific activator of Cdk5, display cortical lamination defects, seizures, and adult lethality. Neuron *18*, 29–42.

Chao, W.-T., and Kunz, J. (2009). Focal adhesion disassembly requires clathrin-dependent endocytosis of integrins. FEBS Lett. *583*, 1337–1343.

Chen, B., Wang, S.S., Hattox, A.M., Rayburn, H., Nelson, S.B., and McConnell, S.K. (2008). The Fezf2-Ctip2 genetic pathway regulates the fate choice of subcortical projection neurons in the developing cerebral cortex. Proc. Natl. Acad. Sci. U.S.A. *105*, 11382–11387.

Chevaleyre, V., and Siegelbaum, S.A. (2010). Strong CA2 pyramidal neuron synapses define a powerful disynaptic cortico-hippocampal loop. Neuron *66*, 560–572.

Claiborne, B.J., Amaral, D.G., and Cowan, W.M. (1986). A light and electron microscopic analysis of the mossy fibers of the rat dentate gyrus. J. Comp. Neurol. *246*, 435–458.

Cobos, I., Calcagnotto, M.E., Vilaythong, A.J., Thwin, M.T., Noebels, J.L., Baraban, S.C., and Rubenstein, J.L.R. (2005). Mice lacking Dlx1 show subtype-specific loss of interneurons, reduced inhibition and epilepsy. Nat. Neurosci. *8*, 1059–1068.

Cohen, P.E., Zhu, L., Nishimura, K., and Pollard, J.W. (2002). Colony-stimulating factor 1 regulation of neuroendocrine pathways that control gonadal function in mice. Endocrinology *143*, 1413–1422.

Conde, C., and Cáceres, A. (2009). Microtubule assembly, organization and dynamics in axons and dendrites. Nature Reviews Neuroscience *10*, 319–332.

Corbo, J.C., Deuel, T.A., Long, J.M., LaPorte, P., Tsai, E., Wynshaw-Boris, A., and Walsh, C.A. (2002). Doublecortin is required in mice for lamination of the hippocampus but not the neocortex. J. Neurosci. *22*, 7548–7557.

Cossart, R., Dinocourt, C., Hirsch, J.C., Merchan-Perez, A., De Felipe, J., Ben-Ari, Y., Esclapez, M., and Bernard, C. (2001). Dendritic but not somatic GABAergic inhibition is decreased in experimental epilepsy. Nat. Neurosci. *4*, 52–62.

Costa, M.R., Bucholz, O., Schroeder, T., and Götz, M. (2009). Late origin of glia-restricted progenitors in the developing mouse cerebral cortex. Cereb. Cortex *19 Suppl 1*, i135–143.

D'Agostino, M.D., Bernasconi, A., Das, S., Bastos, A., Valerio, R.M., Palmini, A., Costa, J.C. da, Scheffer, I.E., Berkovic, S., Guerrini, R., et al. (2002). Subcortical band heterotopia (SBH) in males: clinical, imaging and genetic findings in comparison with females. Brain *125*, 2507–2522.

Daboussi, L., Costaguta, G., and Payne, G.S. (2012). Phosphoinositide-mediated clathrin adaptor progression at the trans-Golgi network. Nat. Cell Biol. *14*, 239–248.

Danglot, L., Triller, A., and Marty, S. (2006). The development of hippocampal interneurons in rodents. Hippocampus *16*, 1032–1060.

Datson, N.A., Meijer, L., Steenbergen, P.J., Morsink, M.C., van der Laan, S., Meijer, O.C., and de Kloet, E.R. (2004). Expression profiling in laser-microdissected hippocampal subregions in rat brain reveals large subregion-specific differences in expression. Eur. J. Neurosci. *20*, 2541–2554.

Datson, N.A., Morsink, M.C., Steenbergen, P.J., Aubert, Y., Schlumbohm, C., Fuchs, E., and de Kloet, E.R. (2009). A molecular blueprint of gene expression in hippocampal subregions CA1, CA3, and DG is conserved in the brain of the common marmoset. Hippocampus *19*, 739–752.

Dayanithi, G., Forostyak, O., Ueta, Y., Verkhratsky, A., and Toescu, E.C. (2012). Segregation of calcium signalling mechanisms in magnocellular neurones and terminals. Cell Calcium *51*, 293–299.

DeFelipe, J., Hendry, S.H., Jones, E.G., and Schmechel, D. (1985). Variability in the terminations of GABAergic chandelier cell axons on initial segments of pyramidal cell axons in the monkey sensory-motor cortex. J. Comp. Neurol. *231*, 364–384.

Deguchi, Y., Donato, F., Galimberti, I., Cabuy, E., and Caroni, P. (2011). Temporally matched subpopulations of selectively interconnected principal neurons in the hippocampus. Nat. Neurosci. *14*, 495–504.

Dehay, C., and Kennedy, H. (2007). Cell-cycle control and cortical development. Nature Reviews Neuroscience *8*, 438–450.

Demarque, M., Represa, A., Becq, H., Khalilov, I., Ben-Ari, Y., and Aniksztejn, L. (2002). Paracrine intercellular communication by a Ca2+- and SNARE-independent release of GABA and glutamate prior to synapse formation. Neuron *36*, 1051–1061.

Denaxa, M., Chan, C.H., Schachner, M., Parnavelas, J.G., and Karagogeos, D. (2001). The adhesion molecule TAG-1 mediates the migration of cortical interneurons from the ganglionic eminence along the corticofugal fiber system. Development *128*, 4635–4644.

Denaxa, M., Kyriakopoulou, K., Theodorakis, K., Trichas, G., Vidaki, M., Takeda, Y., Watanabe, K., and Karagogeos, D. (2005). The adhesion molecule TAG-1 is required for proper migration of the superficial migratory stream in the medulla but not of cortical interneurons. Developmental Biology *288*, 87–99.

Deuel, T.A.S., Liu, J.S., Corbo, J.C., Yoo, S.-Y., Rorke-Adams, L.B., and Walsh, C.A. (2006). Genetic interactions between doublecortin and doublecortin-like kinase in neuronal migration and axon outgrowth. Neuron *49*, 41–53.

Deverman, B.E., and Patterson, P.H. (2009). Cytokines and CNS Development. Neuron *64*, 61–78.

DiMauro, S., and Schon, E.A. (2008). Mitochondrial disorders in the nervous system. Annu. Rev. Neurosci. *31*, 91–123.

Dobyns, W.B., Elias, E.R., Newlin, A.C., Pagon, R.A., and Ledbetter, D.H. (1992). Causal heterogeneity in isolated lissencephaly. Neurology *42*, 1375–1388.

Dobyns, W.B., and Truwit, C.L. (1995). Lissencephaly and other malformations of cortical development: 1995 update. Neuropediatrics *26*, 132–147.

Dobyns, W.B., Truwit, C.L., Ross, M.E., Matsumoto, N., Pilz, D.T., Ledbetter, D.H., Gleeson, J.G., Walsh, C.A., and Barkovich, A.J. (1999). Differences in the gyral pattern distinguish chromosome 17-linked and X-linked lissencephaly. Neurology *53*, 270–277.

Dompierre, J.P., Godin, J.D., Charrin, B.C., Cordelières, F.P., King, S.J., Humbert, S., and Saudou, F. (2007). Histone deacetylase 6 inhibition compensates for the transport deficit in Huntington's disease by increasing tubulin acetylation. J. Neurosci. *27*, 3571–3583.

Dong, H.-W., Swanson, L.W., Chen, L., Fanselow, M.S., and Toga, A.W. (2009). Genomic-anatomic evidence for distinct functional domains in hippocampal field CA1. Proc. Natl. Acad. Sci. U.S.A. *106*, 11794–11799.

Dulabon, L., Olson, E.C., Taglienti, M.G., Eisenhuth, S., McGrath, B., Walsh, C.A., Kreidberg, J.A., and Anton, E.S. (2000). Reelin binds alpha3beta1 integrin and inhibits neuronal migration. Neuron *27*, 33–44.

Eisenstat, D.D., Liu, J.K., Mione, M., Zhong, W., Yu, G., Anderson, S.A., Ghattas, I., Puelles, L., and Rubenstein, J.L. (1999). DLX-1, DLX-2, and DLX-5 expression define distinct stages of basal forebrain differentiation. J. Comp. Neurol. *414*, 217–237.

Elias, L.A.B., Turmaine, M., Parnavelas, J.G., and Kriegstein, A.R. (2010). Connexin 43 mediates the tangential to radial migratory switch in ventrally derived cortical interneurons. J. Neurosci. *30*, 7072–7077.

Elias, L.A.B., Wang, D.D., and Kriegstein, A.R. (2007). Gap junction adhesion is necessary for radial migration in the neocortex. Nature *448*, 901–907.

Englund, C., Fink, A., Lau, C., Pham, D., Daza, R.A.M., Bulfone, A., Kowalczyk, T., and Hevner, R.F. (2005). Pax6, Tbr2, and Tbr1 Are Expressed Sequentially by Radial Glia, Intermediate Progenitor Cells, and Postmitotic Neurons in Developing Neocortex. J. Neurosci. *25*, 247–251.

Erblich, B., Zhu, L., Etgen, A.M., Dobrenis, K., and Pollard, J.W. (2011). Absence of Colony Stimulation Factor-1 Receptor Results in Loss of Microglia, Disrupted Brain Development and Olfactory Deficits. PLoS ONE *6*, e26317.

Erickson, H.P. (2000). Gamma-tubulin nucleation: template or protofilament? Nat. Cell Biol. *2*, E93–96.

Espinosa, A., Gil-Sanz, C., Yanagawa, Y., and Fairén, A. (2009). Two separate subtypes of early non-subplate projection neurons in the developing cerebral cortex of rodents. Front. Neuroanat. *3*, 27.

Estivill-Torrus, G., Pearson, H., van Heyningen, V., Price, D.J., and Rashbass, P. (2002). Pax6 is required to regulate the cell cycle and the rate of progression from symmetrical to asymmetrical division in mammalian cortical progenitors. Development *129*, 455–466.

Ezratty, E.J., Partridge, M.A., and Gundersen, G.G. (2005). Microtubule-induced focal adhesion disassembly is mediated by dynamin and focal adhesion kinase. Nat. Cell Biol. *7*, 581–590.

Fahrion, J.K., Komuro, Y., Li, Y., Ohno, N., Littner, Y., Raoult, E., Galas, L., Vaudry, D., and Komuro, H. (2012). Rescue of neuronal migration deficits in a mouse model of fetal Minamata disease by increasing neuronal Ca2+ spike frequency. PNAS *109*, 5057–5062.

Fairén, A., Cobas, A., and Fonseca, M. (1986). Times of generation of glutamic acid decarboxylase immunoreactive neurons in mouse somatosensory cortex. J. Comp. Neurol. *251*, 67–83.

Fanselow, M.S., and Dong, H.-W. (2010). Are the dorsal and ventral hippocampus functionally distinct structures? Neuron *65*, 7–19.

Farías, G.G., Alfaro, I.E., Cerpa, W., Grabowski, C.P., Godoy, J.A., Bonansco, C., and Inestrosa, N.C. (2009). Wnt-5a/JNK signaling promotes the clustering of PSD-95 in hippocampal neurons. J. Biol. Chem. *284*, 15857–15866.

Fichera, M., Lo Giudice, M., Falco, M., Sturnio, M., Amata, S., Calabrese, O., Bigoni, S., Calzolari, E., and Neri, M. (2004). Evidence of kinesin heavy chain (KIF5A) involvement in pure hereditary spastic paraplegia. Neurology *63*, 1108–1110.

Fish, J.L., Dehay, C., Kennedy, H., and Huttner, W.B. (2008). Making bigger brains-the evolution of neural-progenitor-cell division. J. Cell. Sci. *121*, 2783–2793.

Flames, N., Long, J.E., Garratt, A.N., Fischer, T.M., Gassmann, M., Birchmeier, C., Lai, C., Rubenstein, J.L.R., and Marín, O. (2004). Short- and long-range attraction of cortical GABAergic interneurons by neuregulin-1. Neuron *44*, 251–261.

Flavell, S.W., and Greenberg, M.E. (2008). Signaling mechanisms linking neuronal activity to gene expression and plasticity of the nervous system. Annu. Rev. Neurosci. *31*, 563–590.

Fluegge, D., Moeller, L.M., Cichy, A., Gorin, M., Weth, A., Veitinger, S., Cainarca, S., Lohmer, S., Corazza, S., Neuhaus, E.M., et al. (2012). Mitochondrial Ca(2+) mobilization is a key element in olfactory signaling. Nat. Neurosci. *15*, 754–762.

Fode, C., Ma, Q., Casarosa, S., Ang, S.L., Anderson, D.J., and Guillemot, F. (2000). A role for neural determination genes in specifying the dorsoventral identity of telencephalic neurons. Genes Dev. *14*, 67–80.

Forman, M.S., Squier, W., Dobyns, W.B., and Golden, J.A. (2005). Genotypically defined lissencephalies show distinct pathologies. J. Neuropathol. Exp. Neurol. *64*, 847–857.

Fourniol, F.J., Sindelar, C.V., Amigues, B., Clare, D.K., Thomas, G., Perderiset, M., Francis, F., Houdusse, A., and Moores, C.A. (2010). Template-free 13-protofilament microtubule-MAP assembly visualized at 8 A resolution. J. Cell Biol. *191*, 463–470.

Francis, F., Koulakoff, A., Boucher, D., Chafey, P., Schaar, B., Vinet, M.C., Friocourt, G., McDonnell, N., Reiner, O., Kahn, A., et al. (1999). Doublecortin is a developmentally regulated, microtubule-associated protein expressed in migrating and differentiating neurons. Neuron *23*, 247–256.

Franco, S.J., Gil-Sanz, C., Martinez-Garay, I., Espinosa, A., Harkins-Perry, S.R., Ramos, C., and Müller, U. (2012). Fate-restricted neural progenitors in the mammalian cerebral cortex. Science *337*, 746–749.

Franco, S.J., Martinez-Garay, I., Gil-Sanz, C., Harkins-Perry, S.R., and Müller, U. (2011). Reelin regulates cadherin function via Dab1/Rap1 to control neuronal migration and lamination in the neocortex. Neuron *69*, 482–497.

Frankel, W.N., Taylor, L., Beyer, B., Tempel, B.L., and White, H.S. (2001). Electroconvulsive Thresholds of Inbred Mouse Strains. Genomics *74*, 306–312.

Freund, T.F. (2003). Interneuron Diversity series: Rhythm and mood in perisomatic inhibition. Trends Neurosci. *26*, 489–495.

Freund, T.F., and Buzsáki, G. (1996). Interneurons of the hippocampus. Hippocampus *6*, 347–470.

Friocourt, G., Chafey, P., Billuart, P., Koulakoff, A., Vinet, M.C., Schaar, B.T., McConnell, S.K., Francis, F., and Chelly, J. (2001). Doublecortin interacts with mu subunits of clathrin adaptor complexes in the developing nervous system. Mol. Cell. Neurosci. *18*, 307–319.

Friocourt, G., Koulakoff, A., Chafey, P., Boucher, D., Fauchereau, F., Chelly, J., and Francis, F. (2003). Doublecortin Functions at the Extremities of Growing Neuronal Processes. Cereb. Cortex *13*, 620–626.

Friocourt, G., Marcorelles, P., Saugier-Veber, P., Quille, M.-L., Marret, S., and Laquerrière, A. (2011). Role of cytoskeletal abnormalities in the neuropathology and pathophysiology of type I lissencephaly. Acta Neuropathol. *121*, 149–170.

Frotscher, M., Haas, C.A., and Förster, E. (2003). Reelin controls granule cell migration in the dentate gyrus by acting on the radial glial scaffold. Cereb. Cortex *13*, 634–640.

Frotscher, M., and Heimrich, B. (1993). Formation of layer-specific fiber projections to the hippocampus in vitro. Proc. Natl. Acad. Sci. U.S.A. *90*, 10400–10403.

Gal, J.S., Morozov, Y.M., Ayoub, A.E., Chatterjee, M., Rakic, P., and Haydar, T.F. (2006). Molecular and morphological heterogeneity of neural precursors in the mouse neocortical proliferative zones. J. Neurosci. *26*, 1045–1056.

Galimberti, I., Bednarek, E., Donato, F., and Caroni, P. (2010). EphA4 signaling in juveniles establishes topographic specificity of structural plasticity in the hippocampus. Neuron *65*, 627–642.

Garaschuk, O., Hanse, E., and Konnerth, A. (1998). Developmental profile and synaptic origin of early network oscillations in the CA1 region of rat neonatal hippocampus. J. Physiol. (Lond.) *507 (Pt 1)*, 219–236.

García-Moreno, F., Vasistha, N.A., Trevia, N., Bourne, J.A., and Molnár, Z. (2012). Compartmentalization of cerebral cortical germinal zones in a lissencephalic primate and gyrencephalic rodent. Cereb. Cortex *22*, 482–492.

Garver, T.D., Ren, Q., Tuvia, S., and Bennett, V. (1997). Tyrosine phosphorylation at a site highly conserved in the L1 family of cell adhesion molecules abolishes ankyrin binding and increases lateral mobility of neurofascin. J. Cell Biol. *137*, 703–714.

Gaspard, N., and Vanderhaeghen, P. (2011). Laminar fate specification in the cerebral cortex. F1000 Biol Rep *3*, 6.

Gdalyahu, A., Ghosh, I., Levy, T., Sapir, T., Sapoznik, S., Fishler, Y., Azoulai, D., and Reiner, O. (2004). DCX, a new mediator of the JNK pathway. EMBO J. *23*, 823–832.

Gelman, D.M., Martini, F.J., Nóbrega-Pereira, S., Pierani, A., Kessaris, N., and Marín, O. (2009). The Embryonic Preoptic Area Is a Novel Source of Cortical GABAergic Interneurons. J. Neurosci. *29*, 9380–9389.

Giagtzoglou, N., Ly, C.V., and Bellen, H.J. (2009). Cell adhesion, the backbone of the synapse: “vertebrate” and “invertebrate” perspectives. Cold Spring Harb Perspect Biol *1*, a003079.

Gilmore, E.C., Ohshima, T., Goffinet, A.M., Kulkarni, A.B., and Herrup, K. (1998). Cyclin-dependent kinase 5-deficient mice demonstrate novel developmental arrest in cerebral cortex. J. Neurosci. *18*, 6370–6377.

Gleeson, J.G., Allen, K.M., Fox, J.W., Lamperti, E.D., Berkovic, S., Scheffer, I., Cooper, E.C., Dobyns, W.B., Minnerath, S.R., Ross, M.E., et al. (1998). Doublecortin, a brain-specific gene mutated in human X-linked lissencephaly and double cortex syndrome, encodes a putative signaling protein. Cell *92*, 63–72.

Gleeson, J.G., Lin, P.T., Flanagan, L.A., and Walsh, C.A. (1999). Doublecortin is a microtubule-associated protein and is expressed widely by migrating neurons. Neuron *23*, 257–271.

Glezer, I., Simard, A.R., and Rivest, S. (2007). Neuroprotective role of the innate immune system by microglia. Neuroscience *147*, 867–883.

Glickfeld, L.L., Roberts, J.D., Somogyi, P., and Scanziani, M. (2009). Interneurons hyperpolarize pyramidal cells along their entire somatodendritic axis. Nat. Neurosci. *12*, 21–23.

Gonzales, R.B., DeLeon Galvan, C.J., Rangel, Y.M., and Claiborne, B.J. (2001). Distribution of thorny excrescences on CA3 pyramidal neurons in the rat hippocampus. J. Comp. Neurol. *430*, 357–368.

González-Billault, C., Del Río, J.A., Ureña, J.M., Jiménez-Mateos, E.M., Barallobre, M.J., Pascual, M., Pujadas, L., Simó, S., Torre, A.L., Gavin, R., et al. (2005). A role of MAP1B in Reelin-dependent neuronal migration. Cereb. Cortex *15*, 1134–1145.

Gopal, P.P., Simonet, J.C., Shapiro, W., and Golden, J.A. (2010). Leading process branch instability in Lis1+/- nonradially migrating interneurons. Cereb. Cortex *20*, 1497–1505.

Grigoriou, M., Tucker, A.S., Sharpe, P.T., and Pachnis, V. (1998). Expression and regulation of Lhx6 and Lhx7, a novel subfamily of LIM homeodomain encoding genes, suggests a role in mammalian head development. Development *125*, 2063–2074.

Griveau, A., Borello, U., Causeret, F., Tissir, F., Boggetto, N., Karaz, S., and Pierani, A. (2010). A novel role for Dbx1-derived Cajal-Retzius cells in early regionalization of the cerebral cortical neuroepithelium. PLoS Biol. *8*, e1000440.

van Groen, T., Miettinen, P., and Kadish, I. (2003). The entorhinal cortex of the mouse: organization of the projection to the hippocampal formation. Hippocampus *13*, 133–149.

Grove, E.A., and Tole, S. (1999). Patterning events and specification signals in the developing hippocampus. Cereb. Cortex *9*, 551–561.

Grove, E.A., Tole, S., Limon, J., Yip, L., and Ragsdale, C.W. (1998). The hem of the embryonic cerebral cortex is defined by the expression of multiple Wnt genes and is compromised in Gli3-deficient mice. Development *125*, 2315–2325.

Guerrini, R. (11). Epilepsy in children. The Lancet *367*, 499–524.

Guerrini, R., and Parrini, E. (2010). Neuronal migration disorders. Neurobiol. Dis. *38*, 154–166.

Gulyás, A.I., and Freund, T.F. (1996). Pyramidal cell dendrites are the primary targets of calbindin D28k-immunoreactive interneurons in the hippocampus. Hippocampus *6*, 525–534.

Gupta, A., Tsai, L.-H., and Wynshaw-Boris, A. (2002). LIFE IS A JOURNEY: A GENETIC LOOK AT NEOCORTICAL DEVELOPMENT. Nature Reviews Genetics *3*, 342–355.

Guzik, B.W., and Goldstein, L.S. (2004). Microtubule-dependent transport in neurons: steps towards an understanding of regulation, function and dysfunction. Current Opinion in Cell Biology *16*, 443–450.

Hack, I., Hellwig, S., Junghans, D., Brunne, B., Bock, H.H., Zhao, S., and Frotscher, M. (2007). Divergent roles of ApoER2 and Vldlr in the migration of cortical neurons. Development *134*, 3883–3891.

Hanashima, C., Li, S.C., Shen, L., Lai, E., and Fishell, G. (2004). Foxg1 suppresses early cortical cell fate. Science *303*, 56–59.

Hand, R., Bortone, D., Mattar, P., Nguyen, L., Heng, J.I.-T., Guerrier, S., Boutt, E., Peters, E., Barnes, A.P., Parras, C., et al. (2005). Phosphorylation of Neurogenin2 specifies the migration properties and the dendritic morphology of pyramidal neurons in the neocortex. Neuron *48*, 45–62.

Hansen, D.V., Lui, J.H., Parker, P.R.L., and Kriegstein, A.R. (2010). Neurogenic radial glia in the outer subventricular zone of human neocortex. Nature *464*, 554–561.

Hatten, M.E. (1999). Central Nervous System Neuronal Migration. Annual Review of Neuroscience *22*, 511–539.

Haubensak, W., Attardo, A., Denk, W., and Huttner, W.B. (2004). Neurons arise in the basal neuroepithelium of the early mammalian telencephalon: A major site of neurogenesis. PNAS *101*, 3196–3201.

Häussler, U., Bielefeld, L., Froriep, U.P., Wolfart, J., and Haas, C.A. (2012). Septotemporal position in the hippocampal formation determines epileptic and neurogenic activity in temporal lobe epilepsy. Cereb. Cortex *22*, 26–36.

Haverfield, E.V., Whited, A.J., Petras, K.S., Dobyns, W.B., and Das, S. (2009). Intragenic deletions and duplications of the LIS1 and DCX genes: a major disease-causing mechanism in lissencephaly and subcortical band heterotopia. European Journal of Human Genetics *17*, 911–918.

He, S., Ma, J., Liu, N., and Yu, X. (2010). Early enriched environment promotes neonatal GABAergic neurotransmission and accelerates synapse maturation. J. Neurosci. *30*, 7910–7916.

He, X., Treacy, M.N., Simmons, D.M., Ingraham, H.A., Swanson, L.W., and Rosenfeld, M.G. (1989). Expression of a large family of POU-domain regulatory genes in mammalian brain development. Nature *340*, 35–41.

Heng, J.I.-T., Nguyen, L., Castro, D.S., Zimmer, C., Wildner, H., Armant, O., Skowronska-Krawczyk, D., Bedogni, F., Matter, J.-M., Hevner, R., et al. (2008a). Neurogenin 2 controls cortical neuron migration through regulation of Rnd2. Nature *455*, 114–118.

Heng, J.I.-T., Nguyen, L., Castro, D.S., Zimmer, C., Wildner, H., Armant, O., Skowronska-Krawczyk, D., Bedogni, F., Matter, J.-M., Hevner, R., et al. (2008b). Neurogenin 2 controls cortical neuron migration through regulation of Rnd2. Nature *455*, 114–118.

Henley, J.R., Huang, K., Wang, D., and Poo, M. (2004). Calcium mediates bidirectional growth cone turning induced by myelin-associated glycoprotein. Neuron *44*, 909–916.

Hennou, S., Khalilov, I., Diabira, D., Ben-Ari, Y., and Gozlan, H. (2002). Early sequential formation of functional GABA(A) and glutamatergic synapses on CA1 interneurons of the rat foetal hippocampus. Eur. J. Neurosci. *16*, 197–208.

Henrique, D., Hirsinger, E., Adam, J., Le Roux, I., Pourquié, O., Ish-Horowicz, D., and Lewis, J. (1997). Maintenance of neuroepithelial progenitor cells by Delta-Notch signalling in the embryonic chick retina. Curr. Biol. *7*, 661–670.

Henze, D.A., McMahon, D.B.T., Harris, K.M., and Barrionuevo, G. (2002). Giant miniature EPSCs at the hippocampal mossy fiber to CA3 pyramidal cell synapse are monoquantal. J. Neurophysiol. *87*, 15–29.

Herbomel, P., Thisse, B., and Thisse, C. (2001). Zebrafish early macrophages colonize cephalic mesenchyme and developing brain, retina, and epidermis through a M-CSF receptor-dependent invasive process. Dev. Biol. *238*, 274–288.

Hernández-Miranda, L.R., Parnavelas, J.G., and Chiara, F. (2010). Molecules and mechanisms involved in the generation and migration of cortical interneurons. ASN Neuro *2*, e00031.

Herron, L.R., Hill, M., Davey, F., and Gunn-Moore, F.J. (2009). The intracellular interactions of the L1 family of cell adhesion molecules. Biochem. J. *419*, 519–531.

Hertz, L., Dringen, R., Schousboe, A., and Robinson, S.R. (1999). Astrocytes: glutamate producers for neurons. J. Neurosci. Res. *57*, 417–428.

Hevner, R.F., Shi, L., Justice, N., Hsueh, Y., Sheng, M., Smiga, S., Bulfone, A., Goffinet, A.M., Campagnoni, A.T., and Rubenstein, J.L. (2001). Tbr1 regulates differentiation of the preplate and layer 6. Neuron *29*, 353–366.

Hiesberger, T., Trommsdorff, M., Howell, B.W., Goffinet, A., Mumby, M.C., Cooper, J.A., and Herz, J. (1999). Direct binding of Reelin to VLDL receptor and ApoE receptor 2 induces tyrosine phosphorylation of disabled-1 and modulates tau phosphorylation. Neuron *24*, 481–489.

Hines, J.H., Abu-Rub, M., and Henley, J.R. (2010). Asymmetric endocytosis and remodeling of beta1-integrin adhesions during growth cone chemorepulsion by MAG. Nat. Neurosci. *13*, 829–837.

Horesh, D., Sapir, T., Francis, F., Wolf, S.G., Caspi, M., Elbaum, M., Chelly, J., and Reiner, O. (1999). Doublecortin, a Stabilizer of Microtubules. Hum. Mol. Genet. *8*, 1599–1610.

Hortsch, M. (1996). The L1 family of neural cell adhesion molecules: old proteins performing new tricks. Neuron *17*, 587–593.

Howell, B.W., Gertler, F.B., and Cooper, J.A. (1997). Mouse disabled (mDab1): a Src binding protein implicated in neuronal development. EMBO J. *16*, 121–132.

Hu, H., Marton, T.F., and Goodman, C.S. (2001). Plexin B mediates axon guidance in Drosophila by simultaneously inhibiting active Rac and enhancing RhoA signaling. Neuron *32*, 39–51.

Hudmon, A., and Schulman, H. (2002). Neuronal CA2+/calmodulin-dependent protein kinase II: the role of structure and autoregulation in cellular function. Annu. Rev. Biochem. *71*, 473–510.

Hui, C.C., and Joyner, A.L. (1993). A mouse model of greig cephalopolysyndactyly syndrome: the extra-toesJ mutation contains an intragenic deletion of the Gli3 gene. Nat. Genet. *3*, 241–246.

Hunter, K.E., and Hatten, M.E. (1995). Radial glial cell transformation to astrocytes is bidirectional: regulation by a diffusible factor in embryonic forebrain. Proc. Natl. Acad. Sci. U.S.A. *92*, 2061–2065.

Huttner, W.B., and Brand, M. (1997). Asymmetric division and polarity of neuroepithelial cells. Curr. Opin. Neurobiol. *7*, 29–39.

Iannetti, P., Spalice, A., Atzei, G., Boemi, S., and Trasimeni, G. (1996). Neuronal migrational disorders in children with epilepsy: MRI, interictal SPECT and EEG comparisons. Brain Dev. *18*, 269–279.

Imayoshi, I., Shimogori, T., Ohtsuka, T., and Kageyama, R. (2008). Hes genes and neurogenin regulate non-neural versus neural fate specification in the dorsal telencephalic midline. Development *135*, 2531–2541.

Iwabuchi, M., Maekawa, F., Tanaka, K., and Ohki-Hamazaki, H. (2006). Overexpression of gastrin-releasing peptide receptor induced layer disorganization in brain. Neuroscience *138*, 109–122.

Jacobsen, C.T., and Miller, R.H. (2003). Control of astrocyte migration in the developing cerebral cortex. Dev. Neurosci. *25*, 207–216.

Jaglin, X.H., Hjerling-Leffler, J., Fishell, G., and Batista-Brito, R. (2012). The origin of neocortical nitric oxide synthase-expressing inhibitory neurons. Front Neural Circuits *6*, 44.

Janssen, A., Gressens, P., Grabenbauer, M., Baumgart, E., Schad, A., Vanhorebeek, I., Brouwers, A., Declercq, P.E., Fahimi, D., Evrard, P., et al. (2003). Neuronal migration depends on intact peroxisomal function in brain and in extraneuronal tissues. J. Neurosci. *23*, 9732–9741.

Jenkins, S.M., Kizhatil, K., Kramarcy, N.R., Sen, A., Sealock, R., and Bennett, V. (2001). FIGQY phosphorylation defines discrete populations of L1 cell adhesion molecules at sites of cell-cell contact and in migrating neurons. J. Cell. Sci. *114*, 3823–3835.

Jin, J., Suzuki, H., Hirai, S.-I., Mikoshiba, K., and Ohshima, T. (2010). JNK phosphorylates Ser332 of doublecortin and regulates its function in neurite extension and neuronal migration. Dev Neurobiol *70*, 929–942.

Johansen, M.L., Bak, L.K., Schousboe, A., Iversen, P., Sørensen, M., Keiding, S., Vilstrup, H., Gjedde, A., Ott, P., and Waagepetersen, H.S. (2007). The metabolic role of isoleucine in detoxification of ammonia in cultured mouse neurons and astrocytes. Neurochem. Int. *50*, 1042–1051.

Jonas, P., Bischofberger, J., Fricker, D., and Miles, R. (2004). Interneuron Diversity series: Fast in, fast out--temporal and spatial signal processing in hippocampal interneurons. Trends Neurosci. *27*, 30–40.

Jones, E.G., and Rakic, P. (2010). Radial columns in cortical architecture: it is the composition that counts. Cereb. Cortex *20*, 2261–2264.

Jossin, Y., and Cooper, J.A. (2011). Reelin, Rap1 and N-cadherin orient the migration of multipolar neurons in the developing neocortex. Nat. Neurosci. *14*, 697–703.

Jovanovic, J.N., and Thomson, A.M. (2011). Development of cortical GABAergic innervation. Front Cell Neurosci *5*, 14.

Kamakura, S., Oishi, K., Yoshimatsu, T., Nakafuku, M., Masuyama, N., and Gotoh, Y. (2004). Hes binding to STAT3 mediates crosstalk between Notch and JAK-STAT signalling. Nat. Cell Biol. *6*, 547–554.

Kamichi, S., Wada, E., Aoki, S., Sekiguchi, M., Kimura, I., and Wada, K. (2005). Immunohistochemical localization of gastrin-releasing peptide receptor in the mouse brain. Brain Res. *1032*, 162–170.

Kappeler, C., Dhenain, M., Phan Dinh Tuy, F., Saillour, Y., Marty, S., Fallet-Bianco, C., Souville, I., Souil, E., Pinard, J.-M., Meyer, G., et al. (2007). Magnetic resonance imaging and histological studies of corpus callosal and hippocampal abnormalities linked to doublecortin deficiency. J. Comp. Neurol. *500*, 239–254.

Kappeler, C., Saillour, Y., Baudoin, J.-P., Tuy, F.P.D., Alvarez, C., Houbron, C., Gaspar, P., Hamard, G., Chelly, J., Métin, C., et al. (2006). Branching and nucleokinesis defects in migrating interneurons derived from doublecortin knockout mice. Hum. Mol. Genet. *15*, 1387–1400.

Karle, K.N., Möckel, D., Reid, E., and Schöls, L. (2012). Axonal transport deficit in a KIF5A(-/-) mouse model. Neurogenetics *13*, 169–179.

Kato, M., and Dobyns, W.B. (2003). Lissencephaly and the molecular basis of neuronal migration. Hum. Mol. Genet. *12 Spec No 1*, R89–96.

Kawaguchi, Y., Katsumaru, H., Kosaka, T., Heizmann, C.W., and Hama, K. (1987). Fast spiking cells in rat hippocampus (CA1 region) contain the calcium-binding protein parvalbumin. Brain Res. *416*, 369–374.

Kawaguchi, Y., and Kubota, Y. (1997). GABAergic cell subtypes and their synaptic connections in rat frontal cortex. Cereb. Cortex *7*, 476–486.

Kawauchi, T., Chihama, K., Nabeshima, Y., and Hoshino, M. (2003). The in vivo roles of STEF/Tiam1, Rac1 and JNK in cortical neuronal migration. The EMBO Journal *22*, 4190–4201.

Kawauchi, T., Chihama, K., Nabeshima, Y., and Hoshino, M. (2006). Cdk5 phosphorylates and stabilizes p27kip1 contributing to actin organization and cortical neuronal migration. Nat. Cell Biol. *8*, 17–26.

Kawauchi, T., Chihama, K., Nishimura, Y.V., Nabeshima, Y., and Hoshino, M. (2005). MAP1B phosphorylation is differentially regulated by Cdk5/p35, Cdk5/p25, and JNK. Biochem. Biophys. Res. Commun. *331*, 50–55.

Kawauchi, T., Sekine, K., Shikanai, M., Chihama, K., Tomita, K., Kubo, K., Nakajima, K., Nabeshima, Y.-I., and Hoshino, M. (2010). Rab GTPases-dependent endocytic pathways regulate neuronal migration and maturation through N-cadherin trafficking. Neuron *67*, 588–602.

Keays, D.A., Tian, G., Poirier, K., Huang, G.-J., Siebold, C., Cleak, J., Oliver, P.L., Fray, M., Harvey, R.J., Molnár, Z., et al. (2007). Mutations in alpha-tubulin cause abnormal neuronal migration in mice and lissencephaly in humans. Cell *128*, 45–57.

Kelava, I., Reillo, I., Murayama, A.Y., Kalinka, A.T., Stenzel, D., Tomancak, P., Matsuzaki, F., Lebrand, C., Sasaki, E., Schwamborn, J.C., et al. (2012). Abundant occurrence of basal radial glia in the subventricular zone of embryonic neocortex of a lissencephalic primate, the common marmoset Callithrix jacchus. Cereb. Cortex *22*, 469–481.

Keng, W.T., Pilz, D.T., Minns, B., and FitzPatrick, D.R. (2003). A3243G mitochondrial mutation associated with polymicrogyria. Dev Med Child Neurol *45*, 704–708.

Kerjan, G., and Gleeson, J.G. (2007). A missed exit: Reelin sets in motion Dab1 polyubiquitination to put the break on neuronal migration. Genes Dev. *21*, 2850–2854.

Kessaris, N., Fogarty, M., Iannarelli, P., Grist, M., Wegner, M., and Richardson, W.D. (2005). Competing waves of oligodendrocytes in the forebrain and postnatal elimination of an embryonic lineage. Nature Neuroscience *9*, 173–179.

Khalilov, I., Chazal, G., Chudotvorova, I., Pellegrino, C., Corby, S., Ferrand, N., Gubkina, O., Nardou, R., Tyzio, R., Yamamoto, S., et al. (2011). Enhanced Synaptic

Activity and Epileptiform Events in the Embryonic KCC2 Deficient Hippocampus. Front Cell Neurosci *5*,.

Khazipov, R., Esclapez, M., Caillard, O., Bernard, C., Khalilov, I., Tyzio, R., Hirsch, J., Dzhala, V., Berger, B., and Ben-Ari, Y. (2001). Early development of neuronal activity in the primate hippocampus in utero. J. Neurosci. *21*, 9770–9781.

Khazipov, R., Khalilov, I., Tyzio, R., Morozova, E., Ben-Ari, Y., and Holmes, G.L. (2004). Developmental changes in GABAergic actions and seizure susceptibility in the rat hippocampus. Eur. J. Neurosci. *19*, 590–600.

Khazipov, R., Leinekugel, X., Khalilov, I., Gaiarsa, J.L., and Ben-Ari, Y. (1997). Synchronization of GABAergic interneuronal network in CA3 subfield of neonatal rat hippocampal slices. J. Physiol. (Lond.) *498 (Pt 3)*, 763–772.

Kiernan, B.W., Götz, B., Faissner, A., and ffrench-Constant, C. (1996). Tenascin-C inhibits oligodendrocyte precursor cell migration by both adhesion-dependent and adhesion-independent mechanisms. Mol. Cell. Neurosci. *7*, 322–335.

Kim, E., and Sheng, M. (2004). PDZ domain proteins of synapses. Nat. Rev. Neurosci. *5*, 771–781.

Kim, M.H., Cierpicki, T., Derewenda, U., Krowarsch, D., Feng, Y., Devedjiev, Y., Dauter, Z., Walsh, C.A., Otlewski, J., Bushweller, J.H., et al. (2003). The DCX-domain tandems of doublecortin and doublecortin-like kinase. Nat. Struct. Biol. *10*, 324–333.

Kizhatil, K., Wu, Y.-X., Sen, A., and Bennett, V. (2002). A new activity of doublecortin in recognition of the phospho-FIGQY tyrosine in the cytoplasmic domain of neurofascin. J. Neurosci. *22*, 7948–7958.

Kjonigsen, L.J., Leergaard, T.B., Witter, M.P., and Bjaalie, J.G. (2011). Digital atlas of anatomical subdivisions and boundaries of the rat hippocampal region. Front Neuroinform *5*, 2.

Ko, J., Humbert, S., Bronson, R.T., Takahashi, S., Kulkarni, A.B., Li, E., and Tsai, L.H. (2001). p35 and p39 are essential for cyclin-dependent kinase 5 function during neurodevelopment. J. Neurosci. *21*, 6758–6771.

Köhler, C. (1986). Intrinsic connections of the retrohippocampal region in the rat brain. II. The medial entorhinal area. J. Comp. Neurol. *246*, 149–169.

Koizumi, H., Higginbotham, H., Poon, T., Tanaka, T., Brinkman, B.C., and Gleeson, J.G. (2006). Doublecortin maintains bipolar shape and nuclear translocation during migration in the adult forebrain. Nat. Neurosci. *9*, 779–786.

Komuro, H., and Rakic, P. (1992). Selective role of N-type calcium channels in neuronal migration. Science *257*, 806–809.

Komuro, H., and Rakic, P. (1996). Intracellular Ca2+ Fluctuations Modulate the Rate of Neuronal Migration. Neuron *17*, 275–285.

Kosaka, T., Katsumaru, H., Hama, K., Wu, J.Y., and Heizmann, C.W. (1987). GABAergic neurons containing the Ca2+-binding protein parvalbumin in the rat hippocampus and dentate gyrus. Brain Res. *419*, 119–130.

Kozorovitskiy, Y., Saunders, A., Johnson, C.A., Lowell, B.B., and Sabatini, B.L. (2012). Recurrent network activity drives striatal synaptogenesis. Nature *485*, 646–650.

Kriebel, M., Metzger, J., Trinks, S., Chugh, D., Harvey, R.J., Harvey, K., and Volkmer, H. (2011). The cell adhesion molecule neurofascin stabilizes axo-axonic GABAergic terminals at the axon initial segment. J. Biol. Chem. *286*, 24385–24393.

Kriegstein, A., Noctor, S., and Martínez-Cerdeño, V. (2006). Patterns of neural stem and progenitor cell division may underlie evolutionary cortical expansion. Nature Reviews Neuroscience *7*, 883–890.

Kriegstein, A.R., and Götz, M. (2003). Radial glia diversity: a matter of cell fate. Glia *43*, 37–43.

Kriegstein, A.R., and Noctor, S.C. (2004). Patterns of neuronal migration in the embryonic cortex. Trends Neurosci. *27*, 392–399.

Krysko, O., Hulshagen, L., Janssen, A., Schütz, G., Klein, R., De Bruycker, M., Espeel, M., Gressens, P., and Baes, M. (2007). Neocortical and cerebellar developmental abnormalities in conditions of selective elimination of peroxisomes from brain or from liver. J. Neurosci. Res. *85*, 58–72.

Kuiper, J.W.P., Oerlemans, F.T.J.J., Fransen, J.A.M., and Wieringa, B. (2008). Creatine kinase B deficient neurons exhibit an increased fraction of motile mitochondria. BMC Neurosci *9*, 73.

Kumar, R.A., Pilz, D.T., Babatz, T.D., Cushion, T.D., Harvey, K., Topf, M., Yates, L., Robb, S., Uyanik, G., Mancini, G.M.S., et al. (2010). TUBA1A mutations cause wide spectrum lissencephaly (smooth brain) and suggest that multiple neuronal migration pathways converge on alpha tubulins. Hum. Mol. Genet. *19*, 2817–2827.

Kwan, K.Y., Lam, M.M.S., Krsnik, Z., Kawasawa, Y.I., Lefebvre, V., and Sestan, N. (2008). SOX5 postmitotically regulates migration, postmigratory differentiation, and projections of subplate and deep-layer neocortical neurons. Proc. Natl. Acad. Sci. U.S.A. *105*, 16021–16026.

Lai, T., Jabaudon, D., Molyneaux, B.J., Azim, E., Arlotta, P., Menezes, J.R.L., and Macklis, J.D. (2008). SOX5 controls the sequential generation of distinct corticofugal neuron subtypes. Neuron *57*, 232–247.

Lalancette-Hébert, M., Gowing, G., Simard, A., Weng, Y.C., and Kriz, J. (2007). Selective ablation of proliferating microglial cells exacerbates ischemic injury in the brain. J. Neurosci. *27*, 2596–2605.

Lamonica, B.E., Lui, J.H., Wang, X., and Kriegstein, A.R. (2012). OSVZ progenitors in the human cortex: an updated perspective on neurodevelopmental disease. Current Opinion in Neurobiology.

van Landeghem, F.K.H., Weiss, T., and von Deimling, A. (2007). Expression of PACAP and glutamate transporter proteins in satellite oligodendrocytes of the human CNS. Regulatory Peptides *142*, 52–59.

Lapray, D., Popova, I.Y., Kindler, J., Jorquera, I., Becq, H., Manent, J.-B., Luhmann, H.J., and Represa, A. (2010). Spontaneous epileptic manifestations in a DCX knockdown model of human double cortex. Cereb. Cortex *20*, 2694–2701.

Lee, S., Hjerling-Leffler, J., Zagha, E., Fishell, G., and Rudy, B. (2010). The largest group of superficial neocortical GABAergic interneurons expresses ionotropic serotonin receptors. J. Neurosci. *30*, 16796–16808.

Lee, S.M., Tole, S., Grove, E., and McMahon, A.P. (2000). A local Wnt-3a signal is required for development of the mammalian hippocampus. Development *127*, 457–467.

Leger, P.-L., Souville, I., Boddaert, N., Elie, C., Pinard, J.M., Plouin, P., Moutard, M.L., des Portes, V., Van Esch, H., Joriot, S., et al. (2008). The location of DCX mutations predicts malformation severity in X-linked lissencephaly. Neurogenetics *9*, 277–285.

Lein, E.S., Hawrylycz, M.J., Ao, N., Ayres, M., Bensinger, A., Bernard, A., Boe, A.F., Boguski, M.S., Brockway, K.S., Byrnes, E.J., et al. (2007). Genome-wide atlas of gene expression in the adult mouse brain. Nature *445*, 168–176.

Lein, E.S., Zhao, X., and Gage, F.H. (2004). Defining a molecular atlas of the hippocampus using DNA microarrays and high-throughput in situ hybridization. J. Neurosci. *24*, 3879–3889.

Letinic, K., Zoncu, R., and Rakic, P. (2002). Origin of GABAergic neurons in the human neocortex. Nature *417*, 645–649.

Leventer, R.J., Cardoso, C., Ledbetter, D.H., and Dobyns, W.B. (2001). LIS1 missense mutations cause milder lissencephaly phenotypes including a child with normal IQ. Neurology *57*, 416–422.

Li, J., Lee, W.-L., and Cooper, J.A. (2005a). NudEL targets dynein to microtubule ends through LIS1. Nat. Cell Biol. *7*, 686–690.

Li, W., Lee, J., Vikis, H.G., Lee, S.-H., Liu, G., Aurandt, J., Shen, T.-L., Fearon, E.R., Guan, J.-L., Han, M., et al. (2004). Activation of FAK and Src are receptor-proximal events required for netrin signaling. Nat. Neurosci. *7*, 1213–1221.

Li, X., Gao, X., Liu, G., Xiong, W., Wu, J., and Rao, Y. (2008). Netrin signal transduction and the guanine nucleotide exchange factor DOCK180 in attractive signaling. Nat. Neurosci. *11*, 28–35.

Li, Y., Jia, Y.-C., Cui, K., Li, N., Zheng, Z.-Y., Wang, Y.-Z., and Yuan, X.-B. (2005b). Essential role of TRPC channels in the guidance of nerve growth cones by brain-derived neurotrophic factor. Nature *434*, 894–898.

Liesi, P., and Wright, J.M. (1996). Weaver granule neurons are rescued by calcium channel antagonists and antibodies against a neurite outgrowth domain of the B2 chain of laminin. J. Cell Biol. *134*, 477–486.

Lin, X., Parisiadou, L., Gu, X.-L., Wang, L., Shim, H., Sun, L., Xie, C., Long, C.-X., Yang, W.-J., Ding, J., et al. (2009). Leucine-rich repeat kinase 2 regulates the progression of neuropathology induced by Parkinson's-disease-related mutant alpha-synuclein. Neuron *64*, 807–827.

Liu, J.S., Schubert, C.R., Fu, X., Fourniol, F.J., Jaiswal, J.K., Houdusse, A., Stultz, C.M., Moores, C.A., and Walsh, C.A. (2012). Molecular Basis for Specific Regulation of Neuronal Kinesin-3 Motors by Doublecortin Family Proteins. Mol. Cell.

Lodato, S., Rouaux, C., Quast, K.B., Jantrachotechatchawan, C., Studer, M., Hensch, T.K., and Arlotta, P. (2011). Excitatory Projection Neuron Subtypes Control the Distribution of Local Inhibitory Interneurons in the Cerebral Cortex. Neuron *69*, 763–779.

Lois, C., García-Verdugo, J.M., and Alvarez-Buylla, A. (1996). Chain migration of neuronal precursors. Science *271*, 978–981.

Long, J.E., Cobos, I., Potter, G.B., and Rubenstein, J.L.R. (2009). Dlx1&2 and Mash1 transcription factors control MGE and CGE patterning and differentiation through parallel and overlapping pathways. Cereb. Cortex *19 Suppl 1*, i96–106.

López-Bendito, G., Sánchez-Alcañiz, J.A., Pla, R., Borrell, V., Picó, E., Valdeolmillos, M., and Marín, O. (2008). Chemokine signaling controls intracortical migration and final distribution of GABAergic interneurons. J. Neurosci. *28*, 1613–1624.

López-Bendito, G., Shigemoto, R., Fairén, A., and Luján, R. (2002). Differential distribution of group I metabotropic glutamate receptors during rat cortical development. Cereb. Cortex *12*, 625–638.

Lu, Q.R., Yuk, D., Alberta, J.A., Zhu, Z., Pawlitzky, I., Chan, J., McMahon, A.P., Stiles, C.D., and Rowitch, D.H. (2000). Sonic hedgehog--regulated oligodendrocyte lineage genes encoding bHLH proteins in the mammalian central nervous system. Neuron *25*, 317–329.

Lui, J.H., Hansen, D.V., and Kriegstein, A.R. (2011). Development and Evolution of the Human Neocortex. Cell *146*, 18–36.

Maduzia, L.L., and Padgett, R.W. (1997). Drosophila MAD, a member of the Smad family, translocates to the nucleus upon stimulation of the dpp pathway. Biochem. Biophys. Res. Commun. *238*, 595–598.

Malone, C.J., Misner, L., Le Bot, N., Tsai, M.-C., Campbell, J.M., Ahringer, J., and White, J.G. (2003). The C. elegans hook protein, ZYG-12, mediates the essential attachment between the centrosome and nucleus. Cell *115*, 825–836.

Manent, J.-B., Demarque, M., Jorquera, I., Pellegrino, C., Ben-Ari, Y., Aniksztejn, L., and Represa, A. (2005). A noncanonical release of GABA and glutamate modulates neuronal migration. J. Neurosci. *25*, 4755–4765.

Manent, J.-B., Jorquera, I., Ben-Ari, Y., Aniksztejn, L., and Represa, A. (2006). Glutamate acting on AMPA but not NMDA receptors modulates the migration of hippocampal interneurons. J. Neurosci. *26*, 5901–5909.

Manent, J.-B., Wang, Y., Chang, Y., Paramasivam, M., and LoTurco, J.J. (2009). Dcx reexpression reduces subcortical band heterotopia and seizure threshold in an animal model of neuronal migration disorder. Nature Medicine *15*, 84–90.

Maness, P.F., and Schachner, M. (2007). Neural recognition molecules of the immunoglobulin superfamily: signaling transducers of axon guidance and neuronal migration. Nat. Neurosci. *10*, 19–26.

Mann, F., Miranda, E., Weinl, C., Harmer, E., and Holt, C.E. (2003). B-type Eph receptors and ephrins induce growth cone collapse through distinct intracellular pathways. J. Neurobiol. *57*, 323–336.

Manna, T., Grenningloh, G., Miller, H.P., and Wilson, L. (2007). Stathmin family protein SCG10 differentially regulates the plus and minus end dynamics of microtubules at steady state in vitro: implications for its role in neurite outgrowth. Biochemistry *46*, 3543–3552.

Marin, O., Anderson, S.A., and Rubenstein, J.L. (2000). Origin and molecular specification of striatal interneurons. J. Neurosci. *20*, 6063–6076.

Marín, O., and Rubenstein, J.L.R. (2003). Cell migration in the forebrain. Annu. Rev. Neurosci. *26*, 441–483.

Marín, O., Valdeolmillos, M., and Moya, F. (2006). Neurons in motion: same principles for different shapes? Trends Neurosci. *29*, 655–661.

Marín, O., Yaron, A., Bagri, A., Tessier-Lavigne, M., and Rubenstein, J.L. (2001). Sorting of striatal and cortical interneurons regulated by semaphorin-neuropilin interactions. Science *293*, 872–875.

Marks, B., and McMahon, H.T. (1998). Calcium triggers calcineurin-dependent synaptic vesicle recycling in mammalian nerve terminals. Curr. Biol. *8*, 740–749.

Martínez, A., Lübke, J., Del Río, J.A., Soriano, E., and Frotscher, M. (1996). Regional variability and postsynaptic targets of chandelier cells in the hippocampal formation of the rat. J. Comp. Neurol. *376*, 28–44.

Martínez-Cerdeño, V., Cunningham, C.L., Camacho, J., Antczak, J.L., Prakash, A.N., Cziep, M.E., Walker, A.I., and Noctor, S.C. (2012). Comparative Analysis of the Subventricular Zone in Rat, Ferret and Macaque: Evidence for an Outer Subventricular Zone in Rodents. PLoS ONE *7*, e30178.

Martini, F.J., Valiente, M., López Bendito, G., Szabó, G., Moya, F., Valdeolmillos, M., and Marín, O. (2009). Biased selection of leading process branches mediates chemotaxis during tangential neuronal migration. Development *136*, 41–50.

Matsumoto, N., Leventer, R.J., Kuc, J.A., Mewborn, S.K., Dudlicek, L.L., Ramocki, M.B., Pilz, D.T., Mills, P.L., Das, S., Ross, M.E., et al. (2001). Mutation analysis of the DCX gene and genotype/phenotype correlation in subcortical band heterotopia. Eur. J. Hum. Genet. *9*, 5–12.

Matter, K., Bucher, K., and Hauri, H.P. (1990). Microtubule perturbation retards both the direct and the indirect apical pathway but does not affect sorting of plasma membrane proteins in intestinal epithelial cells (Caco-2). EMBO J. *9*, 3163–3170.

McBain, C.J., and Fisahn, A. (2001). Interneurons unbound. Nature Reviews Neuroscience *2*, 11–23.

McConnell, S.K. (1995). Constructing the cerebral cortex: neurogenesis and fate determination. Neuron *15*, 761–768.

McConnell, S.K., and Kaznowski, C.E. (1991). Cell cycle dependence of laminar determination in developing neocortex. Science *254*, 282–285.

McKenney, R.J., Vershinin, M., Kunwar, A., Vallee, R.B., and Gross, S.P. (2010). LIS1 and NudE induce a persistent dynein force-producing state. Cell *141*, 304–314.

McKhann II, G.., Wenzel, H.., Robbins, C.., Sosunov, A.., and Schwartzkroin, P.. (2003). Mouse strain differences in kainic acid sensitivity, seizure behavior, mortality, and hippocampal pathology. Neuroscience *122*, 551–561.

Mei, D., Parrini, E., Pasqualetti, M., Tortorella, G., Franzoni, E., Giussani, U., Marini, C., Migliarini, S., and Guerrini, R. (2007). Multiplex ligation-dependent probe amplification detects DCX gene deletions in band heterotopia. Neurology *68*, 446–450.

Menendez de la Prida, L., Bolea, S., and Sanchez-Andres, J.V. (1996). Analytical characterization of spontaneous activity evolution during hippocampal development in the rabbit. Neurosci. Lett. *218*, 185–187.

Meyer, G., Soria, J.M., Martínez-Galán, J.R., Martín-Clemente, B., and Fairén, A. (1998). Different origins and developmental histories of transient neurons in the marginal zone of the fetal and neonatal rat cortex. J. Comp. Neurol. *397*, 493–518.

Meyer, H.S., Wimmer, V.C., Hemberger, M., Bruno, R.M., de Kock, C.P.J., Frick, A., Sakmann, B., and Helmstaedter, M. (2010a). Cell type-specific thalamic innervation in a column of rat vibrissal cortex. Cereb. Cortex *20*, 2287–2303.

Meyer, H.S., Wimmer, V.C., Oberlaender, M., de Kock, C.P.J., Sakmann, B., and Helmstaedter, M. (2010b). Number and laminar distribution of neurons in a thalamocortical projection column of rat vibrissal cortex. Cereb. Cortex *20*, 2277–2286.

Michaelson, M.D., Bieri, P.L., Mehler, M.F., Xu, H., Arezzo, J.C., Pollard, J.W., and Kessler, J.A. (1996). CSF-1 deficiency in mice results in abnormal brain development. Development *122*, 2661–2672.

Miles, R., Tóth, K., Gulyás, A.I., Hájos, N., and Freund, T.F. (1996). Differences between somatic and dendritic inhibition in the hippocampus. Neuron *16*, 815–823.

Miller, R.H., and Szigeti, V. (1991). Clonal analysis of astrocyte diversity in neonatal rat spinal cord cultures. Development *113*, 353–362.

Milligan, C.E., Levitt, P., and Cunningham, T.J. (1991). Brain macrophages and microglia respond differently to lesions of the developing and adult visual system. J. Comp. Neurol. *314*, 136–146.

Miyata, T., Kawaguchi, A., Okano, H., and Ogawa, M. (2001). Asymmetric inheritance of radial glial fibers by cortical neurons. Neuron *31*, 727–741.

Miyata, T., Kawaguchi, A., Saito, K., Kawano, M., Muto, T., and Ogawa, M. (2004). Asymmetric production of surface-dividing and non-surface-dividing cortical progenitor cells. Development *131*, 3133–3145.

Miyoshi, G., Butt, S.J.B., Takebayashi, H., and Fishell, G. (2007). Physiologically distinct temporal cohorts of cortical interneurons arise from telencephalic Olig2-expressing precursors. J. Neurosci. *27*, 7786–7798.

Miyoshi, G., and Fishell, G. (2011). GABAergic interneuron lineages selectively sort into specific cortical layers during early postnatal development. Cereb. Cortex *21*, 845–852.

Miyoshi, G., and Fishell, G. (2012). Dynamic FoxG1 Expression Coordinates the Integration of Multipolar Pyramidal Neuron Precursors into the Cortical Plate. Neuron *74*, 1045–1058.

Mizuguchi, R., Sugimori, M., Takebayashi, H., Kosako, H., Nagao, M., Yoshida, S., Nabeshima, Y., Shimamura, K., and Nakafuku, M. (2001). Combinatorial roles of olig2 and neurogenin2 in the coordinated induction of pan-neuronal and subtype-specific properties of motoneurons. Neuron *31*, 757–771.

Mizuno, M., and Singer, S.J. (1994). A possible role for stable microtubules in intracellular transport from the endoplasmic reticulum to the Golgi apparatus. J. Cell. Sci. *107 (Pt 5)*, 1321–1331.

Mohrmann, R., Lessmann, V., and Gottmann, K. (2003). Developmental maturation of synaptic vesicle cycling as a distinctive feature of central glutamatergic synapses. Neuroscience *117*, 7–18.

Molnár, G., Oláh, S., Komlósi, G., Füle, M., Szabadics, J., Varga, C., Barzó, P., and Tamás, G. (2008). Complex events initiated by individual spikes in the human cerebral cortex. PLoS Biol. *6*, e222.

Montag-Sallaz, M., Schachner, M., and Montag, D. (2002). Misguided axonal projections, neural cell adhesion molecule 180 mRNA upregulation, and altered

behavior in mice deficient for the close homolog of L1. Mol. Cell. Biol. *22*, 7967–7981.

Monuki, E.S., Porter, F.D., and Walsh, C.A. (2001). Patterning of the dorsal telencephalon and cerebral cortex by a roof plate-Lhx2 pathway. Neuron *32*, 591–604.

Moody, T.W., Getz, R., O'Donohue, T.L., and Rosenstein, J.M. (1988). Localization of receptors for bombesin-like peptides in the rat brain. Ann. N. Y. Acad. Sci. *547*, 114–130.

Moody, W.J., and Bosma, M.M. (2005). Ion channel development, spontaneous activity, and activity-dependent development in nerve and muscle cells. Physiol. Rev. *85*, 883–941.

Moores, C.A., Perderiset, M., Francis, F., Chelly, J., Houdusse, A., and Milligan, R.A. (2004). Mechanism of Microtubule Stabilization by Doublecortin. Molecular Cell *14*, 833–839.

Moores, C.A., Perderiset, M., Kappeler, C., Kain, S., Drummond, D., Perkins, S.J., Chelly, J., Cross, R., Houdusse, A., and Francis, F. (2006). Distinct roles of doublecortin modulating the microtubule cytoskeleton. EMBO J. *25*, 4448–4457.

Morante-Oria, J., Carleton, A., Ortino, B., Kremer, E.J., Fairén, A., and Lledo, P.-M. (2003). Subpallial origin of a population of projecting pioneer neurons during corticogenesis. PNAS *100*, 12468–12473.

Mórotz, G.M., De Vos, K.J., Vagnoni, A., Ackerley, S., Shaw, C.E., and Miller, C.C.J. (2012). Amyotrophic lateral sclerosis-associated mutant VAPBP56S perturbs calcium homeostasis to disrupt axonal transport of mitochondria. Hum. Mol. Genet. *21*, 1979–1988.

Morris, N.R. (2000). Nuclear migration. From fungi to the mammalian brain. J. Cell Biol. *148*, 1097–1101.

Morris-Rosendahl, D.J., Najm, J., Lachmeijer, A.M.A., Sztriha, L., Martins, M., Kuechler, A., Haug, V., Zeschnigk, C., Martin, P., Santos, M., et al. (2008). Refining the phenotype of alpha-1a Tubulin (TUBA1A) mutation in patients with classical lissencephaly. Clin. Genet. *74*, 425–433.

Murtie, J.C., Zhou, Y.-X., Le, T.Q., Vana, A.C., and Armstrong, R.C. (2005). PDGF and FGF2 pathways regulate distinct oligodendrocyte lineage responses in experimental demyelination with spontaneous remyelination. Neurobiol. Dis. *19*, 171–182.

Muzio, L., Di Benedetto, B., DiBenedetto, B., Stoykova, A., Boncinelli, E., Gruss, P., and Mallamaci, A. (2002). Emx2 and Pax6 control regionalization of the pre-neuronogenic cortical primordium. Cereb. Cortex *12*, 129–139.

Muzio, L., Soria, J.M., Pannese, M., Piccolo, S., and Mallamaci, A. (2005). A mutually stimulating loop involving emx2 and canonical wnt signalling specifically

promotes expansion of occipital cortex and hippocampus. Cereb. Cortex *15*, 2021–2028.

Nadarajah, B., Brunstrom, J.E., Grutzendler, J., Wong, R.O.L., and Pearlman, A.L. (2001). Two modes of radial migration in early development of the cerebral cortex. Nature Neuroscience *4*, 143–150.

Nadarajah, B., and Parnavelas, J.G. (2002). Modes of neuronal migration in the developing cerebral cortex. Nat. Rev. Neurosci. *3*, 423–432.

Naderi, J., Lopez, C., and Pandey, S. (2006). Chronically increased oxidative stress in fibroblasts from Alzheimer's disease patients causes early senescence and renders resistance to apoptosis by oxidative stress. Mech. Ageing Dev. *127*, 25–35.

Nakahira, E., and Yuasa, S. (2005). Neuronal generation, migration, and differentiation in the mouse hippocampal primoridium as revealed by enhanced green fluorescent protein gene transfer by means of in utero electroporation. J. Comp. Neurol. *483*, 329–340.

Nakashiba, T., Young, J.Z., McHugh, T.J., Buhl, D.L., and Tonegawa, S. (2008). Transgenic inhibition of synaptic transmission reveals role of CA3 output in hippocampal learning. Science *319*, 1260–1264.

Nakashima, K., Takizawa, T., Ochiai, W., Yanagisawa, M., Hisatsune, T., Nakafuku, M., Miyazono, K., Kishimoto, T., Kageyama, R., and Taga, T. (2001). BMP2-mediated alteration in the developmental pathway of fetal mouse brain cells from neurogenesis to astrocytogenesis. Proc. Natl. Acad. Sci. U.S.A. *98*, 5868–5873.

Nakashima, K., Yanagisawa, M., Arakawa, H., Kimura, N., Hisatsune, T., Kawabata, M., Miyazono, K., and Taga, T. (1999). Synergistic signaling in fetal brain by STAT3-Smad1 complex bridged by p300. Science *284*, 479–482.

Nam, S.C., Kim, Y., Dryanovski, D., Walker, A., Goings, G., Woolfrey, K., Kang, S.S., Chu, C., Chenn, A., Erdelyi, F., et al. (2007). Dynamic features of postnatal subventricular zone cell motility: a two-photon time-lapse study. J. Comp. Neurol. *505*, 190–208.

Namihira, M., Kohyama, J., Semi, K., Sanosaka, T., Deneen, B., Taga, T., and Nakashima, K. (2009). Committed neuronal precursors confer astrocytic potential on residual neural precursor cells. Dev. Cell *16*, 245–255.

Nasrallah, I.M., McManus, M.F., Pancoast, M.M., Wynshaw-Boris, A., and Golden, J.A. (2006). Analysis of non-radial interneuron migration dynamics and its disruption in Lis1+/- mice. J. Comp. Neurol. *496*, 847–858.

Navarro-Quiroga, I., Chittajallu, R., Gallo, V., and Haydar, T.F. (2007). Long-term, selective gene expression in developing and adult hippocampal pyramidal neurons using focal in utero electroporation. J. Neurosci. *27*, 5007–5011.

Newrzella, D., Pahlavan, P.S., Krüger, C., Boehm, C., Sorgenfrei, O., Schröck, H., Eisenhardt, G., Bischoff, N., Vogt, G., Wafzig, O., et al. (2007). The functional

genome of CA1 and CA3 neurons under native conditions and in response to ischemia. BMC Genomics *8*, 370.

Ngugi, A.K., Kariuki, S.M., Bottomley, C., Kleinschmidt, I., Sander, J.W., and Newton, C.R. (2011). Incidence of epilepsy A systematic review and meta-analysis. Neurology *77*, 1005–1012.

Nguyen, L., Besson, A., Roberts, J.M., and Guillemot, F. (2006). Coupling cell cycle exit, neuronal differentiation and migration in cortical neurogenesis. Cell Cycle *5*, 2314–2318.

Nieto, M., Monuki, E.S., Tang, H., Imitola, J., Haubst, N., Khoury, S.J., Cunningham, J., Gotz, M., and Walsh, C.A. (2004). Expression of Cux-1 and Cux-2 in the subventricular zone and upper layers II-IV of the cerebral cortex. J. Comp. Neurol. *479*, 168–180.

Nikolic, M., Chou, M.M., Lu, W., Mayer, B.J., and Tsai, L.H. (1998). The p35/Cdk5 kinase is a neuron-specific Rac effector that inhibits Pak1 activity. Nature *395*, 194–198.

Nissenkorn, A., Michelson, M., Ben-Zeev, B., and Lerman-Sagie, T. (2001). Inborn errors of metabolism: a cause of abnormal brain development. Neurology *56*, 1265–1272.

Noctor, S.C., Flint, A.C., Weissman, T.A., Wong, W.S., Clinton, B.K., and Kriegstein, A.R. (2002). Dividing Precursor Cells of the Embryonic Cortical Ventricular Zone Have Morphological and Molecular Characteristics of Radial Glia. J. Neurosci. *22*, 3161–3173.

Noctor, S.C., Martínez-Cerdeño, V., Ivic, L., and Kriegstein, A.R. (2004). Cortical neurons arise in symmetric and asymmetric division zones and migrate through specific phases. Nat. Neurosci. *7*, 136–144.

Noebels, J.L. (2003). The biology of epilepsy genes. Annu. Rev. Neurosci. *26*, 599–625.

Nogales, E., Wolf, S.G., and Downing, K.H. (1998). Structure of the alpha beta tubulin dimer by electron crystallography. Nature *391*, 199–203.

Nosten-Bertrand, M., Kappeler, C., Dinocourt, C., Denis, C., Germain, J., Phan Dinh Tuy, F., Verstraeten, S., Alvarez, C., Métin, C., Chelly, J., et al. (2008). Epilepsy in Dcx knockout mice associated with discrete lamination defects and enhanced excitability in the hippocampus. PLoS ONE *3*, e2473.

Nowakowski, R.S., and Rakic, P. (1979). The mode of migration of neurons to the hippocampus: a Golgi and electron microscopic analysis in foetal rhesus monkey. J. Neurocytol. *8*, 697–718.

O'Leary, D.D., Bicknese, A.R., De Carlos, J.A., Heffner, C.D., Koester, S.E., Kutka, L.J., and Terashima, T. (1990). Target selection by cortical axons: alternative mechanisms to establish axonal connections in the developing brain. Cold Spring Harb. Symp. Quant. Biol. *55*, 453–468.

O'Leary, D.D., and Sahara, S. (2008). Genetic regulation of arealization of the neocortex. Curr. Opin. Neurobiol. *18*, 90–100.

O'Leary, D.D., and Wilkinson, D.G. (1999). Eph receptors and ephrins in neural development. Curr. Opin. Neurobiol. *9*, 65–73.

Ochiai, W., Yanagisawa, M., Takizawa, T., Nakashima, K., and Taga, T. (2001). Astrocyte differentiation of fetal neuroepithelial cells involving cardiotrophin-1-induced activation of STAT3. Cytokine *14*, 264–271.

Ohkubo, N., Lee, Y.-D., Morishima, A., Terashima, T., Kikkawa, S., Tohyama, M., Sakanaka, M., Tanaka, J., Maeda, N., Vitek, M.P., et al. (2003). Apolipoprotein E and Reelin ligands modulate tau phosphorylation through an apolipoprotein E receptor/disabled-1/glycogen synthase kinase-3beta cascade. FASEB J. *17*, 295–297.

Ohkubo, Y., Chiang, C., and Rubenstein, J.L.R. (2002). Coordinate regulation and synergistic actions of BMP4, SHH and FGF8 in the rostral prosencephalon regulate morphogenesis of the telencephalic and optic vesicles. Neuroscience *111*, 1–17.

Ohshima, T., Hirasawa, M., Tabata, H., Mutoh, T., Adachi, T., Suzuki, H., Saruta, K., Iwasato, T., Itohara, S., Hashimoto, M., et al. (2007). Cdk5 is required for multipolar-to-bipolar transition during radial neuronal migration and proper dendrite development of pyramidal neurons in the cerebral cortex. Development *134*, 2273–2282.

Ohtsuka, T., Sakamoto, M., Guillemot, F., and Kageyama, R. (2001). Roles of the Basic Helix-Loop-Helix Genes Hes1 and Hes5 in Expansion of Neural Stem Cells of the Developing Brain. J. Biol. Chem. *276*, 30467–30474.

Oláh, S., Füle, M., Komlósi, G., Varga, C., Báldi, R., Barzó, P., and Tamás, G. (2009). Regulation of cortical microcircuits by unitary GABA-mediated volume transmission. Nature *461*, 1278–1281.

Ono, K., Yasui, Y., Rutishauser, U., and Miller, R.H. (1997). Focal ventricular origin and migration of oligodendrocyte precursors into the chick optic nerve. Neuron *19*, 283–292.

Palade, G. (1975). Intracellular aspects of the process of protein synthesis. Science *189*, 347–358.

Paolicelli, R.C., Bolasco, G., Pagani, F., Maggi, L., Scianni, M., Panzanelli, P., Giustetto, M., Ferreira, T.A., Guiducci, E., Dumas, L., et al. (2011). Synaptic pruning by microglia is necessary for normal brain development. Science *333*, 1456–1458.

Papadopoulos, M.C., and Verkman, A.S. (2007). Aquaporin-4 and brain edema. Pediatr. Nephrol. *22*, 778–784.

Paradis, S., Harrar, D.B., Lin, Y., Koon, A.C., Hauser, J.L., Griffith, E.C., Zhu, L., Brass, L.F., Chen, C., and Greenberg, M.E. (2007). An RNAi-based approach identifies molecules required for glutamatergic and GABAergic synapse development. Neuron *53*, 217–232.

Parra, P., Gulyás, A.I., and Miles, R. (1998). How many subtypes of inhibitory cells in the hippocampus? Neuron *20*, 983–993.

Parras, C.M., Schuurmans, C., Scardigli, R., Kim, J., Anderson, D.J., and Guillemot, F. (2002). Divergent functions of the proneural genes Mash1 and Ngn2 in the specification of neuronal subtype identity. Genes Dev. *16*, 324–338.

Pellerin, L., Bouzier-Sore, A.-K., Aubert, A., Serres, S., Merle, M., Costalat, R., and Magistretti, P.J. (2007). Activity-dependent regulation of energy metabolism by astrocytes: an update. Glia *55*, 1251–1262.

Pernet, V., Joly, S., Christ, F., Dimou, L., and Schwab, M.E. (2008). Nogo-A and myelin-associated glycoprotein differently regulate oligodendrocyte maturation and myelin formation. J. Neurosci. *28*, 7435–7444.

Petrovich, G.D., Canteras, N.S., and Swanson, L.W. (2001). Combinatorial amygdalar inputs to hippocampal domains and hypothalamic behavior systems. Brain Res. Brain Res. Rev. *38*, 247–289.

Pierani, A., and Wassef, M. (2009). Cerebral cortex development: From progenitors patterning to neocortical size during evolution. Dev. Growth Differ. *51*, 325–342.

Pilz, D.T., Matsumoto, N., Minnerath, S., Mills, P., Gleeson, J.G., Allen, K.M., Walsh, C.A., Barkovich, A.J., Dobyns, W.B., Ledbetter, D.H., et al. (1998). LIS1 and XLIS (DCX) mutations cause most classical lissencephaly, but different patterns of malformation. Hum. Mol. Genet. *7*, 2029–2037.

Pinto, L., and Götz, M. (2007). Radial glial cell heterogeneity--the source of diverse progeny in the CNS. Prog. Neurobiol. *83*, 2–23.

Piper, M., Salih, S., Weinl, C., Holt, C.E., and Harris, W.A. (2005). Endocytosis-dependent desensitization and protein synthesis-dependent resensitization in retinal growth cone adaptation. Nat. Neurosci. *8*, 179–186.

Piskorowski, R.A., and Chevaleyre, V. (2012). Synaptic integration by different dendritic compartments of hippocampal CA1 and CA2 pyramidal neurons. Cell. Mol. Life Sci. *69*, 75–88.

Pleasure, S.J., Collins, A.E., and Lowenstein, D.H. (2000). Unique expression patterns of cell fate molecules delineate sequential stages of dentate gyrus development. J. Neurosci. *20*, 6095–6105.

Polleux, F., Whitford, K.L., Dijkhuizen, P.A., Vitalis, T., and Ghosh, A. (2002). Control of cortical interneuron migration by neurotrophins and PI3-kinase signaling. Development *129*, 3147–3160.

Portera-Cailliau, C., Price, D.L., and Martin, L.J. (1997). Excitotoxic neuronal death in the immature brain is an apoptosis-necrosis morphological continuum. J. Comp. Neurol. *378*, 70–87.

des Portes, V., Francis, F., Pinard, J.M., Desguerre, I., Moutard, M.L., Snoeck, I., Meiners, L.C., Capron, F., Cusmai, R., Ricci, S., et al. (1998a). doublecortin is the

major gene causing X-linked subcortical laminar heterotopia (SCLH). Hum. Mol. Genet. *7*, 1063–1070.

des Portes, V., Pinard, J.M., Billuart, P., Vinet, M.C., Koulakoff, A., Carrié, A., Gelot, A., Dupuis, E., Motte, J., Berwald-Netter, Y., et al. (1998b). A novel CNS gene required for neuronal migration and involved in X-linked subcortical laminar heterotopia and lissencephaly syndrome. Cell *92*, 51–61.

Pouille, F., and Scanziani, M. (2001). Enforcement of temporal fidelity in pyramidal cells by somatic feed-forward inhibition. Science *293*, 1159–1163.

van Praag, H., Kempermann, G., and Gage, F.H. (2000). Neural consequences of environmental enrichment. Nat. Rev. Neurosci. *1*, 191–198.

Prasad, A.N., Bunzeluk, K., Prasad, C., Chodirker, B.N., Magnus, K.G., and Greenberg, C.R. (2007). Agenesis of the corpus callosum and cerebral anomalies in inborn errors of metabolism. Congenit Anom (Kyoto) *47*, 125–135.

Pulvers, J.N., Bryk, J., Fish, J.L., Wilsch-Bräuninger, M., Arai, Y., Schreier, D., Naumann, R., Helppi, J., Habermann, B., Vogt, J., et al. (2010). Mutations in mouse Aspm (abnormal spindle-like microcephaly associated) cause not only microcephaly but also major defects in the germline. Proc. Natl. Acad. Sci. U.S.A. *107*, 16595–16600.

Qian, X., Shen, Q., Goderie, S.K., He, W., Capela, A., Davis, A.A., and Temple, S. (2000). Timing of CNS cell generation: a programmed sequence of neuron and glial cell production from isolated murine cortical stem cells. Neuron *28*, 69–80.

Qiao, J., Kang, J., Ishola, T.A., Rychahou, P.G., Evers, B.M., and Chung, D.H. (2008). Gastrin-releasing peptide receptor silencing suppresses the tumorigenesis and metastatic potential of neuroblastoma. Proc. Natl. Acad. Sci. U.S.A. *105*, 12891–12896.

Qin, J., Mizuguchi, M., Itoh, M., and Takashima, S. (2000). Immunohistochemical expression of doublecortin in the human cerebrum: comparison of normal development and neuronal migration disorders. Brain Res. *863*, 225–232.

Quélin, C., Saillour, Y., Souville, I., Poirier, K., N'guyen-Morel, M.A., Vercueil, L., Millisher-Bellaiche, A.E., Boddaert, N., Dubois, F., Chelly, J., et al. (2012). Mosaic DCX deletion causes subcortical band heterotopia in males. Neurogenetics.

Quinn, J.C., Molinek, M., Martynoga, B.S., Zaki, P.A., Faedo, A., Bulfone, A., Hevner, R.F., West, J.D., and Price, D.J. (2007). Pax6 controls cerebral cortical cell number by regulating exit from the cell cycle and specifies cortical cell identity by a cell autonomous mechanism. Dev. Biol. *302*, 50–65.

Raff, M.C., Miller, R.H., and Noble, M. (1983). A glial progenitor cell that develops in vitro into an astrocyte or an oligodendrocyte depending on culture medium. Nature *303*, 390–396.

Rakic, P. (1972). Mode of cell migration to the superficial layers of fetal monkey neocortex. The Journal of Comparative Neurology *145*, 61–83.

Rakic, P. (1978). Neuronal migration and contact guidance in the primate telencephalon. Postgrad Med J *54 Suppl 1*, 25–40.

Rakic, P. (1995). A small step for the cell, a giant leap for mankind: a hypothesis of neocortical expansion during evolution. Trends Neurosci. *18*, 383–388.

Rallu, M., Corbin, J.G., and Fishell, G. (2002). Parsing the prosencephalon. Nat. Rev. Neurosci. *3*, 943–951.

Ramírez-Amaya, V., Balderas, I., Sandoval, J., Escobar, M.L., and Bermúdez-Rattoni, F. (2001). Spatial long-term memory is related to mossy fiber synaptogenesis. J. Neurosci. *21*, 7340–7348.

Ravelli, R.B.G., Gigant, B., Curmi, P.A., Jourdain, I., Lachkar, S., Sobel, A., and Knossow, M. (2004). Insight into tubulin regulation from a complex with colchicine and a stathmin-like domain. Nature *428*, 198–202.

Reillo, I., Romero, C. de J., García-Cabezas, M.Á., and Borrell, V. (2011). A Role for Intermediate Radial Glia in the Tangential Expansion of the Mammalian Cerebral Cortex. Cereb. Cortex *21*, 1674–1694.

Reiner, A. (1991). A comparison of neurotransmitter-specific and neuropeptide-specific neuronal cell types present in the dorsal cortex in turtles with those present in the isocortex in mammals: implications for the evolution of isocortex. Brain Behav. Evol. *38*, 53–91.

Reiner, O., Carrozzo, R., Shen, Y., Wehnert, M., Faustinella, F., Dobyns, W.B., Caskey, C.T., and Ledbetter, D.H. (1993). Isolation of a Miller-Dieker lissencephaly gene containing G protein beta-subunit-like repeats. Nature *364*, 717–721.

Richardson, W.D., Kessaris, N., and Pringle, N. (2006). Oligodendrocyte wars. Nature Reviews Neuroscience *7*, 11–18.

Rieger, S., Volkmann, K., and Köster, R.W. (2008). Polysialyltransferase expression is linked to neuronal migration in the developing and adult zebrafish. Dev. Dyn. *237*, 276–285.

Del Río, J.A., Heimrich, B., Borrell, V., Förster, E., Drakew, A., Alcántara, S., Nakajima, K., Miyata, T., Ogawa, M., Mikoshiba, K., et al. (1997). A role for Cajal-Retzius cells and reelin in the development of hippocampal connections. Nature *385*, 70–74.

Robin, P., Rossignol, B., and Raymond, M.N. (1995). Effect of microtubule network disturbance by nocodazole and docetaxel (Taxotere) on protein secretion in rat extraorbital lacrimal and parotid glands. Eur. J. Cell Biol. *67*, 227–237.

Robles, E., Huttenlocher, A., and Gomez, T.M. (2003). Filopodial calcium transients regulate growth cone motility and guidance through local activation of calpain. Neuron *38*, 597–609.

Rodal, A.A., Motola-Barnes, R.N., and Littleton, J.T. (2008). Nervous wreck and Cdc42 cooperate to regulate endocytic actin assembly during synaptic growth. J. Neurosci. *28*, 8316–8325.

Rollenhagen, A., Sätzler, K., Rodríguez, E.P., Jonas, P., Frotscher, M., and Lübke, J.H.R. (2007). Structural determinants of transmission at large hippocampal mossy fiber synapses. J. Neurosci. *27*, 10434–10444.

Rooney, C., White, G., Nazgiewicz, A., Woodcock, S.A., Anderson, K.I., Ballestrem, C., and Malliri, A. (2010). The Rac activator STEF (Tiam2) regulates cell migration by microtubule-mediated focal adhesion disassembly. EMBO Reports *11*, 292–298.

Ross, M.E., Allen, K.M., Srivastava, A.K., Featherstone, T., Gleeson, J.G., Hirsch, B., Harding, B.N., Andermann, E., Abdullah, R., Berg, M., et al. (1997). Linkage and physical mapping of X-linked lissencephaly/SBH (XLIS): a gene causing neuronal migration defects in human brain. Hum. Mol. Genet. *6*, 555–562.

Rothman, S.M. (1999). Mutations of the mitochondrial genome: clinical overview and possible pathophysiology of cell damage. Biochem. Soc. Symp. *66*, 111–122.

Rouach, N., Koulakoff, A., Abudara, V., Willecke, K., and Giaume, C. (2008). Astroglial metabolic networks sustain hippocampal synaptic transmission. Science *322*, 1551–1555.

Rowitch, D.H., and Kriegstein, A.R. (2010). Developmental genetics of vertebrate glial-cell specification. Nature *468*, 214–222.

Rubin, A.N., Alfonsi, F., Humphreys, M.P., Choi, C.K.P., Rocha, S.F., and Kessaris, N. (2010). The germinal zones of the basal ganglia but not the septum generate GABAergic interneurons for the cortex. J. Neurosci. *30*, 12050–12062.

Rudy, B., Fishell, G., Lee, S., and Hjerling-Leffler, J. (2011). Three groups of interneurons account for nearly 100% of neocortical GABAergic neurons. Dev Neurobiol *71*, 45–61.

Rusnak, F., and Mertz, P. (2000). Calcineurin: form and function. Physiol. Rev. *80*, 1483–1521.

Ryan, S.D., Bhanot, K., Ferrier, A., De Repentigny, Y., Chu, A., Blais, A., and Kothary, R. (2012). Microtubule stability, Golgi organization, and transport flux require dystonin-a2-MAP1B interaction. J. Cell Biol. *196*, 727–742.

Sabo, S.L., Gomes, R.A., and McAllister, A.K. (2006). Formation of presynaptic terminals at predefined sites along axons. J. Neurosci. *26*, 10813–10825.

Saillour, Y., Carion, N., Quelin, C., Leger, P.-L., Boddaert, N., Elie, C., Toutain, A., Mercier, S., Barthez, M.A., Milh, M., et al. (2009). LIS1-related isolated lissencephaly: spectrum of mutations and relationships with malformation severity. Arch. Neurol. *66*, 1007–1015.

Sapir, T., Elbaum, M., and Reiner, O. (1997). Reduction of microtubule catastrophe events by LIS1, platelet-activating factor acetylhydrolase subunit. EMBO J. *16*, 6977–6984.

Sapir, T., Horesh, D., Caspi, M., Atlas, R., Burgess, H.A., Wolf, S.G., Francis, F., Chelly, J., Elbaum, M., Pietrokovski, S., et al. (2000). Doublecortin mutations cluster in evolutionarily conserved functional domains. Hum. Mol. Genet. *9*, 703–712.

Sapir, T., Shmueli, A., Levy, T., Timm, T., Elbaum, M., Mandelkow, E.-M., and Reiner, O. (2008). Antagonistic effects of doublecortin and MARK2/Par-1 in the developing cerebral cortex. J. Neurosci. *28*, 13008–13013.

Sawamoto, K., Wichterle, H., Gonzalez-Perez, O., Cholfin, J.A., Yamada, M., Spassky, N., Murcia, N.S., Garcia-Verdugo, J.M., Marin, O., Rubenstein, J.L.R., et al. (2006). New neurons follow the flow of cerebrospinal fluid in the adult brain. Science *311*, 629–632.

Scardigli, R., Bäumer, N., Gruss, P., Guillemot, F., and Le Roux, I. (2003). Direct and concentration-dependent regulation of the proneural gene Neurogenin2 by Pax6. Development *130*, 3269–3281.

Schaar, B.T., Kinoshita, K., and McConnell, S.K. (2004). Doublecortin Microtubule Affinity Is Regulated by a Balance of Kinase and Phosphatase Activity at the Leading Edge of Migrating Neurons. Neuron *41*, 203–213.

Schaar, B.T., and McConnell, S.K. (2005). Cytoskeletal coordination during neuronal migration. Proc. Natl. Acad. Sci. U.S.A. *102*, 13652–13657.

Schaefer, M.K.E., Schmalbruch, H., Buhler, E., Lopez, C., Martin, N., Guénet, J.-L., and Haase, G. (2007). Progressive motor neuronopathy: a critical role of the tubulin chaperone TBCE in axonal tubulin routing from the Golgi apparatus. J. Neurosci. *27*, 8779–8789.

Schimmang, T., Lemaistre, M., Vortkamp, A., and Rüther, U. (1992). Expression of the zinc finger gene Gli3 is affected in the morphogenetic mouse mutant extra-toes (Xt). Development *116*, 799–804.

Schousboe, A., and Waagepetersen, H.S. (2006). Glial modulation of GABAergic and glutamat ergic neurotransmission. Curr Top Med Chem *6*, 929–934.

Schuurmans, C., and Guillemot, F. (2002). Molecular mechanisms underlying cell fate specification in the developing telencephalon. Curr. Opin. Neurobiol. *12*, 26–34.

Scuderi, C., Borgione, E., Castello, F., Lo Giudice, M., Fichera, M., Elia, M., Amato, C., Savio, M., Di Blasi, F.D., Vitello, G.A., et al. (2010). Coexistence of mitochondrial and nuclear DNA mutations in a woman with mitochondrial encephalomyopathy and double cortex. Mitochondrion *10*, 548–554.

Seress, L., Abrahám, H., Hajnal, A., Lin, H., and Totterdell, S. (2005). NOS-positive local circuit neurons are exclusively axo-dendritic cells both in the neo- and archi-cortex of the rat brain. Brain Res. *1056*, 183–190.

Sheldon, M., Rice, D.S., D'Arcangelo, G., Yoneshima, H., Nakajima, K., Mikoshiba, K., Howell, B.W., Cooper, J.A., Goldowitz, D., and Curran, T. (1997). Scrambler and yotari disrupt the disabled gene and produce a reeler-like phenotype in mice. Nature *389*, 730–733.

Shen, Q., Wang, Y., Dimos, J.T., Fasano, C.A., Phoenix, T.N., Lemischka, I.R., Ivanova, N.B., Stifani, S., Morrisey, E.E., and Temple, S. (2006). The timing of cortical neurogenesis is encoded within lineages of individual progenitor cells. Nat. Neurosci. *9*, 743–751.

Shi, P., Wei, Y., Zhang, J., Gal, J., and Zhu, H. (2010). Mitochondrial dysfunction is a converging point of multiple pathological pathways in amyotrophic lateral sclerosis. J. Alzheimers Dis. *20 Suppl 2*, S311–324.

Shieh, J.C., Schaar, B.T., Srinivasan, K., Brodsky, F.M., and McConnell, S.K. (2011). Endocytosis regulates cell soma translocation and the distribution of adhesion proteins in migrating neurons. PLoS ONE *6*, e17802.

Shitamukai, A., Konno, D., and Matsuzaki, F. (2011). Oblique radial glial divisions in the developing mouse neocortex induce self-renewing progenitors outside the germinal zone that resemble primate outer subventricular zone progenitors. J. Neurosci. *31*, 3683–3695.

Shmueli, A., Gdalyahu, A., Sapoznik, S., Sapir, T., Tsukada, M., and Reiner, O. (2006). Site-specific dephosphorylation of doublecortin (DCX) by protein phosphatase 1 (PP1). Molecular and Cellular Neuroscience *32*, 15–26.

Shu, T., Ayala, R., Nguyen, M.-D., Xie, Z., Gleeson, J.G., and Tsai, L.-H. (2004). Ndel1 operates in a common pathway with LIS1 and cytoplasmic dynein to regulate cortical neuronal positioning. Neuron *44*, 263–277.

Sicca, F., Kelemen, A., Genton, P., Das, S., Mei, D., Moro, F., Dobyns, W.B., and Guerrini, R. (2003). Mosaic mutations of the LIS1 gene cause subcortical band heterotopia. Neurology *61*, 1042–1046.

Siddiqui, T.J., and Craig, A.M. (2011). Synaptic organizing complexes. Curr. Opin. Neurobiol. *21*, 132–143.

Siegenthaler, J.A., Ashique, A.M., Zarbalis, K., Patterson, K.P., Hecht, J.H., Kane, M.A., Folias, A.E., Choe, Y., May, S.R., Kume, T., et al. (2009). Retinoic acid from the meninges regulates cortical neuron generation. Cell *139*, 597–609.

Silberberg, G., and Markram, H. (2007). Disynaptic inhibition between neocortical pyramidal cells mediated by Martinotti cells. Neuron *53*, 735–746.

Simon, A., Oláh, S., Molnár, G., Szabadics, J., and Tamás, G. (2005). Gap-junctional coupling between neurogliaform cells and various interneuron types in the neocortex. J. Neurosci. *25*, 6278–6285.

Simpson, P.B., and Armstrong, R.C. (1999). Intracellular signals and cytoskeletal elements involved in oligodendrocyte progenitor migration. Glia *26*, 22–35.

Slomianka, L., Amrein, I., Knuesel, I., Sørensen, J.C., and Wolfer, D.P. (2011). Hippocampal pyramidal cells: the reemergence of cortical lamination. Brain Struct Funct *216*, 301–317.

Smart, I.H.M., Dehay, C., Giroud, P., Berland, M., and Kennedy, H. (2002). Unique morphological features of the proliferative zones and postmitotic compartments of the neural epithelium giving rise to striate and extrastriate cortex in the monkey. Cereb. Cortex *12*, 37–53.

Solecki, D.J. (2012). Sticky situations: recent advances in control of cell adhesion during neuronal migration. Current Opinion in Neurobiology.

Solecki, D.J., Trivedi, N., Govek, E.-E., Kerekes, R.A., Gleason, S.S., and Hatten, M.E. (2009). Myosin II motors and F-actin dynamics drive the coordinated movement of the centrosome and soma during CNS glial-guided neuronal migration. Neuron *63*, 63–80.

Sommer, L., Ma, Q., and Anderson, D.J. (1996). neurogenins, a novel family of atonal-related bHLH transcription factors, are putative mammalian neuronal determination genes that reveal progenitor cell heterogeneity in the developing CNS and PNS. Mol. Cell. Neurosci. *8*, 221–241.

Soria, J.M., and Fairén, A. (2000). Cellular mosaics in the rat marginal zone define an early neocortical territorialization. Cereb. Cortex *10*, 400–412.

Soria, J.M., Martínez-Galán, J.R., Luján, R., Valdeolmillos, M., and Fairén, A. (1999). Functional NMDA and GABAA receptors in pioneer neurons of the cortical marginal zone. Eur. J. Neurosci. *11*, 3351–3354.

Sousa, V.H., Miyoshi, G., Hjerling-Leffler, J., Karayannis, T., and Fishell, G. (2009). Characterization of Nkx6-2-derived neocortical interneuron lineages. Cereb. Cortex *19 Suppl 1*, i1–10.

Spruston, N. (2008). Pyramidal neurons: dendritic structure and synaptic integration. Nature Reviews Neuroscience *9*, 206–221.

Stan, A., Pielarski, K.N., Brigadski, T., Wittenmayer, N., Fedorchenko, O., Gohla, A., Lessmann, V., Dresbach, T., and Gottmann, K. (2010). Essential cooperation of N-cadherin and neuroligin-1 in the transsynaptic control of vesicle accumulation. Proc. Natl. Acad. Sci. U.S.A. *107*, 11116–11121.

Stanfield, B.B., and Cowan, W.M. (1979). The development of the hippocampus and dentate gyrus in normal and reeler mice. J. Comp. Neurol. *185*, 423–459.

Stevens, H.E., Smith, K.M., Rash, B.G., and Vaccarino, F.M. (2010). Neural stem cell regulation, fibroblast growth factors, and the developmental origins of neuropsychiatric disorders. Front Neurosci *4*,.

Steward, O. (1976). Topographic organization of the projections from the entorhinal area to the hippocampal formation of the rat. J. Comp. Neurol. *167*, 285–314.

Storrie, B., and Nilsson, T. (2002). The Golgi apparatus: balancing new with old. Traffic *3*, 521–529.

Stoykova, A., Treichel, D., Hallonet, M., and Gruss, P. (2000). Pax6 modulates the dorsoventral patterning of the mammalian telencephalon. J. Neurosci. *20*, 8042–8050.

Streit, W.J., and Xue, Q.-S. (2009). Life and death of microglia. J Neuroimmune Pharmacol *4*, 371–379.

Stults, N.L., Fechheimer, M., and Cummings, R.D. (1989). Relationship between Golgi architecture and glycoprotein biosynthesis and transport in Chinese hamster ovary cells. J. Biol. Chem. *264*, 19956–19966.

Stumpff, J. (2012). Measuring microtubule thickness: an exercise in cooperativity. Dev. Cell *23*, 1–2.

Sun, K.-H., de Pablo, Y., Vincent, F., Johnson, E.O., Chavers, A.K., and Shah, K. (2008). Novel genetic tools reveal Cdk5's major role in Golgi fragmentation in Alzheimer's disease. Mol. Biol. Cell *19*, 3052–3069.

Sun, Y., Nadal-Vicens, M., Misono, S., Lin, M.Z., Zubiaga, A., Hua, X., Fan, G., and Greenberg, M.E. (2001). Neurogenin promotes neurogenesis and inhibits glial differentiation by independent mechanisms. Cell *104*, 365–376.

Supèr, H., Martínez, A., Del Río, J.A., and Soriano, E. (1998). Involvement of distinct pioneer neurons in the formation of layer-specific connections in the hippocampus. J. Neurosci. *18*, 4616–4626.

Szabadics, J., Varga, C., Molnár, G., Oláh, S., Barzó, P., and Tamás, G. (2006). Excitatory effect of GABAergic axo-axonic cells in cortical microcircuits. Science *311*, 233–235.

Tabata, H., and Nakajima, K. (2003). Multipolar migration: the third mode of radial neuronal migration in the developing cerebral cortex. J. Neurosci. *23*, 9996–10001.

Takahashi, T., Goto, T., Miyama, S., Nowakowski, R.S., and Caviness, V.S., Jr (1999). Sequence of neuron origin and neocortical laminar fate: relation to cell cycle of origin in the developing murine cerebral wall. J. Neurosci. *19*, 10357–10371.

Takahashi, T., Nowakowski, R.S., and Caviness, V.S., Jr (1995). Early ontogeny of the secondary proliferative population of the embryonic murine cerebral wall. J. Neurosci. *15*, 6058–6068.

Takasaki, C., Yamasaki, M., Uchigashima, M., Konno, K., Yanagawa, Y., and Watanabe, M. (2010). Cytochemical and cytological properties of perineuronal oligodendrocytes in the mouse cortex. Eur. J. Neurosci. *32*, 1326–1336.

Takizawa, T., Nakashima, K., Namihira, M., Ochiai, W., Uemura, A., Yanagisawa, M., Fujita, N., Nakao, M., and Taga, T. (2001). DNA methylation is a critical cell-intrinsic determinant of astrocyte differentiation in the fetal brain. Dev. Cell *1*, 749–758.

Tanaka, D., Nakaya, Y., Yanagawa, Y., Obata, K., and Murakami, F. (2003). Multimodal tangential migration of neocortical GABAergic neurons independent of GPI-anchored proteins. Development *130*, 5803–5813.

Tanaka, D.H., Maekawa, K., Yanagawa, Y., Obata, K., and Murakami, F. (2006). Multidirectional and multizonal tangential migration of GABAergic interneurons in the developing cerebral cortex. Development *133*, 2167–2176.

Tanaka, D.H., Yanagida, M., Zhu, Y., Mikami, S., Nagasawa, T., Miyazaki, J., Yanagawa, Y., Obata, K., and Murakami, F. (2009). Random walk behavior of migrating cortical interneurons in the marginal zone: time-lapse analysis in flat-mount cortex. J. Neurosci. *29*, 1300–1311.

Tanaka, T., Serneo, F.F., Higgins, C., Gambello, M.J., Wynshaw-Boris, A., and Gleeson, J.G. (2004a). Lis1 and doublecortin function with dynein to mediate coupling of the nucleus to the centrosome in neuronal migration. J. Cell Biol. *165*, 709–721.

Tanaka, T., Serneo, F.F., Tseng, H.-C., Kulkarni, A.B., Tsai, L.-H., and Gleeson, J.G. (2004b). Cdk5 Phosphorylation of Doublecortin Ser297 Regulates Its Effect on Neuronal Migration. Neuron *41*, 215–227.

Tanaka, T., Veeranna, Ohshima, T., Rajan, P., Amin, N.D., Cho, A., Sreenath, T., Pant, H.C., Brady, R.O., and Kulkarni, A.B. (2001). Neuronal cyclin-dependent kinase 5 activity is critical for survival. J. Neurosci. *21*, 550–558.

Tanemura, K., Murayama, M., Akagi, T., Hashikawa, T., Tominaga, T., Ichikawa, M., Yamaguchi, H., and Takashima, A. (2002). Neurodegeneration with tau accumulation in a transgenic mouse expressing V337M human tau. J. Neurosci. *22*, 133–141.

Taniguchi, Y., Young-Pearse, T., Sawa, A., and Kamiya, A. (2012). In utero electroporation as a tool for genetic manipulation in vivo to study psychiatric disorders: from genes to circuits and behaviors. Neuroscientist *18*, 169–179.

Tarabykin, V., Stoykova, A., Usman, N., and Gruss, P. (2001). Cortical upper layer neurons derive from the subventricular zone as indicated by Svet1 gene expression. Development *128*, 1983–1993.

Taverna, E., and Huttner, W.B. (2010). Neural progenitor nuclei IN motion. Neuron *67*, 906–914.

Taylor, K.R., Holzer, A.K., Bazan, J.F., Walsh, C.A., and Gleeson, J.G. (2000). Patient mutations in doublecortin define a repeated tubulin-binding domain. J. Biol. Chem. *275*, 34442–34450.

Teuling, E., van Dis, V., Wulf, P.S., Haasdijk, E.D., Akhmanova, A., Hoogenraad, C.C., and Jaarsma, D. (2008). A novel mouse model with impaired dynein/dynactin function develops amyotrophic lateral sclerosis (ALS)-like features in motor neurons and improves lifespan in SOD1-ALS mice. Hum. Mol. Genet. *17*, 2849–2862.

Thompson, C.L., Pathak, S.D., Jeromin, A., Ng, L.L., MacPherson, C.R., Mortrud, M.T., Cusick, A., Riley, Z.L., Sunkin, S.M., Bernard, A., et al. (2008). Genomic anatomy of the hippocampus. Neuron *60*, 1010–1021.

Thored, P., Heldmann, U., Gomes-Leal, W., Gisler, R., Darsalia, V., Taneera, J., Nygren, J.M., Jacobsen, S.-E.W., Ekdahl, C.T., Kokaia, Z., et al. (2009). Long-term accumulation of microglia with proneurogenic phenotype concomitant with persistent neurogenesis in adult subventricular zone after stroke. Glia *57*, 835–849.

Thyberg, J., and Moskalewski, S. (1985). Microtubules and the organization of the Golgi complex. Exp. Cell Res. *159*, 1–16.

Tilney, L.G., Bryan, J., Bush, D.J., Fujiwara, K., Mooseker, M.S., Murphy, D.B., and Snyder, D.H. (1973). Microtubules: evidence for 13 protofilaments. J. Cell Biol. *59*, 267–275.

Tint, I., Jean, D., Baas, P.W., and Black, M.M. (2009). Doublecortin Associates with Microtubules Preferentially in Regions of the Axon Displaying Actin-Rich Protrusive Structures. J. Neurosci. *29*, 10995–11010.

Tiveron, M.-C., Rossel, M., Moepps, B., Zhang, Y.L., Seidenfaden, R., Favor, J., König, N., and Cremer, H. (2006). Molecular interaction between projection neuron precursors and invading interneurons via stromal-derived factor 1 (CXCL12)/CXCR4 signaling in the cortical subventricular zone/intermediate zone. J. Neurosci. *26*, 13273–13278.

Togashi, H., Abe, K., Mizoguchi, A., Takaoka, K., Chisaka, O., and Takeichi, M. (2002). Cadherin regulates dendritic spine morphogenesis. Neuron *35*, 77–89.

Togashi, K., von Schimmelmann, M.J., Nishiyama, M., Lim, C.-S., Yoshida, N., Yun, B., Molday, R.S., Goshima, Y., and Hong, K. (2008). Cyclic GMP-gated CNG channels function in Sema3A-induced growth cone repulsion. Neuron *58*, 694–707.

Tojima, T., Akiyama, H., Itofusa, R., Li, Y., Katayama, H., Miyawaki, A., and Kamiguchi, H. (2007). Attractive axon guidance involves asymmetric membrane transport and exocytosis in the growth cone. Nat. Neurosci. *10*, 58–66.

Tojima, T., Hines, J.H., Henley, J.R., and Kamiguchi, H. (2011). Second messengers and membrane trafficking direct and organize growth cone steering. Nat. Rev. Neurosci. *12*, 191–203.

Tojima, T., Itofusa, R., and Kamiguchi, H. (2010). Asymmetric clathrin-mediated endocytosis drives repulsive growth cone guidance. Neuron *66*, 370–377.

Tole, S., Christian, C., and Grove, E.A. (1997). Early specification and autonomous development of cortical fields in the mouse hippocampus. Development *124*, 4959–4970.

Tole, S., and Grove, E.A. (2001). Detailed field pattern is intrinsic to the embryonic mouse hippocampus early in neurogenesis. J. Neurosci. *21*, 1580–1589.

Toyo-oka, K., Shionoya, A., Gambello, M.J., Cardoso, C., Leventer, R., Ward, H.L., Ayala, R., Tsai, L.-H., Dobyns, W., Ledbetter, D., et al. (2003). 14-3-3epsilon is important for neuronal migration by binding to NUDEL: a molecular explanation for Miller-Dieker syndrome. Nat. Genet. *34*, 274–285.

Traub, R.D., Bibbig, A., LeBeau, F.E.N., Buhl, E.H., and Whittington, M.A. (2004). Cellular mechanisms of neuronal population oscillations in the hippocampus in vitro. Annu. Rev. Neurosci. *27*, 247–278.

Tricoire, L., Pelkey, K.A., Erkkila, B.E., Jeffries, B.W., Yuan, X., and McBain, C.J. (2011). A blueprint for the spatiotemporal origins of mouse hippocampal interneuron diversity. J. Neurosci. *31*, 10948–10970.

Trommsdorff, M., Gotthardt, M., Hiesberger, T., Shelton, J., Stockinger, W., Nimpf, J., Hammer, R.E., Richardson, J.A., and Herz, J. (1999). Reeler/Disabled-like disruption of neuronal migration in knockout mice lacking the VLDL receptor and ApoE receptor 2. Cell *97*, 689–701.

Tsai, H.-H., Frost, E., To, V., Robinson, S., Ffrench-Constant, C., Geertman, R., Ransohoff, R.M., and Miller, R.H. (2002). The chemokine receptor CXCR2 controls positioning of oligodendrocyte precursors in developing spinal cord by arresting their migration. Cell *110*, 373–383.

Tsai, H.-H., and Miller, R.H. (2002). Glial cell migration directed by axon guidance cues. Trends Neurosci. *25*, 173–175; discussion 175–176.

Tsai, J.-W., Bremner, K.H., and Vallee, R.B. (2007). Dual subcellular roles for LIS1 and dynein in radial neuronal migration in live brain tissue. Nat. Neurosci. *10*, 970–979.

Tsai, J.-W., Chen, Y., Kriegstein, A.R., and Vallee, R.B. (2005). LIS1 RNA interference blocks neural stem cell division, morphogenesis, and motility at multiple stages. J. Cell Biol. *170*, 935–945.

Tsai, J.-W., Lian, W.-N., Kemal, S., Kriegstein, A.R., and Vallee, R.B. (2010). Kinesin 3 and cytoplasmic dynein mediate interkinetic nuclear migration in neural stem cells. Nature Neuroscience *13*, 1463–1471.

Tsai, L.-H., and Gleeson, J.G. (2005). Nucleokinesis in neuronal migration. Neuron *46*, 383–388.

Tsukada, M., Prokscha, A., Ungewickell, E., and Eichele, G. (2005). Doublecortin association with actin filaments is regulated by neurabin II. J. Biol. Chem. *280*, 11361–11368.

Turner, J.R., and Tartakoff, A.M. (1989). The response of the Golgi complex to microtubule alterations: the roles of metabolic energy and membrane traffic in Golgi complex organization. J. Cell Biol. *109*, 2081–2088.

Tuvia, S., Garver, T.D., and Bennett, V. (1997). The phosphorylation state of the FIGQY tyrosine of neurofascin determines ankyrin-binding activity and patterns of cell segregation. Proc. Natl. Acad. Sci. U.S.A. *94*, 12957–12962.

Tyzio, R., Represa, A., Jorquera, I., Ben-Ari, Y., Gozlan, H., and Aniksztejn, L. (1999). The Establishment of GABAergic and Glutamatergic Synapses on CA1 Pyramidal Neurons is Sequential and Correlates with the Development of the Apical Dendrite. J. Neurosci. *19*, 10372–10382.

Vasudevan, A., Long, J.E., Crandall, J.E., Rubenstein, J.L.R., and Bhide, P.G. (2008). Compartment-specific transcription factors orchestrate angiogenesis gradients in the embryonic brain. Nat. Neurosci. *11*, 429–439.

Verrotti, A., Spalice, A., Ursitti, F., Papetti, L., Mariani, R., Castronovo, A., Mastrangelo, M., and Iannetti, P. (2010). New trends in neuronal migration disorders. Eur. J. Paediatr. Neurol. *14*, 1–12.

Verstreken, P., Ly, C.V., Venken, K.J.T., Koh, T.-W., Zhou, Y., and Bellen, H.J. (2005). Synaptic mitochondria are critical for mobilization of reserve pool vesicles at Drosophila neuromuscular junctions. Neuron *47*, 365–378.

Voigt, T. (1989). Development of glial cells in the cerebral wall of ferrets: direct tracing of their transformation from radial glia into astrocytes. J. Comp. Neurol. *289*, 74–88.

Wada, E., Way, J., Lebacq-Verheyden, A.M., and Battey, J.F. (1990). Neuromedin B and gastrin-releasing peptide mRNAs are differentially distributed in the rat nervous system. J. Neurosci. *10*, 2917–2930.

Walton, N.M., Sutter, B.M., Laywell, E.D., Levkoff, L.H., Kearns, S.M., Marshall, G.P., 2nd, Scheffler, B., and Steindler, D.A. (2006). Microglia instruct subventricular zone neurogenesis. Glia *54*, 815–825.

Wang, G.X., and Poo, M.-M. (2005). Requirement of TRPC channels in netrin-1-induced chemotropic turning of nerve growth cones. Nature *434*, 898–904.

Wang, X., Tsai, J.-W., LaMonica, B., and Kriegstein, A.R. (2011). A new subtype of progenitor cell in the mouse embryonic neocortex. Nat. Neurosci. *14*, 555–561.

Wang, Z., Wang, B., Yang, L., Guo, Q., Aithmitti, N., Songyang, Z., and Zheng, H. (2009). Presynaptic and postsynaptic interaction of the amyloid precursor protein promotes peripheral and central synaptogenesis. J. Neurosci. *29*, 10788–10801.

Washbourne, P., Liu, X.-B., Jones, E.G., and McAllister, A.K. (2004). Cycling of NMDA receptors during trafficking in neurons before synapse formation. J. Neurosci. *24*, 8253–8264.

Wehland, J., Henkart, M., Klausner, R., and Sandoval, I.V. (1983). Role of microtubules in the distribution of the Golgi apparatus: effect of taxol and microinjected anti-alpha-tubulin antibodies. Proc. Natl. Acad. Sci. U.S.A. *80*, 4286–4290.

Weimann, J.M., Zhang, Y.A., Levin, M.E., Devine, W.P., Brûlet, P., and McConnell, S.K. (1999). Cortical neurons require Otx1 for the refinement of exuberant axonal projections to subcortical targets. Neuron *24*, 819–831.

Wen, Z., Guirland, C., Ming, G.-L., and Zheng, J.Q. (2004). A CaMKII/calcineurin switch controls the direction of Ca(2+)-dependent growth cone guidance. Neuron *43*, 835–846.

Wichterle, H., Turnbull, D.H., Nery, S., Fishell, G., and Alvarez-Buylla, A. (2001). In utero fate mapping reveals distinct migratory pathways and fates of neurons born in the mammalian basal forebrain. Development *128*, 3759–3771.

Williams, M.E., Wilke, S.A., Daggett, A., Davis, E., Otto, S., Ravi, D., Ripley, B., Bushong, E.A., Ellisman, M.H., Klein, G., et al. (2011). Cadherin-9 regulates synapse-specific differentiation in the developing hippocampus. Neuron *71*, 640–655.

Wilson, S.W., and Rubenstein, J.L. (2000). Induction and dorsoventral patterning of the telencephalon. Neuron *28*, 641–651.

Wodarz, A., and Huttner, W.B. (2003). Asymmetric cell division during neurogenesis in Drosophila and vertebrates. Mech. Dev. *120*, 1297–1309.

Woodruff, A., Xu, Q., Anderson, S.A., and Yuste, R. (2009). Depolarizing effect of neocortical chandelier neurons. Front Neural Circuits *3*, 15.

Woodruff, A.R., Monyer, H., and Sah, P. (2006). GABAergic excitation in the basolateral amygdala. J. Neurosci. *26*, 11881–11887.

Wu, C., Cui, B., He, L., Chen, L., and Mobley, W.C. (2009). The coming of age of axonal neurotrophin signaling endosomes. J Proteomics *72*, 46–55.

Wu, S.-X., Goebbels, S., Nakamura, K., Nakamura, K., Kometani, K., Minato, N., Kaneko, T., Nave, K.-A., and Tamamaki, N. (2005). Pyramidal neurons of upper cortical layers generated by NEX-positive progenitor cells in the subventricular zone. Proc. Natl. Acad. Sci. U.S.A. *102*, 17172–17177.

Xie, Z., Sanada, K., Samuels, B.A., Shih, H., and Tsai, L.H. (2003). Serine 732 phosphorylation of FAK by Cdk5 is important for microtubule organization, nuclear movement, and neuronal migration. Cell *114*, 469–482.

Xu, X., and Callaway, E.M. (2009). Laminar specificity of functional input to distinct types of inhibitory cortical neurons. J. Neurosci. *29*, 70–85.

Yap, C.C., Vakulenko, M., Kruczek, K., Motamedi, B., Digilio, L., Liu, J.S., and Winckler, B. (2012). Doublecortin (DCX) Mediates Endocytosis of Neurofascin Independently of Microtubule Binding. J. Neurosci. *32*, 7439–7453.

Yoshida, M., Assimacopoulos, S., Jones, K.R., and Grove, E.A. (2006). Massive loss of Cajal-Retzius cells does not disrupt neocortical layer order. Development *133*, 537–545.

Yu, X., and Zecevic, N. (2011). Dorsal radial glial cells have the potential to generate cortical interneurons in human but not in mouse brain. J. Neurosci. *31*, 2413–2420.

Zemlyak, I., Sapolsky, R., and Gozes, I. (2009). NAP protects against cytochrome c release: inhibition of the initiation of apoptosis. Eur. J. Pharmacol. *618*, 9–14.

Zeng, Y.-S., and C. Xu, Z. (2000). Co-existence of necrosis and apoptosis in rat hippocampus following transient forebrain ischemia. Neuroscience Research *37*, 113–125.

Zerlin, M., Levison, S.W., and Goldman, J.E. (1995). Early patterns of migration, morphogenesis, and intermediate filament expression of subventricular zone cells in the postnatal rat forebrain. J. Neurosci. *15*, 7238–7249.

Zhao, Y., Sheng, H.Z., Amini, R., Grinberg, A., Lee, E., Huang, S., Taira, M., and Westphal, H. (1999). Control of hippocampal morphogenesis and neuronal differentiation by the LIM homeobox gene Lhx5. Science *284*, 1155–1158.

Zheng, J.Q. (2000). Turning of nerve growth cones induced by localized increases in intracellular calcium ions. Nature *403*, 89–93.

Zhou, C., Qiu, Y., Pereira, F.A., Crair, M.C., Tsai, S.Y., and Tsai, M.J. (1999). The nuclear orphan receptor COUP-TFI is required for differentiation of subplate neurons and guidance of thalamocortical axons. Neuron *24*, 847–859.

Zhou, Q., Wang, S., and Anderson, D.J. (2000). Identification of a novel family of oligodendrocyte lineage-specific basic helix-loop-helix transcription factors. Neuron *25*, 331–343.

Zimmer, C., Lee, J., Griveau, A., Arber, S., Pierani, A., Garel, S., and Guillemot, F. (2010). Role of Fgf8 signalling in the specification of rostral Cajal-Retzius cells. Development *137*, 293–302.

Zsiros, V., and Maccaferri, G. (2005). Electrical coupling between interneurons with different excitable properties in the stratum lacunosum-moleculare of the juvenile CA1 rat hippocampus. J. Neurosci. *25*, 8686–8695.

(2006). The Hippocampus Book (Oxford University Press, USA).